



저작자표시-비영리-변경금지 2.0 대한민국

이용자는 아래의 조건을 따르는 경우에 한하여 자유롭게

- 이 저작물을 복제, 배포, 전송, 전시, 공연 및 방송할 수 있습니다.

다음과 같은 조건을 따라야 합니다:



저작자표시. 귀하는 원저작자를 표시하여야 합니다.



비영리. 귀하는 이 저작물을 영리 목적으로 이용할 수 없습니다.



변경금지. 귀하는 이 저작물을 개작, 변형 또는 가공할 수 없습니다.

- 귀하는, 이 저작물의 재이용이나 배포의 경우, 이 저작물에 적용된 이용허락조건을 명확하게 나타내어야 합니다.
- 저작권자로부터 별도의 허가를 받으면 이러한 조건들은 적용되지 않습니다.

저작권법에 따른 이용자의 권리는 위의 내용에 의하여 영향을 받지 않습니다.

이것은 [이용허락규약\(Legal Code\)](#)을 이해하기 쉽게 요약한 것입니다.

[Disclaimer](#)

이학박사 학위논문

Rhodium-Catalyzed Asymmetric Cyclization of Alkynes

로듐 촉매에 의한 알카인의
비대칭 고리화 반응

2019 년 2 월

서울대학교 대학원

화학부 유기화학 전공

최 경 민

Abstract

Described here is the development of rhodium-catalyzed asymmetric cyclization reactions of alkynes. For the amplification of synthetic utilities of transition metal vinylidene mediated catalysis in carbocyclization reactions (Chapter 1), a rhodium-catalyzed intramolecular alkenylation of enamines tethered with terminal alkyne was developed (Chapter 2). By using a rhodium-vinylidene complex as a catalytic intermediate, *5-endo-dig* Conia-ene type process could be achieved with alkynylamine substrates. Furthermore, chiral enamines derived from chiral primary amines could induce diastereoselectivity in the C–C bond formation, giving rise to cyclopentenes that have a chiral quaternary carbon.

In contrast to the works described above for the *anti*-Markovnikov carbofunctionalization of terminal alkynes, following studies focused on a rhodium-catalyzed vicinal carbofunctionalization of alkynes with organoboron compounds (Chapter 3). In a rhodium-catalyzed tandem addition–cyclization of alkynylimines, a single rhodium catalyst mediated a sequential inter- and intramolecular 1,2-carborhodations, providing alkylidene cyclobutylamines (Chapter 4). We have shown that hydrolysis-prone aliphatic sulfonylimines could participate in a tandem process, and the exploration of chiral diene ligands enabled the asymmetric induction making chiral cyclobutylamine with excellent enantioselectivity. With the feasibility of catalytic alkenyl addition to the C=N bond, the scope of the C=N bond was expanded by using sulfonylhydrazones instead of imines (Chapter 5). Under mild and operationally simple reaction conditions, traceless endocyclic alkene synthesis could be achieved based on the merger of rhodium-catalysis and pericyclic rearrangement. Mechanistically, alkynylhydrazones gave cyclic hydrazide intermediate by the rhodium-catalysis with organoboronic acids, and it was decomposed to the product *via* allylic diazene with the

extrusion of dinitrogen gas. Furthermore, chiral diene ligands could induce enantioselective addition of the alkenyl rhodium intermediate to the C=N bond, affording an enantioenriched C–N stereocenter whose chirality is transferred to an allylic position *via* stereospecific rearrangement.

Keyword: rhodium, alkyne, cyclization, vinylidene,
tandem cyclization, retro-ene reaction

Student Number: 2013-22942

Table of Contents

Abstract	1
Table of Contents	3
List of Tables	7
List of Schemes	9
List of Figures	16
Abbreviations.....	17
Abstract in Korean	250
Appendix	252

Chapter 1. Transition Metal Vinylidene Mediated Catalytic Carbocyclization of Alkynes

1.1 Introduction	19
1.2 Carbocyclization by nucleophilic addition	
1.2.1 Enol and enamine nucleophiles	19
1.2.2 Alkene and alkyne nucleophiles	21
1.2.3 Carbocyclization initiated by oxygen nucleophiles	25
1.3 Carbocyclization by pericyclic reaction	
1.3.1 Electrocyclization	29
1.3.2 Cycloaddition	31
1.3.3 Sigmatropic rearrangement	34
1.4 Carbocyclization with disubstituted metal vinylidenes	36
1.5 Conclusion	45
1.6 Reference	47

Chapter 2. Rhodium-Catalyzed Carbocyclization of Alkynylamines

2.1 Introduction	50
2.2 Results and discussion	
2.2.1 Carbocyclization of <i>N</i> -benzyl alkynylamine	55
2.2.2 Substrate scope	58
2.2.3 Asymmetric carbocyclization of alkynylamines	60
2.2.4 Proposed mechanism and mechanistic studies	63
2.2.5 Dual catalysis: Merging rhodium-catalysis with organocatalysis	70
2.3 Conclusion and future studies	80
2.4 Reference	83
2.5 Experimental section	
2.5.1 General remarks	85
2.5.2 Synthesis and characterization for compounds	
2.5.2.1 General procedure for alkylation of β -ketoesters	85
2.5.2.2 General procedure for the alkynylamines	88
2.5.2.3 General procedure for the rhodium-catalyzed carbocyclization of alkynylamines	93
2.5.3 Determination of the enantiomeric excess	96

Chapter 3. Rhodium-Catalyzed Tandem Addition–Cyclization Reactions of Alkynes with Organoborons

3.1 Introduction	99
3.2 Tandem addition–cyclization with unsaturated carbon–heteroatom bonds	100

3.3 Tandem addition–cyclization with unsaturated carbon–carbon bonds	105
3.4 Conclusion	113
3.5 Reference	114

Chapter 4. Rhodium-Catalyzed Tandem Addition–Cyclization of Alkynylimines

4.1 Introduction	116
4.2 Results and discussion	
4.2.1 Substrate scope	120
4.2.2 Asymmetric carbocyclization of alkynylimine	123
4.3 Conclusion	126
4.4 Reference	127
4.5 Experimental section	
4.5.1 General remarks	128
4.5.2 Synthesis and characterization for substrates	128
4.5.3 General procedure for the rhodium-catalyzed tandem cyclization	131
4.5.4 Characterization for products	132
4.5.5 Procedure for enantioselective rhodium-catalyzed tandem cyclization	138
4.5.6 Preparation of the rhodium-diene complex 4.25	138

Chapter 5. Rhodium-Catalyzed Tandem Addition–Cyclization–Rearrangement of Alkynylhydrazones

5.1 Introduction	139
5.2 Results and discussion	
5.2.1 Preliminary results	146
5.2.2 Optimization of reaction conditions	150
5.2.3 Substrate scope of organoboronic acids	153
5.2.4 Substrate scope of alkynylhydrazones	157
5.2.5 Arylative ring contraction of cyclohexenones	170
5.2.6 Competition experiments with alkynylaldehyde	173
5.2.7 Asymmetric carbocyclization of alkynylhydrazones	175
5.2.8 Mechanistic studies	182
5.3 Conclusion	186
5.4 Reference	187
5.5 Experimental section	
5.5.1 General remarks	190
5.5.2 Synthesis and characterization for substrates	191
5.5.3 General procedure for the rhodium-catalyzed tandem reaction	215
5.5.4 Characterization for products	216
5.5.5 Competition experiments with alkynylaldehyde	246
5.5.6 Determination of the absolute stereochemistry of 5.35	247
5.5.7 Mechanistic studies	249

List of Tables

Chapter 2

Table 2.1 Phosphine ligand screening	56
Table 2.2 Base screening	57
Table 2.3 Solvent screening	58
Table 2.4 Chiral auxiliary and temperature effects on carbocyclization	62
Table 2.5 Ligand screening experiments	72
Table 2.6 Rh(I)/amine equivalent screening experiments	73
Table 2.7 Primary amine catalyst screening experiments	75
Table 2.8 Rh(I) and Ru(II) precatalyst screening	76
Table 2.9 Brønsted acid screening results	77
Table 2.10 The effects of additives on Rh(I)-catalyzed carbocyclization of an alkynylamine	79

Chapter 4

Table 4.1 Substrate scope of arylboronic acids	120
Table 4.2 Substrate scope for an internal alkyne	122
Table 4.3 Chiral ligand screening for enantioselective cyclization	124

Chapter 5

Table 5.1 Preliminary solvent screening	147
Table 5.2 Solvent screening with toluene and methanol	150
Table 5.3 Alcohol solvent screening	151
Table 5.4 The scope of phenylboronic acid derivatives	154
Table 5.5 The scope of heteroaryl boronic acids	155
Table 5.6 The scope of phenylboronic acids with a TsN-tethered substrate	165
Table 5.7 Pyrroline and pyrrolinone synthesis by Rh(I)-catalysis	167

Table 5.8 The scope of phenylboronic acids with 5.101 under modified conditions	168
Table 5.9 Tandem fragmentation–condensation of α,β -epoxyketones	172
Table 5.10 Enantioselective Rh(I)-catalysis in methanol solvent	176
Table 5.11 Condition optimization using aqueous aprotic solvent	177
Table 5.12 Enantioselective Rh(I)-catalysis in aqueous toluene solvent	178-179
Table 5.13 The scope of the Rh(I)-catalyzed asymmetric tandem addition–cyclization–rearrangement with organoboronic acids	181

List of Schemes

Chapter 1

Scheme 1.1 Mo(0)-catalyzed cycloisomerization of an alkynylmalonate ...	20
Scheme 1.2 W(0)-mediated cyclization of alkyne-tethered silyl enol ethers	20
Scheme 1.3 Rh(I)-catalyzed cycloisomerization of <i>N</i> -propargylenamines	21
Scheme 1.4 Ru(II)-catalyzed cycloisomerization of an ethynylstilbene	22
Scheme 1.5 Ru(II)-catalyzed tandem carbocyclization of an ethynylstyrene	22
Scheme 1.6 Ru(II)-catalyzed cycloisomerization of a 1,5-enyne	23
Scheme 1.7 Ru(II)-catalyzed carboxylative carbocyclization of a 1,6-diyne	24
Scheme 1.8 Ru(II)- and Rh(I)-mediated cycloaromatization of enediynes .	25
Scheme 1.9 Ru(II)-catalyzed hydrative carbocyclization of a 1,5-enyne ..	26
Scheme 1.10 Ru(II)-catalyzed decarbonylative carbocyclization	27
Scheme 1.11 Ru(II)-catalyzed carbocyclization of epoxyalkynes with oxygen transfer	28
Scheme 1.12 Ru(II)-catalyzed oxygenative [2+2] cycloaddition of a sulfoxyenyne	29
Scheme 1.13 Ru(II)-catalyzed 6 π -electrocyclization of dienyne	30
Scheme 1.14 W(0)- and Ru(II)-catalyzed cycloisomerization of aromatic enynes	31
Scheme 1.15 Pd(II)- and Ni ₂ -catalyzed vinylidene transfer reactions	32
Scheme 1.16 Ru(0)-catalyzed carbonylative carbocyclization of a diyne ...	32
Scheme 1.17 Rh(I)-catalyzed cycloisomerization of a 1,6-enyne	33
Scheme 1.18 Rh(I)-catalyzed dimerization of an arylacetylene	34

Scheme 1.19 Ru(II)-catalyzed cycloisomerization of a 2-alkyl arylacetylene	35
Scheme 1.20 Re(I)-catalyzed formal [4+3] cycloaddition	36
Scheme 1.21 Rh(I)-catalyzed tandem carbocyclization of a haloenyne	37
Scheme 1.22 Rh(I)-catalyzed [2+2] cycloaddition of an alkyne and an enoate	37
Scheme 1.23 Rh(I)-catalyzed cycloisomerization of a 1,6-allenyne	38
Scheme 1.24 Au(I)-catalyzed tandem cycloisomerization of diynes	39
Scheme 1.25 Proposed mechanism for Au(I)-catalyzed cycloisomerization	39
Scheme 1.26 Au-catalyzed tandem cycloisomerization of an allenyne	40
Scheme 1.27 Au(I)-catalyzed carbocyclization of monoalkynes	41
Scheme 1.28 Au(I)-catalyzed carbocyclization of diynes	42
Scheme 1.29 Au(I)-catalyzed tandem cycloaddition–rearrangement of a diyne and an alkene	43
Scheme 1.30 Au(I)-catalyzed reconstitutive cycloisomerization of a hexynyl tosylate	44
Scheme 1.31 Au(I)-catalyzed decarbonylative carbocyclization of a diyne	44
Scheme 1.32 Au(I)-catalyzed oxygenative carbocyclization of a diyne	45

Chapter 2

Scheme 2.1 Hf(IV)-catalyzed 5- <i>endo</i> -dig carbocyclization	51
Scheme 2.2 Au(I)-catalyzed enantioselective 5- <i>endo</i> -dig cycloisomerization	51
Scheme 2.3 Au(I)-catalyzed 5- <i>endo</i> -dig cycloisomerization	52
Scheme 2.4 La(III)/Ag(I) co-catalyzed cycloisomerization	53
Scheme 2.5 Zn(II)/Yb(III) co-catalyzed cycloisomerization	53

Scheme 2.6 General scheme for the rhodium-catalyzed cyclization reactions of alkynyl enamines	55
Scheme 2.7 Synthesis of the <i>N</i> -benzyl alkynyl enamine 2.19	56
Scheme 2.8 5- <i>endo</i> -dig carbocyclization of alkynyl enamines	59
Scheme 2.9 Cyclization of alkynyl enamines for the 6- <i>endo</i> product	60
Scheme 2.10 Working hypothesis for the asymmetric carbocyclization of an alkynyl enamine using a chiral enamine	61
Scheme 2.11 Preliminary result of asymmetric carbocyclization of an alkynyl enamine	61
Scheme 2.12 Proposed mechanism for rhodium-catalyzed carbocyclization	63
Scheme 2.13 Deuterium-labeling experiments for mechanistic studies	64
Scheme 2.14 Poor reactivity of phenyl substituted alkynyl enamines without a base	65
Scheme 2.15 Rh(I)-catalyzed carbocyclization under oxidative conditions	66
Scheme 2.16 Observation of the oxygenative addition before carbocyclization	67
Scheme 2.17 Au(I)-catalyzed asymmetric carbocyclization of an alkynyl enamine	68
Scheme 2.18 Rh(I)-catalyzed carbocyclization of the internal alkyne-tethered enamine.....	68
Scheme 2.19 Rh(I)/amine-catalyzed carbocyclization of an alkynyl β -keto ester	70
Scheme 2.20 ^1H NMR experiments for <i>in situ</i> synthesis of an alkynyl enamine	71
Scheme 2.21 The effects of DABCO and water additives	74
Scheme 2.22 Rh(I)-catalyzed dimerization of an alkynyl β -ketoester	78
Scheme 2.23 Further mechanistic studies	81
Scheme 2.24 Further studies for dual catalytic carbocyclization	82

Scheme 2.25 Stereoisomerism of S2.6	96
---	----

Chapter 3

Scheme 3.1 Types of Rh(I)-catalyzed tandem addition–cyclization reactions	100
Scheme 3.2 Rh(I)-catalyzed asymmetric arylative cyclization of an alkynal	101
Scheme 3.3 Rh(I)-catalyzed arylative cyclization of an alkynyl ester	101
Scheme 3.4 Rh(I)-catalyzed tandem addition–cyclization of alkynyl ketones	103
Scheme 3.5 Rh(I)-catalyzed enantioselective tandem addition–cyclization of alkynyl ketones	104
Scheme 3.6 Rh(I)-catalyzed arylative cyclization of an alkynyl isocyanate and an alkynyl nitrile	105
Scheme 3.7 Rh(I)-catalyzed arylative cyclization of 1,6-enynes	106
Scheme 3.8 Rh(I)-catalyzed arylative cyclization of an alkynyl allyl ether	107
Scheme 3.9 Rh(I)-catalyzed asymmetric arylative cyclization of an alkynyl enoate	108
Scheme 3.10 Rh(I)-catalyzed enantioselective synthesis of spirocarbocycle	109
Scheme 3.11 Rh(I)-catalyzed arylative desymmetrization of an alkynyldienone	110
Scheme 3.12 Rh(I)-catalyzed arylative cyclization for azacycles	111
Scheme 3.13 Rh(I)-catalyzed arylative cyclization of an allenyne	111
Scheme 3.14 Rh(I)-catalyzed arylative cyclization of 1,6-diynes	112

Chapter 4

Scheme 4.1 Rh(I)-catalyzed carbofunctionalization of terminal alkynes	117
Scheme 4.2 Rh(I)-catalyzed tandem addition–cyclization of an alkynylimine	118
Scheme 4.3 Mechanistic explanations for Rh(I)-catalyzed tandem addition– cyclization of an alkynylimine with phenylboronic acid	119
Scheme 4.4 Rh(I)-catalyzed alkenylative cyclization of an alkynylimine	121
Scheme 4.5 Rh(I)-catalyzed arylyative cyclization with phenylzinc iodide	122
Scheme 4.6 Synthesis of chiral diene 4.22	123
Scheme 4.7 Preparation of the rhodium–diene complex 4.25 and its performance in the arylyative cyclization	125

Chapter 5

Scheme 5.1 Transition metal catalyzed C–C bond formation of hydrazones	140
Scheme 5.2 Pd(0)-catalyzed cross-coupling reaction of a <i>N</i> -tosylhydrazone	140
Scheme 5.3 Pd- or Ir-catalyzed stereospecific allylic reduction reactions	141
Scheme 5.4 Ru(II)-catalyzed carbonyl addition reaction of a hydrazone ...	142
Scheme 5.5 La(III)-catalyzed traceless allene synthesis	143
Scheme 5.6 Using a hydrazone as a radical acceptor in transition metal catalysis	144
Scheme 5.7 Our efforts on merging organic reactions with retro-ene reactions	146

Scheme 5.8 Preliminary result of Rh(I)-catalyzed tandem addition– cyclization–rearrangement of an alkynylhydrazone	147
Scheme 5.9 The effect of added rhodium catalyst on tandem reaction	148
Scheme 5.10 The generation and the effect of <i>p</i> TolSO ₂ H on the rhodium catalyst	149
Scheme 5.11 The effect of temperature control on the Rh(I)-catalysis	150
Scheme 5.12 Rh(I)-catalysis with two equivalents of phenylboronic acid .	151
Scheme 5.13 Addition of NaOAc after the Rh(I)-catalysis	152
Scheme 5.14 Detrimental effects of reaction temperature and a sulfinic acid	153
Scheme 5.15 Effect of the pyridine additive on the Rh(I)-catalysis	155
Scheme 5.16 The scope of alkenylboronic acids	156
Scheme 5.17 Results of the Rh(I)-catalysis with cyclopropylboronic acid	157
Scheme 5.18 Attempts for the synthesis of a 4-membered ring	157
Scheme 5.19 Results of Me- and <i>i</i> Pr-substituted alkynylhydrazones	158
Scheme 5.20 Rh(I)-catalyzed tandem reactions of a terminal alkyne substrate	159
Scheme 5.21 The <i>gem</i> -disubstituent effects on the Rh(I)-catalysis	160
Scheme 5.22 Preparation of the cyclohexane-fused alkynylhydrazones ...	161
Scheme 5.23 Synthesis of the <i>trans</i> - or <i>cis</i> -hydrindenes	161
Scheme 5.24 Synthesis of cyclohexane-fused alkynylhydrazones which have methyl carboxylate	162
Scheme 5.25 Synthesis of the <i>trans</i> - and <i>cis</i> -hydrindenes which have methyl carboxylate	163
Scheme 5.26 Synthesis of indene from a benzaldehyde hydrazone	164
Scheme 5.27 Results from TsN-tethered substrates possessing terminal or aryl alkyne	166
Scheme 5.28 Synthesis of a dihydrofuran	168
Scheme 5.29 Synthesis of a cyclohexene and undesired hydroarylation ...	169

Scheme 5.30 Synthesis of a dihydronaphthalene	170
Scheme 5.31 Arylative ring contraction of cyclohexenones	171
Scheme 5.32 Synthesis of α,β -epoxyketones	171
Scheme 5.33 Rh(I)-catalyzed arylative cyclization of alkynylhydrazones derived from α,β -epoxyketones	173
Scheme 5.34 Rh(I)-catalyzed hydroarylation of an alkynal	174
Scheme 5.35 Competition experiment between an alkynylhydrazone and an alkynylaldehyde	174
Scheme 5.36 Preparation of the rhodium-diene complex and its performance in the Rh(I)-catalysis	180
Scheme 5.37 Rh(I)-catalyzed asymmetric tandem reaction of an <i>i</i> Pr-substituted alkynylhydrazone	182
Scheme 5.38 Rh(I)-catalyzed asymmetric arylative cyclization of an alkynyl <i>N</i> -Boc-hydrazone	182
Scheme 5.39 Deprotection and aerobic oxidation of the cyclopentyl carbazate	183
Scheme 5.40 Isolation of the cyclic hydrazide intermediate 5.169	184
Scheme 5.41 Tandem elimination and retro-ene rearrangement of the cyclic hydrazide	184
Scheme 5.42 Proposed mechanism	185

List of Figures

Chapter 2

- Figure 2.1** Proposed transition state of asymmetric carbocyclization of
an alkynylamine 69
- Figure 2.2** Chromatographic traces of **S2.6** from racemic **2.33** 97
- Figure 2.3** Chromatographic traces of **S2.6** from chiral **2.33** 97

Chapter 4

- Figure 4.1** ORTEP diagram of **4.2** drawn with 50% probability of ellipsoid
..... 118

Chapter 5

- Figure 5.1** Stereochemical model for explanation of stereospecificity in
hydrindene formations 164

List of Abbreviations

Ac	acetyl
acac	acetylacetonato
aq	aqueous
Ar	aryl
BINAP	2,2'-bis(diphenylphosphino)-1,1'-binaphtyl
Bn	benzyl
Boc	<i>tert</i> -butyloxycarbonyl
bod	bicyclo[2.2.2]octane-2,5-diene
Bu	butyl
Bz	benzoyl
Cbz	carboxybenzyl (benzyloxycarbonyl)
COD	1,5-cyclooctadiene
coe	cyclooctene
Cp	cyclopentadienyl
Cp*	pentamethylcyclopentadienyl
Cy	cyclohexyl
DABCO	1,4-diazabicyclo[2.2.2]octane
dba	Dibenzylideneacetone
DBU	1,8-Diazabicyclo(5.4.0)undec-7-ene
DCE	1,2-dichloroethane
DCM	dichloromethane
DMAP	4-dimethylaminopyridine
DMF	<i>N,N</i> -dimethylformamide
dmpe	1,2-Bis(dimethylphosphino)ethane
DMSO	dimethylsulfoxide
dppf	1,1'-bis(diphenylphosphino)ferrocene
dppm	bis(diphenylphosphino)methane
dppp	1,3- bis(diphenylphosphino)propane
dr	diastereomeric ratio
dtbpy	4,4'-Di- <i>tert</i> -butyl-2,2'-dipyridyl
EA	ethyl acetate
ee	enantiomeric excess

Et	ethyl
HFIP	1,1,1,3,3,3-Hexafluoro-2-propanol
IPNBSH	<i>N</i> -isopropylidene- <i>N'</i> -2-nitrobenzenesulfonylhydrazide
LDA	lithium diisopropylamide
Me	methyl
MOM	methoxymethyl
MS	molecular sieve
NBA	<i>N</i> -bromoacetamide
nb	norbornadiene
NBS	<i>N</i> -bromosuccinimide
Ns	nitrobenzenesulfonyl
Oct	octyl
Ph	phenyl
ppy	phenylpyridine
Pr	propyl
Py	pyridine
TBS	<i>tert</i> -butyldimethylsilyl
TEA	triethylamine
Tf	trifluoromethanesulfonyl
TFA	trifluoroacetic acid
TFE	2,2,2-trifluoroethanol
THF	tetrahydrofuran
TIPS	triisopropylsilyl
TMS	trimethylsilyl
Tp	trispyrazolylborate
Ts	<i>p</i> -toluenesulfonyl

Chapter 1. Transition Metal Vinylidene Mediated Catalytic Carbocyclization of Alkynes

1.1 Introduction

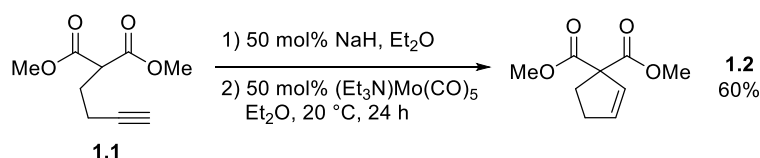
Alkyne is a fundamental functional group of organic compounds that extensively used in organic synthesis.¹ Especially, terminal alkynes have been broadly applied in various C–C bond forming processes. Due to its high *s*-character, the C–H bond of the terminal carbon atom can be deprotonated and used as carbon nucleophiles. Furthermore, the high degree of unsaturation has led the organic chemists to utilize it as carbon electrophiles for the synthesis of highly functionalized molecules.² In efforts to search for distinct methods for functionalization of terminal alkynes with *anti*-Markovnikov selectivity, various transition metal vinylidene mediated organic reactions have been developed.³ This chapter will describe intramolecular carbofunctionalization reactions using transition metal vinylidene mediated catalysis that have been used for the synthesis of carbocyclic compounds.

1.2 Carbocyclization by nucleophilic addition

1.2.1 Enol and enamine nucleophiles

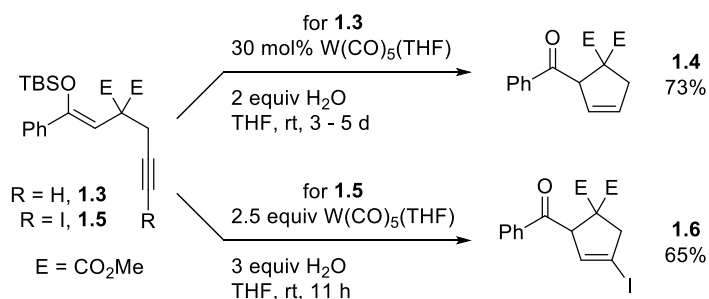
In 1997, molybdenum-catalyzed *5-endo-dig* carbocyclization of

alkynylmalonate was reported (Scheme 1.1).⁴ Despite its low turnover number and narrow substrate scope, this reaction suggested that C–C bond formation between transition metal vinylidene intermediate and stabilized carbanion could be feasible.



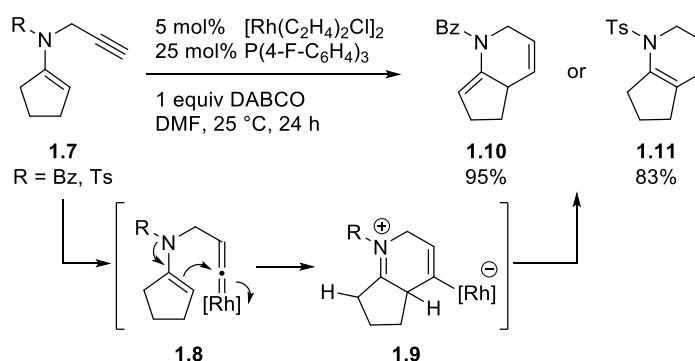
Scheme 1.1 Mo(0)-catalyzed cycloisomerization of an alkynylmalonate

Silyl enol ethers could participate in metal vinylidene mediated catalysis. As shown in Scheme 1.2, terminal alkyne-tethered silyl enol ether **1.3** gave cyclopentene **1.4** under tungsten catalysis.^{5a} This strategy has been extended to iodoalkyne substrate **1.5**, showing the migration of iodine atom attached to the alkyne as a result of cyclization, which is the evidence of metal vinylidene intermediate.^{5b}



Scheme 1.2 W(0)-mediated cyclization of alkyne-tethered silyl enol ethers

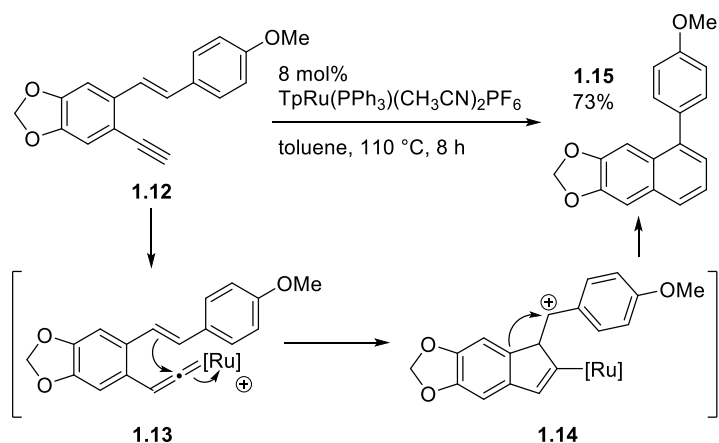
Enamines, one of the well-known carbon nucleophiles, could be engaged in a rhodium-catalyzed *6-endo-dig* cycloisomerization (Scheme 1.3).⁶ The *N*-protected alkynyl enamines **1.7** were cyclized to alkenyl rhodium **1.9** via rhodium vinylidene complex **1.8**. The rhodium catalyst was regenerated giving rise to **1.10** or **1.11**, depending on the protecting group of the enamines.



Scheme 1.3 Rh(I)-catalyzed cycloisomerization of *N*-propargylenamines

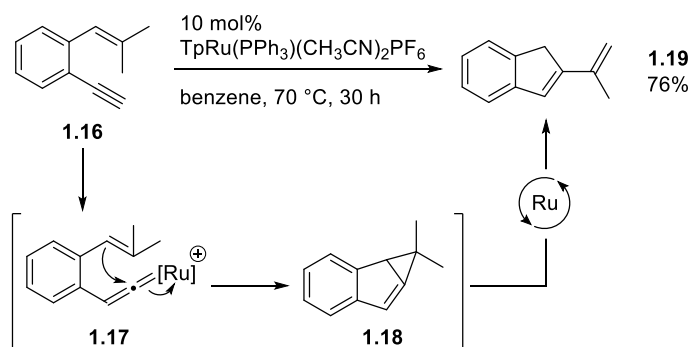
1.2.2 Alkene and alkyne nucleophiles

Less polarized alkenes and alkynes have reactivity towards transition metal vinylidene intermediates. In 2003, the ruthenium-catalyzed cycloisomerization of ethynylstilbene **1.12** was reported (Scheme 1.4).⁷ Under toluene reflux conditions, the cationic ruthenium vinylidene **1.13** could be intercepted by π -electrons of the alkene, and the cyclized intermediate **1.14** proceeded further skeletal rearrangement to give 1-aryl naphthalene **1.15**.



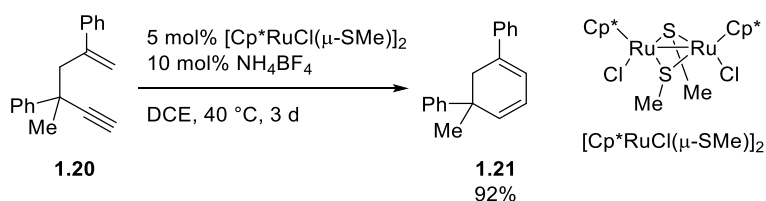
Scheme 1.4 Ru(II)-catalyzed cycloisomerization of an ethynylstilbene

The tandem cycloisomerization of ethynylstyrene **1.16** by a single ruthenium catalyst was observed in 2004.⁸ As depicted in Scheme 1.5, the ruthenium catalyst mediated formal [2+1] cycloaddition, converting metal vinylidene **1.17** to **1.18**, and, *via* further ring-opening rearrangement, to indene **1.19**.



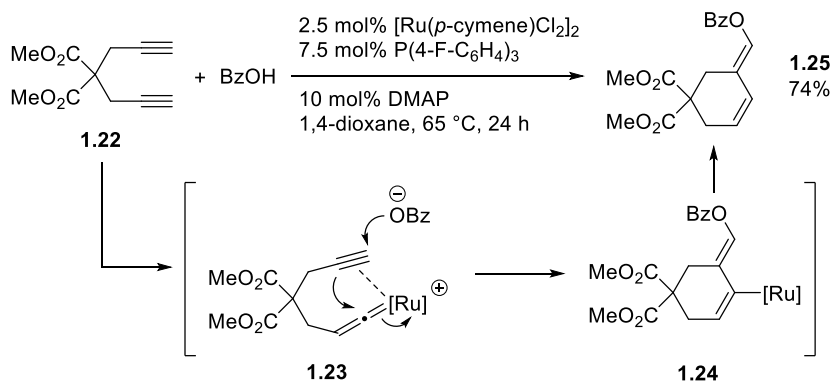
Scheme 1.5 Ru(II)-catalyzed tandem carbocyclization of an ethynylstyrene

A dimeric ruthenium thiolate complex, $[\text{Cp}^*\text{RuCl}(\mu\text{-SMe})]_2$, has been known to mediate catalytic 6-*endo* cycloisomerization of skipped enyne **1.20** via metal vinylidene intermediate (Scheme 1.6).⁹ In contrast with the examples of conjugated enynes in Scheme 1.4 and 1.5, enyne **1.20** undergoes simple intramolecular alkenylation of the styrene without further skeletal rearrangement.



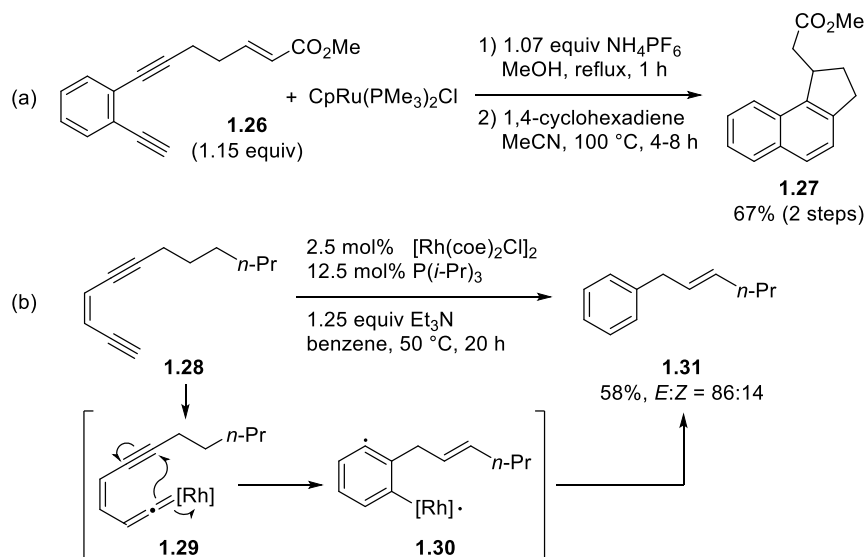
Scheme 1.6 Ru(II)-catalyzed cycloisomerization of a 1,5-enyne

Alkynes have been shown to participate in C–C bond formation through a metal vinylidene intermediate acting as a nucleophile (Scheme 1.7).¹⁰ In a ruthenium-catalyzed carbocyclization reaction of diyne **1.22**, one of the alkynes attacked the ruthenium vinylidene of **1.23** with the assistance of carboxylate anion, resulting in the (*E*)-selective 6-*endo* cyclization.



Scheme 1.7 Ru(II)-catalyzed carboxylative carbocyclization of a 1,6-diyne

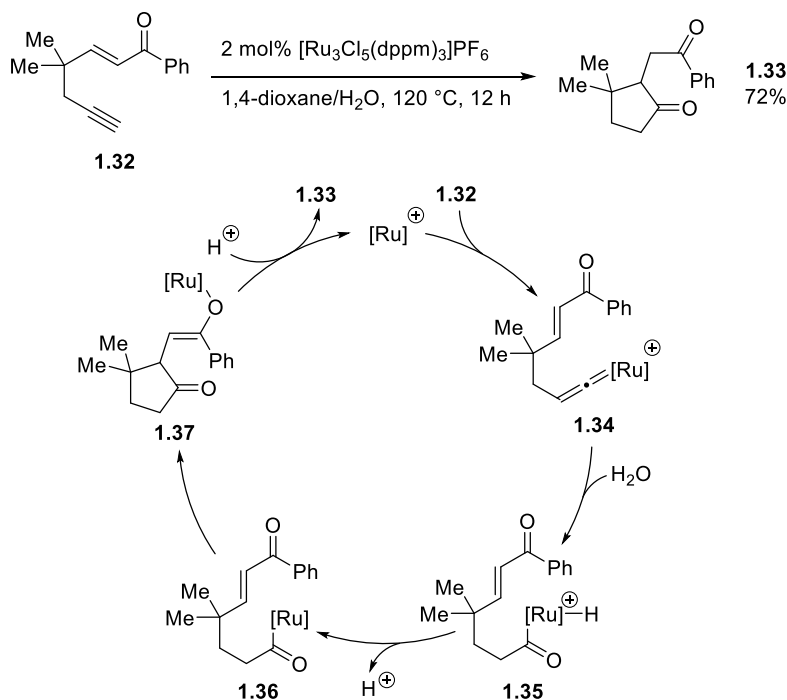
Some transition metal vinylidene complexes have shown a distinct mechanism in cycloaromatization of enediyne substrates. In 1995, the ruthenium-mediated cycloaromatization with concomitant ring closure was reported (Scheme 1.8a).^{11a} The ruthenium-vinylidene complex prepared from aromatic diyne **1.26** was heated with a hydrogen source to give naphthalene **1.27**. One year later, the catalytic derivative of this cycloaromatization reaction was reported (Scheme 1.8b).^{11b} Both of the work proposed the mechanism involving metal vinylidenes, which proceeds through a Myers-Saito type cyclization to form diradical intermediate like **1.30**.



Scheme 1.8 Ru(II)- and Rh(I)-mediated cycloaromatization of enediyne

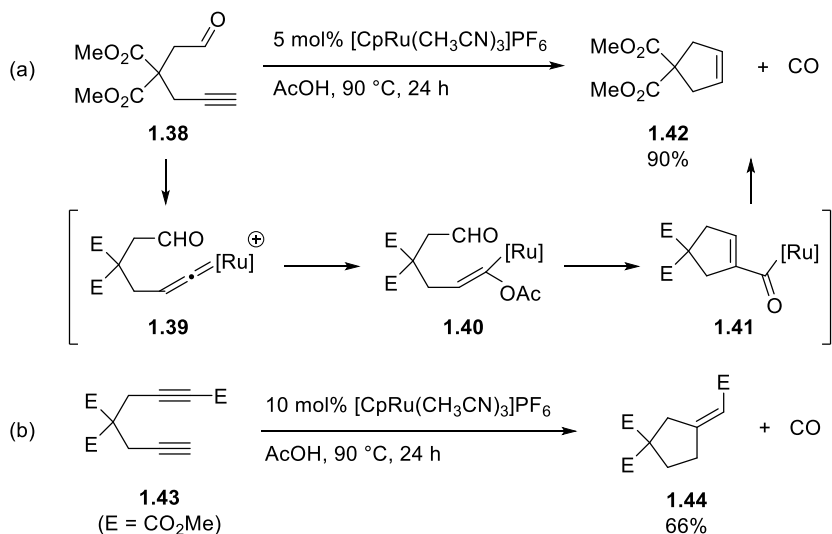
1.2.3 Carbocyclization initiated by oxygen nucleophiles

Oxygen nucleophiles have been shown to engage in transition metal vinylidene mediated catalytic carbocyclization. As depicted in Scheme 1.9, hydrative carbocyclization of alkyne-tethered α,β -unsaturated ketone **1.32** could be feasible using a ruthenium catalyst.^{12a} In the proposed mechanistic scenario, acyl ruthenium intermediate **1.36** generated from metal vinylidene **1.34** and water cyclized to give cyclopentanone **1.33**. This intramolecular hydrative alkyne addition could be extended to intermolecular processes.^{12b}



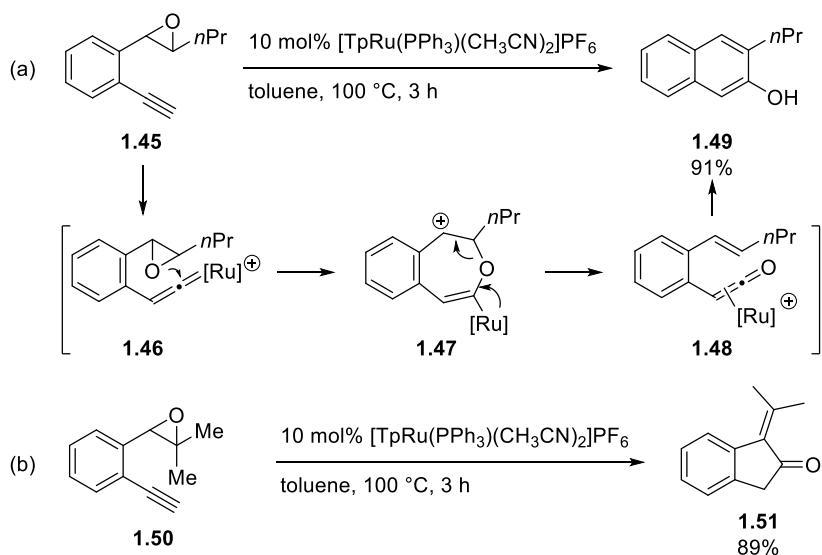
Scheme 1.9 Ru(II)-catalyzed hydrative carbocyclization of a 1,5-enyne

Carboxylates could add to metal vinylidene directly to form carbocyclic structures. In the decarbonylative cyclization of alkynal **1.38**, carbocyclization takes place *via* alkenyl ruthenium **1.40**, which is generated by the addition of an acetate to ruthenium vinylidene **1.39** (Scheme 1.10a).^{13a} A similar ruthenium-catalyzed decarbonylative strategy could be applied to 1,6-diyne **1.43**, showing a reaction pathway distinct from the ruthenium-phosphine ligand conditions as shown in Scheme 1.7 (Scheme 1.10b).^{13b}



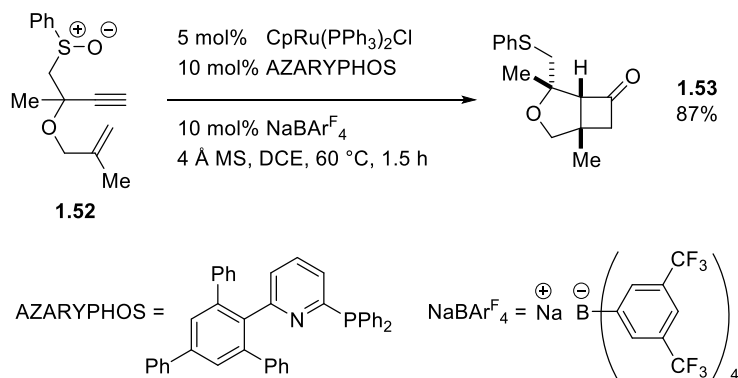
Scheme 1.10 Ru(II)-catalyzed decarbonylative carbocyclization

Oxygen atom transfer from oxidants to metal vinylidene complexes has been shown to enable oxidative functionalization reactions.¹⁴ Such an example is the ruthenium-catalyzed cycloisomerization of ethynyl styrene oxide **1.45** (Scheme 1.11).¹⁵ The translocation of the oxygen atom from the epoxide to the ruthenium vinylidene in **1.46** occurred, giving ruthenium ketene intermediate **1.48** which underwent 6π -electrocyclization. In contrast, the trisubstituted styrene oxide **1.50** gave 2-indanone **1.51** product through a carbocation intermediate generated by the same ruthenium ketene intermediate.



Scheme 1.11 Ru(II)-catalyzed carbocyclization of epoxyalkynes *via* oxygen transfer

In addition to epoxides, sulfoxide nucleophiles could act as a potential oxidant for ruthenium-ketene mediated transformations. As shown in Scheme 1.12, the ruthenium complex with P,N-bidentate ligand AZARYPHOS mediated the intramolecular oxygenative [2+2] cycloaddition reaction of sulfoxyenyne **1.52**.¹⁶ A reaction mechanism has been proposed, wherein a ketene intermediate, derived from the internal redox between the ruthenium vinylidene complex and the sulfoxide, undergoes intramolecular cycloaddition reaction with a tethered alkene.

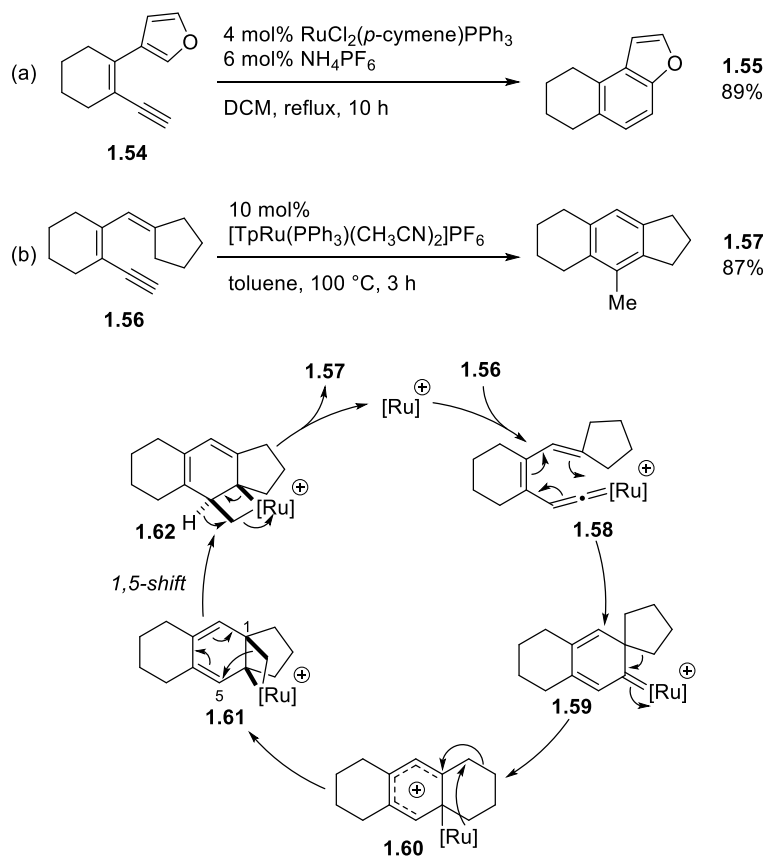


Scheme 1.12 Ru(II)-catalyzed oxygenative [2+2] cycloaddition of a sulfoxyenyne

1.3 Carbocyclization by pericyclic reaction

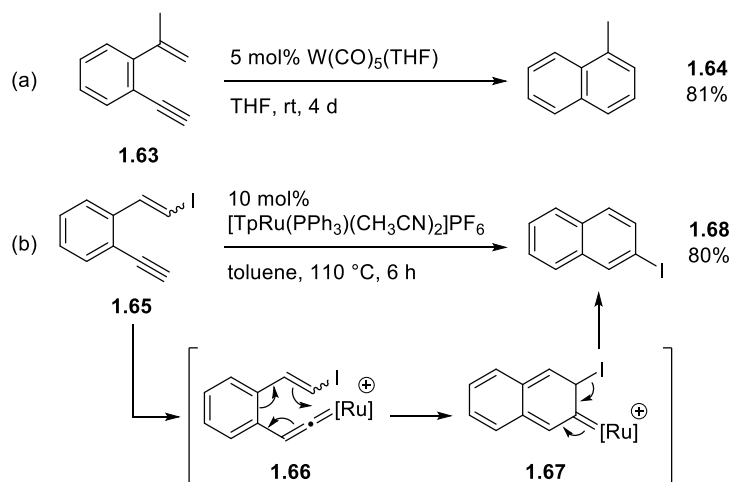
1.3.1 Electrocyclization

Each of the two π -bonds in metal vinylidene complexes has been known to participate in pericyclic reactions. One of the early examples of this process was reported in 1996 (Scheme 1.13a).^{17a} Under cationic ruthenium catalytic conditions, furanyl enyne **1.54** gave the cycloisomerized benzofuran **1.55** via 6π -electrocyclization reaction of ruthenium vinylidene intermediate. Additional skeletal rearrangement of the Fischer carbene intermediate **1.59** generated from electrocyclization was accompanied when simple dienyne **1.56** was exposed to the similar catalytic conditions (Scheme 1.13b).^{17b}



Scheme 1.13 Ru(II)-catalyzed 6 π -electrocyclization of dienynes

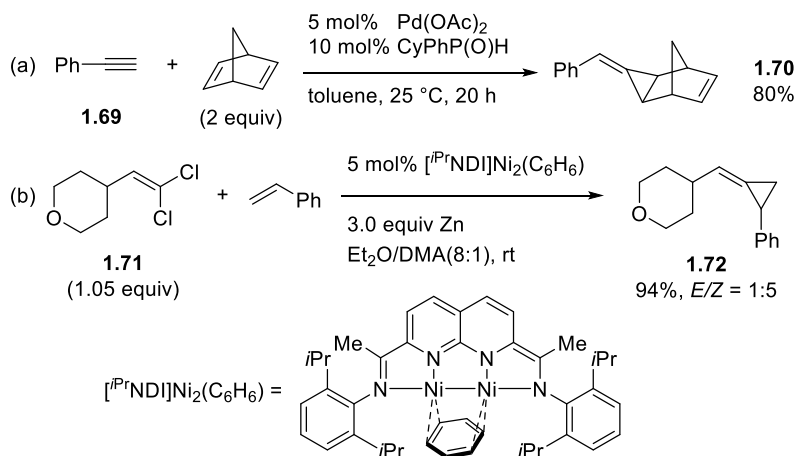
Similar carbocyclization reactions involving electrocyclization of benzene-fused 1,5-enynes has been reported. Cycloisomerization of ethynyl styrene **1.63** could be feasible by a tungsten catalyst at room temperature, which are milder reaction conditions than those for cyclization of dienyne substrates (Scheme 1.14a).^{18a} Furthermore, a ruthenium catalyst has brought about aromative cycloisomerization of alkyne tethered iodostyrene **1.65** with concomitant 1,2-iodine shift (Scheme 1.14b).^{18b}



Scheme 1.14 W(0)- and Ru(II)-catalyzed cycloisomerization of aromatic enynes

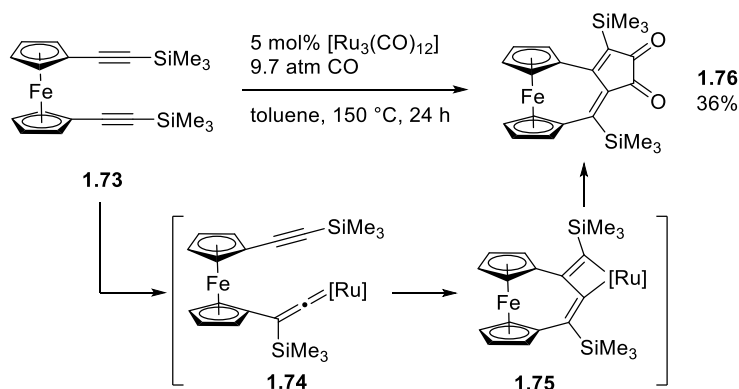
1.3.2 Cycloaddition

The vinylidene transfer reaction, a [2+1] cycloaddition of metal vinylidenes with alkenes, has been achieved (Scheme 1.15a).¹⁹ A palladium vinylidene complex derived from phenylacetylene **1.69** reacted with one π -bond of norbornadiene to give a benzylidene cyclopropane **1.70** at room temperature. Similar transfer of metal unsaturated carbenes and its asymmetric derivatives have been known to be feasible using different catalytic conditions.²⁰ Recently, catalytic reductive vinylidene transfer reaction using 1,1-dichloroalkene instead of alkynes, as a precursor for metal vinylidene species was reported (Scheme 1.15b).²¹ In the presence of dinickel catalyst and the excess amount of a zinc reductant, reductive generation of a dinickel vinylidene complex followed by [2+1] cycloaddition to alkene has been achieved with a broad substrate scope.



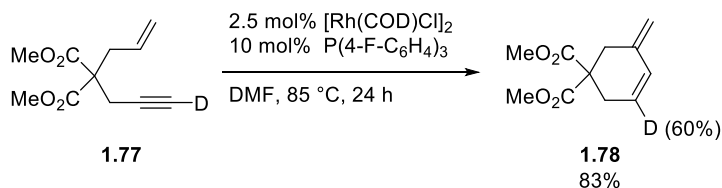
Scheme 1.15 Pd(II)- and Ni₂-catalyzed vinylidene transfer reactions

The [2+2] cycloaddition of metal vinylidenes and alkynes was proposed as a crucial mechanistic step in the ruthenium-catalyzed carbonylative cyclization of diyne **1.73** (Scheme 1.16).²² In the presence of carbon monoxide, ruthenacyclobutene intermediate **1.75** generated from silicon-migrated ruthenium vinylidene complex **1.74** gave cyclic diketone **1.76** with the incorporation of two CO molecules.



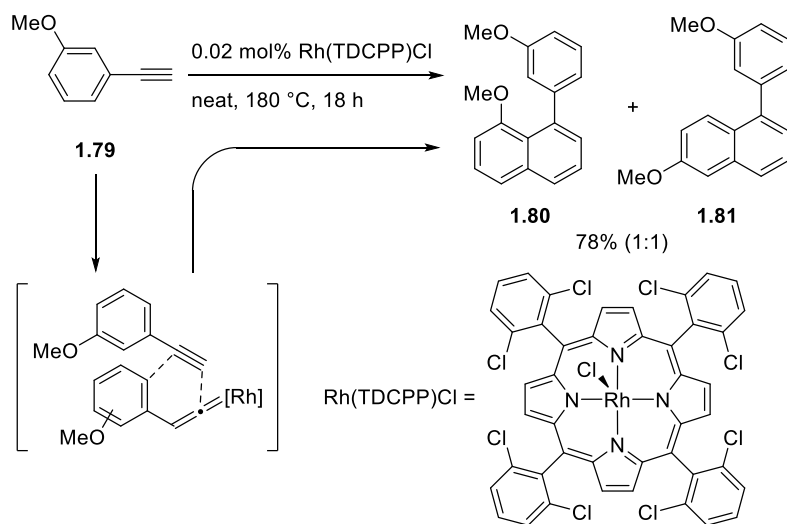
Scheme 1.16 Ru(0)-catalyzed carbonylative carbocyclization of a diyne

In contrast to a silylated metallacyclobutene intermediate requiring carbon monoxide for catalyst turnover, metallacyclobutane complexes generated from a metal vinylidene and an alkene could give cycloisomerized products without CO. Under rhodium/phosphine catalytic conditions, 1,6-enyne **1.77** yielded cyclohexene **1.78** in excellent yield (Scheme 1.17).²³ The deuterium labeling experiments strongly supported the rhodium vinylidene mediated mechanism, including [2+2] cycloaddition of a rhodium vinylidene with an alkene.²⁴



Scheme 1.17 Rh(I)-catalyzed cycloisomerization of a 1,6-enyne

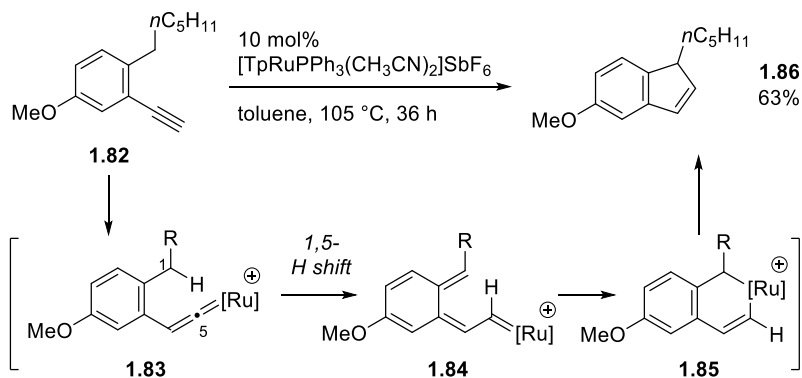
The $\text{C}_\alpha=\text{C}_\beta$ bond of a metal vinylidene could participate in [4+2] cycloaddition as a part of a diene unit. As shown in Scheme 1.18, dimerization of arylacetylene **1.79** was mediated by rhodium porphyrin catalyst, giving rise to the regioisomeric mixture of aryl naphthalenes **1.80** and **1.81**.²⁵



Scheme 1.18 Rh(I)-catalyzed dimerization of an arylacetylene

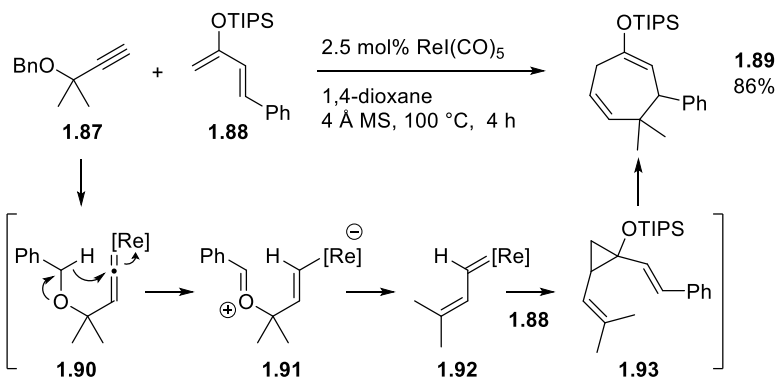
1.3.3 Sigmatropic rearrangement

The sp^3 -hydrogen atom at the C_5 position of 3-en-1-yne systems can move to the C_α of metal vinylidene *via* 1,5-sigmatropic rearrangement. The 2-hexyl-substituted arylacetylene **1.82** was converted to indene **1.86** in moderate yield under ruthenium catalysis (Scheme 1.19).²⁶ Mechanistically, the ruthenium vinylidene complex **1.83** was proposed as an intermediate, which undergoes 1,5-hydride shift and 6π -electrocyclization, followed by reductive elimination of **1.85**, to yield the cycloisomerized product.



Scheme 1.19 Ru(II)-catalyzed cycloisomerization of a 2-alkyl arylacetylene

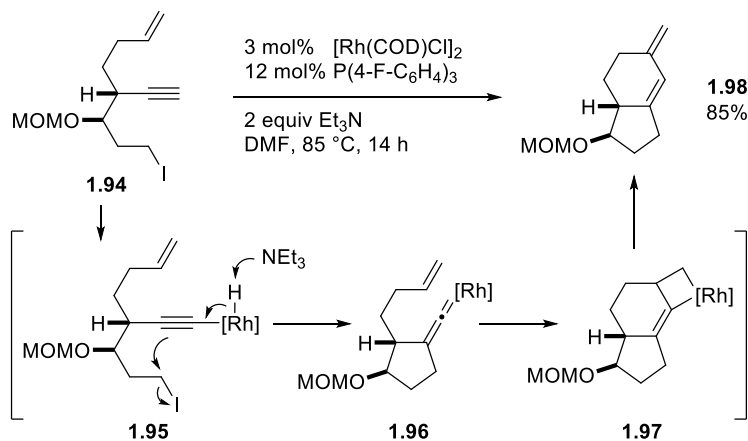
The 1,5-sigmatropic rearrangement of a metal vinylidene complexes has been known to give another catalytic intermediate for carbocyclization. In the rhenium-catalyzed formal [4+3] cycloaddition reaction of propargylic benzyl ether **1.87** and siloxydiene **1.88**, rhenium carbene **1.92** was proposed as a critical intermediate, which arose from the 1,5-hydride shift of rhenium vinylidene **1.90** (Scheme 1.20).²⁷ Subsequent to elimination of benzaldehyde, the resulting rhenium carbene **1.92** undergoes [2+1] cycloaddition with a π -bond of silyl enol ether **1.88** to give cyclopropane **1.93** which yields the siloxycycloheptadiene **1.89** after the Cope rearrangement.



Scheme 1.20 Re(I)-catalyzed formal [4+3] cycloaddition

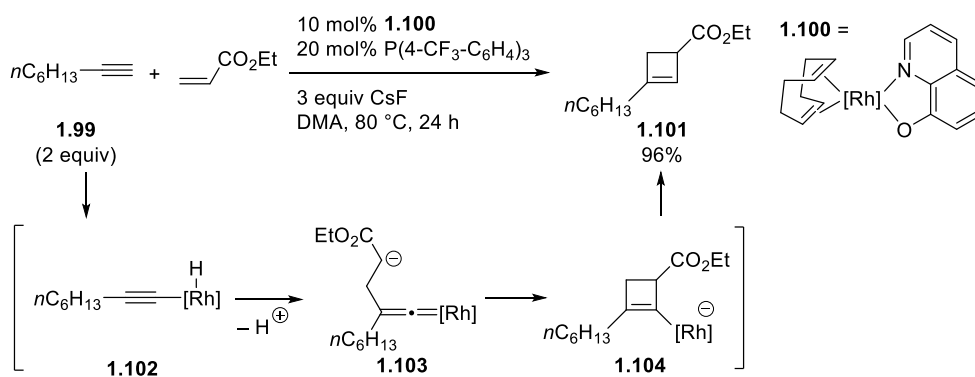
1.4 Carbocyclization with disubstituted metal vinylidenes

One of the ways to access β,β -disubstituted metal vinylidene is introducing electrophiles at a metal vinylidene-formation stage. Although the use of disubstituted metal vinylidene complexes as a catalytic intermediate is quite problematic due to a competitive formation of monosubstituted metal vinylidene, a rhodium-catalyzed tandem carbocyclization of haloenyne **1.94** has been developed (Scheme 1.21).²⁸ In combination with facile 5-membered ring formation, a rhodium catalyst could promote the transformation of haloenyne **1.94** to 5/6-fused bicycle **1.98** *via* [2+2] cycloaddition of the rhodium vinylidene and the alkene.



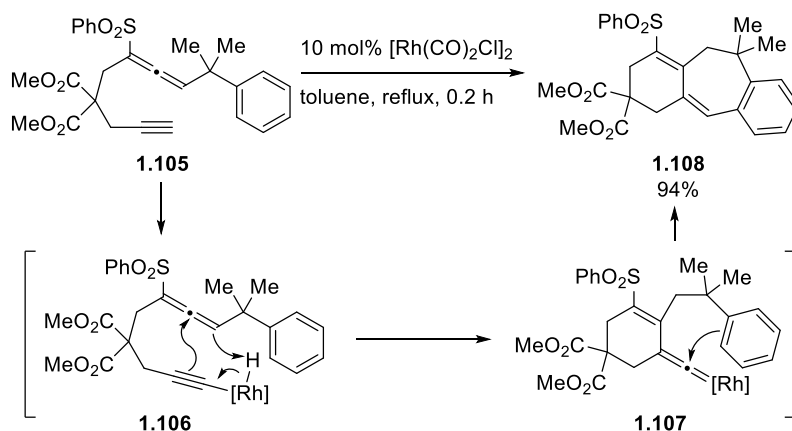
Scheme 1.21 Rh(I)-catalyzed tandem carbocyclization of a haloenyne

Disubstituted metal vinylidenes could be accessed in an intermolecular manner. In the rhodium-catalyzed [2+2] cycloaddition of alkyne **1.99** and ethyl acrylate, an intermolecular C–C bond formation produced disubstituted rhodium vinylidene **1.103**, which underwent ring closure to give rise to cyclobutene **1.101** (Scheme 1.22).²⁹



Scheme 1.22 Rh(I)-catalyzed [2+2] cycloaddition of an alkyne and an enoate

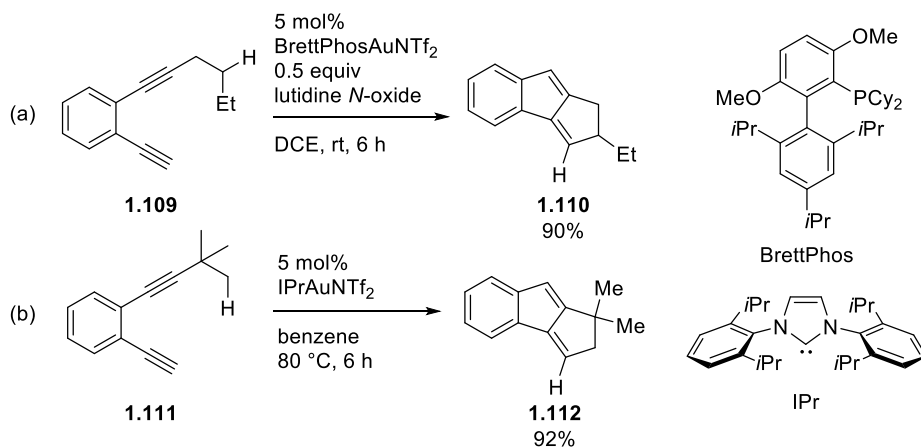
In the rhodium-catalyzed tandem cycloisomerization of 1,6-alleneyne **1.105**, an intramolecular ene-type process could give the disubstituted metal vinylidene intermediate **1.107** (Scheme 1.23).³⁰ The resulting rhodium vinylidene **1.107** was trapped by an aryl group through a Friedel-Crafts type cyclization, yielding 5/7-fused carbocycle **1.108**.



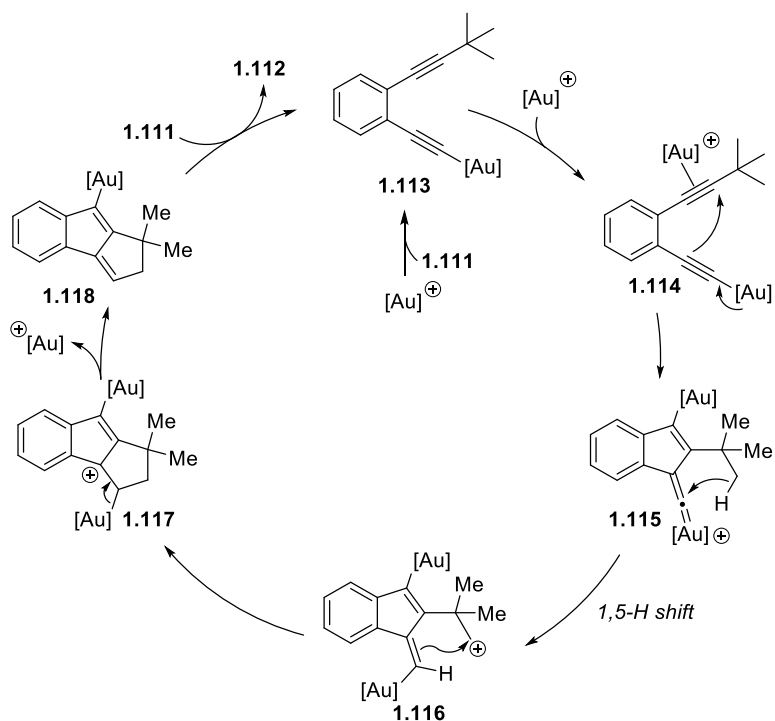
Scheme 1.23 Rh(I)-catalyzed cycloisomerization of a 1,6-alleneyne

The gold vinylidene mediated catalysis has emerged and advanced explosively since dual-gold catalytic carbocyclization reactions were reported in 2012 (Scheme 1.24).³¹ In these transformations mediated by a single phosphine/gold or NHC/gold catalyst, benzene-tethered diynes **1.109** and **1.111** were converted to the 5/5-fused bicyclic dienes **1.110** and **1.112**, respectively. In the proposed mechanistic scenario, alkynyl gold complex **1.114** proceeds 5-*endo*-dig cyclization with the internal alkyne, which is activated by another gold catalyst (Scheme 1.25). The resulting disubstituted gold vinylidene **1.115** undergoes formal C–H insertion at the aliphatic chain

attached to the alkyne that occurs through 1,5-hydride shift followed by carbocation rearrangements.

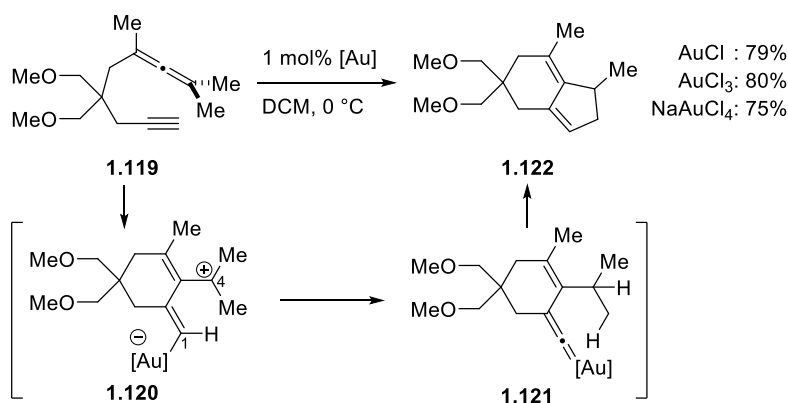


Scheme 1.24 Au(I)-catalyzed tandem cycloisomerization of diynes



Scheme 1.25 Proposed mechanism for Au(I)-catalyzed cycloisomerization

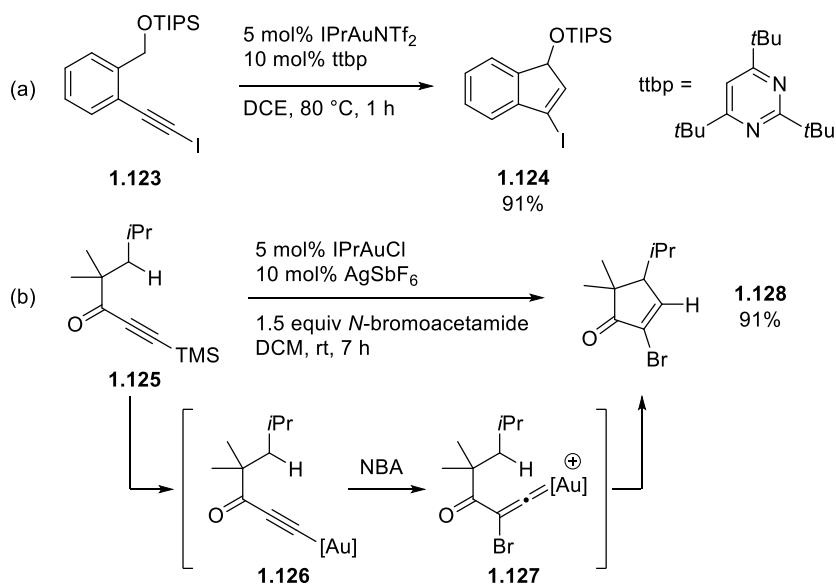
A gold-catalyzed tandem cycloisomerization involving C–H insertion has been carried out with 1,6-allenynes **1.119** (Scheme 1.26).³² A gold(I) or even gold(III) catalyst could mediate the formation of disubstituted gold vinylidene **1.121** at 0 °C *via* 1,4-hydride shift from an alkenyl gold to a tertiary carbocation. Further transformations including C–H insertion took place from gold vinylidene **1.121**, to yield the 6/5-fused cyclic product **1.122**.



Scheme 1.26 Au-catalyzed tandem cycloisomerization of an allenyne

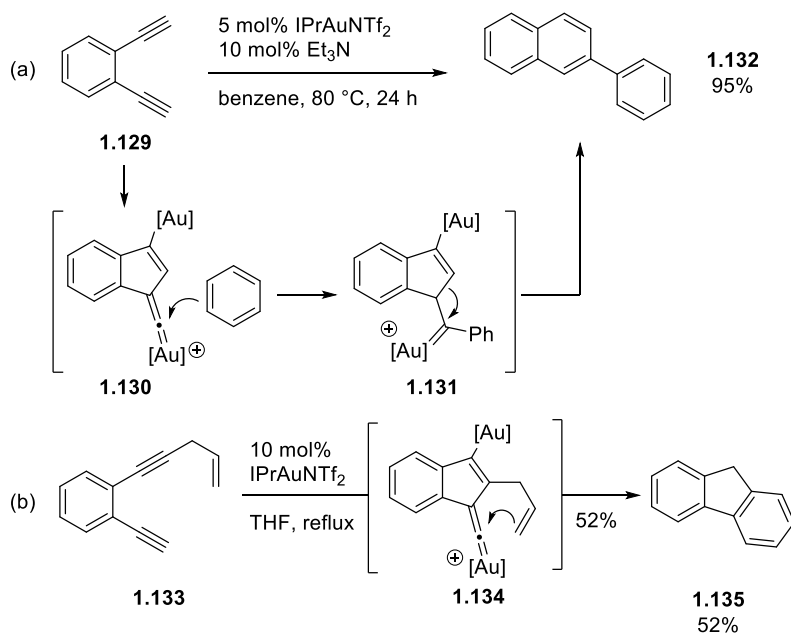
The transformation utilizing disubstituted gold vinylidene complexes capable of C–H insertion could be achieved with monoalkyne substrates possessing a heteroatom. A gold/NHC catalyst promoted the reaction of iodoalkyne **1.123** to afford 1-iodoindene **1.124** *via* formation of gold vinylidene intermediate along with the migration of iodine atom (Scheme 1.27a).^{33a} Recently, bromonium-triggered intermolecular generation of a disubstituted gold vinylidene was reported (Scheme 1.27b).^{33b} When silylated

ynone **1.125** was exposed to a gold/NHC catalyst and *N*-bromoacetamide at room temperature, β -bromination occurred to give 2-bromocyclopentenone **1.128** via bromine substituted gold vinylidene **1.127** which underwent an intramolecular C–H insertion.



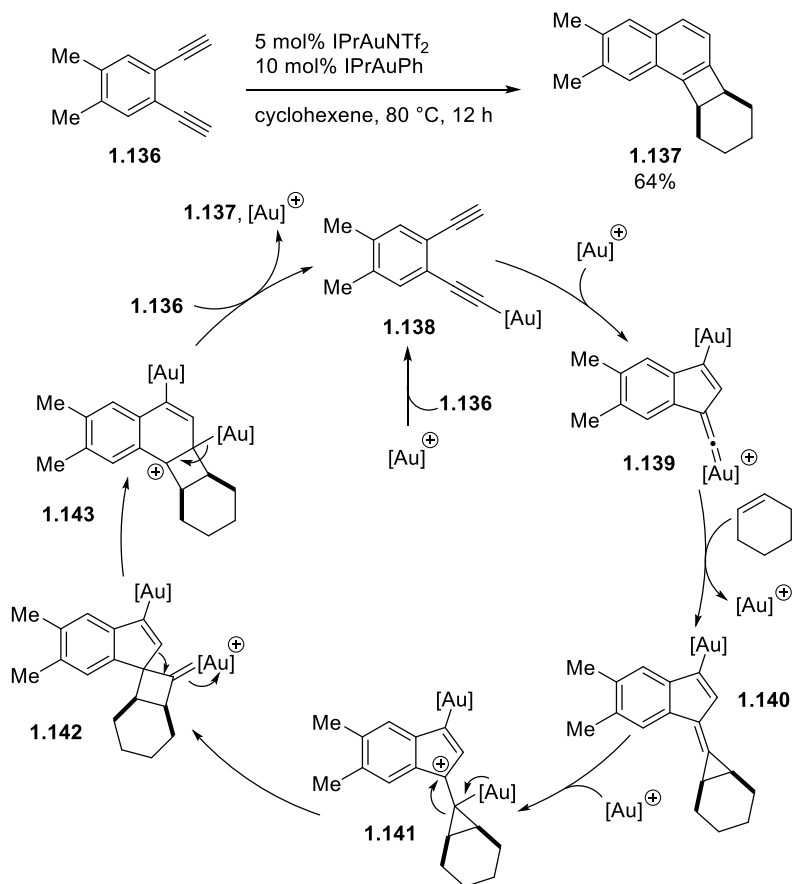
Scheme 1.27 Au(I)-catalyzed carbocyclization of monoalkynes

The highly electrophilic nature of gold vinylidene complexes has been shown in C–C bond forming reactions with nonpolarized alkenes and arenes. The gold-catalyzed arylyative cycloaromatization of diyne **1.129** to aryl naphthalene **1.132** was reported. (Scheme 1.28a).³⁴ In the proposed mechanism, disubstituted gold vinylidene **1.130** is intercepted by benzene via a Friedel-Craft type pathway. In the case of alkenes, an intramolecular carbocyclization with disubstituted gold vinylidene **1.134** could be feasible, giving rise to the fluorene **1.135** (Scheme 1.28b).³⁵



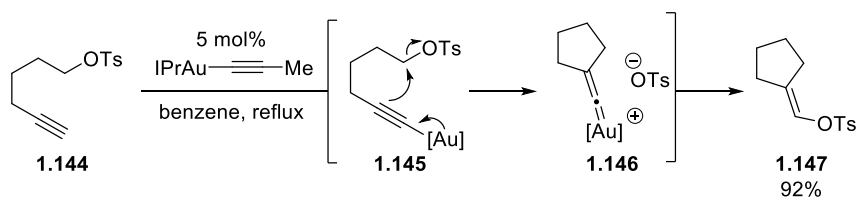
Scheme 1.28 Au(I)-catalyzed carbocyclization of diynes

The vinylidene transfer reaction of a disubstituted gold vinylidene and alkene has been suggested to be a key event in the gold-catalyzed formal cycloaromatization–cycloaddition of arene-tethered diyne **1.136** and cyclohexene (Scheme 1.29).³⁶ In the proposed mechanism, the gold vinylidene **1.139** is trapped with the C=C bond of cyclohexene to produce [2+1] cycloadduct **1.140**. After further gold mediated transformations involving a Wagner-Meerwein type rearrangement, the highly strained cyclobutane-fused carbocycle **1.137** could be obtained in moderate yield.



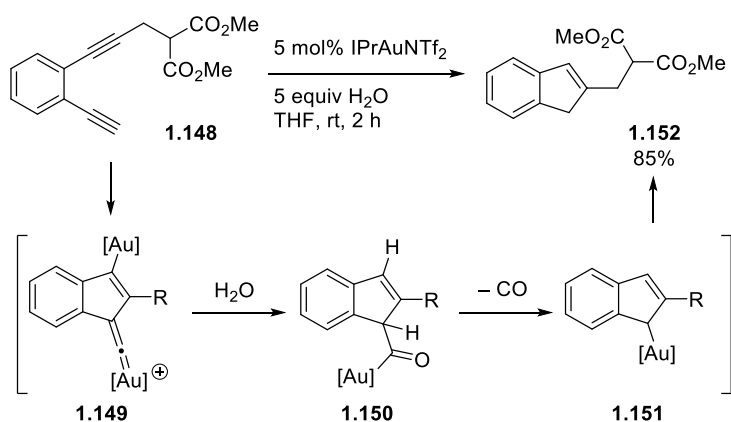
Scheme 1.29 Au(I)-catalyzed tandem cycloaddition–rearrangement of a diyne and an alkene

A disubstituted gold vinylidene complex could be accessed by β -alkylation with an intramolecular electrophile like the case of rhodium catalysis in Scheme 1.21.²⁸ With an alkynyl gold precatalyst, hexynyl tosylate **1.144** underwent reconstitutive cycloisomerization to give rise to vinyl tosylate **1.147** (Scheme 1.30).³⁷ The proposed mechanism includes the formation of disubstituted gold vinylidene **1.146** by β -alkylation and recombination of the gold vinylidene and a tosylate anion.



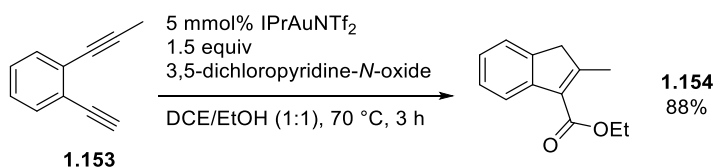
Scheme 1.30 Au(I)-catalyzed reconstitutive cycloisomerization of a hexynyl tosylate

A neutral oxygen nucleophile, water, has been found to be capable of reacting with disubstituted gold vinylidene leading to decarbonylative transformations. As depicted in Scheme 1.31, arene-tethered diyne **1.148** provided indene **1.152** by the gold catalyst in the presence of an excess amount of water.³⁸ The disubstituted gold vinylidene **1.149** was captured by water to give acyl gold complex **1.150**, which entered on a decarbonylative pathway as previously shown in Scheme 1.10.¹³



Scheme 1.31 Au(I)-catalyzed decarbonylative carbocyclization of a diyne

The oxygen atom of *N*-oxides could be transferred to disubstituted gold vinylidenes. Under gold catalysis using a stoichiometric pyridine *N*-oxide oxidant, oxygenative carbocyclization of diyne **1.153** was feasible to afford indenoate ester **1.154** in good yield (Scheme 1.32).³⁹ This example showcases an oxygenative mechanism distinct from the well-known α -oxo gold carbenoid mediated catalysis.



Scheme 1.32 Au(I)-catalyzed oxygenative carbocyclization of a diyne

1.5 Conclusion

In this chapter, transition metal vinylidene mediated carbocyclization reactions of alkynes have been discussed. In contrast to the traditional π -activation strategies for C–C bond formations of alkynes, metal vinylidene intermediates switch the regioselectivity to the *anti*-Markovnikov manner, and provide diversified *endo* cyclic alkenes (Section 1.2). The reactions employ various carbon nucleophiles ranging from polarized carbon nucleophiles to less reactive C=C bonds, and even oxygen nucleophiles have been used for the addition-induced carbocyclization. By rendering the β -carbon of terminal alkynes to a sp^2 -hybridized carbon atom, metal vinylidene complexes mediated a variety of pericyclic reactions which had been difficult

to perform (Section 1.3). Both the carbon–metal and carbon–carbon π -bonds in metal vinylidene complexes have participated in pericyclic processes, some of which accompany further rearrangements to yield carbocycles of higher molecular complexity. The β -alkylation with a tethered alkyl halide has been used to construct carbocycles *via* formation of a disubstituted metal vinylidene intermediate (Section 1.4). Notably, gold mediated vinylidene catalysis, which has appeared in the literature more recently, has shown unique dual gold activation mechanisms, leading to formation of novel carbocycles through accompanying C–H insertion reactions.

Although a great deal of efforts to develop the transition metal vinylidene mediated carbocyclization reactions have been made, there remains much room for improvement. Firstly, most of the catalysis uses second (Ru, Rh, and Pd) or third (W, Re, and Au) row transition metals. Thus, the development of methodologies using earth-abundant first row transition metals will be required. Secondly, the development of asymmetric protocols for these carbocyclization reactions will be of significant value. In contrast to the transition metal allenylidene mediated catalysis that has established a variety of enantioselective C–C bond formations using ruthenium or copper catalysts, there are only quite limited asymmetric examples for metal vinylidene mediated catalysis. Therefore, further exploration of transition metals and chiral ligand systems for asymmetric carbocyclization will greatly expand the usefulness of metal vinylidenes in organic synthesis.

1.6 Reference

- ¹ *Modern Alkyne Chemistry: Catalytic and Atom-Economic Transformations*; Trost, B. M.; Li, C.-J. Wiley-VCH; Weinheim, 2015.
- ² Beller, M.; Seayad, J.; Tillack, A.; Jiao, H. *Angew. Chem. Int. Ed.* **2014**, *43*, 3368.
- ³ (a) Bruneau, C.; Dixneuf, P. H. *Angew. Chem. Int. Ed.* **2006**, *45*, 2176. (b) Trost, B. M.; McClory, A.; *Chem. Asian J.* **2008**, *3*, 164.
- ⁴ McDonald, F. E.; Olson, T. C. *Tetrahedron Lett.* **1997**, *38*, 7691.
- ⁵ (a) Maeyama, K.; Iwasawa, N. *J. Am. Chem. Soc.* **1998**, *120*, 1928. (b) Miura, T.; Iwasawa, N. *J. Am. Chem. Soc.* **2002**, *124*, 518.
- ⁶ Kim, H.; Lee, C. *J. Am. Chem. Soc.* **2006**, *128*, 6336.
- ⁷ Shen, H.-C.; Pal, S.; Lian, J.-J.; Liu, R.-S. *J. Am. Chem. Soc.* **2003**, *125*, 15762.
- ⁸ Madhushaw; R. J.; Lo, C.-Y.; Hwang, C.-W.; Su, M.-D.; Shen, H.-C.; Pal, S.; Shaikh, I. R.; Liu, R.-S. *J. Am. Chem. Soc.* **2004**, *126*, 15560.
- ⁹ Fukamizu, K.; Miyake, Y.; Nishibayashi, Y. *Angew. Chem. Int. Ed.* **2009**, *48*, 2534.
- ¹⁰ Kim, H.; Goble, S. D.; Lee, C. *J. Am. Chem. Soc.* **2007**, *129*, 1030.
- ¹¹ (a) Wang, Y.; Finn, M. G. *J. Am. Chem. Soc.* **1995**, *117*, 8045. (b) Ohe, K.; Kojima, M.-a.; Yonehara, K.; Uemura, S. *Angew. Chem. Int. Ed. Engl.* **1996**, *35*, 1823.
- ¹² (a) Chen, Y.; Ho, D. M.; Lee, C. *J. Am. Chem. Soc.* **2005**, *127*, 12184. (b) Chen, Y.; Park, S. H.; Lee, C. W.; Lee, C. *Chem. Asian J.* **2011**, *6*, 2000.
- ¹³ (a) Varela, J. A.; González-Rodríguez, C.; Rubín, S. G.; Castedo, L.; Saá, C. *J. Am. Chem. Soc.* **2006**, *128*, 9576. (b) González-Rodríguez, C.; Varela, J. A.; Castedo, L.; Saá, C. *J. Am. Chem. Soc.* **2007**, *129*, 12916.
- ¹⁴ For rhodium-catalyzed oxygenative transformations of terminal alkynes, see: (a) Kim, I.; Lee, C. *Angew. Chem. Int. Ed.* **2013**, *52*, 10023. (b) Kim, I.; Roh, S. W.; Lee, D. G.; Lee, C. *Org. Lett.* **2014**, *16*, 2482. (c) Zeng, H.; Li, C.-J. *Angew. Chem. Int. Ed.* **2014**, *53*, 13862.
- ¹⁵ (a) Madhushaw, R. J.; Lin, M.-Y.; Sohel, S. M. A.; Liu, R.-S. *J. Am. Chem. Soc.* **2004**, *126*, 6895. (b) Ming-Yuan, L.; Madhushaw, R. J.; Liu, R.-S. *J. Org. Chem.* **2004**, *69*, 7700.
- ¹⁶ Wang, Y.; Zheng, Z.; Zhang, L. *Angew. Chem. Int. Ed.* **2014**, *53*, 9572.
- ¹⁷ (a) Merlic, C. A.; Pauly, M. E. *J. Am. Chem. Soc.* **1996**, *118*, 11319. (b) Lian, J.-J.; Odedra, A.; Wu, C.-J.; Liu, R.-S. *J. Am. Chem. Soc.* **2005**, *127*, 4186.
- ¹⁸ (a) Maeyama, K.; Iwasawa, N. *J. Org. Chem.* **1999**, *64*, 1344. (b) Shen, H.-C.; Pal, S.; Lian, J.-J.; Liu, R.-S. *J. Am. Chem. Soc.* **2003**, *125*, 15762.

- ¹⁹ Bigeault, J.; Giordano, L.; Buono, G. *Angew. Chem. Int. Ed.* **2005**, *44*, 4753.
- ²⁰ For Pt-catalyzed reaction, see: (a) Bigeault, J.; Giordano, L.; de Raggi, I.; Gimbert, Y.; Buono, G. *Org. Lett.* **2007**, *9*, 3567; For Pd allenylidene transfer, see: (b) Bigeault, J.; de Raggi, I.; Gimbert, Y.; Giordano, L.; Buono, G. *Synlett* **2008**, *7*, 1071; For its enantioselective derivative, see: (c) Gatineau, D.; Moraleda, D.; Naubron, J.-B.; Bürgi, T.; Giordano, L.; Buono, G. *Tetrahedron: Asymmetry* **2009**, *20*, 1912.
- ²¹ Pal, S.; Zhou, Y.-Y.; Uyeda, C. *J. Am. Chem. Soc.* **2017**, *139*, 11686.
- ²² Onitsuka, K.; Katayama, H.; Sonogashira, K.; Ozawa, F. *J. Chem. Soc., Chem. Commun.* **1995**, 2267.
- ²³ Kim, H.; Lee, C. *J. Am. Chem. Soc.* **2005**, *127*, 10180.
- ²⁴ For the other examples of carbocyclization involving [2+2] cycloaddition from metal vinylidenes, see: (a) Grigg, R.; Stevenson, P.; Worakun, T. *Tetrahedron* **1988**, *44*, 4967. (b) Matsuda, T.; Kato, K.; Goya, T.; Shimada, S.; Murakami, M. *Chem. Eur. J.* **2016**, *22*, 1941.
- ²⁵ Elakkari, E.; Floris, B.; Galloni, P.; Tagliatesta, P. *Eur. J. Org. Chem.* **2005**, 889.
- ²⁶ (a) Datta, S.; Odedra, A.; Liu, R.-S. *J. Am. Chem. Soc.* **2005**, *127*, 11606. (b) Odedra, A.; Datta, S.; Liu, R.-S. *J. Org. Chem.* **2007**, *72*, 3289.
- ²⁷ Sogo, H.; Iwasawa, N. *Angew. Chem. Int. Ed.* **2016**, *55*, 10057.
- ²⁸ Joo, J. M.; Yuan, Y.; Lee, C. *J. Am. Chem. Soc.* **2006**, *128*, 14818.
- ²⁹ Sakai, K.; Kochi, T.; Kakiuchi, F. *Org. Lett.* **2013**, *15*, 1024.
- ³⁰ Kawaguchi, Y.; Yasuda, S.; Kaneko, A.; Oura, Y.; Mukai, C. *Angew. Chem. Int. Ed.* **2014**, *53*, 7608.
- ³¹ (a) Ye, L.; Wang, Y.; Aue, D. H.; Zhang, L. *J. Am. Chem. Soc.* **2012**, *134*, 31. (b) Hashmi, A. S. K.; Braun, I.; Nösel, P.; Schädlich, J.; Wieteck, M.; Rudolph, M.; Rominger, F. *Angew. Chem. Int. Ed.* **2012**, *51*, 4456.
- ³² Lemière, G.; Gandon, V.; Agenet, N.; Goddard, J.-P.; de Kozak, A.; Aubert, C.; Fensterbank, L.; Malacria, M. *Angew. Chem. Int. Ed.* **2006**, *45*, 7596.
- ³³ (a) Morán-Poladura, P.; Rubio, E.; González, J. M. *Angew. Chem. Int. Ed.* **2015**, *54*, 3052. (b) Wang, Y.; Zarca, M.; Gong, L.-Z.; Zhang, L. *J. Am. Chem. Soc.* **2016**, *138*, 7516.
- ³⁴ (a) Hashmi, A. S. K.; Braun, I.; Rudolph, M.; Rominger, F. *Organometallics* **2012**, *31*, 644. For the intramolecular arylyative cycloaromatizations, see: (b) Hashmi, A. S. K.; Wieteck, M.; Braun, I.; Nösel, P.; Jongbloed, L.; Rudolph, M.; Rominger, F. *Adv. Synth. Catal.* **2012**, *354*, 555.

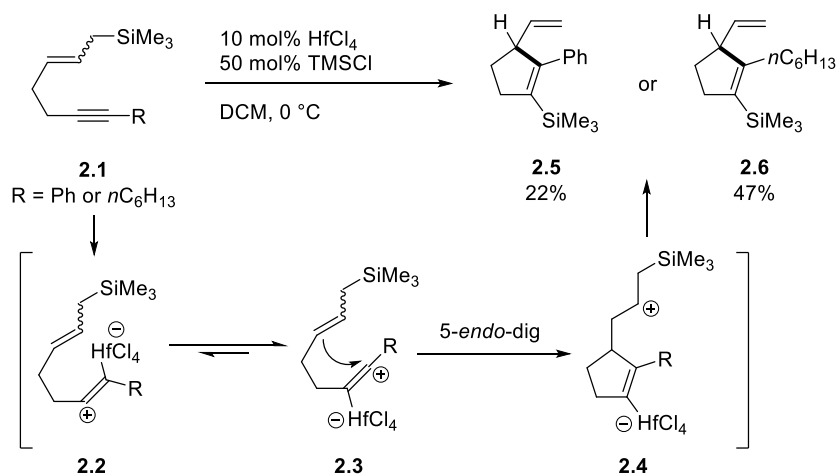
- ³⁵ Bucher, J.; Wurm, T.; Taschinski, S.; Sachs, E.; Ascough, D.; Rudolph, M.; Rominger, F.; Hashmi, A. S. K. *Adv. Synth. Catal.* **2017**, *359*, 225.
- ³⁶ Hashmi, A. S. K.; Wieteck, M.; Braun, I. Rudolph, M.; Rominger, F. *Angew. Chem. Int. Ed.* **2012**, *51*, 10633.
- ³⁷ Bucher, J.; Wurm, T.; Nalivela, K. S.; Rudolph, M.; Rominger, F.; Hashmi, A. S. K. *Angew. Chem. Int. Ed.* **2014**, *53*, 3854.
- ³⁸ Bucher, J.; Stöber, T.; Rudolph, M.; Rominger, F.; Hashmi, A. S. K. *Angew. Chem. Int. Ed.* **2015**, *54*, 1666.
- ³⁹ Yu, C.; Ma, X.; Chen, B.; Tang, B.; Paton, R. S.; Zhang, G. *Eur. J. Org. Chem.* **2017**, 1561.

Chapter 2. Rhodium-Catalyzed Carbocyclization of Alkynylamines

2.1 Introduction

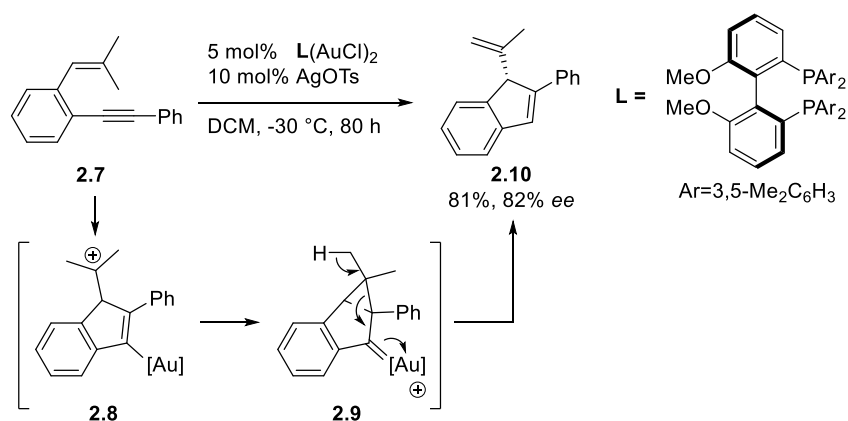
Development of methodologies to construct carbocyclic structures has been invaluable due to the affluence of carbocycles in Nature, as well as the significance of making new C–C bonds in organic synthesis. In this context, the transition metal catalyzed carbocyclization of alkynes has been explored and used extensively for decades using the π -unsaturation for atom-economical transformations. In this section, transition metal catalyzed 5-*endo*-dig carbocyclization reactions of enyne derivatives will be discussed briefly. In doing so, transition metal vinylidene mediated reactions are excluded because these reactions have been discussed in the previous chapter.¹

An early example of transition metal catalyzed carbocyclization of enyne was reported in 1998.² In the presence of a catalytic amount hafnium complex and a substoichiometric amount of TMSCl, the alkyne-tethered allyl silanes **2.1** was cyclized to silyl cyclopentenes **2.5** and **2.6** *via* zwitterionic intermediates involving a vinyl cation (Scheme 2.1). The authors proposed that exclusive *endo*-selective 5-, 6-, and 7-carbocyclization could occur due to the sterical and electronical preference of vinyl cation **2.3**.



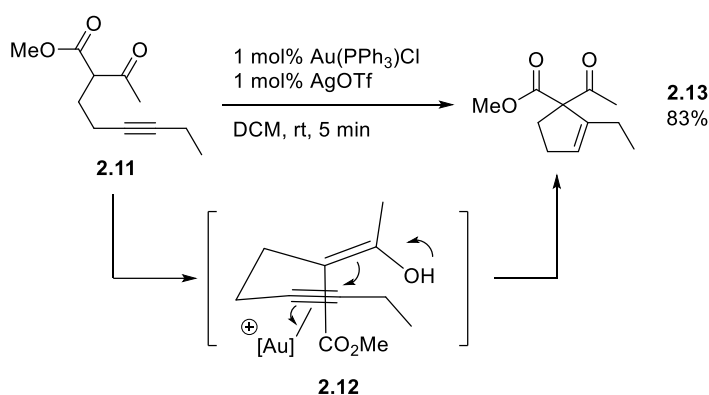
Scheme 2.1 Hf(IV)-catalyzed 5-*endo*-dig carbocyclization

An electrophilic cationic gold catalyst can be used in 5-*endo*-dig carbocyclizations for less polarized arene-tethered enynes. As depicted in Scheme 2.3, a gold/biphep catalyst could mediate the enantioselective cycloisomerization of enyne **2.7**, *via* tertiary carbocation and gold carbene intermediates, to give the chiral vinyl indene **2.10**.³ The tertiary carbocation **2.8** could also be captured by external alcohol derivatives to generate its corresponding alkoxy-cyclized products.



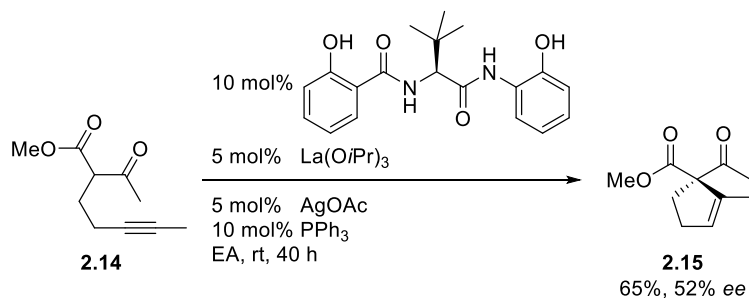
Scheme 2.2 Au(I)-catalyzed enantioselective 5-*endo*-dig cycloisomerization

Alkenes derived from the enol form of β -ketoesters have been known to participate in enyne cycloisomerizations. The 3-hexyne-substituted methyl acetoacetate **2.11** was cycloisomerized to cyclopentene **2.13** rapidly in the presence of 1 mol% of cationic gold catalyst (Scheme 2.3).⁴ The authors have argued that the reaction mechanism involves a nucleophilic addition of an enol to gold alkyne complex **2.12**.



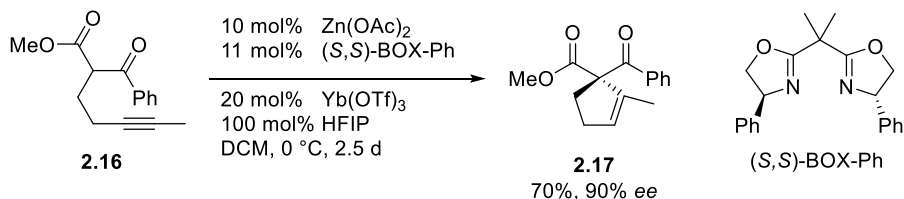
Scheme 2.3 Au(I)-catalyzed 5-*endo*-dig cycloisomerization

Since the Toste group reported the first catalytic enantioselective Conia-ene reaction *via* 5-*exo*-dig cyclization,⁵ there have been several asymmetric examples of similar reactions. In the lanthanum/silver-catalyzed asymmetric carbocyclization of the alkynyl β -ketoester **2.14**, the chiral lanthanum catalyst acted as a hard Lewis acid to form a chiral enolate, which underwent 5-*endo*-dig cyclization, giving the cycloisomerized product **2.15** (Scheme 2.4).⁶ There is only a single example of 5-*endo*-dig cycloisomerization, albeit showing only modest enantiomeric excess.



Scheme 2.4 La(III)/Ag(I) co-catalyzed cycloisomerization

In 2012, enantioselective 5-*endo*-dig carbocyclization was reported using zinc and ytterbium catalysts cooperatively (Scheme 2.5).⁷ Under chiral zinc and ytterbium catalyzed conditions, β -ketoester **2.16**, tethered with an internal alkyne, was converted to its cyclic isomer **2.17** in moderate yield and good enantioselectivity. In the proposed mechanistic picture, a chiral zinc enolate derived from zinc/BOX complex undergoes nucleophilic attack to a ytterbium alkyne complex. Although this work afforded cyclopentenes having a chiral quaternary carbon center, high enantioselectivity was limited to benzoyl acetate substrate. There is no example of terminal alkyne substrates.

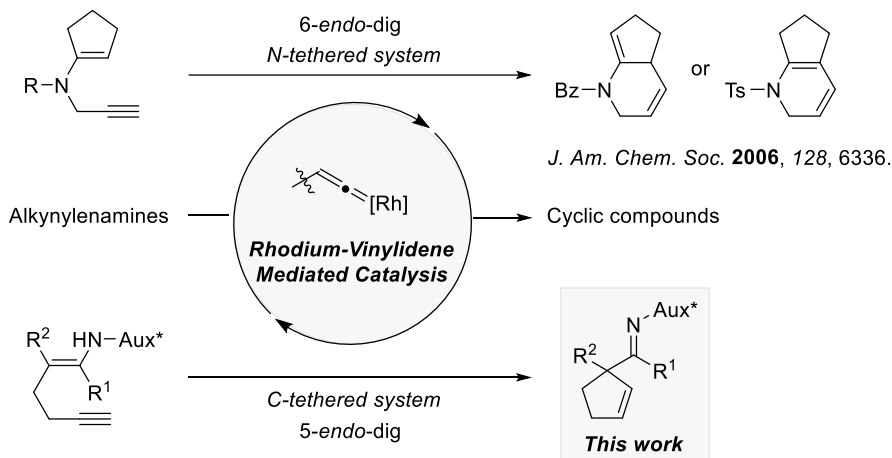


Scheme 2.5 Zn(II)/Yb(III) co-catalyzed cycloisomerization

In summary, transition metal catalyzed 5-*endo*-dig carbocyclizations have been discussed. A variety of alkenes, ranging from less polarized alkenes

to enol ethers, could engage in the carbocyclization with alkynes. These reactions are initiated by the formation of metal alkyne π -complexes, which have a lower LUMO than free alkynes and make C–C bonds with carbon nucleophiles. Moreover, recently, cooperative catalytic systems, where enolates are generated, have been developed for the synthesis of cyclopentenes with a quaternary stereocenter.⁸ Notwithstanding these efforts, the use of enyne substrates that have a terminal alkyne is still limited, because metal alkyne π -complexes have high propensity to follow Markovnikov selectivity.⁹

Described here is the development of the rhodium-catalyzed 5-*endo*-dig carbocyclization of alkyne-tethered enamines. To make C–C bond formation with terminal alkynes take place in an *anti*-Markovnikov fashion, the rhodium catalyzed conditions previously reported in the cycloisomerization of *N*-propargyl enamines has been employed (Scheme 2.6).¹⁰ Furthermore, it was anticipated that the rhodium-catalyzed asymmetric alkenylation reactions could be achieved by introducing chiral auxiliary at the enamine. This reaction would constitute the first example of asymmetric carbocyclization *via* a rhodium vinylidene intermediate.¹¹ In particular, substrate design of alkynyl enamines, investigation of chiral auxiliaries, preliminary mechanistic studies, and rhodium/amine dual-catalytic carbocyclization reactions will be discussed.

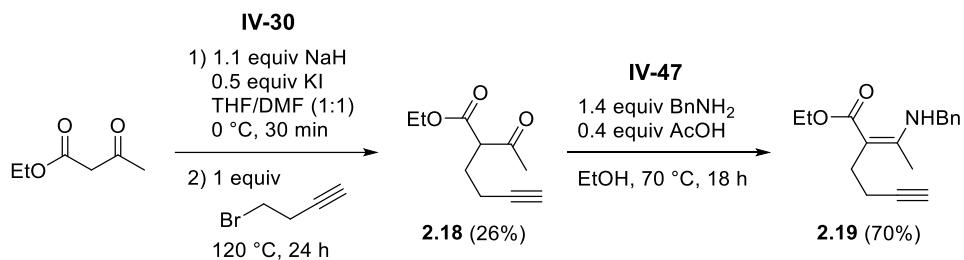


Scheme 2.6 General scheme for the rhodium-catalyzed cyclization reactions of alkynyl enamines

2.2 Results and discussion

2.2.1 Carbocyclization of *N*-benzyl alkynylamine

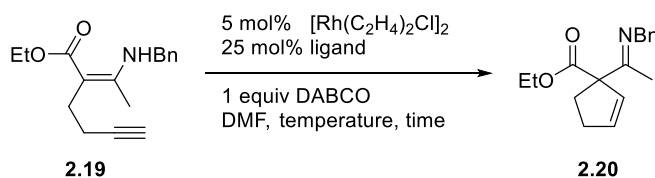
In designing an appropriate substrate, the following requirements seemed to be needed for asymmetric carbocyclization reactions based on the previous work. First of all, the C₂-position of enamines should be disubstituted, because racemization of the chiral product can take place through iminium-enamine tautomerizations. Secondly, the cyclization between prochiral enamine and alkyne should take place with a single *E* or *Z* configuration of the enamine. For these reasons, alkyne-tethered fully substituted enamine **2.19** has been prepared by alkylation of ethyl acetoacetate with 4-bromo-1-butyne followed by condensation with benzylamine (Scheme 2.7).



Scheme 2.7 Synthesis of the *N*-benzyl alkynylenamine **2.19**

Under the conditions employed in the previous work of 6-*endo*-dig cycloisomerization of *N*-propargylenamines, no cyclized product was observed. However, heating reaction temperature to 50 °C gave the desired product **2.20** in moderate yield (Table 2.1, Entry 1). Further phosphine ligand screening was conducted, but did not improve the reaction yield (Table 2.1, Entry 2-6).

Table 2.1 Phosphine ligand screening



Entry	Ligand	Temperature	Time	Yield ^a
1	P(4-F-C ₆ H ₄) ₃	50 °C	22 h	67%
2	P(4-Cl-C ₆ H ₄) ₃	50 °C	17 h	33%
3	P(3,5-CF ₃ -C ₆ H ₄) ₃	85 °C	15 h	11%
4	PPh ₃	50 °C	17 h	37%
5	P(4-F-C ₆ H ₄) ₃	85 °C	26 h	23%
6	P(2-furyl) ₃	85 °C	15 h	14%

^aYields were determined by ¹H NMR using anisole as an internal standard.

The base has shown effects different from those found in the previous work (Table 2.2). Although DABCO was still the optimal base, the desired cyclization took place even without a base at a higher temperature (Entry 6). These results indicated that high acidity of the iminium N–H bond could serve as a proton source to protonate the carbon–rhodium bond in the turnover step without a proton shuttle.

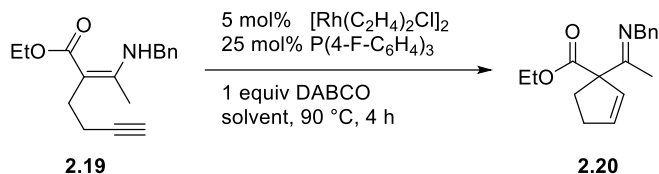
Table 2.2 Base screening

Entry	Base	Temperature	Time	Yield ^a
1	DABCO	50 °C	22 h	67%
2	DABCO	90 °C	4 h	46%
3	DBU	50 °C	24 h	21%
4	TEA	90 °C	4 h	48%
5	2,6-di- <i>t</i> BuPy	90 °C	4 h	35%
6	none	90 °C	4 h	46%

^aYields were determined by ¹H NMR using anisole as an internal standard.

Having examined the base effect, we then conducted solvent screening experiments (Table 2.3). Nonpolar toluene gave a better result rather than polar DMF solvent (Entry 1 and 4), indicating the presence of an intramolecular electrostatic interaction between the iminium cation and the alkenyl rhodium anion. These results also suggest the possibility that cyclization and proton transfer might occur in a concerted manner without going through a zwitterionic intermediate.

Table 2.3 Solvent screening

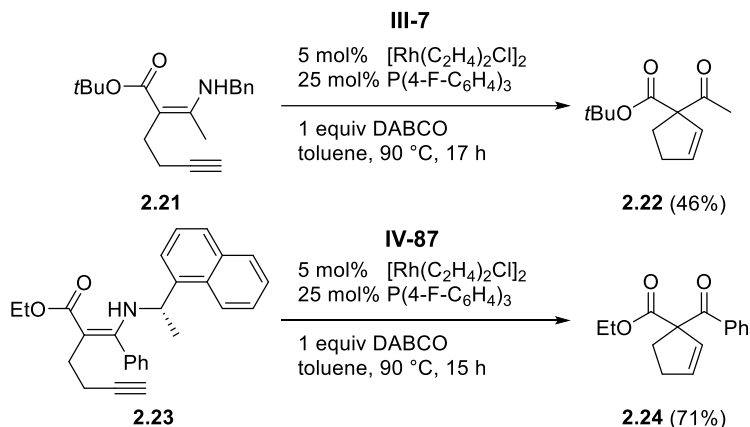


Entry	Solvent	Yield ^a
1	DMF	46%
2	MeCN	42%
3	1,4-dioxane	54%
4	toluene	74%

^aYields were determined by ¹H NMR using anisole as an internal standard.

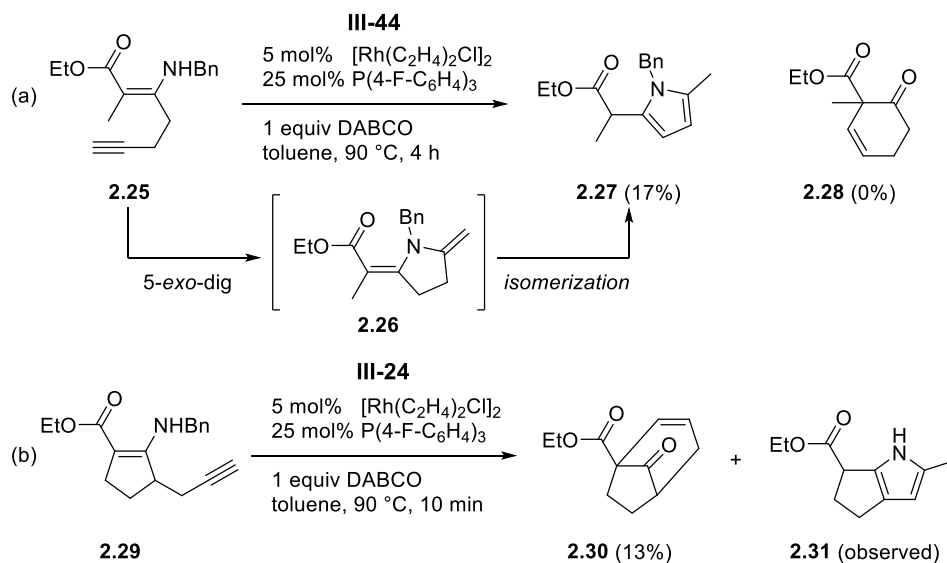
2.2.2 Substrate scope

With the partially optimized protocols in hand, we investigated rhodium-catalyzed carbocyclization of alkynyl enamines possessing a different substituent. With the alkynyl enamines derived from *tert*-butyl acetoacetate and ethyl benzoacetate, the reaction worked well in moderate yields (Scheme 2.8). Especially, the reaction of alkynyl enamine **2.23**, conjugated by a phenyl group, required a higher temperature and a longer reaction time than those of methyl substituted alkynyl enamine **2.19**.



Scheme 2.8 5-*endo*-dig carbocyclization of alkynyl enamines

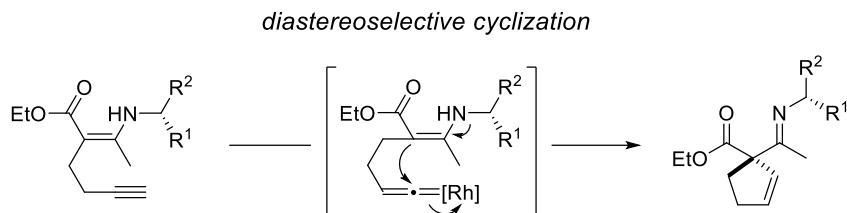
When enamines prepared from a propargylated acetoacetate were exposed to the rhodium catalyzed conditions, unexpected 5-*exo*-dig cyclization took place dominantly giving rise to pyrrole **2.27** (Scheme 2.9a). The high degree of freedom of alkynyl group may induce the azacyclization, so we used alkynyl enamine **2.29** which has more rigidity to avoid undesired 5-*exo* cyclization (Scheme 2.9b). In spite of the fused pyrrole **2.31** was still observed as a major product, desired 6-*endo* product **2.30** could be isolated suggesting the possibilities to be improved.



Scheme 2.9 Cyclization of alkynyl enamines for the 6-*endo* product

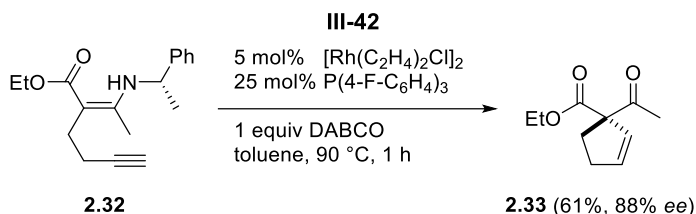
2.2.3 Asymmetric carbocyclization of alkynyl enamines

It has been shown that achiral *N*-benzyl alkynyl enamines can afford corresponding endocyclic alkenes in previous sections. To expand the usefulness of this methodology, we went back to the original objective of performing the reaction with asymmetric induction. As illustrated in Scheme 2.10, chiral enamines from commercially available primary amine¹² can act as a chiral nucleophile in the carbocyclization to react with a rhodium vinylidene electrophile, leading to a diastereomeric product with construction of a quaternary stereocenter.



Scheme 2.10 Working hypothesis for the asymmetric carbocyclization of an alkynyl enamine using chiral enamine

Under this hypothesis, the chiral alkynyl enamine **2.32** derived from (*S*)- α -methylbenzylamine was exposed to the optimized conditions (Scheme 2.11). Fortunately, the desired product **2.33** was generated in moderate yield with good enantioselectivity presumably *via* hydrolysis of the imine formed under rhodium-catalyzed conditions.¹³

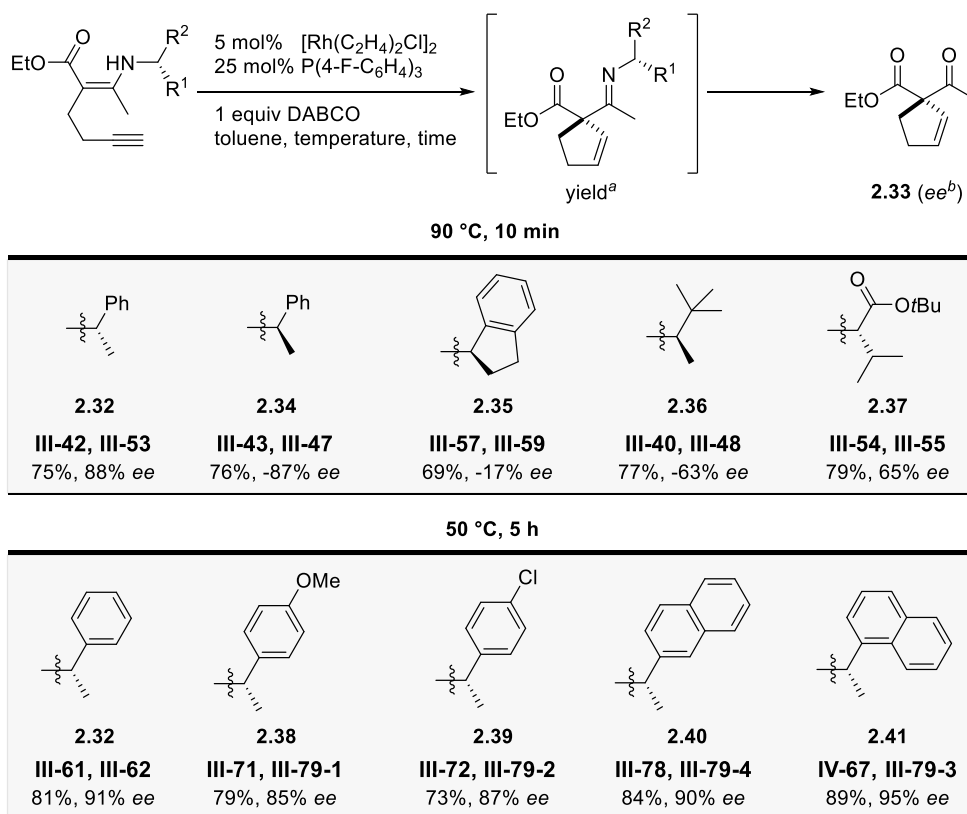


Scheme 2.11 Preliminary result of asymmetric carbocyclization of an alkynyl enamine

With the promising result of asymmetric carbocyclization, the effects of the auxiliary on diastereoselectivity were investigated (Table 2.4). A variety of chiral primary amines possessing indanyl, *t*-butyl, and amino acid-derived substituents were tested. However, none of these amines gave a

higher stereoselectivity. We noticed that the reaction was completed at 90 °C in only 10 minutes during these experiments. Thus, the reaction temperature was decreased from 90 °C to 50 °C in the hope of enhancing the stereoselectivity. As we expected, both the reaction yield and the stereoselectivity were improved significantly. Further investigation of chiral primary amines revealed 1-naphthyl substituted amine to be optimal, giving excellent yield and stereoselectivity.

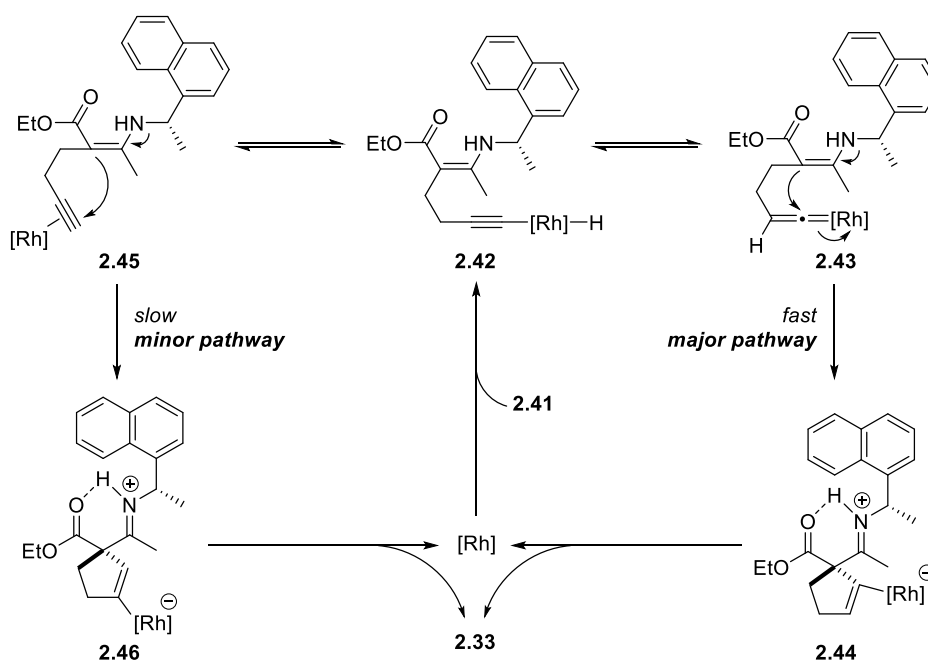
Table 2.4 Chiral auxiliary and temperature effects on carbocyclization



^aYields were determined by ¹H NMR using 1,3,5-trimethoxybenzene as an internal standard. ^bee of **2.33** were determined by chiral HPLC after reduction of ketone.

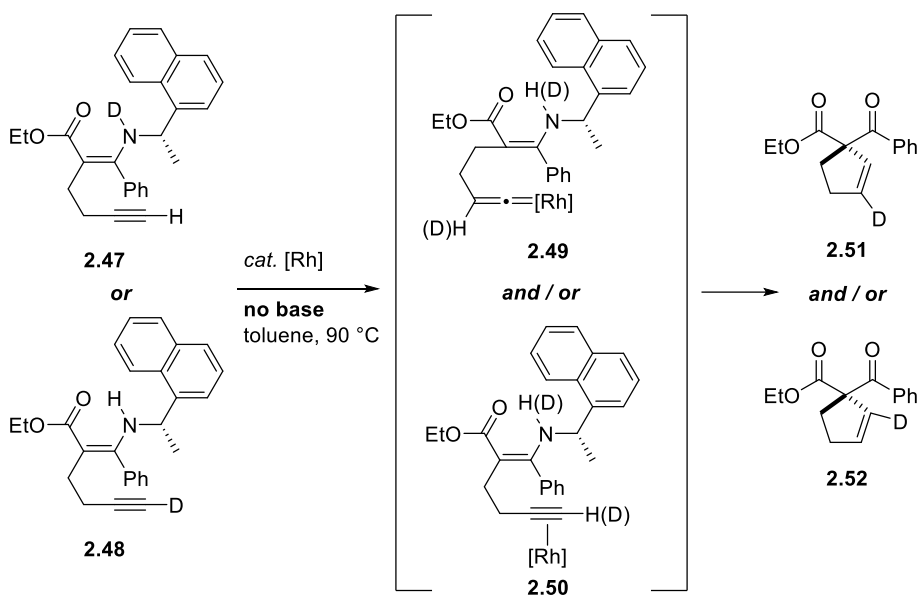
2.2.4 Proposed mechanism and mechanistic studies

We have developed the rhodium-catalyzed asymmetric carbocyclization of alkynyl enamines using a chiral auxiliary. Based on these results, mechanistic studies were conducted to elucidate the exact catalytic reaction pathway. A mechanism is described in Scheme 2.12, suggesting two possible reaction pathways. In the first proposed mechanism, rhodium vinylidene complex **2.43** mediates the C–C bond forming event. In the other case, the rhodium catalyst acts as a Lewis acid to activate π -bond of the alkyne. In both cases, the turnover of the rhodium catalyst was mediated by DABCO, shuttling proton from the iminium to the alkenyl rhodium complex.



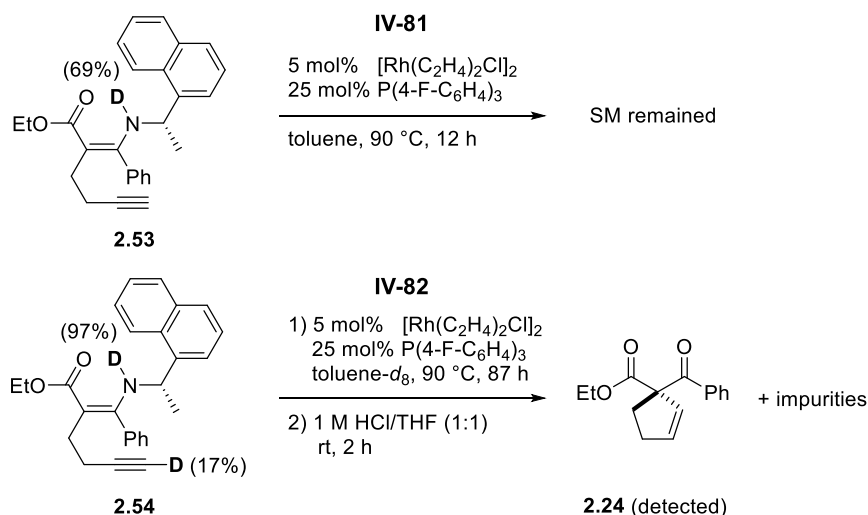
Scheme 2.12 Proposed mechanism for rhodium-catalyzed carbocyclization

A useful way in determining the reaction mechanism is deuterium-labeling experiments (Scheme 2.13). If N-D alkynylenamine **2.47** or C-D alkynylenamine **2.48** was subjected to the rhodium-catalyzed conditions, they could give the deuterated cyclopentene **2.51** or **2.52** depending on the reaction mechanism. Also, the reaction of phenyl substituted alkynylenamine without a base additive could suppress the chance of proton mixing.



Scheme 2.13 Deuterium-labeling experiments for mechanistic studies

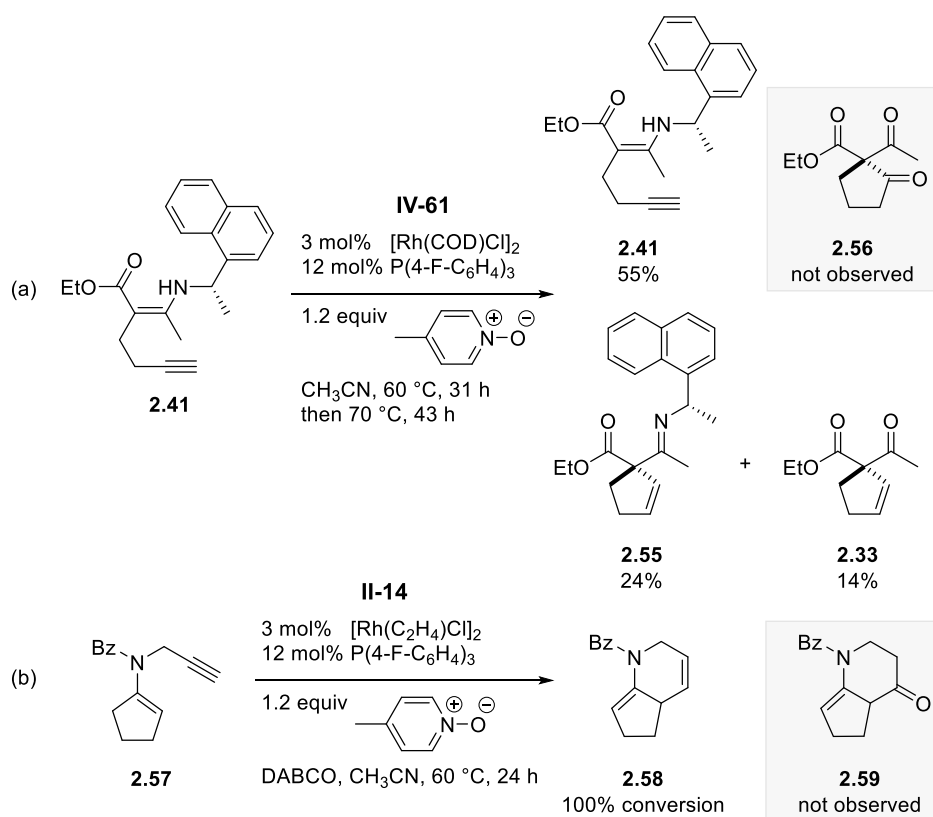
With the deuterated alkynylenamines in hand, we conducted the rhodium-catalyzed carbocyclizations without a base at 90 °C (Scheme 2.14). However, alkynylenamine **2.53** did not react at all for 12 h, and gave only trace amount of product **2.24** after a prolonged time, in contrast with the results from an acetoacetate-derived system (Table 2.2, Entry 6). To conclude these results, the future studies will require the results of the same reaction with DABCO, along with deuterium-labeling experiments with the standard substrate **2.41**.



Scheme 2.14 Poor reactivity of phenyl substituted alkynylenamines without a base

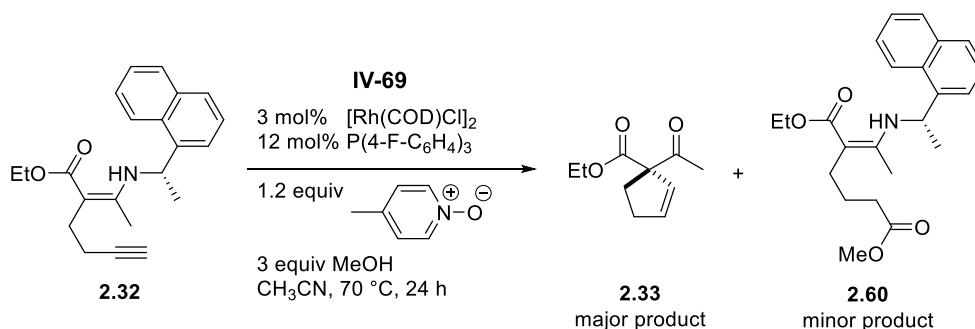
In 2013, our group reported the rhodium vinylidene mediated oxygenative functionalization reactions of terminal alkynes using a rhodium-ketene as a catalytic intermediate.¹⁴ To prove the presence of the rhodium vinylidene intermediate, we attempted to obtain the oxygenated carbocycle

2.56 under oxidative conditions (Scheme 2.15). However, under the rhodium catalyzed conditions with picoline *N*-oxide, neither the C- (**2.41**) or N-tethered (**2.57**) alkynyl substrate gave oxidized carbocycles **2.56** or **2.59**, but produced endocyclic alkenes **2.55** and **2.58**, respectively. These results mean that **1**) the carbocyclization was too fast for the rhodium vinylidene to be oxidized to a ketene, **2**) a rhodium-ketene intermediate could not react with the enamine, or **3**) the cyclization did not involve a rhodium vinylidene intermediate.



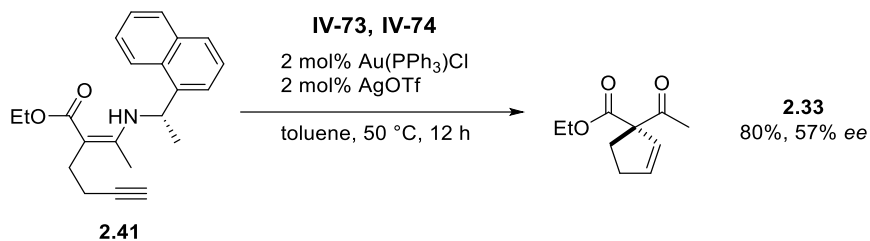
Scheme 2.15 Rh(I)-catalyzed carbocyclization under oxidative conditions

Next, we performed a quenching experiment using methanol as a nucleophile to check the existence of a rhodium-ketene intermediate (Scheme 2.16). As a result, the oxygenative addition product **2.60** was observed in the ^1H NMR spectrum of a crude product, supporting the presence of the rhodium-ketene intermediate generated from a rhodium vinylidene.



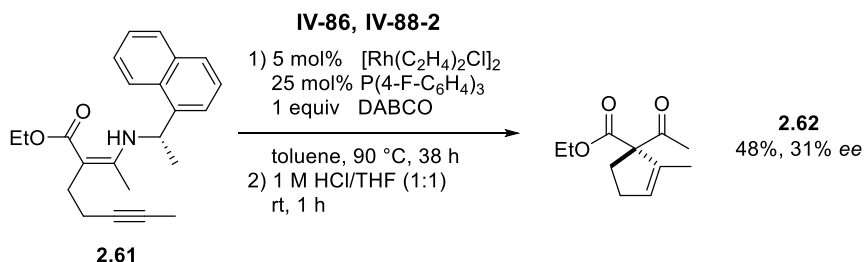
Scheme 2.16 Observation of the oxygenative addition before carbocyclization

A cationic gold(I) catalyst, known as an efficient catalyst for *5-endo*-dig carbocyclization of alkyne β -keto esters, was tested for the carbocyclization of alkyne enamines in order to compare the reaction profiles of gold and rhodium catalysis (Scheme 2.17). Under gold catalysis in toluene at 50°C , alkyne enamine **2.41** reacted well giving rise to the desired carbocycle **2.33**, but the enantiomeric excess was lower than that from the rhodium catalyzed conditions.



Scheme 2.17 Au(I)-catalyzed asymmetric carbocyclization of an alkynyl enamine

Alkyl-substituted internal alkynes have been known as a poor reactant in transition metal vinylidene mediated catalysis. When we applied the rhodium catalyzed conditions to the internal alkyne-tethered enamine **2.61** (Scheme 2.18), surprisingly, 1-methyl cyclopentene **2.62** was isolated in moderate yield. However, the poor stereochemical outcome and the requirement of a higher temperature and a longer reaction time suggest that this internal alkyne substrate follows a mechanism different than terminal alkynes.



Scheme 2.18 Rh(I)-catalyzed carbocyclization of the internal alkyne-tethered enamine

Based on the results of the carbocyclization through π -alkyne pathways, we suggest that these reactions are going through the transition states where the catalysts are far away from the chiral auxiliary (Figure 2.1). On the contrary, the reactions described in table 2.4 give excellent stereochemical outcomes. In these reactions occurring through a rhodium vinylidene involved transition state, the rhodium carbene center feels more steric differentiation influenced by the chiral auxiliary than those in π -alkyne pathways.

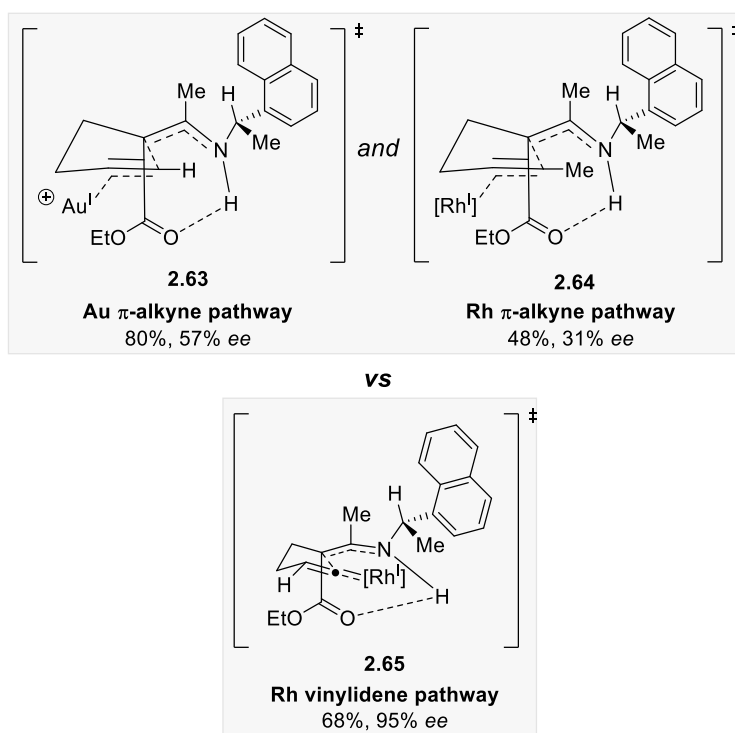
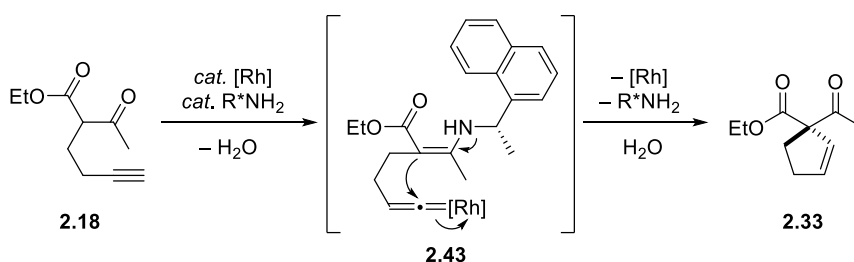


Figure 2.1 Proposed transition state of asymmetric carbocyclization of an alkynylamine

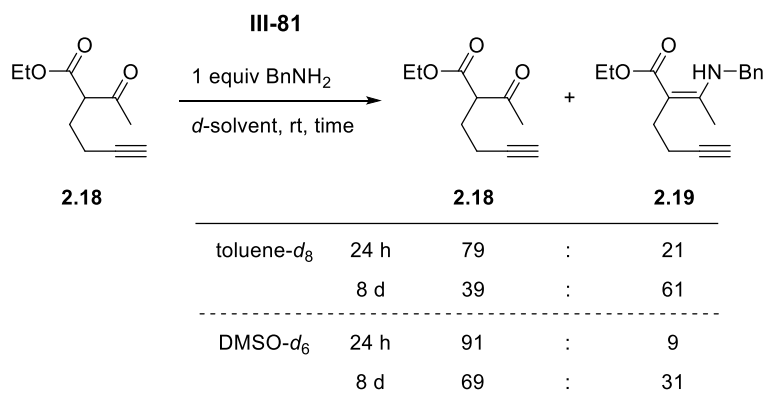
2.2.5 Dual catalysis: Merging rhodium-catalysis with organocatalysis

The rhodium-catalyzed carbocyclization of alkynylamines has shown moderate yield and high stereoselectivity, leading to the formation of cyclopentenes which have quaternary stereogenic carbon centers. However, there is a limitation of requiring a stoichiometric amount of a chiral primary amine to prepare the alkynylamines before the rhodium catalysis. For these reasons, we propose the synergistic cooperative catalysis merging transition metal- and organocatalysis.^{15,16} As shown in Scheme 2.19, both of the rhodium and primary amine catalysts react with the terminal alkyne and the ketone, respectively, giving rise to the rhodium vinylidene-tethered enamine **2.43** *in situ* which brings about formation of carbocycle **2.33**.¹⁷ The following sections will describe the development of the rhodium/primary amine co-catalyzed carbocyclization of alkynyl β -keto esters.¹⁸



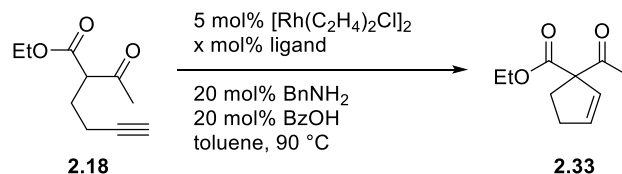
Scheme 2.19 Rh(I)/amine-catalyzed carbocyclization of an alkynyl β -keto ester

Before the optimization of the reaction conditions, we conducted ^1H NMR experiment to verify the feasibility of *in situ* generation of alkynyl enamine (Scheme 2.20). A 1:1 mixture of alkynyl β -keto ester **2.18** and benzylamine produced *N*-benzyl alkynyl enamine **2.19** in the absence of a Brønsted acid additive, regardless of whether nonpolar toluene or polar DMSO was used as a solvent. Interestingly, toluene, which had been found to be the best solvent for the rhodium-catalyzed carbocyclization of alkynyl enamines, showed faster conversion rate than DMSO.



Scheme 2.20 ^1H NMR experiments for *in situ* synthesis of an alkynyl enamine

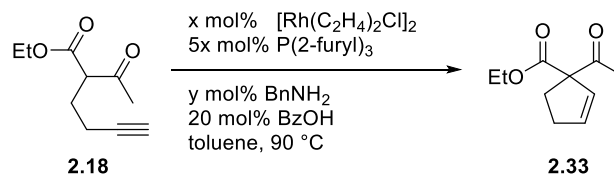
With 20 mol% of benzylamine and benzoic acid, ligand screening experiments were conducted (Table 2.5). In contrast to the stoichiometric carbocyclization reactions where $\text{P}(4\text{-F-C}_6\text{H}_4)_3$ gave the best results, only $\text{P}(2\text{-furyl})_3$ gave rise to the desired carbocycle **2.33** in low yield (Entry 1-4 vs 5). Increasing the amount of phosphine ligand did not improve the yield, and the reaction was blocked when the stoichiometric amount of ligand was used (Entry 5-8).¹⁹

Table 2.5 Ligand screening experiments

Exp. #	Entry	Ligand (x)	Time	Yield ^a
III-95-1	1	$\text{P}(4\text{-F-C}_6\text{H}_4)_3$ (25)	7 h	trace
III-95-3	2	PPh_3 (25)	7 h	trace
III-95-4	3	$\text{P}(4\text{-Me-C}_6\text{H}_4)_3$ (25)	21 h	trace
III-93	4	$\text{P}(4\text{-MeO-C}_6\text{H}_4)_3$ (25)	8 h	trace
III-95-2	5	$\text{P}(2\text{-furyl})_3$ (25)	21 h	5%
III-99-1	6	none	21 h	trace
III-99-2	7	$\text{P}(2\text{-furyl})_3$ (50)	21 h	5%
III-99-3	8	$\text{P}(2\text{-furyl})_3$ (100)	21 h	trace

^aYields were determined by ¹H NMR using 1,3,5-trimethoxybenzene as an internal standard

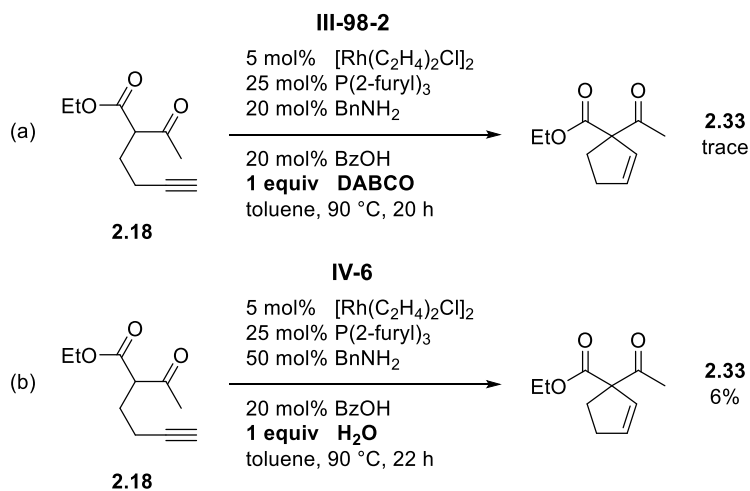
With these preliminary results in hand, the effects of the rhodium/amine equivalent on carbocyclization were investigated (Table 2.6). Increasing the amount of the amine catalyst compared to that of the rhodium catalyst gave higher yields, but the results could not be improved further (Entry 1-4). In the presence of a 2.5 mol% rhodium catalyst, the yields of the desired product did not increase in spite of a longer reaction time (Entry 5-9), suggesting a possibility of an interaction between the rhodium and amine catalysts.

Table 2.6 Rh(I)/amine equivalent screening experiments

Exp. #	Entry	Rh (x)	Amine (y)	Amine/Rh	Time	Yield ^a
III-95-2	1	5	20	2	22 h	5%
III-97-1	2	5	50	5	48 h	22%
III-97-2	3	5	100	10	9 h	15%
III-97-3	4	5	200	20	72 h	24%
IV-4-1	5	2.5	20	4	32 h	5%
IV-4-2	6	2.5	40	8	32 h	8%
IV-4-3	7	2.5	50	10	32 h	9%
IV-4-4	8	2.5	60	12	48 h	8%
IV-4-5	9	2.5	100	20	48 h	13%

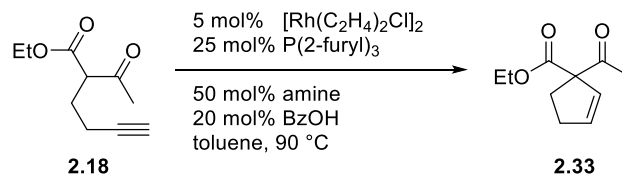
^aYields were determined by ^1H NMR using 1,3,5-trimethoxybenzene as an internal standard

DABCO has been found to be an optimal additive in the stoichiometric carbocyclization of alkylenamines, but the addition of DABCO did not give any improved results (Scheme 2.21a). In addition, a stoichiometric amount of water, added to facilitate the hydrolysis of imine intermediate, brought about decrease in the yield of carbocycle **2.33**, suggesting that hydrolysis of the imine was not a crucial cause of low yields (Scheme 2.21b).



Scheme 2.21 The effects of DABCO and water additives

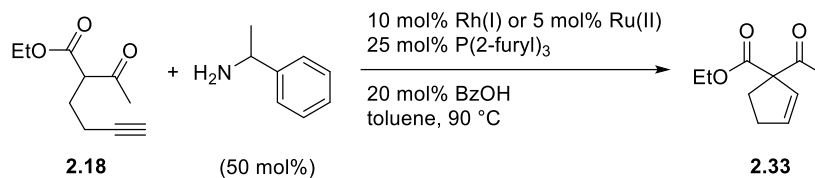
In 2003, the Lautens group suggested a possible poisoning pathway of a rhodium catalyst by a primary amine.²⁰ In their work of rhodium-catalyzed ring opening reactions of oxabicyclic alkenes, a rhodium(I) catalyst decomposed with α -oxidation of amine, giving rise to a rhodium(III) hydride species. To avoid this catalytic dead-end pathway, the screening experiments of the primary amines with various α -substituents were performed (Table 2.7). As a result, α -methyl benzylamine was found to give a slightly better result than benzylamine (Entry 1-2), but a primary amine possessing a tertiary alkyl substituent led to the formation of the product in only 4% probably due to the steric hindrance during the condensation step (Entry 3).

Table 2.7 Primary amine catalyst screening experiments

Exp. #	Entry	Amine	Time	Yield ^a
III-97-1	1		48 h	22%
IV-8	2		41 h	26%
IV-13	3		41 h	4%

^aYields were determined by ^1H NMR using 1,3,5-trimethoxybenzene as an internal standard

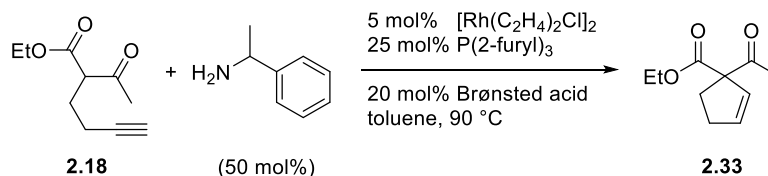
Then we conducted the screening of rhodium(I) and ruthenium(II) precatalysts to identify the effects of anionic ligands attached to a transition metal (Table 2.8). Although $[\text{Rh}(\text{C}_2\text{H}_4)_2\text{Cl}]_2$ was still the best precatalyst, we observed the feasibility of dual-catalytic carbocyclization by using a ruthenium catalyst, the yield comparable to that of the rhodium could be attained only after a prolonged reaction time (Entry 6).

Table 2.8 Rh(I) and Ru(II) precatalyst screening

Exp. #	Entry	Precatalyst	Time	Yield ^a
IV-8	1	$[\text{Rh}(\text{C}_2\text{H}_4)_2\text{Cl}]_2$	41 h	26%
IV-14-1	2	$[\text{Rh}(\text{COD})\text{Cl}]_2$	20 h	20%
IV-14-2	3	$[\text{Rh}(\text{COD})\text{OH}]_2$	41 h	10%
IV-14-3	4	$[\text{Rh}(\text{COD})\text{OMe}]_2$	24 h	11%
IV-16	5	$[\text{Rh}(\text{COD})_2]\text{BF}_4$	18 h	<14%
IV-14-5	6	$\text{CpRu}(\text{PPh}_3)\text{Cl}$	8 d	25%

^aYields were determined by ¹H NMR using 1,3,5-trimethoxybenzene as an internal standard

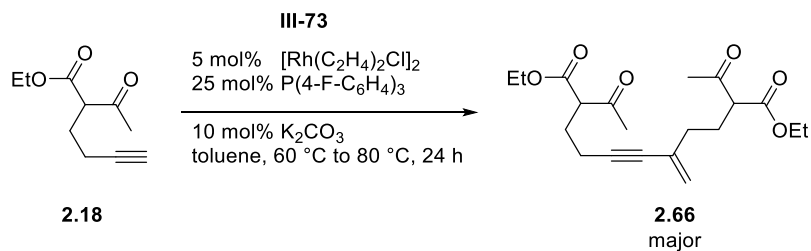
A Brønsted acid catalyst can promote both the condensation and hydrolysis processes. To facilitate these processes effectively, we performed Brønsted acid screening experiments (Table 2.9). However, the reactions using a variety of Brønsted acid with different *pKa* values resulted in the yield similar to those with benzoic acid, also showing that condensation and hydrolysis processes were not critical factors for a high yield.

Table 2.9 Brønsted acid screening results

Exp. #	Entry	Acid	Time	Yield ^a
IV-8	1	BzOH	41 h	26%
IV-14-5	2	none	19 h	15%
IV-15-1	3	4-NO ₂ -BzOH	48 h	4%
IV-15-2	4	AcOH	19 h	24%
IV-15-3	5	<i>p</i> TsOH·H ₂ O	19 h	23%
IV-15-4			8 d	25%

^aYields were determined by ¹H NMR using 1,3,5-trimethoxybenzene as an internal standard

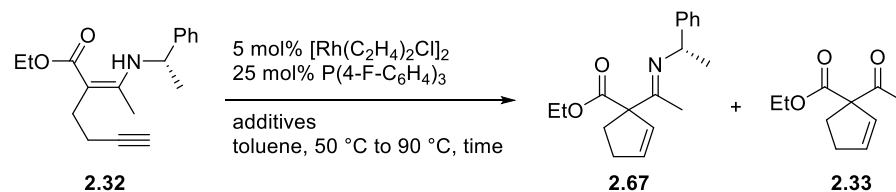
Notwithstanding the extensive screening experiments of metals, amines, acids, and their equivalents, we have not been able to improve the reaction yield, which is lower than the amount of primary amines. One of the major problems is the background reaction of alkynyl β -ketoesters under the rhodium conditions (Scheme 2.22). In the presence of a catalytic amount of rhodium and an inorganic base, we could observe formation of dimer **2.66** as a major product, a major side product during the screening experiments.



Scheme 2.22 Rh(I)-catalyzed dimerization of an alkyne β -ketoester

As already mentioned in table 2.6, there is another possible deleterious factor in the dual-catalytic reaction that the rhodium and amine catalysts can quench their catalytic activity each other. To figure out these undesired interactions between the rhodium and primary amine, we conducted a rhodium-catalyzed carbocyclization of a preformed alkyneamine with primary amine and/or Brønsted acid additives (Table 2.10). As expected, only 20 mol% of a primary amine additive had adverse effects as compared with the original result (Entry 1 vs 2), and so did a Brønsted acid additive (Entry 3). These deleterious effects were even augmented when both the amine and Brønsted acid were put in the flask at the same time (Entry 4). From these results, we concluded that reactivity quenching between the rhodium and amine catalysts was a serious problem in proceeding the desired dual-catalysis.

Table 2.10 The effects of additives on Rh(I)-catalyzed carbocyclization of an alkynylenamine



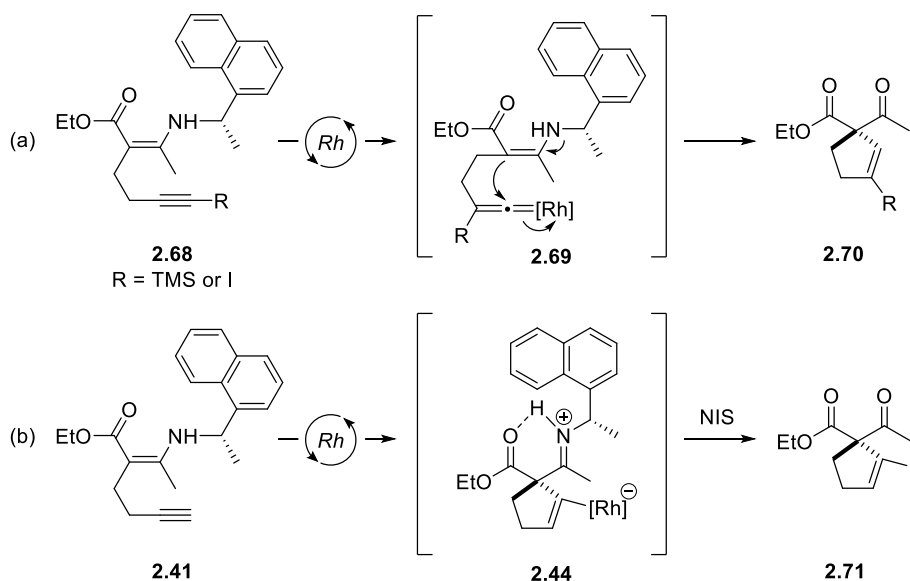
Exp. #	Entry	DABCO (mol %)	$\text{H}_2\text{N-Ph}$ (mol %)	4-NO ₂ -BzOH (mol %)	Time	Conversion	2.67	2.33	Yield ^a
III-61	1	100	0	0	50 °C, 5 h	100%	81%	-	81%
V-53-1	2	100	20	0	90 °C, 5 h ^b	80%	60%	-	60%
V-53-2	3	100	0	20	50 °C, 5 h	90%	66%	-	66%
V-53-3	4	100	20	20	90 °C, 5 h ^b	68%	21%	25%	46%
V-53-4	5	20	0	0	90 °C, 3 h ^b	91%	74%	-	74%
V-53-5	6	0	20	0	90 °C, 5 h ^b	59%	40%	-	40%
V-53-6	7	0	0	20	90 °C, 5 h ^b	60%	-	15%	15%
V-53-7	8	0	20	20	90 °C, 5 h ^b	64%	9%	28%	37%
V-53-8	9	0	100	0	90 °C, 5 h ^b	27%	<26%	-	<26%
V-53-9	10	0	0	100	90 °C, 5 h ^b	81%	-	15%	15%

^aYields were determined by ¹H NMR using 1,3,5-trimethoxybenzene as an internal standard. ^b50 °C for 24 h before warming to 90 °C.

2.3. Conclusion and Future studies

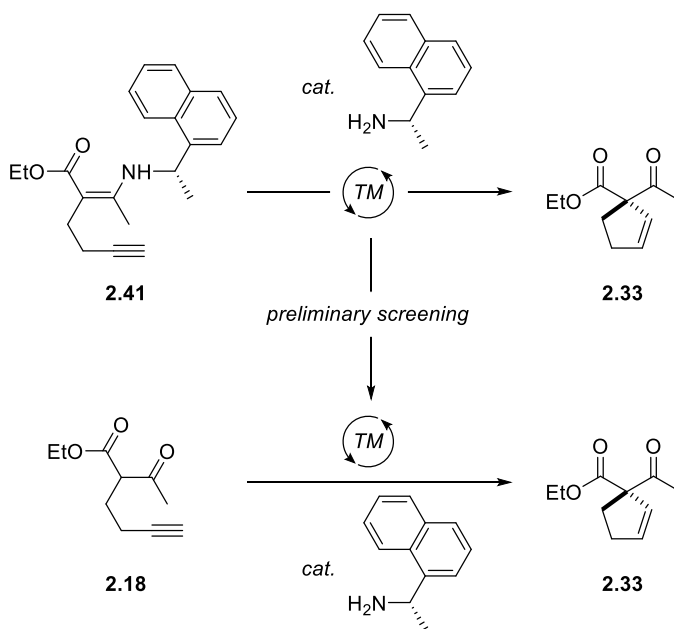
In summary, we have developed the rhodium-catalyzed 5-*endo*-dig carbocyclization of alkynyl enamines. In the presence of a rhodium/triarylphosphine catalyst, *N*-benzyl alkynyl enamines produced 3,3-dicarbonyl cyclopentenones in good yields (Section 2.2.1 and 2.2.2). Furthermore, chiral alkynyl enamines derived from (*S*)-1-(1-naphthyl)ethylamine could induce diastereoselectivity in the cyclizing event, giving rise to the product possessing a quaternary stereogenic center with high enantiopurity (Section 2.2.3). Although we have not obtained the direct evidence of a rhodium vinylidene involved mechanism, the existence of rhodium vinylidene intermediate in this reaction conditions has been confirmed by using oxygenative conditions with picoline-*N*-oxide (Section 2.2.4). Based on these data, we proposed and investigated the rhodium/amine dual-catalytic carbocyclization of alkynyl β -ketoesters. However, we have not been able to induce the turnover of the primary amine catalyst due to the reactivity quenching between rhodium and amine catalysts (Section 2.2.5). Although this work has not been completed, it has not only expanded the scope of the rhodium-catalyzed carbocyclization of alkynyl enamines from the synthesis of azacycles to carbocycles but also achieved asymmetric induction using a chiral auxiliary for the enamine.

Future studies will include further mechanistic studies to prove that the rhodium-catalyzed carbocyclization of alkynylenamine proceeds through a rhodium vinylidene intermediate. Although we already have the indirect evidence for a rhodium vinylidene intermediate by detecting the oxygenated product **2.60**, disubstituted rhodium vinylidene mediated carbocyclizations using silyl- or iodoalkynes can give more straightforward evidence of the mechanism (Scheme 2.23a).²¹ In addition, trapping the alkenyl rhodium intermediate **2.44** not by proton transfer, but by halonium sources can verify exact reaction intermediate (Scheme 2.23b).²²



Scheme 2.23 Further mechanistic studies

For the transition metal/amine dual-catalytic carbocyclization reactions, identification of a transition metal catalyst compatible with primary amines, instead of a rhodium catalyst, should be done. As a preliminary study, we propose a high-throughput screening experiment of various transition metal catalysts on carbocyclization of alkynyl enamine with or without primary amine additive (Scheme 2.24). If a hit shows similar adequate results regardless of primary amine additives, further research can be conducted for the development of a dual-catalytic carbocyclization of alkynyl β -ketoesters.



Scheme 2.24 Further studies for dual catalytic carbocyclization

2.4 Reference

- ¹ For the reviews on transition metal vinylidene mediated catalysis, see: (a) Bruneau, C.; Dixneuf, P. H. *Angew. Chem. Int. Ed.* **2006**, *45*, 2176. (b) Trost, B. M.; McClory, A. *Chem. Asian J.* **2008**, *3*, 164.
- ² Imamura, K.; Yoshikawa, E.; Gevorgyan, V.; Yamamoto, Y. *J. Am. Chem. Soc.* **1998**, *120*, 5339.
- ³ Martínez, A.; García-García, P.; Fernández-Rodríguez, M. A.; Rodríguez, F.; Sanz, R. *Angew. Chem. Int. Ed.* **2010**, *49*, 4633.
- ⁴ (a) Staben, S. T.; Kennedy-Smith, J. J.; Toste, F. D. *Angew. Chem. Int. Ed.* **2004**, *43*, 5350. For iron(III)-catalyzed 5-endo-dig carbocyclizations, see: (b) Chan, L. Y.; Kim, S.; Park, Y.; Lee, P. H. *J. Org. Chem.* **2012**, *77*, 5239.
- ⁵ Corkey, B. K.; Toste, F. D. *J. Am. Chem. Soc.* **2005**, *127*, 17168.
- ⁶ Matsuzawa, A.; Mashiko, T.; Kumagai, N.; Shibasaki, M. *Angew. Chem. Int. Ed.* **2011**, *50*, 7616.
- ⁷ Suzuki, S.; Tokunaga, E.; Reddy, D. S.; Matsumoto, T.; Shiro, M.; Shibata, N. *Angew. Chem. Int. Ed.* **2012**, *51*, 4131.
- ⁸ For the review on the catalytic enantioselective synthesis of quaternary carbon stereocenter, see: Quasdorf, K. W.; Overman, L. E. *Nature* **2014**, *516*, 181.
- ⁹ For the review on the catalytic Markovnikov and *anti*-Markovnikov functionalization of alkenes and alkynes, see: Beller, M.; Seayad, J.; Tillack, A.; Jiao, H. *Angew. Chem. Int. Ed.* **2004**, *43*, 3368.
- ¹⁰ Kim, H.; Lee, C. *J. Am. Chem. Soc.* **2006**, *128*, 6336.
- ¹¹ For the recent example of the construction of alkene-substituted chiral quaternary carbon center by using chiral auxiliary of enamine, see: Picazo, E.; Anthony, S. M.; Giroud, M.; Simon, A.; Miller, M. A.; Houk, K. N.; Garg, N. K. *J. Am. Chem. Soc.* **2018**, *140*, 7605.
- ¹² For the commercially available chiral primary amine, Chipros[®] produced by BASF, see: <http://www.intermediates.basf.com/chemicals/chiral-intermediates/amines>
- ¹³ For the determination of enantiomeric excess, see experimental section.
- ¹⁴ (a) Kim, I.; Lee, C. *Angew. Chem. Int. Ed.* **2013**, *52*, 10023. (b) Kim, I.; Roh, S. W.; Lee, D. G.; Lee, C. *Org. Lett.* **2014**, *16*, 2482.
- ¹⁵ For the review on synergistic catalysis, see: Allen, A. E.; MacMillan, D. W. C. *Chem. Sci.* **2012**, *3*, 633.

- ¹⁶ For the reviews on merging transition metal and organocatalysis, see: (a) Du, Z.; Shao, Z. *Chem. Soc. Rev.* **2013**, *42*, 1337. (b) Deng, Y.; Kumar, S.; Wang, H. *Chem. Commun.* **2014**, *50*, 4272.
- ¹⁷ For the review on the asymmetric enamine catalysis, see: Mukherjee, S.; Yang, J. W.; Hoffmann, S.; List, B. *Chem. Rev.* **2007**, *107*
- ¹⁸ For the rhodium/secondary amine co-catalyzed α -alkenylation of ketones with internal alkynes, see: Mo, F.; Lim, H. N.; Dong, G. *J. Am. Chem. Soc.* **2015**, *137*, 15518.
- ¹⁹ For using the excess amount of phosphine ligand to suppress undesirable processes, see: Trost, B. M.; Rhee, Y. H. *J. Am. Chem. Soc.* **2003**, *125*, 7482.
- ²⁰ Lautens, M.; Fagnou, K.; Yang, D. *J. Am. Chem. Soc.* **2003**, *125*, 14884.
- ²¹ For the silicon migrations, see: (a) Kim, H.; Lee, C. *J. Am. Chem. Soc.* **2005**, *127*, 10180. For the iodine migrations, see: (b) Miura, T.; Iwasawa, N. *J. Am. Chem. Soc.* **2002**, *124*, 518.
- ²² For the trapping of alkenylsilver intermediate by *N*-iodosuccinimide, see: Heinrich, C. F.; Fabre, I.; Miesch, L. *Angew. Chem. Int. Ed.* **2016**, *55*, 5170.

2.5 Experimental section

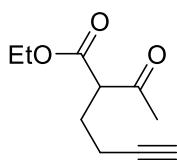
2.5.1 General remarks

All solvents were dried by passing through activated alumina columns. Commercially available reagents were used without further purification. Thin layer chromatography (TLC) was performed using Silicycle 60 F254 plates. TLC plates were visualized by exposure to UV light (254 nm) and/or stained by ceric ammonium molybdate, or potassium permanganate solutions. Flash column chromatography was performed on Silicycle silica gel 60 (40-63 μm) using the indicated solvent system. ^1H and ^{13}C NMR spectra were recorded in CDCl_3 , unless otherwise noted, on an Agilent MR DD2 400 MHz, Oxford AS500 spectrometers. Chemical shifts in ^1H NMR spectra were reported in parts per million (ppm) on the δ scale from an internal standard of residual chloroform (7.26 ppm). Data for ^1H NMR are reported as follows: chemical shift, multiplicity (s = singlet, d = doublet, t = triplet, q = quartet, p = quintet, m = multiplet, br s = broad singlet), coupling constant in Hertz (Hz) and integration. Data for ^{13}C NMR spectra are reported in terms of chemical shift in ppm from the central peak of CDCl_3 (77.0 ppm).

2.5.2 Synthesis and characterization for compounds

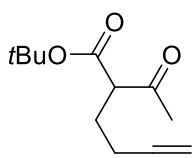
2.5.2.1 General procedure for alkylation of β -ketoesters

β -ketoesters (1.2 equiv) was added dropwise to solution of KI (0.5 equiv) and NaH (1.1 equiv) in THF/DMF (1:1, 0.5 M) at 0 $^\circ\text{C}$. The reaction mixture was stirred for 30 min at room temperature, and 4-bromo-1-alkyne (1 equiv) was added. After stirring at 120 $^\circ\text{C}$ for overnight, the reaction mixture was cooled down to room temperature and washed with 3 N *aq.* HCl three times and brine, then dried over MgSO_4 . After concentration, pure alkynyl β -ketoester was purified by flash column chromatography or distillation with Kugelrohr apparatus.



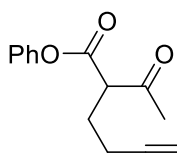
Ethyl 2-acetylhex-5-ynoate (**2.18**)

Clear oil; $^1\text{H NMR}$ (500 MHz, CDCl_3) δ 4.21 (qd, $J = 7.3$, 1.3 Hz, 2H), 3.72 (t, $J = 7.2$ Hz, 1H), 2.28 (s, 3H), 2.27 – 2.23 (m, 2H), 2.10 – 2.05 (m, 2H), 2.00 (t, $J = 2.7$ Hz, 1H), 1.29 (td, $J = 7.1$, 1.1 Hz, 3H); $^{13}\text{C NMR}$ (100 MHz, CDCl_3) δ 202.56, 169.20, 82.51, 69.75, 61.50, 57.83, 29.39, 26.32, 16.28, 14.03.



tert-butyl 2-acetylhex-5-ynoate (**S2.1**)

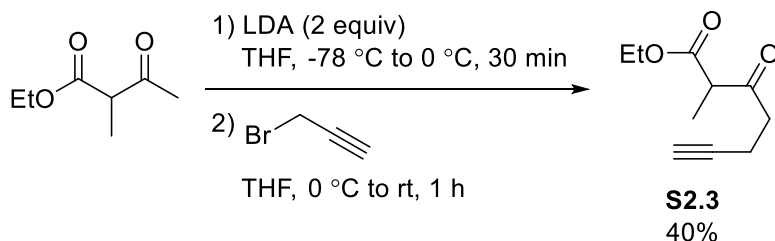
$^1\text{H NMR}$ (500 MHz, CDCl_3) δ 3.61 (t, $J = 7.3$ Hz, 1H), 2.27 (s, 3H), 2.24 (td, $J = 7.1$, 2.5 Hz, 2H), 2.05 – 1.98 (m, 3H), 1.47 (s, 9H); $^{13}\text{C NMR}$ (100 MHz, CDCl_3) δ 202.79, 168.27, 82.63, 82.02, 69.58, 58.85, 29.24, 27.79, 26.27, 16.17.



Phenyl 2-acetylhex-5-ynoate (**S2.2**)

$^1\text{H NMR}$ (500 MHz, CDCl_3) δ 8.04 (dd, $J = 8.4$, 1.3 Hz, 2H), 7.64 – 7.57 (m, 1H), 7.53 – 7.46 (m, 2H), 4.62 (t, $J = 7.0$ Hz, 1H), 4.17 (qd, $J = 7.1$, 2.2 Hz, 2H), 2.41 – 2.28 (m, 2H), 2.27 – 2.19 (m, 2H), 2.04 (t, $J = 2.6$ Hz, 1H), 1.19 (td, $J = 7.1$, 1.5 Hz, 3H).

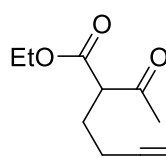
(3-26)



Ethyl 2-methyl-3-oxohept-6-ynoate (**S2.3**)

To a solution of diisopropylamine (2.8 ml, 20 mmol, 2 equiv) in THF (25 ml, 0.4 M) was added *n*-BuLi (1.6 M in *n*-hexane, 12.5 ml, 2 equiv) dropwise at -78 °C. After stirring at 0 °C for 30 min, the reaction mixture was cooled down to -78 °C again. Ethyl 2-methyl-3-oxobutanoate (1.5 ml, 10 mmol, 1 equiv) was added dropwise and the reaction mixture was stirred at 0 °C for 30 min. After the addition of propargyl bromide (1.1 ml, 10 mmol, 1 equiv) in one portion, the reaction mixture was stirred at room temperature for 1 h. The reaction was quenched by the addition of AcOH and water. The organic layer extracted with diethyl ether was washed with brine. After drying over MgSO₄, the desired product was purified by flash column chromatography.

R_f = 0.46 (Hex/EA = 5:1); **¹H NMR (400 MHz, CDCl₃)** δ 4.20 (q, *J* = 7.2 Hz, 2H), 3.53 (q, *J* = 7.2 Hz, 1H), 2.93 – 2.67 (m, 2H), 2.48 (td, *J* = 7.1, 2.6 Hz, 2H), 1.95 (t, *J* = 2.6 Hz, 1H), 1.36 (d, *J* = 7.1 Hz, 3H), 1.28 (t, *J* = 7.1 Hz, 3H).



Ethyl 2-acetylhept-5-ynoate (**S2.5**)

R_f = 0.46 (Hex/EA = 5:1); **¹H NMR (500 MHz, CDCl₃)** δ 4.21 (qd, *J* = 7.1, 1.7 Hz, 2H), 3.69 (t, *J* = 7.2 Hz, 1H), 2.28 (s, 3H), 2.25 – 2.14 (m, 2H), 2.02 (q, *J* = 7.1 Hz, 2H), 1.78 (t, *J* = 2.5 Hz, 3H), 1.29 (t, *J* = 7.1 Hz, 3H).

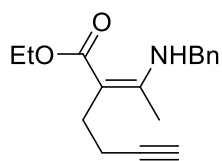
2.5.2.2 General procedure for the alkynylamines

Procedure A

A mixture of alkynyl β -ketoester (1 equiv), primary amine (1.1 equiv), and acetic acid (0.1 equiv) was placed in an ultrasound bath at room temperature for an appropriate time. The reaction was monitored by ^1H NMR, and after the full conversion of the substrate, ethanol was added and the crude solution was dried over NaSO_4 . After concentration, alkynylamine was purified by filtration with short column of basic alumina.

Procedure B

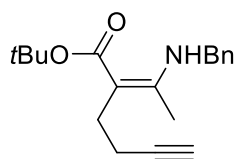
A mixture of alkynyl β -ketoester (1 equiv), primary amine (1.4 equiv), and acetic acid (0.4 equiv) in ethanol was heated to $70\text{ }^\circ\text{C}$ for an appropriate time. The reaction mixture was dried over Na_2SO_4 , and alkynylamine was purified by filtration with short column of basic alumina.



Alkynylamine **2.19**

$R_f = 0.37$ (Hex/EA = 5:1); ^1H NMR (400 MHz, CDCl_3)

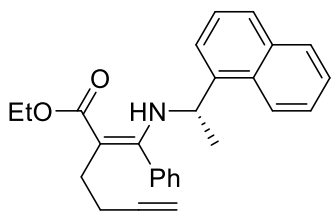
δ 9.81 (s, 1H), 7.40 – 7.31 (m, 2H), 7.31 – 7.21 (m, 3H), 4.45 (dd, $J = 13.0, 5.8$ Hz, 2H), 4.24 – 4.08 (m, 2H), 2.63 – 2.43 (m, 2H), 2.35 – 2.17 (m, 2H), 2.08 – 1.97 (m, 3H), 1.97 – 1.88 (m, 1H), 1.35 – 1.22 (m, 3H); ^{13}C NMR (100 MHz, CDCl_3) δ 170.66, 160.52, 139.08, 128.69, 127.16, 126.68, 91.67, 85.02, 68.13, 58.73, 47.10, 26.77, 19.63, 15.23, 14.61.



Alkynylenamine **2.21**

R_f = 0.56 (Hex/EA = 5:1); **¹H NMR (400 MHz, CDCl₃)**

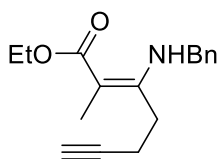
δ 9.73 (s, 1H), 7.34 (dd, J = 11.3, 4.1 Hz, 2H), 7.28 – 7.21 (m, 3H), 4.42 (d, J = 6.3 Hz, 2H), 2.24 (td, J = 7.6, 2.6 Hz, 2H), 1.97 (s, 3H), 1.90 (td, J = 2.6, 1.0 Hz, 1H), 1.48 (s, 9H).



Alkynylenamine **2.23**

R_f = 0.56 (Hex/EA = 5:1); **¹H NMR (400 MHz,**

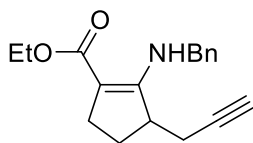
CDCl₃) δ 9.82 (d, J = 8.8 Hz, 1H), 7.79 (d, J = 8.1 Hz, 1H), 7.70 (dd, J = 6.9, 2.1 Hz, 1H), 7.50 – 7.27 (m, 7H), 7.17 (t, J = 7.5 Hz, 1H), 6.80 (t, J = 7.6 Hz, 1H), 6.35 (d, J = 7.7 Hz, 1H), 4.89 – 4.78 (m, 1H), 4.35 – 4.21 (m, 2H), 2.18 – 2.01 (m, 4H), 1.79 (s, 1H), 1.51 (d, J = 6.8 Hz, 3H), 1.36 (t, J = 7.1 Hz, 3H); **¹³C NMR (100 MHz, CDCl₃)** δ 171.01, 162.59, 141.71, 134.72, 133.48, 129.72, 128.61, 128.27, 128.22, 127.99, 127.87, 127.43, 127.14, 125.65, 125.24, 122.92, 121.99, 93.89, 84.96, 67.74, 59.14, 49.86, 27.53, 24.30, 19.69, 14.61.



Alkynylenamine **2.25**

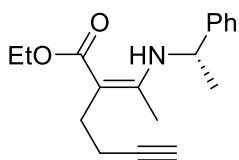
R_f = 0.43 (Hex/EA = 5:1); **¹H NMR (400 MHz, CDCl₃)**

δ 9.54 (s, 1H), 7.33 (dd, J = 9.7, 4.9 Hz, 2H), 7.28 (d, J = 0.4 Hz, 3H), 4.46 (d, J = 6.3 Hz, 2H), 4.13 (q, J = 7.1 Hz, 2H), 2.63 – 2.55 (m, 2H), 2.31 (ddd, J = 10.0, 7.2, 2.7 Hz, 2H), 2.01 (t, J = 2.7 Hz, 1H), 1.83 (s, 3H), 1.28 (t, J = 7.1 Hz, 3H).



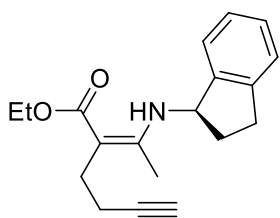
Alkynylenamine **2.29**

$R_f = 0.54$ (Hex/EA = 5:1); $^1\text{H NMR}$ (500 MHz, CDCl_3) δ 7.71 – 7.63 (m, 1H), 7.36 – 7.31 (m, 2H), 7.27 (t, $J = 3.3$ Hz, 3H), 4.44 (d, $J = 6.6$ Hz, 2H), 4.22 – 4.09 (m, 2H), 2.62 – 2.53 (m, 1H), 2.48 (ddd, $J = 14.1, 8.3, 2.3$ Hz, 1H), 2.41 (dt, $J = 17.0, 3.3$ Hz, 1H), 2.24 (ddd, $J = 17.0, 9.9, 2.7$ Hz, 1H), 1.98 (t, $J = 2.7$ Hz, 1H), 1.96 – 1.91 (m, 2H), 1.27 (t, $J = 7.1$ Hz, 3H).



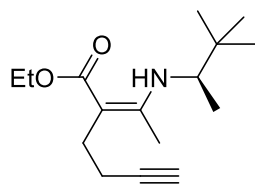
Alkynylenamine **2.32**

$^1\text{H NMR}$ (500 MHz, CDCl_3) δ 9.81 (d, $J = 6.9$ Hz, 1H), 7.37 – 7.31 (m, 2H), 7.27 – 7.20 (m, 3H), 4.66 (p, $J = 6.9$ Hz, 1H), 4.25 – 4.11 (m, 2H), 2.58 – 2.40 (m, 2H), 2.23 (tt, $J = 16.6, 8.5$ Hz, 2H), 1.87 (s, 3+1H), 1.52 (d, $J = 6.8$ Hz, 3H), 1.31 (t, $J = 7.1$ Hz, 3H); $^{13}\text{C NMR}$ (100 MHz, CDCl_3) δ 170.71, 160.17, 145.43, 128.69, 126.89, 125.43, 91.67, 84.97, 68.06, 58.74, 53.20, 26.63, 25.15, 19.57, 15.65, 14.63.



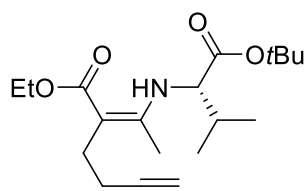
Alkynylenamine **2.35**

$^1\text{H NMR}$ (400 MHz, CDCl_3) δ 9.66 (d, $J = 8.2$ Hz, 1H), 7.34 – 7.27 (m, 1H), 7.24 – 7.16 (m, 3H), 5.05 (q, $J = 7.9$ Hz, 1H), 4.08 (q, $J = 7.1$ Hz, 2H), 3.00 (ddd, $J = 15.8, 8.7, 2.9$ Hz, 1H), 2.91 – 2.77 (m, 1H), 2.61 – 2.52 (m, 3H), 2.34 – 2.25 (m, 2H), 2.22 (s, 3H), 1.96 (t, $J = 2.5$ Hz, 1H), 1.94 – 1.84 (m, 1H), 1.24 (t, $J = 7.1$ Hz, 3H); $^{13}\text{C NMR}$ (100 MHz, CDCl_3) δ 170.52, 159.48, 143.61, 142.77, 127.80, 126.81, 124.73, 123.77, 91.31, 85.18, 68.10, 58.64, 58.49, 35.71, 30.05, 26.90, 19.66, 15.77, 14.61.



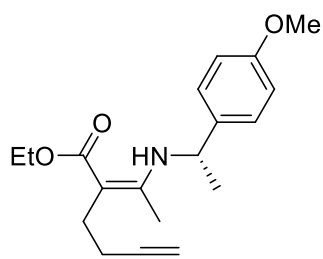
Alkynylenamine **2.36**

¹H NMR (400 MHz, CDCl₃) δ 9.61 (d, *J* = 9.7 Hz, 1H), 4.15 – 4.01 (m, 2H), 3.26 (dq, *J* = 10.1, 6.6 Hz, 1H), 2.47 (t, *J* = 7.5 Hz, 2H), 2.26 – 2.16 (m, 2H), 1.99 (s, 3H), 1.88 (t, *J* = 2.6 Hz, 1H), 1.23 (t, *J* = 7.1 Hz, 3H), 1.06 (d, *J* = 6.6 Hz, 3H), 0.90 (s, 9H); **¹³C NMR (100 MHz, CDCl₃)** δ 170.66, 160.11, 89.65, 85.21, 67.92, 58.45, 57.42, 35.00, 26.86, 26.32, 19.72, 17.42, 15.13, 14.64.



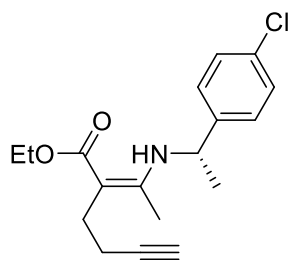
Alkynylenamine **2.37**

¹H NMR (400 MHz, CDCl₃) δ 9.66 (d, *J* = 8.9 Hz, 1H), 4.19 – 4.10 (m, 2H), 3.82 (dd, *J* = 9.0, 5.4 Hz, 1H), 2.51 (t, *J* = 7.6 Hz, 2H), 2.25 (ddd, *J* = 8.0, 7.5, 3.9 Hz, 2H), 2.16 (td, *J* = 13.6, 6.9 Hz, 1H), 1.96 (s, 3H), 1.94 – 1.90 (m, 1H), 1.46 (s, 9H), 1.26 (td, *J* = 6.9, 2.9 Hz, 3H), 1.02 (dd, *J* = 6.9, 3.3 Hz, 6H); **¹³C NMR (100 MHz, CDCl₃)** δ 171.29, 170.39, 159.15, 92.68, 85.01, 81.47, 68.01, 62.54, 58.73, 31.68, 27.94, 26.95, 19.53, 19.16, 18.05, 15.32, 14.55.



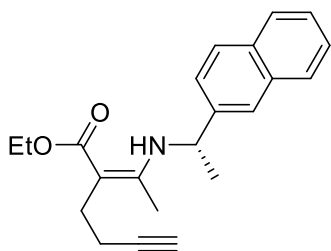
Alkynylenamine **2.38**

¹H NMR (400 MHz, CDCl₃) δ 9.75 (d, *J* = 7.2 Hz, 1H), 7.13 (d, *J* = 8.7 Hz, 2H), 6.82 (d, *J* = 8.7 Hz, 2H), 4.58 (p, *J* = 6.8 Hz, 1H), 4.22 – 4.04 (m, 2H), 3.75 (s, 3H), 2.54 – 2.36 (m, 2H), 2.19 (td, *J* = 7.4, 2.6 Hz, 2H), 1.84 (s, 3+1H), 1.45 (d, *J* = 6.8 Hz, 3H), 1.26 (t, *J* = 7.1 Hz, 3H); **¹³C NMR (100 MHz, CDCl₃)** δ 170.68, 160.21, 158.45, 137.52, 126.50, 114.02, 91.50, 84.98, 68.07, 58.70, 55.20, 52.59, 26.63, 25.24, 19.58, 15.59, 14.64.



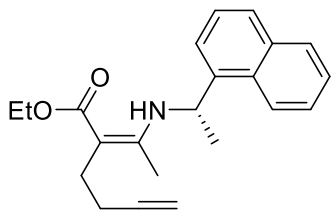
Alkynylenamine **2.39**

¹H NMR (400 MHz, CDCl₃) δ 9.77 (d, *J* = 7.1 Hz, 1H), 7.32 – 7.27 (m, 2H), 7.20 – 7.14 (m, 2H), 4.63 (p, *J* = 6.9 Hz, 1H), 4.23 – 4.10 (m, 2H), 2.56 – 2.37 (m, 2H), 2.22 (td, *J* = 7.3, 2.6 Hz, 2H), 1.86 (t, *J* = 2.6 Hz, 1H), 1.84 (s, 3H), 1.48 (d, *J* = 6.8 Hz, 3H), 1.29 (dd, *J* = 10.5, 3.7 Hz, 3H); **¹³C NMR (100 MHz, CDCl₃)** δ 170.73, 159.83, 144.03, 132.58, 128.85, 126.85, 92.15, 84.88, 68.12, 58.83, 52.62, 26.55, 25.04, 19.53, 15.66, 14.60.



Alkynylenamine **2.40**

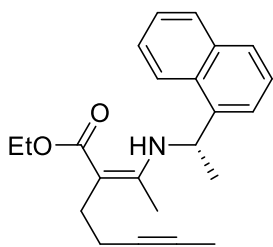
¹H NMR (400 MHz, CDCl₃) δ 9.91 (d, *J* = 7.0 Hz, 1H), 7.84 – 7.76 (m, 3H), 7.67 (s, 1H), 7.50 – 7.39 (m, 2H), 7.37 (dd, *J* = 8.5, 1.8 Hz, 1H), 4.80 (p, *J* = 6.8 Hz, 1H), 4.26 – 4.11 (m, 2H), 2.56 – 2.38 (m, 2H), 2.28 – 2.17 (m, 2H), 1.87 (s, 3H), 1.83 (t, *J* = 2.6 Hz, 1H), 1.58 (d, *J* = 6.8 Hz, 3H), 1.31 (t, *J* = 7.1 Hz, 3H); **¹³C NMR (100 MHz, CDCl₃)** δ 170.80, 160.28, 142.97, 133.46, 132.59, 128.64, 127.81, 127.65, 126.19, 125.70, 123.97, 123.85, 91.81, 84.95, 68.17, 58.81, 53.37, 26.61, 25.06, 19.59, 15.78, 14.69.



Alkynylenamine **2.41**

¹H NMR (400 MHz, CDCl₃) δ 9.98 (d, *J* = 6.5 Hz, 1H), 8.05 (d, *J* = 8.4 Hz, 1H), 7.89 (d, *J* = 8.0 Hz, 1H), 7.75 (dd, *J* = 6.4, 2.7 Hz, 1H), 7.59 – 7.48 (m, 2H), 7.45 (ddd, *J* = 5.2, 4.3, 1.4 Hz, 2H), 5.46 (p, *J* = 6.8 Hz, 1H), 4.32 – 4.14 (m, 2H), 2.66 – 2.33 (m, 2H), 2.24 (dt, *J* = 8.1, 4.0 Hz, 2H), 1.87

– 1.82 (m, 1H), 1.79 (s, 3H), 1.65 (d, $J = 6.7$ Hz, 3H), 1.33 (td, $J = 7.1$, 1.6 Hz, 3H); ^{13}C NMR (100 MHz, CDCl_3) δ 170.83, 160.24, 141.06, 133.84, 129.85, 129.12, 127.45, 126.26, 125.92, 125.56, 122.51, 122.03, 92.06, 84.94, 68.18, 58.83, 49.32, 26.63, 23.98, 19.62, 15.60, 14.69

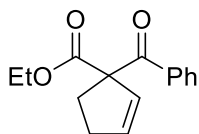


Alkynylamine **2.61**

^1H NMR (400 MHz, CDCl_3) δ 9.97 (d, $J = 6.8$ Hz, 1H), 8.05 (d, $J = 8.4$ Hz, 1H), 7.88 (d, $J = 8.0$ Hz, 1H), 7.74 (t, $J = 4.7$ Hz, 1H), 7.52 (dt, $J = 14.5$, 6.9 Hz, 2H), 7.45 (d, $J = 4.7$ Hz, 2H), 5.45 (p, $J = 6.7$ Hz, 1H), 4.27 – 4.14 (m, 2H), 2.51 – 2.34 (m, 2H), 2.17 (dt, $J = 9.1$, 4.5 Hz, 2H), 1.78 (s, 3H), 1.68 – 1.61 (m, 3+3H), 1.32 (t, $J = 7.1$ Hz, 3H); ^{13}C NMR (100 MHz, CDCl_3) δ 170.95, 160.08, 141.16, 133.83, 129.85, 129.11, 127.38, 126.22, 125.96, 125.54, 122.45, 122.04, 92.42, 79.59, 75.36, 58.77, 49.29, 27.08, 24.00, 19.92, 15.44, 14.69, 3.44.

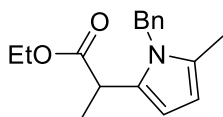
2.5.2.3 General procedure for the rhodium-catalyzed carbocyclization of alkynylamines

A mixture of $[\text{Rh}(\text{C}_2\text{H}_4)_2\text{Cl}]_2$ (0.015 mmol, 5 mol%), $\text{P}(4\text{-F-C}_6\text{H}_4)_3$ (0.075 mmol, 25 mol%), and DABCO (0.3 mmol, 1 equiv) in toluene was stirred for 10 min at room temperature under the argon atmosphere. To the solution was added alkynylamine and the reaction mixture was heated to 50 °C or 90 °C. The reaction was monitored by TLC and after an appropriate time, the solvent was evaporated *in vacuo*. The residue was dissolved in 1 N *aq.*HCl/THF (1:1) and stirred for 1 h. The organic layer was extracted four times with diethyl ether, and then washed with water, 3 N *aq.*HCl, and brine. After the drying by Na_2SO_4 and concentration, desired product was purified by flash column chromatography.



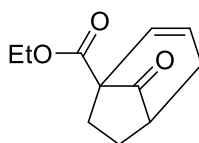
Ethyl 1-benzoylcyclopent-2-ene-1-carboxylate (**2.24**)

¹H NMR (400 MHz, CDCl₃) δ 7.89 (d, *J* = 7.8 Hz, 2H), 7.52 (t, *J* = 7.4 Hz, 1H), 7.42 (t, *J* = 7.7 Hz, 2H), 6.03 (dt, *J* = 5.0, 2.1 Hz, 1H), 5.93 (dt, *J* = 5.5, 2.0 Hz, 1H), 4.08 (q, *J* = 7.1 Hz, 2H), 2.74 (dt, *J* = 16.1, 6.1 Hz, 1H), 2.67 – 2.38 (m, 3H), 1.02 (t, *J* = 7.1 Hz, 3H); **¹³C NMR (100 MHz, CDCl₃)** δ 195.69, 172.63, 135.75, 135.15, 132.91, 129.66, 128.76, 128.50, 70.89, 61.52, 32.25, 31.88, 13.75.



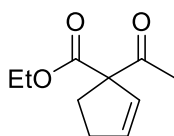
Ethyl 2-(1-benzyl-5-methyl-1*H*-pyrrol-2-yl)propanoate (**2.27**)

R_f = 0.59 (Hex/EA = 5:1); **¹H NMR (400 MHz, CDCl₃)** δ 7.28 (t, *J* = 7.6 Hz, 2H), 7.22 (d, *J* = 7.2 Hz, 1H), 6.83 (d, *J* = 8.1 Hz, 2H), 6.07 (d, *J* = 3.4 Hz, 1H), 5.93 (d, *J* = 3.4 Hz, 1H), 5.12 (q, *J* = 17.4 Hz, 2H), 4.04 – 3.81 (m, 2H), 3.59 (q, *J* = 7.1 Hz, 1H), 2.12 (s, 3H), 1.43 (dd, *J* = 7.2, 1.0 Hz, 3H), 1.12 (td, *J* = 7.1, 1.1 Hz, 3H); **¹³C NMR (100 MHz, CDCl₃)** δ 173.82, 138.35, 130.85, 129.09, 128.61, 126.99, 125.44, 106.21, 105.36, 60.71, 46.64, 37.68, 17.31, 13.97, 12.38.



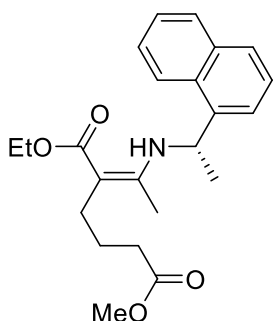
Ethyl 8-oxobicyclo[3.2.1]oct-2-ene-1-carboxylate (**2.30**)

R_f = 0.38 (Hex/EA = 5:1); **¹H NMR (500 MHz, CDCl₃)** δ 6.10 (dd, *J* = 9.4, 2.1 Hz, 1H), 5.66 (ddd, *J* = 9.2, 4.5, 1.8 Hz, 1H), 4.30 – 4.19 (m, 2H), 2.95 (d, *J* = 17.5 Hz, 1H), 2.66 – 2.53 (m, 2H), 2.51 (s, 1H), 2.42 – 2.32 (m, 1H), 2.28 – 2.19 (m, 1H), 1.83 – 1.75 (m, 1H), 1.30 (t, *J* = 7.1 Hz, 3H).



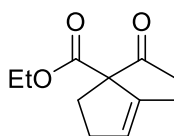
Ethyl 1-acetylcyclopent-2-ene-1-carboxylate (**2.33**)

$R_f = 0.48$ (Hex/EA = 5:1); $^1\text{H NMR}$ (500 MHz, CDCl_3) δ 6.02 (dt, $J = 5.6, 2.2$ Hz, 1H), 5.86 (dt, $J = 5.6, 2.1$ Hz, 1H), 4.27 – 4.13 (m, 2H), 2.55 – 2.31 (m, 4H), 2.19 (s, 3H), 1.27 (t, $J = 7.1$ Hz, 3H); $^{13}\text{C NMR}$ (100 MHz, CDCl_3) δ 203.79, 171.76, 136.25, 128.70, 73.55, 61.42, 31.89, 30.00, 26.40, 14.01.



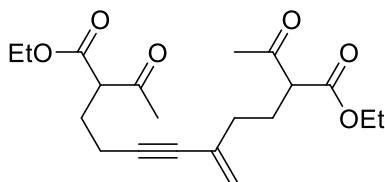
Enecarbamate **2.60**

$^1\text{H NMR}$ (400 MHz, CDCl_3 , proposed, selected peaks) δ 9.88 (d, $J = 6.9$ Hz, 1H, NH), 5.40 – 5.33 (m, 1H, NCH), 3.63 (s, 3H, OCH₃), 1.96 (t, $J = 2.1$ Hz, 2H, CH₂CO₂Me).



Ethyl 1-acetyl-2-methylcyclopent-2-ene-1-carboxylate (**2.62**)

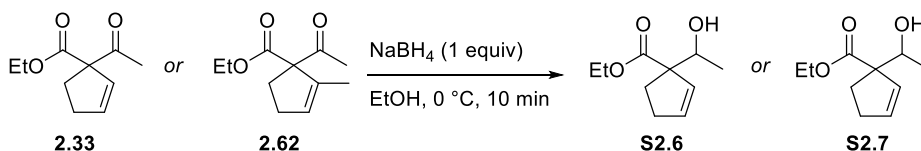
$^1\text{H NMR}$ (400 MHz, CDCl_3) δ 5.70 (dt, $J = 4.6, 1.9$ Hz, 1H), 4.23 (qd, $J = 7.1, 3.0$ Hz, 2H), 2.63 (dddd, $J = 13.8, 8.5, 5.3, 3.0$ Hz, 1H), 2.50 – 2.27 (m, 2H), 2.27 – 2.19 (m, 1H), 2.18 (d, $J = 3.0$ Hz, 3H), 1.87 – 1.80 (m, 3H), 1.29 (td, $J = 7.1, 3.0$ Hz, 3H).



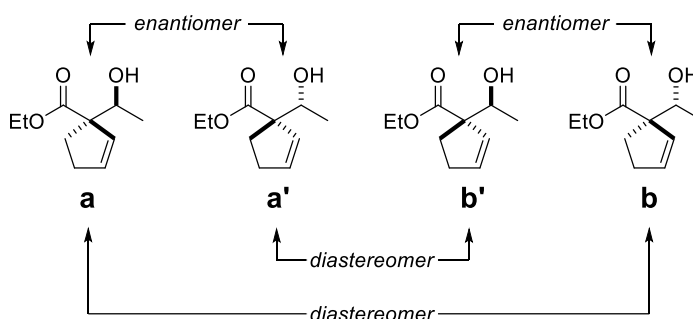
Dimer **2.66**

$^1\text{H NMR}$ (400 MHz, CDCl_3) δ 5.28 (d, $J = 11.8$ Hz, 2H), 4.30 – 4.12 (m, 8H), 3.68 (t, $J = 7.7$ Hz, 1H), 3.57 (t, $J = 7.7$ Hz, 1H), 2.90 (d, $J = 7.7$ Hz, 2H), 2.70 (d, $J = 7.7$ Hz, 2H), 1.28 (td, $J = 7.2$ Hz, 12H).

2.5.3 Determination of the enantiomeric excess



To a solution of carbocycle in ethanol was added NaBH_4 (1 equiv) at $0\text{ }^\circ\text{C}$, then the reaction mixture was stirred for 10 min. After the addition of $\text{aq. NH}_4\text{Cl}$, the organic layer was extracted three times with EA. The resulting organic layer washed with brine and dried over Na_2SO_4 . After the concentration, the secondary alcohol was purified by flash column chromatography and its enantiomeric excess was determined by following chiral HPLC analysis.



Scheme 2.25 Stereoisomerism of **S2.6**

In the chiral chromatographic traces of **S2.6** derived from racemic **2.33**, the integrated area of one single peak (A_a) is same as in one of the overlapped peaks ($A_{a'}$) because the reduction of **2.33** with sodium borohydride isn't enantioselective reaction (Figure 2.2). From this chemical hypothesis, the diastereomeric ratio of this reduction process could be determined as following calculation.

$$A_a = 1367.6 \quad A_{a'} + A_b + A_{b'} = 4490.1$$

$$dr = A_a + A_{a'} : A_b + A_{b'} = 2735.2 : 3122.5 = 1 : 1.1416$$

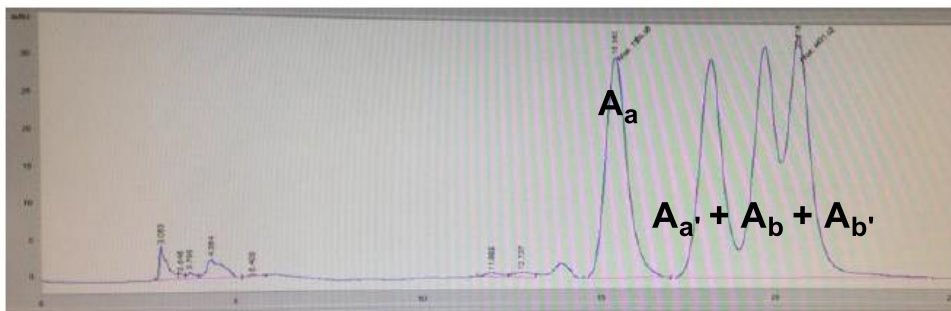


Figure 2.2 Chromatographic traces of **S2.6** from racemic **2.33**

Using the diastereomeric ratio, the enantiomeric excess of **2.33** could be determined by chiral HPLC analysis of reduced secondary alcohol **S2.6**.

$$A_a = 199.2 \quad A_{a'} + A_b + A_{b'} = 6659.9$$

$$A_b = 1.1416A_a \quad A_{b'} = 1.1416A_{a'}$$

$$A_{a'} = \frac{6659.9 - 1.1416A_a}{2.1416} = 3003.6$$

$$ee = 100 \times \frac{A_a - A_{a'}}{A_a + A_{a'}} = 100 \times \frac{2804.4}{3202.8} = 88\%$$

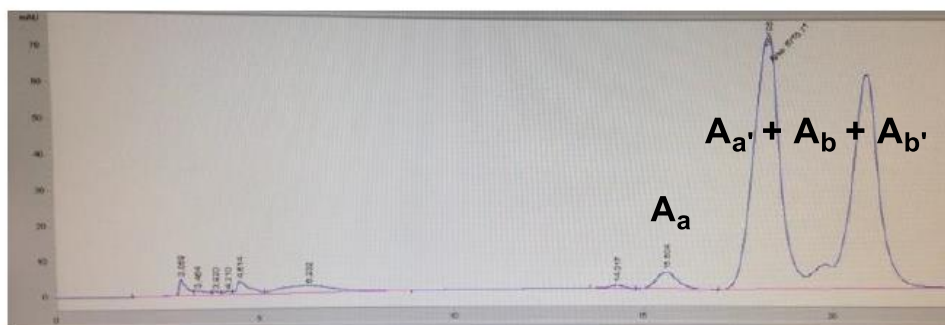
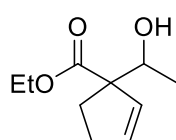


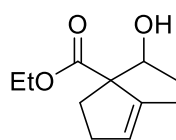
Figure 2.3 Chromatographic traces of **S2.6** from chiral **2.33**



Ethyl 1-(1-hydroxyethyl)cyclopent-2-ene-1-carboxylate

(**S2.6**, diastereomeric mixture, $dr=1.1416:1$)

$R_f = 0.31, 0.25$ (Hex/EA = 5:1); $^1\text{H NMR}$ (500 MHz, CDCl_3) δ 5.97 (ddt, $J = 13.0, 5.6, 2.3$ Hz, 1H), 5.68 (ddt, $J = 12.7, 5.6, 2.2$ Hz, 1H), 4.22 – 4.12 (m, 2H), 4.05 – 3.95 (m, 1H), 2.62 – 2.34 (m, 2+1H), 2.32 – 2.18 (m, 1H), 2.04 (dddd, $J = 19.1, 14.4, 8.9, 5.3$ Hz, 1H), 1.27 (td, $J = 7.1, 1.2$ Hz, 3H), 1.13 (dd, $J = 6.4, 5.0$ Hz, 3H); **Chiral HPLC**: Chiralpak IA, 1.0 ml/min, Hex/*i*PA=99:1, 15.4 min (first diastereomer), 18.1, 19.6, 20.5 min (the other diastereomers).



Ethyl 1-(1-hydroxyethyl)-2-methylcyclopent-2-ene-1-carboxylate

(**S2.7**, diastereomeric mixture, $dr=4.4505:1$, major)

$^1\text{H NMR}$ (400 MHz, CDCl_3) δ 5.65 (d, $J = 1.4$ Hz, 1H), 4.39 – 4.26 (m, 1H), 4.23 – 4.07 (m, 2H), 2.49 – 2.14 (m, 3H), 2.09 (s, 1H), 1.94 (ddd, $J = 16.8, 10.2, 5.1$ Hz, 1H), 1.78 (dd, $J = 3.5, 2.0$ Hz, 3H), 1.26 (t, $J = 7.1$ Hz, 3H), 1.12 (d, $J = 6.3$ Hz, 3H); **Chiral HPLC**: Chiralpak IA, 1.0 ml/min, Hex/*i*PA=99:1, 11.3, 12.2 min (three diastereomers), 14.2 min (the other diastereomer).

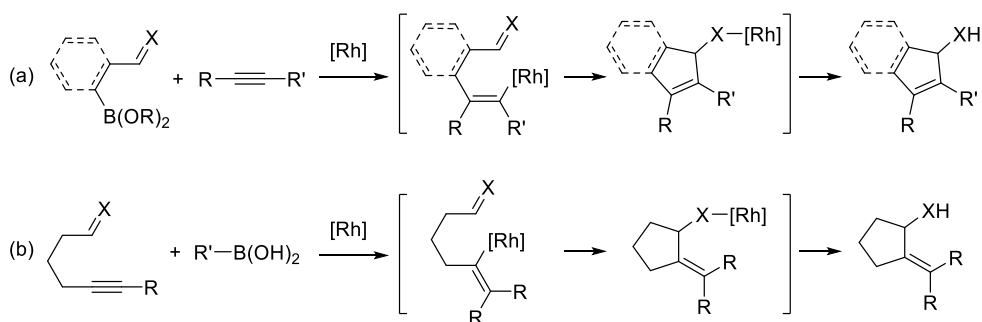
Chapter 3. Rhodium-Catalyzed Tandem Addition– Cyclization Reactions of Alkynes with Organoborons

3.1 Introduction

The rhodium-catalyzed tandem addition–cyclization of alkynes with organoboron reagents has been a powerful method for the synthesis of carbo- and heterocyclic compounds.¹ By employing a single rhodium catalyst with organoboron compounds, sequential inter- and intramolecular C–C bond formation are mediated in tandem. Practically, these cascade cyclization reactions have been known to follow three fundamental mechanistic steps: 1) transmetalation from organoboron to rhodium, 2) *syn*-carbometallation of organorhodium species to the alkyne, and then 3) nucleophilic addition or migratory insertion of alkenyl rhodium intermediate to another π -bond.

With its inherent high synthetic efficiency for the synthesis of cyclic compounds, a number of methodologies have been developed. In the reaction pathways as described in Scheme 3.1, there are two distinct types of tandem cyclization, depending on how alkyne, organoboron, and another π -bond are linked. Firstly, reactions can occur between organoboron compounds tethered with active π -bond and external alkyne substrates, giving rise to endocyclic alkene products (Scheme 3.1a). On the other hand, the external organoboron

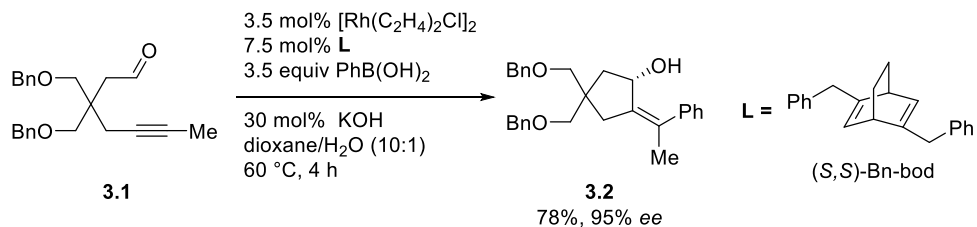
compounds could bring carbon functionalities to the enyne substrates, which finally give alkylidene-substituted cyclic products (Scheme 3.1b). This chapter will focus on the latter cases with emphasis placed on the π -bonds, rather than the alkyne or organoboron moieties.



Scheme 3.1 Types of Rh(I)-catalyzed tandem addition–cyclization reactions

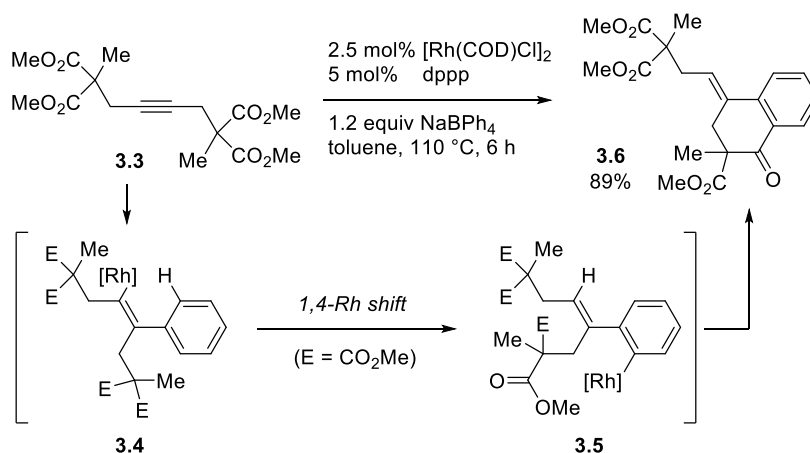
3.2 Tandem addition–cyclization with unsaturated carbon–heteroatom bonds

Early examples of tandem addition–cyclization reactions have used unsaturated carbon–heteroatom bonds tethered with alkynes as a substrate. As illustrated in Scheme 3.2, arylative carbocyclization of alkynyl aldehyde **3.1** could be feasible by a rhodium catalyst and arylboronic acids.² Furthermore, asymmetric induction which gives the chiral allylic alcohol **3.2** has been achieved with a chiral diene ligand.



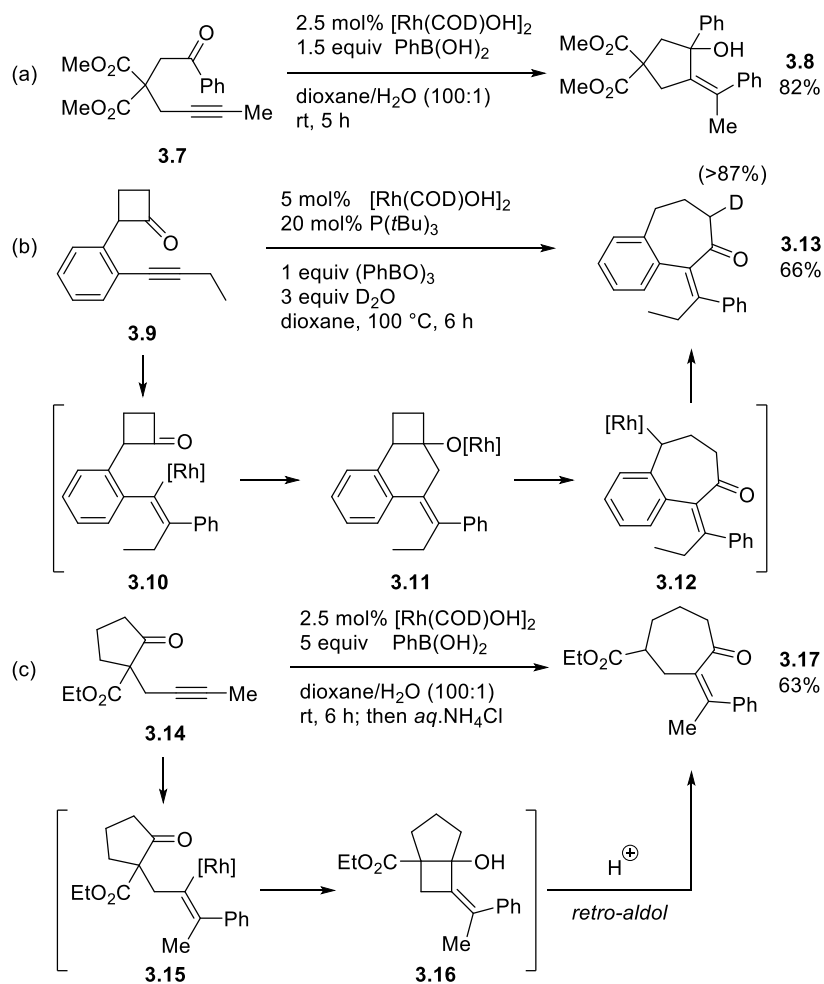
Scheme 3.2 Rh(I)-catalyzed asymmetric arylation of an alkyne

An alkenyl rhodium intermediate could induce the nucleophilic substitution reaction to the ester. Under the catalysis of rhodium/phosphine complex, symmetrical alkynyl ester **3.3** was converted to α -tetralone derivative **3.6** in good yield (Scheme 3.3).³ It was proposed that nucleophilic substitution occurred from aryl rhodium intermediate **3.5**, which derived from alkenyl rhodium **3.4** *via* 1,4-rhodium shift.⁴ Although highly anhydrous conditions and higher temperatures were required to prohibit protodemetalation of organorhodium species, this work verified the reactivity of ester groups in tandem addition–cyclization reactions.



Scheme 3.3 Rh(I)-catalyzed arylation of an alkynyl ester

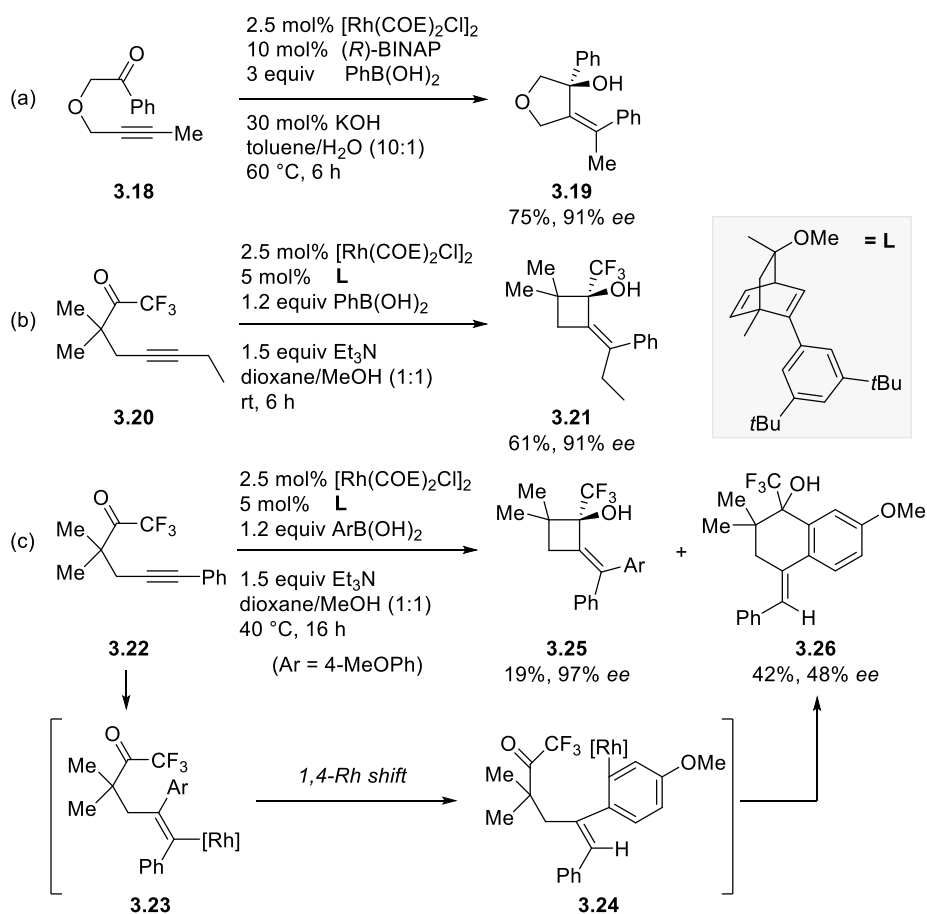
A rhodium-catalyzed tandem addition–cyclization reactions could be applied for the synthesis of tertiary allylic alcohols from alkyne-tethered ketones at room temperature (Scheme 3.4a).⁵ In addition to simple addition–cyclization, several alkynyl ketone substrates could induce further ring-expansion reactions. As depicted in Scheme 3.4b, the aryl alkyne-substituted cyclobutanone **3.9** was converted to 7-membered ring ketone **3.13** under similar rhodium-catalyzed conditions.⁶ With assistance from ring strain of 4-membered ring, 4/6-fused tertiary alkoxide **3.11** brought about ring-expansion to give **3.12**, which underwent protodemetalation of a rhodium enolate. In addition to cyclobutanones, β -carbonyl groups attached to ketones also led to similar ring-expansion cascades by retro-aldol process (Scheme 3.4c).⁷ When propargyl β -ketoester **3.14** was exposed to the rhodium catalyst and phenylboronic acid, cycloheptanone **3.17** was obtained in moderate yield after the acidic treatment of tandem cyclized intermediate **3.16**.



Scheme 3.4 Rh(I)-catalyzed tandem addition–cyclization of alkynyl ketones

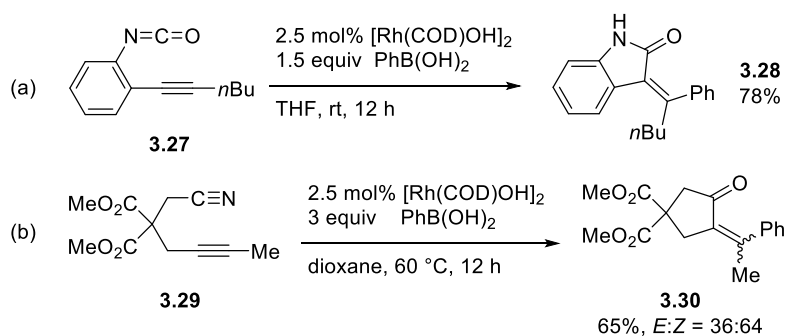
A stereogenic center of tertiary allylic alcohols has been controlled by a rhodium catalyst with chiral ligands. In 2014, a range of rhodium-catalyzed tandem addition–cyclization reactions were reported for the enantioselective synthesis of both hetero- and carbocycles (Scheme 3.5). The reaction using chiral BINAP as a ligand for the rhodium catalyst provided chiral tetrahydrofuran **3.19** or pyrrolidine products from oxygen- or nitrogen-

tethered alkynyl ketones (Scheme 3.5a).⁸ The length of carbon tether could be modulated as shown in the synthesis of cyclobutanol (Scheme 3.5b).⁹ Interestingly, when arylalkyne-tethered ketone **3.22** was used as a substrate, the 6-membered ring alcohol **3.26** was formed as the major product through the aryl rhodium intermediate **3.24** derived from *syn*-carbometalation with reversed regioselectivity followed by 1,4-Rh shift (Scheme 3.5c).



Scheme 3.5 Rh(I)-catalyzed enantioselective tandem addition–cyclization of alkynyl ketones

The *sp*-carbon of carbon–heteroatom bonds has participated in the rhodium-catalyzed tandem addition–cyclization reactions. In the rhodium-catalyzed arylyative cyclization reaction, alkynyl isocyanate **3.27** gave oxindole **3.28** in good yield (Scheme 3.6a).¹⁰ Furthermore, the first example of using unsaturated carbon–nitrogen bond in the rhodium-catalyzed tandem cyclization was reported in 2005 (Scheme 3.6b).¹¹ Under rhodium catalysis, alkynyl nitrile **3.29** afforded 2-alkylidene cyclopentanone **3.30** as a mixture of alkene isomers.

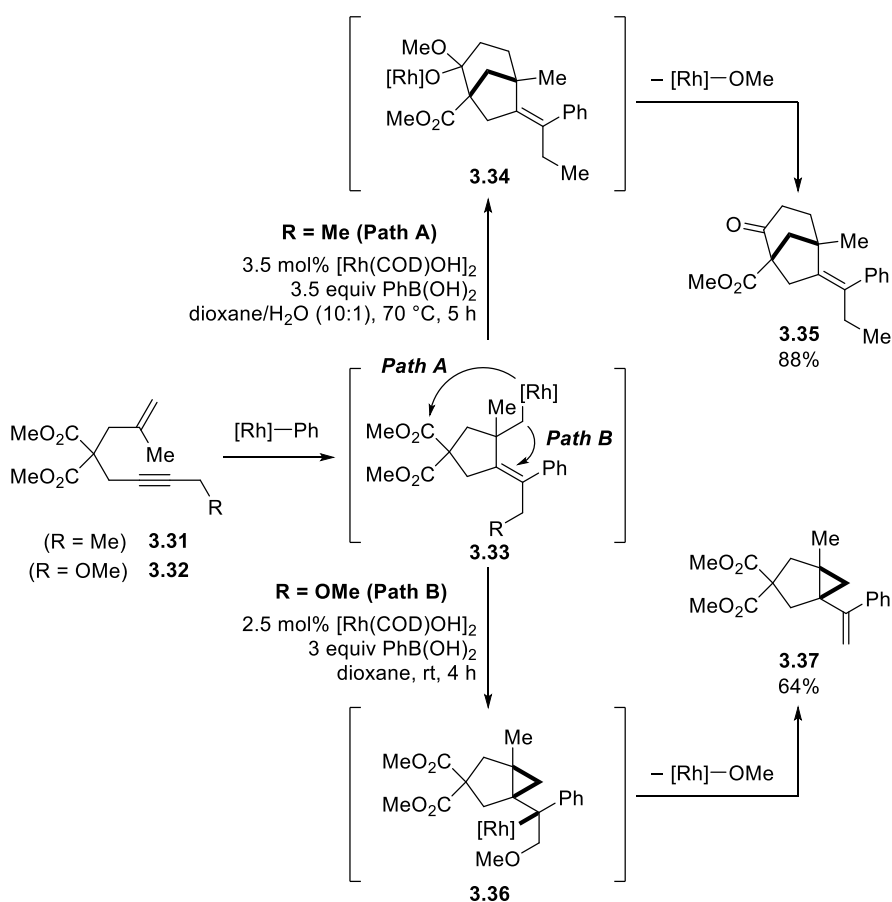


Scheme 3.6 Rh(I)-catalyzed arylyative cyclization of an alkynyl isocyanate and an alkynyl nitrile.

3.3 Tandem addition–cyclization with unsaturated carbon–carbon bonds

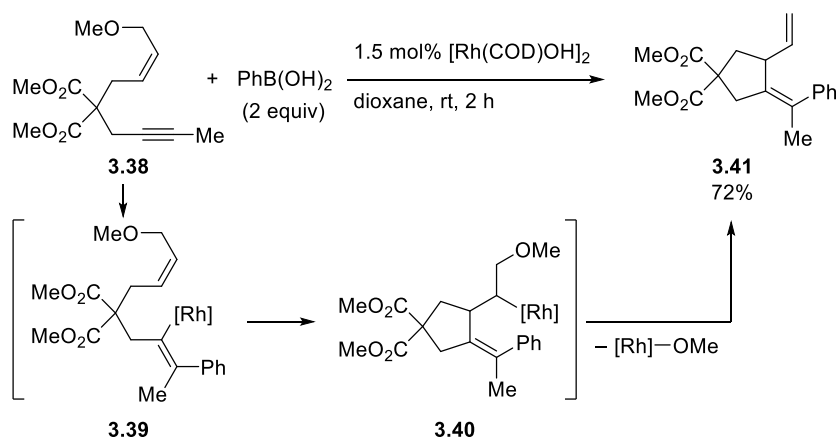
The alkenes have been used as acceptors in rhodium-catalyzed cyclization cascades. In contrast with unsaturated carbon–heteroatom bonds where the rhodium catalyst was regenerated by protonation, less polarized alkenes require an additional functional group to make the rhodium

commence catalysis again. As described in Scheme 3.7, 1,6-enynes showed distinct mechanistic pathways giving rise to different bicyclic carbocycles. When 1,6-enyne **3.31** was subject to the rhodium-catalyzed conditions, alkyl rhodium intermediate **3.33** brought about additional ring closure to the ester to give the bridged bicycle **3.35** (Path A).^{2,3} On the other hand, similar 1,6-enyne **3.32**, containing a methoxymethyl group, underwent addition–cyclization followed by *syn*-carbomatalation into the alkene affording cyclopropane-fused bicycle **3.37** (Path B).¹²



Scheme 3.7 Rh(I)-catalyzed arylative cyclization of 1,6-enynes

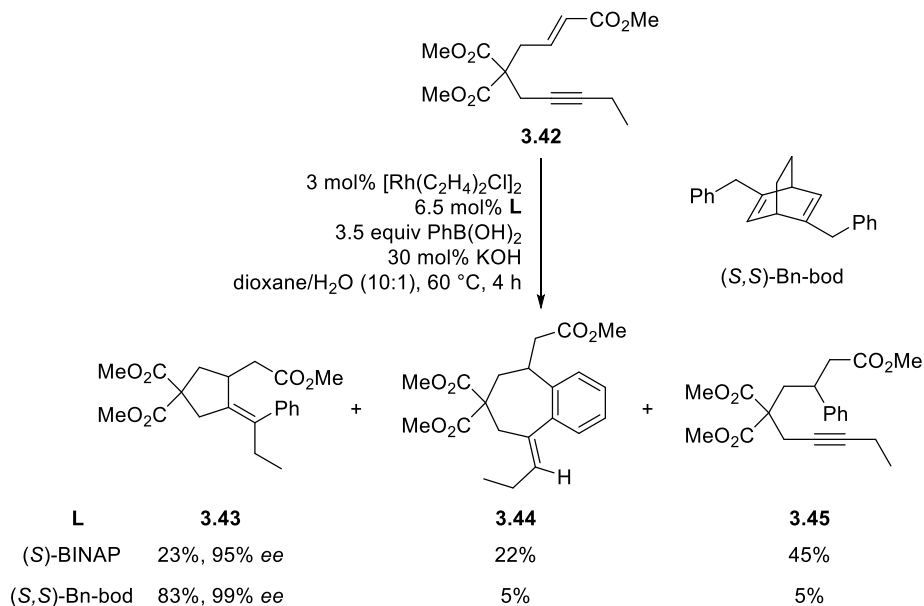
The turnover of the rhodium catalyst by β -alkoxy elimination could be applied to alkyne-tethered allyl ether **3.38** (Scheme 3.8).¹³ In the proposed mechanism, the aryl rhodium complex mediated sequential migratory insertion into alkyne and alkene moieties, giving carbocycle **3.41** in moderate yield. Besides, the authors observed that simple hydroarylation of an alkyne substrate with no tethered alkene was hard to take place (10%), suggesting that intramolecular coordination of the alkene to the rhodium center could facilitate the initial carbometalation of the alkyne.



Scheme 3.8 Rh(I)-catalyzed arylative cyclization of an alkyne allyl ether

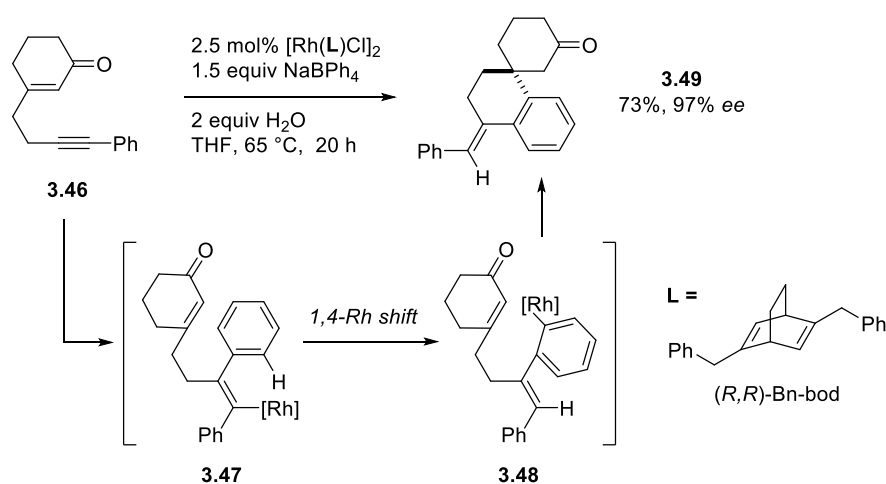
α,β -Unsaturated carbonyl derivatives have been used as substrates for the rhodium-catalyzed 1,4-addition reactions.¹⁴ However, when these systems were tethered with alkynes, the reactivity difference between the

alkyne and the α,β -unsaturated carbonyl group brought about distinct carbocyclization reactions. In 2005, Hayashi group reported the rhodium-catalyzed arylation cyclization of alkyne-tethered enoate **3.42** (Scheme 3.9).¹⁵ In the presence of a rhodium catalyst and phenylboronic acid, different product distributions were observed depending on the ligand. Although both chiral phosphine and chiral diene ligands displayed excellent enantioselectivities, the 1:1:2 mixture of the desired product (**3.43**), another carbocycle derived from reversed carbometalation (**3.44**), and direct 1,4-adduct (**3.45**) was obtained when chiral BINAP was used. On the contrary, a chiral bod ligand showed excellent product selectivity giving the desired carbocycle **3.43** as a major product.



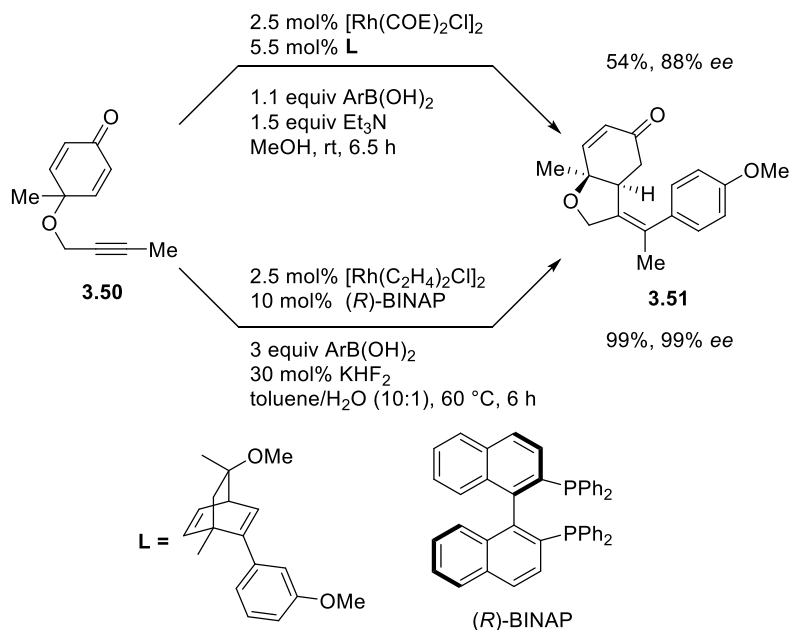
Scheme 3.9 Rh(I)-catalyzed asymmetric arylation cyclization of an alkyne enoate

The regioselectivity of *syn*-carbometalation in the rhodium-catalyzed tandem addition–cyclization was switched when aryl alkyne substrates were used instead of alkyl alkynes. As depicted in Scheme 3.10, under the catalysis of a rhodium/chiral bod complex, cyclohexenone **3.46** with a phenylacetylene moiety gave rise to spirocycle **3.49** possessing a quaternary stereocenter in excellent enantioselectivity.¹⁶



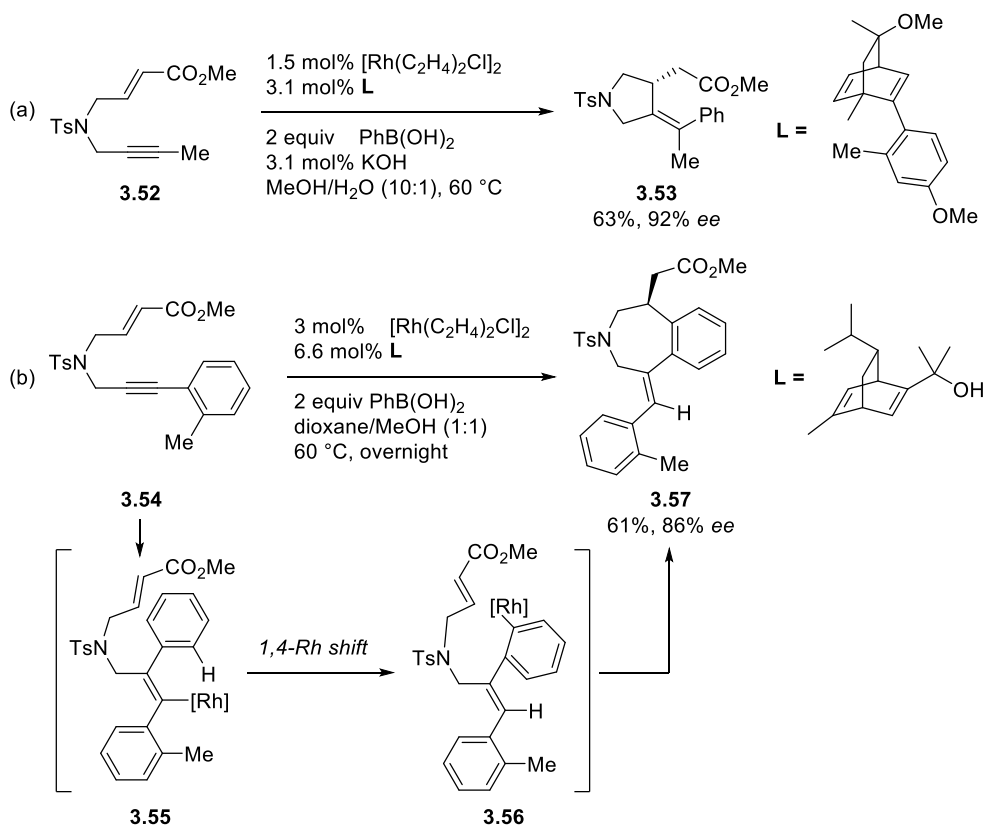
Scheme 3.10 Rh(I)-catalyzed enantioselective synthesis of spirocarbocycle

The rhodium-catalyzed tandem addition–cyclization reactions with concomitant desymmetrization have been reported (Scheme 3.11).¹⁷ Under rhodium catalyzed conditions with arylboronic acid, the alkyne-substituted cyclohexadione **3.50** was converted to heterocycle **3.51**. The enantiomeric differentiation of two C=C bonds was achieved using chiral diene or phosphine ligands, among which BINAP gave better yield and enantioselectivity than the chiral diene.



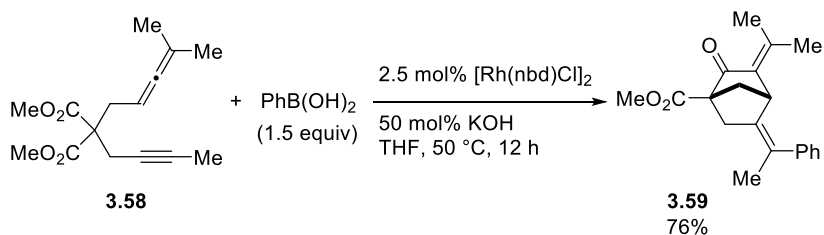
Scheme 3.11 Rh(I)-catalyzed arylation and cyclization of an alkynyldienone

In the arylation reactions for the synthesis of azacycles, a substrate-controlled divergent approach has been reported. The chiral rhodium catalyst mediated the arylation of alkynyl enoate **3.52** to give pyrrolidine **3.53** in excellent enantioselectivity (Scheme 3.12a).¹⁸ On the other hand, enyne **3.54** substituted with an aryl alkyne resulted in chiral benzazepine **3.57** (Scheme 3.12b).¹⁹ These results were derived from reversed selectivity in *syn*-carbometalation, as mentioned in Scheme 3.5 and 3.10.



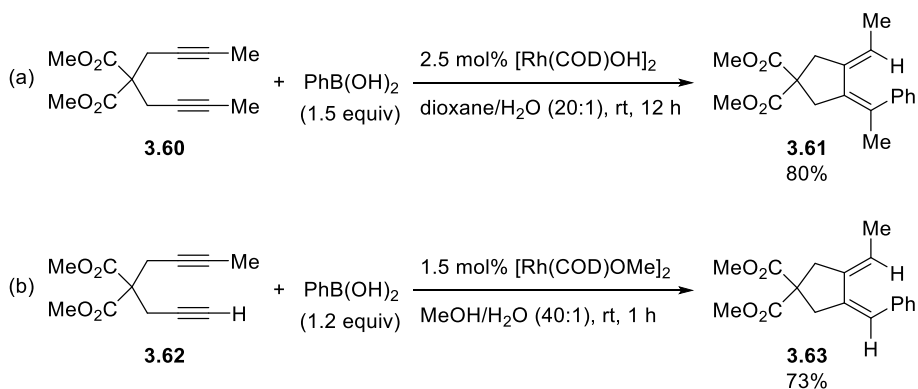
Scheme 3.12 Rh(I)-catalyzed arylative cyclization for azacycles

Allenes can participate in the rhodium-catalyzed tandem cyclization with alkynes. As shown in Scheme 3.13, bicycloheptanone **3.59** was obtained in moderate yield when allenyne **3.58** was treated with the rhodium catalyst and phenylboronic acid.²⁰



Scheme 3.13 Rh(I)-catalyzed arylative cyclization of an allenyne

The migratory insertion of the alkenyl rhodium intermediate can occur at the other alkyne. In the rhodium-catalyzed arylation cyclization reaction, symmetrical 1,6-diyne **3.60** gave dialkylidene cyclopentane **3.61** (Scheme 3.14a).²¹ Unlike the alkyl rhodium intermediate, the alkenyl rhodium species generated from the second carbometalation could be trapped by protodemetalation to provide the desired product. When similar reaction conditions were applied to the unsymmetrical 1,6-diyne **3.62** possessing both internal and terminal alkyne, the initial carbometalation occurred selectively at the terminal alkyne, giving rise to cyclopentane **3.63** (Scheme 3.14b).²²



Scheme 3.14 Rh(I)-catalyzed arylation cyclization of 1,6-diyne

3.4 Conclusion

In this chapter, rhodium-catalyzed tandem addition–cyclization reactions of alkynes have been discussed with respect to the secondary π -systems of substrates. A variety of unsaturated carbon–heteroatom (Section 3.2) and carbon–carbon bonds (Section 3.3) could participate in the cyclizing event. There are two roles of the secondary π -bond: 1) it acts a directing group which directs the regioselectivity in *syn*-carbometalation. 2) it is a reaction partner for cyclization, trapping the alkenyl rhodium intermediate.

In some cases, the 1,4-rhodium shift of alkenyl rhodium complexes to aryl rhodium complexes gave more expanded cyclic products. Furthermore, substrates possessing aryl alkyne showed reversed regioselectivity in *syn*-carbometalation of organorhodium species, giving rise to different cyclic products with the concomitant 1,4-rhodium shift.

However, the scope of unsaturated carbon–nitrogen bond was extremely limited in the rhodium-catalyzed tandem addition–cyclization in comparison with unsaturated carbon–oxygen and carbon–carbon bonds. Because of the significance of amino functional groups in organic synthesis, further investigation would be desirable which uncovers the reactivity of C=N bonds such as imines and hydrazones for the advancement of this field.

3.5 Reference

- ¹ (a) Miura, T.; Murakami, M. *Chem. Commun.* **2007**, 217. (b) Youn, S. W. *Eur. J. Org. Chem.* **2009**, 2009, 2597.
- ² Shintani, R.; Okamoto, K.; Otomaru, Y.; Ueyama, K.; Hayashi, T. *J. Am. Chem. Soc.* **2005**, *127*, 54.
- ³ Miura, T.; Sasaki, T.; Nakazawa, H.; Murakami, M. *J. Am. Chem. Soc.* **2005**, *127*, 1390.
- ⁴ (a) Oguma, K.; Miura, M.; Satoh, T.; Nomura, M. *J. Am. Chem. Soc.* **2000**, *122*, 10464. (b) Hayashi, T.; Inoue, K.; Taniguchi, N.; Ogasawara, M. *J. Am. Chem. Soc.* **2001**, *123*, 9918. (c) Ma, S.; Gu, Z. *Angew. Chem. Int. Ed.* **2005**, *44*, 7512.
- ⁵ Miura, T.; Shimada, M.; Murakami, M. *Synlett* **2005**, 667. and ref 3.
- ⁶ Matsuda, T.; Makino, M.; Murakami, M. *Angew. Chem. Int. Ed.* **2005**, *44*, 4608.
- ⁷ (a) Miura, T.; Shimada, M.; Murakami, M. *Angew. Chem. Int. Ed.* **2005**, *44*, 7598. (b) Miura, T.; Shimada, M.; Murakami, M. *Tetrahedron* **2007**, *63*, 6131.
- ⁸ Li, Y.; Xu, M.-H. *Org. Lett.* **2014**, *16*, 2712.
- ⁹ Johnson, T.; Choo, K.-L.; Lautens, M. *Chem. Eur. J.* **2014**, *20*, 14194.
- ¹⁰ Miura, T.; Takahashi, Y.; Murakami, M. *Org. Lett.* **2007**, *9*, 5075.
- ¹¹ Miura, T.; Nakazawa, H.; Murakami, M. *Chem. Commun.* **2005**, 2855.
- ¹² Miura, T.; Sasaki, T.; Harumashi, T.; Murakami, M. *J. Am. Chem. Soc.* **2006**, *128*, 2516.
- ¹³ Miura, T.; Shimada, M.; Murakami, M. *J. Am. Chem. Soc.* **2005**, *127*, 1094.
- ¹⁴ (a) Hayashi, T.; Yamasaki, K. *Chem. Rev.* **2003**, *103*, 2829. (b) Fagnou, K.; Lautens, M. *Chem. Rev.* **2003**, *103*, 169. (c) Tian, P.; Dong, H.-Q.; Lin, G.-Q. *ACS Catal.* **2012**, *2*, 95.
- ¹⁵ Shintani, R.; Tsurusaki, A.; Okamoto, K.; Hayashi, T. *Angew. Chem. Int. Ed.* **2005**, *44*, 3909.
- ¹⁶ Shintani, R.; Isobe, S.; Takeda, M.; Hayashi, T. *Angew. Chem. Int. Ed.* **2010**, *49*, 3795.
- ¹⁷ (a) Keilitz, J.; Newman, S. G.; Lautens, M. *Org. Lett.* **2013**, *15*, 1148. (b) He, Z.-T.; Tian, B.; Fukui, Y.; Tong, X.; Tian, P.; Lin, G.-Q. *Angew. Chem. Int. Ed.* **2013**, *52*, 5314.
- ¹⁸ Serpier, F.; Flamme, B.; Brayer, J.-L.; Folléas, B.; Darses, S. *Org. Lett.* **2015**, *17*, 1720.

- ¹⁹ Claraz, A.; Serpier, F.; Darses, S. *ACS Catal.* **2017**, *7*, 3410.
- ²⁰ Miura, T.; Ueda, K.; Takahashi, Y.; Murakami, M. *Chem. Commun.* **2008**, 5366.
- ²¹ Miura, T.; Yamauchi, M.; Murakami, M. *Synlett* **2007**, 2029.
- ²² Artok, L.; Kuş, M.; Ürer, B. N.; Türkmen, G.; Aksın-Artok, Ö. *Org. Biomol. Chem.* **2010**, *8*, 2060.

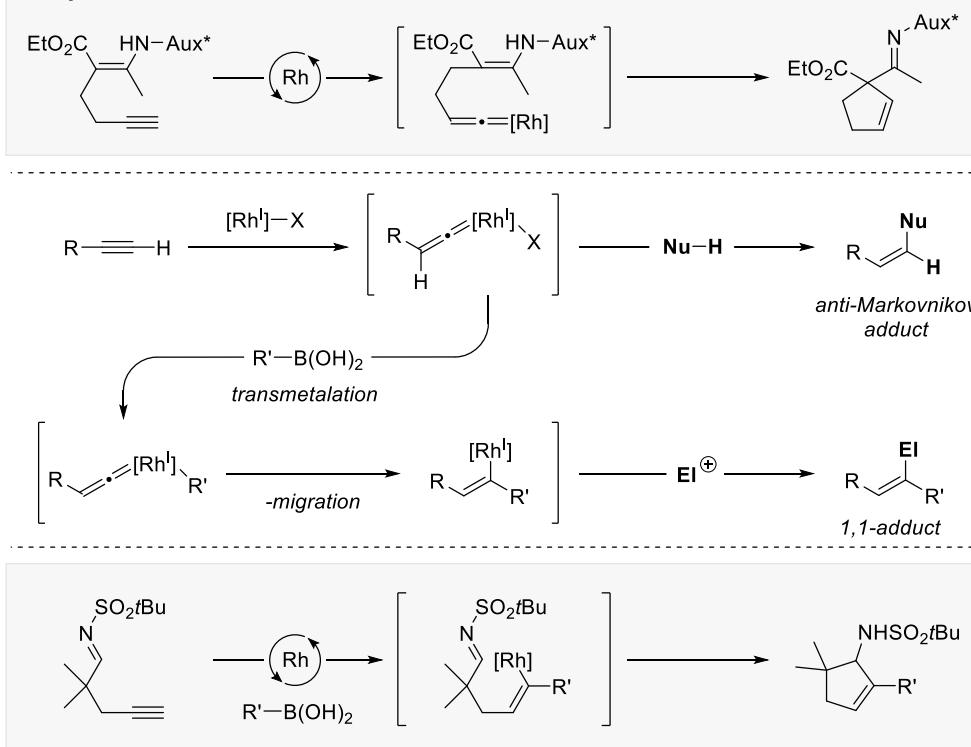
Chapter 4. Rhodium-Catalyzed Tandem Addition– Cyclization of Alkynylimines

4.1 Introduction

In Chapter 2, the rhodium-catalyzed carbocyclization of alkynyl enamines has been discussed. The reactions used the alkyne as an electrophile *via* rhodium vinylidene complex to make a C–C bond with the carbon nucleophile, the enamine. With the promising results in hand, we proposed an alternative reaction pathway wherein alkynes used as electrophiles could be converted to nucleophilic species to undergo further C–C bond formations.

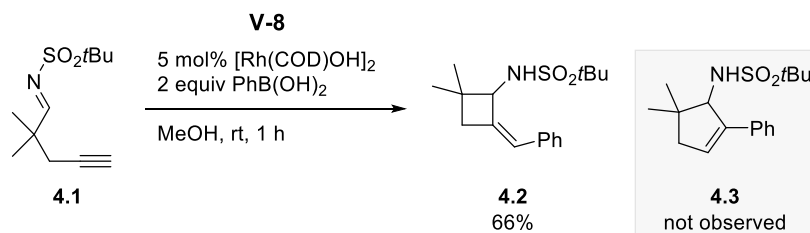
In the hypothesis described in Scheme 4.1, the electrophilic rhodium vinylidene complexes derived from terminal alkynes undergo transmetalation in the presence of organoboronic acids. The resulting organorhodium vinylidene complex might give a nucleophilic alkenyl rhodium species through α -migration, which could then be trapped by carbon electrophiles.¹ As a preliminary study, an imine, the corresponding electrophile of an enamine, can make a C–C bond with the alkenyl rhodium intermediate through concomitant ring closure.

Chapter 2



Scheme 4.1 Rh(I)-catalyzed carbofunctionalization of terminal alkynes

With these hypotheses, we prepared sulfonylimine **4.1** tethered with a terminal alkyne, and exposed it to the rhodium hydroxo precatalyst and 2 equivalents of phenylboronic acid in methanol solvent (Scheme 4.2). To our surprise, alkyneimine **4.1** gave not cyclopentenylamine **4.3**, but benzylidene cyclobutylamine **4.2**, whose structure was confirmed by X-ray crystallography (Figure 4.1).^{2,3}



Scheme 4.2 Rh(I)-catalyzed tandem addition–cyclization of an alkynylimine

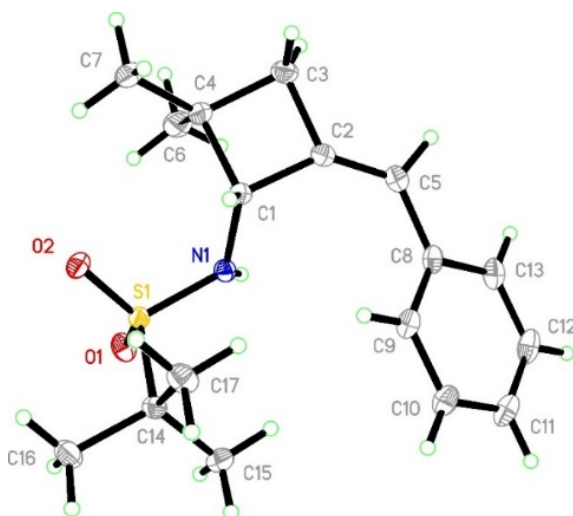
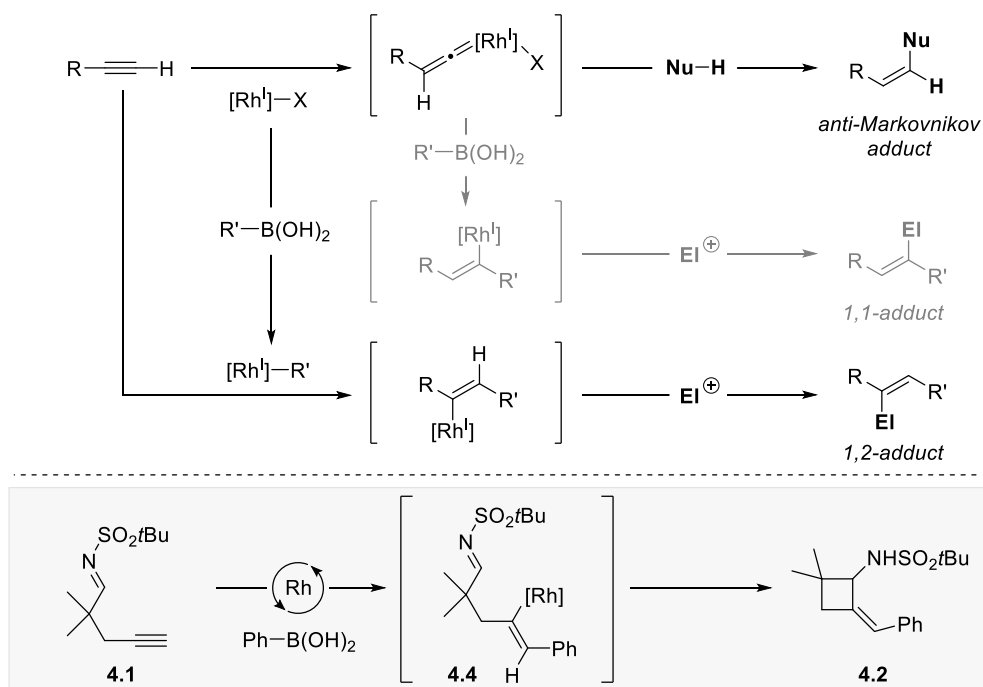


Figure 4.1 ORTEP diagram of **4.2** drawn with 50% probability of ellipsoid

Having the results described in Scheme 4.2, we went back to our original hypothesis and tried to explain these unexpected results. In practice, the rhodium catalyst mediated *syn*-carbometalation to the alkyne *via* organorhodium complex derived from transmetalation, before the formation of rhodium vinylidene complex. (Scheme 4.3). The resulting alkenyl rhodium intermediate acted as a nucleophile to give cyclobutylamine **4.2** by cyclization with the sulfonylimine.⁴



Scheme 4.3 Mechanistic explanations for Rh(I)-catalyzed tandem addition–cyclization of an alkynylimine with phenylboronic acid

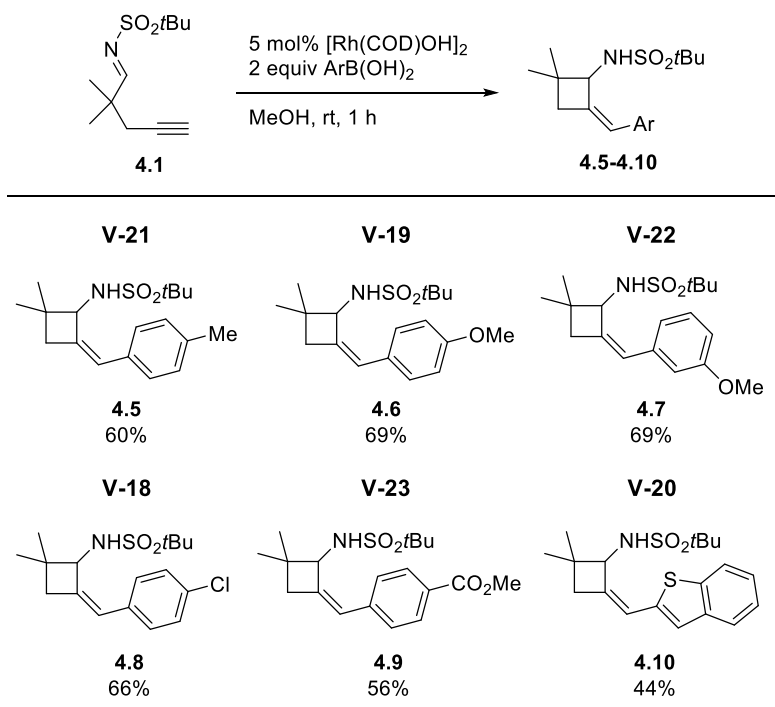
In this chapter, our investigations on the rhodium-catalyzed tandem addition–cyclization of alkynylimines will be discussed.⁵ With organoboron and organozinc reagents, a single rhodium catalyst could mediate sequential 1,2-carbomeatlation to alkyne and sulfonylimine moieties, giving rise to 4-membered cyclic amine products.⁶ Furthermore, this strategy could be expanded to an enantioselective variation where a chiral diene ligand for the rhodium catalyst determines the facial selectivity of imine C=N bond, leading to the chiral allylic stereogenic center.

4.2 Results and discussion

4.2.1 Substrate scope

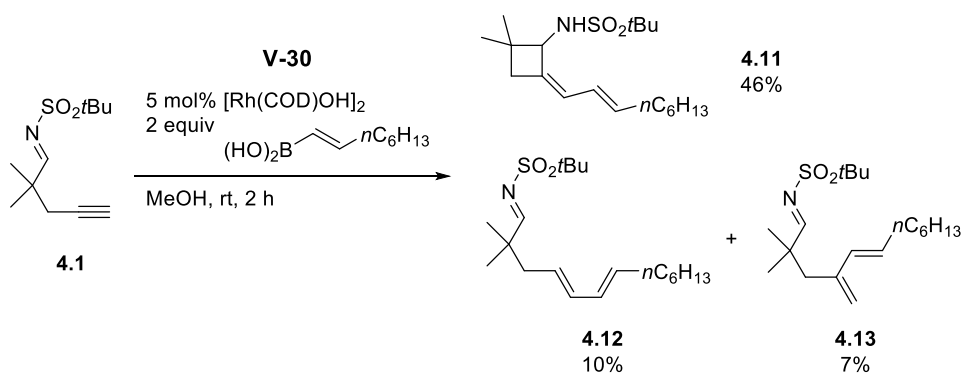
With the optimal reaction conditions in hand,² the scope of the rhodium-catalyzed arylyative cyclization was examined regarding arylboronic acids (Table 4.1). Arylboronic acids with varying electronic properties showed moderate yield in providing corresponding cyclobutylamines. However, fast protodeborylation led to slightly diminished yield of **4.10** when benzo[*b*]thien-2-ylboronic acid was used.

Table 4.1 Substrate scope of arylboronic acids



All reactions were carried out with **4.1** (0.20 mmol), $\text{ArB}(\text{OH})_2$ (0.40 mmol), and $[\text{Rh}(\text{COD})\text{OH}]_2$ (0.01 mmol) in MeOH (0.05 M) at rt for 1 h. Isolated yield.

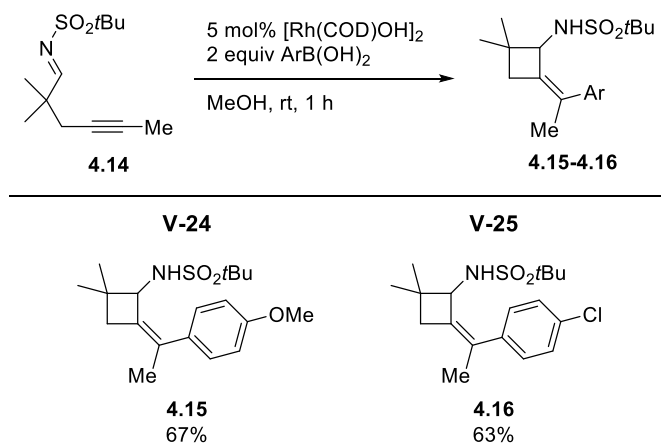
(*E*)-alkenyl boronic acid could give the desired cyclobutylamine **4.1** in moderate yield along with a regioisomeric mixture of hydroalkenylated sulfonylimines **4.12** and **4.13** (Scheme 4.4). These results suggested that 1,4-rhodium shift would be more feasible in the alkenyl rhodium intermediate after the initial *syn*-carbometalation.⁷



Scheme 4.4 Rh(I)-catalyzed alkenylative cyclization of an alkynylimine

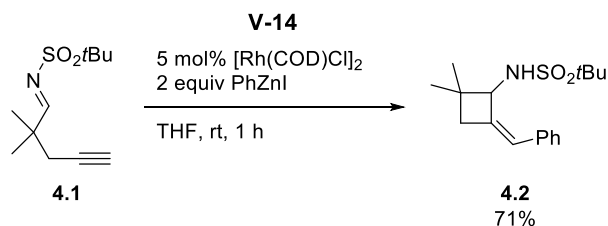
The rhodium-catalyzed tandem addition–cyclization of alkynyl imines does not follow a vinylidene mediated mechanism. Thus, these reaction conditions were applied to alkynylimine **4.14** possessing an internal alkyne (Table 4.2). Cyclobutylamines **4.15** and **4.16** was obtained in similar yields to that of terminal alkyne substrate **4.1**.

Table 4.2 Substrate scope for an internal alkyne



All reactions were carried out with **4.14** (0.20 mmol), $\text{ArB}(\text{OH})_2$ (0.40 mmol), and $[\text{Rh}(\text{COD})\text{OH}]_2$ (0.01 mmol) in MeOH (0.05 M) at rt for 1 h. Isolated yield.

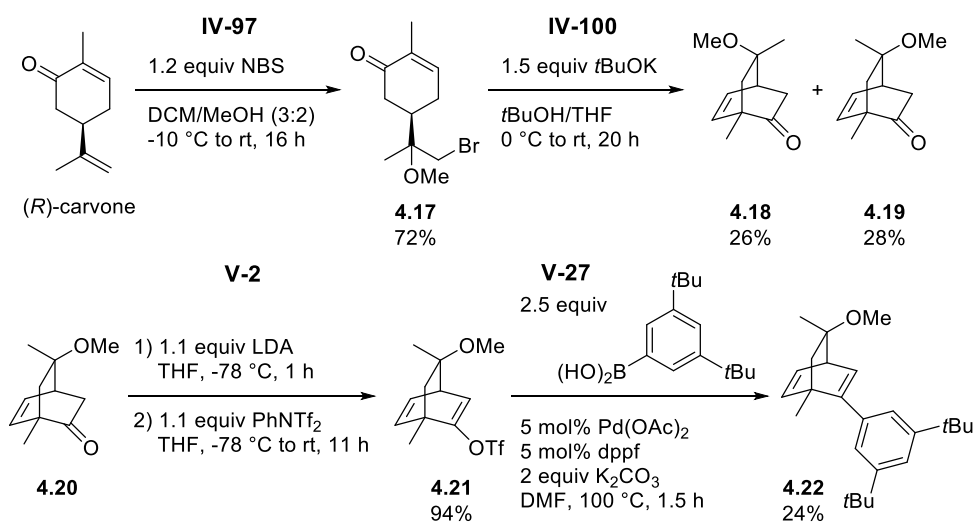
Next, we examined the tandem addition–cyclization reaction with organozinc reagents known to participate in transmetalation with rhodium catalysts.⁸ Interestingly, arylative cyclization occurred with phenylzinc iodide using a catalytic rhodium chloro complex in THF, affording **4.2** in good yield (Scheme 4.5).



Scheme 4.5 Rh(I)-catalyzed arylative cyclization with phenylzinc iodide

4.2.2 Asymmetric carbocyclization of alkynylimine

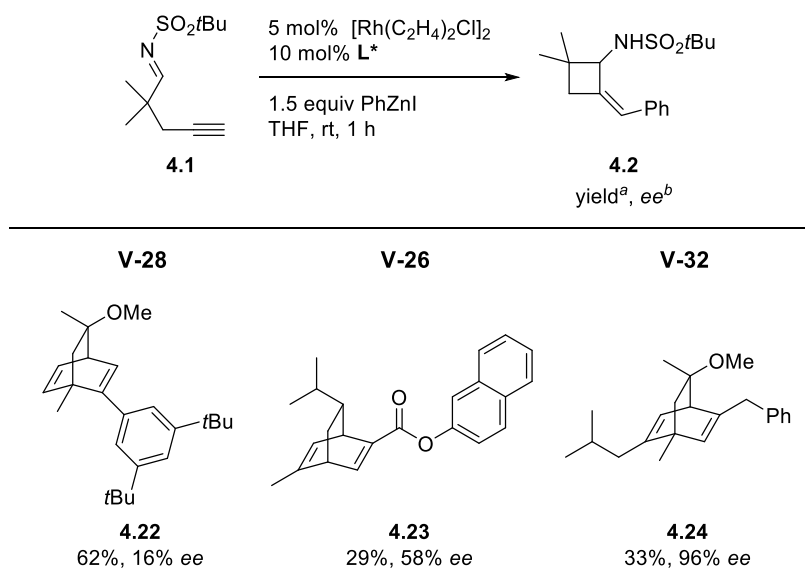
Having established the feasibility of the rhodium-catalyzed arylyative cyclization with phenylzinc iodide, we then tried to make an enantioenriched allylic C–N stereocenter by employing chiral diene ligands.⁹ Before the evaluation of a series of chiral diene ligands, we prepared the chiral diene **4.22** which proved to be the most effective ligand in the rhodium-catalyzed enantioselective arylyative cyclization for the synthesis of cyclobutanols.^{6d} From the natural terpenoid (*R*)-(-)-carvone, the chiral diene **4.22** was synthesized by the following procedure (Scheme 4.6).



Scheme 4.6 Synthesis of chiral diene **4.22**

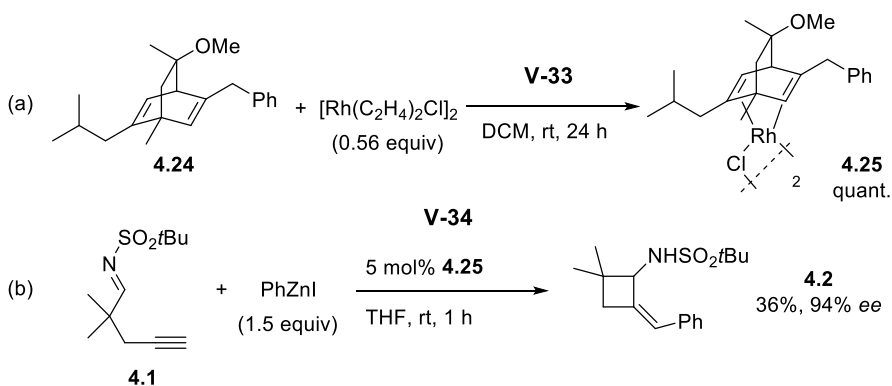
With an assortment of chiral diene ligands in hand, we examined them in the rhodium-catalyzed arylation cyclization using $[\text{Rh}(\text{C}_2\text{H}_4)\text{Cl}]_2$ and phenylzinc iodide (Table 4.3). It was found that the commercially available chiral diene **4.24** developed by Carreira displayed the highest enantioselectivity in spite of low yield.¹⁰ Other chiral dienes **4.22** and **4.23** proved to be less effective in the enantioselective arylation cyclization resulting in varying yields and enantiomeric excesses.¹¹

Table 4.3 Chiral ligand screening for enantioselective cyclization



^aAll reactions were carried out with **4.1** (0.20 mmol), PhZnI (0.30 mmol), and $[\text{Rh}(\text{C}_2\text{H}_4)\text{Cl}]_2$ (0.01 mmol) in THF (0.05 M) at rt for 1 h. Isolated yield. ^bee were determined by chiral HPLC.

Then we set out to prepare the rhodium-diene complex in advance and use it in the arylation cyclization to improve both yield and enantioselectivity. The rhodium chiral diene complex **4.25** was prepared quantitatively from chiral diene **4.24** and $[\text{Rh}(\text{C}_2\text{H}_4)\text{Cl}]_2$ (Scheme 4.7a).^{11b} However, the reaction with the rhodium-diene complex **4.25** gave the results similar to the *in situ* prepared catalyst within an error range (Scheme 4.7b).



Scheme 4.7 Preparation of the rhodium-diene complex **4.25** and its performance in the arylation cyclization

4.3 Conclusion

In summary, the rhodium-catalyzed tandem addition–cyclization reaction of alkynylimines has been described. This methodology provides aryl- or alkenyl-substituted alkylidene cyclobutylamines from alkyne-tethered sulfonylimines in moderate yields.¹² Using a single rhodium catalyst under mild reaction conditions, we have shown that hydrolysis-prone aliphatic sulfonylimines could participate in the tandem reaction.¹³ This was the first example of converting highly electrophilic imines to 4-membered rings instead of intermolecular 1,2-adduct by using terminal or internal alkynes as a mechanistic pivot. Moreover, the reaction can also be rendered asymmetric by using chiral diene ligands, making allylic C–N stereocenters with excellent enantioselectivity.

4.4 Reference

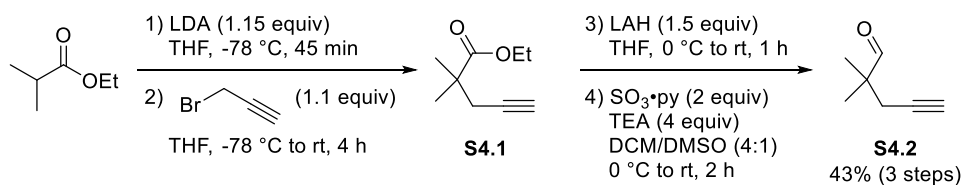
- ¹ Wiedmann, R.; Steinert, P.; Schafer, M.; Werner, H. *J. Am. Chem. Soc.* **1993**, *115*, 9864.
- ² For more details in reaction development and preliminary studies, see: Joo, J. M. (2008). *Studies on the rhodium-catalyzed alkyne functionalization reactions and their application to the total synthesis of 3-demethoxyerythratidinone* (Doctoral dissertation). Princeton University.
- ³ Crystallographic data for **4.2** have been deposited with the Cambridge Crystallographic Data Centre as supplementary publication no. CCDC 1062537.
- ⁴ For the review on the rhodium-catalyzed asymmetric addition reactions to imines, see: Tian, P.; Dong, H.-Q.; Lin, G.-Q. *ACS Catal.* **2012**, *2*, 95.
- ⁵ (a) Miura, T.; Murakami, M. *Chem. Commun.* **2007**, 217. (b) Youn, S. W. *Eur. J. Org. Chem.* **2009**, 2597.
- ⁶ For the seminal works on the rhodium-catalyzed arylation cyclizations for 4-membered rings, see: (a) Miura, T.; Shimada, M.; Murakami, M. *Tetrahedron* **2007**, *63*, 6131. (b) Chen, Y.; Lee, C. *J. Am. Chem. Soc.* **2006**, *128*, 15598. (c) Chen, Y.; Lee, C. *J. Am. Chem. Soc.* **2012**, *134*, 20564. (d) Johnson, T.; Choo, K.-L.; Lautens, M. *Chem. Eur. J.* **2014**, *20*, 14194.
- ⁷ Ma, S.; Gu, Z. *Angew. Chem. Int. Ed.* **2005**, *44*, 7512.
- ⁸ (a) Shintani, R.; Tokunaga, N.; Doi, H.; Hayashi, T. *J. Am. Chem. Soc.* **2004**, *126*, 6240. (b) Nishimura, T.; Yasuhara, Y.; Hayashi, T. *Org. Lett.* **2006**, *8*, 979.
- ⁹ (a) Johnson, J. B.; Rovis, T. *Angew. Chem. Int. Ed.* **2008**, *47*, 840. (b) Defieber, C.; Grützmacher, H.; Carreira, E. M. *Angew. Chem. Int. Ed.* **2008**, *47*, 4482.
- ¹⁰ Paquin, J.-F.; Stephenson, C. R. J.; Defieber, C.; Carreira, E. M. *Org. Lett.* **2005**, *7*, 3821.
- ¹¹ For selected examples using **4.23** in the Rh-catalyzed arylations, see: (a) Okamoto, K.; Hayashi, T.; Rawal, V. H. *Chem. Commun.* **2009**, 4815. (b) Shintani, R.; Takeda, M.; Tsuji, T.; Hayashi, T. *J. Am. Chem. Soc.* **2010**, *132*, 13168. (c) Sasaki, K.; Nishimura, T.; Shintani, R.; Kantchev, E. A. B.; Hayashi, T. *Chem. Sci.* **2012**, *3*, 1278. (d) Zhang, L.; Qureshi, Z.; Sonaglia, L.; Lautens, M. *Angew. Chem. Int. Ed.* **2014**, *53*, 13850.
- ¹² Brandi, A.; Cicchi, S.; Cordero, F. M.; Goti, A. *Chem. Rev.* **2014**, *114*, 7317.
- ¹³ For selected examples on Rh-catalyzed arylation reactions of aliphatic sulfonylimines, see: (a) Trincado, M.; Ellman, J. A. *Angew. Chem. Int. Ed.* **2008**, *47*, 5623. (b) Cui, Z.; Yu, H.-J.; Yang, R.-F.; Gao, W.-Y.; Feng, C.-G.; Lin, G.-Q. *J. Am. Chem. Soc.* **2011**, *133*, 12394.

4.5 Experimental section

4.5.1 General remarks

All solvents were dried by passing through activated alumina columns. Commercially available reagents were used without further purification. Thin layer chromatography (TLC) was performed using Silicycle 60 F254 plates. TLC plates were visualized by exposure to UV light (254 nm) and/or stained by anisaldehyde, ceric ammonium molybdate, or potassium permanganate solutions. Flash column chromatography was performed on Silicycle silica gel 60 (40-63 μm) using the indicated solvent system. ^1H and ^{13}C NMR spectra were recorded in CDCl_3 , unless otherwise noted, on a Agilent MR DD2 400 MHz, Oxford AS500 spectrometers. Chemical shifts in ^1H NMR spectra were reported in parts per million (ppm) on the δ scale from an internal standard of residual chloroform (7.26 ppm). Data for ^1H NMR are reported as follows: chemical shift, multiplicity (s = singlet, d = doublet, t = triplet, q = quartet, m = multiplet, br s = broad singlet), coupling constant in Hertz (Hz) and integration. Data for ^{13}C NMR spectra are reported in terms of chemical shift in ppm from the central peak of CDCl_3 (77.0 ppm). FT-IR spectra were obtained on Thermoscientific Nicolet iS10 and reported in frequency of the absorption (cm^{-1}). Optical Rotations were measured in a 50.00 mm cell with a Jasco P-1030 polarimeter equipped with a sodium lamp (589 nm). High resolution mass spectra (HRMS) were obtained from the Organic Chemistry Research Center at Sogang University.

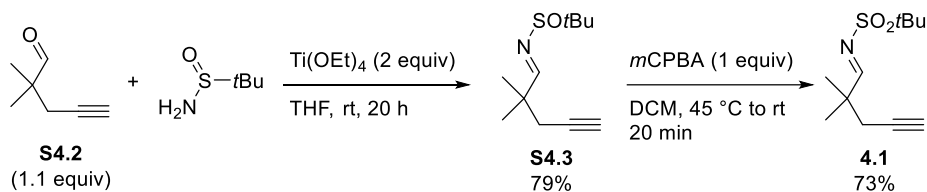
4.5.2 Synthesis and characterization for substrates



To a solution of diisopropylamine (5.5 ml, 39 mmol, 1.3 equiv) in THF was added *n*BuLi (21.6 ml, 34.5 mmol, 1.15 equiv) dropwise at -78 °C. After stirring for 30 min at that temperature, a solution of ethyl isobutyrate (4.1 ml, 30 mmol, 1 equiv) in THF was added dropwise. The reaction mixture was stirred for 45 min at -78 °C and propargyl bromide (3.7 ml, 33 mmol, 1.1 equiv) was added. The reaction flask was allowed to warm slowly to room temperature and quenched with *aq.*NH₄Cl after 4 h. The aqueous layer was extracted by diethyl ether, and the collected organic phase was washed with brine, dried over MgSO₄, and concentrated to afford alkynylester **S4.1** without further purification.

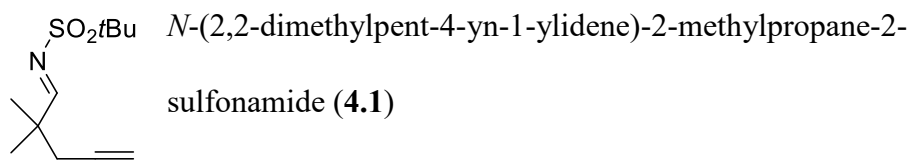
A solution of **S4.1** in THF was added dropwise to a solution of LAH (1797.6 mg, 45 mmol, 1.5 equiv) in THF (176.5 ml, 0.17 M) at 0 °C under N₂ atmosphere. After stirring at room temperature for 1 h, the reaction mixture was cooled down to 0 °C, quenched by *sat. aq.*Na₂SO₄, and stirred for 15 min. The heterogeneous mixture was filtered through short pad of Celite, and concentrated *in vacuo* to give pure alkynyl alcohol without further purification

To a solution of alkynyl alcohol in DCM/DMSO (4:1, 100 ml) was added TEA (16.7 ml, 120 mmol, 4 equiv) and SO₃·py (9744.5 mg, 60 mmol, 2 equiv) successively at 0 °C. After 15 min, the reaction mixture was allowed to warm to room temperature and quenched by water after 2 h. The aqueous layer was extracted by DCM, and the collected organic phase was washed with water five times and brine, dried over Na₂SO₄, and concentrated below room temperature. The crude residue was purified by flash column chromatography to give the pure alkynyl aldehyde **S4.2** as a volatile oil (1418.5 mg, 12.9 mmol, 43% overall yield for 3 steps).

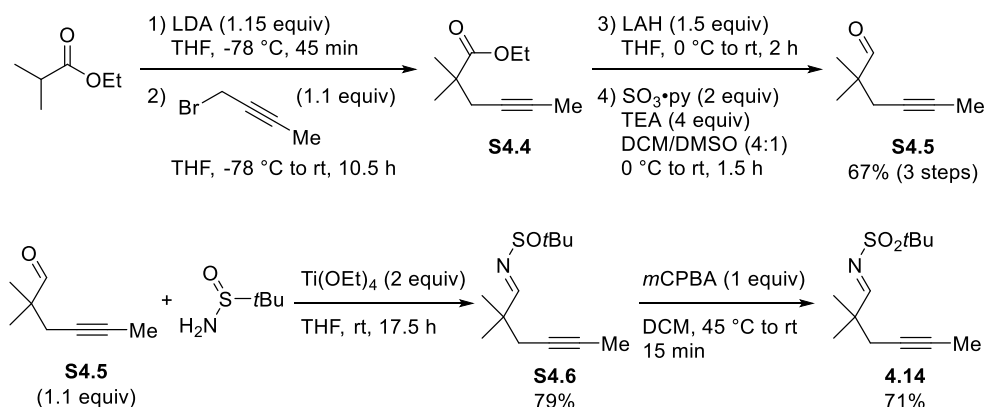


To a solution of alkynyl aldehyde **S4.2** (774.6 mg, 7.0 mmol) in THF (7.8 ml, 0.9 M) were added Ti(OEt)_4 (3240.9 mg, 14.1 mmol, 2 equiv) and *tert*-butylsulfonamide (878.6 mg, 7.0 mmol, 1 equiv) at room temperature. After stirring at room temperature for 20 h, MeOH was added and *aq.* NaHCO_3 was also added until completion of precipitation of titanium salt. The heterogeneous mixture was filtered through a Na_2SO_4 . After concentration, the crude material was purified by flash column chromatography to afford alkynyl sulfinamide **S4.3** (1187.8 mg, 5.6 mmol, 79%) as a yellow oil.

To a solution of alkynyl sulfinamide **S4.3** (1187.8 mg, 5.6 mmol) in DCM (11.1 ml, 0.5 M) was added *m*CPBA (1372.6 mg, 70~75%, 5.6 mmol, 1 equiv) slowly at 45 °C. The reaction mixture was allowed to cool to room temperature and stirred for 20 min. The reaction mixture was diluted with DCM, washed with *sat. aq.* NaHCO_3 five times, and dried over Na_2SO_4 . After concentration, the residue was purified by flash column chromatography to get alkynyl sulfonylimine **4.1** (937.3 mg, 4.1 mmol, 73%) as a white solid.



$R_f = 0.50$ (Hex/EA = 3:1); **m.p.** 37–38 °C; $^1\text{H NMR}$ (500 MHz, CDCl_3) δ 8.52 (s, 1H), 2.46 (d, $J = 2.6$ Hz, 2H), 2.05 (t, $J = 2.6$ Hz, 1H), 1.46 (s, 9H), 1.30 (s, 6H); $^{13}\text{C NMR}$ (125 MHz, CDCl_3) δ 185.1, 80.3, 71.5, 58.3, 41.3, 28.8, 24.0, 24.0; **IR (film, cm^{-1})** 3275, 2977, 2119, 1634, 1306, 1127; **HRMS (EI)** calcd for $\text{C}_{11}\text{H}_{19}\text{NNaO}_2\text{S}$ $[\text{M}+\text{Na}]^+$ 252.1034, found 252.1026.



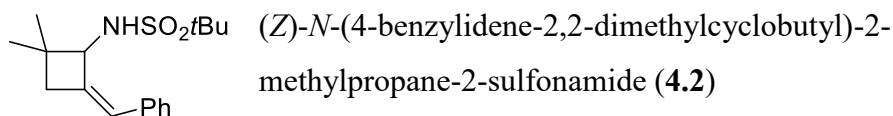
N-(2,2-dimethylhex-4-ynylidene)-2-methylpropane-2-sulfonamide (**4.14**)

$R_f = 0.37$ (Hex/EA = 4:1); $^1\text{H NMR}$ (500 MHz, CDCl_3) δ 8.50 (s, 1H), 2.37 (q, $J = 2.5$ Hz, 2H), 1.75 (t, $J = 2.5$ Hz, 3H), 1.44 (s, 9H), 1.24 (s, 6H); $^{13}\text{C NMR}$ (125 MHz, CDCl_3) δ 186.1, 78.8, 75.1, 58.3, 41.7, 29.7, 24.0, 24.0, 3.6; **IR** (film, cm^{-1}) 3293, 2976, 2923, 1634, 1481, 1307, 1209, 1128; **HRMS** (ESI-TOF) calcd for $\text{C}_{12}\text{H}_{22}\text{NO}_2\text{S}$ $[\text{M}+\text{H}]^+$ 244.1371, found 244.1380.

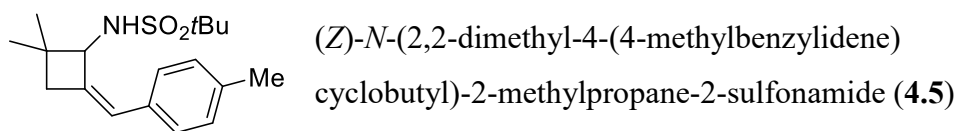
4.5.3 General procedure for the rhodium-catalyzed tandem cyclization

To a 10 ml round bottom flask equipped with a magnetic stirring bar was added alkynylimine (0.20 mmol, 1 equiv) in MeOH (4.0 ml, 0.05 M). $[\text{Rh}(\text{COD})\text{OH}]_2$ (0.010 mmol, 0.05 equiv) and organoboronic acid (0.40 mmol, 2 equiv) were then added to the reaction flask in one portion at room temperature. The mixture was stirred at room temperature for 1 to 2 h and concentrated residue was loaded directly onto a silica gel column to get the corresponding carbocycle product.

4.5.4 Characterization for products

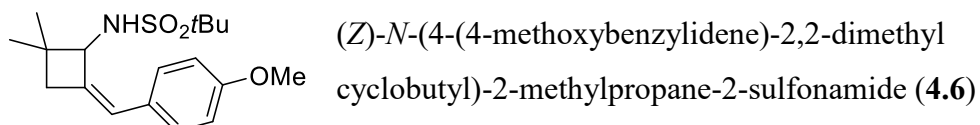


Following the general procedure, alkynylimine **4.1** (42.4 mg, 0.18 mmol) was reacted with [Rh(COD)OH]₂ (4.6 mg, 0.0092 mmol) and PhB(OH)₂ (45.1 mg, 0.37 mmol) in MeOH (3.7 mL) for 1 h to give cyclized product **4.2** (37.5 mg, 0.12 mmol, 66%) as a white solid after purification by flash column chromatography. **R_f** = 0.51 (Hex/EA = 3:1); **m.p.** 80–82 °C; **¹H NMR (500 MHz, CDCl₃)** δ 7.34-7.28 (m, 4H), 7.24-7.18 (m, 1H), 6.36 (d, *J* = 2.1 Hz, 1H), 4.51 (d, *J* = 9.2 Hz, 1H), 3.81 (d, *J* = 9.5 Hz, 1H), 2.38 (d, *J* = 15.0 Hz, 1H), 2.25 (dt, *J* = 15.0, 1.2 Hz, 1H), 1.31 (s, 3H), 1.30 (s, 9H), 1.14 (s, 3H); **¹³C NMR (125 MHz, CDCl₃)** δ 139.6, 135.7, 128.9, 128.4, 127.1, 125.5, 64.2, 60.1, 41.4, 39.1, 27.9, 24.2, 22.4; **IR (film, cm⁻¹)** 3272, 2955, 1451, 1321, 1298, 1128; **HRMS (EI)** calcd for C₁₇H₂₅NNaO₂S [M+Na]⁺ 330.1504, found 330.1500; **Chiral HPLC**: Chiralpak IA, 1.0 mL/min, Hex/*i*-PA = 99:1, 8.8 min (major), 10.8 min (minor); **[α]_D²⁵** = + 31.26 (c=0.10 g/100 mL, CHCl₃, 96% *ee*).

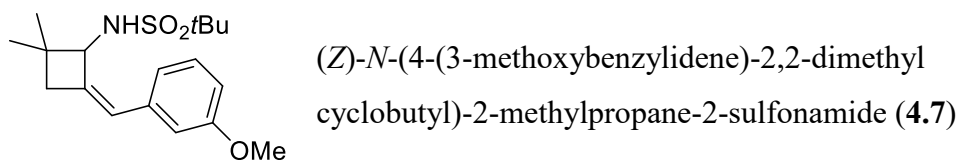


Following the general procedure, alkynylimine **4.1** (44.6 mg, 0.19 mmol) was reacted with [Rh(COD)OH]₂ (4.6 mg, 0.0097 mmol) and 4-methylphenylboronic acid (52.9 mg, 0.39 mmol) in MeOH (3.9 mL) for 1 h to give cyclized product **4.5** (37.4 mg, 0.12 mmol, 60%) as a white solid after purification by flash column chromatography. **R_f** = 0.65 (Hex:EA = 3:1); **m.p.** 87–88 °C; **¹H NMR (500 MHz, CDCl₃)** δ 7.20 (d, *J* = 8.0 Hz, 2H), 7.11 (d, *J* = 7.9 Hz, 2H), 6.31 (d, *J* = 2.1 Hz, 1H), 4.50 (dt, *J* = 9.4, 2.5 Hz, 1H), 3.84 (d, *J* = 9.4 Hz, 1H), 2.36 (d, *J* = 15.2 Hz, 1H), 2.32 (s, 3H), 2.23 (ddd, *J* =

15.3, 3.1, 2.0 Hz, 1H), 1.31 (s, 9H), 1.30 (s, 3H), 1.13 (s, 3H); ^{13}C NMR (125 MHz, CDCl_3) δ 138.33, 136.71, 132.62, 128.96, 128.62, 125.26, 64.07, 59.96, 41.27, 38.92, 27.74, 24.10, 22.32, 21.19; IR (neat, cm^{-1}) 3273, 2954, 1321, 1296, 1128, 1112, 758; HRMS (EI) calcd for $\text{C}_{18}\text{H}_{27}\text{NNaO}_2\text{S}$ 344.1660, found 344.1656.

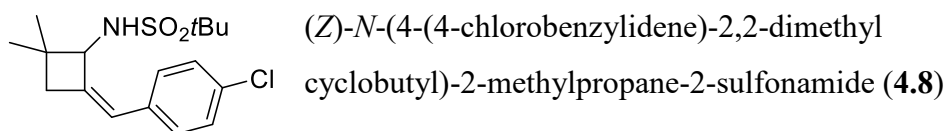


Following the general procedure, alkynylimine **4.1** (42.1 mg, 0.18 mmol) was reacted with $[\text{Rh}(\text{COD})\text{OH}]_2$ (4.3 mg, 0.0092 mmol) and 4-methoxyphenylboronic acid (58.7 mg, 0.37 mmol) in MeOH (3.7 mL) for 1 h to give cyclized product **4.6** (43 mg, 0.13 mmol, 69%) as a colorless liquid after purification by flash column chromatography. $R_f = 0.45$ (Hex:EA = 3:1); ^1H NMR (500 MHz, CDCl_3) δ 7.26-7.22 (m, 2H), 6.86-6.82 (m, 2H), 6.28 (d, $J = 2.3$ Hz, 1H), 4.50 (dt, $J = 9.3, 2.8$ Hz, 1H), 3.85 (d, $J = 9.4$ Hz, 1H), 3.79 (s, 3H), 2.36 (d, $J = 15.3$ Hz, 1H), 2.26-2.19 (m, 1H), 1.33 (s, 9H), 1.30 (s, 3H), 1.13 (s, 3H); ^{13}C NMR (125 MHz, CDCl_3) δ 158.63, 137.20, 129.91, 128.11, 124.85, 113.75, 77.25, 77.00, 76.74, 63.97, 59.92, 55.32, 41.29, 38.94, 27.74, 24.16, 22.35; IR (neat, cm^{-1}) 3284, 2956, 1511, 1320, 1297, 1249, 1128, 756; HRMS (EI) calcd for $\text{C}_{18}\text{H}_{27}\text{NNaO}_3\text{S}$ $[\text{M}+\text{Na}]^+$ 360.1609, found 360.1604.

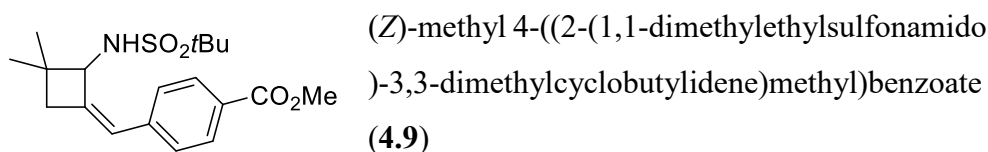


Following the general procedure, alkynylimine **4.1** (45.1 mg, 0.20 mmol) was reacted with $[\text{Rh}(\text{COD})\text{OH}]_2$ (4.6 mg, 0.0098 mmol) and 3-methoxyphenylboronic acid (59.8 mg, 0.39 mmol) in MeOH (3.9 mL) for 1

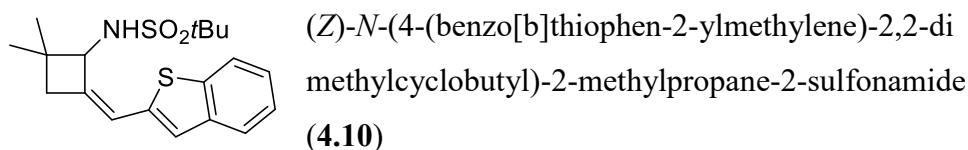
h to give cyclized product **4.7** (45.6 mg, 0.14 mmol, 69%) as a colorless liquid after purification by flash column chromatography. **R_f** = 0.52 (Hex:EA =3:1); **¹H NMR (500 MHz, CDCl₃)** δ 7.24 (t, *J* = 7.9 Hz, 1H), 6.91 (d, *J* = 7.5 Hz, 1H), 6.80 (d, *J* = 1.4 Hz, 1H), 6.77 (dd, *J* = 8.2, 2.0 Hz, 1H), 6.35 (d, *J* = 2.2 Hz, 1H), 4.50 (dt, *J* = 9.4, 2.5 Hz, 1H), 3.83 (s, 1H), 3.82 (s, 3H), 2.38 (d, *J* = 15.3 Hz, 1H), 2.25 (ddd, *J* = 15.3, 3.1, 1.9 Hz, 1H), 1.32 (s, 3H), 1.29 (s, 9H), 1.14 (s, 3H); **¹³C NMR (125 MHz, CDCl₃)** δ 159.46, 139.78, 137.00, 129.28, 125.11, 121.19, 114.55, 112.26, 64.04, 59.94, 55.16, 41.22, 38.93, 27.73, 24.04, 22.22; **IR (neat, cm⁻¹)** 3281, 2957, 1318, 1295, 1128, 1114, 756; **HRMS (EI)** calcd for C₁₈H₂₇NNaO₃S [M+Na]⁺ 360.1609, found 360.1605.



Following the general procedure, alkynylimine **4.1** (43.8 mg, 0.19 mmol) was reacted with [Rh(COD)OH]₂ (4.5 mg, 0.0095 mmol) and 4-chlorophenylboronic acid (62.9 mg, 0.38 mmol) in MeOH (3.8 mL) for 1 h to give cyclized product **5d** (43.2 mg, 0.13 mmol, 66%) as a white solid after purification by flash column chromatography. **R_f** = 0.61 (Hex:EA =3:1); **m.p.** 90-91 °C; **¹H NMR (500 MHz, CDCl₃)** δ 7.36-7.16 (m, 4H), 6.29 (dd, *J* = 4.6, 2.3 Hz, 1H), 4.51 (dt, *J* = 9.8, 2.6 Hz, 1H), 3.81 (d, *J* = 9.7 Hz, 1H), 2.37 (d, *J* = 15.5 Hz, 1H), 2.24 (ddd, *J* = 15.5, 3.2, 2.0 Hz, 1H), 1.32 (s, 9H), 1.31 (s, 3H), 1.13 (s, 3H); **¹³C NMR (125 MHz, CDCl₃)** δ 140.55, 133.84, 132.74, 130.00, 128.43, 124.22, 63.83, 59.97, 41.25, 38.99, 27.75, 24.12, 22.28; **IR (neat, cm⁻¹)** 3274, 2956, 1491, 1318, 1297, 1127, 1113, 758; **HRMS (EI)** calcd for C₁₇H₂₄CINNaO₂S [M+Na]⁺ 364.1114, found 364.1107.

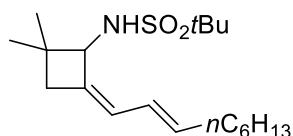


Following the general procedure, alkynylimine **4.1** (45.4 mg, 0.20 mmol) was reacted with [Rh(COD)OH]₂ (4.7 mg, 0.0099 mmol) and 4-(methoxycarbonyl)phenylboronic acid (71.3 mg, 0.40 mmol) in MeOH (4.0 mL) for 1 h to give cyclized product **4.9** (40.2 mg, 0.11 mmol, 56%) as a white solid after purification by flash column chromatography. *R_f* = 0.45 (Hex:EA = 3:1); **m.p.** 160–161 °C; ¹H NMR (500 MHz, CDCl₃) δ 7.98 (d, *J* = 8.2 Hz, 2H), 7.38 (d, *J* = 8.2 Hz, 2H), 6.37 (d, *J* = 2.0 Hz, 1H), 4.56 (dt, *J* = 9.7, 2.5 Hz, 1H), 3.90 (s, 3H), 3.85 (d, *J* = 9.8 Hz, 1H), 2.40 (d, *J* = 15.7 Hz, 1H), 2.33-2.23 (m, 1H), 1.32 (s, 12H), 1.15 (s, 3H); ¹³C NMR (125 MHz, CDCl₃) δ 166.81, 142.58, 140.01, 129.58, 128.66, 128.44, 124.65, 64.03, 60.03, 52.04, 41.40, 39.00, 27.75, 24.12, 22.29; IR (neat, cm⁻¹) 3279, 2953, 1707, 1315, 1298, 1280, 1116, 760; HRMS (EI) calcd for C₁₉H₂₇NNaO₄S 388.1558, found 388.1553.



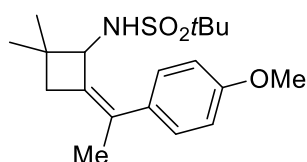
Following the general procedure, alkynylimine **4.1** (41.9 mg, 0.18 mmol) was reacted with [Rh(COD)OH]₂ (4.3 mg, 0.0091 mmol) and thianaphthene-2-boronic acid (65.0 mg, 0.37 mmol) in MeOH (3.7 mL) for 1 h to give cyclized product **4.10** (29.3 mg, 0.081 mmol, 44%) as a white solid after purification by flash column chromatography. *R_f* = 0.58 (Hex:EA = 3:1); **m.p.** 100–101 °C; ¹H NMR (500 MHz, CDCl₃) δ 7.74 (d, *J* = 7.9 Hz, 1H), 7.70 (d, *J* = 7.9 Hz, 1H), 7.34-7.24 (m, 2H), 7.22 (d, *J* = 4.6 Hz, 1H), 6.45 (d, *J* = 1.9 Hz, 1H), 4.51 (dt, *J* = 9.6, 3.0 Hz, 1H), 4.05 (d, *J* = 9.6 Hz, 1H), 2.40 (dd, *J* = 15.7, 1.8 Hz, 1H), 2.34-2.24 (m, 1H), 1.33 (s, 3H), 1.29 (s, 9H), 1.17 (s, 3H); ¹³C

NMR (125 MHz, CDCl₃) δ 142.51, 140.01, 139.85, 137.85, 124.47, 124.23, 123.40, 123.35, 121.96, 118.06, 64.18, 60.10, 41.27, 38.94, 27.68, 24.04, 22.33; **IR (neat, cm⁻¹)** 3279, 2957, 1318, 1297, 1126, 886, 755, 708; **HRMS (EI)** calcd for C₁₉H₂₅NNaO₂S₂ 386.1224, found 386.1220.



N-((*Z*)-2,2-dimethyl-4-((*E*)-non-2-en-1-ylidene)cyclobutyl)-2-methylpropane-2-sulfonamide (**4.11**)

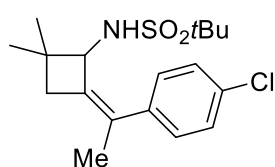
Following the general procedure, alkynylimine **4.1** (43.5 mg, 0.19 mmol) was reacted with [Rh(COD)OH]₂ (4.5 mg, 0.0095 mmol) and *trans*-1-octen-1-ylboronic acid (60.4 mg, 0.38 mmol) in MeOH (3.8 mL) for 2 h to give cyclized product **4.11** (29.8 mg, 0.087 mmol, 46%) as a white solid along with protodemethylated byproducts **4.12** and **4.13** as a colorless oil after purification by flash column chromatography. To separate dienyylimine byproduct **4.12** and **4.13** completely, addition reduction by LAH was conducted. **R_f** = 0.57 (Hex:EA = 4:1); **m.p.** 56–58 °C; **¹H NMR (500 MHz, CDCl₃)** δ 6.45 (dd, *J* = 15.0, 11.4 Hz, 1H), 5.89 (d, *J* = 11.2 Hz, 1H), 5.63-5.53 (m, 1H), 4.24 (d, *J* = 10.5 Hz, 1H), 4.18 (d, *J* = 10.6 Hz, 1H), 2.22 (d, *J* = 15.7 Hz, 1H), 2.12 (d, *J* = 16.2 Hz, 1H), 2.07 (q, *J* = 14.4, 7.3 Hz, 2H), 1.46 (s, 9H), 1.33-1.25 (m, 8H), 1.24 (s, 3H), 1.10 (s, 3H), 0.88 (t, *J* = 6.8 Hz, 3H); **¹³C NMR (125 MHz, CDCl₃)** δ 137.31, 134.54, 125.59, 125.30, 63.79, 59.93, 40.06, 38.69, 32.83, 31.71, 29.23, 28.90, 27.42, 24.31, 22.59, 22.33, 14.09; **IR (neat, cm⁻¹)** 3299, 2926, 1727, 1456, 1298, 1129, 969, 893, 806, 738; **HRMS (EI)** calcd for C₁₉H₃₅NNaO₂S 364.2286, found 364.2282.



(*Z*)-*N*-(4-(1-(4-methoxyphenyl)ethylidene)-2,2-dimethylcyclobutyl)-2-methylpropane-2-sulfonamide (**4.15**)

Following the general procedure, alkynylimine **4.14** (46.2 mg, 0.19 mmol)

was reacted with $[\text{Rh}(\text{COD})\text{OH}]_2$ (4.5 mg, 0.0095 mmol) and 4-methoxyphenylboronic acid (60.7 mg, 0.38 mmol) in MeOH (3.8 mL) for 1 h to give cyclized product **4.15** (44.6 mg, 0.13 mmol, 67%) as a white crystal after purification by flash column chromatography. $R_f = 0.46$ (Hex:EA = 3:1); **m.p.** 121–124 °C; $^1\text{H NMR}$ (500 MHz, CDCl_3) δ 7.16–7.12 (m, 2H), 6.89–6.82 (m, 2H), 4.26 (d, $J = 9.1$ Hz, 1H), 3.77 (s, 3H), 3.60 (d, $J = 9.1$ Hz, 1H), 2.32–2.22 (m, 2H), 1.85 (dd, $J = 3.2, 1.5$ Hz, 3H), 1.27 (s, 3H), 1.11 (s, 3H), 1.09 (s, 9H); $^{13}\text{C NMR}$ (125 MHz, CDCl_3) δ 158.59, 133.65, 131.72, 131.52, 128.76, 113.99, 77.26, 77.01, 76.75, 63.81, 59.60, 55.35, 39.90, 38.09, 27.64, 23.91, 23.84, 22.90, 20.03; **IR** (neat, cm^{-1}) 3293, 2955, 1511, 1323, 1296, 1245, 1127, 1107, 831, 760; **HRMS** (EI) calcd for $\text{C}_{19}\text{H}_{29}\text{NNaO}_3\text{S}$ $[\text{M}+\text{Na}]^+$ 374.1766, found 374.1761.



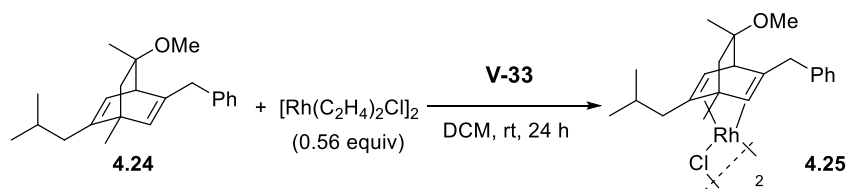
(*Z*)-*N*-(4-(1-(4-chlorophenyl)ethylidene)-2,2-dimethylcyclobutyl)-2-methylpropane-2-sulfonamide (**4.16**)

Following the general procedure, alkynylimine **4.14** (47.9 mg, 0.20 mmol) was reacted with $[\text{Rh}(\text{COD})\text{OH}]_2$ (4.6 mg, 0.0098 mmol) and 4-chlorophenylboronic acid (64.8 mg, 0.39 mmol) in MeOH (3.9 mL) for 1 h to give cyclized product **4.16** (44.4 mg, 0.12 mmol, 63%) as a white solid after purification by flash column chromatography. $R_f = 0.60$ (Hex:EA = 3:1); **m.p.** 143–146 °C; $^1\text{H NMR}$ (500 MHz, CDCl_3) δ 7.31–7.27 (m, 2H), 7.18–7.13 (m, 2H), 4.24 (d, $J = 9.6$ Hz, 1H), 3.54 (d, $J = 9.6$ Hz, 1H), 2.34–2.22 (m, 2H), 1.85 (dd, $J = 3.3, 1.6$ Hz, 3H), 1.27 (s, 3H), 1.11 (s, 3H), 1.09 (s, 9H); $^{13}\text{C NMR}$ (100 MHz, CDCl_3) δ 139.69, 133.39, 132.73, 131.11, 129.07, 128.62, 63.64, 59.62, 39.77, 38.18, 27.60, 23.73, 22.83, 19.89; **IR** (neat, cm^{-1}) 3292, 2931, 1489, 1322, 1295, 1127, 1104, 759; **HRMS** (EI) for $\text{C}_{18}\text{H}_{26}\text{ClNNaO}_2\text{S}$ $[\text{M}+\text{Na}]^+$ 378.1270, found 378.1265.

4.5.5 Procedure for enantioselective rhodium-catalyzed tandem cyclization

To a 10 ml round bottom flask were added $[\text{Rh}(\text{C}_2\text{H}_4)_2\text{Cl}]_2$ (0.010 mmol, 0.05 equiv), chiral diene **4.22-4.24** (0.020 mmol, 0.1 equiv) and THF (2.8 ml). After stirring for 15 min at room temperature, a solution of alkynylimine **4.1** (0.20 mmol in 1.2 ml of THF) was added followed by addition of phenylzinc iodide (0.30 mmol, 1.5 equiv). After stirring for 1 h, the reaction mixture was treated with 2 N HCl (0.5 ml) and filtered through a short pad of silica gel. The filtrate was concentrated, and the residue was purified by flash column chromatography to give the cyclized product **4.2**.

4.5.6 Preparation of the rhodium-diene complex **4.25**



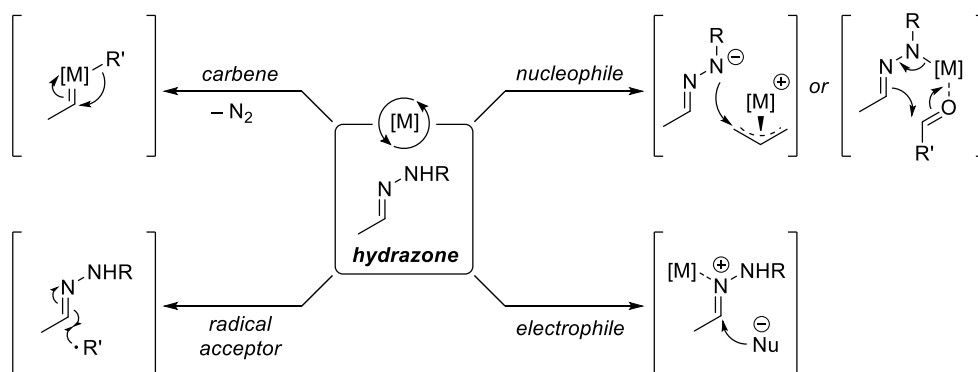
A solution of **4.24** (35.4 mg, 0.11 mmol) and $[\text{Rh}(\text{C}_2\text{H}_4)_2\text{Cl}]_2$ (23.8 mg, 0.061 mmol) in DCM (2.2 ml, 0.05 M) was stirred at room temperature for 12 h. After concentration of the reaction mixture, the residue was subjected to silica gel column to afford the rhodium-diene complex **4.25** (51.0 mg, 0.057 mmol, quant.) as a yellow solid.

Chapter 5. Rhodium-Catalyzed Tandem Addition–Cyclization–Rearrangement of Alkynylhydrazones

5.1 Introduction

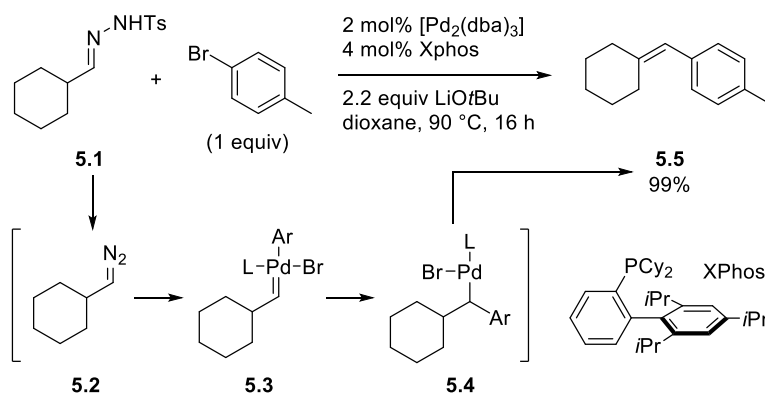
Hydrazones are a condensate of hydrazine and carbonyl derivatives, of which the formation of a C=N–N bond has been utilized extensively as carbonyl characterization in classical organic chemistry. They have also been used as precursors to synthesize alkenes in Bamford-Stevens reaction and Shapiro reaction, as well as an intermediate of Wolff-Kishner reduction to afford methylene groups from ketones.^{1,2} Furthermore, because of their ambiphilic reactivity, hydrazones have been utilized in C–C bond forming processes with a variety of carbon nucleophiles and electrophiles.^{3,4}

Recently, hydrazones have emerged as a versatile reactant in transition metal mediated catalytic C–C bond formations. As depicted in Scheme 5.1, there have been reported four distinct roles of hydrazones in transition metal mediated reactions. In this section, each representative works of using hydrazones as diazo precursors, nucleophiles, electrophiles, and radical acceptors with transition metal catalysts will be discussed briefly.



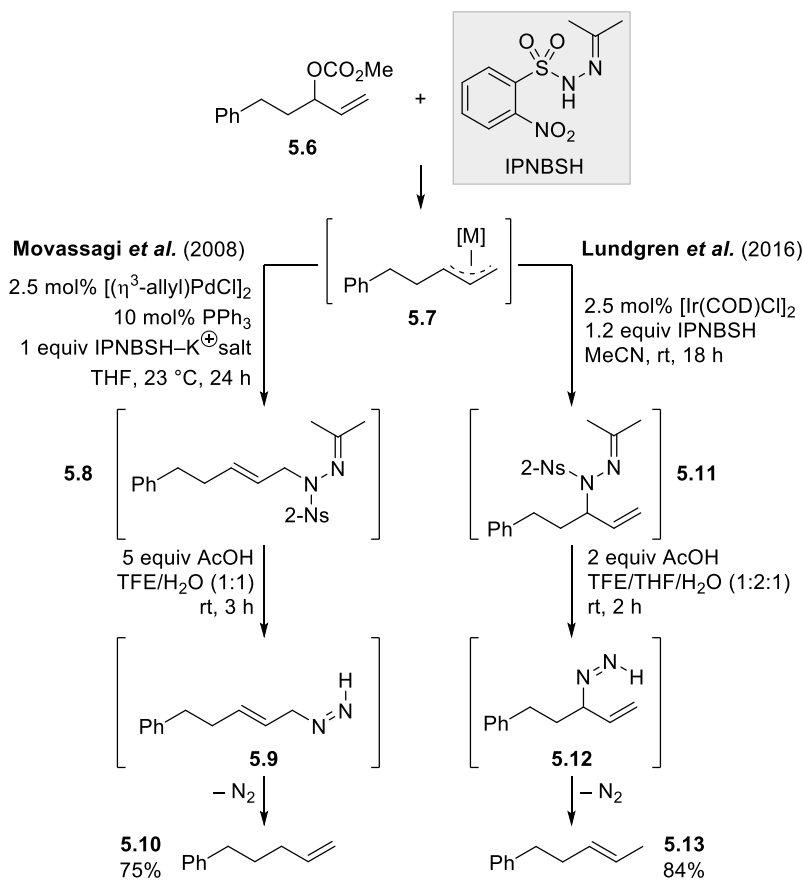
Scheme 5.1 Transition metal catalyzed C–C bond formation of hydrazones

In 2007, the palladium-catalyzed cross-coupling reaction of *N*-tosylhydrazone **5.1** with an aryl halide was reported (Scheme 5.2).⁵ The authors used sulfonylhydrazones as a precursor for diazo compound **5.2** in the presence of a base to produce palladium carbene **5.3**. After the α -migration of an aryl moiety in **5.4**, the subsequent β -hydride elimination gave the desired coupling product **5.5**. Since this seminal work was reported, a number of cross-coupling reactions of sulfonylhydrazones have emerged extensively.⁶



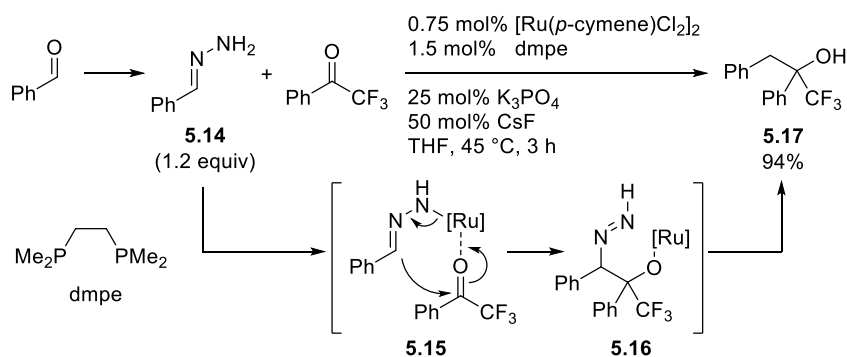
Scheme 5.2 Pd(0)-catalyzed cross-coupling reaction of a *N*-tosylhydrazone

In the presence of a base, hydrazones which have a N–H bond can be deprotonated to act as a nucleophile. In conjunction of this reactivity with transition metal catalysis, two stereospecific allylic reduction reactions of allylic carbonate **5.6** were reported.⁷ As described in Scheme 5.3, the linear (**5.8**) and branched (**5.11**) *N*-allyl hydrazones could be accessed with IPNBSH using a palladium or iridium catalyst, respectively.⁸ Following unmasking processes involving acidic hydrolysis and sulfinic acid elimination, the resulting allylic diazene intermediate **5.9** and **5.12** underwent a retro-ene reaction to afford the allylic reduction products **5.10** and **5.13** respectively.⁹



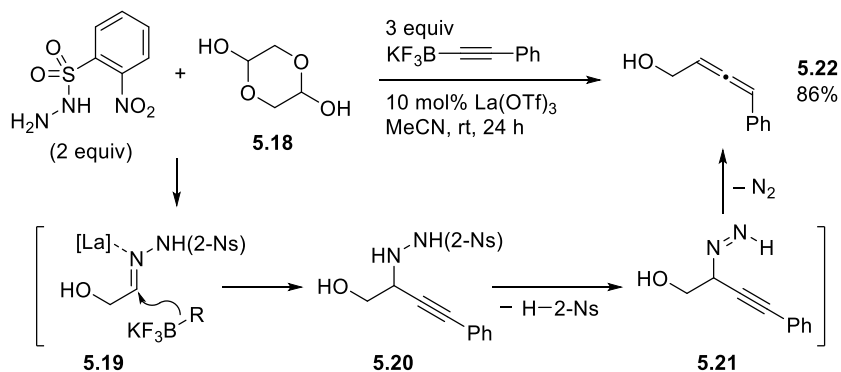
Scheme 5.3 Pd- or Ir-catalyzed stereospecific allylic reduction reactions

Hydrazones which have no substituents at the terminal nitrogen atom can be deprotonated in the presence of a Lewis acid and a mild base. In 2017, the ruthenium-catalyzed carbonyl addition reaction of hydrazones was reported (Scheme 5.4).¹⁰ Using hydrazone **5.14** as a carbanion equivalent, a reductive C–C coupling with another carbonyl compound was achieved in the presence of the ruthenium catalyst.¹¹



Scheme 5.4 Ru(II)-catalyzed carbonyl addition reaction of a hydrazone

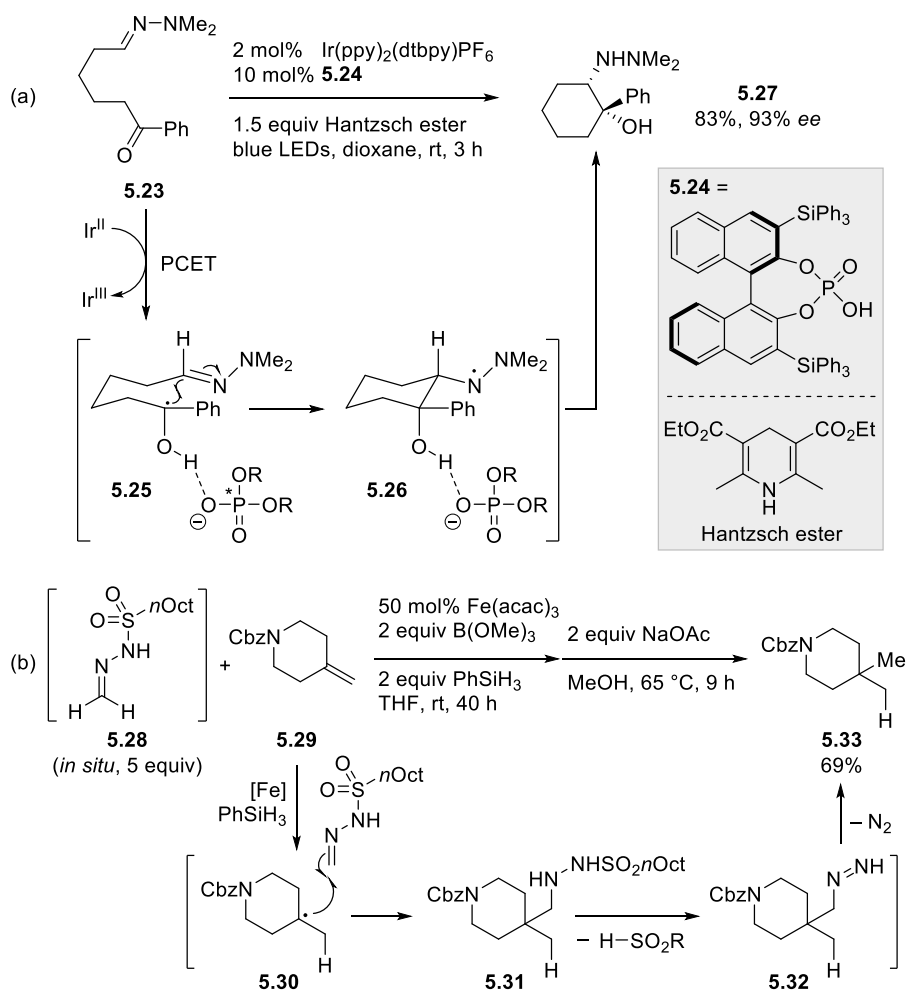
A Lewis acid catalyst could mediate both *in situ* hydrazone formation and nucleophilic addition. As shown in Scheme 5.5, the Thomson group reported a traceless synthesis of allenes by a lanthanum catalyst.¹² In their work, the lanthanum catalyst facilitated the *in situ* formation of hydrazone **5.19** as well as a Petasis-type reaction with an alkynyl tetrafluoroborate giving rise to propargyl hydrazide **5.20**. Subsequently, the unstable hydrazide **5.20** decomposed to allene **5.22** spontaneously, with the extrusion of dinitrogen gas *via* a diazene intermediate as shown in Scheme 5.3.¹³



Scheme 5.5 La(III)-catalyzed traceless allene synthesis

A carbon-centered radical species have been known to react with a C=N bond of hydrazones leading to the formation of a C–C bond.¹⁴ Recently, organic reactions involving radical species have been known to be feasible by transition metal catalysts, and the examples of using a hydrazone as a radical acceptor were reported. In 2013, the catalytic asymmetric aza-pinacol cyclization of ketohydrazone **5.23** was reported (Scheme 5.6a).¹⁵ Under visible light irradiation, proton-coupled electron transfer (PCET) mediated by the iridium photoredox catalyst and phosphoric acid **5.24** led to ketyl radical **5.25**. Following stereoselective aza-pinacol cyclization occurred through the addition of the ketyl radical to the hydrazone, whose facial selectivity was controlled by the chiral conjugate base of **5.24**. This reaction provided chiral *syn*-1,2-amino alcohol derivatives with excellent diastereo- and enantioselectivity. Meanwhile, the formal hydromethylation of unactivated alkenes was achieved with a sulfonylhydrazone by a substoichiometric iron catalyst (Scheme 5.6b).¹⁶ In the presence of an iron catalyst and phenylsilane

as a reductant, carbon-centered 3°-radical **5.30** was generated, and added to the *in situ* generated sulfonylhydrazone **5.28**. Further solvent exchange and heating with an inorganic base induced both elimination of the sulfonic acid and liberation of dinitrogen gas, providing formal hydromethylated product **5.33** in moderate yield. Although there were a few examples in catalytic protocols, this work suggested a solution for the unsolved problem of chemoselective direct olefin hydromethylation.

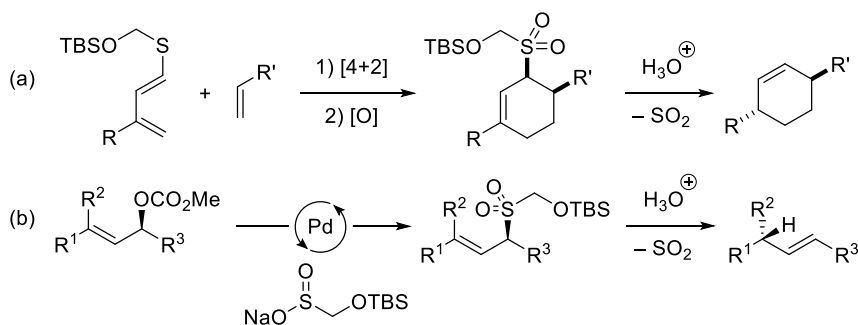


Scheme 5.6 Using a hydrazone as a radical acceptor in transition metal catalysis

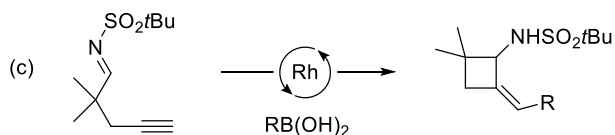
Our group recently reported works merging organic reactions with a retro-ene reaction. These reactions have shown that various sulfonyl motifs could be introduced as precursors of allylic sulfinic acids with the formation of carbon–carbon or carbon–heteroatom bonds, ultimately resulting in the alkene products that are inaccessible *via* direct reaction routes (Scheme 5.7a and 5.7b).¹⁷

In conjunction with our efforts to develop tandem retro-ene reactions, the rhodium-catalyzed tandem addition–cyclization–rearrangement of alkynylhydrazones has been studied and the results will be described in this chapter (Scheme 5.7d).¹⁸ With the feasibility of the catalytic alkenyl addition to the C=N bond of sulfonylimines in hand (Scheme 5.7c), we proposed the same catalytic alkenyl addition to the C=N bond would take place in sulfonylhydrazones under rhodium catalysis.¹⁹ Following elimination of the sulfinic acid, the allylic diazene intermediate affords endocyclic alkene products *via* pericyclic rearrangement described in Scheme 5.3. Specifically, optimization of the reaction conditions, substrate scope of organoboronic acids and alkynylhydrazones, their applications in ring-size alteration, evaluation of chiral ligands, and mechanistic studies will be discussed.

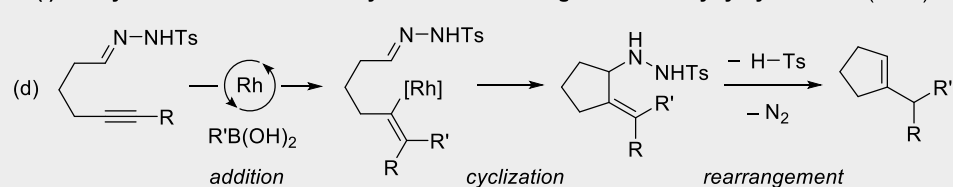
Tandem C–C or C–S Bond Formation and Retro-Ene Reactions (2014, 2018)



Rh(I)-Catalyzed Tandem Addition–Cyclization of Alkynylimines (2015)



Rh(I)-catalyzed Tandem Addition–Cyclization–Rearrangement of Alkynylhydrazones (2018)

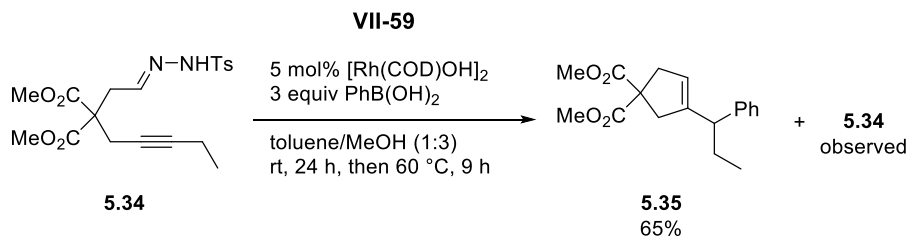


Scheme 5.7 Our efforts on merging organic reactions with retro-ene reactions

5.2 Results and discussion

5.2.1 Preliminary results

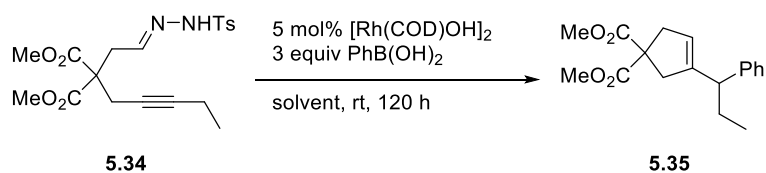
Our studies were initiated with alkynyl hydrazone **5.34** tethered with a dimethyl malonate (Scheme 5.8). As we anticipated from the previous results in Chapter 4, the rhodium catalyst and three equivalents of phenylboronic acid gave desired cyclopentene **5.35** in moderate yield at room temperature. However, at some point, no further conversion of starting hydrazone **5.34** was observed even at a higher temperature up to 60 °C.



Scheme 5.8 Preliminary result of Rh(I)-catalyzed tandem addition–cyclization–rearrangement of an alkynylhydrazone

We then set out to examine the reaction in other solvents which have been used in the rhodium-catalyzed arylation cyclization reactions (Table 5.1). Although toluene and methanol solvents displayed better yield than those obtained in ethereal solvents, the unreacted substrate was remained even after five days (Entry 1-4).

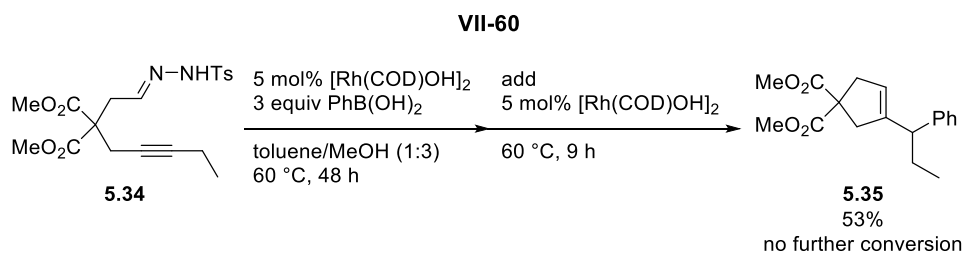
Table 5.1 Preliminary solvent screening



Exp. #	Entry	Solvent	Yield ^a
VII-62	1	toluene	50%
VII-63-1	2	MeOH	56%
VII-63-2	3	1,4-dioxane	28%
VII-63-3	4	THF	27%

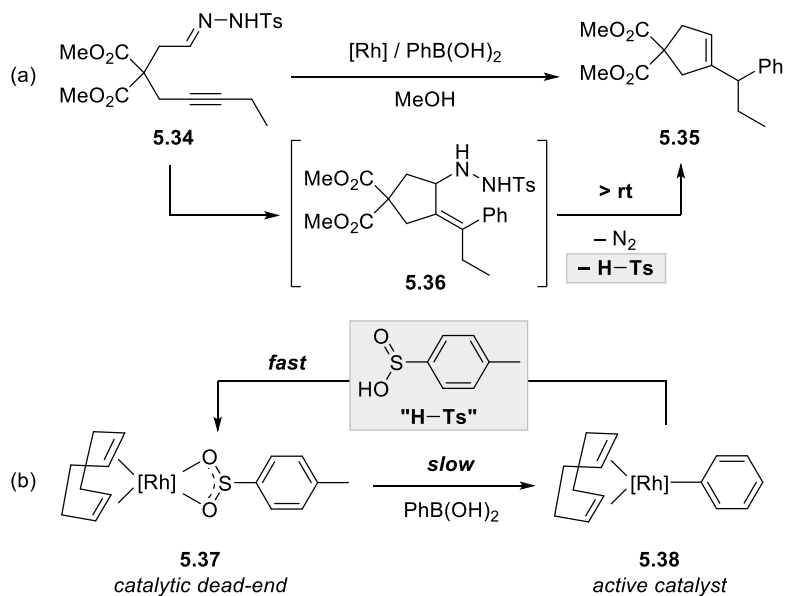
^aYields were determined by ¹H NMR using 1,3,5-trimethoxybenzene as an internal standard.

From these preliminary results, we surmised that the rhodium catalyst turned unreactive during the reaction process. To confirm this possibility, we put a 5 mol% rhodium catalyst after the reaction was performed for two days at 60 °C (Scheme 5.9). Interestingly, remaining alkynylhydrazone **5.34** did not react any more with the added rhodium catalyst, meaning that some species, which was more abundant than the rhodium catalyst, quenched the active rhodium catalyst.



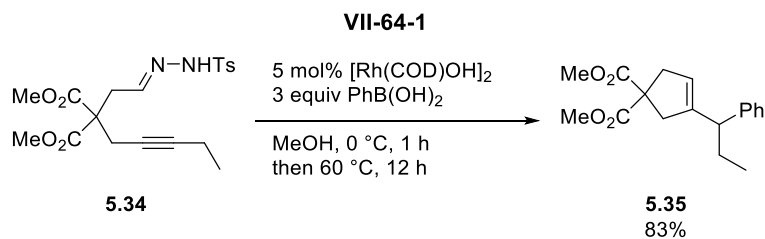
Scheme 5.9 The effect of added rhodium catalyst on tandem reaction

The reaction described in Scheme 5.9 showed that the active rhodium catalyst was trapped by a byproduct derived from the desired reaction. We thought that the highly acidic *p*-toluenesulfinic acid, which was a byproduct of elimination generating the allylic diazene intermediate (Scheme 5.10a), captured the active phenyl rhodium complex rapidly converting to inactive rhodium sulfinate complex **5.37** and benzene (Scheme 5.10b).²⁰



Scheme 5.10 The generation and the effect of *p*TolSO₂H on the rhodium catalyst

To avoid elimination of *p*-toluenesulfonic acid, we decreased the reaction temperature from room temperature to 0 °C. To our astonishment, the desired tandem addition–cyclization of alkynylhydrazone **5.34** proceeded readily in only an hour, giving rise to cyclic hydrazide intermediate **5.36** which was observed by TLC (Scheme 5.11). Heating the reaction mixture after the full conversion of the alkynylhydrazone led to elimination and rearrangement, giving cyclopentene **5.35** in high yield.

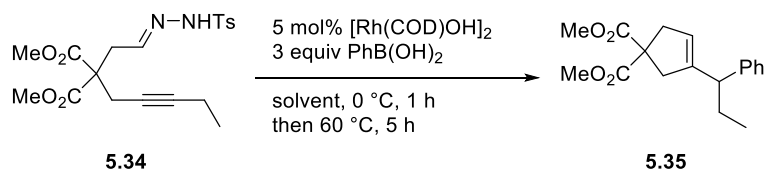


Scheme 5.11 The effect of temperature control on the Rh(I)-catalysis

5.2.2 Optimization of reaction conditions

With the preliminary reaction conditions in hand, the effect of the solvent was reexamined with a mixture of toluene and methanol that was found to be optimal (Table 5.2). In contrast to the reactions performed at room temperature, methanol solvent displayed much better result than toluene where a large portion of the alkynylhydrazone substrate remained unreacted. (Entry 1 vs 4).

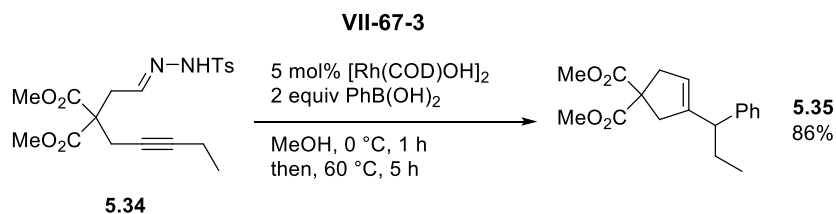
Table 5.2 Solvent screening with toluene and methanol



Exp. #	Entry	Solvent	Yield ^a
VII-71	1	toluene	46% ^b
VII-65-2	2	toluene/MeOH (1:1)	84%
VII-65-3	3	toluene/MeOH (1:3)	85%
VII-65-4	4	MeOH	84%

^aIsolated yield. ^bYield was determined by ¹H NMR using 1,3,5-trimethoxybenzene as an internal standard.

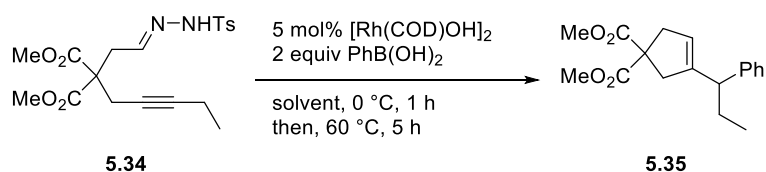
Because two equivalents of phenylboronic acid gave the yield similar to that with three equivalents, we used two equivalents of organoboronic acid for further studies (Scheme 5.12).



Scheme 5.12 Rh(I)-catalysis with two equivalents of phenylboronic acid

The additional screening of alcoholic solvents was conducted (Table 5.3). A series of alcohol solvents which could affect on each reaction step were evaluated, however, methanol proved to be the best solvent for the rhodium catalysis.

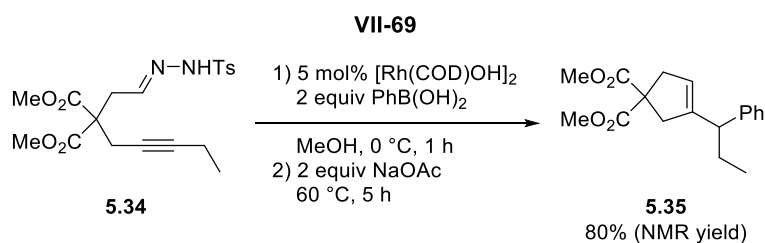
Table 5.3 Alcohol solvent screening



Exp. #	Entry	Solvent	Yield ^a
VII-67-3	1	MeOH	96%
VII-68-2	2	EtOH	43%
VII-68-3	3	<i>i</i> PrOH	21%
VII-68-4	4	CF ₃ CH ₂ OH	16%
VII-68-6	5	HFIP	-

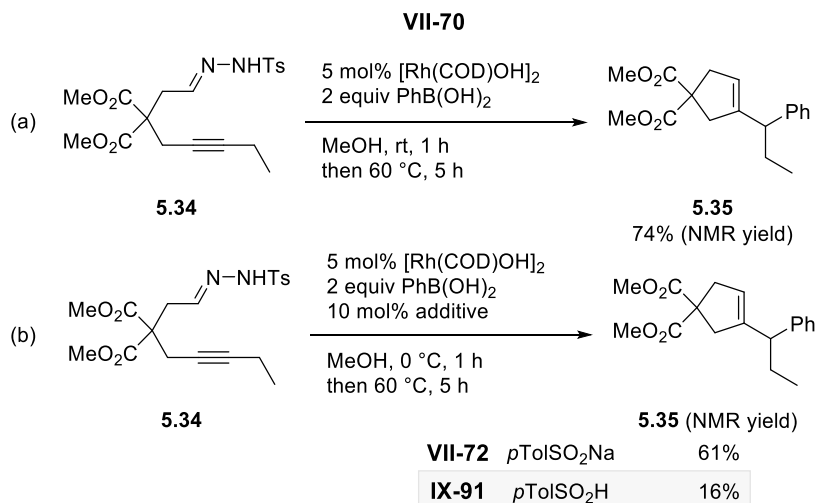
^aYields were determined by ¹H NMR using 1,3,5-trimethoxybenzene as an internal standard.

To facilitate elimination of *p*-toluenesulfonic acid from the cyclic hydrazide intermediate, we added sodium acetate before elevating reaction temperature (Scheme 5.13).²¹ In spite of the faster conversion rate of the cyclic hydrazide intermediate (in 3 h), the addition of sodium acetate resulted in a diminished yield of cyclopentene **5.35**.



Scheme 5.13 Addition of NaOAc after the Rh(I)-catalysis

We then set out to confirm the effects of temperature and the sulfonic acid under the optimized reaction conditions. In contrast with the observation of full conversion within an hour at 0 °C, the reaction conducted at room temperature gave unreacted alkynehydrazone **5.34** after the same reaction time (Scheme 5.14a). In the experiments with *p*-toluenesulfonic acid or its conjugated sodium base, the sulfonic acid suppressed the reaction, bringing about the color change of the reaction mixture from yellow to dark orange (Scheme 5.14b).

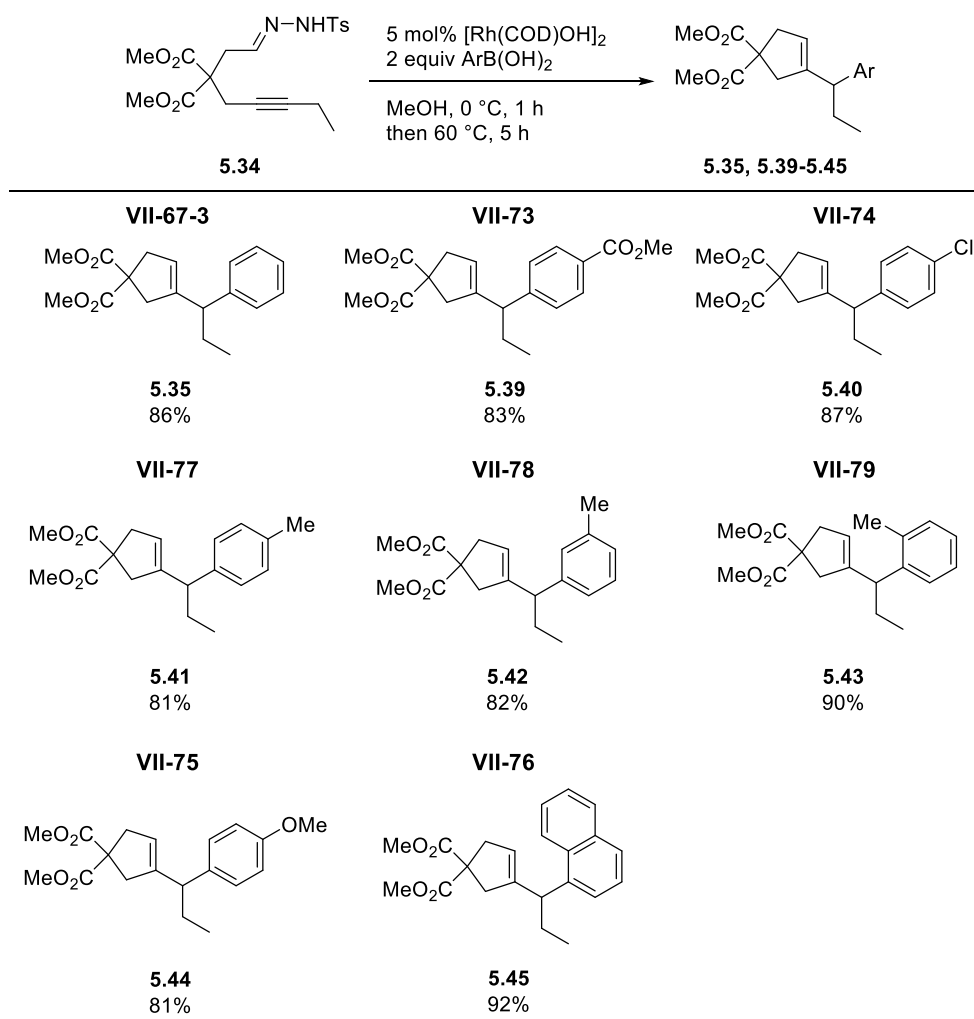


Scheme 5.14 Detrimental effects of reaction temperature and a sulfonic acid

5.2.3 Substrate scope of organoboronic acids

Having established the feasibility of the rhodium-catalyzed tandem addition–cyclization–rearrangement, we then set out to examine the scope of phenylboronic acid derivatives (Table 5.4). An array of phenylboronic acids bearing methyl ester (**5.39**), chloride (**5.40**), and methoxy (**5.41**) functional groups were proved to be competent participants in this reaction. In particular, arylboronic acids with an ortho-substituent (**5.43** and **5.45**) displayed increased yield of the corresponding cyclopentenes than other phenylboronic acids, suggesting that 1,4-rhodium shift might occur in the alkenyl rhodium intermediate before the addition to the C=N bond of the hydrazone.

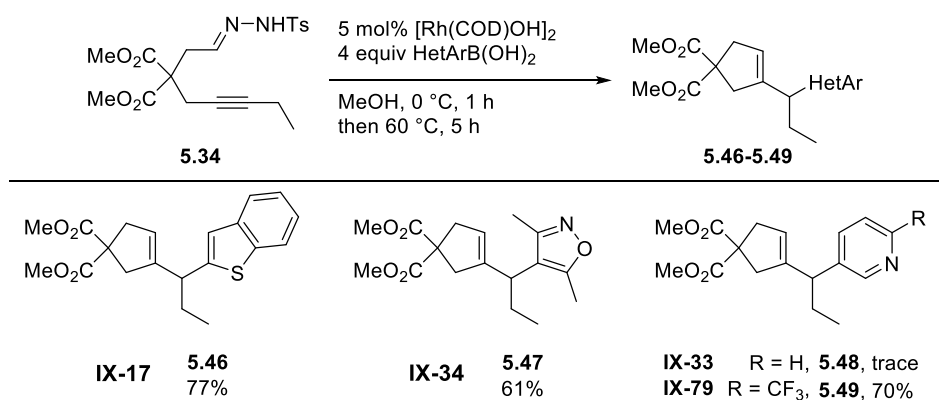
Table 5.4 The scope of phenylboronic acid derivatives



Reaction conditions: **5.34** (0.2 mmol), ArB(OH)₂ (0.4 mmol), and [Rh(COD)OH]₂ (0.01 mmol) in MeOH (2 ml). Isolated yield.

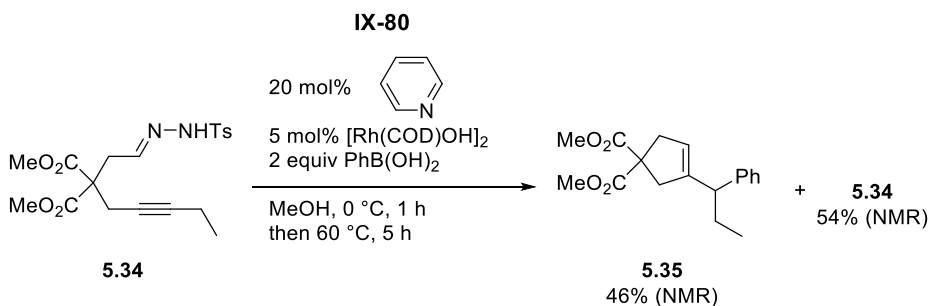
In the case of heteroarylboronic acids, the major problem was low yield and conversion due to their fast protodeborylation. For this reason, four equivalents of heteroarylboronic acids were used to obtain the corresponding cyclopentenes which have benzothiophene (**5.46**), isoxazoline (**5.47**), and substituted pyridine (**5.49**) (Table 5.5).

Table 5.5 The scope of heteroaryl boronic acids



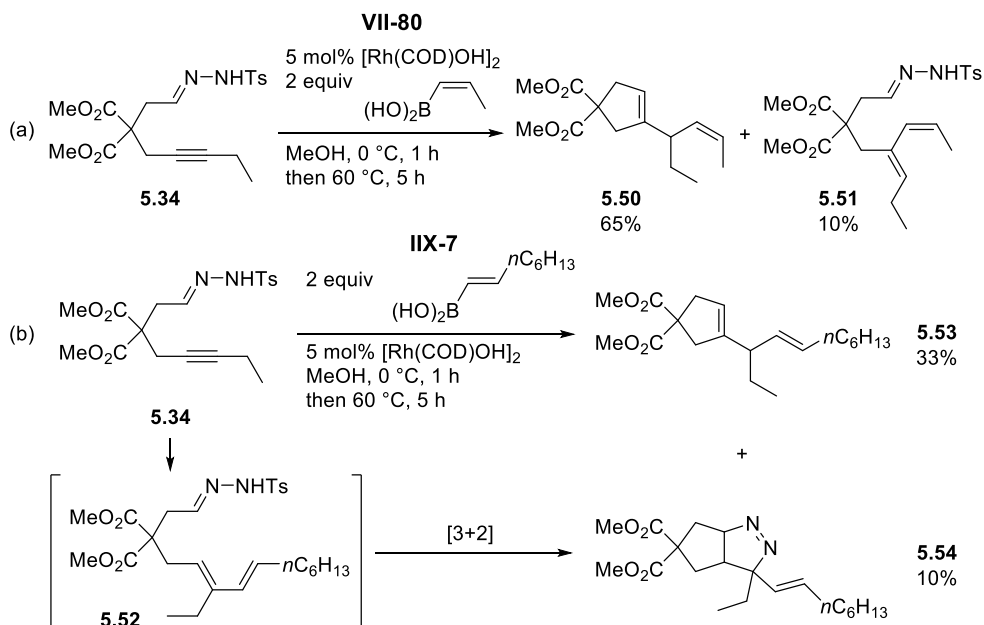
Reaction conditions: **5.34** (0.2 mmol), HetArB(OH)₂ (0.8 mmol), and [Rh(COD)OH]₂ (0.01 mmol) in MeOH (2 ml). Isolated yield.

One of the interesting features in Table 5.5 is that the unsubstituted 3-pyridinylboronic acid gave only a trace amount of the product. We carried out the experiment as described in Scheme 5.15 to identify the effect of pyridine byproduct from protodeborylation. In consequence, the addition of a catalytic amount of pyridine suppressed the reaction with phenylboronic acid. This result indicates that pyridine could occupy the vacant site of the active rhodium catalyst and suppress the coordination of the substrate, resulting in no further conversion.



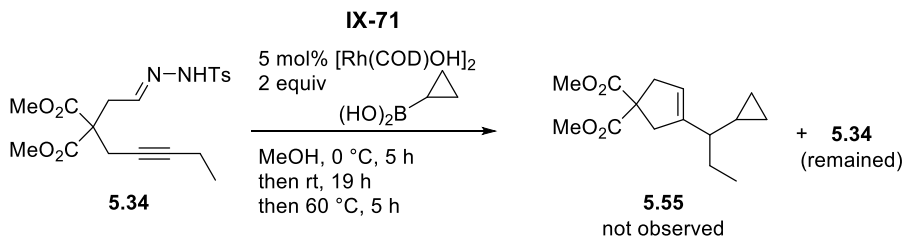
Scheme 5.15 Effect of the pyridine additive on the Rh(I)-catalysis

Alkenylboronic acids also participated in the rhodium-catalyzed tandem reaction (Scheme 5.16). When *cis*-propenyl boronic acid was used, formation of a 2:1 mixture of the desired cyclopentene **5.50** and hydroalkenylated hydrazone **5.51** which had inverted regioselectivity was observed in the ¹H NMR spectrum of a crude product. Interestingly, *trans*-octenyl boronic acid gave the desired product **5.53** in 33% yield and fused dihydropyrazole **5.54** in 10% yield (Scheme 5.16b). We thought that side product **5.54** was yielded from hydroalkenylated hydrazone **5.52** which might be derived from the 1,4-rhodium shift of the alkenyl rhodium intermediate followed by protoderhodation.



Scheme 5.16 The scope of alkenylboronic acids

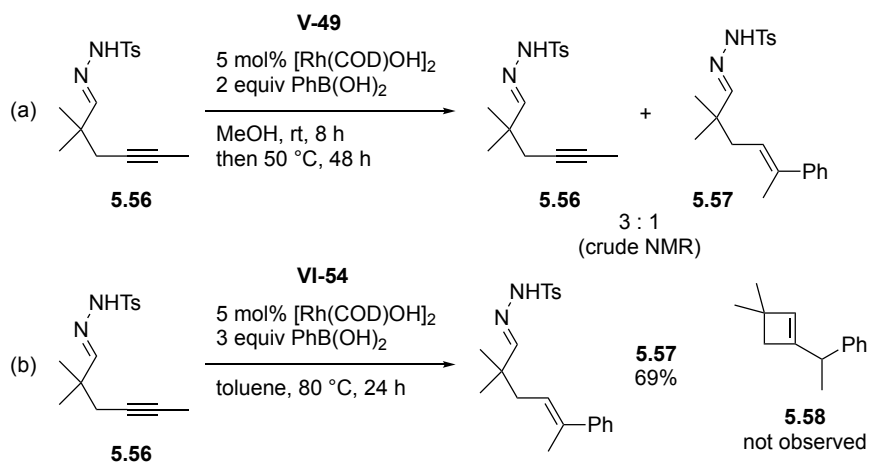
In contrast to the (hetero)aryl- and alkenylboronic acids, the cyclopropyl boronic acid did not give any desired product at all, leaving the unreacted alkynylhydrazone (Scheme 5.17).²²



Scheme 5.17 Results of the Rh(I)-catalysis with cyclopropylboronic acid

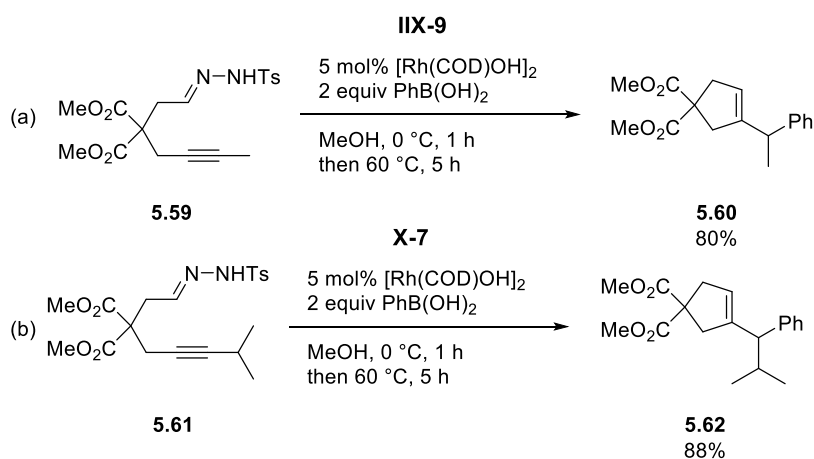
5.2.4 Substrate scope of alkynylhydrazones

The rhodium-catalyzed tandem reaction was further examined for the synthesis of cyclobutenes rather than cyclopentenes (Scheme 5.18). However, alkynylhydrazone **5.56** gave only simple hydroarylated product **5.57** even at an elevated temperature.



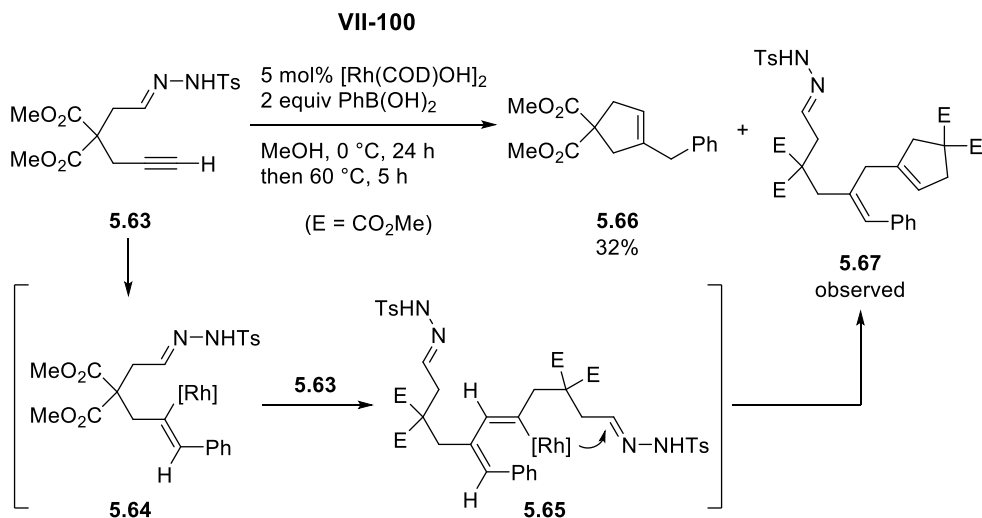
Scheme 5.18 Attempts for the synthesis of a 4-membered ring

As a variation of standard substrate **5.34**, sulfonylhydrazones tethered with methyl- (**5.59**) and isopropyl-substituted alkynes (**5.61**) were subjected to the standard conditions (Scheme 5.19). Both of the alkynylhydrazones proved to be viable substrates to give the corresponding cyclopentenes, not affected by the bulkiness of the substituent.



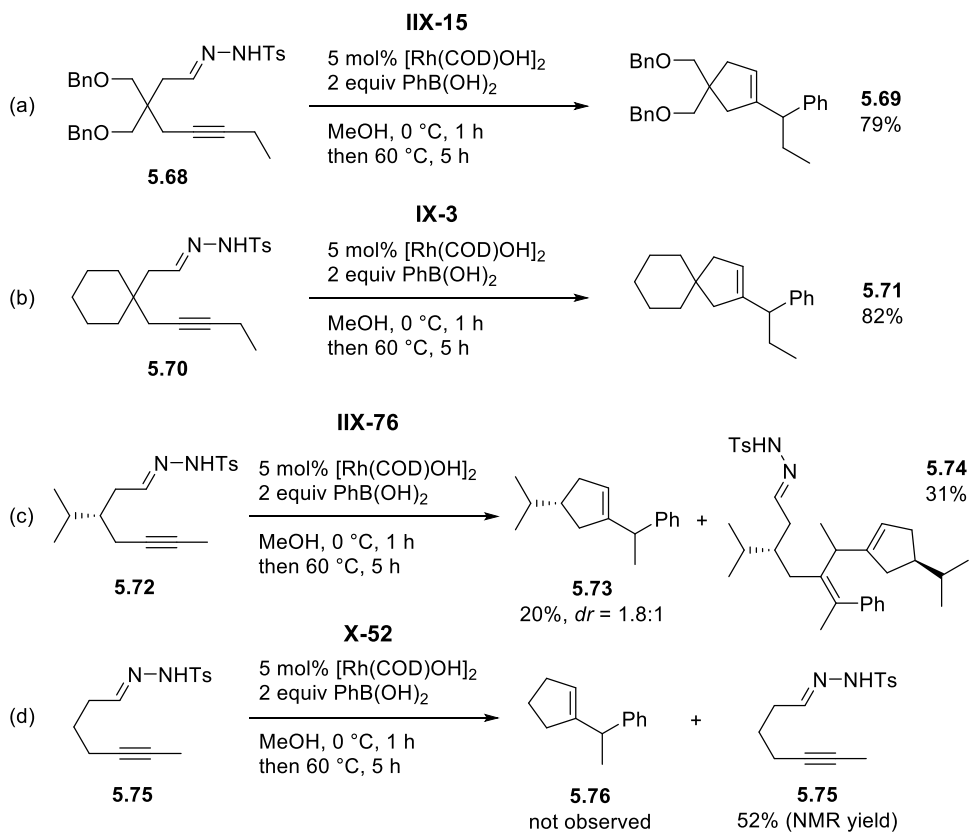
Scheme 5.19 Results of Me- and *i*Pr-substituted alkynylhydrazones

In case of the terminal alkyne-tethered *N*-tosylhydrazone **5.63**, it gave dimeric side product **5.67** via an intermolecular addition of **5.64** to **5.63** followed by concomitant cyclization (Scheme 5.20).²³



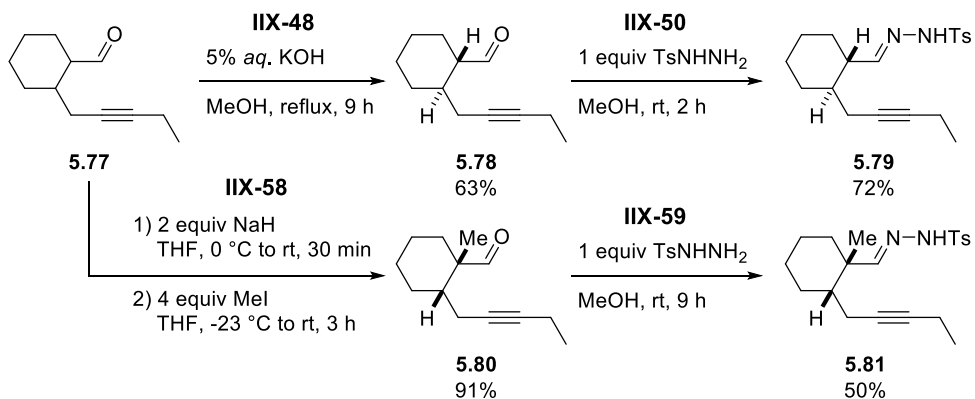
Scheme 5.20 Rh(I)-catalyzed tandem reactions of a terminal alkyne substrate

To identify the *gem*-dialkyl effect on the rhodium-catalyzed tandem addition–cyclization–rearrangement, alkynylhydrazones with different carbon tethers instead of the malonate were investigated (Scheme 5.21).²⁴ As we anticipated, the desired rhodium catalysis worked well with alkynyl hydrazones **5.68** and **5.70** regardless of the two substituents on the tether (Scheme 5.21a and 5.21b). However, monosubstituted substrate **5.72** gave only 20% yield of the desired cyclopentene **5.73** together with dimeric side product **5.74** as depicted in Scheme 5.20 (Scheme 5.21c). Furthermore, sulfonylhydrazone **5.75** derived from the unsubstituted 5-heptynal did not react at all, concluding that the *gem*-disubstituent effect was crucial in the rhodium-catalyzed tandem reactions (Scheme 5.21d).²⁵



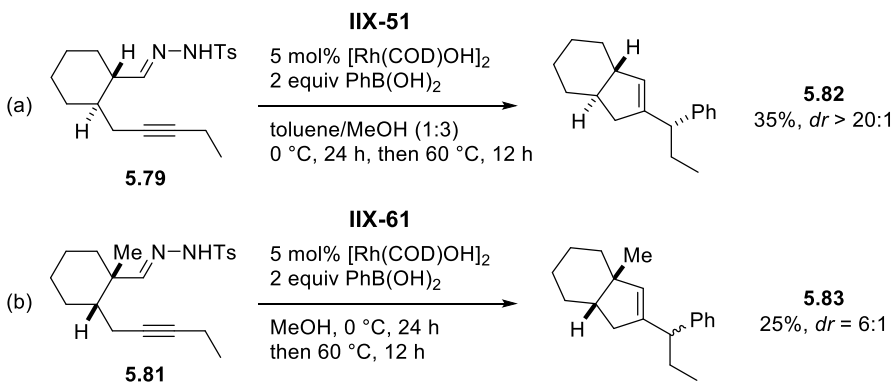
Scheme 5.21 The *gem*-disubstituent effects on the Rh(I)-catalysis

The substrate scope was further explored by using alkynylhydrazones that were bound to a cyclohexane to access fused-bicycles. Both of the cyclohexane-tethered alkynylhydrazones which have *trans*- (**5.79**) or *cis*-junction (**5.81**) were prepared by using thermodynamic equilibrium or kinetic methylation, respectively (Scheme 5.22).



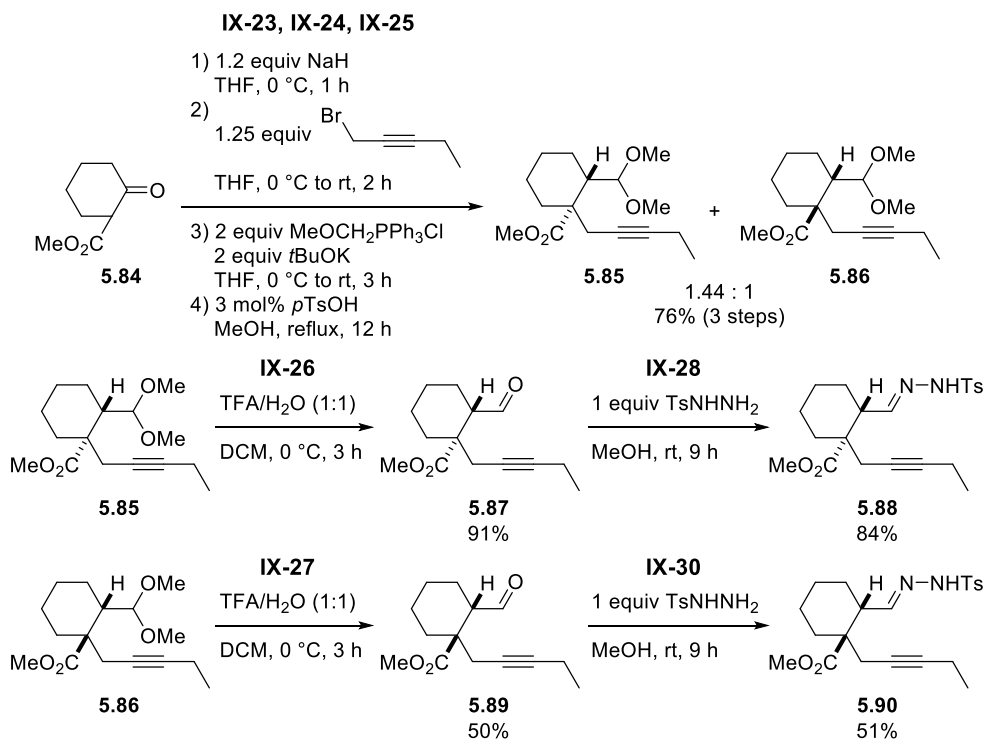
Scheme 5.22 Preparation of the cyclohexane-fused alkylnylhydrazones

Although *trans*-fused alkylnylhydrazone **5.79** provided corresponding fused-hydrindene **5.82** as a single diastereomer, the yield was only 35% (Scheme 5.23a). Similarly, *cis*-fused alkylnylhydrazone **5.81** gave *cis*-hydrindene **5.83** in low yield and moderate diastereoselectivity (Scheme 5.23b). The low yields of **5.82** and **5.83** would be derived from the *gem*-disubstituent effect as mentioned in Scheme 5.21c.



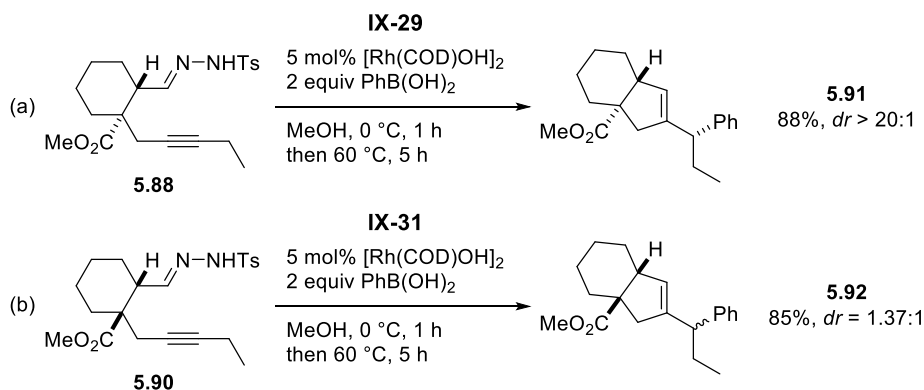
Scheme 5.23 Synthesis of the *trans*- or *cis*-hydrindenes

Then we tried to satisfy the requirement of the *gem*-disubstituent by putting an additional methyl carboxylate substituent on the tether (Scheme 5.24). Two diastereomeric alkynylacetal **5.85** and **5.86** were separated, and each of them was subjected to hydrolysis to obtain *trans*- (**5.88**) and *cis*-alkynylhydrazone (**5.90**).



Scheme 5.24 Synthesis of cyclohexane-fused alkynylhydrazones which have methyl carboxylate

As we anticipated, both **5.88** and **5.90** proved to be competent participants in the reaction to provide hydrindenes with stereospecificity similar to previous results (Scheme 5.25).



Scheme 5.25 Synthesis of the *trans*- and *cis*-hydrindenes which have methyl carboxylate

The different stereochemical outcomes derived from *trans*- and *cis*-junction indicated high stereospecificity of the cyclization step comprising the cascade process. A stereochemical model can be proposed to explain these stereospecificities during cyclization as illustrated in Figure 5.1. In the case of the alkenyl rhodium intermediate that has a *trans*-junction, the pseudoequatorial orientation of the *N*-sulfonylhydrazone group in **5.93** would be favorable than pseudoaxial one (**5.94**) due to its *syn*-pentane interaction with an axial methyl carboxylate. On the other hand, the steric hindrance occurred in both pseudoequatorial (**5.95**) and pseudoaxial orientation (**5.96**) of *cis*-fused alkenyl rhodium intermediates, bringing about a decrease of the energy difference and leading to low stereospecificity.

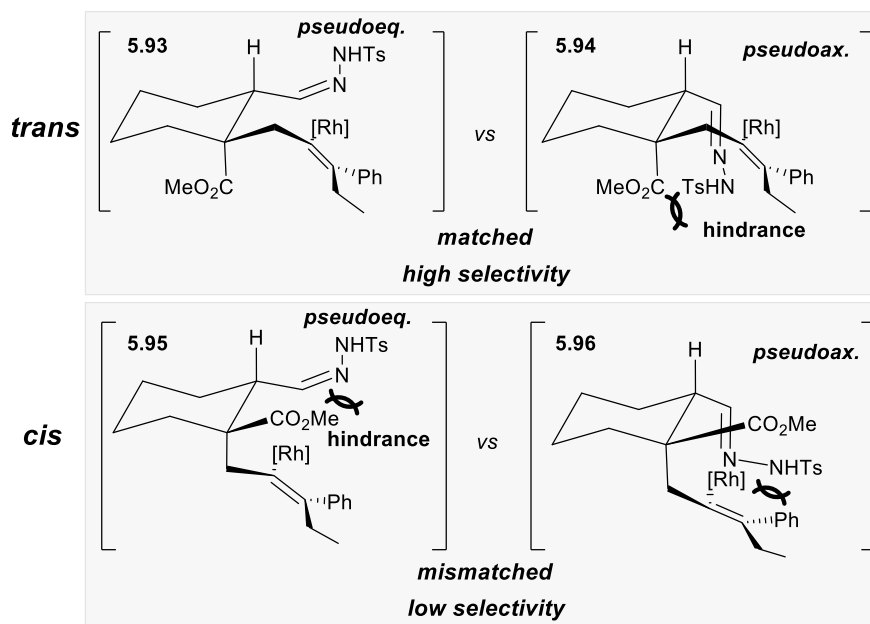
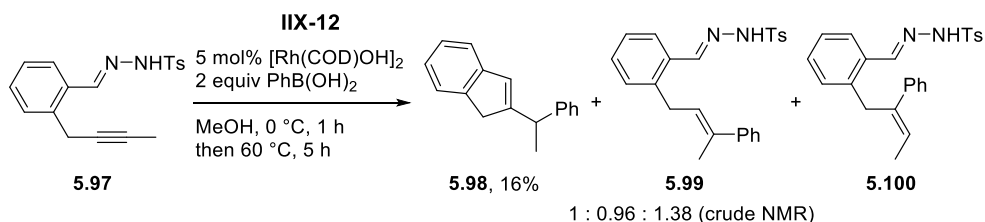


Figure 5.1 Stereochemical model for explanation of stereospecificity in hydride formations

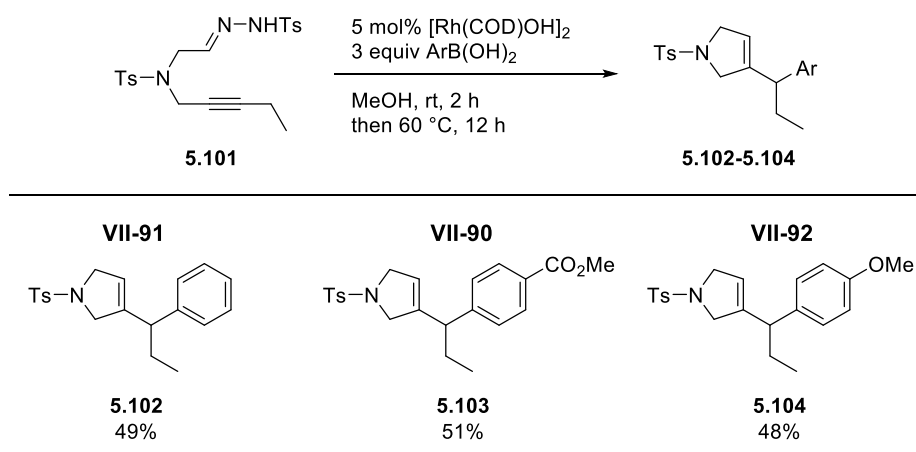
Alkynylhydrazone **5.97** derived from a benzaldehyde substrate was found to participate in the reaction (Scheme 5.26). However, it gave only 16% isolated yield of indene **5.98** and a regioisomeric mixture of hydroarylated hydrazones **5.99** and **5.100**.



Scheme 5.26 Synthesis of indene from a benzaldehyde hydrazone

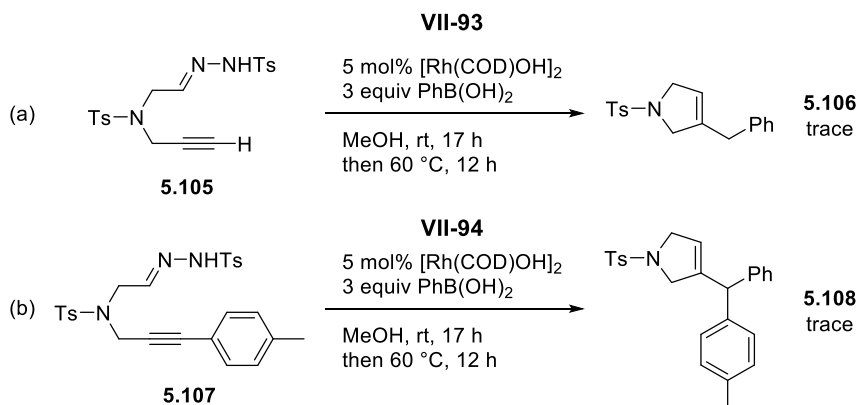
For the synthesis of heterocycles, we explored sulfonamide-tethered alkynylhydrazone **5.101** under the optimized reaction conditions. However, a slower reaction rate than that of carbon-tethered substrates left substrate **5.101** unreacted (2 equivalents of PhB(OH)₂ at 0 °C). Fortunately, elimination of the sulfinic acid from the cyclic hydrazone intermediate, which was a major problem of catalytic dead end, also slower than that of carbocyclic hydrazone **5.36**. Finally, we elevated the temperature from 0 °C to room temperature and used three equivalents of phenylboronic acid to achieve full conversion of the substrate (Table 5.6). Although the pyrroline formation was less efficient than cyclopentenes, a series of phenylboronic acids possessing different substituent could participate in this reaction to afford the corresponding heterocycles.^{26,27}

Table 5.6 The scope of phenylboronic acids with a TsN-tethered substrate



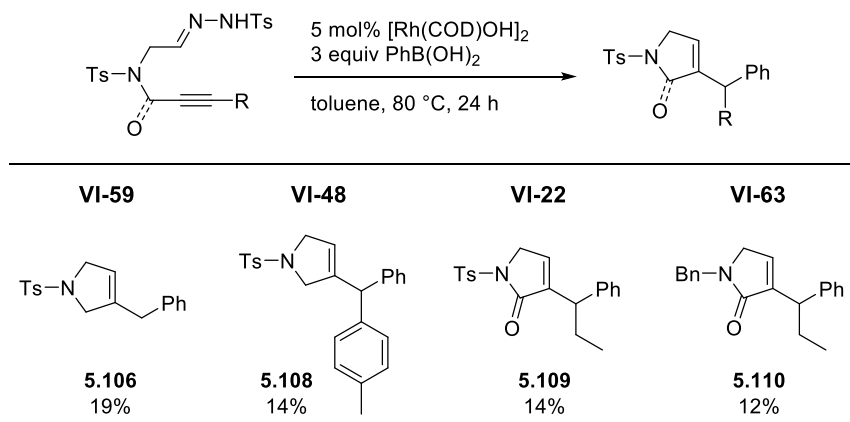
Reaction conditions: **5.101** (0.2 mmol), ArB(OH)₂ (0.6 mmol), and [Rh(COD)OH]₂ (0.01 mmol) in MeOH (2 ml). Isolated yield.

In contrast to alkynylhydrazone **5.101**, sulfonamide-tethered terminal alkyne (**5.105**) or aryl alkyne (**5.107**) gave trace amounts of the desired products **5.106** and **5.108** (Scheme 5.27). These results were possibly due to low solubility of the substrates in methanol, and their low innate reactivity in cyclization (**5.105**) or initial carbometalation (**5.107**).



Scheme 5.27 Results from TsN-tethered substrates possessing terminal or aryl alkyne

With the observation of slow elimination of the sulfinic acid, we used less polar toluene solvent under a higher temperature to facilitate cyclization and inhibit elimination simultaneously. Even though there was no significant improvement, we could access pyrrolines **5.106** and **5.108** as well as TsN- and BnN-tethered pyrrolinones **5.109** and **5.110** (Table 5.7).

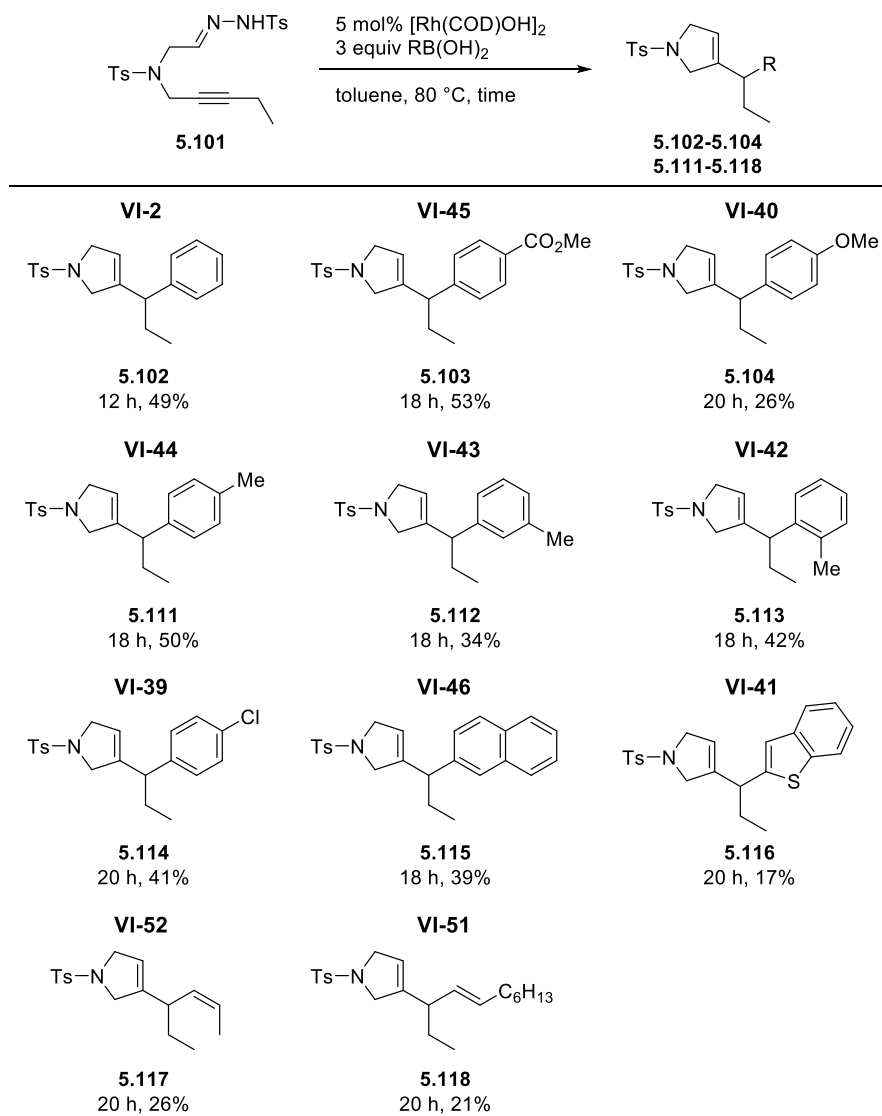
Table 5.7 Pyrroline and pyrrolinone synthesis by Rh(I)-catalysis

Reaction conditions: Alkynylhydrazone (0.2 mmol), ArB(OH)₂ (0.6 mmol), and [Rh(COD)OH]₂ (0.01 mmol) in MeOH (2 ml). Isolated yield.

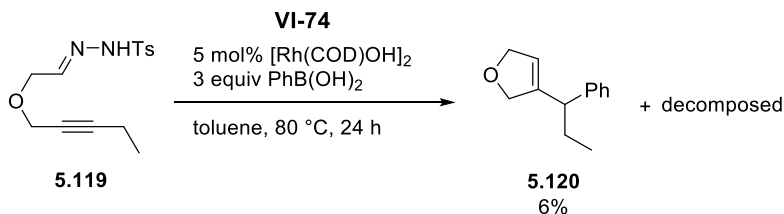
Since running the reaction in toluene at 80 °C gave better results for sulfonamide-tethered alkynylhydrazones, we conducted tandem cyclization again with various organoboronic acids (Table 5.8). However, although no unreacted substrate or side product was detected, no improvement of yield was observed on the standard conditions as depicted in Table 5.6. The exact reason for the low yields of the reactions with sulfonamide-tethered hydrazones remained elusive, except for the observation that these substrates required longer reaction times.

Alkynylhydrazone **5.119** possessing an ether linkage did not react under methanolic conditions and gave the desired dihydrofuran **5.120** only in 6% yield when it was subjected to toluene heating conditions (Scheme 5.28).

Table 5.8 The scope of organoboronic acids with **5.101** under modified conditions

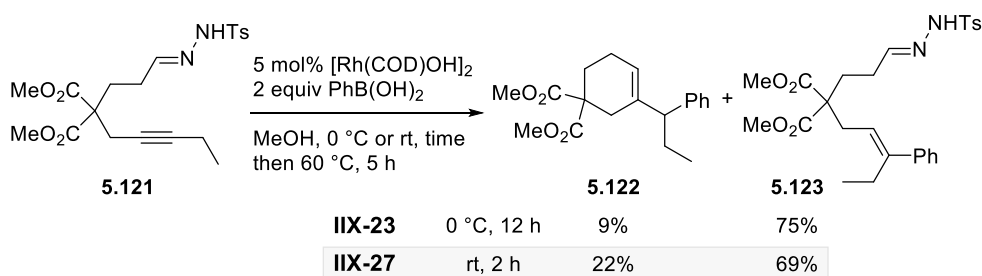


Reaction conditions: **5.101** (0.2 mmol), RB(OH)_2 (0.6 mmol), and $[\text{Rh(COD)OH}]_2$ (0.01 mmol) in toluene (2 ml). Isolated yield.



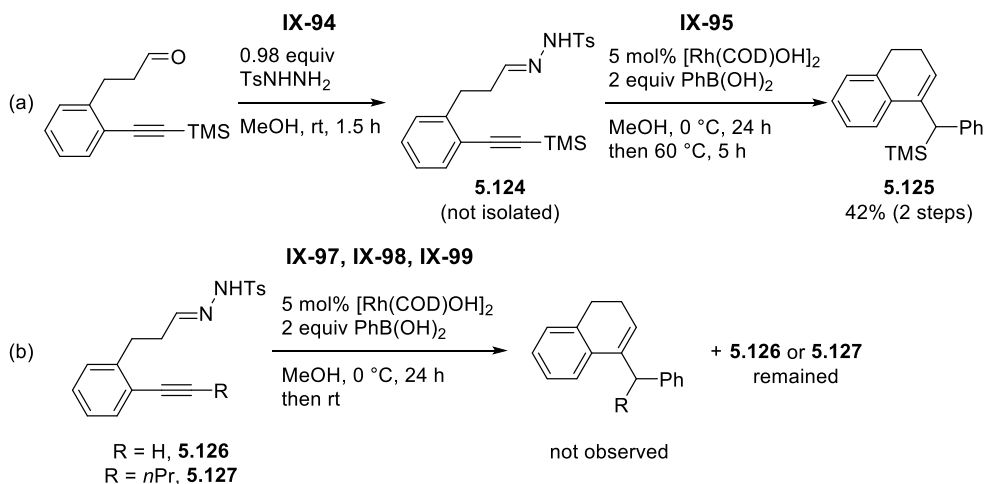
Scheme 5.28 Synthesis of a dihydrofuran

Synthesis of cyclohexene **5.122** was unfruitful as the reaction of alkynylhydrazone **5.121** gave poor results (Scheme 5.29). With this substrate the major side pathway was protodemetalation of the alkenyl rhodium intermediate, more challenging to cyclize, giving rise to alkenylhydrazone **5.123** in moderate yield. To overcome the product selectivity between cyclohexene **5.122** and side product **5.123**, we elevated the reaction temperature to room temperature. However, the hydroarylated hydrazone **5.123** was obtained as the major product along with only 22% yield of the desired cyclohexene **5.122**.



Scheme 5.29 Synthesis of a cyclohexene and undesired hydroarylation

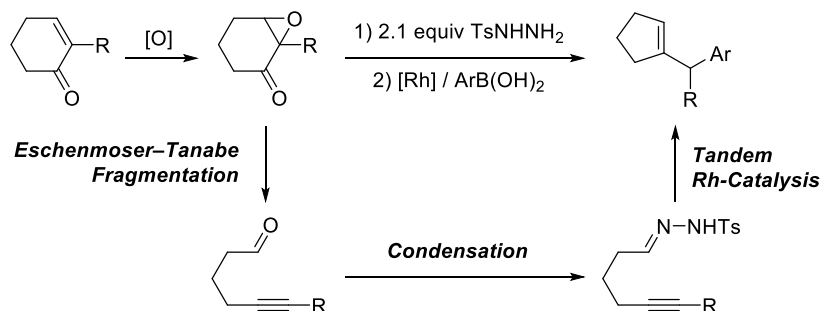
Alkynylhydrazone **5.124**, derived from an aryl-tethered aldehyde *in situ*, was a viable participant of the rhodium-catalyzed tandem reaction (Scheme 5.30). Interestingly, the reaction was dependent on the substituent of an ethynyl group. Only the trimethylsilyl-substituted alkyne gave the desired benzene-fused cyclohexene **5.125**, whereas terminal (**5.126**) and *n*-propyl (**5.127**) alkynes did not react.



Scheme 5.30 Synthesis of a dihydronaphthalene

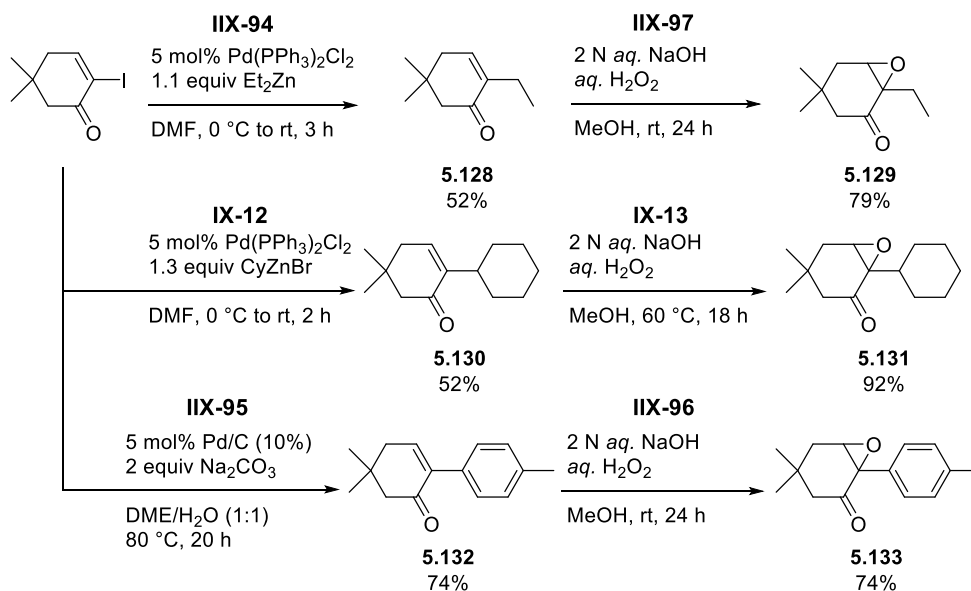
5.2.5 Arylative ring contraction of cyclohexenones

One of the general methods for the synthesis of alkynals is the Eschenmoser–Tanabe fragmentation.²⁸ These alkynals are precursors of alkynylhydrazones, which were the substrate for the rhodium catalysis. To expand the utility of the rhodium-catalyzed tandem addition–cyclization–rearrangement, we examined the possibility of developing an efficient ring-size alteration strategy of cyclohexenes to cyclopentenes by channeling the reaction with the Eschenmoser–Tanabe fragmentation. As described in Scheme 5.31, treatment of an α,β -epoxyketone derived from a cyclohexenone with two equivalents of *p*-toluene sulfonyl hydrazide was expected to afford the alkynylhydrazone *via* fragmentation and *in situ* condensation of the resulting aldehyde. The rhodium-catalyzed cascade process could then furnish cyclopentenes with the introduction of aryl group from arylboronic acids.



Scheme 5.31 Arylative ring contraction of cyclohexenones

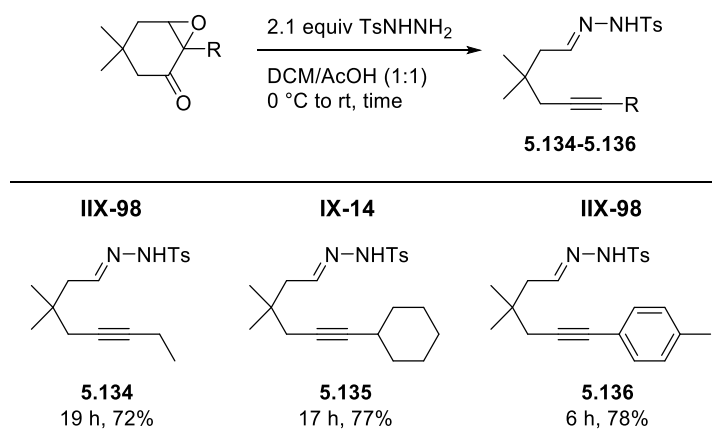
We initiated our studies with the preparation of a series of α,β -epoxyketones (Scheme 5.32). From the iodocyclohexenone, the palladium-catalyzed cross-coupling followed by nucleophilic oxidation gave corresponding primary alkyl- (**5.129**), secondary alkyl- (**5.131**), and aryl- (**5.133**) substituted epoxyketones in good yields.



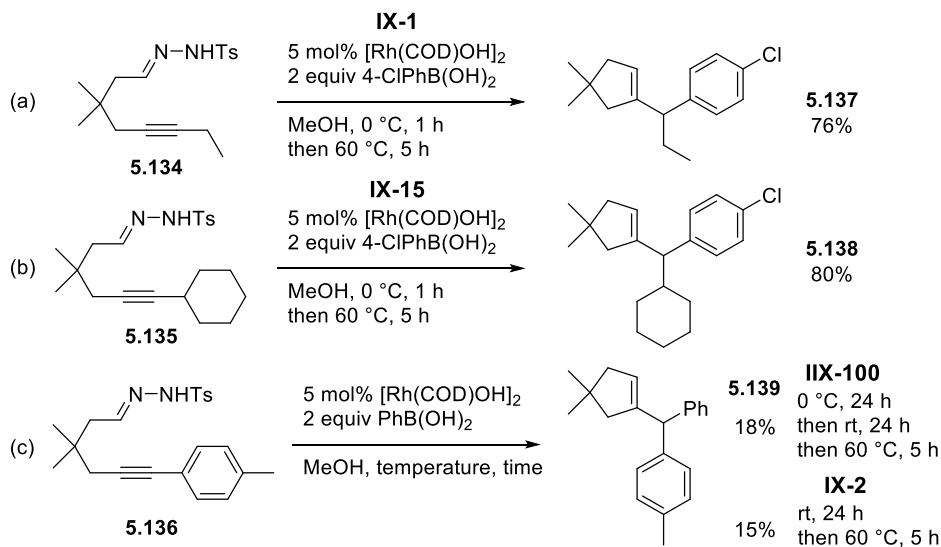
Scheme 5.32 Synthesis of α,β -epoxyketones

The tandem Eschenmoser–Tanabe fragmentation–condensation of α,β -epoxyketones cleanly provided the corresponding alkynylhydrazones in moderate yield regardless of the substituents (Table 5.9).

Table 5.9 Tandem fragmentation–condensation of α,β -epoxyketones



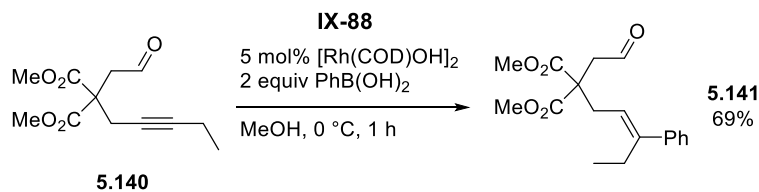
Having the alkynylhydrazones from the tandem fragmentation–condensation in hand, we conducted the rhodium-catalyzed arylation cyclizations using these alkynylhydrazones. When the alkyl-substituted alkynes with a pendent sulfonylhydrazone were used as a substrate, the desired cyclopentenes **5.137** and **5.138** were produced in good yield (Scheme 5.33a and 5.33b). However, the reaction of *N*-sulfonylhydrazone **5.136** tethered with a toluene-substituted alkyne gave the product only in 18% yield (Scheme 5.33c). It was probably due to the inverse 1,2-carbometalation preference as dealt with in Chapter 3.²⁹



Scheme 5.33 Rh(I)-catalyzed arylation cyclization of alkynylhydrazones derived from α,β -epoxyketones

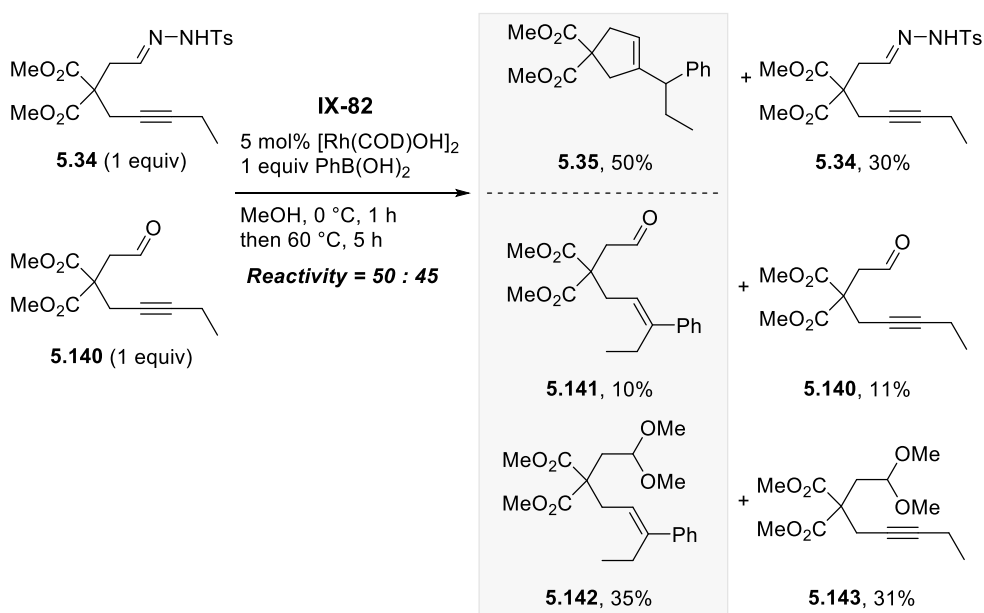
5.2.6 Competition experiment with alkynylaldehyde

The initial studies of the rhodium-catalyzed tandem addition–cyclization were focused on the identification of unsaturated carbon–heteroatom bonds that could capture the alkenyl rhodium intermediate. In particular, the alkynylaldehyde was one of the substrates subjected to the rhodium-catalyzed tandem process.³⁰ To understand an intrinsic reactivity of the alkynyl hydrazones, we evaluated the relative reactivity of the alkynylhydrazone using the alkynal as a reference substrate. Before comparing their reactivity, we exposed alkynal **5.140** to the standard reaction conditions for the alkynylhydrazones (Scheme 5.34). Surprisingly, alkynal **5.140** gave hydroarylated hydrazone **5.141**, not an arylation cyclization product, meaning that the aldehyde was not engaged in the cyclization reaction at 0 °C.



Scheme 5.34 Rh(I)-catalyzed hydroarylation of an alkynyl

Using phenylboronic acid as a limiting reagent, we then carried out a competition experiment between alkynylhydrazone **5.34** and alkynyl **5.140** (Scheme 5.35). Alkynylhydrazone **5.34** displayed slightly better reactivity than alkynyl **5.140** in reacting with the phenylrhodium complex (cf. **5.38** in Scheme 5.10). In summary, in the rhodium-catalyzed cascade processes, a *N*-tosylhydrazone is more reactive than an aldehyde in terms of both initial carbometalation and cyclization with the alkenyl rhodium intermediate.



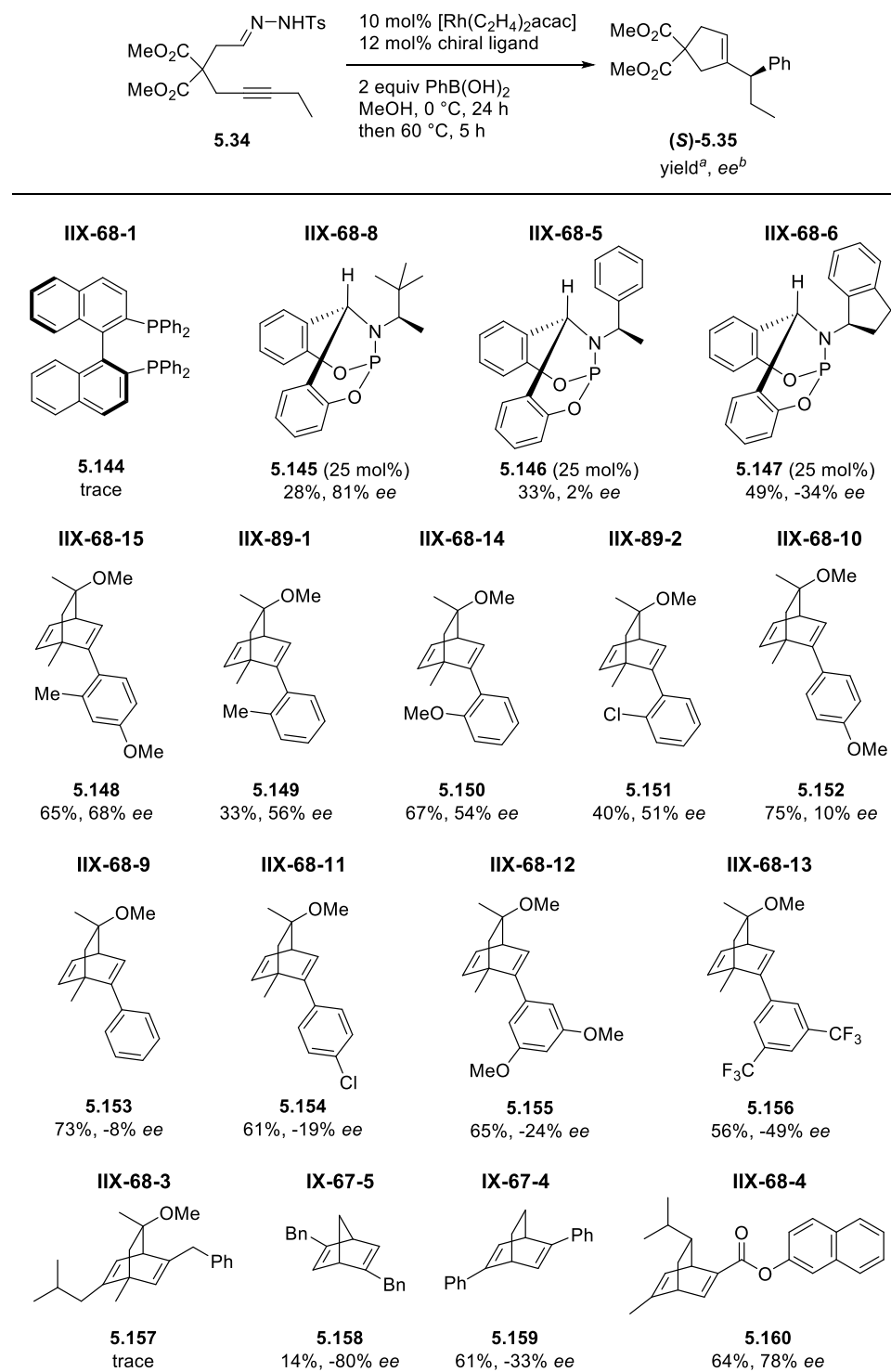
Scheme 5.35 Competition experiment between an alkynylhydrazone and an alkynylaldehyde

5.2.7 Asymmetric carbocyclization of alkynylhydrazones

Our investigations moved on to the development of an enantioselective variant of the rhodium-catalyzed tandem process. To establish the C–N stereocenter asymmetrically, the use of chiral ligands in place of COD was expected to induce enantioselective addition of the alkenyl rhodium intermediate to the C=N bond of the hydrazone.³¹ Subsequently, elimination of the sulfinic acid from the chiral cyclic hydrazide would generate the allylic diazene intermediate which could undergo stereospecific rearrangement leading to the cyclopentenones attached with a secondary-alkyl stereocenter.

The preliminary studies for the asymmetric induction were conducted in methanol solvent with [Rh(C₂H₄)acac] precatalyst and a series of chiral ligands as described in Table 5.10. In the case of chiral phosphine ligands, although all of them showed low yields of the desired product, BRIPHOS ligand **5.145** gave moderate enantioselectivity of the (*S*)-**5.35**.^{32,33} After further screening experiments with a number of chiral diene ligands, however, we concluded that improvement of the enantioselectivity over 90% *ee* was difficult to achieve under this reaction conditions.

Table 5.10 Enantioselective Rh(I)-catalysis in methanol solvent

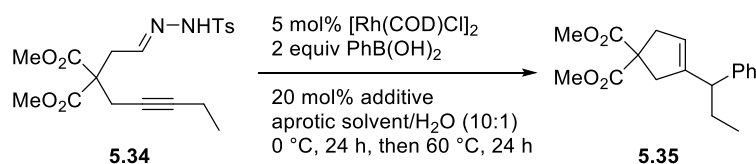


^aReaction conditions: **5.34** (0.1 mmol), $\text{PhB}(\text{OH})_2$ (0.2 mmol), $[\text{Rh}(\text{C}_2\text{H}_4)_2\text{acac}]$ (0.01 mmol), and chiral ligand (0.012 mmol) in MeOH (1 ml). Isolated yield.

^bEnantiomeric excess determined by chiral HPLC.

The hydrogen bonding interaction between the *N*-sulfonylhydrazone moiety and methanol was suspected to prohibit enantioselective addition. Aqueous aprotic solvents were employed with a catalytic amount of a base additive to suppress the undesired hydrogen bonding network (Table 5.11). Fortunately, toluene and aqueous potassium hydroxide solution with [Rh(COD)Cl]₂ catalyst proved to be the most effective in producing the desired product.

Table 5.11 Condition optimization using aqueous aprotic solvent



Exp. #	Entry	Solvent	Additive	Yield
X-13-1	1	toluene	Et ₃ N	n.d.
X-13-2	2	toluene	0.2 N KOH	84%
X-13-3	3	toluene	0.2 N K ₂ CO ₃	80%
X-13-4	4	toluene	0.2 N KHCO ₃	82%
X-13-13	5	toluene	0.2 N NaHCO ₃	81%
X-13-5~8	6-9	1,4-dioxane (rt)	as in entry 1-4	SM remained
X-13-9~12	10-13	THF	as in entry 1-4	SM remained

Reaction conditions: **5.34** (0.1 mmol), PhB(OH)₂ (0.2 mmol), [Rh(COD)Cl]₂ (0.05 mmol), and additive (0.02 mmol) in solvent. Isolated yield. n.d. = not determined

Additional screening experiments were carried out with chiral ligands under the optimized reaction conditions in toluene solvent (Table 5.12). In general, fluctuations of yield and *ee* were observed with most of the ligands. Interestingly, chiral diene **5.160**, which gave 64% yield and 78% *ee* in methanol, showed quite improved results (66% yield, 85% *ee*). Further optimization of the substituents resulted in the formation of the desired product (*S*)-**5.35** in the highest *ee* of 92% and good yield, when chiral diene **5.164** was used for the rhodium catalyst.³⁴

To improve both yield and enantioselectivity, we then set out to make a rhodium-chiral diene complex instead of mixing the precatalyst and the ligand before the reaction. Although the rhodium-chiral diene complex **5.165** was prepared in low yield, it gave rise to slightly improved results in both yield and enantioselectivity (Scheme 5.36).

Table 5.12 Enantioselective Rh(I)-catalysis in aqueous toluene solvent

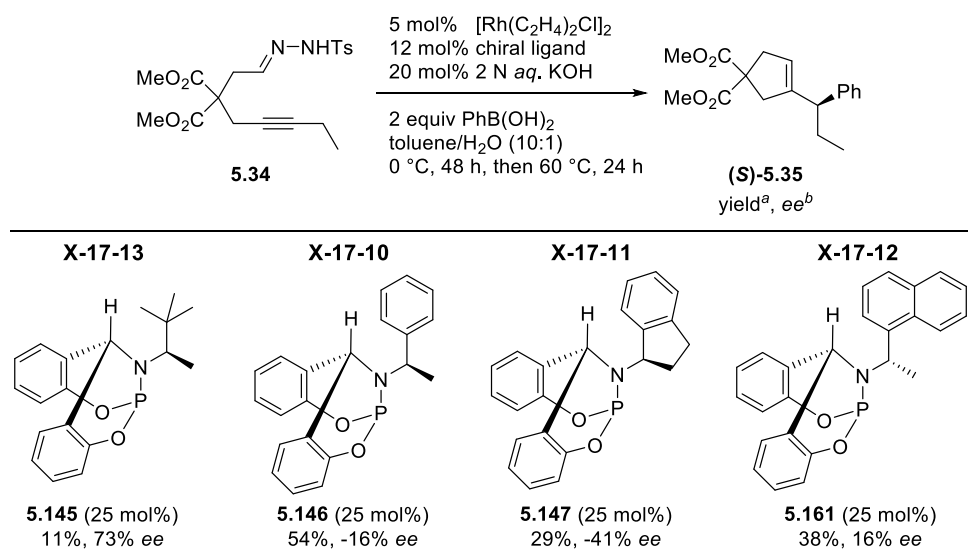
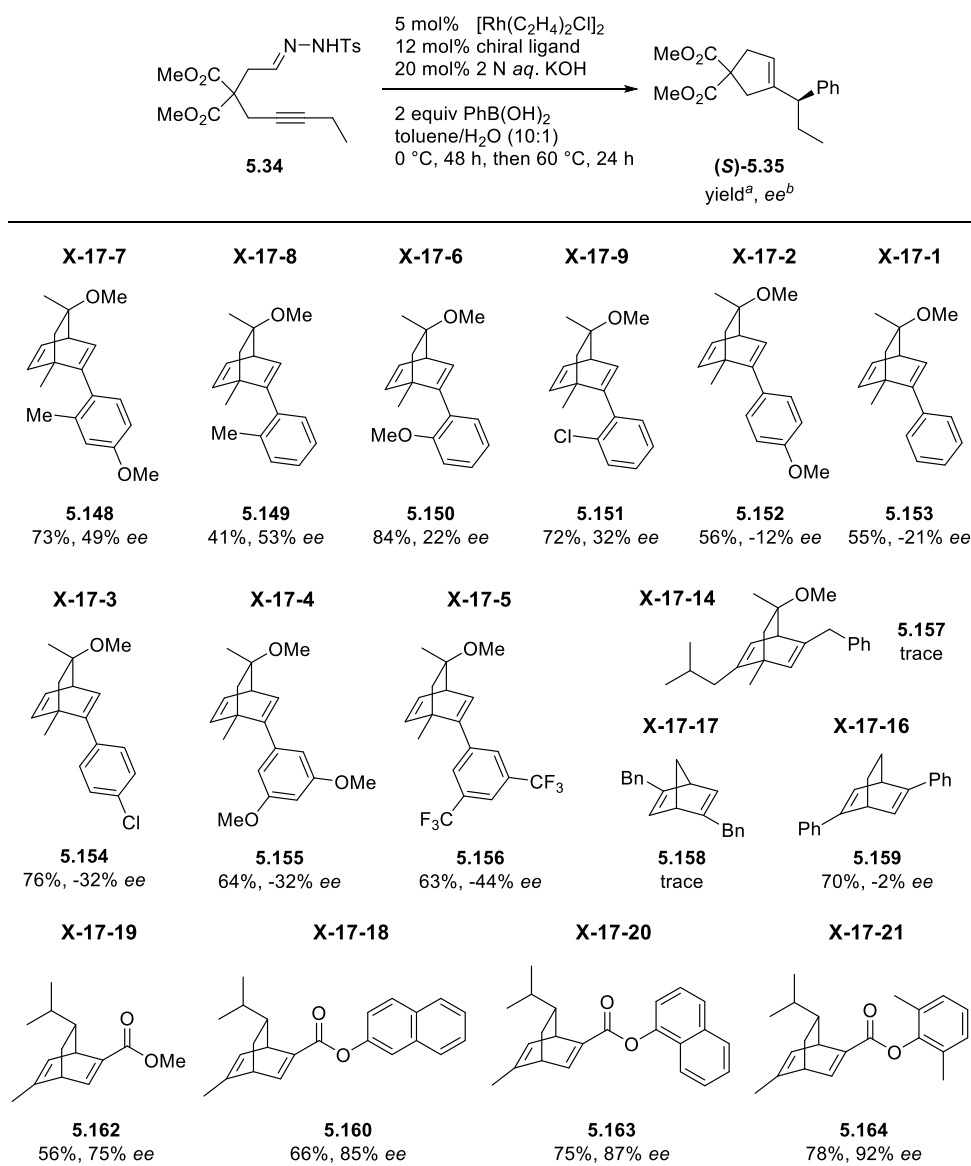
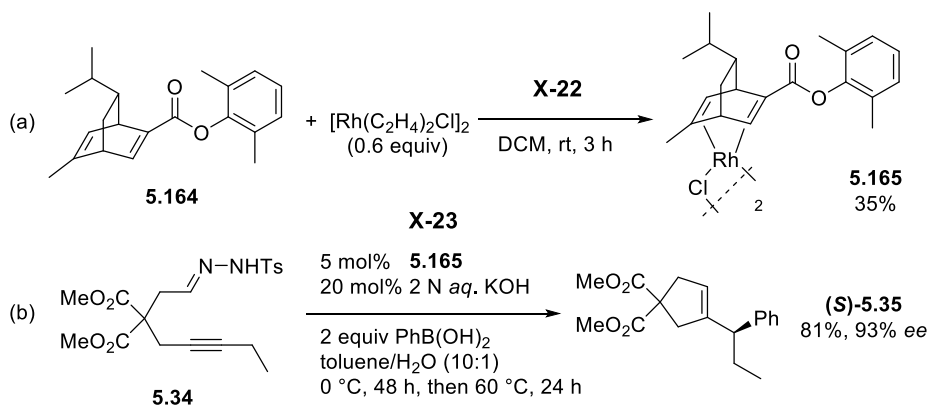


Table 5.12 (Continued)



^aReaction conditions: **5.34** (0.1 mmol), $\text{PhB}(\text{OH})_2$ (0.2 mmol), $[\text{Rh}(\text{C}_2\text{H}_4)_2\text{acac}]$ (0.01 mmol), and chiral ligand (0.012 mmol) in MeOH (1 ml). Isolated yield.

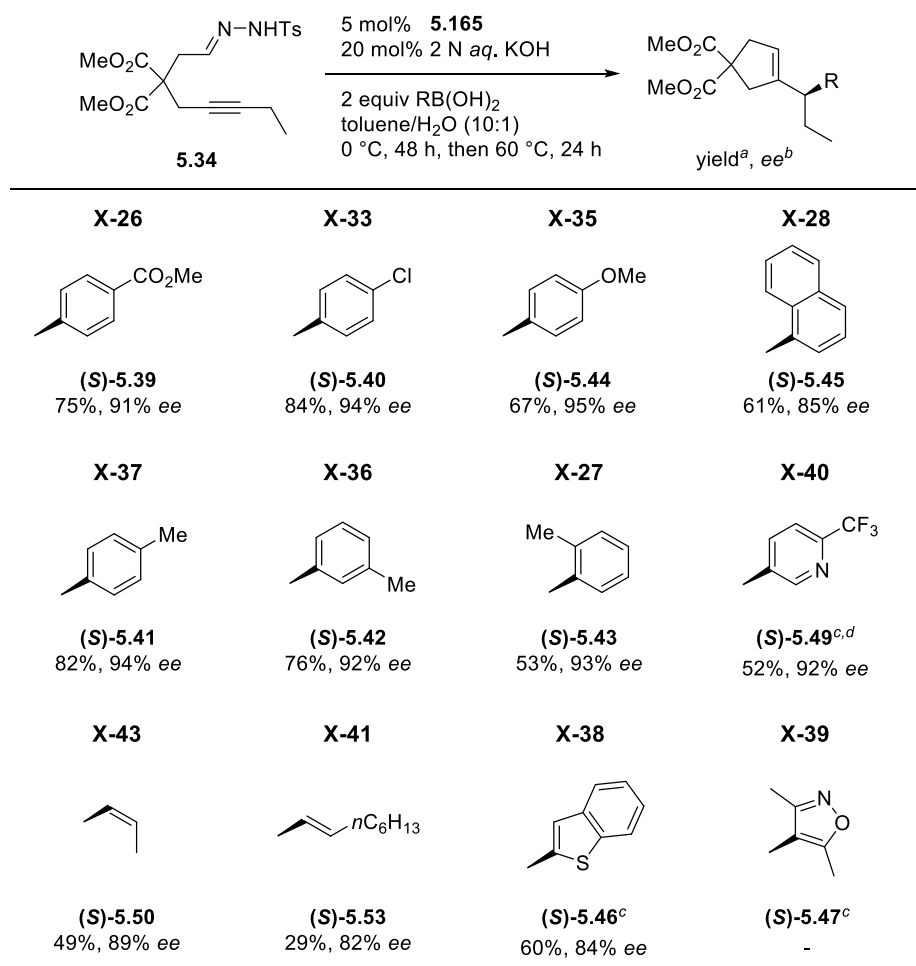
^bEnantiomeric excess determined by chiral HPLC.



Scheme 5.36 Preparation of the rhodium-diene complex and its performance in the Rh(I)-catalysis

Having the established reaction conditions for the asymmetric variation, the rhodium-catalyzed enantioselective cascade was further examined using a variety of organoboronic acids (Table 5.13). In most cases, the reaction using the rhodium-diene complex **5.165** gave the corresponding chiral cyclopentenes with high enantioselectivity regardless of both steric and electronic variation in the arylboronic acids. Although the reactions with the organoboronic acids possessing 1-naphthyl and alkenyl groups gave slightly lower enantioselectivity than those of the others, a high level of enantioselectivity was maintained. In the case of heteroaryl boronic acids, the enantioselective reactions proceeded well except for 3,5-dimethyl-4-isoxazolylboronic acid which did not give desired product **5.47** at all.

Table 5.13 The scope of the Rh(I)-catalyzed asymmetric tandem addition–cyclization–rearrangement with organoboronic acids



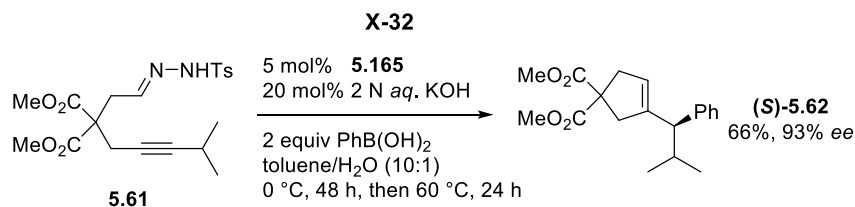
^aReaction conditions: **5.34** (0.1 mmol), RB(OH)₂ (0.2 mmol), **5.165** (0.005 mmol), and 2 N KOH (0.02 mmol) in aqueous toluene (1 ml). Isolated yield.

^bEnantiomeric excess determined by chiral HPLC and/or ¹H NMR shift experiment.

^c4 equiv of organoboronic acid.

^dToluene/MeOH/H₂O (8:2:1) solvent.

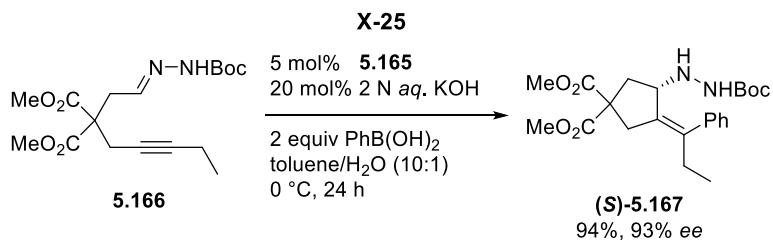
An additional experiment to expand the scope of the alkyne was performed with *N*-tosylhydrazone **5.61** possessing an isopropyl substituent at the alkyne. Under the optimized conditions, (*S*)-**5.62** was obtained in good yield and excellent enantioselectivity (Scheme 5.37).



Scheme 5.37 Rh(I)-catalyzed asymmetric tandem reaction of an *iPr*-substituted alkynylhydrazone

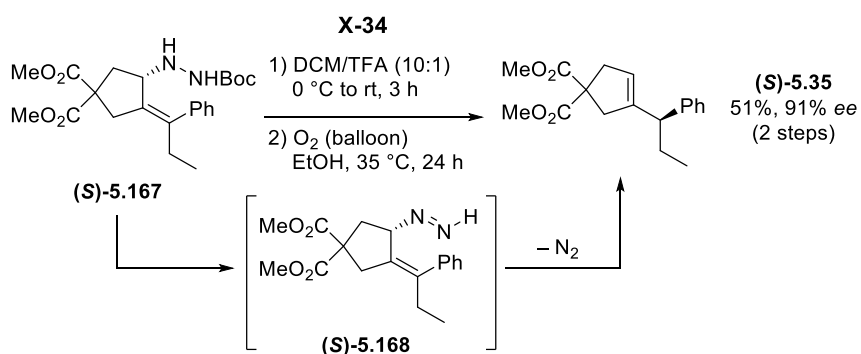
5.2.8 Mechanistic studies

To elucidate the reaction mechanism, we initially focused on the isolation of cyclic hydrazone intermediate **5.36** from alkynylhydrazone **5.34**. Unfortunately, cyclic *N*-tosyl hydrazone intermediate **5.36** was too unstable to be isolated by flash column chromatography. Thus, we tried to access *N*-Boc protected cyclic hydrazone **5.167** which could not undergo elimination to generate the allylic diazene (Scheme 5.38). Using rhodium-chiral diene complex **5.165**, the reaction of alkynyl *N*-Boc-hydrazone **5.166** with phenylboronic acid gave allylic carbazate **5.167** in high yield and enantioselectivity.



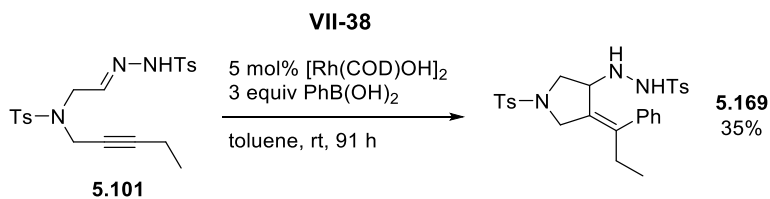
Scheme 5.38 Rh(I)-catalyzed asymmetric arylation and cyclization of an alkynyl *N*-Boc-hydrazone

The cyclic hydrazide **5.167** was subjected to deprotection and aerobic oxidation to obtain cyclopentene **5.35** maintaining high enantiomeric excess (Scheme 5.39). The product had the same (*S*)-configuration as that arising from the enantioselective reaction of alkynyl *N*-Ts-hydrazone **5.34** using the same catalyst. These results described in Scheme 5.38 and 5.39 indicate that the rhodium catalyst mediates tandem arylation cyclization *via* the alkenyl rhodium intermediate, and the resulting cyclic hydrazide undergoes elimination of the sulfinic acid followed by the allylic diazene rearrangement to give the endocyclic alkene product.



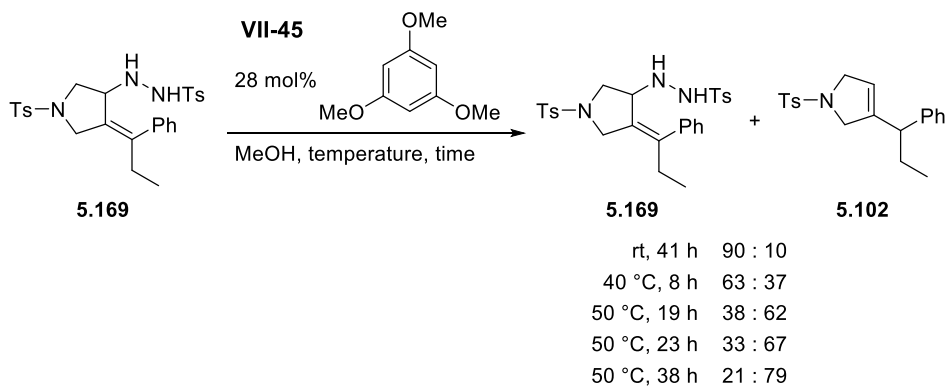
Scheme 5.39 Deprotection and aerobic oxidation of the cyclopentyl carbazate

In contrast to the alkynylhydrazones with a dimethyl malonate tether, cyclic hydrazide **5.169** from sulfonamide-tethered alkynylhydrazone **5.101** could be isolated by flash column chromatography (Scheme 5.40).



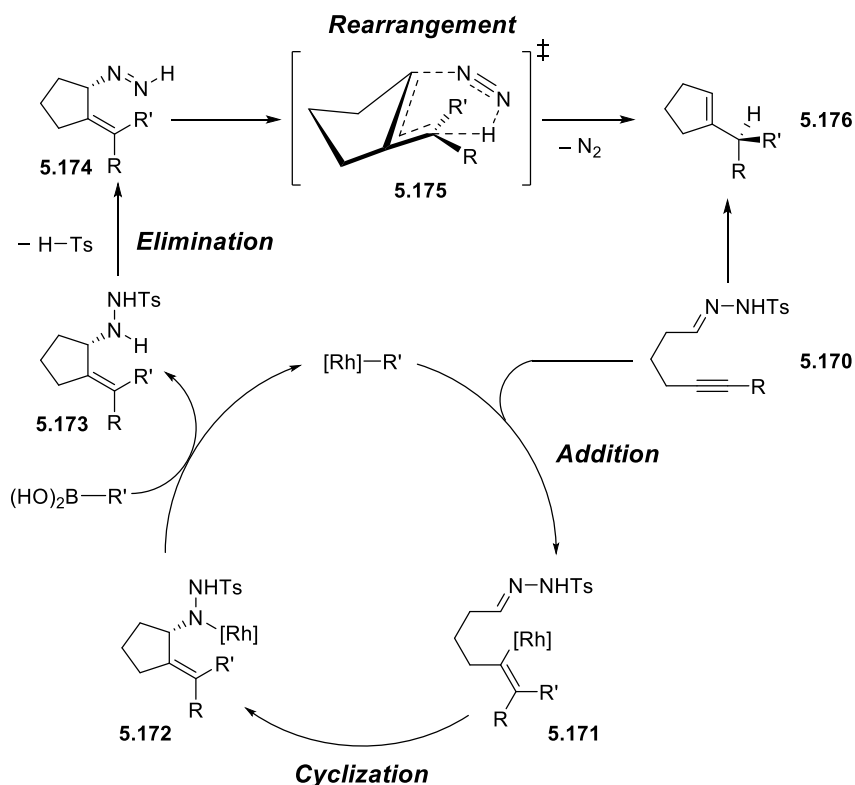
Scheme 5.40 Isolation of the cyclic hydrazide intermediate **5.169**

Then we put isolated cyclic hydrazide **5.169** into methanol solvent to induce elimination and the retro-ene rearrangement (Scheme 5.41). Upon elevating the temperature, **5.169** was converted to pyrroline **5.102** gradually, indicating that the cyclic hydrazide derived from the alkynylhydrazone was the actual reaction intermediate of the cascade process.



Scheme 5.41 Tandem elimination and retro-ene rearrangement of the cyclic hydrazide

From results described in Scheme 5.38 to 5.41, we propose the possible reaction mechanism of the rhodium-catalyzed tandem addition–cyclization–rearrangement (Scheme 5.42). At the first stage, the organorhodium species generated by transmetalation with the organoboronic acids mediates a sequential inter- and intramolecular 1,2-carborhodations of alkynylhydrazone **5.170** leading to cyclic hydrazide intermediate **5.173**. Subsequently, upon warming the reaction mixture, cyclic hydrazide **5.173** decomposes to allylic diazene intermediate **5.174**, which is rearranged to cyclopentene **5.176** with the extrusion of dinitrogen gas.³⁵



Scheme 5.42 Proposed mechanism

5.3 Conclusion

In summary, we have developed a novel annulation method of alkynylhydrazones by merging a rhodium-catalyzed tandem addition–cyclization with a retro-ene reaction. Expanding the synthetic utility of the rhodium-catalysis with C=N bonds, this reaction can provide a variety of 2°-alkyl-substituted cyclic alkenes from alkyne-tethered *N*-sulfonylhydrazones and organoboronic acids under mild and operationally simple conditions. The developed methodology can be fused with the Eschenmoser–Tanabe fragmentation, enabling an efficient ring-size alteration strategy for the conversion of cyclohexenones to functionalized cyclopentenones. Furthermore, by employing a chiral diene ligand for the rhodium catalyst, the reaction can be carried out to construct an enantioenriched C–N stereocenter whose chirality is transferred to an allylic position *via* stereospecific rearrangement. Mechanistically, alkynylhydrazone gives a cyclic hydrazide intermediate by the rhodium catalysis, which decomposes to an allylic diazene and the desired product spontaneously at an elevated temperature (Section 5.2.8).

5.4 Reference

- ¹ (a) Bamford, W. R.; Stevens, T. S. *J. Chem. Soc.* **1952**, 4735. (b) Shapiro, R. H.; Lipton, M. F.; Kolonko, K. J.; Buswell, R. L.; Capuano, L. A. *Tetrahedron Lett.* **1975**, *16*, 1811.
- ² (a) Kishner, N. *J. Russ. Phys. Chem. Soc.* **1911**, *43*, 582. (b) Wolff, L. *Liebigs Ann. Chem.* **1912**, *394*, 86.
- ³ For selected examples using hydrazones as the acceptor of organometallic nucleophiles, see: (a) Vedejs, E.; Stolle, W. T.; *Tetrahedron Lett.* **1977**, *18*, 135.; (b) Myers, A. G.; Kukkola, P. J. *J. Am. Chem. Soc.* **1990**, *112*, 8208. (c) Myers, A. G.; Movassaghi, M. *J. Am. Chem. Soc.* **1998**, *120*, 8891. (d) Marxer, A.; Horvath, M. *Helv. Chim. Acta* **1964**, *47*, 1101. (e) Takahashi, H.; Tomita, K.; Otomasu, H. *J. Chem. Soc., Chem. Commun.* **1979**, 668. (f) Kobayashi, S.; Sugiura, M.; Ogawa, C. *Adv. Synth. Catal.* **2004**, *346*, 1023. (g) Kobayashi, S.; Mori, Y.; Fossey, J. S.; Salter, M. M. *Chem. Rev.* **2011**, *111*, 2626.
- ⁴ For selected examples using (*R*)- or (*S*)-1-amino-2-methoxymethylpyrrolidine (SAMP or RAMP) mediated asymmetric alkylation reactions, see: (a) Corey, E. J.; Enders, D. *Tetrahedron Lett.* **1976**, *17*, 3. (b) Enders, D.; Eichenauer, H. *Angew. Chem. Int. Ed. Engl.* **1976**, *15*, 549. (c) Enders, D.; Eichenauer, H. *Tetrahedron Lett.* **1977**, *18*, 191. (d) Job, A.; Janeck, C. F.; Bettray, W.; Peters, R.; Enders, D. *Tetrahedron* **2002**, *58*, 2253.
- ⁵ Barluenga, J.; Moriel, P.; Valdés, C.; Aznar, F. *Angew. Chem. Int. Ed.* **2007**, *46*, 5587.
- ⁶ For the reviews on transition metal catalyzed cross-coupling reactions of sulfonylhydrazones, see: (a) Shao, Z.; Zhang, H. *Chem. Soc. Rev.* **2012**, *41*, 560. (b) Xia, Y.; Qiu, D.; Wang, Z. *Chem. Rev.* **2017**, *117*, 13810.
- ⁷ Pd: (a) Movassaghi, M.; Ahmad, O. K. *Angew. Chem. Int. Ed.* **2008**, *47*, 8909. Ir: (b) Lundgren, R. J.; Thomas, B. N. *Chem. Commun.* **2016**, *52*, 958.
- ⁸ Movassaghi, M.; Ahmad, O. K. *J. Org. Chem.* **2007**, *72*, 1838.
- ⁹ For the seminal work on the allylic diazene rearrangement, see: (a) Sato, T.; Homma, I.; Nakamura, S. *Tetrahedron Lett.* **1969**, *10*, 871. (b) Corey, E. J.; Cane, D. E.; Libit, L. *J. Am. Chem. Soc.* **1971**, *93*, 7016. (c) Hutchins, R. O.; Kacher, M.; Rua, L. *J. Org. Chem.* **1975**, *40*, 923. For a computational study for allylic diazene rearrangement, see: (d) Jabbari, A.; Sorensen E. J.; Houk, K. N. *Org. Lett.* **2006**, *8*, 3105.
- ¹⁰ Wang, H.; Dai, X.-J.; Li, C.-J. *Nat. Chem.* **2017**, *9*, 374.
- ¹¹ For the following studies, see: (a) Chen, N.; Dai, X.-J.; Wang, H.; Li, C.-J. *Angew. Chem. Int. Ed.* **2017**, *56*, 6260. (b) Dai, X.-J.; Wang, H.; Li, C.-J. *Angew. Chem. Int. Ed.* **2017**, *56*, 6302.

- ¹² (a) Mundal, D. A.; Lutz, K. E.; Thomson, R. J. *J. Am. Chem. Soc.* **2012**, *134*, 5782. For their following works in traceless Petasis reactions, see: (b) Diagne, A. B.; Li, S.; Perkowski, G. A.; Mrksich, M.; Thomson, R. J. *ACS Comb. Sci.* **2015**, *17*, 658. (c) Jiang, Y.; Diagne, A. B.; Thomson, R. J.; Schaus, S. E.; *J. Am. Chem. Soc.* **2017**, *139*, 1998. (d) Jiang, Y.; Thomson, R. J.; Schaus, S. E. *Angew. Chem. Int. Ed.* **2017**, *56*, 16631.
- ¹³ For the tandem nucleophilic addition–allylic diazene rearrangement of *N*-sulfonylhydrazones with organolithium reagents, see ref 3b and 3c.
- ¹⁴ (a) Kim, S.; Cho, J. R. *Synlett* **1992**, 629. (b) Kim, S. *Pure Appl. Chem.* **1996**, *68*, 623. (c) Campbell, N. E.; Sammis, G. M. *Angew. Chem. Int. Ed.* **2014**, *53*, 6228.
- ¹⁵ Rono, L. J.; Yayla, H. G.; Wang, D. Y.; Armstrong, M. F.; Knowles, R. R. *J. Am. Chem. Soc.* **2013**, *135*, 17735.
- ¹⁶ (a) Dao, H. T.; Li, C.; Michaudel, Q.; Maxwell, B. D.; Baran, P. S. *J. Am. Chem. Soc.* **2015**, *137*, 8046. For the following studies, see: (b) Saladrigas, M.; Loren, G.; Bonjoch, J.; Bradshaw, B. *ACS Catal.* **2018**, *8*, 11699.
- ¹⁷ (a) Choi, J.; Park, H.; Yoo, H. J.; Kim, S.; Sorensen, E. J.; Lee, C. *J. Am. Chem. Soc.* **2014**, *136*, 9918. (b) Um, H.-S.; Min, J.; An, T.; Choi, J.; Lee, C. *Org. Chem. Front.* **2018**, *5*, 2158.
- ¹⁸ Choi, K.; Park, H.; Lee, C. *J. Am. Chem. Soc.* **2018**, *140*, 10407.
- ¹⁹ Choi, K.; Joo, J. M.; Lee, C. *Tetrahedron* **2015**, *71*, 5910.
- ²⁰ For the effect of anionic ligands on transmetalation of Rh(I)-catalyst, see: (a) Hayashi, T.; Takahashi, M.; Takaya, Y.; Ogasawara, M. *J. Am. Chem. Soc.* **2002**, *124*, 5052. (b) Kina, A.; Yasuhara, Y.; Nishimura, T.; Iwamura, H.; Hayashi, T. *Chem. - Asian J.* **2006**, *1*, 707.
- ²¹ For the use of sodium acetate in elimination of sulfinic acid, see Scheme 5.6b and ref 16.
- ²² For the Rh-catalyzed 1,4-addition of cyclopropylboronic acid, see: Takechi, R.; Nishimura, T. *Chem. Commun.* **2015**, *51*, 8528.
- ²³ For the example of arylyative dimerization *via* intermolecular tandem addition–cyclization process, see ref 19.
- ²⁴ Jung, M. E.; Piizzi, G. *Chem. Rev.* **2005**, *105*, 1735.
- ²⁵ For the *gem*-dialkyl effects on the Rh(I)-catalyzed arylyative cyclization of alkynylketones, see: Johnson, T.; Choo, K.-L.; Lautens, M. *Chem. Eur. J.* **2014**, *20*, 14194.

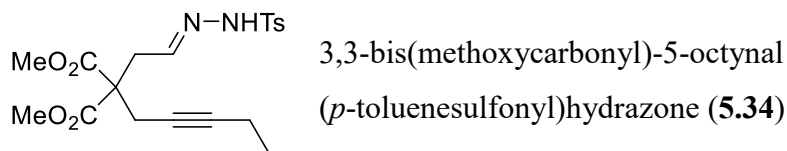
- ²⁶ For the low yields of related Rh(I)-catalyzed arylation cyclization of TsN-tethered substrates, see: Miura, T.; Shimada, M.; Murakami, M. *J. Am. Chem. Soc.* **2005**, *127*, 1094.
- ²⁷ For the synthesis of pyrrolidines using the Rh(I)-catalyzed arylation cyclization, see: Serpier, F.; Flamme, B.; Brayer, J.-L.; Folléas, B.; Darses, S. *Org. Lett.* **2015**, *17*, 1720.
- ²⁸ (a) Eschenmoser, A.; Felix, D.; Ohloff, G. *Helv. Chim. Acta* **1967**, *50*, 708. (b) Schreiber, J.; Felix, D.; Eschenmoser, A.; Winter, M.; Gautschi, F.; Schulte-Elte, K. H.; Sundt, E.; Ohloff, G.; Kalovoda, J.; Kaufmann, H.; Wieland, P.; Anner, G. *Helv. Chim. Acta* **1967**, *50*, 2101. (c) Tanabe, M.; Crowe, D. F.; Dehn, R. L.; Detre, G. *Tetrahedron Lett.* **1967**, *8*, 3739. (d) Tanabe, M.; Crowe, D. F.; Dehn, R. L. *Tetrahedron Lett.* **1967**, *8*, 3943.
- ²⁹ (a) Ref 25. (b) Shintani, R.; Isobe, S.; Takeda, M.; Hayashi, T. *Angew. Chem. Int. Ed.* **2010**, *49*, 3795. (c) Claraz, A.; Serpier, F.; Darses, S. *ACS Catal.* **2017**, *7*, 3410.
- ³⁰ Shintani, R.; Okamoto, K.; Otomaru, Y.; Ueyama, K.; Hayashi, T. *J. Am. Chem. Soc.* **2005**, *127*, 54.
- ³¹ For the reviews on chiral olefin ligands for asymmetric catalysis, see: (a) Johnson, J. B.; Rovis, T. *Angew. Chem. Int. Ed.* **2008**, *47*, 840. (b) Defieber, C.; Grützmacher, H.; Carreira, E. M. *Angew. Chem. Int. Ed.* **2008**, *47*, 4482.
- ³² (a) Lee, A.; Ahn, S.; Kang, K.; Seo, M.-S.; Kim, Y.; Kim, W. Y.; Kim, H. *Org. Lett.* **2014**, *16*, 5490. (b) Lee, A.; Kim, H. *J. Am. Chem. Soc.* **2015**, *137*, 11250. (c) Lee, A.; Kim, H. *J. Org. Chem.* **2016**, *81*, 3520.
- ³³ For the assignment of the absolute configuration of **5.35**, see the Experimental section for details.
- ³⁴ For chiral diene **5.164** and its derivatives, see: Okamoto, K.; Hayashi, T.; Rawal, V. H. *Chem. Commun.* **2009**, 4815.
- ³⁵ For a transition state of the allylic diazene rearrangement by computational studies, see ref 9d.

5.5 Experimental section

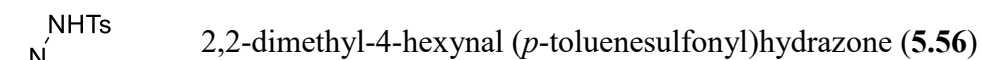
5.5.1 General remarks

All solvents were dried by passing through activated alumina columns of solvent purification systems. Commercially available reagents were used without further purification. Thin layer chromatography (TLC) was performed using Merck Silica gel 60 F254 plates that were visualized by exposure to UV light (254 nm) and/or stained by ceric ammonium molybdate solutions. Flash column chromatography was performed on silica gel (Merck Silica gel 60, 0.040-0.063 Mm) using the indicated solvent system. NMR spectra were recorded in CDCl₃, unless otherwise noted, on an Agilent MR DD2 400 MHz, Varian/Oxford AS500 spectrometers. Chemical shifts in ¹H NMR spectra were reported in parts per million (ppm) on the δ scale from an internal standard of tetramethylsilane (0.00 ppm). Data for ¹H NMR are reported as follows: chemical shift, multiplicity (s = singlet, d = doublet, t = triplet, q = quartet, m = multiplet, br s = broad singlet), coupling constant in Hertz (Hz) and integration. Data for ¹³C NMR spectra are reported in terms of chemical shift in ppm from the central peak of CDCl₃ (77.0 ppm) or DMSO (39.5 ppm). FT-IR spectra were obtained on Thermoscientific Nicolet iS10 or Bruker TENSOR27 and reported in frequency of the absorption (cm⁻¹). Optical Rotations were measured in a 50.00 mm cell with a Jasco P-1030 polarimeter equipped with a sodium lamp (589 nm). High resolution mass spectra (HRMS) were obtained from the Organic Chemistry Research Center at Sogang University.

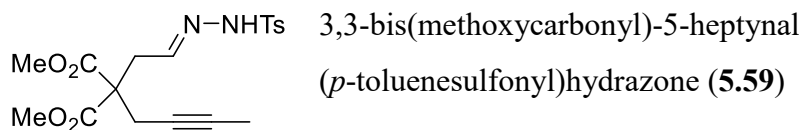
5.5.2 Synthesis and characterization for substrates



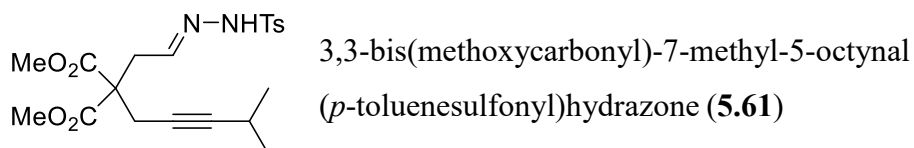
3,3-bis(methoxycarbonyl)-5-octynal (1708.4 mg, 7.11 mmol, 1 equiv) was dissolved in MeOH (17.8 ml, 0.4 M) at rt. *p*-toluenesulfonyl hydrazide (1365.2 mg, 7.11 mmol, 1 equiv) was added to rbf and the reaction mixture was stirred for 2 h at rt. After evaporation of the solvent, crude material was chromatographed on silica gel to give the pure product **5.34** as a clear gum (2550.1 mg, 6.24 mmol, 88%). $R_f = 0.28$ (Hex/EA = 2:1), 0.13 (Hex/EA = 3:1); $^1\text{H NMR}$ (400 MHz, DMSO) δ 11.09 (s, 1H), 7.66 (d, $J = 7.8$ Hz, 2H), 7.40 (d, $J = 7.8$ Hz, 2H), 7.18 (t, $J = 5.3$ Hz, 1H), 3.56 (s, 6H), 2.73 (d, $J = 4.9$ Hz, 2H), 2.56 (s, $J = 9.9$ Hz, 2H), 2.38 (s, 3H), 2.08 (q, $J = 7.4$ Hz, 2H), 0.99 (t, $J = 7.5$ Hz, 3H); $^{13}\text{C NMR}$ (101 MHz, DMSO) δ 169.66, 146.46, 143.61, 136.66, 129.92, 127.57, 85.66, 74.08, 56.02, 53.14, 35.29, 23.52, 21.41, 14.42, 12.01; **IR** (neat, cm^{-1}): 3212, 2955, 2360, 2342, 1739, 1598, 1438, 1165, 1076, 910, 815, 669, 581, 548; **HRMS** (ESI): Calcd for $\text{C}_{19}\text{H}_{24}\text{N}_2\text{NaO}_6\text{S}$ $[\text{M}+\text{Na}]^+$ 431.1253, found 431.1247.



2,2-dimethyl-4-hexynal (130.8 mg, 1.05 mmol, 1 equiv) was dissolved in MeOH (2.1 ml, 0.5 M) at rt. *p*-toluenesulfonyl hydrazide (202.2 mg, 1.05 mmol, 1 equiv) was added and the reaction mixture was stirred for 2 h at rt. After evaporation of the solvent, crude material was chromatographed on silica gel to give the pure product **5.56** as a white solid (307.5 mg, quant). $R_f = 0.26$ (Hex/EA = 3:1); $^1\text{H NMR}$ (400 MHz, CDCl_3) δ 7.81 (d, $J = 8.3$ Hz, 2H), 7.31 (d, $J = 8.4$ Hz, 2H), 7.14 (s, 1H), 2.43 (s, 3H), 2.13 (q, $J = 2.5$ Hz, 2H), 1.70 (t, $J = 2.5$ Hz, 3H), 1.08 (s, 6H).

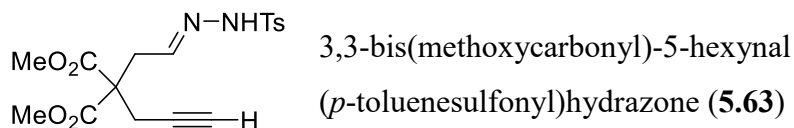


3,3-bis(methoxycarbonyl)-5-heptynal¹ (644.7 mg, 2.85 mmol, 1 equiv) was dissolved in MeOH (7.1 ml, 0.4 M) at rt. *p*-toluenesulfonyl hydrazide (547.1 mg, 2.85 mmol, 1 equiv) was added to rbf and the reaction mixture was stirred for 5 h at rt. After evaporation of the solvent, crude material was chromatographed on silica gel to give the pure product **5.59** as a clear gum (917.7 mg, 2.33 mmol, 82%). R_f = 0.26 (Hex/EA = 2:1), 0.11 (Hex/EA = 3:1); ¹H NMR (400 MHz, DMSO) δ 11.11 (s, 1H), 7.66 (d, J = 7.8 Hz, 2H), 7.40 (d, J = 7.4 Hz, 2H), 7.18 (s, 1H), 3.55 (s, 6H), 2.72 (s, 2H), 2.56 (s, 2H), 2.38 (s, 3H), 1.70 (s, 3H); ¹³C NMR (101 MHz, DMSO) δ 169.66, 146.66, 143.69, 136.53, 129.94, 127.58, 79.80, 73.68, 55.87, 53.18, 35.27, 23.56, 21.42, 3.48; IR (neat, cm⁻¹): 3211, 2955, 2923, 1738, 1598, 1495, 1438, 1364, 1328, 1293, 1216, 1168, 1074, 911, 816, 736, 706, 670, 581, 548; HRMS (ESI): Calcd for C₁₈H₂₂N₂NaO₆S [M+Na]⁺ 417.1096, found 417.1094.

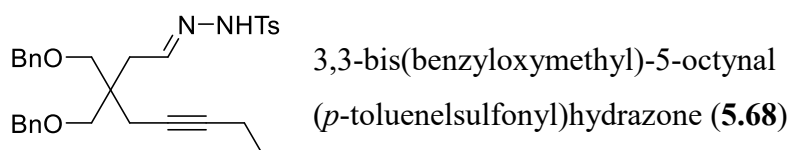


3,3-bis(methoxycarbonyl)-7-methyl-5-octynal (137.3 mg, 0.54 mmol, 1 equiv) was dissolved in MeOH (2.7 ml, 0.2 M) at rt. *p*-toluenesulfonyl hydrazide (102.6 mg, 0.54 mmol, 1 equiv) was added to rbf and the reaction mixture was stirred for 4.5 h at rt. After evaporation of the solvent, crude material was chromatographed on silica gel to give the pure product **5.61** as a clear gum (215.2 mg, 0.51 mmol, 94%). R_f = 0.39 (Hex/EA = 2:1); ¹H NMR (400 MHz, DMSO) δ 11.10 (s, 1H), 7.66 (d, J = 8.1 Hz, 2H), 7.39 (d, J = 8.0 Hz, 2H), 7.19 (t, J = 5.1 Hz, 1H), 3.56 (s, 6H), 2.73 (d, J = 5.1 Hz, 2H), 2.52 (d, J = 17.4 Hz, 2H), 2.48 – 2.40 (m, 0H), 2.38 (s, 3H), 1.03 (d, J = 6.8 Hz, 6H); ¹³C NMR (101 MHz, DMSO) δ 169.18, 146.22, 143.22, 136.11, 129.48, 127.13,

89.43, 73.53, 55.69, 52.69, 52.63, 34.86, 22.94, 20.94, 19.67; **IR** (neat, cm^{-1}): 3206, 2967, 1736, 1437, 1364, 1325, 1292, 1212, 1167, 1075, 910, 815, 670; **HRMS** (ESI): Calcd for $\text{C}_{20}\text{H}_{26}\text{N}_2\text{NaO}_6\text{S}$ $[\text{M}+\text{Na}]^+$ 445.1409, found 445.1408.

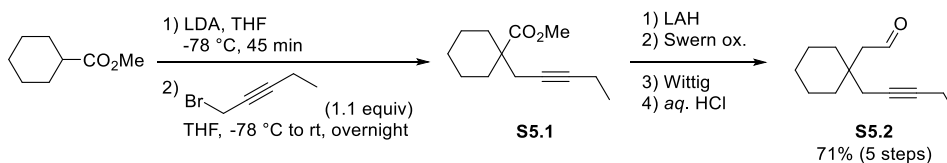


3,3-bis(methoxycarbonyl)-5-hexynal (467.6 mg, 2.2 mmol, 1 equiv) was dissolved in MeOH (5.5 ml, 0.4 M) at rt. *p*-toluenesulfonyl hydrazide (423.1 mg, 2.2 mmol, 1 equiv) was added to rbf and the reaction mixture was stirred for 4.5 h at rt. After evaporation of the solvent, crude material was chromatographed on silica gel to give the pure product **5.63** as a white solid (838.1 mg, 2.2 mmol, quantitative). $R_f = 0.23$ (Hex/EA = 2:1); **^1H NMR (400 MHz, DMSO)** δ 11.12 (s, 1H), 7.66 (d, $J = 8.2$ Hz, 2H), 7.40 (d, $J = 8.0$ Hz, 2H), 7.18 (t, $J = 5.0$ Hz, 1H), 3.56 (s, 6H), 2.97 (t, 1H), 2.74 (s, 1H), 2.59 (d, $J = 2.4$ Hz, 2H), 2.38 (s, 3H); **^{13}C NMR (101 MHz, DMSO)** δ 169.42, 146.46, 143.72, 136.49, 129.97, 127.60, 78.96, 74.96, 55.57, 53.27, 35.12, 23.11, 21.43; **IR** (neat, cm^{-1}): 3278, 3210, 2956, 2360, 2342, 1738, 1598, 1437, 1364, 1326, 1294, 1217, 1168, 1077, 908, 816, 668, 580, 548; **HRMS** (ESI): Calcd for $\text{C}_{17}\text{H}_{20}\text{N}_2\text{NaO}_6\text{S}$ $[\text{M}+\text{Na}]^+$ 403.0940, found 403.0936.



3,3-bis(benzyloxymethyl)-5-octynal¹ (772.8 mg, 2.1 mmol, 1 equiv) was dissolved in MeOH (5.3 ml, 0.4 M) at rt. *p*-toluenesulfonyl hydrazide (407.1 mg, 2.1 mmol, 1 equiv) was added to rbf and the reaction mixture was stirred for 15 h at rt. After evaporation of the solvent, crude material was

chromatographed on silica gel to give the pure product **5.68** as a clear sticky oil (609.2 mg, 1.1 mmol, 54%). $R_f = 0.32$ (Hex/EA = 3:1); $^1\text{H NMR}$ (400 MHz, DMSO) δ 10.94 (s, 1H), 7.67 (d, $J = 8.2$ Hz, 2H), 7.39 – 7.23 (m, $J = 18.0, 13.2, 8.1$ Hz, 13H), 4.32 (s, 4H), 3.17 (q, $J = 9.1$ Hz, 4H), 2.34 (s, 3H), 2.17 (d, $J = 6.0$ Hz, 2H), 2.08 (q, $J = 14.8, 7.4$ Hz, 2H), 2.02 (s, 2H), 0.99 (t, $J = 7.4$ Hz, 3H); $^{13}\text{C NMR}$ (101 MHz, DMSO) δ 149.79, 143.55, 138.77, 136.63, 129.95, 128.61, 127.75, 127.70, 127.61, 84.38, 75.84, 72.82, 71.93, 42.35, 35.71, 22.85, 21.42, 14.62, 12.19; IR (neat, cm^{-1}): 3205, 3063, 3030, 2973, 2859, 1598, 1496, 1453, 1365, 1324, 1167, 1094, 1029, 910, 814, 738, 698, 668, 582, 550; HRMS (ESI): Calcd for $\text{C}_{31}\text{H}_{36}\text{N}_2\text{NaO}_4\text{S}$ $[\text{M}+\text{Na}]^+$ 555.2293, found 555.2290;



2-{1-(2-pentyn-1-yl)cyclohexyl}acetaldehyde (**S5.2**)

To a solution of lithium diisopropylamide prepared by addition of *n*BuLi (2.5 M in Hexane; 6.9 ml, 17.25 mmol, 1.15 equiv) to diisopropylamine (2.8 ml, 19.5 mmol, 1.3 equiv) in THF (35 ml) at -78 °C was added methyl cyclohexylcarboxylate (1.6 ml, 15 mmol, 1 equiv) in THF (5 ml) under N_2 atmosphere. The reaction mixture was stirred for 45 min, and 1-bromo-2-pentyne (1.7 ml, 16.5 mmol, 1.1 equiv) was added. The resulting mixture was allowed to warm to rt and kept for overnight (16 h). The reaction was quenched by the addition of *sat. aq.* NH_4Cl , and aqueous layer was extracted with Et_2O . The collected organic extracts were washed with brine, dried over MgSO_4 , filtered, and concentrated to give alkylated product **S5.1** without further purification.

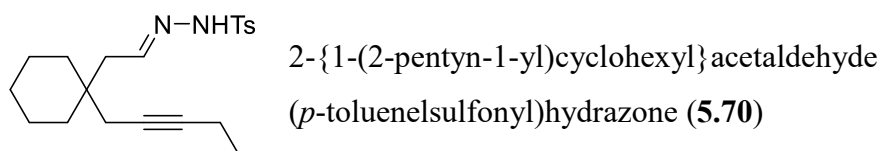
The solution of **S5.1** in THF (15 ml) was added dropwise to a solution of LAH (871.3 mg, 22.5 mmol, 1.5 equiv) in THF (60 ml) at 0 °C under N₂ atmosphere. After stirring at rt for 1 h, the reaction mixture was cooled down to 0 °C, quenched by *sat. aq.* Na₂SO₄, and stirred for 15 min. The heterogeneous mixture was filtered through short pad of Celite, and concentrated *in vacuo* to give pure alkynyl alcohol without further purification.

To a solution of oxalyl chloride (1.6 ml, 18 mmol, 1.2 equiv) in DCM (40 ml) was added dropwise a solution of DMSO (2.6 ml, 36 mmol, 2.4 equiv) in DCM (20 ml) under N₂ atmosphere. After 10 min, a solution of alkynyl alcohol in DCM (15 ml) was added dropwise and resulting mixture was stirred for additional 10 min. The reaction mixture was allowed to warm to 0 °C after addition of TEA (10.0 ml, 72 mmol, 4.8 equiv), and stirred for 2 h. The mixture was poured into *sat. aq.* NH₄Cl, and aqueous layer was extracted with DCM. The combined organic extracts were washed with brine, dried over Na₂SO₄, filtered, and concentrated to give pure alkynal without further purification.

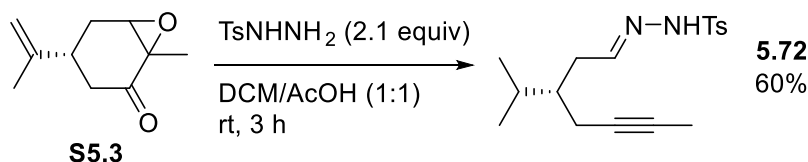
To a suspension of (methoxymethyl)triphenylphosphonium chloride (6296.5 mg, 18 mmol, 1.2 equiv) in dry THF (30 ml) was added *t*BuOK (2061.0 mg, 18 mmol, 1.2 equiv) at 0 °C under N₂ atmosphere. After 20 min, a solution of alkynal in THF (20 ml) was added and resulting mixture was allowed to warm to rt, and stirred for 4 h. The reaction mixture was quenched by H₂O, and aqueous layer was extracted with EA. The combined organic extracts were washed with brine, dried over MgSO₄, filtered, and concentrated *in vacuo* to give methyl vinyl ether for next step without further purification.

The solution of methyl vinyl ether in THF (30 ml) and 2 N *aq.* HCl (20 ml) was stirred at 55 °C for 3 h, and resulting mixture was quenched by *sat. aq.* NaHCO₃, and extracted with Et₂O. The combined organic extracts were dried over Na₂SO₄, concentrated, and purified by flash column chromatography to

give the pure product **S5.2** as a clear slightly yellow oil (2034.2 mg, 10.6 mmol, 71% overall yield for 5 steps). $R_f = 0.44$ (Hex/EA = 10:1); $^1\text{H NMR}$ (400 MHz, CDCl_3) δ 9.90 (t, $J = 2.9$ Hz, 1H), 2.45 (d, $J = 2.9$ Hz, 2H), 2.31 (t, $J = 2.3$ Hz, 2H), 2.22 – 2.10 (m, 2H), 1.57 – 1.35 (m, 10H), 1.12 (t, $J = 7.5$ Hz, 3H); $^{13}\text{C NMR}$ (101 MHz, CDCl_3) δ 203.16, 84.79, 75.92, 51.09, 36.76, 35.52, 28.49, 25.78, 21.48, 14.18, 12.36; **IR** (neat, cm^{-1}): 2927, 2852, 1705, 1455, 1319, 1209, 929, 850; **HRMS** (ESI): Calcd for $\text{C}_{13}\text{H}_{20}\text{NaO}$ $[\text{M}+\text{Na}]^+$ 215.1412, found 215.1410.

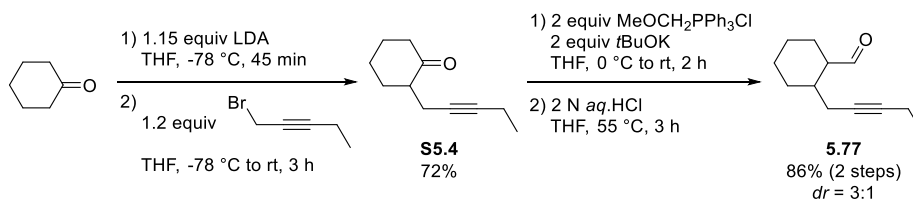


2-{1-(2-pentyn-1-yl)cyclohexyl}acetaldehyde (**S5.2**, 703.4 mg, 3.7 mmol, 1 equiv) was dissolved in MeOH (9.1 ml, 0.4 M) at rt. *p*-toluenesulfonyl hydrazide (702.3 mg, 3.7 mmol, 1 equiv) was added to rbf and the reaction mixture was stirred for 5 h at rt. After evaporation of the solvent, crude material was chromatographed on silica gel to give the pure product **5.70** as a white solid (958.9 mg, 2.7 mmol, 73%). $R_f = 0.39$ (Hex/EA = 3:1); $^1\text{H NMR}$ (400 MHz, DMSO) δ 10.77 (s, 1H), 7.63 (d, $J = 8.1$ Hz, 2H), 7.34 (d, $J = 8.0$ Hz, 2H), 7.20 (t, $J = 6.2$ Hz, 1H), 2.33 (s, 3H), 2.14 – 2.00 (m, 2+2H), 1.87 (s, 2H), 1.21 (s, 6H), 1.13 (d, $J = 13.8$ Hz, 2H), 0.99 (t, $J = 7.4$ Hz, 3+2H); $^{13}\text{C NMR}$ (101 MHz, DMSO) δ 150.11, 143.51, 136.46, 129.83, 127.64, 84.41, 76.70, 39.61, 36.49, 34.46, 27.99, 25.80, 21.40, 21.31, 14.74, 12.23; **IR** (neat, cm^{-1}): 3201, 2925, 2851, 2360, 2342, 1598, 1453, 1364, 1322, 1167, 1093, 1062, 1029, 907, 813, 669, 585, 547; **HRMS** (ESI): Calcd for $\text{C}_{20}\text{H}_{28}\text{N}_2\text{NaO}_2\text{S}$ $[\text{M}+\text{Na}]^+$ 383.1769, found 383.1766.



(*S*)-3-isopropylhept-5-ynal (*p*-toluenesulfonyl)hydrazone (**5.72**)

To a solution of **S5.3** (1691.2 mg, 10 mmol) in DCM/AcOH (1.7 ml/1.7 ml) at -10 °C was added *p*-toluenesulfonyl hydrazide (2122.9 mg, 21 mmol, 2.1 equiv). After stirring for 4 h at rt, the resulting mixture was quenched with *sat. aq.* NaHCO₃, extracted with DCM, dried over Na₂SO₄, and concentrated. The crude material was chromatographed on silica gel to give the hydrazone **5.72** as a white solid (1947.8 mg, 6.1 mmol, 60%). *R_f* = 0.16 (Hex/EA = 5:1), 0.31 (Hex/EA = 3:1); ¹H NMR (selected, 400 MHz, CDCl₃) δ 7.81 (d, *J* = 8.2 Hz, 2H), 7.38 (s, 1H), 7.32 (d, *J* = 7.8 Hz, 2H), 7.18 (t, *J* = 5.6 Hz, 1H), 2.43 (s, 3H), 1.74 (s, 3H), 0.80 (d, *J* = 6.8 Hz, 6H).

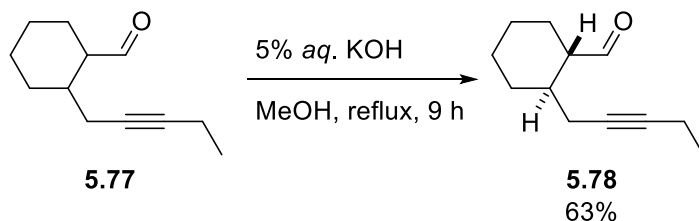


To a solution of diisopropylamine (2.8 ml, 19.5 mmol, 1.3 equiv) in THF was added *n*BuLi (6.9 ml, 17.25 mmol, 1.15 equiv) dropwise at -78 °C. After stirring for 30 min at that temperature, a solution of cyclohexanone (1.6 ml, 15 mmol, 1 equiv) in THF was added dropwise. The reaction mixture was stirred for 45 min at -78 °C and 1-bromo-2-pentyne (1.9 ml, 18 mmol, 1.2 equiv) was added. The reaction flask was allowed to warm slowly to room temperature and quenched with *aq.* NH₄Cl after 2.5 h. The aqueous layer was extracted by diethyl ether, and the collected organic phase was washed with brine, dried over MgSO₄, and concentrated. The crude residue was purified

by flash column chromatography to give the pure pentynyl cyclohexanone **S5.4** (1764.2 mg, 10.7 mmol, 72%) as a clear oil. $R_f = 0.39$ (Hex/EA = 10:1)

To a suspension of (methoxymethyl)triphenylphosphonium chloride (2964.6 mg, 8.4 mmol, 2 equiv) in dry THF (14.1 ml) was added *t*BuOK (970.4 mg, 8.4 mmol, 2 equiv) at 0 °C under N₂ atmosphere. After 20 min, a solution of **S5.4** (696.0 mg, 4.2 mmol) in THF (20 ml) was added and resulting mixture was allowed to warm to rt, and stirred for 2 h. The reaction mixture was quenched by H₂O, and aqueous layer was extracted with EA. The combined organic extracts were washed with brine, dried over MgSO₄, filtered, and concentrated *in vacuo* to give methyl vinyl ether for next step without further purification.

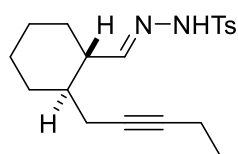
The solution of methyl vinyl ether in THF (12.6 ml) and 2 N *aq.* HCl (8.4 ml) was stirred at 55 °C for 3 h, and resulting mixture was quenched by *sat. aq.* NaHCO₃, and extracted with Et₂O. The combined organic extracts were dried over Na₂SO₄, concentrated, and purified by flash column chromatography to give the pure product **5.77** (650.4 mg, 3.6 mmol, 86% overall yield for 2 steps). $R_f = 0.4$ (Hex/EA = 10:1);



Alkynylaldehyde **5.78**

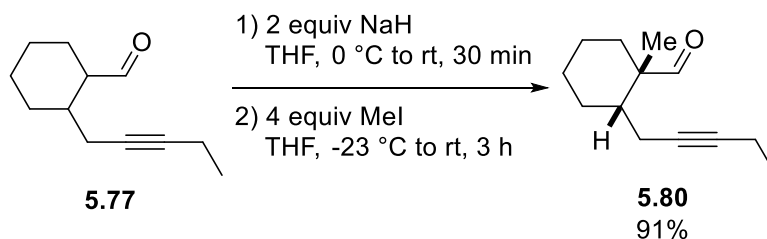
The solution of **5.77** (5.4 mmol) in 5% *aq.* KOH (13.5 ml) and MeOH (13.5 ml) was refluxed for 3 h. The reaction mixture was cooled down to room temperature and extracted by diethyl ether. The combined organic layer was dried over Na₂SO₄, concentrated to give isomerized alkynealdehyde **5.78**

(611.1 mg, 3.4 mmol, 63%) without further purification. $^1\text{H NMR}$ (499 MHz, CDCl_3) δ 9.64 (d, $J = 3.2$ Hz, 1H), 2.31 – 2.05 (m, 6H), 1.88 – 1.66 (m, 6H), 1.43 – 1.24 (m, 2H), 1.11 (t, $J = 7.3$ Hz, 3H).



Alkynylhydrazone **5.79**

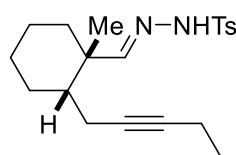
Alkynylaldehyde **5.78** (504.0 mg, 2.8 mmol, 1 equiv) was dissolved in MeOH (7.1 ml, 0.4 M) at rt. *p*-toluenesulfonyl hydrazide (542.8 mg, 2.8 mmol, 1 equiv) was added to rbf and the reaction mixture was stirred for 2 h at rt. The crude mixture was filtered with hexane to give the pure alkynylhydrazone **5.79** as a white solid (705.1 mg, 2.0 mmol, 72%). $R_f = 0.33$ (Hex/EA = 3:1); $^1\text{H NMR}$ (499 MHz, DMSO) δ 10.77 (s, 1H), 7.67 (d, $J = 8.1$ Hz, 2H), 7.39 (d, $J = 8.0$ Hz, 2H), 7.07 (d, $J = 7.0$ Hz, 1H), 2.38 (s, 3H), 2.10 (q, $J = 7.3$ Hz, 2H), 1.90 – 1.73 (m, 3H), 1.64 (dd, $J = 13.9, 4.9$ Hz, 3H), 1.50 (d, $J = 5.6$ Hz, 1H), 1.34 – 1.23 (m, 1H), 1.13 (d, $J = 8.1$ Hz, 3H), 1.03 (t, $J = 7.5$ Hz, 4H); $^{13}\text{C NMR}$ (101 MHz, DMSO) δ 154.99, 143.57, 136.45, 129.86, 127.58, 83.27, 77.78, 45.05, 38.80, 30.86, 30.06, 25.44, 25.15, 23.42, 21.42, 14.71, 12.21.

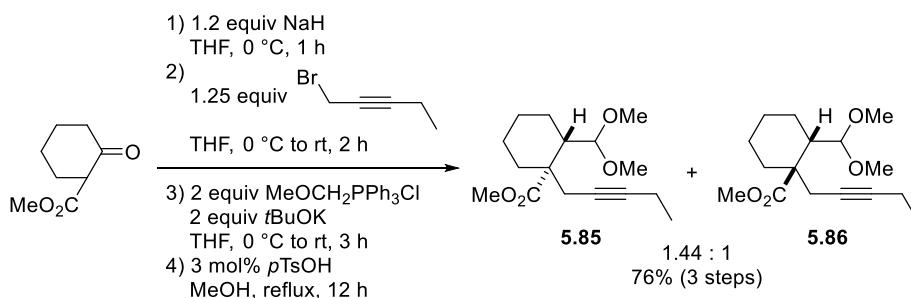


Alkynylaldehyde **5.80**

The solution of sodium hydride (121.9 mg, 3.0 mmol, 2 equiv) in THF (4 ml) was added **5.77** (271.6 mg, 1.5 mmol) in THF (3.1 ml) at 0 °C. After stirring for 30 min at room temperature, the reaction mixture was cooled down to -

23 °C and methyl iodide (0.39 ml, 6.1 mmol, 4 equiv) in THF (0.5 ml) was added. After stirring for 3 h at room temperature, the reaction was quenched by *aq.*NH₄Cl and the mixture was extracted by diethyl ether. Washing with brine, drying over MgSO₄, and flash column chromatography gave the methylate alkynal **5.80** (267.9 mg, 1.4 mmol, 91%). *R_f* = 0.56 (Hex/EA = 10:1);


 Alkynylhydrazone **5.81**
 Alkynylaldehyde **5.80** (267.9 mg, 1.4 mmol, 1 equiv) was dissolved in MeOH (3.5 ml, 0.4 M) at rt. *p*-toluenesulfonyl hydrazide (254.1 mg, 1.3 mmol, 0.95 equiv) was added to rbf and the reaction mixture was stirred for 28 h at rt. After evaporation of the solvent, crude material was chromatographed on silica gel to give the pure product **5.81** as a clear gum (253.2 mg, 0.7 mmol, 50%). *R_f* = 0.42 (Hex/EA = 3:1); ¹H NMR (400 MHz, CDCl₃) δ 7.79 (d, *J* = 8.0 Hz, 2H), 7.31 (d, *J* = 7.9 Hz, 2H), 7.28 – 7.22 (m, 1H), 2.43 (s, 3H), 2.18 – 2.06 (m, 3H), 1.81 (d, *J* = 14.0 Hz, 1H), 1.66 (d, *J* = 9.4 Hz, 3H), 1.52 – 1.18 (m, 6H), 1.09 (t, *J* = 7.3 Hz, 3H), 1.04 (s, 3H).



To a suspension of NaH (889.6 mg, 22.2 mmol, 1.2 equiv) in dry THF (80 ml) was added a solution of methyl 2-oxocyclohexanecarboxylate (2.9 ml, 18.5

mmol, 1 equiv) in THF (13 ml) dropwise at 0 °C under N₂ atmosphere. After 1 h, 1-bromo-2-pentyne (2.4 ml, 23.2 mmol, 1.25 equiv) was added. The reaction mixture was allowed to warm to rt, stirred for 24 h, and quenched with H₂O. The aqueous layer was extracted with Et₂O, and the collected organic extracts were dried over MgSO₄, filtered, and concentrated to give pure alkylated product without further purification.

To a suspension of (methoxymethyl)triphenylphosphonium chloride (9722.1 mg, 27.8 mmol, 2 equiv) in dry THF (36 ml) was added *t*BuOK (3182.3 mg, 27.8 mmol, 2 equiv) at 0 °C under N₂ atmosphere. After 30 min, a solution of the alkylated product (3088.9 mg, 13.9 mmol, 1 equiv) in THF (10 ml) was added and resulting mixture was allowed to warm to rt, and stirred for 3 h. The reaction mixture was quenched by H₂O, and aqueous layer was extracted with EA. The combined organic extracts were washed with brine, dried over MgSO₄, filtered, and concentrated *in vacuo* to give methyl vinyl ether for next step without further purification.

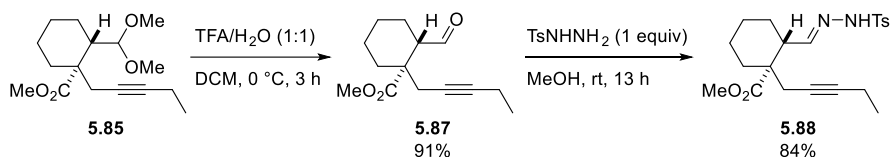
To a solution of methyl vinyl ether in MeOH (56 ml, 0.25 M) was added *p*TsOH·H₂O (80.9 mg, 0.42 mmol, 3 mol%), and resulting mixture was stirred for 22 h under reflux. After a complete consumption of starting material, reaction mixture was cooled down to rt, then concentrated *in vacuo*. The organic residue was treated with *sat. aq.* NaHCO₃, and extracted with DCM. The combined organic extracts were dried over Na₂SO₄, filtered, and concentrated *n vacuo*. The crude material was chromatographed on silica gel to give the diastereomeric products **5.85** and **5.86** as a clear oil (2978.3 mg, 10.5 mmol, 76%, *dr* = 1.44:1).

(±)-(1*R*,2*R*)-1-methoxycarbonyl-1-(2-pentyn-1-yl)cyclohexane-2-carbaldehyde dimethyl acetal (**5.85**)

R_f = 0.45 (Hex/EA = 5:1); **¹H NMR (400 MHz, CDCl₃)** δ 4.45 (d, *J* = 6.2 Hz, 1H), 3.66 (s, 3H), 3.31 (d, *J* = 7.2 Hz, 6H), 2.80 (dt, *J* = 16.5, 2.1 Hz, 1H), 2.48 (dt, *J* = 16.6, 2.1 Hz, 1H), 2.15 (qt, *J* = 7.4, 2.1 Hz, 2H), 2.02 (dd, *J* = 12.3, 6.1 Hz, 1H), 1.89 – 1.72 (m, 2H), 1.72 – 1.57 (m, 4H), 1.55 – 1.42 (m, 1H), 1.28 (dt, *J* = 15.2, 6.7 Hz, 1H), 1.10 (t, *J* = 7.5 Hz, 3H); **¹³C NMR (101 MHz, CDCl₃)** δ 175.69, 105.35, 84.36, 75.82, 55.32, 53.28, 51.24, 46.72, 43.75, 31.23, 27.44, 23.58, 22.50, 21.89, 14.30, 12.38; **IR (neat, cm⁻¹):** 2938, 2862, 1726, 1681, 1450, 1201, 1124, 1070, 998, 951; **HRMS (ESI):** Calcd for C₁₆H₂₆NaO₄ [M+Na]⁺ 305.1729, found 305.1726. Relative stereochemistry was confirmed by 1D NOE experiments.

(±)-(1*R*,2*S*)-1-methoxycarbonyl-1-(2-pentyn-1-yl)cyclohexane-2-carbaldehyde dimethyl acetal (**5.86**)

R_f = 0.37 (Hex/EA = 5:1); **¹H NMR (400 MHz, CDCl₃)** δ 4.03 (d, *J* = 7.2 Hz, 1H), 3.68 (s, 3H), 3.28 (d, *J* = 4.9 Hz, 6H), 2.61 (d, *J* = 16.5 Hz, 1H), 2.43 (d, *J* = 16.5 Hz, 1H), 2.31 (ddd, *J* = 11.0, 7.2, 3.9 Hz, 1H), 2.21 – 2.08 (m, 3H), 1.79 – 1.52 (m, 4H), 1.41 – 1.18 (m, 3H), 1.10 (t, *J* = 7.5 Hz, 3H); **¹³C NMR (101 MHz, CDCl₃)** δ 176.98, 105.90, 83.22, 76.28, 55.83, 52.33, 51.56, 47.20, 44.03, 33.32, 24.91, 22.78, 21.04, 19.03, 14.29, 12.51; **IR (neat, cm⁻¹):** 2939, 2862, 1731, 1676, 1453, 1285, 1225, 1150, 1128, 1065; **HRMS (ESI):** Calcd for C₁₆H₂₆NaO₄ [M+Na]⁺ 305.1729, found 305.1726.

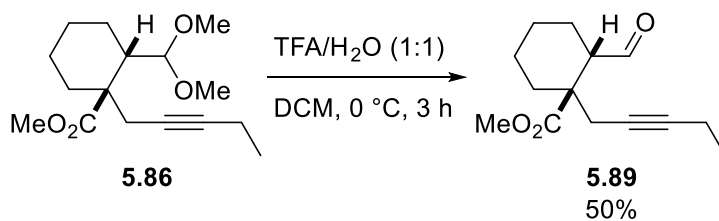


(±)-(1*R*,2*R*)-1-methoxycarbonyl-1-(2-pentyn-1-yl)cyclohexane-2-carbaldehyde (*p*-toluenesulfonyl)hydrazone (**5.88**)

To a solution of **5.85** (637.9 mg, 2.3 mmol) in DCM/H₂O (5.6 ml/1.4 ml) at 0 °C was added TFA (1.4 ml), and resulting mixture was stirred at 0 °C for 3 h. After quenching a reaction with *sat. aq.* NaHCO₃, organic extracts were collected with DCM. The combined organic extracts were dried over Na₂SO₄, filtered, and concentrated to give the aldehyde **5.87** without further purification (crude, 488.3 mg, 2.1 mmol, 91%).

5.87 was dissolved in MeOH (5.2 ml, 0.4 M) at rt. *p*-toluenesulfonyl hydrazide (396.7 mg, 2.1 mmol, 1 equiv) was added to rbf and the reaction mixture was stirred for 13 h at rt. After evaporation of the solvent, crude material was chromatographed on silica gel to give the pure product **5.88** as a white gum (702.2 mg, 1.7 mmol, 84% for 2 steps).

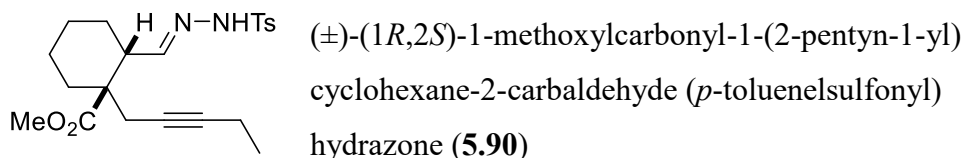
R_f = 0.22 (Hex/EA = 3:1); **¹H NMR (400 MHz, CDCl₃)** δ 7.82 (d, *J* = 8.1 Hz, 2H), 7.64 (s, 1H), 7.37 (d, *J* = 7.2 Hz, 1H), 7.30 (d, *J* = 8.1 Hz, 2H), 3.60 (s, 3H), 2.48 – 2.37 (m, 4H), 2.20 – 2.02 (m, 5H), 1.67 – 1.53 (m, 4H), 1.47 – 1.22 (m, 3H), 1.09 (t, *J* = 7.4 Hz, 3H); **¹³C NMR (101 MHz, CDCl₃)** δ 174.79, 154.14, 143.88, 135.35, 129.46, 127.83, 85.17, 74.43, 51.69, 49.59, 46.87, 33.53, 28.64, 26.89, 24.51, 22.68, 21.55, 14.25, 12.36; **IR (neat, cm⁻¹):** 3200, 2936, 2861, 1727, 1598, 1450, 1365, 1322, 1223, 1202, 1186, 1165, 1093, 1038, 998, 953, 919, 814, 706, 669, 611, 548; **HRMS (ESI):** Calcd for C₂₁H₂₈N₂NaO₄S [M+Na]⁺ 427.1667, found 427.1664.



(±)-(1*R*,2*S*)-1-methoxycarbonyl-1-(2-pentyn-1-yl)cyclohexane-2-carbaldehyde (**5.89**)

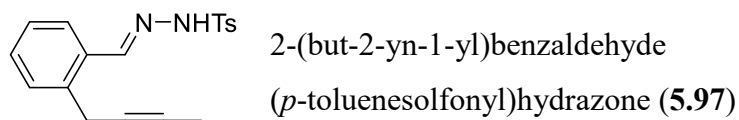
To a solution of **5.86** (554.1 mg, 2.0 mmol) in DCM/H₂O (4.9 ml/1.2 ml) at 0 °C was added TFA (1.2 ml), and resulting mixture was stirred at 0 °C for 3 h. After quenching a reaction with *sat. aq.* NaHCO₃, organic extracts were collected with DCM. The combined organic extracts were dried over Na₂SO₄, filtered, concentrated, and purified by flash column chromatography to give the aldehyde **5.89** as a clear oil (233.4 mg, 1.0 mmol, 50%).

*R*_f = 0.53 (Hex/EA = 5:1); ¹H NMR (400 MHz, CDCl₃) δ 9.85 (s, 1H), 3.77 (s, *J* = 7.2 Hz, 3H), 2.99 (dd, *J* = 8.7, 4.4 Hz, 1H), 2.69 (dt, *J* = 16.8, 2.1 Hz, 1H), 2.58 – 2.50 (m, 1H), 2.10 (qt, *J* = 7.5, 2.3 Hz, 2H), 1.93 – 1.33 (m, 8H), 1.07 (t, *J* = 7.5 Hz, 3H); ¹³C NMR (101 MHz, CDCl₃) δ 202.59, 175.45, 85.53, 75.01, 52.12, 51.96, 48.75, 33.50, 23.41, 22.97, 21.79, 21.67, 13.84, 12.27; IR (neat, cm⁻¹): 2938, 2861, 2360, 2341, 1732, 1452, 1321, 1225, 1143, 1075, 998; HRMS (ESI): Calcd for C₁₄H₂₀NaO₃ [M+Na]⁺ 259.1310, found 259.1310.

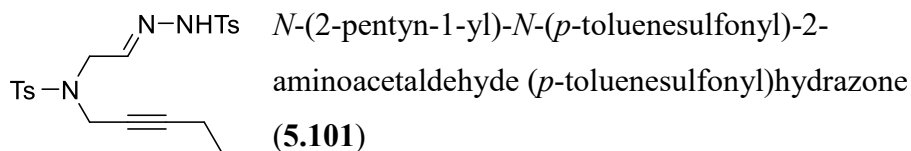


5.89 (139.5 mg, 0.6 mmol, 1 equiv) was dissolved in MeOH (3.0 ml, 0.2 M) at rt. *p*-toluenesulfonyl hydrazide (113.3 mg, 0.6 mmol, 1 equiv) was added to rbf and the reaction mixture was stirred for 9 h at rt. After evaporation of

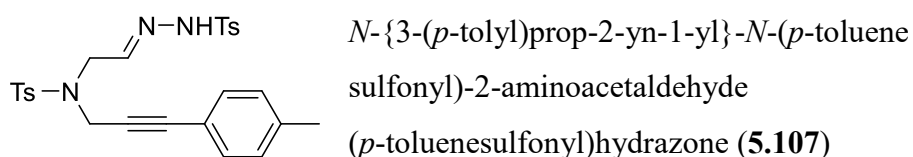
the solvent, crude material was chromatographed on silica gel to give the pure product **5.90** as a white gum (122.2 mg, 0.3 mmol, 51%). $R_f = 0.24$ (Hex/EA = 3:1); $^1\text{H NMR}$ (400 MHz, CDCl_3) δ 7.96 (s, 1H), 7.80 (d, $J = 8.2$ Hz, 2H), 7.31 (d, $J = 8.1$ Hz, 2H), 7.26 (d, $J = 5.5$ Hz, 1H), 3.61 (s, 3H), 2.88 – 2.78 (m, 1H), 2.43 (s, 3H), 2.17 (q, $J = 16.7$ Hz, 2H), 2.07 (q, $J = 7.4$ Hz, 2H), 1.84 – 1.22 (m, 8H), 1.05 (t, $J = 7.5$ Hz, 3H); $^{13}\text{C NMR}$ (101 MHz, CDCl_3) δ 175.33, 152.59, 144.06, 135.16, 129.52, 127.89, 84.55, 74.95, 51.89, 49.37, 43.23, 31.62, 25.14, 23.13, 22.81, 21.56, 21.46, 14.25, 12.34; **IR** (neat, cm^{-1}): 3194, 2936, 2861, 1729, 1598, 1451, 1367, 1324, 1290, 1223, 1185, 1167, 1093, 1037, 945, 922, 814, 706, 678, 582, 548; **HRMS** (ESI): Calcd for $\text{C}_{21}\text{H}_{28}\text{N}_2\text{NaO}_4\text{S}$ $[\text{M}+\text{Na}]^+$ 427.1667, found 427.1664.



2-(but-2-yn-1-yl)benzaldehyde (183.2 mg, 1.16 mmol, 1 equiv) and 4 Å molecular sieves (116 mg, 100 mg/mmol) was in DCM (11.6 ml, 0.1 M) at rt. *p*-toluenesulfonyl hydrazide (222.3 mg, 1.16 mmol, 1 equiv) was added to rbf and the reaction mixture was stirred for 20 h at rt. After cotton filtration, product **5.97** was purified by recrystallization with DCM and petroleum ether as a needle-shaped white crystal (286.9 mg, 0.88 mmol, 76%). $R_f = 0.50$ (Hex/EA = 2:1); $^1\text{H NMR}$ (400 MHz, CDCl_3) δ 8.07 (s, 1H), 7.98 (s, 1H), 7.89 (d, $J = 8.3$ Hz, 2H), 7.66 (d, $J = 7.7$ Hz, 1H), 7.44 (d, $J = 7.6$ Hz, 1H), 7.37 – 7.28 (m, 3H), 7.24 (t, 1H), 3.58 (d, $J = 2.4$ Hz, 2H), 2.41 (s, 3H), 1.79 (t, $J = 2.5$ Hz, 3H). $^{13}\text{C NMR}$ (101 MHz, CDCl_3) δ 146.43, 144.30, 136.43, 135.18, 130.65, 130.31, 129.67, 129.35, 127.99, 126.97, 79.07, 76.11, 23.42, 21.58, 3.57.

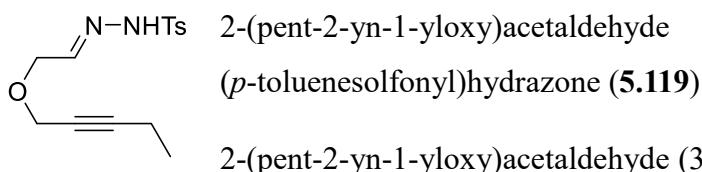


N-(2-pentyn-1-yl)-*N*-(*p*-toluenesulfonyl)-2-aminoacetaldehyde (3025.8 mg, 10.8 mmol, 1 equiv) and 4 Å molecular sieves (1080 mg, 100 mg/mmol) was in DCM (108 ml, 0.1 M) at rt. *p*-toluenesulfonyl hydrazide (2079.6 mg, 10.8 mmol, 1 equiv) was added to rbf and the reaction mixture was stirred for 2 h at rt. After cotton filtration, product **5.101** was purified by recrystallization with hot toluene as a white solid (3592.5 mg, 8.0 mmol, 74%). $R_f = 0.29$ (Hex/EA = 2:1); $^1\text{H NMR}$ (400 MHz, DMSO) δ 11.30 (s, 1H), 7.65 (dd, $J = 12.6, 8.2$ Hz, 4H), 7.39 (dd, $J = 8.1, 2.4$ Hz, 4H), 7.13 (t, $J = 5.1$ Hz, 1H), 3.80 (s, 2H), 3.77 (d, $J = 5.1$ Hz, 2H), 2.39 (s, 3H), 2.37 (s, 3H), 1.88 (q, $J = 7.5$ Hz, 2H), 0.81 (t, $J = 7.5$ Hz, 3H); $^{13}\text{C NMR}$ (101 MHz, DMSO) δ 145.84, 144.03, 143.81, 136.44, 135.57, 130.04, 130.02, 127.88, 127.50, 87.96, 72.33, 48.38, 37.76, 21.43, 21.42, 13.68, 11.84; **IR** (neat, cm^{-1}): 3206, 2978, 2878, 1598, 1445, 1348, 1163, 1091, 1040, 918, 815, 737, 660, 582, 546; **HRMS** (ESI): Calcd for $\text{C}_{21}\text{H}_{25}\text{N}_3\text{NaO}_4\text{S}_2$ $[\text{M}+\text{Na}]^+$ 470.1184, found 470.1177.

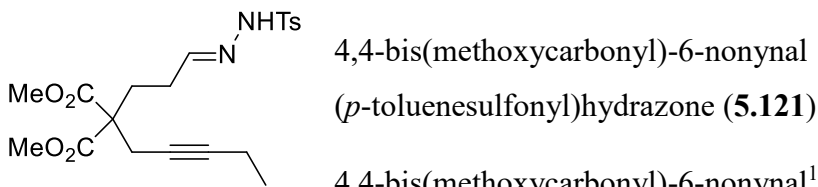


N-{3-(*p*-tolyl)prop-2-yn-1-yl}-*N*-(*p*-toluenesulfonyl)-2-aminoacetaldehyde (244.7 mg, 0.72 mmol, 1 equiv) and 4 Å molecular sieves (72 mg, 100 mg/mmol) was in DCM (7.2 ml, 0.1 M) at rt. *p*-toluenesulfonyl hydrazide (137.6 mg, 0.72 mmol, 1 equiv) was added to rbf and the reaction mixture was stirred for 19 h at rt. After cotton filtration, product **5.107** was purified by recrystallization with hot toluene 149.4 mg, 0.29 mmol, 41%). $R_f = 0.27$ (Hex/EA = 2:1); $^1\text{H NMR}$ (400 MHz, DMSO) δ 11.33 (s, 1H), 7.68 (dd, $J =$

7.7, 6.4 Hz, 4H), 7.35 (d, $J = 6.7$ Hz, 4H), 7.20 (t, $J = 5.0$ Hz, 1H), 7.14 (d, $J = 7.8$ Hz, 2H), 6.97 (d, $J = 7.9$ Hz, 2H), 4.08 (s, 2H), 3.86 (d, $J = 5.0$ Hz, 2H), 2.34 (s, 3H), 2.32 (s, 3H), 2.30 (s, 3H); ^{13}C NMR (101 MHz, DMSO) δ 145.71, 144.17, 143.82, 138.92, 136.41, 135.45, 131.63, 130.18, 130.04, 129.44, 127.90, 127.50, 118.82, 85.68, 81.82, 48.63, 38.12, 21.43, 21.39, 21.37.

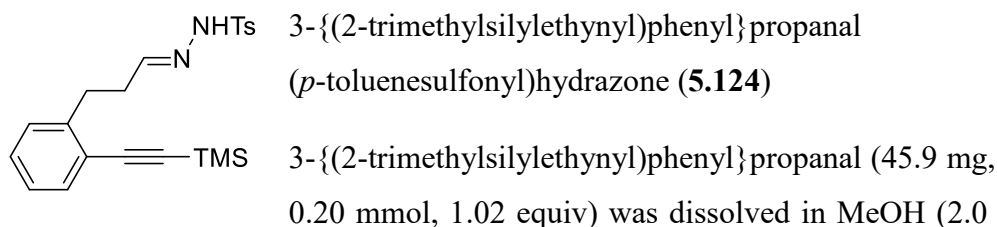


2-(pent-2-yn-1-yloxy)acetaldehyde (32.2 mg, 0.26 mmol, 1 equiv) and 4 Å molecular sieves (25.5 mg, 100 mg/mmol) was in DCM (2.6 ml, 0.1 M) at rt. *p*-toluenesulfonyl hydrazide (49.0 mg, 0.26 mmol, 1 equiv) was added to rbf and the reaction mixture was stirred for 18.5 h at rt. After cotton filtration, product **5.119** was purified by flash column chromatography (16.1 mg, 0.055 mmol, 21%). $R_f = 0.73$ (Hex/EA = 1:1);

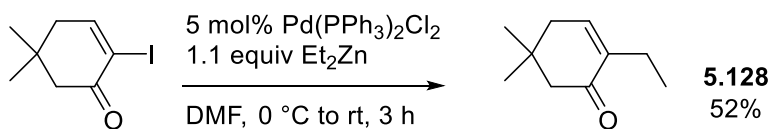


4,4-bis(methoxycarbonyl)-6-nonynal¹ (824.1 mg, 3.2 mmol, 1 equiv) was dissolved in MeOH (8.1 ml, 0.4 M) at rt. *p*-toluenesulfonyl hydrazide (622.2 mg, 3.2 mmol, 1 equiv) was added to rbf and the reaction mixture was stirred for 4 h at rt. After evaporation of the solvent, crude material was chromatographed on silica gel to give the pure product **5.121** as a clear gum (1280.5 mg, 3.0 mmol, 94%). $R_f = 0.25$ (Hex/EA = 2:1); ^1H NMR (400 MHz, DMSO) δ 10.99 (s, 1H), 7.68 (d, $J = 8.2$ Hz, 2H), 7.39 (d, $J = 8.2$ Hz, 2H), 3.65 (s, 6H), 2.67 (s, 2H), 2.38 (s, 3H), 2.14 – 1.95 (m, 6H), 0.98 (t, $J = 7.5$ Hz, 3H); ^{13}C NMR (101 MHz, DMSO) δ 170.39, 150.69, 143.62, 136.62, 129.90, 127.54, 85.30, 74.19, 56.58, 53.16, 28.57,

27.18, 23.16, 21.41, 14.42, 12.02; **IR** (neat, cm^{-1}): 3266, 2954, 1737, 1597, 1438, 1206, 1165, 1083, 960, 815, 736, 666, 548; **HRMS** (ESI): Calcd for $\text{C}_{20}\text{H}_{26}\text{N}_2\text{NaO}_6\text{S}$ $[\text{M}+\text{Na}]^+$ 445.1409, found 445.1407.



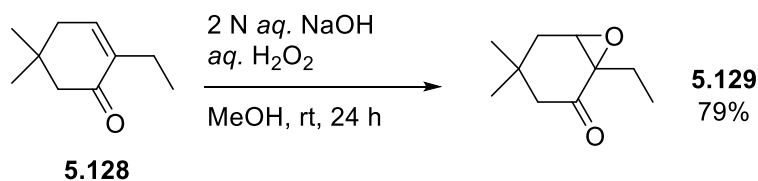
ml, 0.1 M) at rt. *p*-toluenesulfonyl hydrazide (37.1 mg, 0.20 mmol, 1 equiv) was added to rbf and the reaction mixture was stirred for 1.5 h at rt to give the alkynylhydrazone **5.124**. The crude solution was used for Rh-catalysis directly due to its stability issue during flash column chromatography. R_f = 0.16 (Hex/EA = 5:1); **^1H NMR** (400 MHz, CD_3OD) δ 7.73 (d, J = 8.2 Hz, 2H), 7.34 (d, J = 8.1 Hz, 3H), 7.22 (t, J = 5.2 Hz, 1H), 7.20 – 7.06 (m, 3H), 4.86 (s, 1H), 2.89 (t, J = 7.6 Hz, 2H), 2.53 – 2.44 (m, 2H), 2.42 (s, J = 4.0 Hz, 3H), 0.20 (s, J = 13.5 Hz, 9H); **^{13}C NMR** (101 MHz, CD_3OD) δ 152.29, 145.08, 144.34, 137.48, 133.34, 130.61, 130.08, 129.94, 128.77, 127.26, 123.67, 104.66, 99.00, 33.95, 32.19, 21.59, 0.07.



2-ethyl-5,5-dimethylcyclohex-2-en-1-one (**5.128**)

To a solution of 2-iodo-5,5-dimethylcyclohex-2-en-1-one (1170.5 mg, 4.7 mmol) and $\text{Pd}(\text{PPh}_3)_2\text{Cl}_2$ (167.6 mg, 0.23 mmol, 5 mol%) in DMF (23.4 ml) at 0 °C was added diethylzinc (1.0 M in hexane, 5.2 ml, 5.2 mmol, 1.1 equiv) under Ar atmosphere. The resulting mixture was stirred for 3 h at rt, quenched

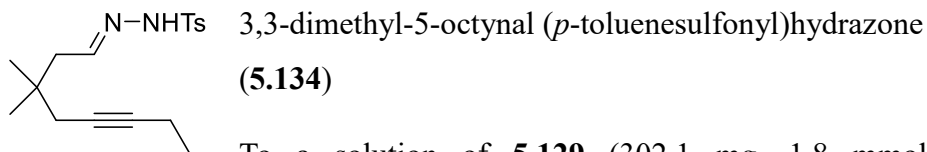
with *aq.* NH₄Cl, and extracted with Et₂O. The combined organic extracts were washed with H₂O (twice) and brine, and dried over MgSO₄. After evaporation of the solvent (temperature of water bath should be kept below 15 °C), crude material was chromatographed on silica gel to give the cross-coupled product **5.128** as a colorless clear liquid (367.8 mg, 2.4 mmol, 52%). *R*_f = 0.38 (Hex/EA = 10:1); ¹H NMR (400 MHz, CDCl₃) δ 6.55 (t, *J* = 4.0 Hz, 1H), 2.28 (s, 2H), 2.26 – 2.18 (m, 4H), 1.06 – 0.96 (s, 6H; t, 3H); ¹³C NMR (101 MHz, CDCl₃) δ 199.46, 141.51, 140.03, 52.05, 40.00, 33.93, 28.16, 22.06, 12.78; IR (neat, cm⁻¹): 2964, 2933, 2874, 1718, 1677, 1620, 1463, 1387, 1369, 1270, 1232, 1195, 1154, 943, 920; HRMS (ESI): Calcd for C₁₀H₁₆NaO [M+Na]⁺ 175.1099, found 175.1096.



1-ethyl-4,4-dimethyl-7-oxabicyclo[4.1.0]heptan-2-one (**5.129**)

To a solution of **5.128** (358.9 mg, 2.4 mmol) in MeOH (24 ml) and 2 N *aq.* NaOH (0.83 ml, 1.7 mmol, 0.7 equiv) was added *aq.* H₂O₂ (34.5%, 1.2 ml, 13.2 mmol, 5.6 equiv) at rt. After stirring for 24 h, the reaction mixture was diluted with H₂O, and extracted with DCM. The combined organic extracts were washed with H₂O, dried over Na₂SO₄, filtered, and concentrated *in vacuo*. The crude material was chromatographed on silica gel to give the epoxy ketone **5.129** as a clear liquid (313.1 mg, 1.9 mmol, 79%). *R*_f = 0.42 (Hex/EA = 10:1); ¹H NMR (400 MHz, CDCl₃) δ 3.37 (d, *J* = 3.6 Hz, 1H), 2.70 (d, *J* = 13.3 Hz, 1H), 2.03 (d, *J* = 15.4 Hz, 1H), 1.95 (td, *J* = 14.4, 7.3 Hz, 1H), 1.83 (d, *J* = 13.3 Hz, 2H), 1.63 (td, *J* = 14.5, 7.5 Hz, 1H), 1.01 (s, 3H), 0.96 (t, *J* = 7.2 Hz, 3H), 0.90 (s, 3H); ¹³C NMR (101 MHz, CDCl₃) δ

207.72, 62.46, 61.94, 48.97, 37.94, 36.70, 30.85, 27.79, 21.82, 8.82; **IR** (neat, cm^{-1}): 2958, 2931, 2872, 1712, 1466, 1370, 1351, 1170, 1112, 1051, 945, 931, 858, 479; **HRMS** (ESI): Calcd for $\text{C}_{10}\text{H}_{16}\text{NaO}_2$ $[\text{M}+\text{Na}]^+$ 191.1048, found 191.1046.



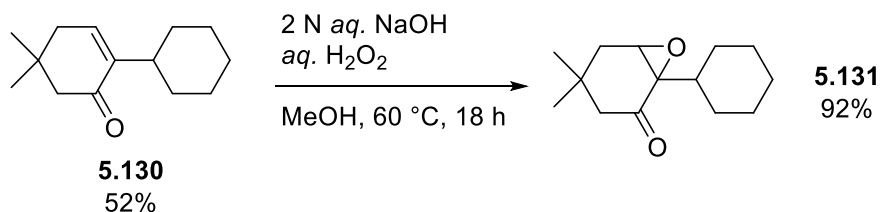
To a solution of **5.129** (302.1 mg, 1.8 mmol) in DCM/AcOH (3.0 ml/3.0 ml) at 0 °C was added *p*-toluenesulfonyl hydrazide (724.0 mg, 3.8 mmol, 2.1 equiv). After stirring for 19 h at rt, the resulting mixture was quenched with *sat. aq.* NaHCO_3 , extracted with DCM, dried over Na_2SO_4 , and concentrated. The crude material was chromatographed on silica gel to give the hydrazone **5.134** as a clear oil (416.8 mg, 1.3 mmol, 72%). R_f = 0.22 (Hex/EA = 5:1); **^1H NMR** (400 MHz, CDCl_3) δ 7.81 (d, J = 8.0 Hz, 3H), 7.31 (d, J = 8.0 Hz, 2H), 7.22 (t, J = 6.2 Hz, 1H), 2.42 (s, 3H), 2.19 (d, J = 6.2 Hz, 2H), 2.18 – 2.10 (m, 2H), 1.92 (s, 2H), 1.10 (t, J = 7.5 Hz, 3H), 0.85 (s, 6H); **^{13}C NMR** (101 MHz, CDCl_3) δ 151.21, 144.10, 135.13, 129.59, 127.86, 84.14, 76.32, 43.24, 34.13, 32.12, 26.63, 21.56, 14.34, 12.37; **IR** (neat, cm^{-1}): 3206, 2963, 2935, 2878, 1599, 1455, 1367, 1324, 1166, 1093, 1040, 918, 814, 706, 668; **HRMS** (ESI): Calcd for $\text{C}_{17}\text{H}_{24}\text{N}_2\text{NaO}_2\text{S}$ $[\text{M}+\text{Na}]^+$ 343.1456, found 343.1454.



2-cyclohexyl-5,5-dimethylcyclohex-2-en-1-one (**5.130**)

To a solution of 2-iodo-5,5-dimethylcyclohex-2-en-1-one (998.3 mg, 4.0 mmol) and $\text{Pd}(\text{PPh}_3)_2\text{Cl}_2$ (143.2 mg, 0.2 mmol, 5 mol%) in DMF (20 ml) at 0 °C was added cyclohexylzinc bromide solution in THF (5 ml) which was made from ZnBr_2 (1194.9 mg, 5.2 mmol, 1.3 equiv) and

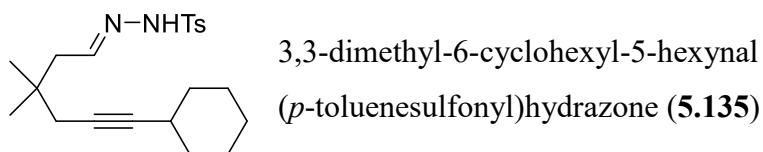
cyclohexylmagnesium bromide (2.0 M in Et₂O, 2.8 ml, 5.6 mmol, 1.4 equiv) under Ar atmosphere. The resulting mixture was stirred for 2 h at rt, quenched with *aq.* NH₄Cl, and extracted with Et₂O. The combined organic extracts were washed with H₂O (twice) and brine, and dried over MgSO₄. After evaporation of the solvent, crude material was chromatographed on silica gel to give the cross-coupled product **5.130** as a colorless clear liquid (428.7 mg, 2.1 mmol, 52%). *R_f* = 0.42 (Hex/EA = 10:1); ¹H NMR (400 MHz, CDCl₃) δ 6.50 (t, *J* = 4.1 Hz, 1H), 2.53 (t, *J* = 11.9 Hz, 1H), 2.27 (s, 2H), 2.24 (d, *J* = 4.1 Hz, 2H), 1.79 – 1.62 (m, 5H), 1.36 (q, *J* = 12.7 Hz, 2H), 1.24 – 1.03 (m, 3H), 1.01 (s, 6H); ¹³C NMR (101 MHz, CDCl₃) δ 199.08, 143.85, 140.24, 52.34, 40.13, 35.73, 33.68, 32.60, 28.13, 26.67, 26.34; IR (neat, cm⁻¹): 2925, 2852, 1674, 1449, 1387, 1368, 1352, 1300, 1270, 1233, 1178, 1138, 1091, 1028, 967, 921, 893, 579; HRMS (ESI): Calcd for C₁₄H₂₂NaO [M+Na]⁺ 229.1568, found 229.1564.



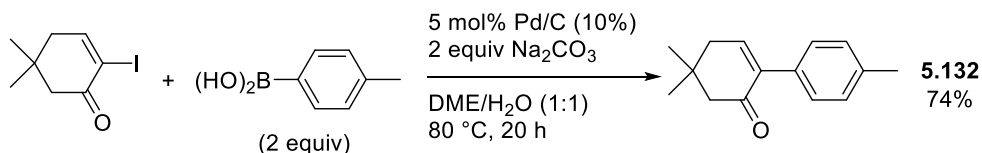
1-cyclohexyl-4,4-dimethyl-7-oxabicyclo[4.1.0]heptan-2-one (**5.131**)

To a solution of **5.130** (190.9 mg, 0.9 mmol) in MeOH (9.3 ml) and 2 N *aq.* NaOH (0.33 ml, 0.6 mmol, 0.7 equiv) was added *aq.* H₂O₂ (34.5%, 0.45 ml, 5.2 mmol, 5.6 equiv) at rt. After stirring at 60 °C for 18 h, the reaction mixture was diluted with H₂O, and extracted with DCM. The combined organic extracts were washed with H₂O, dried over Na₂SO₄, filtered, and concentrated *in vacuo*. The crude material was chromatographed on silica gel to give the epoxy ketone **5.131** as a clear liquid (188.8 mg, 0.8 mmol, 92%). *R_f* = 0.44 (Hex/EA = 10:1); ¹H NMR (400 MHz, CDCl₃) δ 3.38 (d, *J* = 4.5 Hz, 1H),

2.69 (d, $J = 13.5$ Hz, 1H), 2.12 (t, $J = 12.1$ Hz, 1H), 2.01 (d, $J = 15.3$ Hz, 1H), 1.85 – 1.55 (m, 7H), 1.29 (p, $J = 13.1$ Hz, 2H), 1.19 – 1.03 (m, 2H), 1.02 – 0.93 (m, 4H), 0.89 (s, 3H); ^{13}C NMR (101 MHz, CDCl_3) δ 207.46, 64.17, 59.83, 49.32, 37.98, 36.29, 35.03, 30.84, 28.99, 27.70, 26.37, 26.24, 26.02, 25.92; IR (neat, cm^{-1}): 2926, 2854, 1711, 1451, 1421, 1389, 1369, 1346, 1299, 1277, 1235, 1163, 1149, 1101, 1069, 1020, 964, 938, 856, 845, 778, 727, 677, 606, 589, 571, 553, 494; HRMS (ESI): Calcd for $\text{C}_{14}\text{H}_{22}\text{NaO}_2$ $[\text{M}+\text{Na}]^+$ 245.1517, found 245.1515.

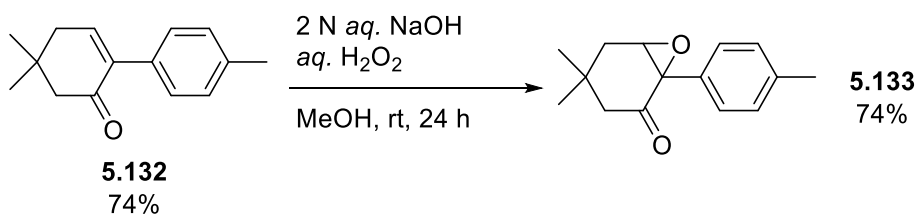


To a solution of **5.131** (188.8 mg, 0.8 mmol) in DCM/AcOH (1.4 ml/1.4 ml) at 0 °C was added *p*-toluenesulfonyl hydrazide (342.4 mg, 1.8 mmol, 2.1 equiv). After stirring for 17 h at rt, the resulting mixture was quenched with *sat. aq.* NaHCO_3 , extracted with DCM, dried over Na_2SO_4 , and concentrated. The crude material was chromatographed on silica gel to give the hydrazone **5.135** as a clear oil (243.7 mg, 0.7 mmol, 77%). $R_f = 0.21$ (Hex/EA = 5:1); ^1H NMR (400 MHz, CDCl_3) δ 7.81 (d, $J = 8.2$ Hz, 2H), 7.57 (d, $J = 9.1$ Hz, 1H), 7.30 (d, $J = 8.0$ Hz, 2H), 7.21 (t, $J = 6.2$ Hz, 1H), 2.42 (s, 3H), 2.33 (s, 1H), 2.20 (d, $J = 6.2$ Hz, 2H), 1.94 (d, $J = 2.0$ Hz, 2H), 1.80 – 1.61 (m, 4H), 1.53 – 1.24 (m, 6H), 0.86 (s, 6H); ^{13}C NMR (101 MHz, CDCl_3) δ 151.18, 144.08, 135.19, 129.57, 127.88, 87.16, 76.88, 43.26, 34.20, 33.05, 32.06, 29.02, 26.69, 25.89, 24.80, 21.56; IR (neat, cm^{-1}): 3203, 2928, 2854, 1598, 1448, 1367, 1328, 1306, 1166, 1094, 1037, 1011, 920, 814, 706, 669, 591, 548; HRMS (ESI): Calcd for $\text{C}_{21}\text{H}_{30}\text{N}_2\text{NaO}_2\text{S}$ $[\text{M}+\text{Na}]^+$ 397.1926, found 397.1924.



2-(*p*-tolyl)-5,5-dimethylcyclohex-2-en-1-one (**5.132**)

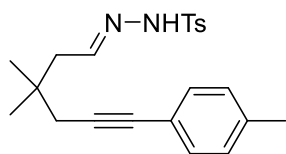
To a solution of 2-iodo-5,5-dimethylcyclohex-2-en-1-one (1029.4 mg, 4.1 mmol) in DME (12.3 ml) and H₂O (12.3 ml) were added Na₂CO₃ (872.6 mg, 8.2 mmol, 2 equiv), 4-methylphenylboronic acid (1142.1 mg, 8.2 mmol, 2 equiv), and 10% Pd/C (219.0 mg, 0.21 mmol, 5 mol%). The mixture was stirred at 80 °C for 20 h, and Pd/C was filtered. The organic mixture was diluted with water and extracted with diethyl ether. The collected organic extracts were dried over MgSO₄ and concentrated. The crude material was chromatographed on a silica gel to give the product **5.132** as a white solid (649.4 mg, 3.0 mmol, 74%). *R*_f = 0.37 (Hex/EA = 10:1); ¹H NMR (400 MHz, CDCl₃) δ 7.21 (d, *J* = 7.9 Hz, 2H), 7.13 (d, *J* = 7.9 Hz, 2H), 6.84 (t, *J* = 4.3 Hz, 1H), 2.41 (s, 2H), 2.37 (d, *J* = 4.3 Hz, 2H), 2.32 (s, 3H), 1.08 (s, 6H); ¹³C NMR (101 MHz, CDCl₃) δ 198.11, 145.12, 139.18, 137.24, 133.39, 128.72, 128.44, 52.67, 40.65, 34.08, 28.28, 21.19.



1-(*p*-tolyl)-4,4-dimethyl-7-oxabicyclo[4.1.0]heptan-2-one (**5.133**)

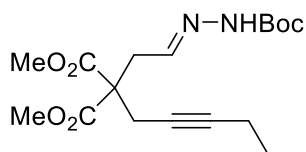
To a solution of **5.132** (633.8 mg, 3.0 mmol) in MeOH (30 ml) and 2 N *aq.* NaOH (1.04 ml, 2.1 mmol, 0.7 equiv) was added *aq.* H₂O₂ (34.5%, 1.44 ml, 16.6 mmol, 5.6 equiv) at rt. After stirring for 24 h, the reaction mixture was diluted with H₂O, and extracted with DCM. The combined organic extracts

were washed with H₂O, dried over Na₂SO₄, filtered, and concentrated *in vacuo*. The crude material was chromatographed on silica gel to give the epoxy ketone **5.133** as a white crystal (504.1 mg, 2.2 mmol, 74%). *R*_f = 0.36 (Hex/EA = 10:1); ¹H NMR (400 MHz, CDCl₃) δ 7.25 (d, *J* = 7.7 Hz, 2H), 7.16 (d, *J* = 7.9 Hz, 2H), 3.42 (d, *J* = 4.5 Hz, 1H), 2.82 (d, *J* = 13.7 Hz, 1H), 2.34 (s, 3H), 2.09 (t, *J* = 16.4 Hz, 1H), 2.05 – 1.89 (m, 2H), 1.06 (s, 6H). ¹³C NMR (101 MHz, CDCl₃) δ 205.73, 138.03, 130.64, 128.82, 127.07, 65.53, 62.34, 49.20, 38.00, 36.49, 30.83, 27.94, 21.23.



3,3-dimethyl-6-(*p*-tolyl)-5-hexynal
(*p*-toluenesulfonyl)hydrazone (**5.136**)

To a solution of **5.133** (494.7 mg, 2.1 mmol) in DCM/AcOH (3.6 ml/3.6 ml) at 0 °C was added *p*-toluenesulfonyl hydrazide (866.0 mg, 4.5 mmol, 2.1 equiv). After stirring for 6 h at rt, the resulting mixture was quenched with *sat. aq.* NaHCO₃, extracted with DCM, dried over Na₂SO₄, and concentrated. The crude material was chromatographed on silica gel to give the hydrazone **5.136** as a clear oil (644.3 mg, 1.7 mmol, 78%). *R*_f = 0.30 (Hex/EA = 3:1); ¹H NMR (400 MHz, CDCl₃) δ 7.80 (d, *J* = 8.1 Hz, 2H), 7.31 (d, *J* = 4.8 Hz, 2H), 7.27 (d, *J* = 7.6 Hz, 2H), 7.10 (d, *J* = 7.9 Hz, 2H), 2.41 (s, 3H), 2.34 (s, 3H), 2.28 (d, *J* = 6.2 Hz, 2H), 2.19 (s, 2H), 0.96 (s, 6H).



3,3-bis(methoxycarbonyl)-5-octynal
(*tert*-butoxycarbonyl)hydrazone (**5.166**)

3,3-bis(methoxycarbonyl)-5-octynal (452.4 mg, 1.9 mmol, 1 equiv) was dissolved in MeOH (4.7 ml, 0.4 M) at rt. *tert*-butyl carbazate (253.9 mg, 1.9 mmol, 1 equiv) was added to rbf and the reaction

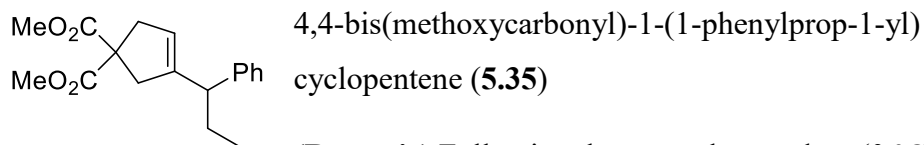
mixture was stirred for 8 h at rt. After evaporation of the solvent, crude material was chromatographed on silica gel to give the pure product **5.166** as a white solid (506.3 mg, 1.4 mmol, 76%). $R_f = 0.35$ (Hex/EA = 2:1); $^1\text{H NMR}$ (400 MHz, CDCl_3) δ 7.67 (s, 1H), 7.23 (s, 1H), 3.75 (d, $J = 1.3$ Hz, 6H), 2.98 (d, $J = 5.5$ Hz, 2H), 2.82 (s, 2H), 2.12 (q, $J = 7.4$ Hz, 2H), 1.49 (s, 9H), 1.08 (t, $J = 7.5$ Hz, 3H); $^{13}\text{C NMR}$ (101 MHz, CDCl_3) δ 170.06, 152.30, 142.38, 85.64, 80.89, 73.23, 56.68, 52.82, 35.50, 28.18, 24.24, 14.02, 12.24; **IR** (neat, cm^{-1}): 3311, 3249, 2978, 2847, 2241, 1748, 1538, 1436, 1368, 1063, 1016, 968, 915, 869, 770, 733, 646, 608; **HRMS (ESI)**: Calcd for $\text{C}_{17}\text{H}_{26}\text{N}_2\text{NaO}_6$ $[\text{M}+\text{Na}]^+$ 377.1689, found 377.1687.

5.5.3 General procedure for the rhodium-catalyzed tandem reaction

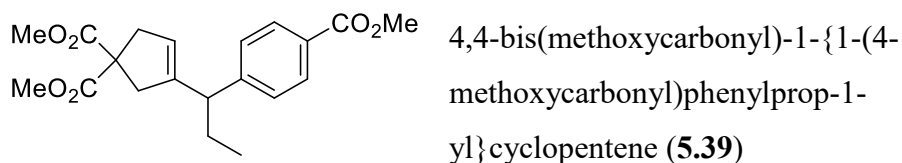
(Racemic) To a alkynylhydrazone (0.20 mmol) in a 20 ml tube vial was added MeOH (2 ml, 0.1 M), and $[\text{Rh}(\text{COD})\text{OH}]_2$ (0.010 mmol, 0.05 equiv). The resulting yellow solution was cooled to 0 °C. $\text{RB}(\text{OH})_2$ (0.40 mmol, 2 equiv) was added and the reaction mixture was stirred at 0 °C for 1 h (check conversion of SM by TLC), then 60 °C for 5 h. After evaporation of the solvent, the crude product was purified by flash chromatography on a silica gel column to give the pure product.

(Asymmetric) To a alkynylhydrazone (0.10 mmol) in a 20 ml tube vial was added toluene (1 ml, 0.1 M) and **5.165** (0.005 mmol, 0.05 equiv). The resulting orange solution was cooled to 0 °C. Aqueous KOH (0.2 M, 0.1 ml, 0.02 mmol, 20 mol%) and $\text{RB}(\text{OH})_2$ (0.20 mmol, 2 equiv) was added and the reaction mixture was stirred at 0 °C for 48 h, then 60 °C for 24 h. After short filtration by Na_2SO_4 and evaporation of the solvent, the crude product was purified by flash chromatography on a silica gel column to give the pure product.

5.5.4 Characterization for products

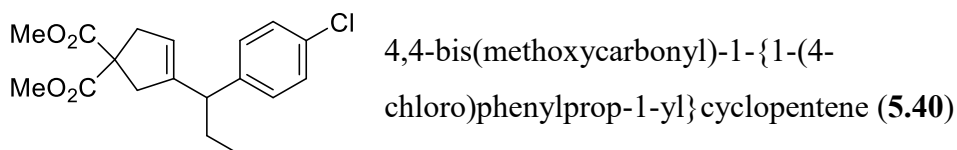


(Racemic) Following the general procedure (0 °C, 1 h, then 60 °C, 5 h), **5.34** (43.8 mg, 0.11 mmol) was reacted with [Rh(cod)OH]₂ (2.5 mg, 0.0054 mmol) and phenylboronic acid (26.1 mg, 0.21 mmol) in MeOH (1.1 ml) to give the product **5.35** as a clear oil (27.8 mg, 0.092 mmol, 86%). **(Asymmetric)** Following the general procedure, **5.34** (48.5 mg, 0.12 mmol) was reacted with **5.165** (5.3 mg, 0.0059 mmol), aqueous KOH (0.12 ml, 0.024 mmol), and phenylboronic acid (29.9 mg, 0.24 mmol) in toluene (1.2 ml) to give the product (*S*)-**5.35** as a clear oil (29.0 mg, 0.096 mmol, 81%, 93% *ee*). $R_f = 0.59$ (Hex/EA = 3:1); ¹H NMR (400 MHz, CDCl₃) δ 7.27 (t, *J* = 7.3 Hz, 2H), 7.18 (t, *J* = 7.0 Hz, 1H), 7.13 (d, *J* = 7.5 Hz, 2H), 5.38 (s, 1H), 3.68 (s, 3H), 3.65 (s, 3H), 3.15 (t, *J* = 7.0 Hz, 1H), 3.08 – 2.93 (m, 2H), 2.76 (q, *J* = 16.6 Hz, 2H), 1.96 – 1.82 (m, 1H), 1.78 – 1.63 (m, 1H), 0.82 (t, *J* = 7.3 Hz, 3H); ¹³C NMR (101 MHz, CDCl₃) δ 172.50, 144.65, 142.83, 128.22, 127.85, 126.19, 120.62, 59.02, 52.68, 52.64, 48.95, 41.68, 40.34, 26.65, 12.30; **IR** (neat, cm⁻¹): 2956, 2932, 2873, 2360, 2341, 1738, 1493, 1452, 1435, 1259, 1198, 1159, 1075, 808, 758, 702, 536; **HRMS (ESI)**: Calcd for C₁₈H₂₂NaO₄ [M+Na]⁺ 325.1416, found 325.1409; **Chiral HPLC**: Chiralpak IA, 1.0 ml/min, Hex/*i*PA=99:1, R_t =6.8 min, 7.7 min; $[\alpha]_D^{22.8} = -1.38$ (*c* = 1.00 g/100 ml, CHCl₃, 93% *ee*).



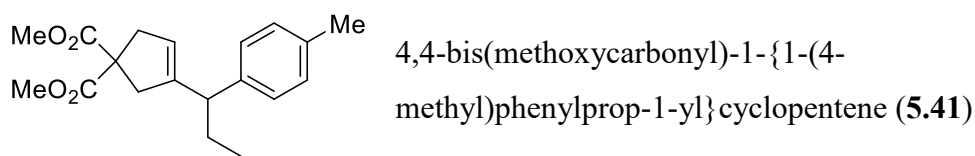
(Racemic) Following the general procedure (0 °C, 1 h, then 60 °C, 5 h), **5.34** (75.9 mg, 0.19 mmol) was reacted with [Rh(cod)OH]₂ (4.4 mg, 0.0093 mmol)

and 4-(methoxycarbonyl)phenylboronic acid (69.0 mg, 0.37 mmol) in MeOH (1.9 ml) to give the product **5.39** as a clear oil (55.6 mg, 0.15 mmol, 83%). (**Asymmetric**) Following the general procedure, **5.34** (48.5 mg, 0.12 mmol) was reacted with **5.165** (5.3 mg, 0.0059 mmol), aqueous KOH (0.12 ml, 0.024 mmol), and (methoxycarbonyl)phenylboronic acid (44.1 mg, 0.24 mmol) in toluene (1.2 ml) to give the product (*S*)-**5.39** as a clear oil (32.3 mg, 0.090 mmol, 75%, 91% *ee*). $R_f = 0.61$ (Hex/EA = 3:1); $^1\text{H NMR}$ (400 MHz, CDCl_3) δ 7.96 (d, $J = 8.3$ Hz, 2H), 7.21 (d, $J = 8.2$ Hz, 2H), 5.40 (s, $J = 1.4$ Hz, 1H), 3.90 (s, 3H), 3.69 (s, 3H), 3.66 (s, 3H), 3.22 (t, $J = 7.1$ Hz, 1H), 3.08 – 2.94 (m, 2H), 2.74 (q, $J = 16.6$ Hz, 2H), 2.02 – 1.85 (m, 1H), 1.80 – 1.64 (m, 1H), 0.81 (t, $J = 7.3$ Hz, 3H); $^{13}\text{C NMR}$ (101 MHz, CDCl_3) δ 172.40, 172.38, 167.05, 148.35, 143.74, 129.64, 128.27, 127.92, 121.36, 58.92, 52.74, 52.71, 51.96, 48.95, 41.66, 40.34, 26.51, 12.20; **IR** (neat, cm^{-1}): 2956, 2874, 1737, 1610, 1435, 1280, 1197, 1178, 1110, 1078, 1019, 967, 807, 772, 710; **HRMS** (**ESI**): Calcd for $\text{C}_{20}\text{H}_{24}\text{NaO}_6$ $[\text{M}+\text{Na}]^+$ 383.1471, found 383.1463; **Chiral HPLC**: Chiralpak IA, 1.0 ml/min, Hex/*i*PA=80:20, R_t =5.1 min, 6.4 min; $[\alpha]_D^{23.1} = +0.46$ ($c = 1.00$ g/100 ml, CHCl_3 , 91% *ee*).



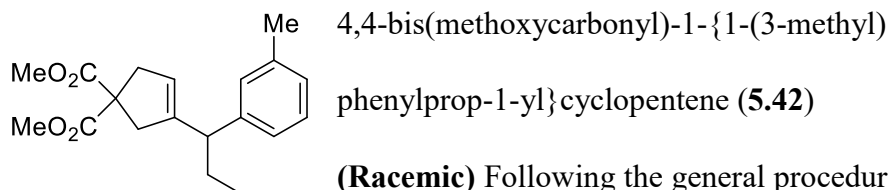
(**Racemic**) Following the general procedure (0 °C, 1 h, then 60 °C, 5 h), **5.34** (84.2 mg, 0.21 mmol) was reacted with $[\text{Rh}(\text{cod})\text{OH}]_2$ (4.8 mg, 0.010 mmol) and 4-chlorophenylboronic acid (67.9 mg, 0.41 mmol) in MeOH (2.1 ml) to give the product **5.40** as a clear oil (60.3 mg, 0.18 mmol, 87%). (**Asymmetric**) Following the general procedure, **5.34** (49.1 mg, 0.12 mmol) was reacted with **5.165** (5.4 mg, 0.0061 mmol), aqueous KOH (0.12 ml, 0.024 mmol), and 4-chlorophenylboronic acid (39.6 mg, 0.24 mmol) in toluene (1.2 ml) to give the product (*S*)-**5.40** as a clear oil (33.9 mg, 0.10 mmol, 84%, 94% *ee*). $R_f =$

0.59 (Hex/EA = 3:1); $^1\text{H NMR}$ (400 MHz, CDCl_3) δ 7.25 (d, $J = 8.2$ Hz, 2H), 7.06 (d, $J = 8.2$ Hz, 2H), 5.37 (s, 1H), 3.69 (s, $J = 0.5$ Hz, 3H), 3.67 (s, $J = 0.5$ Hz, 3H), 3.13 (t, $J = 7.2$ Hz, 1H), 3.08 – 2.94 (m, 2H), 2.74 (q, $J = 16.6$ Hz, 2H), 1.96 – 1.81 (m, 1H), 1.75 – 1.59 (m, 1H), 0.80 (t, $J = 7.3$ Hz, 3H); $^{13}\text{C NMR}$ (101 MHz, CDCl_3) δ 172.44, 172.43, 144.13, 141.31, 131.87, 129.21, 128.37, 121.04, 58.91, 52.73, 52.71, 48.30, 41.65, 40.34, 26.61, 12.20; **IR** (neat, cm^{-1}): 2957, 2932, 2874, 1737, 1492, 1435, 1258, 1190, 1160, 1092, 1015, 968, 832, 804, 536; **HRMS (ESI)**: Calcd for $\text{C}_{18}\text{H}_{21}\text{ClNaO}_4$ [$\text{M}+\text{Na}$] $^+$ 359.1026, found 359.1021; $[\alpha]_D^{23.5} = -1.69$ ($c = 1.00$ g/100 ml, CHCl_3 , 94% *ee*); **Chiral HPLC analysis of 2c-diol after reduction of 2c by LAH**: Chiralpak IA, 1.0 ml/min, Hex/*i*PA=95:5, R_t =17.0 min, 20.3 min.



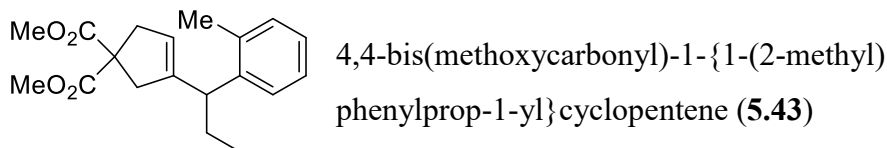
(Racemic) Following the general procedure (0 °C, 1 h, then 60 °C, 5 h), **5.34** (82.9 mg, 0.20 mmol) was reacted with $[\text{Rh}(\text{cod})\text{OH}]_2$ (4.8 mg, 0.010 mmol) and 4-methylphenylboronic acid (56.3 mg, 0.41 mmol) in MeOH (2.0 ml) to give the product **5.41** as a clear oil (51.9 mg, 0.16 mmol, 81%). **(Asymmetric)** Following the general procedure, **5.34** (45.3 mg, 0.11 mmol) was reacted with **5.165** (5.0 mg, 0.0055 mmol), aqueous KOH (0.11 ml, 0.022 mmol), and 4-methylphenylboronic acid (30.8 mg, 0.22 mmol) in toluene (1.1 ml) to give the product (*S*)-**5.41** as a clear oil (28.6 mg, 0.090 mmol, 82%, 94% *ee*). $R_f = 0.62$ (Hex/EA = 3:1); $^1\text{H NMR}$ (400 MHz, CDCl_3) δ 7.08 (d, $J = 7.8$ Hz, 2H), 7.01 (d, $J = 8.0$ Hz, 2H), 5.36 (s, $J = 1.3$ Hz, 1H), 3.69 (s, 3H), 3.66 (s, 3H), 3.12 (t, $J = 7.1$ Hz, 1H), 3.07 – 2.92 (m, 2H), 2.85 – 2.68 (m, 2H), 2.31 (s, 3H), 1.95 – 1.80 (m, 1H), 1.76 – 1.61 (m, 1H), 0.81 (t, $J = 7.3$ Hz, 3H); $^{13}\text{C NMR}$ (101 MHz, CDCl_3) δ 172.57, 172.55, 144.83, 139.78, 135.60, 128.91, 127.71, 120.43, 58.99, 52.68, 52.64, 48.52, 41.68, 40.35, 26.72, 20.98, 12.32;

IR (neat, cm⁻¹): 2956, 2929, 2873, 2360, 2341, 1738, 1513, 1435, 1384, 1257, 1198, 1159, 1078, 968, 805, 536; **HRMS (ESI):** Calcd for C₁₉H₂₄NaO₄ [M+Na]⁺ 339.1572, found 339.1569; [α]_D^{23.7} = -1.82 (*c* = 1.00 g/100 ml, CHCl₃, 94% *ee*); **Chiral HPLC analysis of 2g-diol after reduction of 2g by LAH:** Chiralpak IA, 1.0 ml/min, Hex/*i*PA=95:5, R_t=11.7 min, 12.5 min.

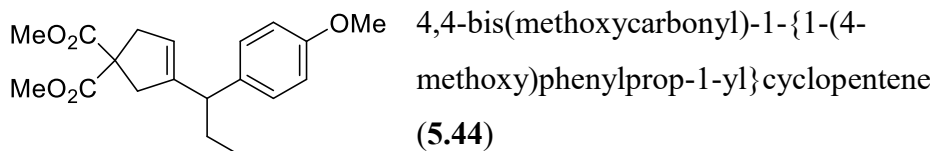


(Racemic) Following the general procedure (0 °C, 1 h, then 60 °C, 5 h), **5.34** (80.6 mg, 0.20 mmol) was reacted with [Rh(cod)OH]₂ (4.6 mg, 0.0099 mmol) and 3-methylphenylboronic acid (53.7 mg, 0.39 mmol) in MeOH (2.0 ml) to give the product **5.42** as a clear oil (51.2 mg, 0.16 mmol, 82%). **(Asymmetric)** Following the general procedure, **5.34** (44.0 mg, 0.11 mmol) was reacted with **5.165** (4.8 mg, 0.0054 mmol), aqueous KOH (0.11 ml, 0.022 mmol), and 3-methylphenylboronic acid (29.3 mg, 0.22 mmol) in toluene (1.1 ml) to give the product (*S*)-**5.42** as a clear oil (26.0 mg, 0.082 mmol, 76%, 92% *ee*). R_f = 0.62 (Hex/EA = 3:1); ¹H NMR (400 MHz, CDCl₃) δ 7.16 (t, *J* = 7.8 Hz, 1H), 7.00 (d, *J* = 7.6 Hz, 1H), 6.92 (d, *J* = 6.6 Hz, 2H), 5.37 (s, *J* = 1.4 Hz, 1H), 3.69 (s, 3H), 3.66 (s, 3H), 3.11 (t, *J* = 7.3 Hz, 1H), 3.07 – 2.92 (m, 2H), 2.77 (q, *J* = 16.6 Hz, 2H), 2.32 (s, 3H), 1.96 – 1.80 (m, 1H), 1.76 – 1.61 (m, 1H), 0.81 (t, *J* = 7.3 Hz, 3H); ¹³C NMR (101 MHz, CDCl₃) δ 172.56, 172.53, 144.73, 142.79, 137.68, 128.64, 128.07, 126.92, 124.84, 120.50, 59.03, 52.68, 52.64, 48.90, 41.68, 40.32, 26.66, 21.45, 12.35; **IR (neat, cm⁻¹):** 2956, 2931, 2873, 1738, 1606, 1435, 1382, 1257, 1197, 1159, 1077, 968, 785, 707; **HRMS (ESI):** Calcd for C₁₉H₂₄NaO₄ [M+Na]⁺ 339.1572, found 339.1568; **Chiral shift analysis by ¹H NMR:** 5 equiv Eu(hfc)₃ in benzene-*d*₆ (0.03 M); **Chiral HPLC:** Chiralpak

IA, 0.5 ml/min, Hex/*i*PA=99:1, R_t =11.9 min, 12.3 min; $[\alpha]_D^{23.5} = -2.82$ ($c = 1.00$ g/100 ml, CHCl_3 , 92% *ee*).

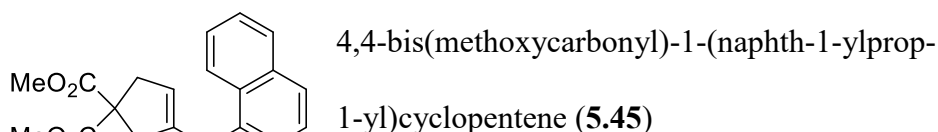


(Racemic) Following the general procedure (0 °C, 1 h, then 60 °C, 5 h), **5.34** (78.8 mg, 0.19 mmol) was reacted with $[\text{Rh}(\text{cod})\text{OH}]_2$ (4.5 mg, 0.0096 mmol) and 2-methylphenylboronic acid (53.5 mg, 0.39 mmol) in MeOH (1.9 ml) to give the product **5.43** as a clear oil (54.9 mg, 0.17 mmol, 90%). **(Asymmetric)** Following the general procedure, **5.34** (50.6 mg, 0.12 mmol) was reacted with **5.165** (5.6 mg, 0.0062 mmol), aqueous KOH (0.12 ml, 0.024 mmol), and 2-methylphenylboronic acid (34.4 mg, 0.25 mmol) in toluene (1.2 ml) to give the product (*S*)-**5.43** as a clear oil (20.6 mg, 0.065 mmol, 53%, 93% *ee*). $R_f = 0.61$ (Hex/EA = 3:1); $^1\text{H NMR}$ (400 MHz, CDCl_3) δ 7.18 – 7.03 (m, 4H), 5.32 (s, $J = 1.4$ Hz, 1H), 3.68 (s, 3H), 3.66 (s, 3H), 3.44 (t, $J = 7.2$ Hz, 1H), 3.08 – 2.91 (m, 2H), 2.74 (q, 2H), 2.30 (s, 3H), 1.99 – 1.83 (m, 1H), 1.79 – 1.63 (m, 1H), 0.84 (t, $J = 7.3$ Hz, 3H); $^{13}\text{C NMR}$ (101 MHz, CDCl_3) δ 172.53, 172.51, 144.26, 140.91, 136.23, 130.17, 126.48, 125.98, 125.86, 120.76, 59.04, 52.68, 52.65, 44.02, 41.71, 40.29, 26.61, 19.68, 12.28; **IR** (neat, cm^{-1}): 2956, 2930, 2873, 1738, 1489, 1456, 1435, 1383, 1257, 1197, 1159, 1077, 968, 815, 795, 758, 739; **HRMS** (ESI): Calcd for $\text{C}_{19}\text{H}_{24}\text{NaO}_4$ $[\text{M}+\text{Na}]^+$ 339.1572, found 339.1568; **Chiral HPLC**: Chiralpak IA, 1.0 ml/min, Hex/*i*PA=99:1, R_t =7.7 min, 9.7 min; $[\alpha]_D^{23.0} = -2.96$ ($c = 1.00$ g/100 ml, CHCl_3 , 93% *ee*).



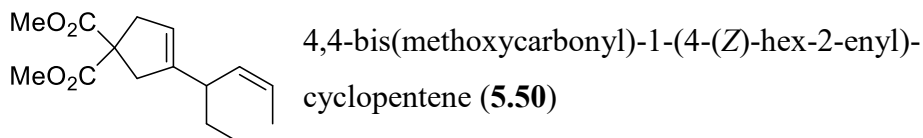
(Racemic) Following the general procedure (0 °C, 1 h, then 60 °C, 5 h), **5.34** (81.9 mg, 0.20 mmol) was reacted with [Rh(cod)OH]₂ (4.7 mg, 0.010 mmol) and 4-methoxyphenylboronic acid (64.1 mg, 0.40 mmol) in MeOH (2.0 ml) to give the product **5.44** as a clear oil (54.3 mg, 0.16 mmol, 81%).

(Asymmetric) Following the general procedure, **5.34** (43.7 mg, 0.11 mmol) was reacted with **5.165** (4.8 mg, 0.0053 mmol), aqueous KOH (0.11 ml, 0.022 mmol), and 4-methoxyphenylboronic acid (34.2 mg, 0.21 mmol) in toluene (1.1 ml) to give the product (*S*)-**5.44** as a clear oil (23.9 mg, 0.072 mmol, 67%, 95% *ee*). **R_f** = 0.52 (Hex/EA = 3:1); **¹H NMR** (400 MHz, CDCl₃) δ 7.04 (d, *J* = 8.6 Hz, 2H), 6.82 (d, *J* = 8.6 Hz, 2H), 5.35 (s, *J* = 1.4 Hz, 1H), 3.78 (s, 3H), 3.69 (s, 3H), 3.66 (s, 3H), 3.10 (t, *J* = 7.2 Hz, 1H), 3.07 – 2.93 (m, 2H), 2.76 (q, *J* = 16.5 Hz, 2H), 1.94 – 1.80 (m, 1H), 1.73 – 1.59 (m, 1H), 0.81 (t, *J* = 7.3 Hz, 3H); **¹³C NMR** (101 MHz, CDCl₃) δ 172.57, 172.55, 157.95, 144.99, 134.92, 128.72, 120.32, 113.59, 58.97, 55.17, 52.69, 52.66, 48.06, 41.69, 40.36, 26.77, 12.29; **IR (neat, cm⁻¹):** 2956, 2933, 2873, 2838, 2360, 2342, 1738, 1611, 1511, 1435, 1251, 1198, 1176, 1077, 1037, 834, 808, 546; **HRMS (ESI):** Calcd for C₁₉H₂₄NaO₅ [M+Na]⁺ 355.1521, found 355.1514; **Chiral HPLC:** Chiralpak IA, 1.0 ml/min, Hex/*i*PA=99:1, R_t=9.4 min, 10.7 min; **[α]_D^{23.0}** = -0.24 (*c* = 1.00 g/100 ml, CHCl₃, 95% *ee*).



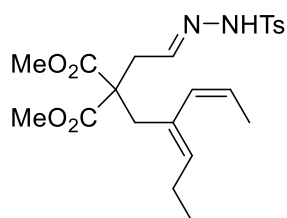
(Racemic) Following the general procedure (0 °C, 1 h, then 60 °C, 5 h), **5.34** (81.7 mg, 0.20 mmol) was reacted with [Rh(cod)OH]₂ (4.7 mg, 0.010 mmol) and naphthalene-1-boronic acid (70.9

mg, 0.40 mmol) in MeOH (2.0 ml) to give the product **5.45** as a clear oil (65.1 mg, 0.18 mmol, 92%). **(Asymmetric)** Following the general procedure, **5.34** (52.8 mg, 0.13 mmol) was reacted with **5.165** (5.8 mg, 0.0065 mmol), aqueous KOH (0.13 ml, 0.026 mmol), and naphthalene-1-boronic acid (45.8 mg, 0.26 mmol) in toluene (1.3 ml) to give the product (*S*)-**5.45** as a clear oil (27.6 mg, 0.078 mmol, 61%, 85% *ee*). $R_f = 0.57$ (Hex/EA = 3:1); $^1\text{H NMR}$ (400 MHz, CDCl_3) δ 8.10 (d, $J = 7.7$ Hz, 1H), 7.90 – 7.81 (m, 1H), 7.71 (d, $J = 8.1$ Hz, 1H), 7.53 – 7.38 (m, 3H), 7.32 (d, $J = 7.1$ Hz, 1H), 5.47 (s, $J = 1.5$ Hz, 1H), 4.03 (t, $J = 6.8$ Hz, 1H), 3.62 (d, $J = 1.5$ Hz, 6H), 3.03 (q, $J = 16.8$ Hz, 2H), 2.83 – 2.66 (m, 2H), 2.15 – 1.99 (m, 1H), 1.99 – 1.83 (m, 1H), 0.89 (t, $J = 7.3$ Hz, 3H); $^{13}\text{C NMR}$ (101 MHz, CDCl_3) δ 172.48, 172.46, 144.37, 138.82, 133.92, 132.14, 128.81, 126.81, 125.67, 125.44, 125.23, 124.33, 123.32, 121.33, 59.08, 52.63, 43.71, 41.87, 40.40, 26.92, 12.59; **IR** (neat, cm^{-1}): 2955, 2926, 2873, 1736, 1434, 1256, 1197, 1162, 1075, 796, 780; **HRMS** (ESI): Calcd for $\text{C}_{22}\text{H}_{24}\text{NaO}_4$ $[\text{M}+\text{Na}]^+$ 375.1572, found 375.1567; **Chiral HPLC**: Chiralpak IA, 1.0 ml/min, Hex/*i*PA=99:1, R_t =8.8 min, 11.2 min; $[\alpha]_D^{23.3} = +33.58$ ($c = 1.00$ g/100 ml, CHCl_3 , 85% *ee*).



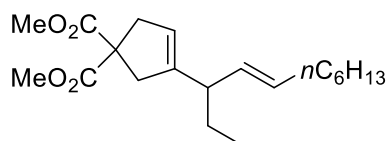
(Racemic) Following the general procedure (0 °C, 1 h, then 60 °C, 5 h), **5.34** (78.6 mg, 0.19 mmol) was reacted with $[\text{Rh}(\text{cod})\text{OH}]_2$ (4.5 mg, 0.0096 mmol) and *cis*-propenylboronic acid (34.8 mg, 0.38 mmol) in MeOH (1.9 ml) to give the product **5.50** as a clear oil (33.4 mg, 0.13 mmol, 65%). **(Asymmetric)** Following the general procedure, **5.34** (42.4 mg, 0.10 mmol) was reacted with **5.165** (4.7 mg, 0.0052 mmol), aqueous KOH (0.10 ml, 0.020 mmol), and *cis*-propenylboronic acid (17.8 mg, 0.21 mmol) in toluene (1.0 ml) to give the product (*S*)-**5.50** as a clear oil (13.5 mg, 0.033 mmol, 49%, 89% *ee*). $R_f = 0.65$

(Hex/EA = 3:1); $^1\text{H NMR}$ (400 MHz, CDCl_3) δ 5.58 – 5.44 (m, 1H), 5.26 – 5.11 (m, 2H), 3.73 (s, 6H), 2.98 (s, 3H), 2.91 (s, 2H), 1.68 – 1.50 (m, 4H), 1.44 – 1.28 (m, 1H), 0.83 (t, $J = 7.4$ Hz, 3H); $^{13}\text{C NMR}$ (101 MHz, CDCl_3) δ 172.71, 144.29, 132.19, 124.51, 119.72, 58.89, 52.71, 41.24, 40.33, 40.08, 26.38, 13.03, 11.64; **IR** (neat, cm^{-1}): 3010, 2957, 2930, 2873, 1738, 1435, 1384, 1255, 1198, 1161, 1075, 967, 811; **HRMS** (ESI): Calcd for $\text{C}_{15}\text{H}_{22}\text{NaO}_4$ $[\text{M}+\text{Na}]^+$ 289.1416, found 289.1410; $[\alpha]_D^{24.0} = +26.97$ ($c = 0.33$ g/100 ml, CHCl_3 , 89% *ee*).



Diénylhydrazone **5.51**

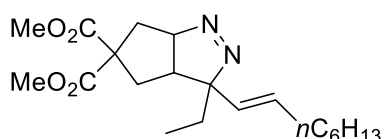
$^1\text{H NMR}$ (400 MHz, CDCl_3) δ 7.81 (d, $J = 8.2$ Hz, 2H), 7.60 (s, 1H), 7.32 (d, $J = 8.1$ Hz, 2H), 7.17 (t, $J = 5.0$ Hz, 1H), 5.50 (d, $J = 11.0$ Hz, 1H), 5.45 (dd, $J = 12.6, 6.1$ Hz, 1H), 5.38 (t, $J = 7.3$ Hz, 1H), 3.55 (s, 6H), 2.76 (s, 2H), 2.70 (d, $J = 5.1$ Hz, 2H), 2.42 (s, 3H), 1.98 – 1.88 (m, 2H), 1.66 (d, $J = 6.2$ Hz, 3H), 0.90 (t, $J = 7.4$ Hz, 3H).



4,4-bis(methoxycarbonyl)-1-(3-(*E*)-undec-4-enyl)-cyclopentene (**5.53**)

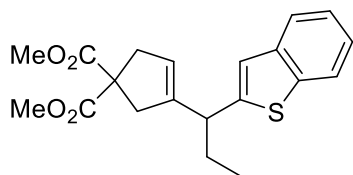
(Racemic) Following the general procedure (0 °C, 24 h, then 60 °C, 5 h), **5.34** (87.8 mg, 0.21 mmol) was reacted with $[\text{Rh}(\text{cod})\text{OH}]_2$ (5.1 mg, 0.011 mmol) and *trans*-1-octen-1-ylboronic acid (68.4 mg, 0.43 mmol) in MeOH (2.1 ml) to give the product **5.53** as a clear oil (23.9 mg, 0.071 mmol, 33%) and byproduct **5.54** as a clear oil (7.5 mg, 0.021 mmol, 10%). **(Asymmetric)** Following the general procedure, **5.34** (43.9 mg, 0.11 mmol) was reacted with **5.165** (4.8 mg, 0.0054 mmol), aqueous KOH (0.11 ml, 0.022 mmol), and *trans*-1-octen-1-ylboronic acid (34.2 mg, 0.21 mmol) in toluene (1.1 ml) to

give the product (*S*)-**5.53** as a clear oil (10.4 mg, 0.031 mmol, 29%, 82% *ee*). $R_f = 0.72$ (Hex/EA = 3:1); $^1\text{H NMR}$ (400 MHz, CDCl_3) δ 5.39 (dt, 1H), 5.22 (dd, $J = 15.3, 8.0$ Hz, 2H), 3.72 (d, $J = 1.2$ Hz, 6H), 2.99 (s, 2H), 2.90 (s, 2H), 2.58 (q, $J = 14.4, 7.3$ Hz, 1H), 1.98 (q, $J = 13.5, 6.7$ Hz, 2H), 1.61 – 1.46 (m, 1H), 1.44 – 1.15 (m, 9H), 0.88 (t, $J = 6.7$ Hz, 3H), 0.82 (t, $J = 7.4$ Hz, 3H); $^{13}\text{C NMR}$ (101 MHz, CDCl_3) δ 172.73, 144.59, 131.41, 131.24, 119.95, 58.87, 52.70, 45.89, 41.17, 40.40, 32.49, 31.68, 29.49, 28.77, 25.98, 22.60, 14.06, 11.80; **IR** (neat, cm^{-1}): 2956, 2927, 2856, 1739, 1435, 1384, 1255, 1197, 1162, 1077, 968, 808; **HRMS (ESI)**: Calcd for $\text{C}_{20}\text{H}_{32}\text{NaO}_4$ $[\text{M}+\text{Na}]^+$ 359.2198, found 359.2192; **Chiral shift analysis by $^1\text{H NMR}$** : 6 equiv $\text{Eu}(\text{hfc})_3$ in benzene- d_6 (0.03 or 0.025 M); **Chiral HPLC**: Chiralpak IA, 1.0 ml/min, Hex/*i*PA=99.7:0.3, $R_t=21.1$ min, 22.5 min; $[\alpha]_D^{22.9} = +13.71$ ($c = 0.47$ g/100 ml, CHCl_3 , 82% *ee*).



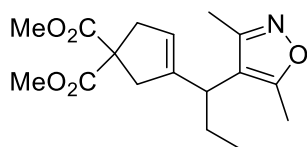
dimethyl (*E*)-3-ethyl-3-(oct-1-en-1-yl)-
3a,4,6,6a-tetrahydrocyclopenta
[c]pyrazole-5,5(3H)-dicarboxylate (**5.54**)

$^1\text{H NMR}$ (400 MHz, CDCl_3) δ 5.42 – 5.21 (m, 2H), 4.76 – 4.65 (m, 1H), 3.76 (s, 3H), 3.71 (s, 3H), 3.04 (dd, $J = 14.6, 9.4$ Hz, 1H), 2.66 (dd, $J = 14.6, 4.7$ Hz, 1H), 2.36 (dt, $J = 11.1, 7.2$ Hz, 1H), 2.27 (td, $J = 15.0, 7.6$ Hz, 1H), 2.15 (dd, $J = 13.1, 7.6$ Hz, 1H), 1.97 (q, $J = 13.4, 6.5$ Hz, 2H), 1.78 (dq, $J = 14.5, 7.4$ Hz, 1H), 1.72 – 1.63 (m, 1H), 1.36 – 1.20 (m, 8H), 1.10 (t, $J = 7.4$ Hz, 3H), 0.87 (t, $J = 6.7$ Hz, 3H); $^{13}\text{C NMR}$ (101 MHz, CDCl_3) δ 171.95, 170.87, 130.99, 128.48, 97.02, 92.34, 60.92, 52.99, 52.83, 44.27, 35.39, 33.70, 32.64, 31.57, 29.02, 28.68, 26.23, 22.54, 14.03, 9.43.



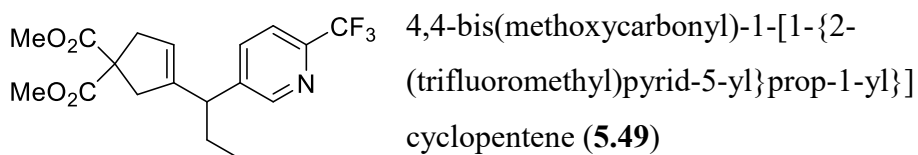
4,4-bis(methoxycarbonyl)-1-{1-(benzo[b]thiophen-2-yl)prop-1-yl}cyclopentene (**5.46**)

(Racemic) Following the general procedure (0 °C, 24 h, then 60 °C, 5 h), **5.34** (79.7 mg, 0.20 mmol) was reacted with [Rh(cod)OH]₂ (4.6 mg, 0.0098 mmol) and benzo[b]thien-2-ylboronic acid (138.9 mg, 0.78 mmol, 4 equiv) in MeOH (2.0 ml) to give the product **5.46** as a red solid (54.1 mg, 0.15 mmol, 77%). **(Asymmetric)** Following the general procedure, **5.34** (43.7 mg, 0.11 mmol) was reacted with **5.165** (4.8 mg, 0.0053 mmol), aqueous KOH (0.11 ml, 0.022 mmol), and benzo[b]thien-2-ylboronic acid (76.2 mg, 0.43 mmol, 4 equiv) in toluene (1.1 ml) to give the product (*S*)-**5.46** as a red solid (23.2 mg, 0.065 mmol, 60%, 84% *ee*). **R_f** = 0.44 (Hex/EA = 5:1); **¹H NMR** (400 MHz, CDCl₃) δ 7.75 (d, *J* = 7.9 Hz, 1H), 7.67 (d, *J* = 7.7 Hz, 1H), 7.36 – 7.19 (m, 2H), 7.03 (s, 1H), 5.49 (s, 1H), 3.68 (d, *J* = 1.8 Hz, 6H), 3.59 (t, *J* = 7.5 Hz, 1H), 3.04 (s, 2H), 2.97 – 2.85 (m, 2H), 2.00 – 1.81 (m, 2H), 0.93 (t, *J* = 7.3 Hz, 3H); **¹³C NMR** (101 MHz, CDCl₃) δ 172.39, 148.12, 143.27, 139.87, 139.29, 123.98, 123.52, 122.89, 122.29, 122.16, 120.63, 58.97, 52.75, 44.76, 40.92, 40.32, 27.10, 12.23; **IR (neat, cm⁻¹):** 2955, 2931, 2873, 1732, 1457, 1434, 1251, 1197, 1162, 1072, 1015, 992, 967, 860, 814, 797, 748, 727, 709, 582, 434; **HRMS (ESI):** Calcd for C₂₀H₂₂NaO₄S [M+Na]⁺ 381.1136, found 381.1133; **Chiral shift analysis by ¹H NMR:** 5 equiv Eu(hfc)₃ in benzene-*d*₆ (0.03 M); **Chiral HPLC analysis of 2k-diol after reduction of 2k by LAH:** Chiralpak IA, 1.0 ml/min, Hex/*i*PA=90:10, R_t=8.7 min, 9.0 min; [**α**]_D^{22.7} = -6.48 (*c* = 1.00 g/100 ml, CHCl₃, 84% *ee*).



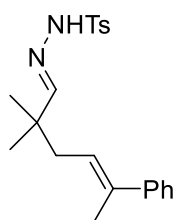
4,4-bis(methoxycarbonyl)-1-{1-(3,5-dimethylisooxazol-4-yl)prop-1-yl}cyclopentene (**5.47**)

Following the general procedure (0 °C, 24 h, then 60 °C, 5 h), **5.34** (81.2 mg, 0.20 mmol) was reacted with [Rh(cod)OH]₂ (4.7 mg, 0.0099 mmol) and 3,5-dimethylisooxazole-4-boronic acid (115.5 mg, 0.80 mmol, 4 equiv) in MeOH (2.0 ml) to give the product **5.47** as a clear oil (38.9 mg, 0.12 mmol, 61%) and recovered starting material **5.34** (21.9 mg, 0.053 mmol, 27%). *R_f* = 0.54 (Hex/EA = 2:1, stained by KMnO₄); ¹H NMR (400 MHz, CDCl₃) δ 5.35 (d, *J* = 1.4 Hz, 1H), 3.71 (d, *J* = 14.1 Hz, 6H), 3.12 – 2.94 (m, 3H), 2.77 (dd, *J* = 57.0, 16.6 Hz, 2H), 2.28 (s, 3H), 2.14 (s, 3H), 2.00 – 1.85 (m, 1H), 1.74 – 1.59 (m, 1H), 0.83 (t, *J* = 7.4 Hz, 3H); ¹³C NMR (101 MHz, CDCl₃) δ 172.37, 172.34, 165.23, 159.43, 142.32, 121.02, 113.11, 58.72, 52.77, 52.74, 42.30, 40.44, 37.37, 24.76, 12.15, 11.19, 10.57; IR (neat, cm⁻¹): 2959, 2934, 2874, 1734, 1629, 1435, 1256, 1198, 1161, 1074, 997, 967, 896, 805, 770; HRMS (ESI): Calcd for C₁₇H₂₃NNaO₅ [M+Na]⁺ 344.1474, found 344.1471.



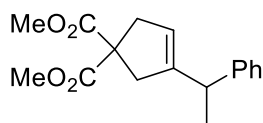
(Racemic) Following the general procedure (0 °C, 24 h, then 60 °C, 5 h), **5.34** (73.5 mg, 0.18 mmol) was reacted with [Rh(cod)OH]₂ (4.2 mg, 0.0090 mmol) and 2-(trifluoromethyl)pyridine-5-boronic acid (140.2 mg, 0.72 mmol, 4 equiv) in MeOH (1.8 ml) to give the product **5.49** as a clear oil (46.5 mg, 0.13 mmol, 70%) and recovered starting material **5.34** (17.4 mg, 0.043 mmol, 24%). **(Asymmetric)** Following the general procedure, **5.34** (39.8 mg, 0.097 mmol) was reacted with **5.165** (4.4 mg, 0.0049 mmol), aqueous KOH (0.10 ml, 0.019 mmol), and 2-(trifluoromethyl)pyridine-5-boronic acid (75.9 mg, 0.39 mmol, 4 equiv) in toluene (0.78 ml) and MeOH (0.19 ml) to give the product (*S*)-**5.49** as a clear oil (18.9 mg, 0.051 mmol, 52%, 92% *ee*). *R_f* = 0.43 (Hex/EA = 3:1); ¹H NMR (400 MHz, CDCl₃) δ 8.53 (s, 1H), 7.69 – 7.59 (m,

2H), 5.45 (s, $J = 1.2$ Hz, 1H), 3.69 (d, $J = 8.0$ Hz, 6H), 3.31 (t, $J = 7.2$ Hz, 1H), 3.03 (s, 2H), 2.77 (q, $J = 16.8$ Hz, 2H), 2.06 – 1.90 (m, 1H), 1.81 – 1.67 (m, 1H), 0.85 (t, $J = 7.3$ Hz, 3H); $^{13}\text{C NMR}$ (101 MHz, CDCl_3) δ 172.18 (s), 172.14 (s), 149.98 (s), 146.38 (q, $J = 34.6$ Hz), 142.53 (s), 141.61 (s), 136.27 (s), 122.70 (d, $J = 1.9$ Hz), 121.59 (q, $J = 273.8$ Hz), 120.16 (dd, $J = 5.0, 2.4$ Hz), 58.86 (s), 52.78 (s), 52.76 (s), 46.18 (s), 41.44 (s), 40.30 (s), 26.41 (s), 12.05 (s); $^{19}\text{F NMR}$ (376 MHz, CDCl_3) δ -67.78; **IR** (neat, cm^{-1}): 2959, 2936, 2876, 1732, 1454, 1435, 1402, 1337, 1254, 1196, 1167, 1131, 1082, 1025, 994, 966, 854, 810, 782, 761, 725; **HRMS** (ESI): Calcd for $\text{C}_{18}\text{H}_{20}\text{F}_3\text{NNaO}_4$ $[\text{M}+\text{Na}]^+$ 394.1242, found 394.1239; **Chiral HPLC**: Chiralpak IA, 1.0 ml/min, Hex/*i*PA=98:2, R_t = 11.0 min, 12.1 min; $[\alpha]_D^{22.9} = +2.67$ ($c = 1.00$ g/100 ml, CHCl_3 , 92% *ee*).



Styrenylhydrazone **5.57**

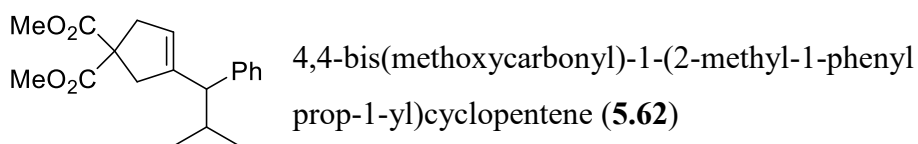
$R_f = 0.66$ (Hex/EA=2:1); $^1\text{H NMR}$ (400 MHz, CDCl_3) δ 7.78 (d, $J = 5.2$ Hz, 2H), 7.33 – 7.24 (m, 5H), 7.21 (d, $J = 5.9$ Hz, 2H), 7.10 (d, $J = 3.4$ Hz, 1H), 5.60 (t, $J = 7.0$ Hz, 1H), 2.38 – 2.34 (m, 3H), 2.25 (d, $J = 5.6$ Hz, 2H), 1.95 (s, 3H), 1.10 – 1.05 (m, 6H).



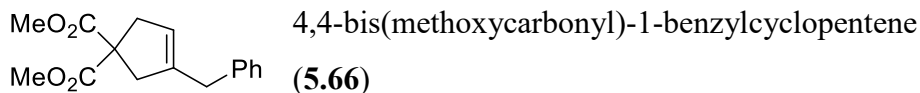
4,4-bis(methoxycarbonyl)-1-(1-phenyleth-1-yl)
cyclopentene (**5.60**)

Following the general procedure (0 °C, 1 h, then 60 °C, 5 h), **5.59** (81.5 mg, 0.21 mmol) was reacted with $[\text{Rh}(\text{cod})\text{OH}]_2$ (4.9 mg, 0.010 mmol) and phenylboronic acid (51.9 mg, 0.41 mmol) in MeOH (2.1 ml) to give the product **5.60** as a clear oil (47.8 mg, 0.17 mmol, 80%). $R_f = 0.71$ (Hex/EA = 2:1); $^1\text{H NMR}$ (400 MHz, CDCl_3) δ 7.28 (t, $J = 7.7$ Hz, 2H), 7.20 (d, $J = 7.4$ Hz, 1H), 7.15 (d, $J = 7.4$ Hz, 2H), 5.35 (s, 1H), 3.70 (s, 3H), 3.66 (s, 3H), 3.43

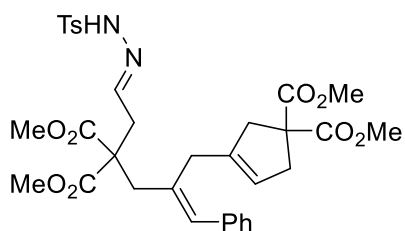
(q, 1H), 3.10 – 2.95 (m, 2H), 2.78 (dd, $J = 38.6, 16.6$ Hz, 2H), 1.39 (d, $J = 7.0$ Hz, 3H); ^{13}C NMR (101 MHz, CDCl_3) δ 172.59, 172.51, 145.59, 144.46, 128.34, 127.29, 126.20, 120.55, 59.13, 52.73, 52.67, 41.97, 41.04, 40.41, 20.46; IR (neat, cm^{-1}): 3435, 2954, 1737, 1493, 1435, 1267, 1199, 1168, 1075, 817, 765, 703, 544; HRMS (ESI): Calcd for $\text{C}_{17}\text{H}_{20}\text{NaO}_4$ $[\text{M}+\text{Na}]^+$ 311.1259, found 311.1256.



(**Racemic**) Following the general procedure (0 °C, 1 h, then 60 °C, 5 h), **5.61** (79.5 mg, 0.19 mmol) was reacted with $[\text{Rh}(\text{cod})\text{OH}]_2$ (4.4 mg, 0.0094 mmol) and phenylboronic acid (47.3 mg, 0.38 mmol) in MeOH (1.9 ml) to give the product **5.62** as a white solid (52.1 mg, 0.16 mmol, 88%). (**Asymmetric**) Following the general procedure, **5.61** (40.5 mg, 0.096 mmol) was reacted with **5.165** (4.3 mg, 0.0048 mmol), aqueous KOH (0.10 ml, 0.019 mmol), and phenylboronic acid (24.1 mg, 0.19 mmol) in toluene (0.96 ml) to give the product (*S*)-**5.62** as a clear oil (20.0 mg, 0.063 mmol, 66%, 93% *ee*). $R_f = 0.44$ (Hex/EA = 5:1); ^1H NMR (400 MHz, CDCl_3) δ 7.26 (t, $J = 7.4$ Hz, 2H), 7.17 (t, $J = 7.3$ Hz, 1H), 7.13 (d, $J = 7.0$ Hz, 2H), 5.41 (s, 1H), 3.66 (d, $J = 10.0$ Hz, 6H), 3.06 – 2.93 (m, 3H), 2.83 (dd, $J = 40.1, 16.8$ Hz, 2H), 2.24 – 2.07 (m, 1H), 0.95 (d, $J = 6.5$ Hz, 3H), 0.71 (d, $J = 6.6$ Hz, 3H); ^{13}C NMR (101 MHz, CDCl_3) δ 172.60, 172.39, 143.96, 142.19, 128.27, 128.14, 126.08, 121.34, 59.04, 55.95, 52.68, 52.64, 40.92, 40.11, 29.93, 21.63, 21.05; IR (neat, cm^{-1}): 2953, 2868, 1733, 1451, 1434, 1252, 1196, 1160, 1071, 968, 797, 757, 702; HRMS (ESI): Calcd for $\text{C}_{19}\text{H}_{24}\text{NaO}_4$ $[\text{M}+\text{Na}]^+$ 339.1572, found 339.1570; Chiral HPLC: Chiralpak IA, 1.0 ml/min, Hex/*i*PA=99:1, $R_t = 6.3$ min, 7.1 min; $[\alpha]_D^{23.4} = -8.20$ ($c = 0.95$ g/100 ml, CHCl_3 , 93% *ee*).

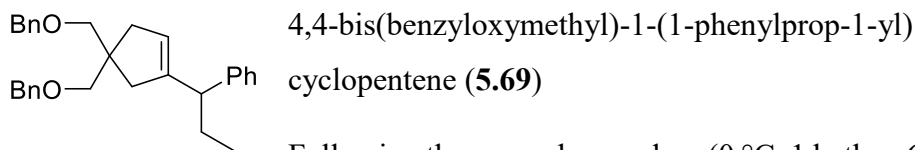


Following the general procedure (0 °C, 24 h, then 60 °C, 5 h), **5.63** (79.2 mg, 0.21 mmol) was reacted with [Rh(cod)OH]₂ (4.9 mg, 0.010 mmol) and phenylboronic acid (52.3 mg, 0.41 mmol) in MeOH (2.1 ml) to give the product **5.66** as a clear oil (18.0 mg, 0.066 mmol, 32%). *R*_f = 0.67 (Hex/EA = 2:1); ¹H NMR (400 MHz, CDCl₃) δ 7.32 – 7.24 (m, 2H), 7.20 (t, *J* = 7.4 Hz, 1H), 7.15 (d, *J* = 7.3 Hz, 2H), 5.22 (s, 1H), 3.71 (s, 6H), 3.37 (s, 2H), 3.00 (d, *J* = 1.8 Hz, 2H), 2.88 (s, 2H); ¹³C NMR (101 MHz, CDCl₃) δ 172.58, 140.85, 138.87, 128.74, 128.31, 126.12, 122.38, 59.21, 52.74, 42.70, 40.57, 37.25; IR (neat, cm⁻¹): 3027, 2953, 2908, 2840, 1734, 1496, 1435, 1255, 1198, 1163, 1074, 996, 968, 787, 758, 702, 585; HRMS (ESI): Calcd for C₁₆H₁₈NaO₄ [M+Na]⁺ 297.1103, found 297.1098.



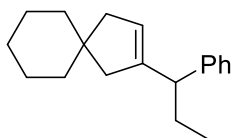
Phenylated dimer **5.67**

¹H NMR (selected, 400 MHz, CDCl₃) δ 6.32 (s, C=CHPh, 1H), 5.17 (s, CCC=CHC, 1H).



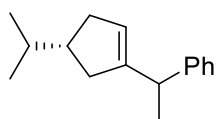
Following the general procedure (0 °C, 1 h, then 60 °C, 5 h), **5.68** (103.2 mg, 0.19 mmol) was reacted with [Rh(cod)OH]₂ (4.6 mg, 0.0097 mmol) and phenylboronic acid (48.7 mg, 0.39 mmol) in MeOH (1.9 ml) to give the product **5.69** as a clear oil (65.2 mg, 0.15 mmol, 79%). *R*_f = 0.52 (Hex/EA = 10:1); ¹H NMR (400 MHz, CDCl₃) δ 7.34 – 7.20 (m, 12H), 7.17 (d, *J* = 7.2 Hz, 1H), 7.12 (d, *J* = 7.3 Hz, 2H), 5.34 (s, 1H), 4.45 (d, *J* =

11.2 Hz, 4H), 3.38 (s, 2H), 3.33 (s, 2H), 3.10 (t, $J = 7.3$ Hz, 2H), 2.23 (s, 2H), 2.09 – 1.96 (m, 2H), 1.92 – 1.78 (m, 1H), 1.76 – 1.60 (m, 1H), 0.80 (t, $J = 7.3$ Hz, 3H); ^{13}C NMR (101 MHz, CDCl_3) δ 145.45, 143.78, 138.93, 138.92, 128.22, 128.21, 128.14, 127.93, 127.38, 127.28, 127.27, 125.94, 121.70, 74.05, 73.94, 73.13, 49.53, 46.84, 40.25, 38.97, 26.69, 12.52; IR (neat, cm^{-1}): 3062, 3027, 2958, 2849, 2359, 2341, 1495, 1453, 1384, 1362, 1099, 734, 697, 669; HRMS (ESI): Calcd for $\text{C}_{30}\text{H}_{34}\text{NaO}_2$ $[\text{M}+\text{Na}]^+$ 449.2457, found 449.2454.



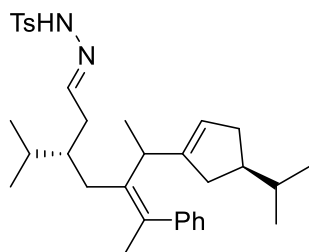
2-(1-phenylprop-1-yl)spiro[4.5]dec-2-ene (**5.71**)

Following the general procedure (0 °C, 1 h, then 60 °C, 5 h), **5.70** (78.0 mg, 0.22 mmol) was reacted with $[\text{Rh}(\text{cod})\text{OH}]_2$ (5.1 mg, 0.011 mmol) and phenylboronic acid (54.4 mg, 0.43 mmol) in MeOH (2.2 ml) to give the product **5.71** as a clear oil (44.9 mg, 0.18 mmol, 82%). $R_f = 0.52$ (Hexane only); ^1H NMR (400 MHz, CDCl_3) δ 7.33 – 7.21 (m, 4H), 7.23 – 7.11 (m, 8H), 5.35 (s, 1H), 3.11 (t, $J = 6.7$ Hz, 2H), 2.13 (s, 2H), 1.91 (s, 2H), 1.90 – 1.80 (m, 1H), 1.76 – 1.59 (m, 1H), 1.44 – 1.21 (m, 10H), 0.82 (t, $J = 7.3$ Hz, 3H); ^{13}C NMR (101 MHz, CDCl_3) δ 145.34, 144.09, 128.08, 127.91, 125.84, 121.90, 49.69, 46.60, 45.13, 42.06, 38.69, 38.50, 26.78, 26.17, 23.53, 23.35, 12.54; IR (neat, cm^{-1}): 3060, 3026, 2923, 2841, 1601, 1492, 1451, 1378, 1316, 1261, 805, 757, 699, 537; HRMS (ESI): Calcd for $\text{C}_{19}\text{H}_{27}$ $[\text{M}+\text{H}]^+$ 255.2113, found 255.2111.



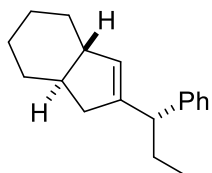
(4R)-isopropyl-1-(1-phenyleth-1-yl)cyclopentene (**5.73**)

$R_f = 0.59$ (Hexane only); ^1H NMR (400 MHz, CDCl_3) δ 7.28 (t, $J = 6.7$ Hz, 2H), 7.18 (t, $J = 6.5$ Hz, 3H), 5.41 (d, $J = 14.3$ Hz, 1H), 3.43 (d, $J = 6.9$ Hz, 1H), 2.40 (dd, $J = 15.3, 7.8$ Hz, 1H), 2.15 (dd, $J = 15.4, 7.4$ Hz, 1H), 2.09 – 1.73 (m, 3H), 1.54 (s, 1H), 1.51 – 1.40 (m, 1H), 1.37 (d, $J = 7.1$ Hz, 3H), 0.82 (dt, $J = 11.0, 6.5$ Hz, 6H).



Dimer 5.74

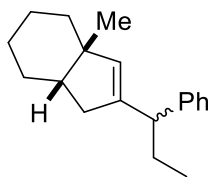
$R_f = 0.55$ (Hex/EA = 3:1); $^1\text{H NMR}$ (400 MHz, CDCl_3) δ 7.78 (d, $J = 8.3$ Hz, 2H), 7.32 – 7.22 (m, 5H), 7.18 (t, $J = 7.2$ Hz, 1H), 6.95 (d, $J = 7.2$ Hz, 2H), 6.81 (t, $J = 5.8$ Hz, 1H), 5.24 (s, 1H), 2.94 (q, $J = 13.6, 7.8$ Hz, 1H), 2.42 (s, 3H), 2.37 – 2.24 (m, 1H), 2.15 – 2.07 (m, 2H), 2.05 – 1.95 (m, 2H), 1.94 – 1.84 (m, 1H), 1.83 – 1.74 (m, 1H), 1.54 – 1.40 (m, 3+2H), 1.34 – 1.20 (m, 2H), 0.99 (d, $J = 6.9$ Hz, 3H), 0.88 – 0.71 (m, 6+2H), 0.67 (t, $J = 7.1$ Hz, 6H).



(±)-(3aR,7aS)-2-((S)-1-phenylprop-1-yl)-3a,4,5,6,7,7a-

hexahydro-1H-indene (**5.82**)

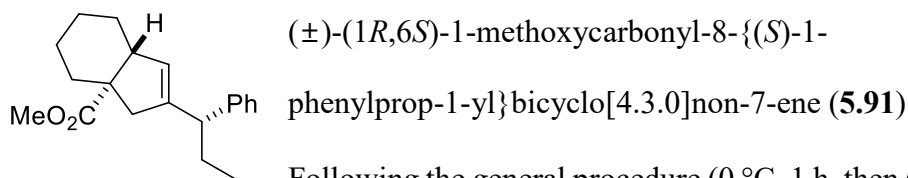
$R_f = 0.48$ (Hexane only); $^1\text{H NMR}$ (400 MHz, CDCl_3) δ 7.48 – 7.05 (m, 5H), 5.55 (s, 1H), 3.18 (s, 1H), 2.16 – 1.81 (m, 4H), 1.71 (s, 5H), 1.50 – 1.05 (m, 5H), 0.83 (dt, $J = 11.5, 5.8$ Hz, 3H); $^{13}\text{C NMR}$ (101 MHz, CDCl_3) δ 147.94, 144.01, 128.52, 128.06, 127.94, 125.82, 51.23, 49.98, 49.82, 39.12, 30.92, 30.21, 26.86, 26.64, 26.61, 12.46.



(±)-(3aS,7aS)-3a-methyl-2-(1-phenylprop-1-yl)-

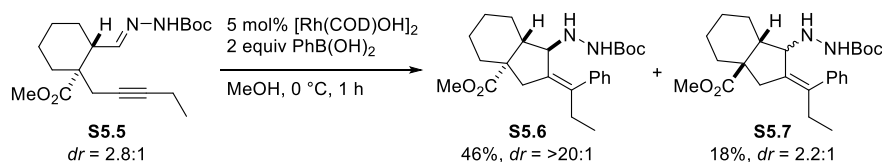
3a,4,5,6,7,7a-hexahydro-1H-indene (**5.83**)

$R_f = 0.56$ (Hexane only); $^1\text{H NMR}$ (400 MHz, CDCl_3) δ 7.30 – 7.21 (m, 2H), 7.21 – 7.11 (m, 3H), 5.34 (d, $J = 13.6$ Hz, 1H), 3.11 (t, $J = 7.5$ Hz, 1H), 2.16 – 2.03 (m, 1H), 1.94 – 1.78 (m, 2H), 1.78 – 1.62 (m, 2H), 1.54 – 1.20 (m, 8H), 1.00 (d, $J = 5.2$ Hz, 3H), 0.84 (t, $J = 7.3$ Hz, 3H); $^{13}\text{C NMR}$ (101 MHz, CDCl_3) δ 144.31, 144.19, 135.31, 128.02, 127.87, 125.77, 49.61, 45.35, 44.40, 38.33, 35.63, 27.20, 26.79, 26.08, 22.91, 21.97, 12.51.



Following the general procedure (0 °C, 1 h, then 60 °C, 5 h), **5.88** (85.8 mg, 0.21 mmol) was reacted with [Rh(cod)OH]₂ (5.0 mg, 0.011 mmol) and phenylboronic acid (53.3 mg, 0.42 mmol) in MeOH (2.1 ml) to give the product **5.91** as a clear oil (55.8 mg, 0.19 mmol, 88%). *R_f* = 0.32 (Hex/EA = 20:1); ¹H NMR (400 MHz, CDCl₃) δ 7.25 (t, *J* = 7.5 Hz, 2H), 7.15 (t, *J* = 7.3 Hz, 1H), 7.10 (d, *J* = 7.3 Hz, 2H), 5.72 (s, 1H), 3.45 (s, 3H), 3.17 (t, *J* = 7.4 Hz, 1H), 2.38 (d, *J* = 12.8 Hz, 1H), 2.26 (d, *J* = 14.8 Hz, 1H), 2.16 (d, *J* = 12.6 Hz, 1H), 2.12 – 2.04 (m, 1H), 2.01 (d, *J* = 14.9 Hz, 1H), 1.88 – 1.62 (m, 4H), 1.59 (d, *J* = 13.8 Hz, 1H), 1.42 (td, *J* = 13.0, 3.7 Hz, 1H), 1.27 (qt, *J* = 12.9, 4.4 Hz, 1H), 1.09 (qt, 1H), 0.81 (t, *J* = 7.3 Hz, 3H); ¹³C NMR (101 MHz, CDCl₃) δ 176.18, 143.40, 143.33, 129.23, 128.05, 127.84, 125.87, 58.30, 53.02, 51.08, 49.38, 44.45, 33.92, 26.22, 25.90, 24.68, 23.71, 12.31; IR (neat, cm⁻¹): 3025, 2930, 2858, 1736, 1492, 1452, 1311, 1260, 1227, 1190, 1169, 1146, 1126, 1002, 814, 762, 701; HRMS (ESI): Calcd for C₂₀H₂₆NaO₂ [M+Na]⁺ 321.1830, found 321.1826.

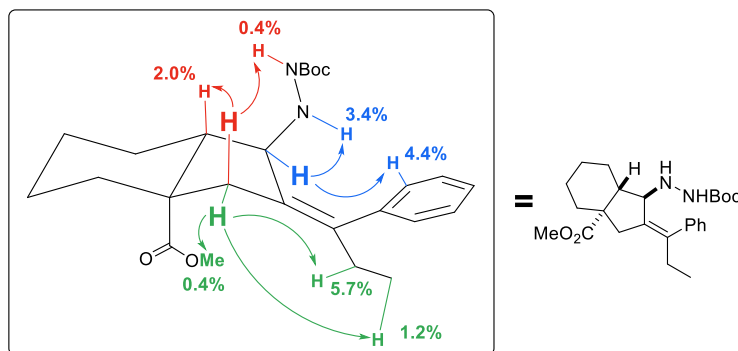
To determine the relative stereochemistry, diastereomeric separation with Boc-hydrazone was conducted.



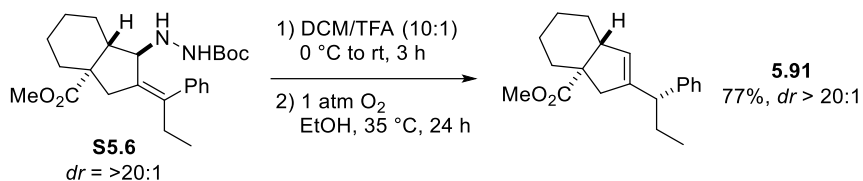
In 20 ml tube vial, **S5.5** (77.9 mg, 0.22 mmol, *dr* = 2.8:1) was dissolved in MeOH (2.2 ml), and [Rh(cod)OH]₂ (5.2 mg, 0.011 mmol) was added. After

the reaction mixture was cooled down to 0 °C, PhB(OH)₂ (55.9 mg, 0.44 mmol) was added and the reaction mixture was stirred for 1 h at 0 °C. After evaporation of the solvent, crude material was chromatographed on silica gel to give the products **S5.6** (44.2 mg, 0.10 mmol, 46%) and **S5.7** (17.1 mg, 0.040 mmol, 18%, *dr* = 2.2:1) as a clear paste (mixture, 33.0 mg, 0.077 mmol, 35%, **S5.6**:**S5.7** = 2.8:1 in crude NMR). **R_f**(**S5.6**) = 0.41 (Hex/EA = 3:1); **¹H NMR (S5.6, 400 MHz, CDCl₃)** δ 7.33 (t, *J* = 7.3 Hz, 2H), 7.25 (t, *J* = 7.3 Hz, 1H), 7.18 (d, *J* = 7.1 Hz, 2H), 5.17 (s, 1H), 4.13 (d, *J* = 10.2 Hz, 1H), 3.70 (s, 3H), 3.11 (s, 1H), 2.74 (d, *J* = 15.5 Hz, 1H), 2.41 (dt, *J* = 14.6, 8.3 Hz, 2H), 2.21 (d, *J* = 14.9 Hz, 2H), 1.93 (d, *J* = 11.3 Hz, 1H), 1.78 (s, 1H), 1.72 – 1.59 (m, 2H), 1.41 (s, 9H), 1.29 – 1.17 (m, 4H), 0.84 (t, *J* = 7.4 Hz, 3H); **IR (S5.6, neat, cm⁻¹)**: 3328, 2932, 2858, 1729, 1507, 1453, 1366, 1248, 1165, 1132, 1084, 1022, 912, 873, 819, 767, 733, 705; **HRMS (ESI)**: Calcd for C₂₅H₃₆N₂NaO₄ [M+Na]⁺ 451.2573, found 451.2570.

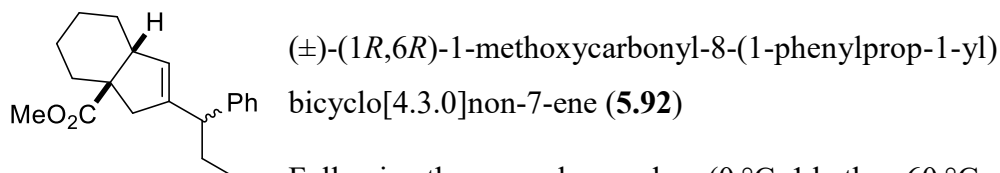
Relative stereochemistry of **S5.6** was confirmed by 1D NOE.



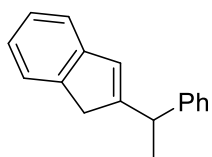
R_f(**S5.7**) = 0.49 (Hex/EA = 3:1); **¹H NMR (S5.7, 400 MHz, CDCl₃)** δ 7.32 (t, *J* = 7.3 Hz, 2H), 7.26 – 7.20 (m, 1H), 7.15 (t, *J* = 9.0 Hz, 2H), 3.69 (minor, s, 3H), 3.66 (major, s, 3H), 2.76 (dd, *J* = 63.3, 16.7 Hz, 1H), 2.51 – 2.32 (m, 1H), 2.29 – 2.15 (m, 1H), 1.89 – 1.37 (m, 8H), 1.35 (minor, s, 9H), 1.33 (major, s, 9H), 0.87 (t, *J* = 7.2 Hz, 3H); **IR (S5.7, neat, cm⁻¹)**: 3390, 2932, 2857, 1727, 1491, 1452, 1367, 1247, 1161, 1015, 871, 767, 738, 703.



S5.6 (44.2 mg, 0.10 mmol) was reacted with DCM/TFA (10:1, 1.1 ml) at rt for 3 h, and then oxidized with O₂ balloon at 35 °C for 24 h to give the single diastereomer **5.91** as a clear oil (23.6 mg, 0.079 mmol, 77%).

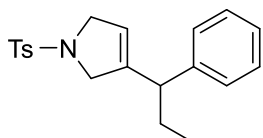


Following the general procedure (0 °C, 1 h, then 60 °C, 5 h), **5.90** (75.6 mg, 0.19 mmol) was reacted with [Rh(cod)OH]₂ (4.4 mg, 0.0093 mmol) and phenylboronic acid (47.0 mg, 0.37 mmol) in MeOH (1.9 ml) to give the product **5.92** as a clear oil (47.4 mg, 0.16 mmol, 85%, *dr* = 1.4:1). *R_f* = 0.28 (Hex/EA = 20:1); ¹H NMR (400 MHz, CDCl₃) δ 7.27 (td, *J* = 7.3, 3.4 Hz, 2H), 7.21 – 7.16 (m, 1H), 7.16 – 7.09 (m, 2H), 5.37 (s, 1H of major diastereomer), 5.34 (s, 1H of minor diastereomer), 3.62 (d, *J* = 6.9 Hz, 3H), 3.22 – 3.03 (m, 2H), 2.46 (t, *J* = 15.4 Hz, 1H), 1.99 – 1.81 (m, 2H), 1.82 – 1.59 (m, 4H), 1.55 – 1.15 (m, 5H), 0.89 – 0.78 (m, 3H); ¹³C NMR (101 MHz, CDCl₃) δ 177.94, 177.89, 144.38 (overlapped), 143.27, 143.20, 128.17, 128.14, 128.05, 127.93, 127.85, 127.81, 126.03, 125.99, 51.61, 51.58, 51.53, 51.37, 49.62, 49.49, 45.86, 45.73, 44.97, 44.94, 31.44, 31.36, 26.70, 26.66, 26.57, 26.44, 22.46, 22.41, 21.98 (overlapped), 12.46, 12.43; IR (neat, cm⁻¹): 3026, 2929, 2855, 1729, 1493, 1450, 1330, 1281, 1227, 1150, 1124, 1031, 805, 760, 700, 541; HRMS (ESI): Calcd for C₂₀H₂₆NaO₂ [M+Na]⁺ 321.1830, found 321.1827.



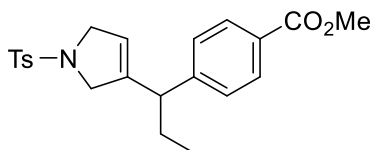
2-(1-phenylethyl)-1*H*-indene (**5.98**)

$R_f = 0.51$ (Hex/EA=20:1); $^1\text{H NMR}$ (499 MHz, CDCl_3) δ 7.33 – 7.26 (m, 4H), 7.24 – 7.18 (m, 4H), 7.11 – 7.05 (m, 1H), 6.61 (s, $J = 1.4$ Hz, 1H), 3.91 (q, $J = 7.0$ Hz, 1H), 3.21 (s, 2H), 1.59 (d, $J = 7.1$ Hz, 3H).



N-(*p*-toluenesulfonyl)-3-(1-phenylpropyl)-2,5-dihydro-1*H*-pyrrole (**5.102**)

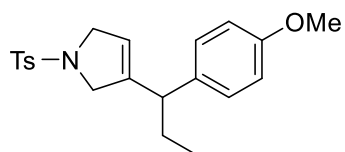
Following the general procedure (rt, 2 h, then 60 °C, 12 h), **5.101** (82.4 mg, 0.18 mmol) was reacted with $[\text{Rh}(\text{cod})\text{OH}]_2$ (4.3 mg, 0.0092 mmol) and phenylboronic acid (69.4 mg, 0.55 mmol) in MeOH (1.8 ml) to give the product **5.102** as a white paste (30.6 mg, 0.089 mmol, 49%). $R_f = 0.59$ (Hex/EA = 2:1); $^1\text{H NMR}$ (400 MHz, CDCl_3) δ 7.61 (d, $J = 6.5$ Hz, 2H), 7.30 – 7.16 (m, 5H), 7.01 (d, $J = 7.5$ Hz, 2H), 5.38 (s, $J = 1.5$ Hz, 1H), 4.11 (s, $J = 1.2$ Hz, 2H), 3.95 – 3.80 (m, 2H), 3.06 (t, $J = 6.3$ Hz, 1H), 2.41 (s, 3H), 1.88 – 1.74 (m, 1H), 1.74 – 1.62 (m, 1H), 0.76 (t, $J = 7.3$ Hz, 3H); $^{13}\text{C NMR}$ (101 MHz, CDCl_3) δ 143.21, 142.68, 141.58, 134.17, 129.64, 128.47, 127.63, 127.31, 126.64, 118.12, 55.73, 55.10, 47.33, 26.56, 21.49, 12.13; **IR** (neat, cm^{-1}): 3061, 3027, 2962, 2927, 2872, 1732, 1658, 1598, 1493, 1453, 1345, 1163, 1095, 1062, 814, 757, 737, 710, 668, 594, 549; **HRMS** (ESI): Calcd for $\text{C}_{20}\text{H}_{23}\text{NNaO}_2\text{S}$ $[\text{M}+\text{Na}]^+$ 364.1347, found 364.1343.



N-(*p*-toluenesulfonyl)-3-{1-(4-methoxycarbonyl)phenylpropyl}-2,5-dihydro-1*H*-pyrrole (**5.103**)

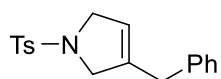
Following the general procedure (rt, 2 h, then 60 °C, 12 h), **5.101** (85.1 mg, 0.19 mmol) was reacted with $[\text{Rh}(\text{cod})\text{OH}]_2$ (4.5 mg, 0.0095 mmol) and 4-(methoxycarbonyl)phenylboronic acid (105.8 mg, 0.57 mmol) in MeOH (1.9

ml) to give the product **5.103** as a white paste (38.7 mg, 0.097 mmol, 51%). **R_f** = 0.49 (Hex/EA = 2:1); **¹H NMR** (400 MHz, CDCl₃) δ 7.92 (d, *J* = 6.5 Hz, 2H), 7.60 (d, *J* = 6.6 Hz, 2H), 7.25 (d, *J* = 6.9 Hz, 2H), 7.07 (d, *J* = 6.7 Hz, 2H), 5.42 (s, 1H), 4.17 – 4.07 (m, 2H), 3.98 – 3.76 (m, 5H), 3.13 (t, *J* = 7.1 Hz, 1H), 2.43 (d, *J* = 2.8 Hz, 3H), 1.91 – 1.78 (m, 1H), 1.75 – 1.61 (m, 1H), 0.76 (t, *J* = 7.3 Hz, 3H); **¹³C NMR** (101 MHz, CDCl₃) δ 166.82, 146.99, 143.36, 141.81, 134.01, 129.85, 129.67, 128.68, 127.67, 127.29, 118.90, 55.61, 55.12, 52.07, 47.27, 26.44, 21.47, 12.04; **IR (neat, cm⁻¹)**: 2961, 2930, 2873, 2359, 2337, 1721, 1610, 1436, 1345, 1281, 1163, 1109, 1019, 966, 861, 816, 773, 726, 709, 669, 600, 549; **HRMS (ESI)**: Calcd for C₂₂H₂₅NNaO₄S [M+Na]⁺ 422.1402, found 422.1397.



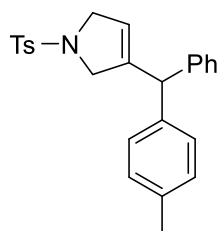
N-(*p*-toluenesulfonyl)-3-{1-(4-methoxyphenyl)propyl}-2,5-dihydro-1*H*-pyrrole (**5.104**)

Following the general procedure (rt, 2 h, then 60 °C, 12 h), **5.101** (86.1 mg, 0.19 mmol) was reacted with [Rh(cod)OH]₂ (4.5 mg, 0.0096 mmol) and 4-methoxyphenylboronic acid (92.3 mg, 0.58 mmol) in MeOH (1.9 ml) to give the product **5.104** as a white paste (34.6 mg, 0.093 mmol, 48%). **R_f** = 0.55 (Hex/EA = 2:1); **¹H NMR** (499 MHz, CDCl₃) δ 7.62 (d, *J* = 7.2 Hz, 2H), 7.27 (d, *J* = 6.6 Hz, 2H), 6.93 (d, *J* = 7.6 Hz, 2H), 6.79 (d, *J* = 7.6 Hz, 2H), 5.36 (s, 1H), 4.10 (s, 2H), 3.87 (d, *J* = 3.9 Hz, 2H), 3.80 (s, *J* = 1.1 Hz, 3H), 3.01 (t, *J* = 7.1 Hz, 1H), 2.42 (s, 3H), 1.83 – 1.73 (m, 1H), 1.69 – 1.56 (m, 1H), 0.75 (t, *J* = 6.9 Hz, 3H); **¹³C NMR** (101 MHz, CDCl₃) δ 158.25, 143.20, 143.07, 134.22, 133.62, 129.62, 128.54, 127.33, 117.80, 113.84, 55.71, 55.22, 55.10, 46.48, 26.63, 21.49, 12.12; **IR (neat, cm⁻¹)**: 2961, 2930, 2871, 2360, 2337, 1611, 1511, 1463, 1344, 1304, 1249, 1163, 1106, 1037, 832, 813, 749, 709, 668, 601, 549; **HRMS (ESI)**: Calcd for C₂₁H₂₅NNaO₃S [M+Na]⁺ 394.1453, found 394.1450.



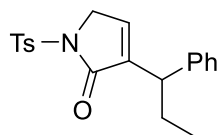
N-(*p*-toluenesulfonyl)-3-(phenylmethyl)-2,5-dihydro-1*H*-pyrrole (**5.106**)

White solid; $R_f = 0.31$ (Hex/EA=5:1); $^1\text{H NMR}$ (400 MHz, CDCl_3) δ 7.67 (d, $J = 8.1$ Hz, 2H), 7.32 – 7.18 (m, 5H), 7.05 (d, $J = 6.9$ Hz, 2H), 5.25 (s, 1H), 4.09 (s, 2H), 3.97 (s, 2H), 3.30 (s, $J = 12.9$ Hz, 2H), 2.43 (s, $J = 6.7$ Hz, 3H); $^{13}\text{C NMR}$ (101 MHz, CDCl_3) δ 143.30, 138.81, 137.51, 134.20, 129.69, 128.58, 128.52, 127.37, 126.56, 119.93, 56.21, 55.02, 35.37, 21.51.



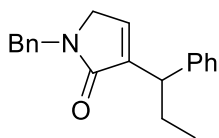
N-(*p*-toluenesulfonyl)-3-{1-phenyl-1-(*p*-tolyl)methyl}-2,5-dihydro-1*H*-pyrrole (**5.108**)

White paste; $R_f = 0.71$ (Hex/EA=2:1); $^1\text{H NMR}$ (400 MHz, CDCl_3) δ 7.68 (d, $J = 8.1$ Hz, 2H), 7.33 (d, $J = 8.0$ Hz, 2H), 7.21 (dd, $J = 10.8, 7.2$ Hz, 3H), 7.05 (d, $J = 7.8$ Hz, 2H), 7.01 (d, $J = 7.0$ Hz, 2H), 6.91 (d, $J = 7.9$ Hz, 2H), 5.08 (s, 1H), 4.59 (s, 1H), 4.13 (s, $J = 2.0$ Hz, 2H), 4.01 (s, 2H), 2.47 (s, 3H), 2.31 (s, 3H); $^{13}\text{C NMR}$ (101 MHz, CDCl_3) δ 143.34, 142.08, 141.00, 137.76, 136.40, 134.09, 129.71, 129.19, 128.46, 128.43, 128.35, 127.49, 126.72, 122.52, 56.37, 55.19, 50.92, 29.67, 20.99.



N-(*p*-toluenesulfonyl)-3-(1-phenylpropyl)-1,5-dihydro-2*H*-pyrrol-2-one (**5.109**)

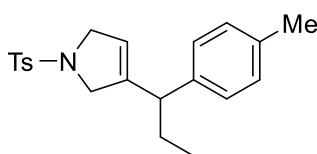
$R_f = 0.47$ (Hex/EA=2:1); $^1\text{H NMR}$ (499 MHz, CDCl_3) δ 7.96 – 7.92 (m, 2H), 7.32 (d, $J = 8.0$ Hz, 2H), 7.27 (d, $J = 7.7$ Hz, 2H), 7.23 – 7.18 (m, 1H), 7.17 (d, $J = 6.9$ Hz, 2H), 6.77 (dd, $J = 3.4, 2.1$ Hz, 1H), 4.35 (qtp, 2H), 3.49 (dd, $J = 8.5, 5.8$ Hz, 1H), 2.43 (s, 3H), 2.02 – 1.93 (m, 1H), 1.80 – 1.70 (m, 1H), 0.79 (t, $J = 7.3$ Hz, 3H); $^{13}\text{C NMR}$ (101 MHz, CDCl_3) δ 168.21, 145.02, 142.89, 140.82, 138.31, 135.32, 129.70, 128.56, 128.00, 127.97, 126.78, 50.14, 44.13, 26.99, 21.66, 12.29.



N-benzyl-3-(1-phenylpropyl)-1,5-dihydro-2*H*-pyrrol-2-one (**5.110**)

R_f = 0.47 (Toluene/EA=4:1); **¹H NMR (400 MHz, CDCl₃)**

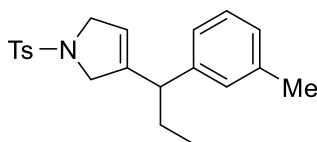
δ 7.35 – 7.26 (m, 7H), 7.21 (d, *J* = 7.3 Hz, 4H), 6.58 (s, 1H), 4.60 (dd, *J* = 47.0, 14.9 Hz, 2H), 3.72 (d, *J* = 7.9 Hz, 2H), 3.68 (d, *J* = 8.8 Hz, 1H), 2.16 – 2.05 (m, 1H), 1.90 – 1.77 (m, 1H), 0.88 (t, *J* = 7.3 Hz, 3H); **¹³C NMR (101 MHz, CDCl₃)** δ 170.87, 143.40, 142.31, 137.36, 134.43, 128.65, 128.37, 128.09, 128.02, 127.44, 126.37, 50.15, 46.30, 44.61, 27.35, 12.47.



N-(*p*-toluenesulfonyl)-3-{1-(4-methylphenyl)propyl}-2,5-dihydro-1*H*-pyrrole (**5.111**)

White paste; **R_f** = 0.70 (Hex/EA=2:1), 0.41 (DCM

only); **¹H NMR (499 MHz, CDCl₃)** δ 7.62 (d, *J* = 8.1 Hz, 2H), 7.26 (d, *J* = 7.5 Hz, 3H), 7.05 (d, *J* = 7.5 Hz, 2H), 6.90 (d, *J* = 7.8 Hz, 2H), 5.36 (s, 1H), 4.10 (dd, *J* = 3.8, 1.9 Hz, 2H), 3.88 (dd, *J* = 2.2, 1.1 Hz, 2H), 3.03 (t, *J* = 7.2 Hz, 1H), 2.32 (s, 3H), 1.84 – 1.72 (m, 1H), 1.70 – 1.59 (m, 1H), 0.75 (t, *J* = 7.3 Hz, 3H); **¹³C NMR (101 MHz, CDCl₃)** δ 143.18, 142.91, 138.53, 136.12, 134.23, 129.61, 129.14, 127.49, 127.32, 117.90, 55.71, 55.09, 46.93, 26.57, 21.49, 20.99, 12.15.

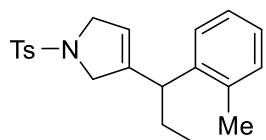


N-(*p*-toluenesulfonyl)-3-{1-(3-methylphenyl)propyl}-2,5-dihydro-1*H*-pyrrole (**5.112**)

White paste; **R_f** = 0.69 (Hex/EA=2:1); **¹H NMR**

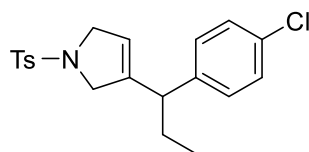
(499 MHz, CDCl₃) δ 7.62 (d, *J* = 7.8 Hz, 2H), 7.27 (d, *J* = 7.1 Hz, 2H), 7.14 (t, *J* = 7.5 Hz, 1H), 7.02 (d, *J* = 7.5 Hz, 1H), 6.81 (d, *J* = 11.8 Hz, 2H), 5.38 (s, 1H), 4.11 (s, 2H), 3.93 – 3.82 (m, 2H), 3.02 (t, *J* = 7.0 Hz, 1H), 2.42 (s, 3H), 2.30 (s, 3H), 1.85 – 1.74 (m, 1H), 1.72 – 1.59 (m, 1H), 0.76 (t, *J* = 7.3

Hz, 3H); ^{13}C NMR (101 MHz, CDCl_3) δ 143.18, 142.77, 141.54, 138.01, 134.20, 129.62, 128.34, 128.32, 127.39, 127.32, 124.63, 117.93, 55.76, 55.10, 47.30, 26.53, 21.49, 21.43, 12.18.



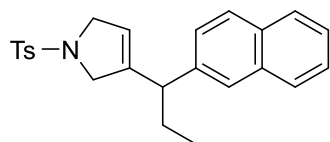
N-(*p*-toluenesulfonyl)-3-{1-(2-methylphenyl)propyl}-2,5-dihydro-1*H*-pyrrole (**5.113**)

White solid; R_f = 0.68 (Hex/EA=2:1); ^1H NMR (499 MHz, CDCl_3) δ 7.60 (d, J = 8.1 Hz, 2H), 7.29 – 7.23 (m, 2H), 7.13 – 7.05 (m, 3H), 6.97 – 6.90 (m, 1H), 5.34 (s, 1H), 4.10 (s, 2H), 3.87 (s, 2H), 3.37 (t, J = 7.0 Hz, 1H), 2.42 (s, 3H), 2.21 (s, 3H), 1.88 – 1.75 (m, 1H), 1.74 – 1.61 (m, 1H), 0.78 (t, J = 7.3 Hz, 3H); ^{13}C NMR (101 MHz, CDCl_3) δ 143.20, 142.34, 139.67, 136.01, 134.15, 130.41, 129.64, 127.29, 126.30, 126.24, 118.32, 55.71, 55.07, 42.39, 26.52, 21.49, 19.60, 12.08.



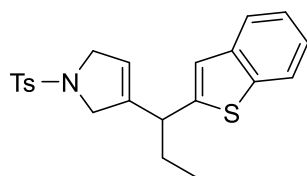
N-(*p*-toluenesulfonyl)-3-{1-(4-chlorophenyl)propyl}-2,5-dihydro-1*H*-pyrrole (**5.114**)

White paste; R_f = 0.61 (Hex/EA=2:1); ^1H NMR (499 MHz, CDCl_3) δ 7.61 (d, J = 8.2 Hz, 2H), 7.27 (d, J = 6.9 Hz, 2H), 7.21 (d, J = 8.4 Hz, 2H), 6.94 (d, J = 8.3 Hz, 2H), 5.41 – 5.36 (m, 1H), 4.12 (s, 2H), 3.85 (dd, J = 33.8, 13.7 Hz, 2H), 3.04 (t, J = 7.2 Hz, 1H), 2.43 (s, 3H), 1.86 – 1.75 (m, 1H), 1.69 – 1.57 (m, 1H), 0.76 (t, J = 7.3 Hz, 3H); ^{13}C NMR (101 MHz, CDCl_3) δ 143.33, 142.22, 140.08, 134.05, 132.35, 129.64, 128.95, 128.62, 127.30, 118.54, 55.57, 55.12, 46.68, 26.47, 21.49, 12.04.



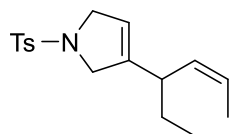
N-(*p*-toluenesulfonyl)-3-{1-(naphth-1-ylprop-1-yl)}-2,5-dihydro-1*H*-pyrrole (**5.115**)

White solid; $R_f = 0.65$ (Hex/EA=2:1); $^1\text{H NMR}$ (**400 MHz, CDCl₃**) δ 7.85 – 7.77 (m, 1H), 7.77 – 7.69 (m, 2H), 7.57 (d, $J = 8.2$ Hz, 2H), 7.51 – 7.43 (m, 3H), 7.17 (d, $J = 8.0$ Hz, 2H), 7.13 (d, $J = 8.5$ Hz, 1H), 5.44 (s, 1H), 4.13 (s, 2H), 3.91 (dd, $J = 29.3, 13.3$ Hz, 2H), 3.24 (t, $J = 6.9$ Hz, 1H), 2.38 (s, 3H), 1.98 – 1.85 (m, 1H), 1.85 – 1.71 (m, 1H), 0.80 (t, $J = 7.3$ Hz, 3H); $^{13}\text{C NMR}$ (**101 MHz, CDCl₃**) δ 143.17, 142.65, 139.03, 134.07, 133.39, 132.41, 129.59, 128.23, 127.59, 127.55, 127.27, 126.37, 126.05, 125.66, 125.59, 118.32, 55.81, 55.16, 47.45, 26.39, 21.46, 12.19.



N-(*p*-toluenesulfonyl)-3-{1-(benzo[*b*]thiophen-2-yl)prop-1-yl}-2,5-dihydro-1*H*-pyrrole (**5.116**)

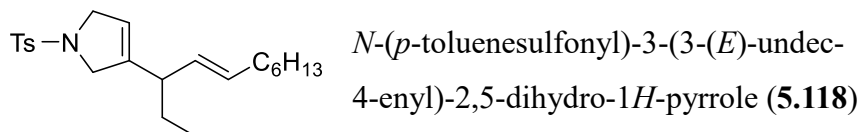
Yellow oil; $^1\text{H NMR}$ (**499 MHz, CDCl₃**) δ 7.73 (d, $J = 7.9$ Hz, 1H), 7.65 (d, $J = 7.7$ Hz, 1H), 7.61 (d, $J = 8.1$ Hz, 2H), 7.37 – 7.27 (m, 3H), 7.20 (d, $J = 7.7$ Hz, 2H), 6.95 (s, 1H), 5.49 (s, 1H), 4.14 (s, 2H), 4.03 (s, 2H), 3.51 (t, $J = 7.3$ Hz, 1H), 2.39 (s, 3H), 1.83 (td, $J = 13.5, 6.7$ Hz, 2H), 0.88 (t, $J = 7.2$ Hz, 3H).



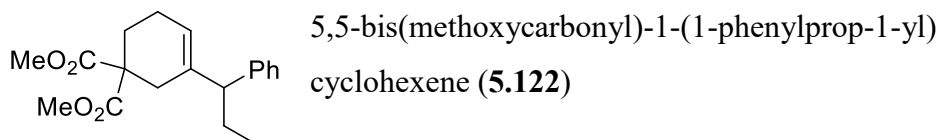
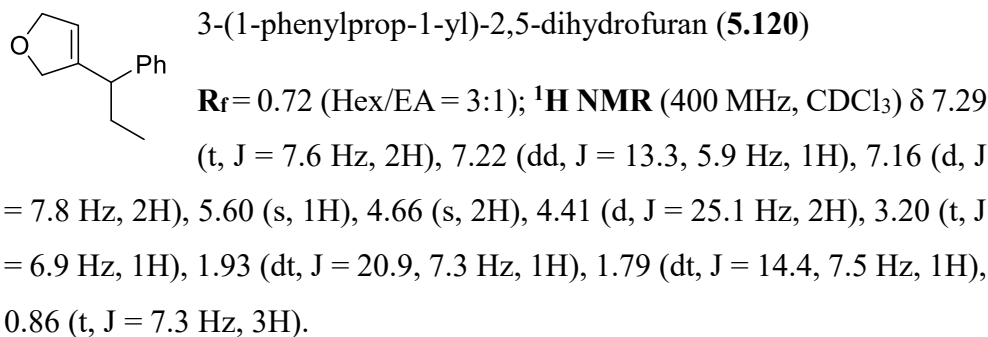
N-(*p*-toluenesulfonyl)-3-(4-(*Z*)-hex-2-enyl)-2,5-dihydro-1*H*-pyrrole (**5.117**)

White paste; $R_f = 0.45$ (Hex/EA=5:1); $^1\text{H NMR}$ (**400 MHz, CDCl₃**) δ 7.71 (d, $J = 8.2$ Hz, 2H), 7.31 (d, $J = 8.4$ Hz, 2H), 5.53 (dq, $J = 13.7, 6.8$ Hz, 1H), 5.29 – 5.24 (m, 1H), 5.11 – 5.03 (m, 1H), 4.07 (d, $J = 4.6$ Hz, 2H), 4.01 (d, $J = 3.6$ Hz, 2H), 2.93 (dd, $J = 14.6, 8.7$ Hz, 1H), 2.43 (s, 3H), 1.55 (s, 3H), 1.54 – 1.47 (m, 1H), 1.36 – 1.27 (m, 1H), 0.79 (t, $J = 7.3$ Hz, 3H); $^{13}\text{C NMR}$ (**101 MHz, CDCl₃**) δ 143.25, 142.23, 134.33, 131.06,

129.64, 127.37, 125.56, 117.42, 55.21, 54.91, 38.52, 26.24, 21.49, 13.00, 11.49.

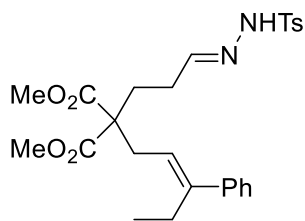


White paste; $R_f = 0.53$ (Hex/EA=5:1), 0.45 (DCM only); $^1\text{H NMR}$ (499 MHz, CDCl_3) δ 7.70 (d, $J = 8.2$ Hz, 2H), 7.31 (d, $J = 8.0$ Hz, 2H), 5.39 – 5.31 (m, 1H), 5.26 (dd, $J = 3.3, 1.8$ Hz, 1H), 5.10 (dd, $J = 15.3, 8.3$ Hz, 1H), 4.11 – 4.07 (m, 2H), 4.03 – 3.96 (m, 2H), 2.51 (dd, $J = 14.9, 7.6$ Hz, 1H), 2.42 (s, 3H), 1.95 (q, $J = 6.7$ Hz, 2H), 1.49 – 1.42 (m, 1H), 1.39 – 1.21 (m, 9H), 0.88 (t, $J = 7.0$ Hz, 3H), 0.78 (t, $J = 7.4$ Hz, 3H); $^{13}\text{C NMR}$ (101 MHz, CDCl_3) δ 143.23, 142.52, 134.30, 132.28, 130.34, 129.63, 127.38, 117.56, 55.23, 55.03, 44.42, 32.39, 31.65, 29.35, 28.79, 25.84, 22.58, 21.47, 14.06, 11.66.



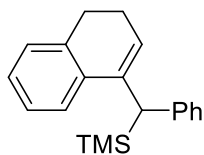
Following the general procedure (rt, 2 h, then 60 °C, 12 h), **5.121** (88.0 mg, 0.21 mmol) was reacted with $[\text{Rh}(\text{cod})\text{OH}]_2$ (4.9 mg, 0.010 mmol) and phenylboronic acid (52.4 mg, 0.42 mmol) in MeOH (2.1 ml)

to give the product **5.122** as a clear oil (14.2 mg, 0.045 mmol, 22%) and **5.123** as a clear gum (71.8 mg, 0.14 mmol, 69%). $R_f = 0.49$ (Hex/EA = 5:1); $^1\text{H NMR}$ (400 MHz, CDCl_3) δ 7.27 (t, $J = 7.3$ Hz, 2H), 7.17 (t, $J = 8.2$ Hz, 3H), 5.58 (s, 1H), 3.59 (s, 3H), 3.57 (s, 3H), 3.05 (t, $J = 7.5$ Hz, 1H), 2.31 (q, $J = 17.0$ Hz, 2H), 2.17 (s, 2H), 2.11 – 1.96 (m, 2H), 1.93 – 1.79 (m, 1H), 1.79 – 1.65 (m, 1H), 0.84 (t, $J = 7.3$ Hz, 3H); $^{13}\text{C NMR}$ (101 MHz, CDCl_3) δ 171.87, 143.30, 137.07, 128.01, 127.93, 125.97, 120.17, 54.45, 53.45, 52.36, 31.79, 27.55, 25.09, 22.56, 12.40; **IR** (neat, cm^{-1}): 3025, 2955, 2874, 1736, 1493, 1452, 1256, 1215, 1086, 952, 761, 702; **HRMS** (ESI): Calcd for $\text{C}_{19}\text{H}_{24}\text{NaO}_4$ $[\text{M}+\text{Na}]^+$ 339.1572, found 339.1568.



(*E*)-4,4-bis(methoxycarbonyl)-7-phenylnon-6-enal (*p*-toluenesulfonyl)hydrazone (**5.123**)

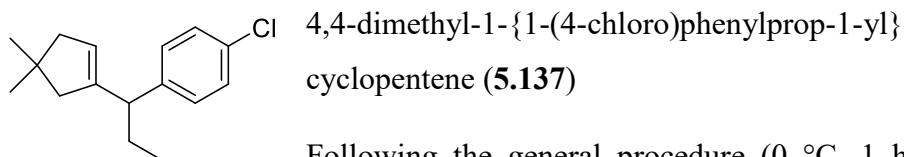
$^1\text{H NMR}$ (400 MHz, CDCl_3) δ 8.12 (s, 1H), 7.79 (d, $J = 8.3$ Hz, 2H), 7.36 – 7.20 (m, 5H), 7.15 (t, $J = 4.8$ Hz, 1H), 5.36 (t, $J = 7.2$ Hz, 1H), 3.72 (s, 6H), 2.80 (d, $J = 7.3$ Hz, 2H), 2.54 – 2.44 (m, 2H), 2.38 (s, 3H), 2.24 – 2.12 (m, 2H), 2.11 – 2.01 (m, 2H), 0.93 (t, $J = 7.6$ Hz, 3H).



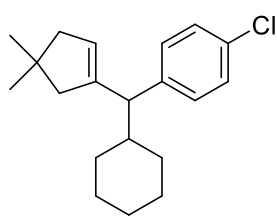
1-((trimethylsilyl)(phenyl))methyl-3,4-dihydronaphthalene (**5.125**)

To a solution of **5.124** generated *in situ* (0.20 mmol) was added $[\text{Rh}(\text{cod})\text{OH}]_2$ (4.6 mg, 0.0098 mmol). After the reaction mixture was cooled down to 0 °C, $\text{PhB}(\text{OH})_2$ (49.1 mg, 0.39 mmol) was added and the reaction mixture was stirred for 24 h at 0 °C, then 5 h at 60 °C. After evaporation of the solvent, crude material was chromatographed on silica gel to give the product **5.125** as a white solid (24.2 mg, 0.083 mmol, 42%, 2 steps

from *p*-toluenesulfonyl hydrazide). $R_f = 0.26$ (Hexane only); $^1\text{H NMR}$ (400 MHz, CDCl_3) δ 7.32 – 7.19 (m, 5H), 7.16 – 6.98 (m, 4H), 6.16 (t, $J = 4.7$ Hz, 1H), 3.44 (s, 1H), 2.85 – 2.65 (m, 2H), 2.42 – 2.29 (m, 2H), 0.06 (s, 9H); $^{13}\text{C NMR}$ (101 MHz, CDCl_3) δ 142.24, 137.11, 136.77, 136.51, 128.09, 127.78, 127.62, 127.29, 126.37, 126.26, 124.72, 123.46, 40.87, 28.45, 23.47, -1.37; **IR** (neat, cm^{-1}): 3057, 3019, 2946, 2884, 2829, 1736, 1597, 1483, 1448, 1363, 1247, 1141, 1078, 1024, 914, 890, 865, 837, 757, 734, 670; **HRMS (ESI)**: Calcd for $\text{C}_{20}\text{H}_{24}\text{NaSi}$ $[\text{M}+\text{Na}]^+$ 315.1545, found 315.1554.

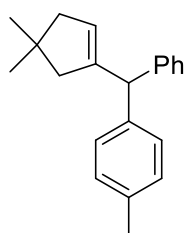


Following the general procedure (0 °C, 1 h, then 60 °C, 5 h), **5.134** (65.9 mg, 0.21 mmol) was reacted with $[\text{Rh}(\text{cod})\text{OH}]_2$ (4.8 mg, 0.010 mmol) and 4-chlorophenylboronic acid (67.7 mg, 0.41 mmol) in MeOH (2.1 ml) to give the product **5.137** as a clear liquid (38.8 mg, 0.16 mmol, 76%). $R_f = 0.63$ (Hexane only); $^1\text{H NMR}$ (400 MHz, CDCl_3) δ 7.23 (d, $J = 8.4$ Hz, 2H), 7.08 (d, $J = 8.3$ Hz, 2H), 5.35 (s, 1H), 3.09 (t, $J = 7.3$ Hz, 1H), 2.19 – 2.05 (m, 2H), 1.94 – 1.78 (m, 3H), 1.73 – 1.58 (m, 1H), 0.99 (d, $J = 14.8$ Hz, 6H), 0.81 (t, $J = 7.3$ Hz, 3H); $^{13}\text{C NMR}$ (101 MHz, CDCl_3) δ 145.38, 142.45, 131.45, 129.22, 128.20, 122.65, 49.06, 48.55, 47.41, 38.21, 29.70, 29.63, 26.59, 12.40; **IR** (neat, cm^{-1}): 3047, 2954, 2929, 2899, 2866, 2838, 1491, 1463, 1408, 1380, 1363, 1308, 1264, 1187, 1092, 1015, 992, 827, 805, 735, 535, 495; **HRMS (ESI)**: Calcd for $\text{C}_{16}\text{H}_{22}\text{Cl}$ $[\text{M}+\text{H}]^+$ 249.1410, found 249.1406.



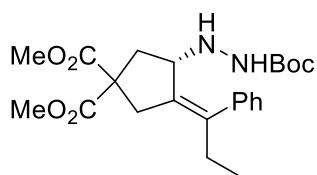
4,4-dimethyl-1-{cyclohexyl-(4-chloro)
phenylmethyl}cyclopentene (**5.138**)

Following the general procedure (0 °C, 1 h, then 60 °C, 5 h), **5.135** (81.3 mg, 0.22 mmol) was reacted with [Rh(cod)OH]₂ (5.1 mg, 0.011 mmol) and 4-chlorophenylboronic acid (71.5 mg, 0.43 mmol) in MeOH (2.2 ml) to give the product **5.138** as a clear liquid (52.4 mg, 0.17 mmol, 80%). *R_f* = 0.69 (Hexane only); ¹H NMR (400 MHz, CDCl₃) δ 7.22 (d, *J* = 8.1 Hz, 2H), 7.06 (d, *J* = 8.3 Hz, 2H), 5.37 (s, 1H), 2.99 (d, *J* = 10.1 Hz, 1H), 2.15 – 2.03 (m, 2H), 1.99 – 1.82 (m, 3H), 1.79 – 1.67 (m, 2H), 1.61 (s, *J* = 7.0 Hz, 2H), 1.37 (d, *J* = 12.8 Hz, 1H), 1.25 (dd, *J* = 25.0, 12.6 Hz, 1H), 1.18 – 1.07 (m, 2H), 0.98 (d, *J* = 9.7 Hz, 6H), 0.88 (ddd, *J* = 14.9, 12.8, 3.3 Hz, 1H), 0.75 – 0.62 (m, 1H); ¹³C NMR (101 MHz, CDCl₃) δ 144.18, 141.54, 131.26, 129.66, 128.07, 123.44, 54.67, 47.90, 47.25, 39.34, 38.17, 32.15, 31.40, 29.89, 29.60, 26.55, 26.38, 26.26; IR (neat, cm⁻¹): 2925, 2852, 1688, 1606, 1490, 1465, 1449, 1408, 1091, 1015, 895, 829, 589, 521, 496; HRMS (ESI): Calcd for C₂₀H₂₈Cl [M+H]⁺ 303.1880, found 303.1888.



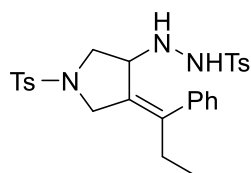
4,4-dimethyl-1-{phenyl-(4-methyl)phenylmethyl}
cyclopentene (**5.139**)

R_f = 0.23 (Hexane only); ¹H NMR (400 MHz, CDCl₃) δ 7.31 – 7.22 (m, 2H), 7.18 (t, *J* = 7.0 Hz, 3H), 7.14 – 7.02 (m, 4H), 5.04 (s, 1H), 4.64 (s, 1H), 2.31 (s, 3H), 2.15 (s, 2H), 2.07 (s, 2H), 1.07 (s, 6H); ¹³C NMR (101 MHz, CDCl₃) δ 145.28, 143.17, 139.90, 135.68, 128.98, 128.89, 128.81, 128.23, 126.74, 126.12, 53.53, 50.03, 47.68, 38.80, 29.97, 21.11.



1-(2-*tert*-butoxycarbonyl)hydrazinyl)-4,4-bis(methoxycarbonyl)-2-(1-(*Z*)-phenylpropylidene)cyclopentane (**5.167**)

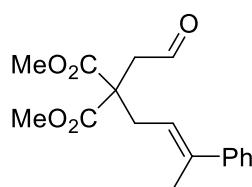
To **5.166** (73.2 mg, 0.21 mmol) in a 20 ml tube vial was added toluene (2.1 ml) and **5.165** (9.3 mg, 0.010 mmol). The resulting orange solution was cooled to 0 °C. Aqueous KOH (0.21 ml, 0.021 mmol) and PhB(OH)₂ (51.9 mg, 0.41 mmol) was added and the reaction mixture was stirred at 0 °C for 24 h. After short filtration by Na₂SO₄ and evaporation of the solvent, the crude product was purified by flash chromatography on a silica gel column to give (*S*)-**5.167** as a clear paste (83.8 mg, 0.19 mmol, 94%, 93% *ee*). *R*_f = 0.48 (Hex/EA = 2:1); ¹H NMR (400 MHz, CDCl₃) δ 7.33 (t, *J* = 7.3 Hz, 2H), 7.29 – 7.20 (m, 1H), 7.15 (d, *J* = 7.0 Hz, 2H), 5.67 (s, 1H), 3.93 (s, 1H), 3.76 (d, *J* = 4.3 Hz, 6H), 3.59 (d, *J* = 9.2 Hz, 1H), 3.33 (d, *J* = 17.0 Hz, 1H), 3.00 (d, *J* = 17.0 Hz, 1H), 2.51 (d, *J* = 13.6 Hz, 1H), 2.45 – 2.26 (m, 2H), 2.21 (dd, *J* = 13.7, 5.3 Hz, 1H), 1.32 (s, 9H), 0.89 (t, *J* = 7.5 Hz, 3H); ¹³C NMR (101 MHz, CDCl₃) δ 172.67, 172.25, 155.85, 141.17, 139.96, 134.31, 128.32, 128.07, 126.81, 79.81, 60.85, 58.28, 52.93, 52.89, 37.84, 36.76, 28.78, 28.22, 12.06; IR (neat, cm⁻¹): 3412, 2972, 1737, 1435, 1392, 1367, 1167, 1089, 870, 768, 704; HRMS (ESI): Calcd for C₂₃H₃₂N₂NaO₆ [M+Na]⁺ 455.2158, found 455.2155; Chiral HPLC: Chiralcel OD-H, 1.0 ml/min, Hex/*i*PA=95:5, *R*_f=5.6 min, 7.7 min; [α]_D^{23.4} = +30.67 ((*S*)-enantiomer, *c* = 1.00 g/100 ml, CHCl₃, 93% *ee*).



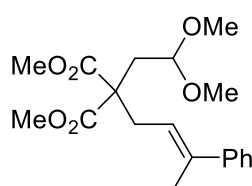
Cyclic hydrazide **5.169**

*R*_f = 0.36 (Hex/EA = 2:1); ¹H NMR (selected, 400 MHz, CDCl₃) δ 3.90 (q, *J* = 14.0 Hz, 1H), 3.81 (s, 1H), 3.39 (dd, *J* = 10.7, 2.7 Hz, 1H), 3.22 (s, 1H), 3.05 (dd, *J* = 10.7, 5.4 Hz, 1H), 2.45 (s, 1H), 2.41 (s, 1H), 2.26 – 2.15 (m, 1H), 0.82 (t, *J* = 7.5 Hz, 3H).

5.5.5 Competition experiments with alkynylaldehyde

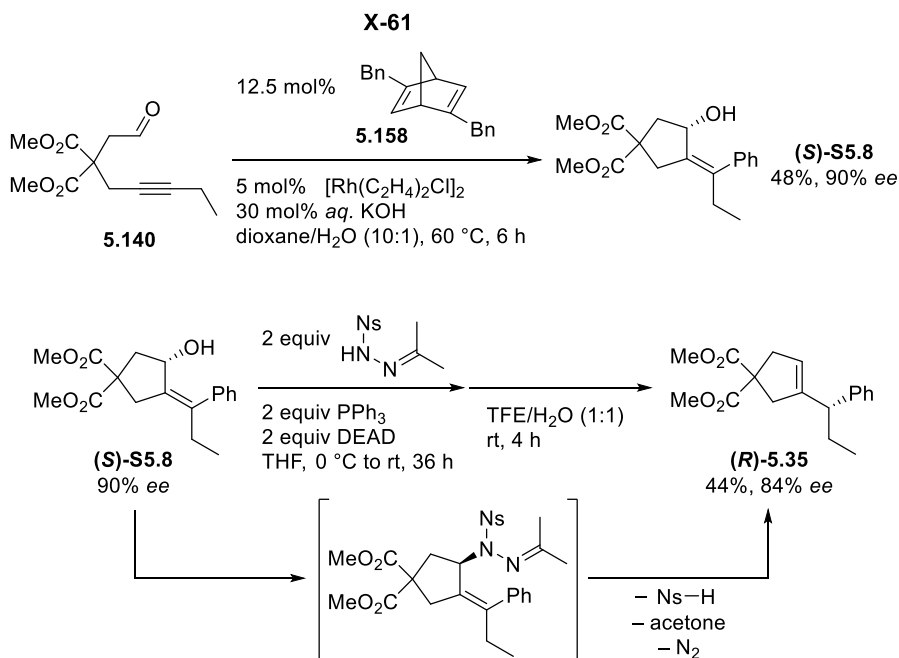
 **(E)-3,3-bis(methoxycarbonyl)-6-phenyl-5-octenal**
(5.141)

To an alkynylaldehyde **5.140** (86.9 mg, 0.36 mmol) in a 20 ml tube vial was added MeOH (3.6 ml), and [Rh(COD)OH]₂ (8.5 mg, 0.018 mmol, 0.05 equiv). The resulting yellow solution was cooled to 0 °C. PhB(OH)₂ (90.9 mg, 0.72 mmol, 2 equiv) was added and the reaction mixture was stirred at 0 °C for 1 h. After evaporation of the solvent, the crude product was purified by flash chromatography on a silica gel column to give the pure product **5.141** as a clear oil (79.3 mg, 0.25 mmol, 69%). *R_f* = 0.39 (Hex/EA = 3:1); ¹H NMR (400 MHz, CDCl₃) δ 9.72 (s, 1H), 7.37 – 7.18 (m, 2H), 5.37 (t, *J* = 7.6 Hz, 1H), 3.77 (s, 2H), 3.05 (s, 1H), 2.95 (d, *J* = 7.6 Hz, 1H), 2.47 (q, *J* = 7.4 Hz, 1H), 0.92 (t, *J* = 7.5 Hz, 3H); ¹³C NMR (101 MHz, CDCl₃) δ 198.77, 170.55, 146.50, 142.32, 128.22, 127.08, 126.43, 120.33, 54.83, 52.95, 46.33, 32.73, 23.00, 13.30.

 **(E)-3,3-bis(methoxycarbonyl)-6-phenyl-5-octenal**
dimethyl acetal (5.142)

¹H NMR (400 MHz, CDCl₃) δ 7.37 – 7.20 (m, 5H), 5.39 (t, *J* = 7.4 Hz, 1H), 4.49 (t, *J* = 5.5 Hz, 1H), 3.72 (s, 6H), 3.31 (s, 6H), 2.88 (d, *J* = 7.4 Hz, 2H), 2.52 (q, *J* = 7.4 Hz, 2H), 2.29 (d, *J* = 5.5 Hz, 2H), 0.95 (t, *J* = 7.5 Hz, 3H); ¹³C NMR (101 MHz, CDCl₃) δ 171.52, 145.64, 142.55, 128.17, 126.91, 126.44, 120.68, 101.92, 55.29, 53.56, 52.45, 36.12, 32.22, 30.28, 23.04, 13.32.

5.5.6 Determination of the absolute stereochemistry of **5.35**

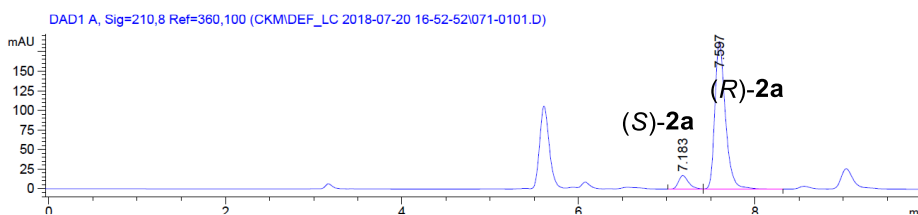


The absolute configuration of **5.35** was determined by the independent synthesis of (*R*)-**5.35** (84% *ee*) through a route combining the protocols of Hayashi and Movassaghi. Following the Hayashi's method for the rhodium-catalyzed arylation cyclization of alkyne, alcohol **S5.8** was prepared in 90% *ee*, whose Mosher's MTPA ester analysis determined the configuration of the major isomer of **S5.8** to be (*S*) that was consistent with Hayashi's assignment. Allylic alcohol (*S*)-**S5.8** was converted to (*R*)-**5.35** by the stereospecific allylic reduction developed by Movassaghi, which involved Mitsunobu inversion of the alcohol with IPNBSH and allylic diazene rearrangement. Comparison of the chiral HPLC chromatograms of cyclopentene **5.35**, obtained respectively from this route and from alkynehydrazone **5.34**, determined the absolute stereochemistry of **5.35**, derived from the asymmetric reaction of alkynehydrazone **5.34** using **5.164**, to be of (*S*)-configuration.

Of note in the result of these correlation experiments is that the C=O and C=N

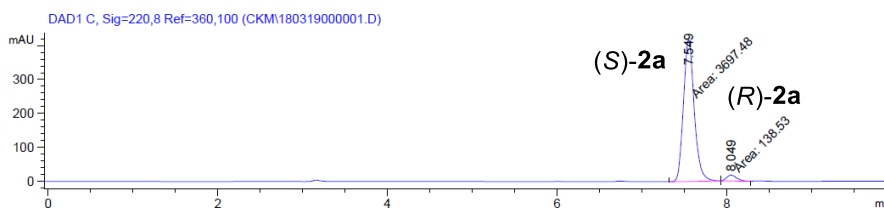
bonds of the aldehyde and hydrazone substrates exhibit opposite enantiofacial preference for the reaction with the same chiral ligand. For example, the reaction of **5.34** with phenylboronic acid using dibenzylnorbonadiene ligand (**5.158**) produced (*R*)-**5.35** in 80% *ee*, indicating the intermediacy of (*R*)-**5.36** (an up C–N bond vis-à-vis the down C–O bond in **S5.8**).

- Chromatographic Traces of (*R*)-**5.35** from **S5.8** (84% *ee*)

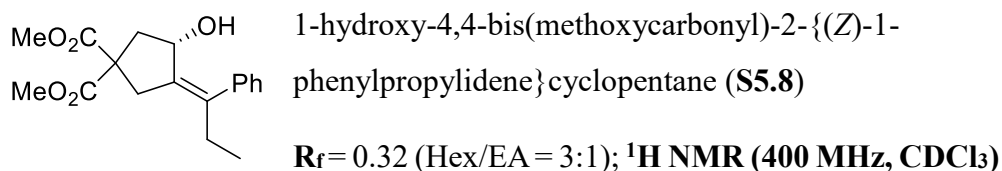


Peak #	RetTime [min]	Type	Width [min]	Area [mAU*s]	Height [mAU]	Area %
1	7.183	VV	0.1203	137.39470	17.36128	8.0627
2	7.597	VB	0.1268	1566.67554	188.86984	91.9373

- Chromatographic Traces of (*S*)-**5.35** from **5.34** (93% *ee*)



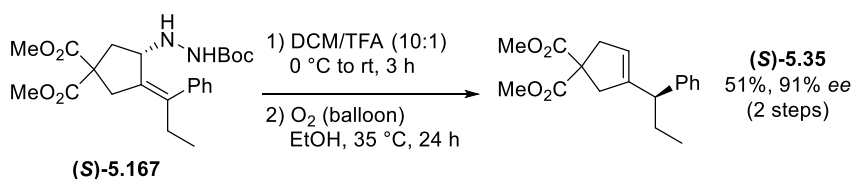
Peak #	RetTime [min]	Type	Width [min]	Area [mAU*s]	Height [mAU]	Area %
1	7.549	MM	0.1475	3697.47681	417.89795	96.3887
2	8.049	MM	0.1346	138.52971	17.15647	3.6113



$R_f = 0.32$ (Hex/EA = 3:1); $^1\text{H NMR}$ (400 MHz, CDCl_3)

δ 7.33 (t, $J = 7.3$ Hz, 2H), 7.29 – 7.25 (m, 1H), 7.21 (d, $J = 7.1$ Hz, 2H), 4.43 (d, $J = 2.9$ Hz, 1H), 3.77 (d, $J = 6.9$ Hz, 6H), 3.40 (d, $J = 17.3$ Hz, 1H), 2.92 (d, $J = 17.3$ Hz, 1H), 2.47 – 2.32 (m, 4H), 1.73 (d, $J = 3.3$ Hz, 1H), 0.92 (t, $J = 7.5$ Hz, 3H); $^{13}\text{C NMR}$ (101 MHz, CDCl_3) δ 172.97, 172.23, 141.13, 140.52, 137.47, 128.26, 128.10, 126.90, 72.10, 58.34, 52.97, 52.90, 52.88, 52.82, 42.52, 36.56, 28.50, 12.02; **Chiral HPLC**: Chiralcel OD-H, 1.0 ml/min, Hex/*i*PA=95:5, R_t =10.1 min, 12.0 min; $[\alpha]_D^{28.7} = +16.09$ ((*S*)-enantiomer, $c = 0.41$ g/100 ml, CHCl_3 , 90% *ee*).

5.5.7 Mechanistic studies



To a solution of (*S*)-**5.167** (53.2 mg, 0.12 mmol, 93% *ee*) in DCM (1.1 ml) was added trifluoroacetic acid (0.11 ml) at 0 °C and resulting reaction mixture was stirred for 3 h at rt. After full conversion of (*S*)-**5.167**, TFA was quenched with *aq.* NaHCO_3 , and aqueous layer was extracted by DCM. Collected organic extracts were dried with Na_2SO_4 , and then concentrated *in vacuo* to give Boc-deprotected allylic hydrazine.

The solution of crude material in EtOH (1.2 ml) was allowed to warm to 35 °C and stirred for 24 h under O_2 balloon. After evaporation of the solvent, crude material was chromatographed on silica gel to give product (*S*)-**5.35** as a clear oil (19.1 mg, 0.063 mmol, 51% for 2 steps, 91% *ee*, 98% *es*).

국문 초록

본 학위 논문에는 로듐 촉매에 의한 비대칭 고리화 반응의 개발에 대한 연구 결과가 수록되어 있다. 고리화 반응을 위한 전이금속-바이닐리딘 매개 촉매 반응의 활용 가능성을 확장시키기 위하여(제 1 장), 말단 알카인에 연결된 엔아민에서 일어나는 로듐 촉매 알켄화 반응에 대한 연구를 수행하였다(제 2 장). 로듐-바이닐리딘 착물을 촉매 중간체로 활용하여 알카인-엔아민의 고리화 반응을 수행하고, 궁극적으로 카이랄 엔아민을 사용한 부분 입체 선택적 탄소-탄소 결합 형성 반응을 통해 카이랄 사차 탄소를 지닌 사이클로펜텐 합성법을 제안한다.

본 논문의 후반부는 로듐 촉매와 유기붕소산에 의한 알카인의 이웃 자리 탄소기능화 반응의 연구 결과를 다루고 있다(제 3 장). 알카인-이민의 로듐 촉매 연쇄 첨가-고리화 반응에서는 단일 로듐 촉매가 순차적인 분자간, 분자내 1,2-탄소로듐화 반응을 매개하여 알킬리덴-사이클로부틸아민의 합성을 가능토록 한다(제 4 장). 또한 로듐 촉매에 배위할 수 있는 카이랄 리간드에 의한 거울상 선택적 반응을 통해 높은 광학 활성을 갖는 사이클로부틸아민의 합성법을 보인다. 앞서 확인한 알켄-로듐 중간체의 탄소-질소 이중 결합 첨가 반응성을 바탕으로 알카인-하이드라존의 로듐 촉매 연쇄 첨가-고리화-재배열 반응을 개발하였다(제 5 장). 본 연구에서는 로듐-촉매 연쇄 고리화 반응과 레트로-엔 반응의 융합을 통해 무흔적 사이클로알켄 합성을 수행하고, 반응 중간체를 분석하여 반응

메커니즘을 규명한다. 로듐-카이랄 리간드 착물은 알켄-로듐 중간체의 비대칭 탄소-질소 이중 결합 첨가 반응을 유도하고, 결과적으로 분자 밖 입체 중심을 지닌 사이클로펜틴을 높은 거울상 순도로 합성한다.

주요어: 로듐, 알카인, 고리화 반응, 바이닐리딘, 연쇄 고리화 반응, 레트로-엔 반응

학 번: 2013-22942

Appendix

Chapter 2

NMR spectra	253
Chiral HPLC data	277

Chapter 4

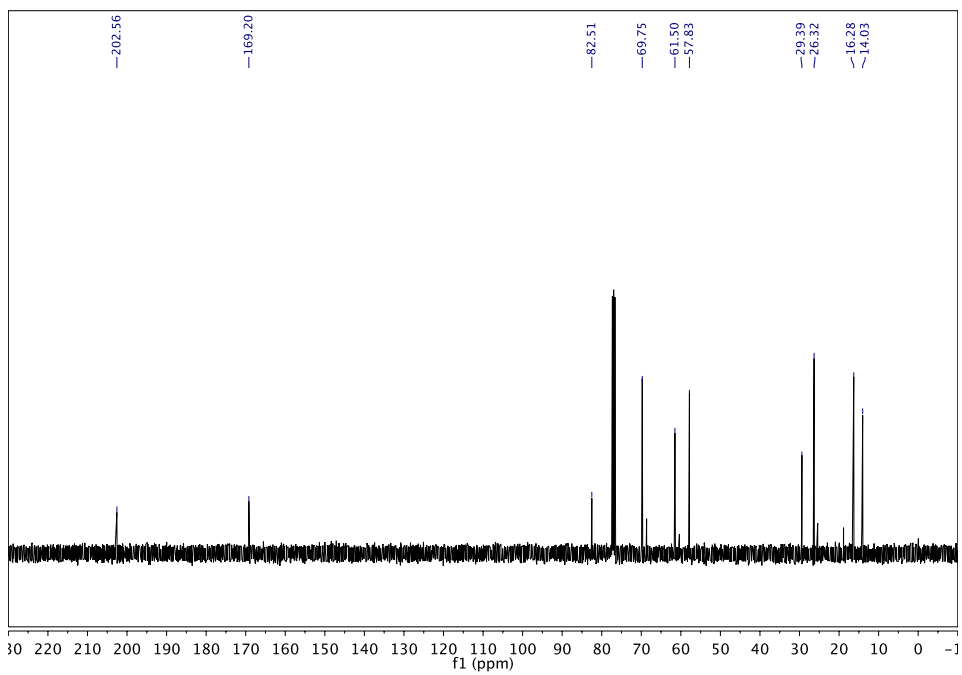
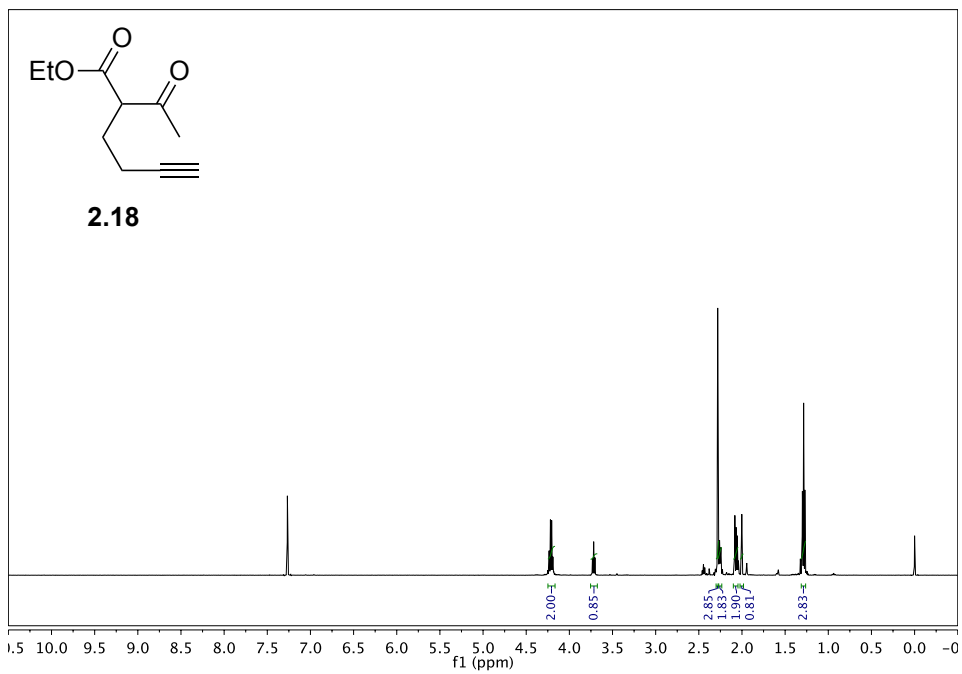
NMR spectra	279
Chiral HPLC data	291

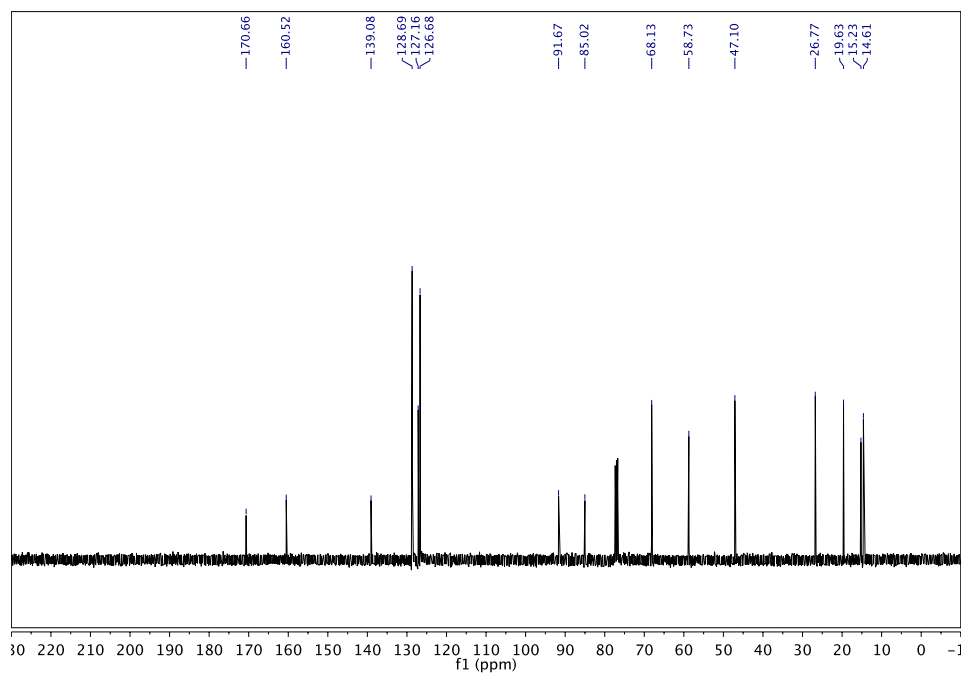
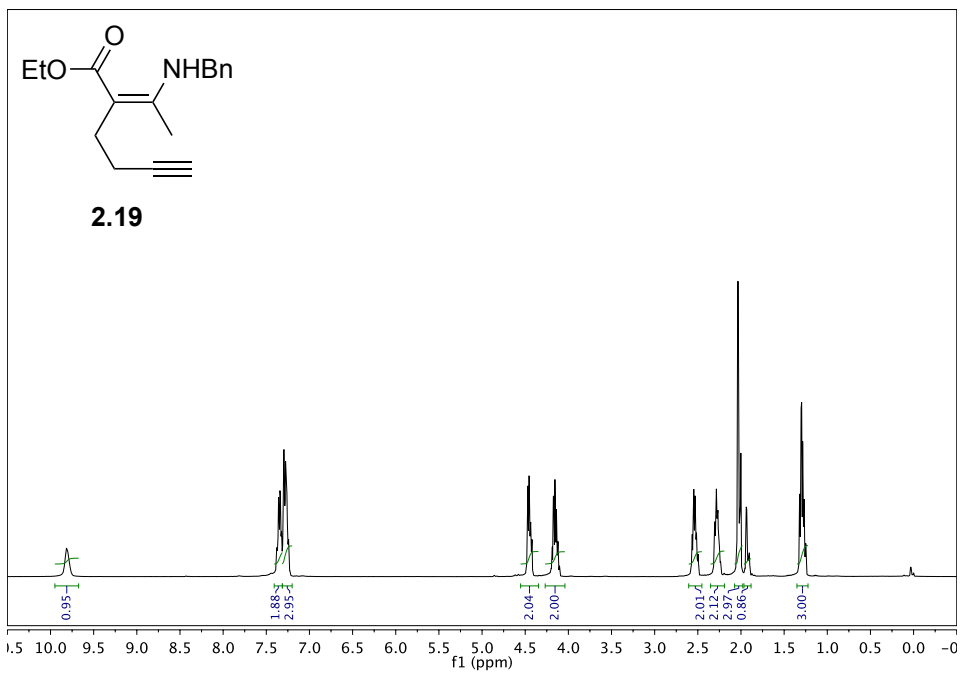
Chapter 5

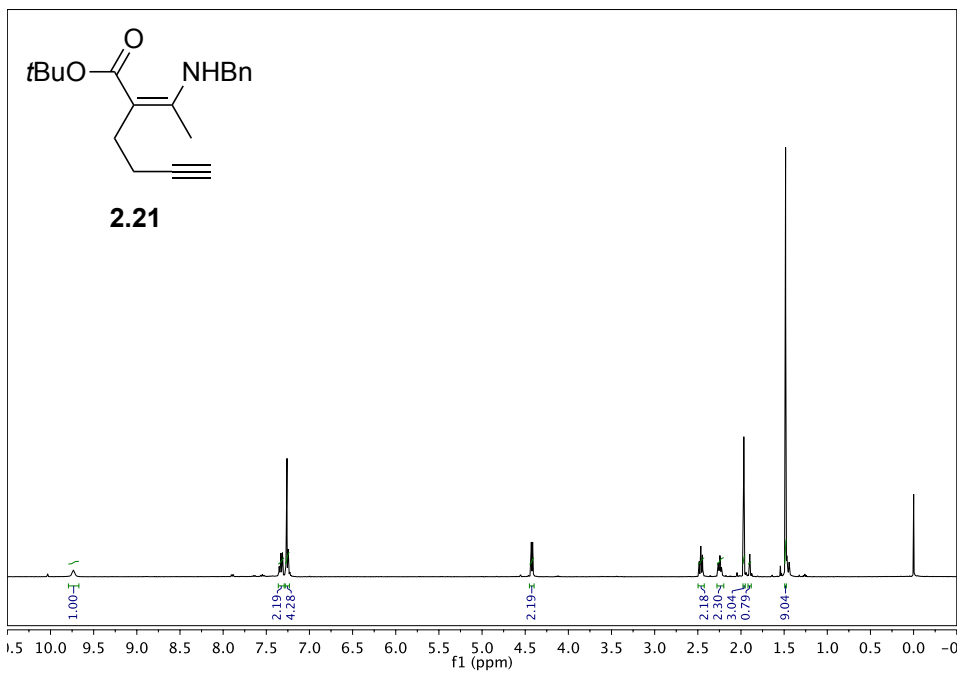
NMR spectra	293
Chiral HPLC data	390

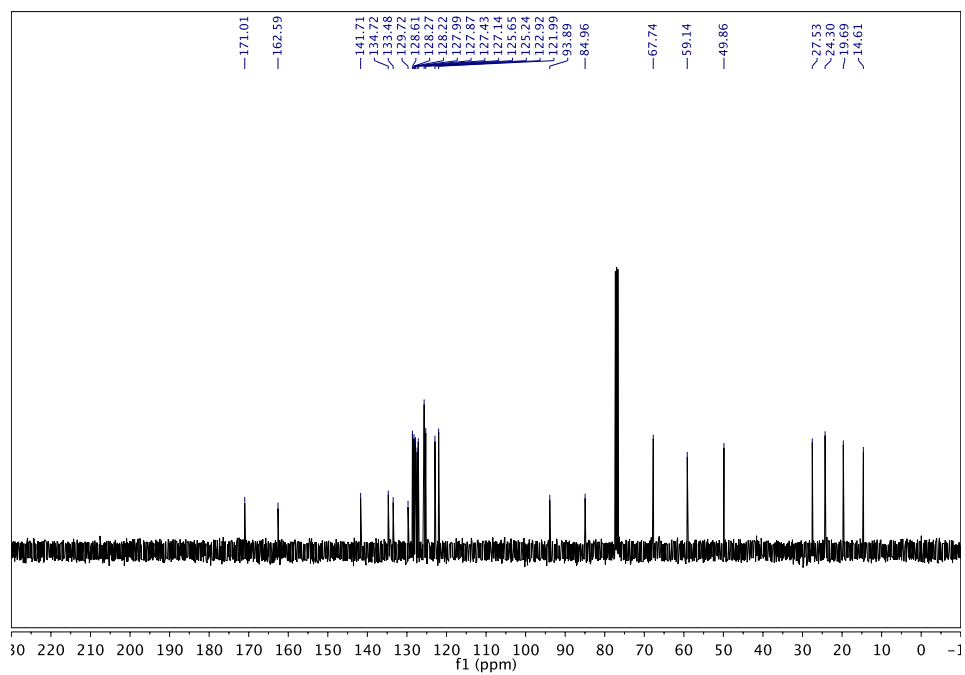
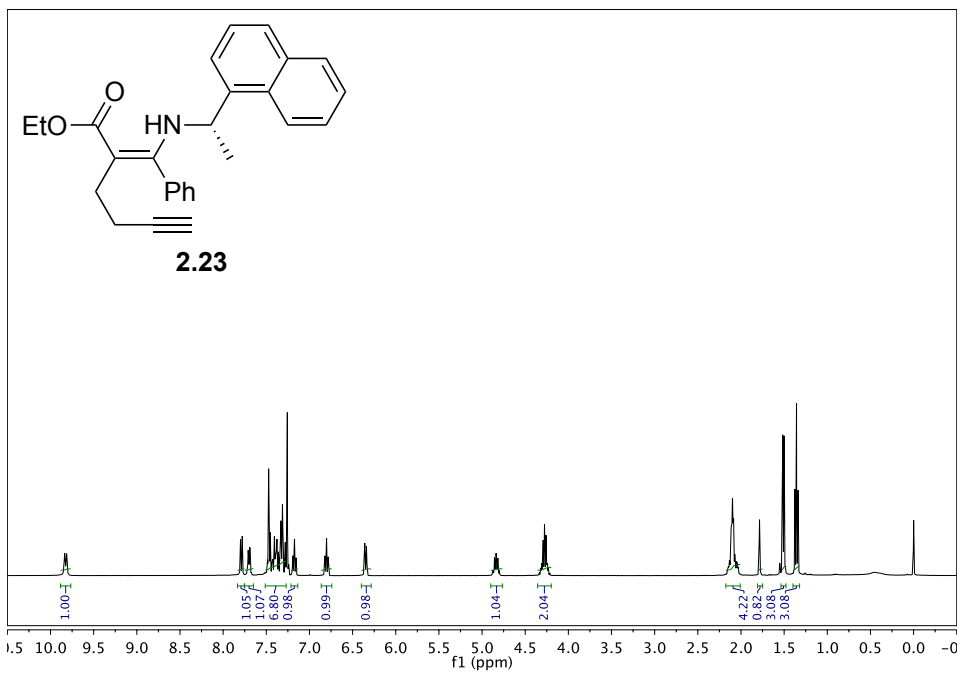
Chapter 2

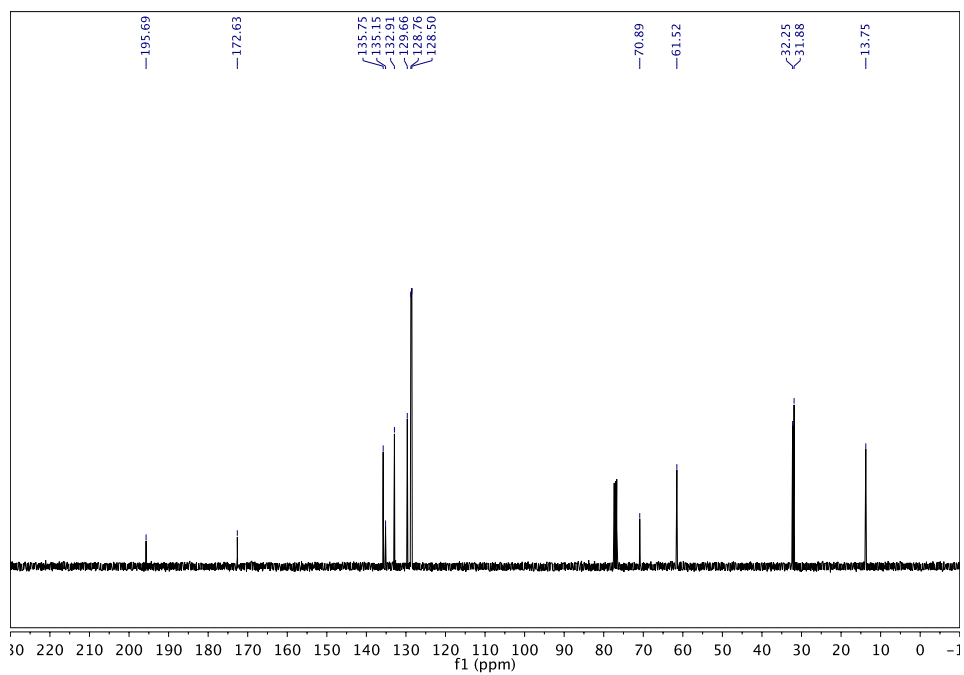
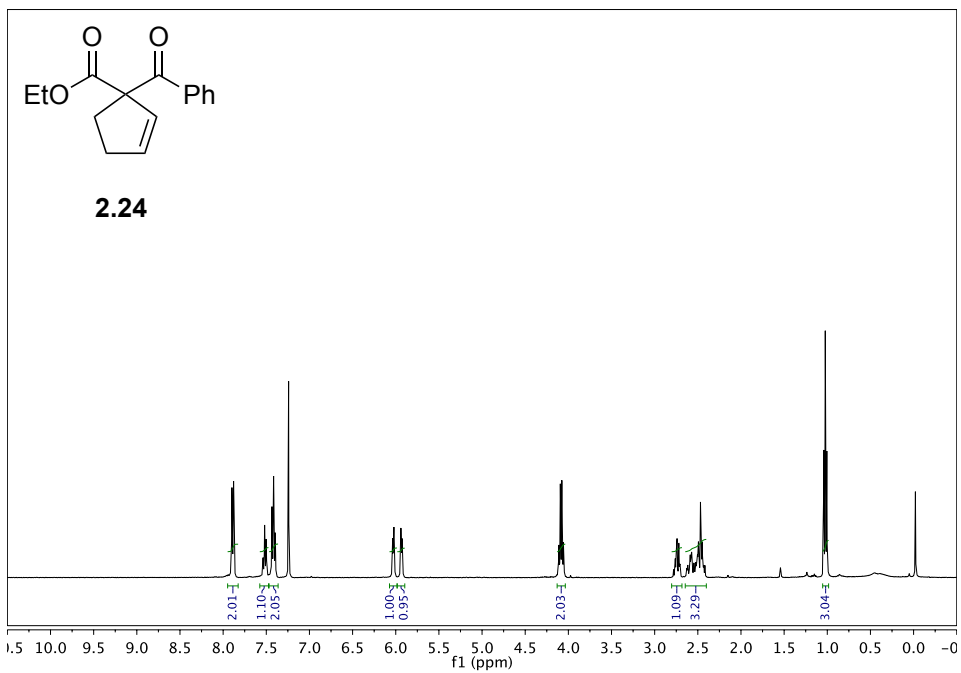
NMR spectra

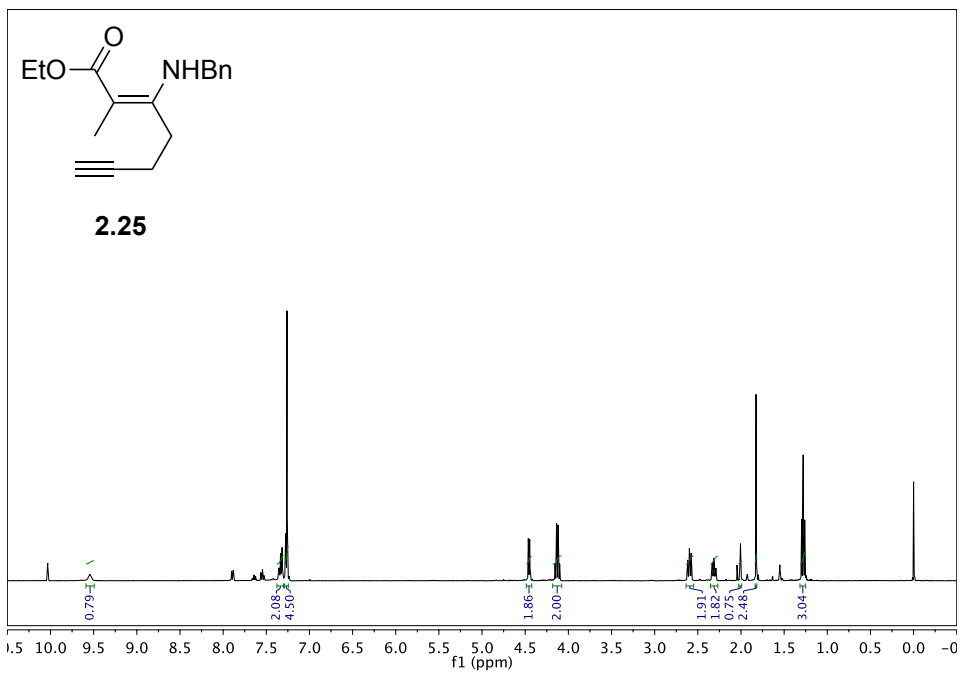


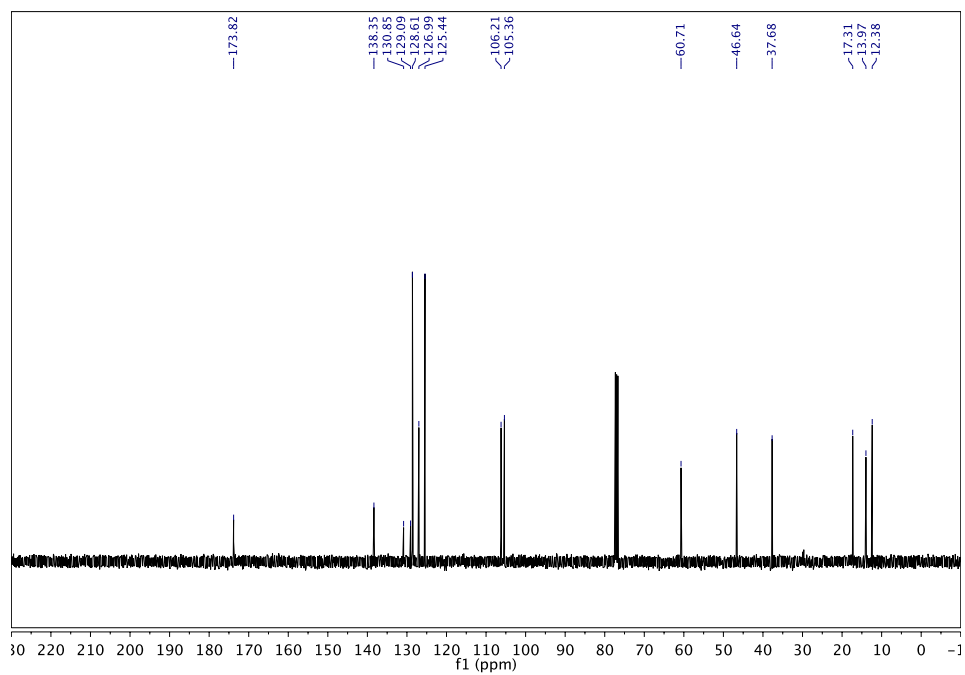
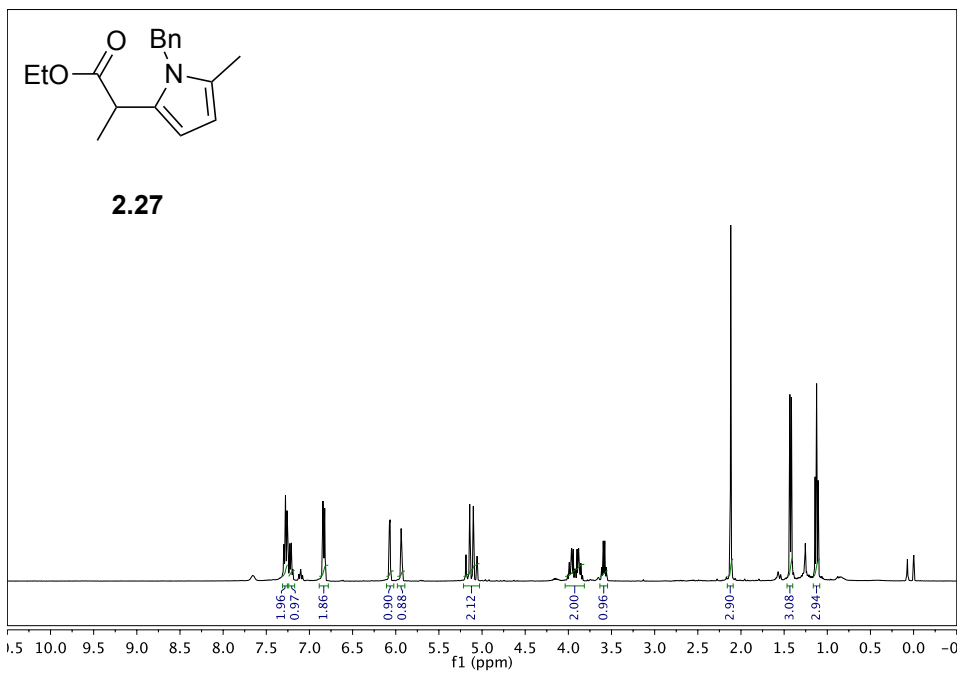


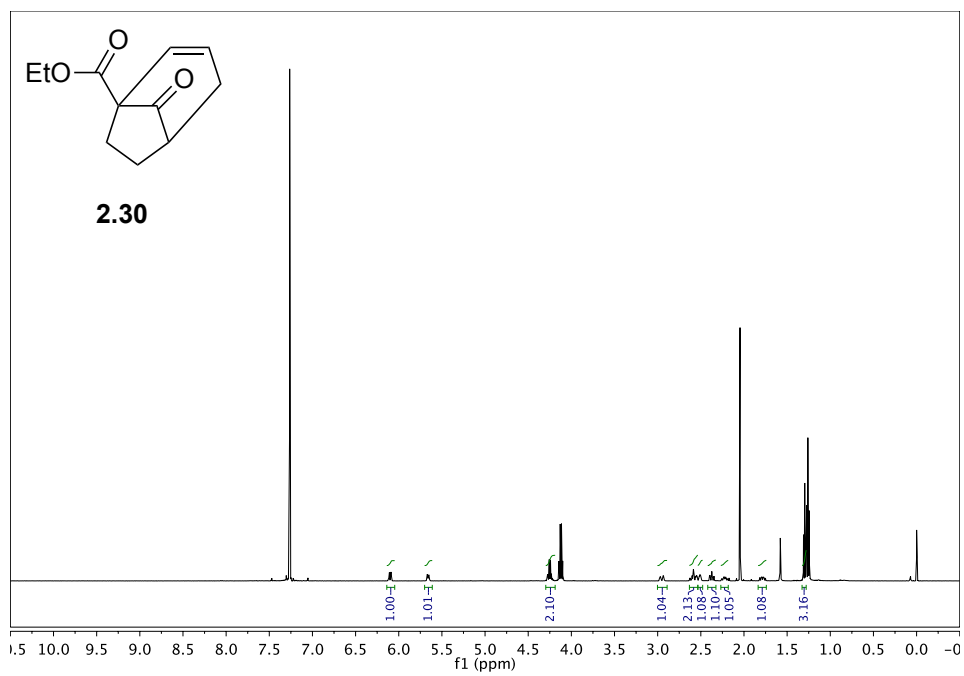
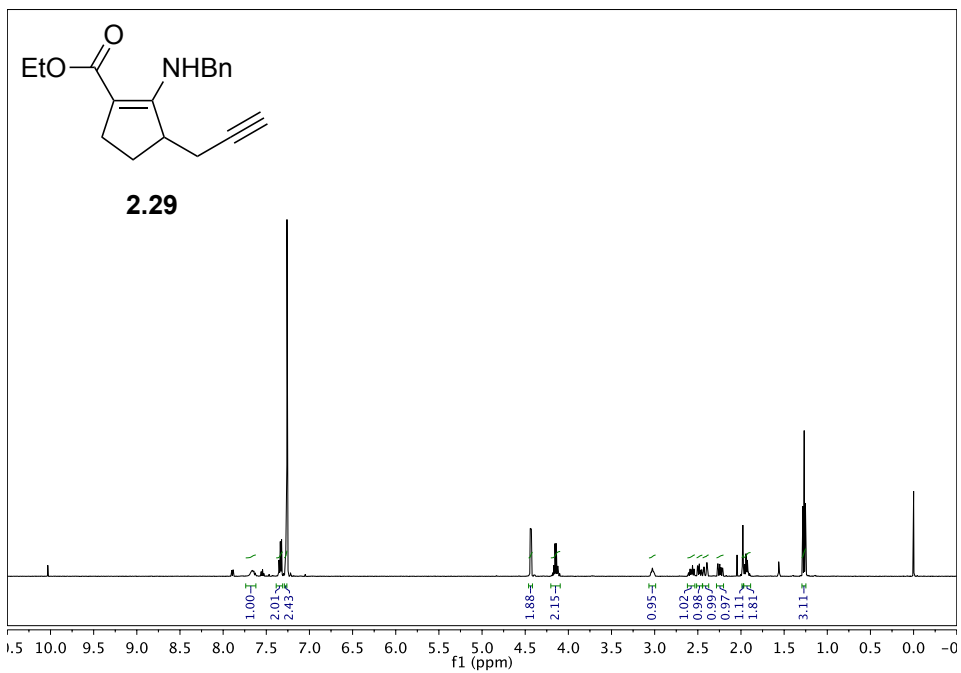


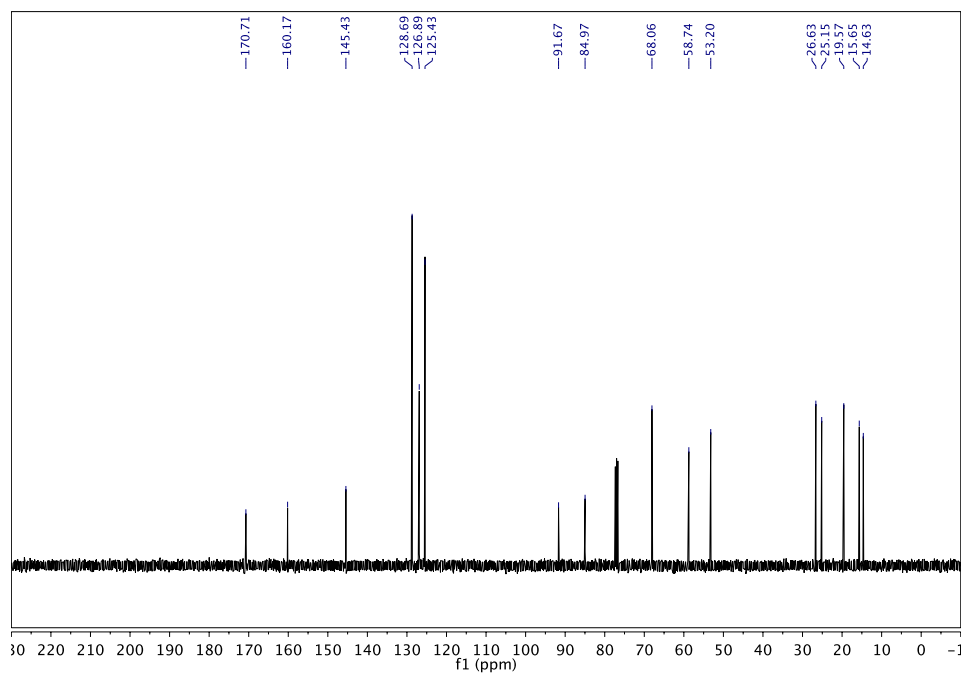
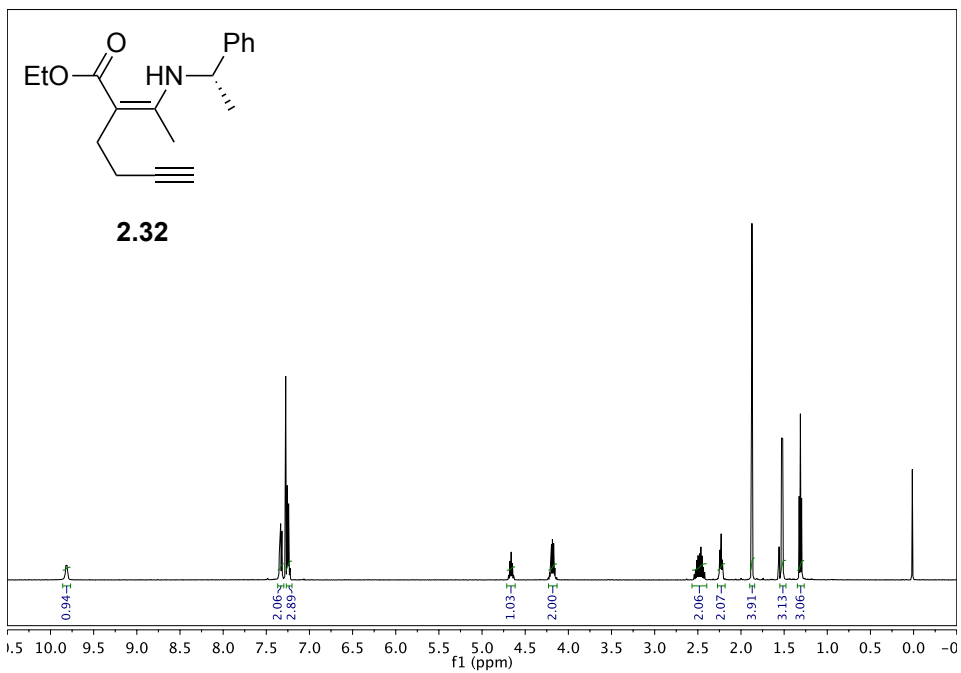


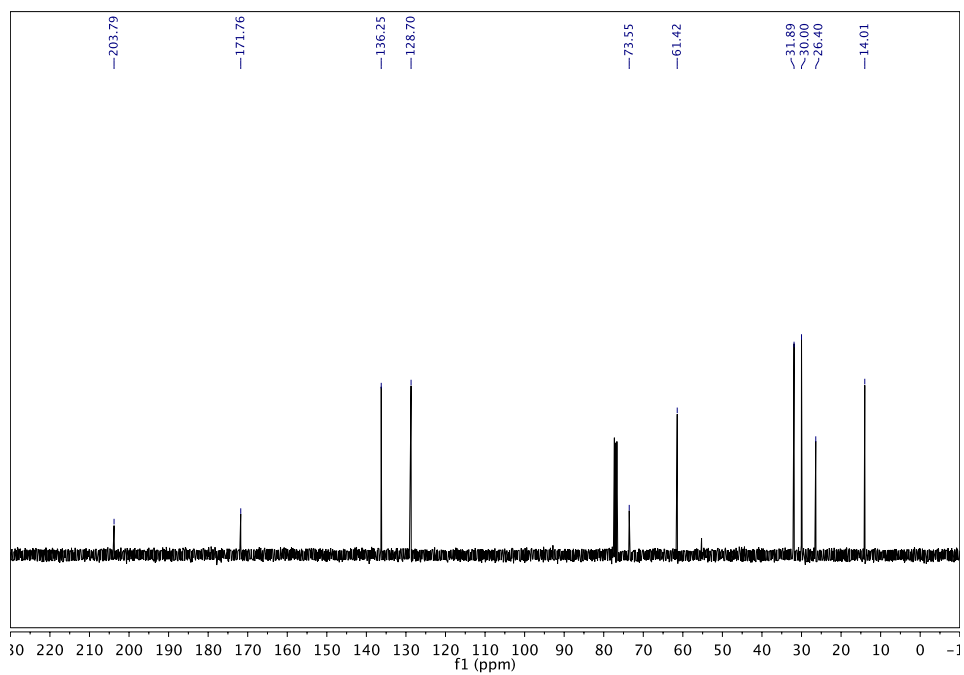
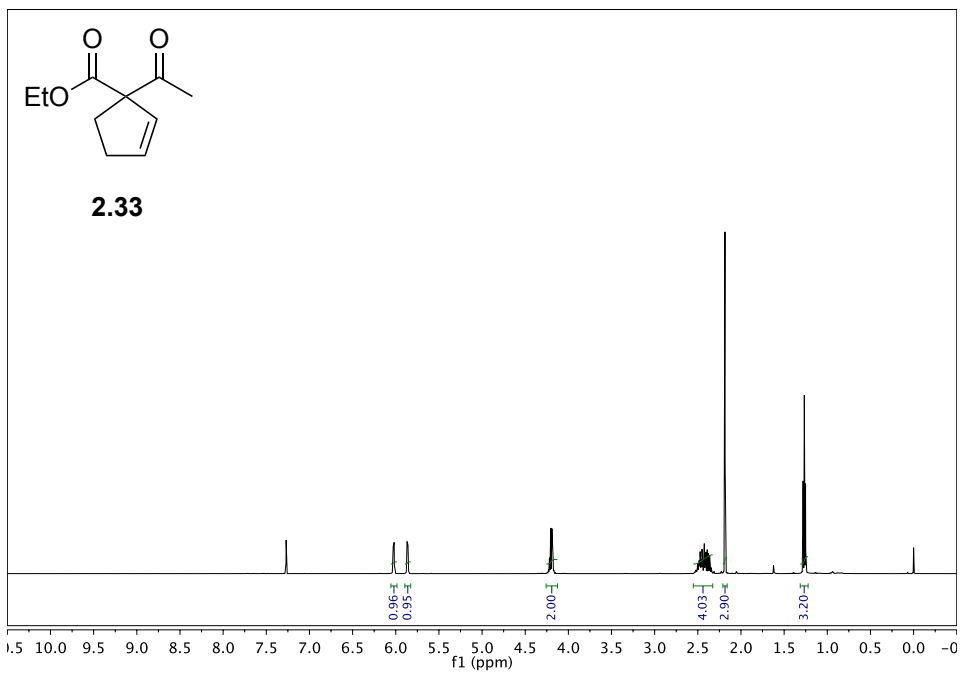


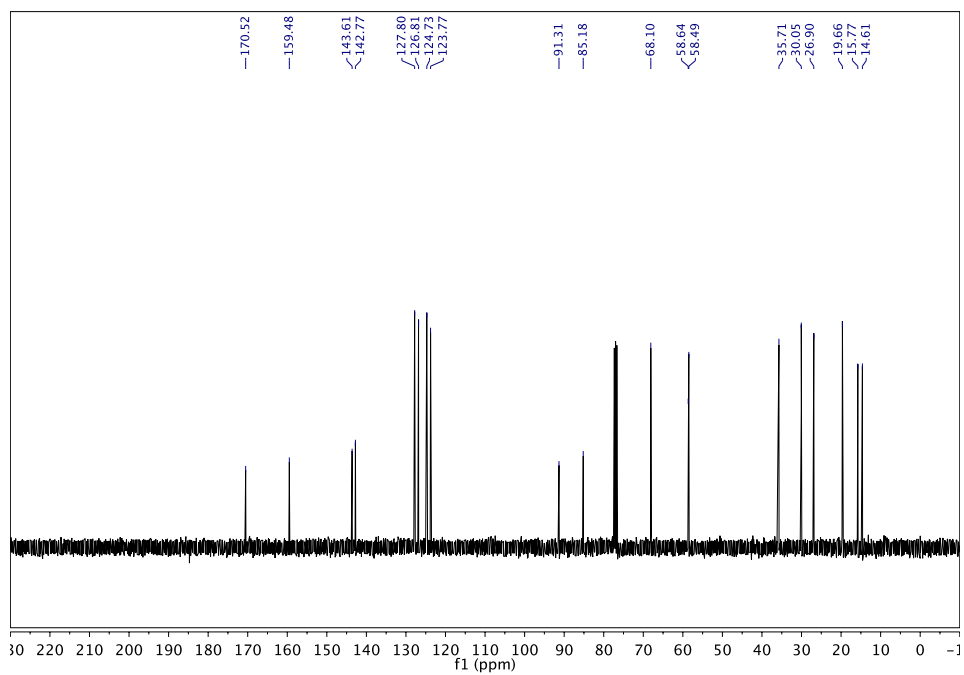
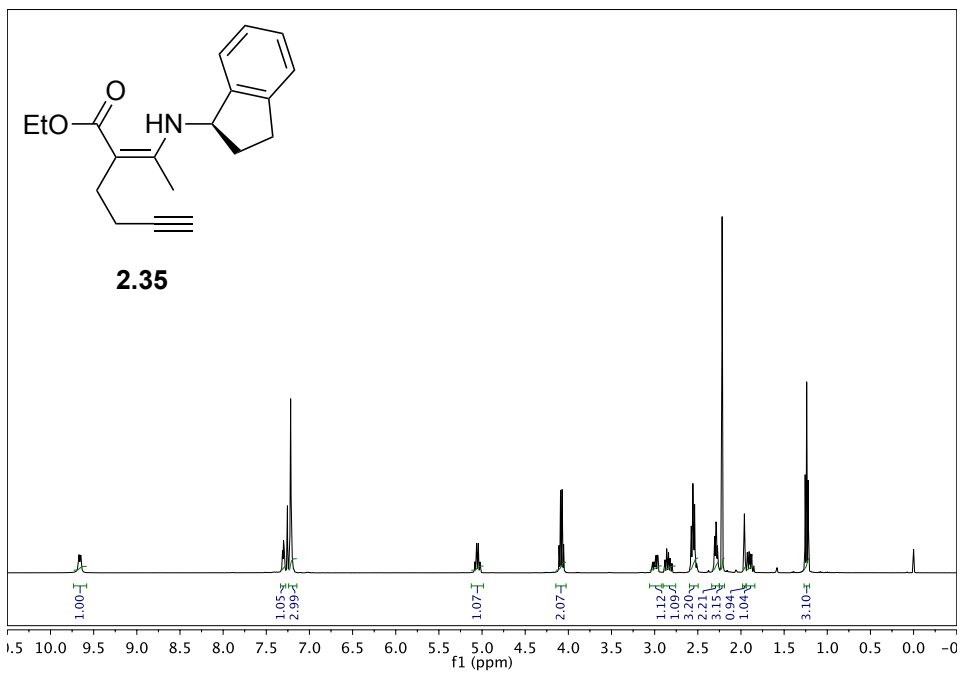


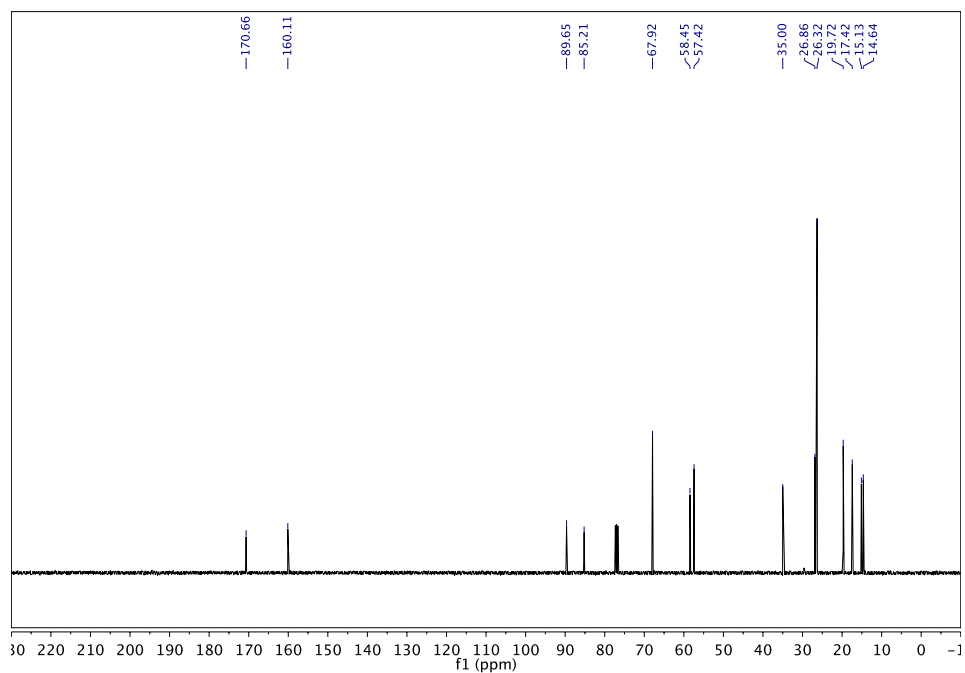
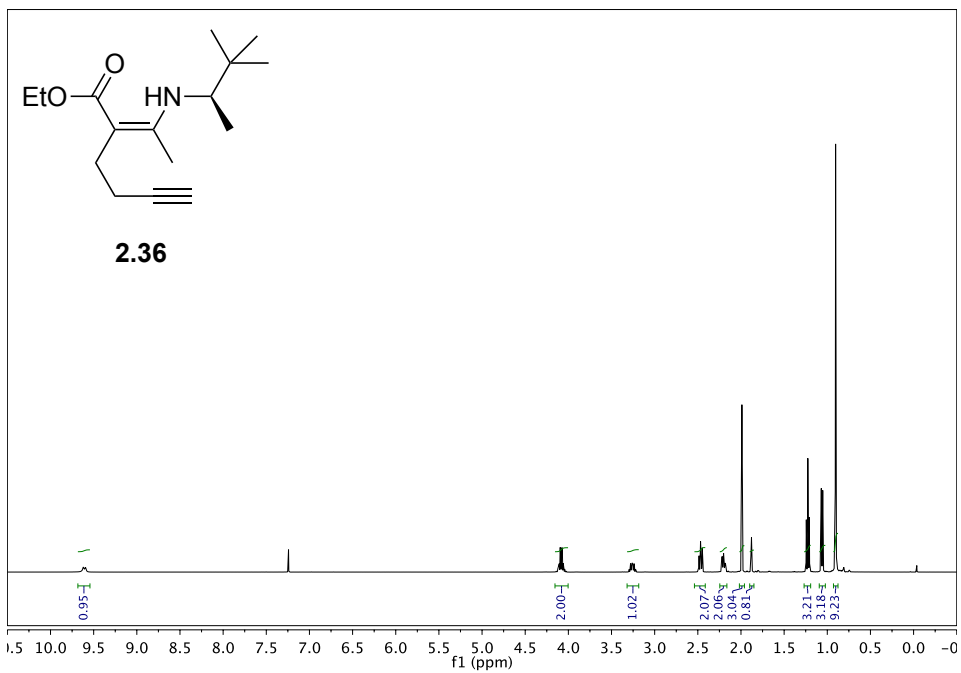


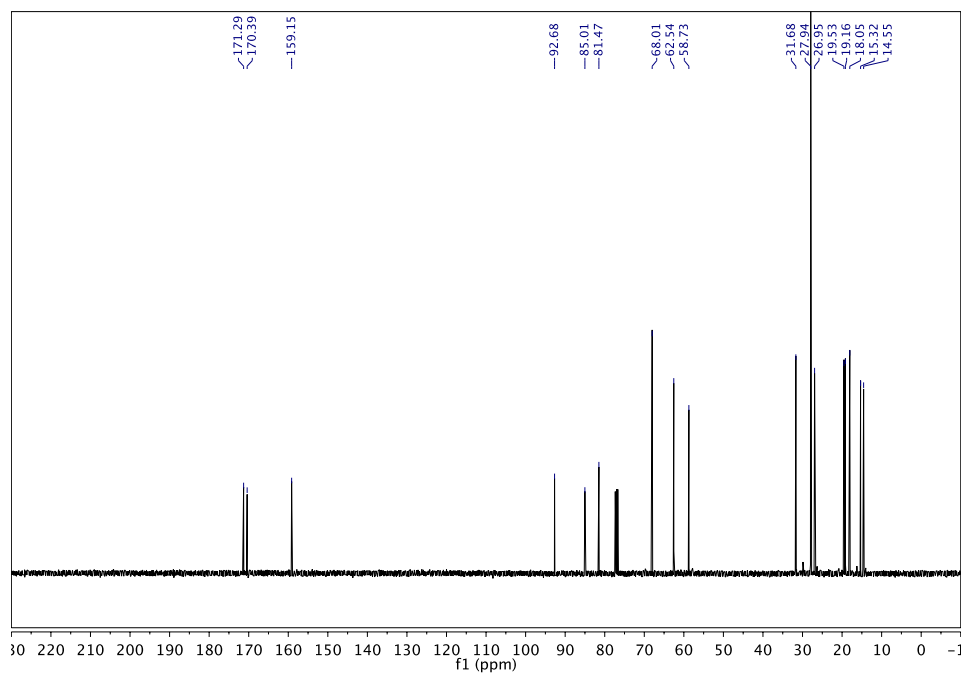
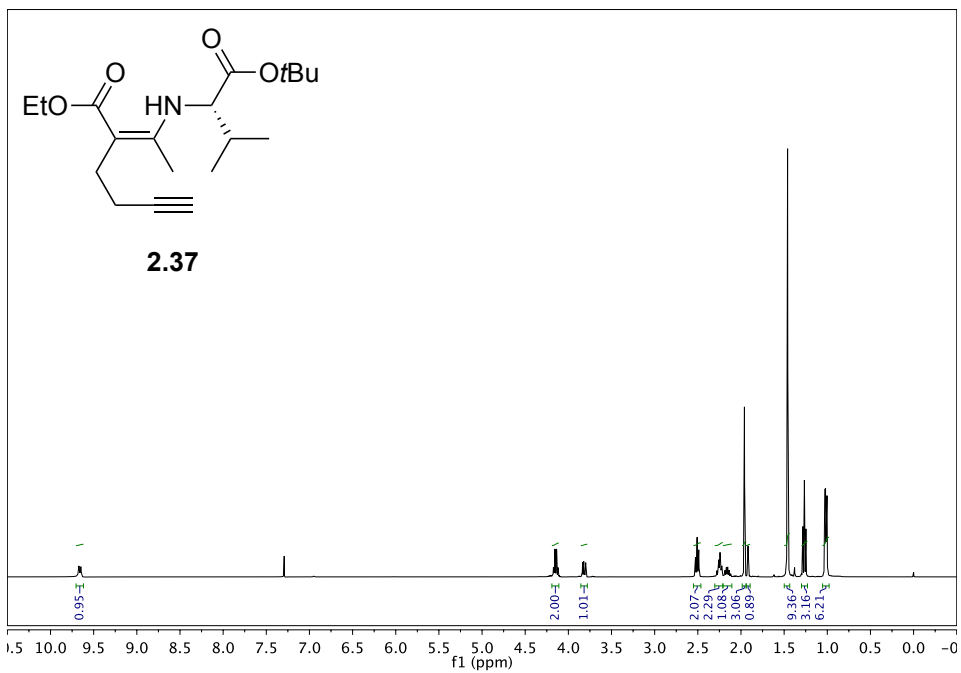


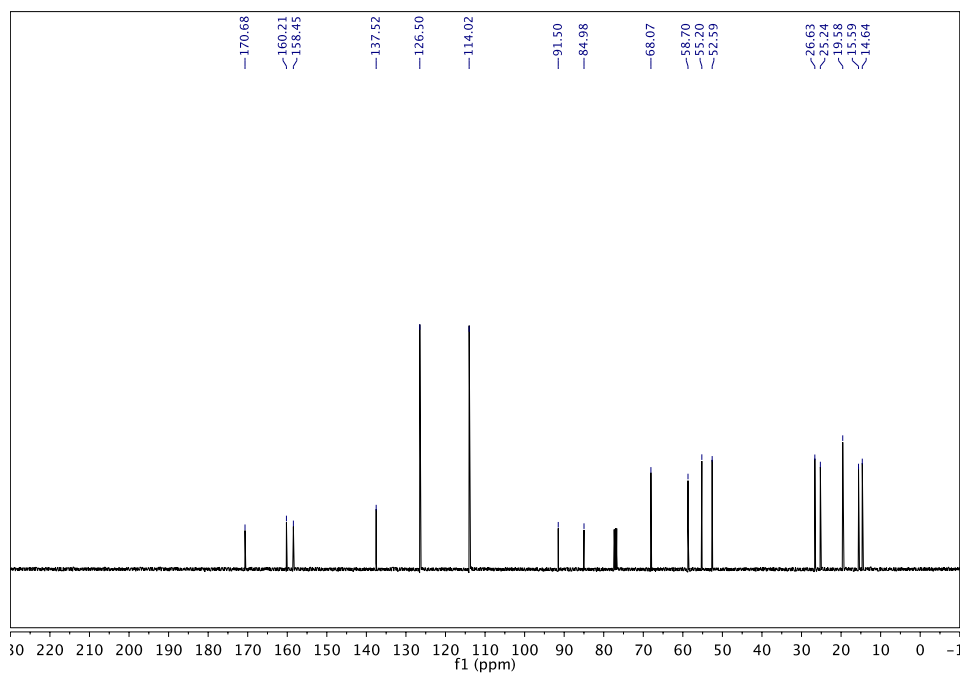
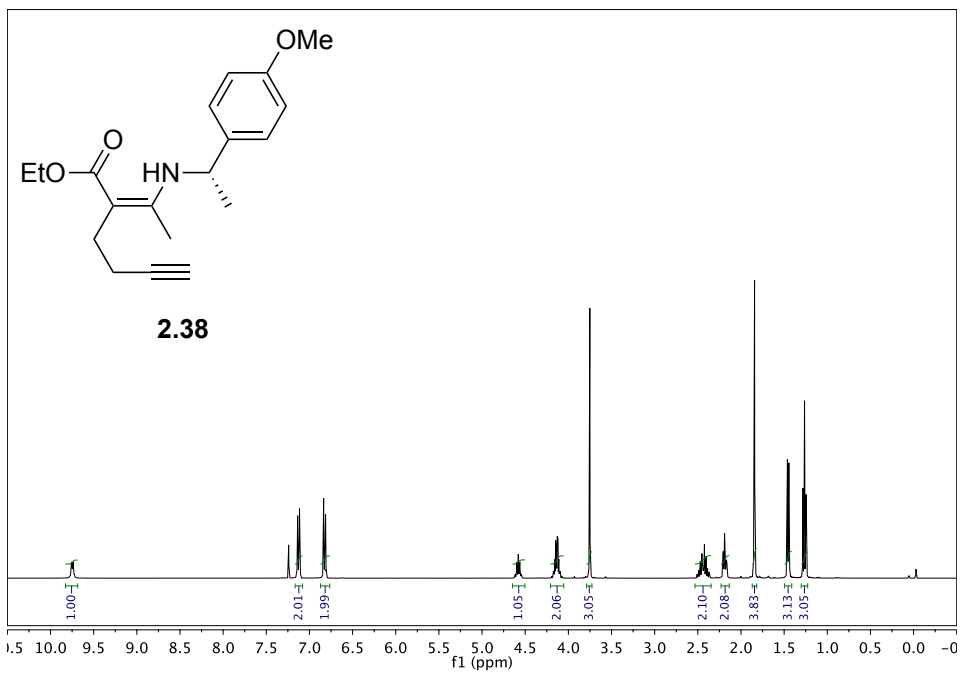


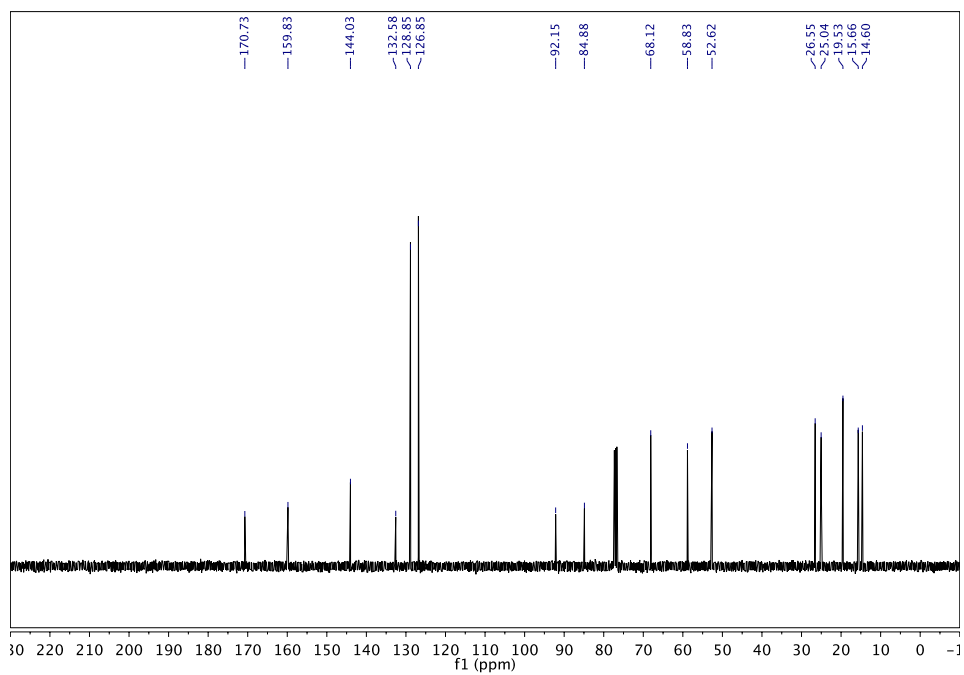
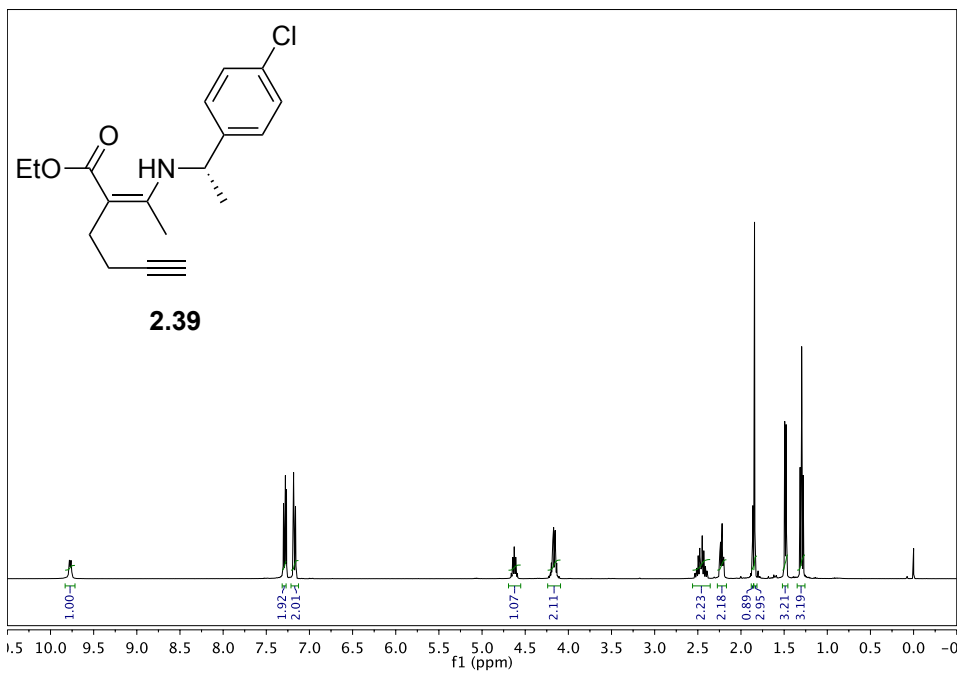


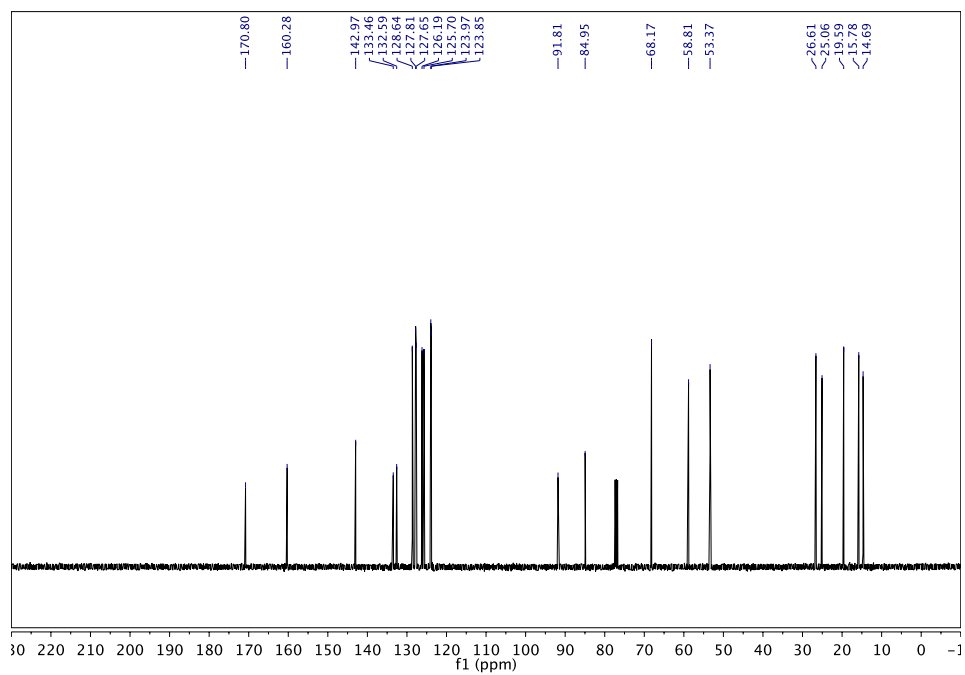
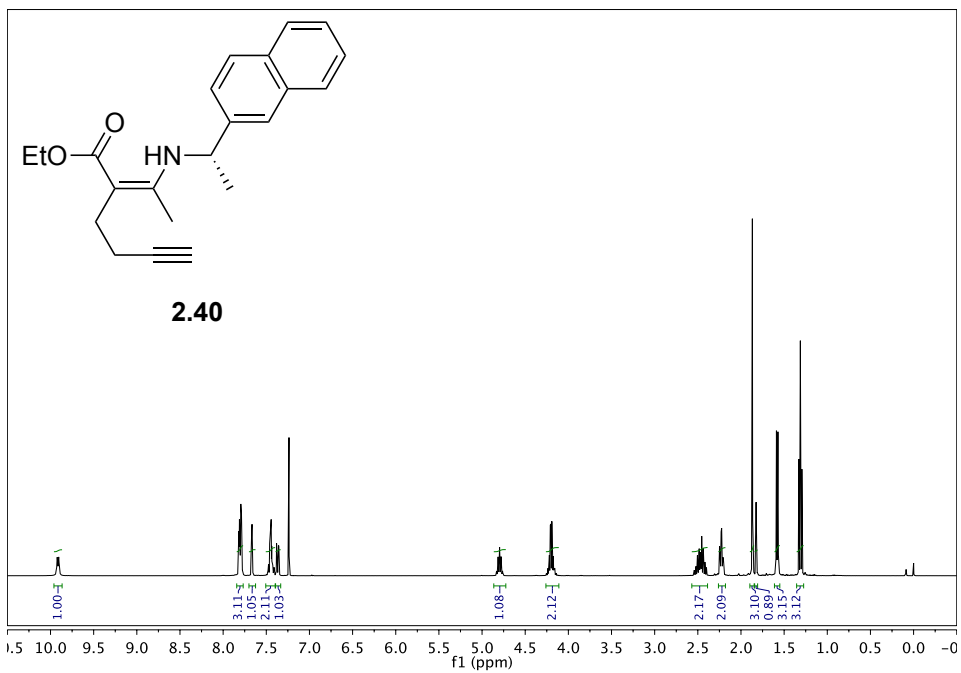


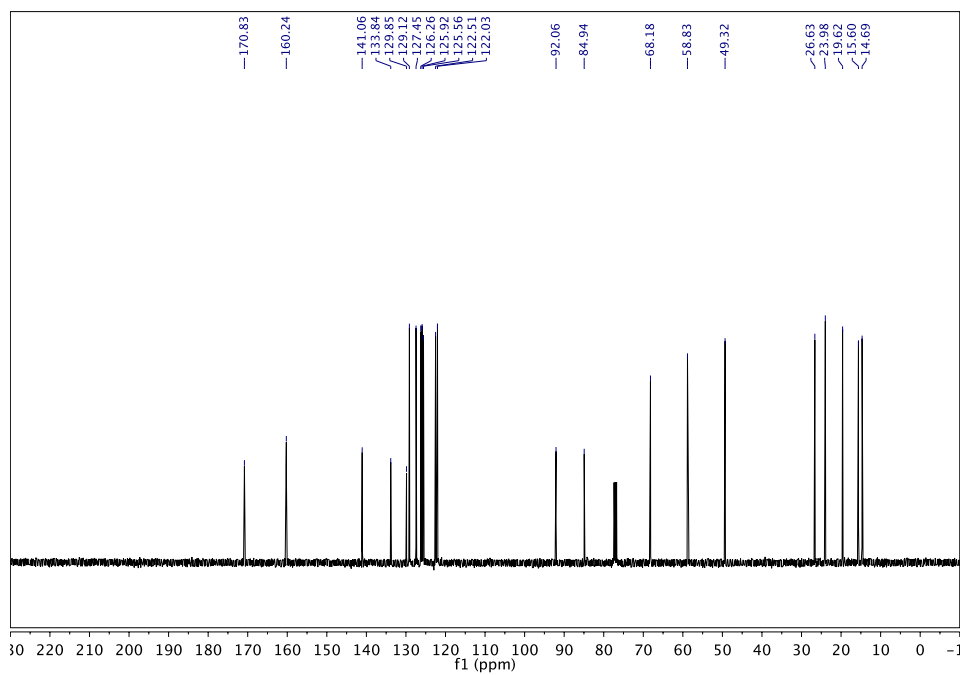
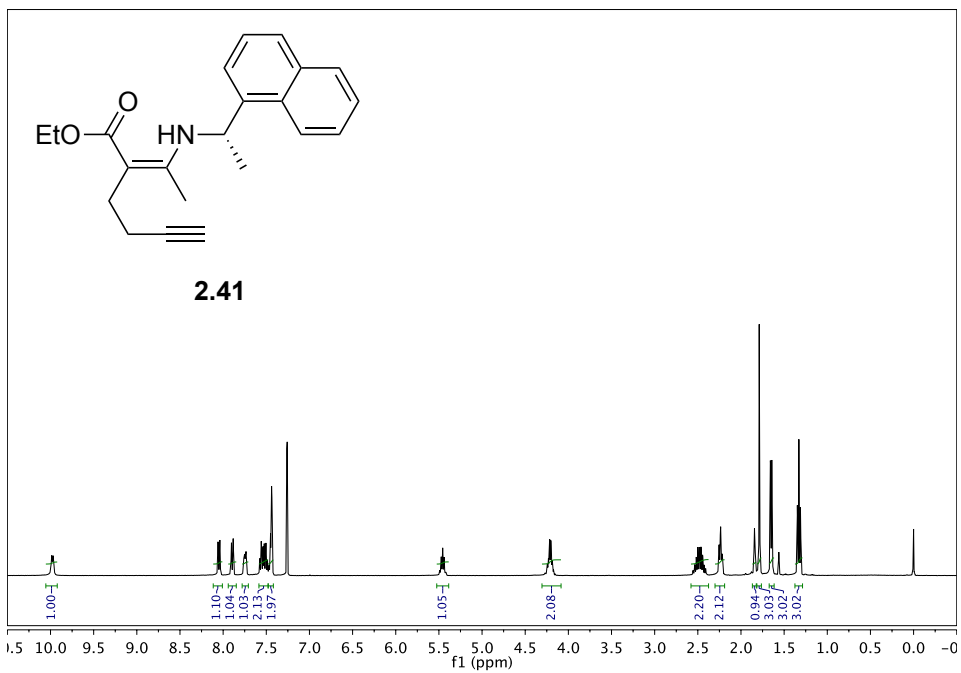


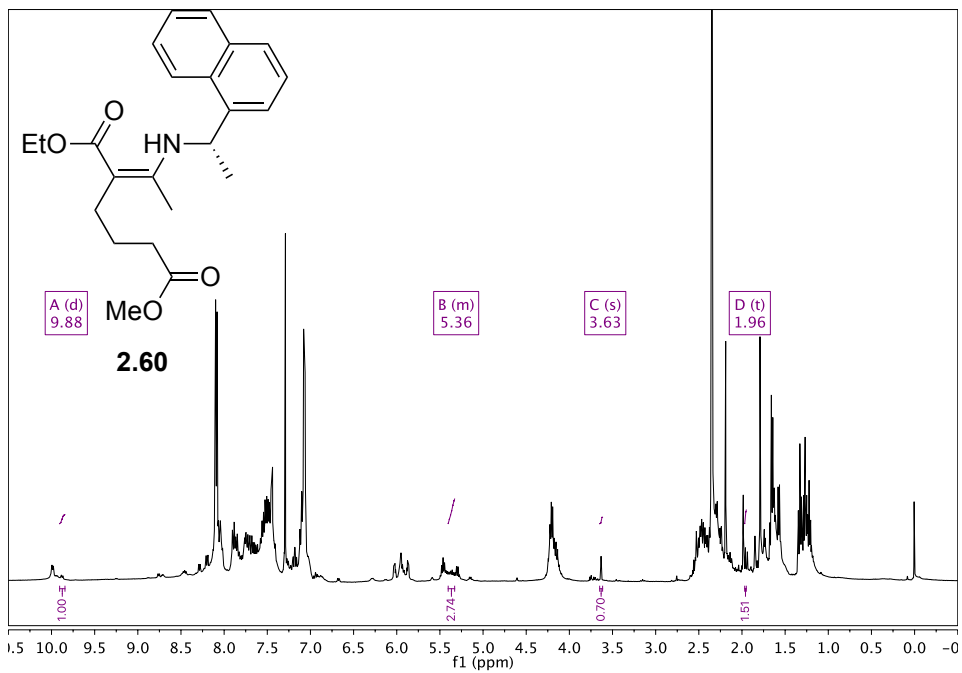


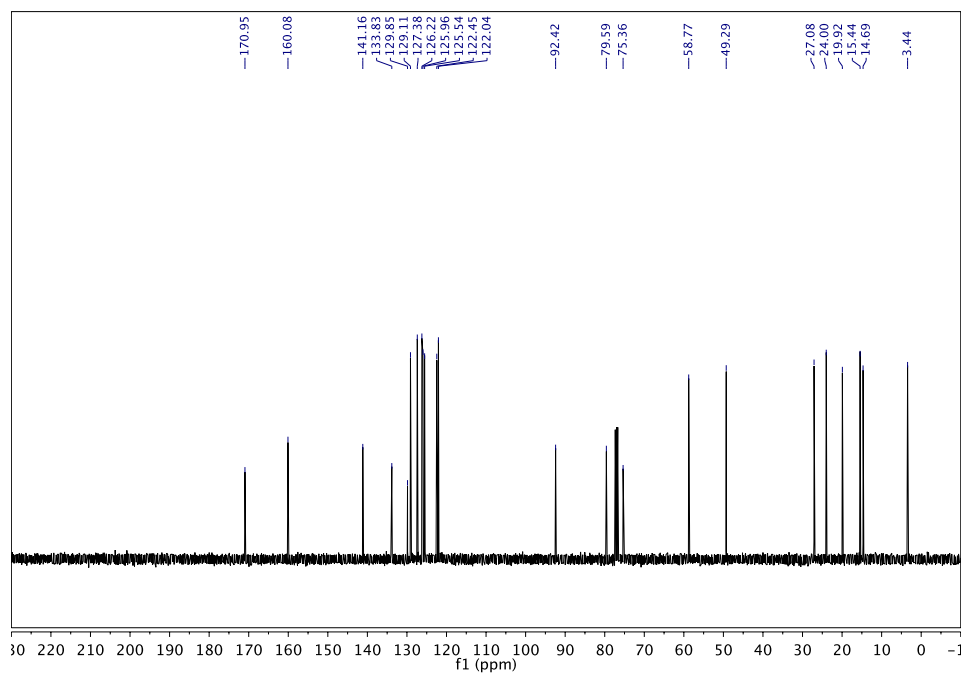
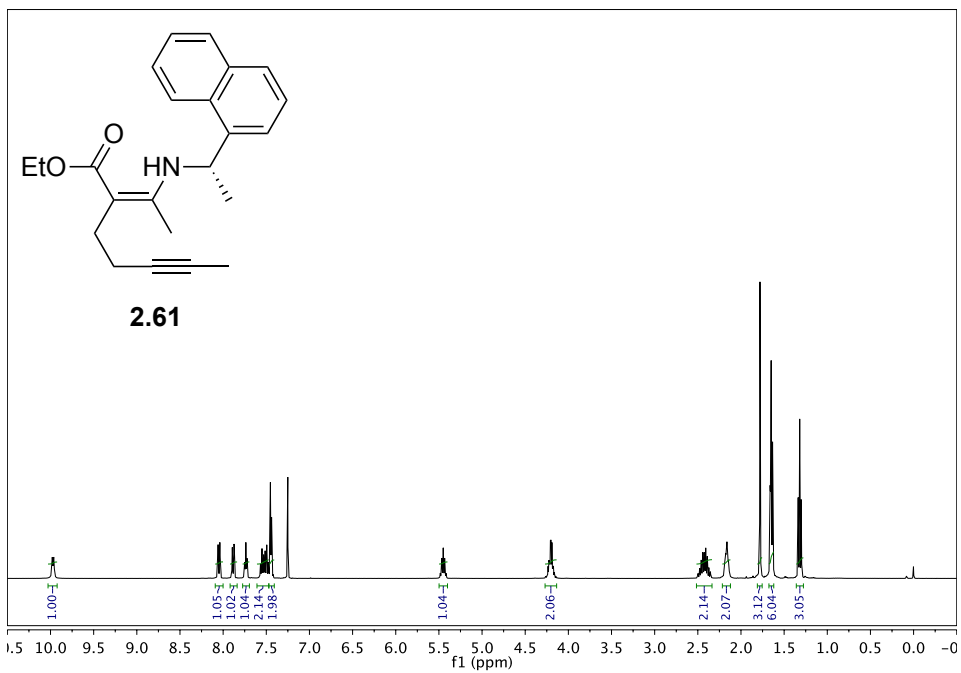


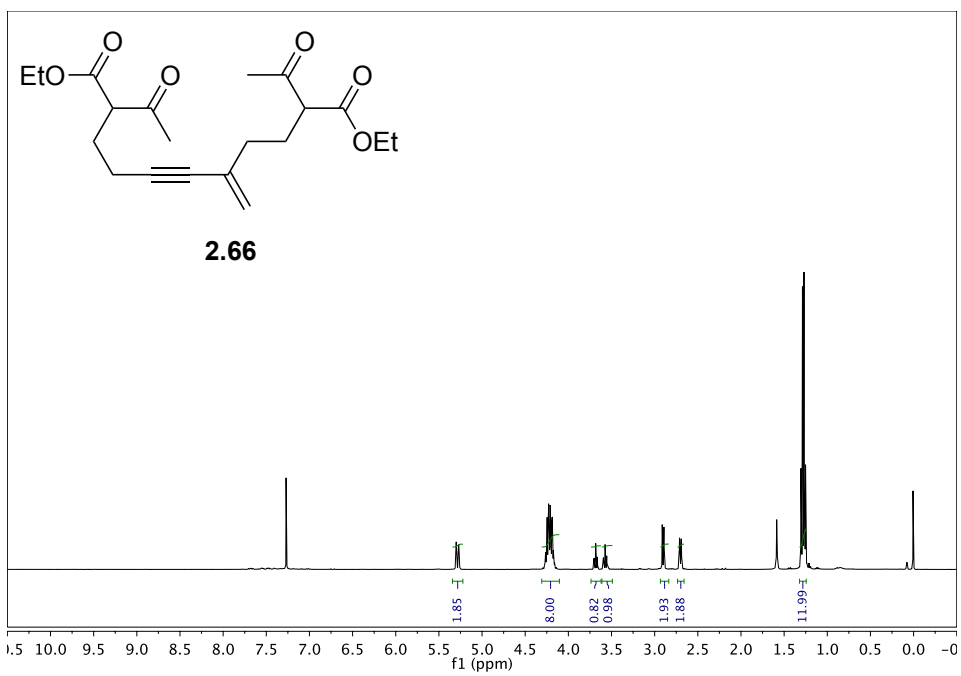
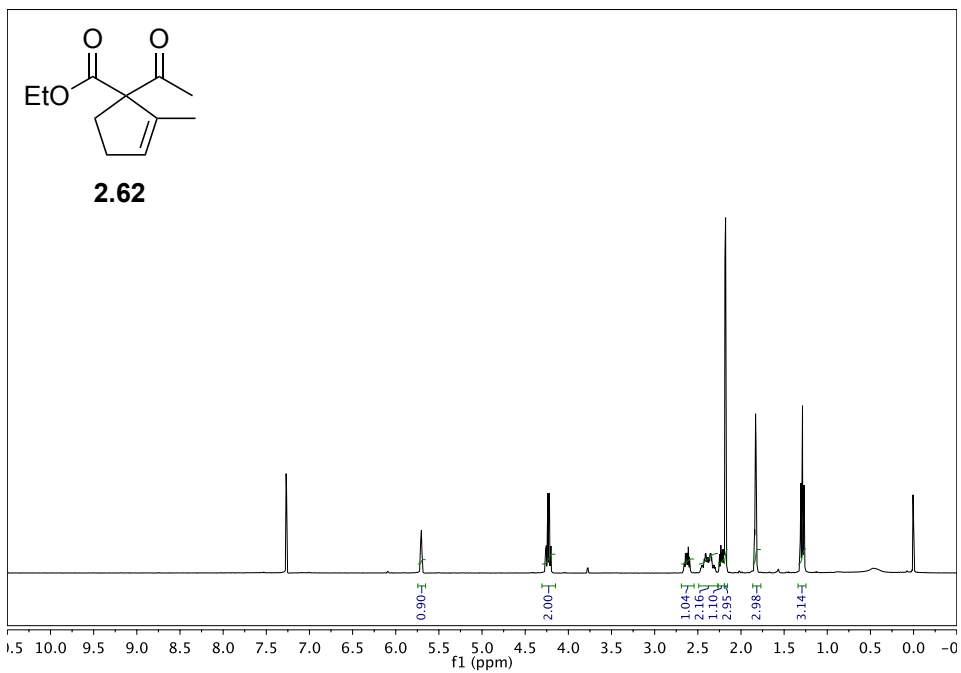


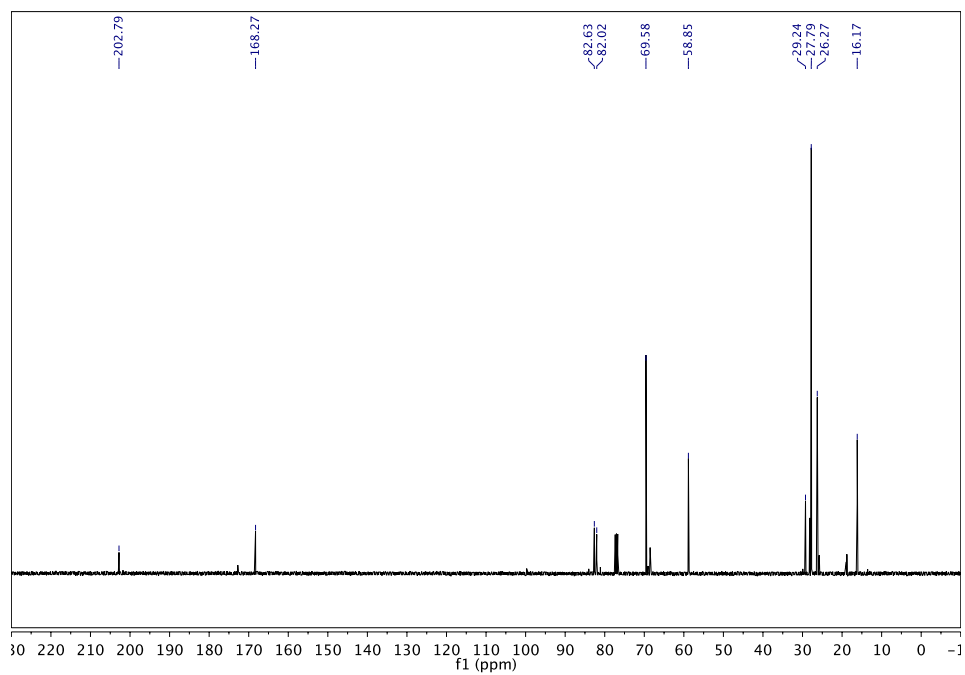
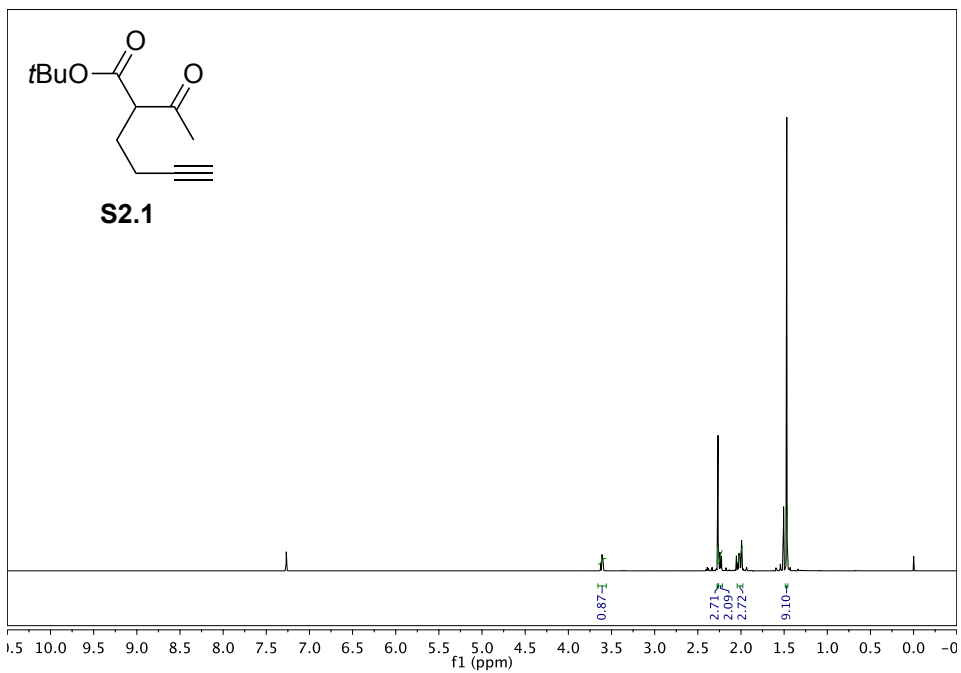


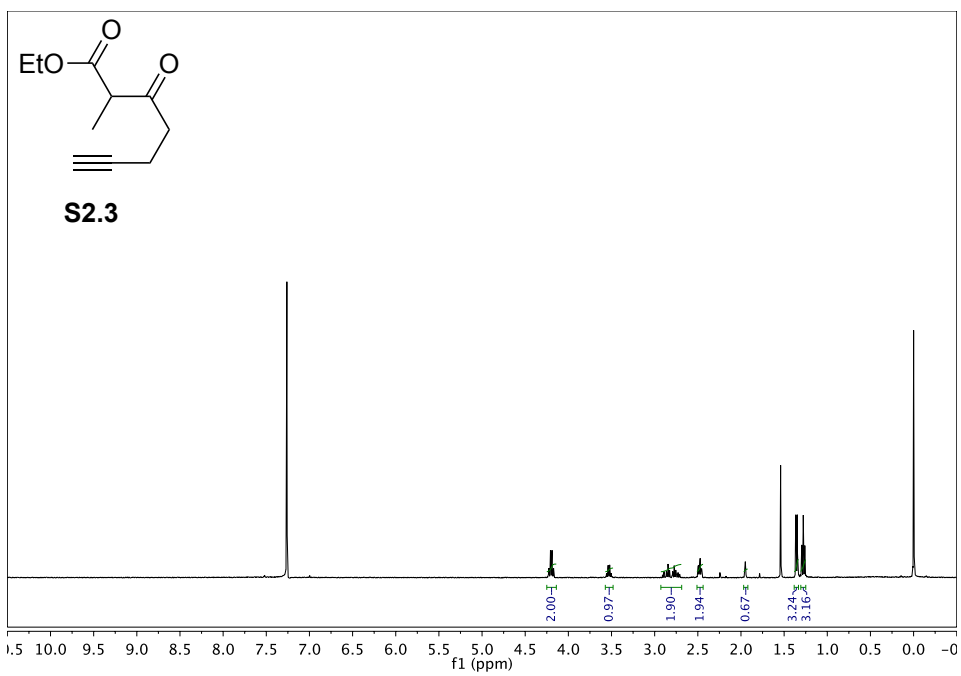
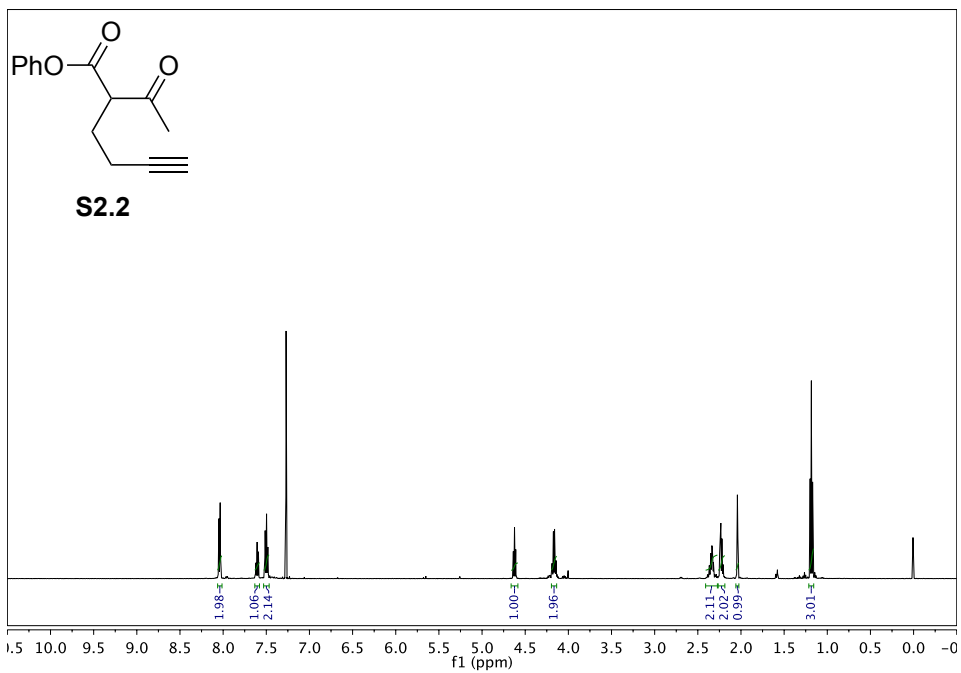


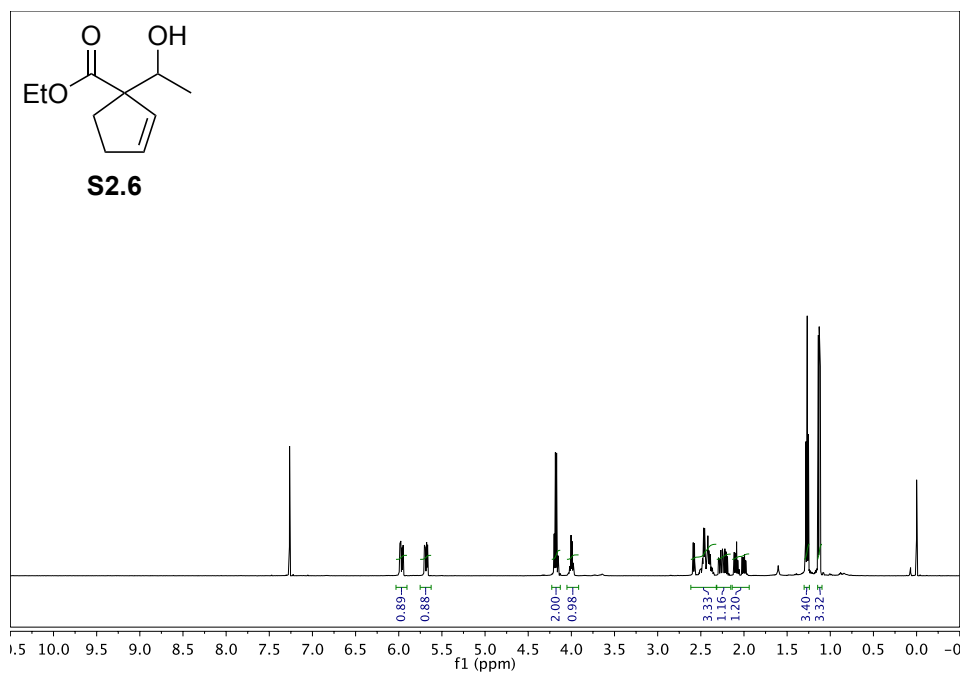
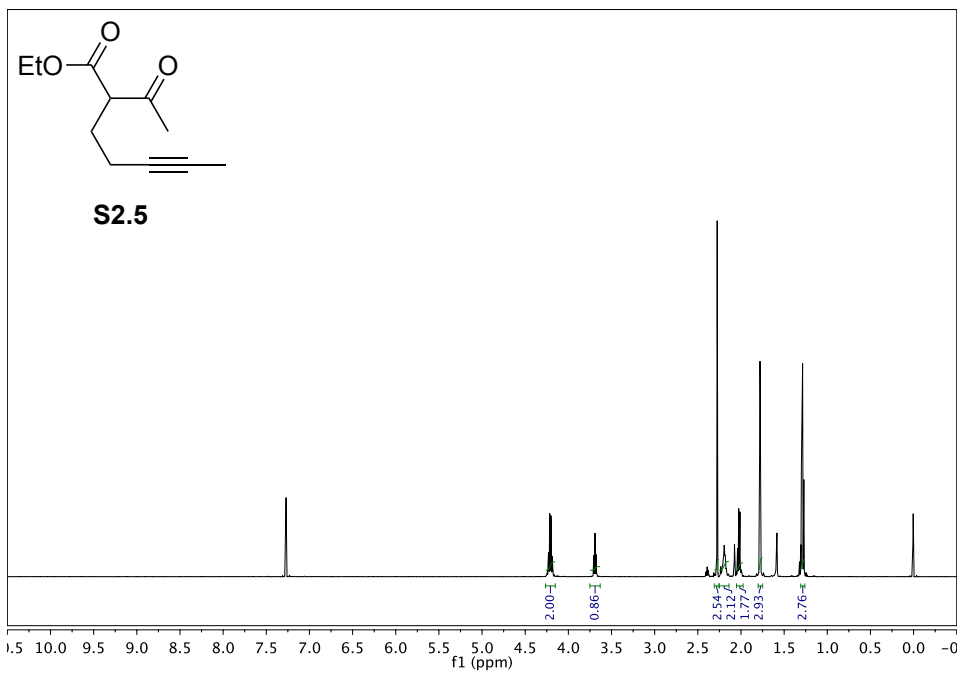


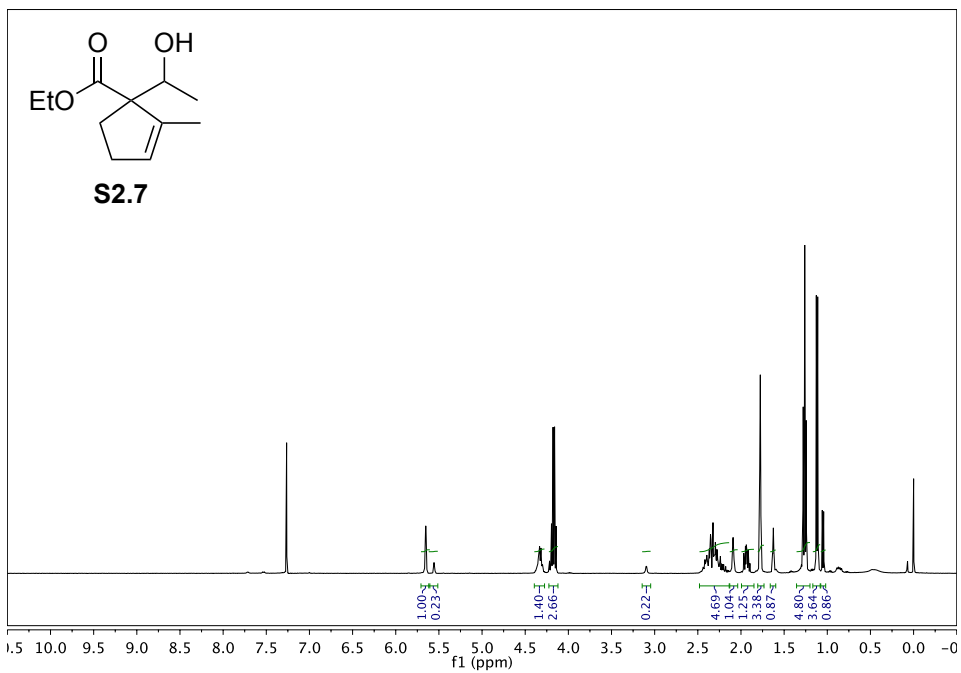












Chiral HPLC data

1. Analytical Method of S2.6 and S2.7

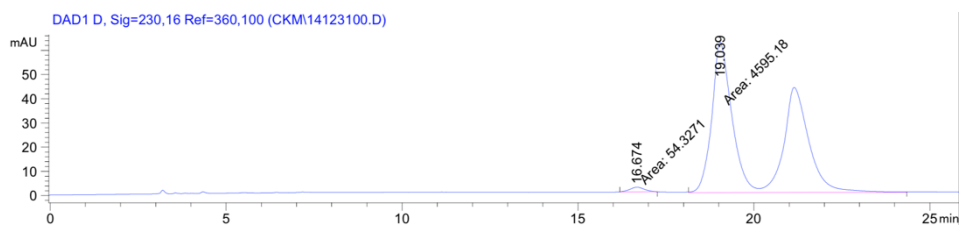
Column: Chiralpak IA

Eluent: Hexane/isopropyl alcohol = 99:1

Flow rate: 1.0 ml/min

Detection Wavelength: 210 nm or 230 nm

2. Chromatographic Trace of a chiral sample S2.6 (95% ee)



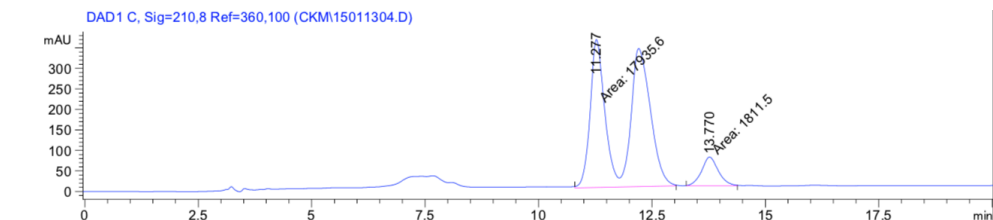
Signal 3: DAD1 D, Sig=230,16 Ref=360,100

Peak #	RetTime [min]	Type	Width [min]	Area [mAU*s]	Height [mAU]	Area %
1	16.674	MM	0.4686	54.32714	1.93241	1.1685
2	19.039	MM	1.2340	4595.17627	62.06411	98.8315

Totals : 4649.50341 63.99652

3. Chromatographic Traces of S2.7

3-1. A racemic sample ($dr = 4.4505:1$)

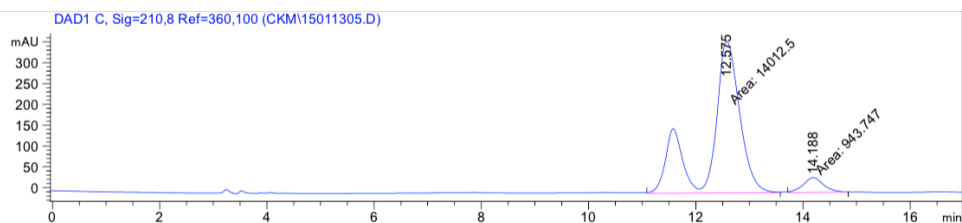


Signal 3: DAD1 C, Sig=210,8 Ref=360,100

Peak #	RetTime [min]	Type	Width [min]	Area [mAU*s]	Height [mAU]	Area %
1	11.277	MM	0.8287	1.79356e4	360.70258	90.8265
2	13.770	MM	0.4303	1811.49719	70.16351	9.1735

Totals : 1.97471e4 430.86609

3-2. A chiral sample (32% ee)



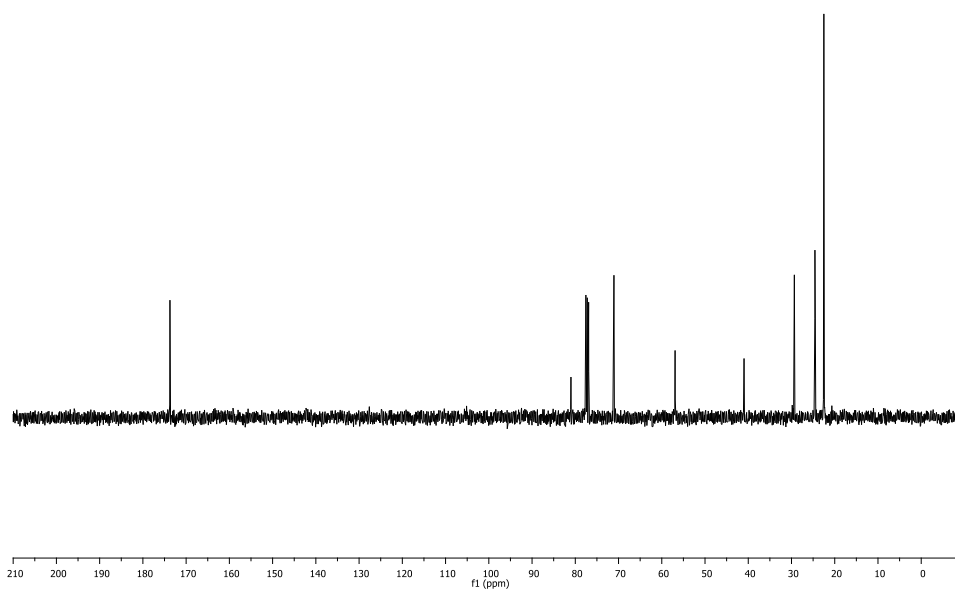
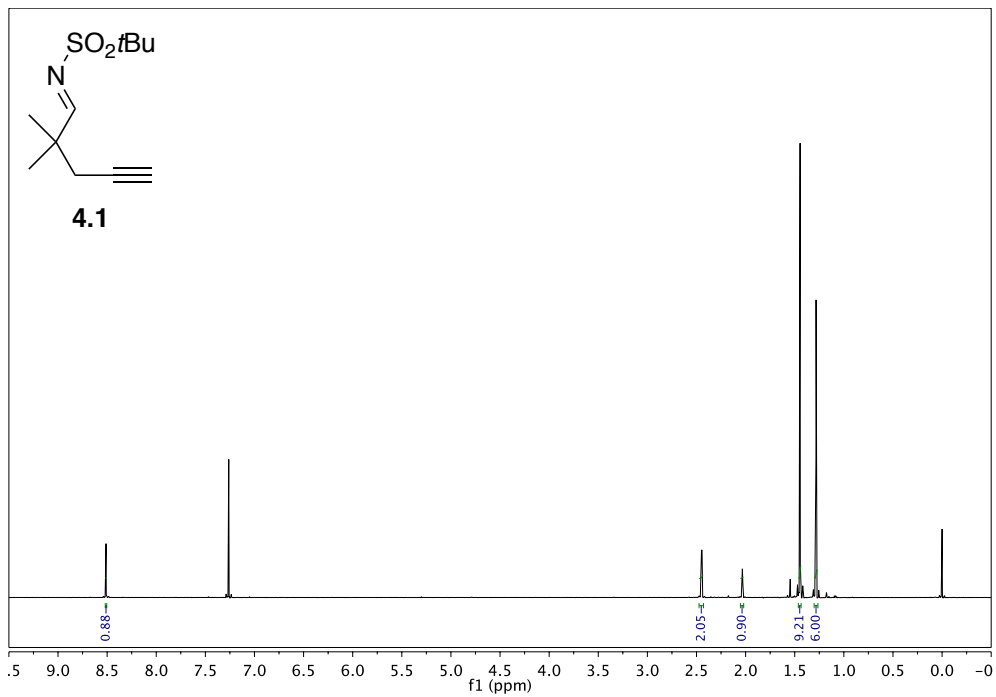
Signal 3: DAD1 C, Sig=210,8 Ref=360,100

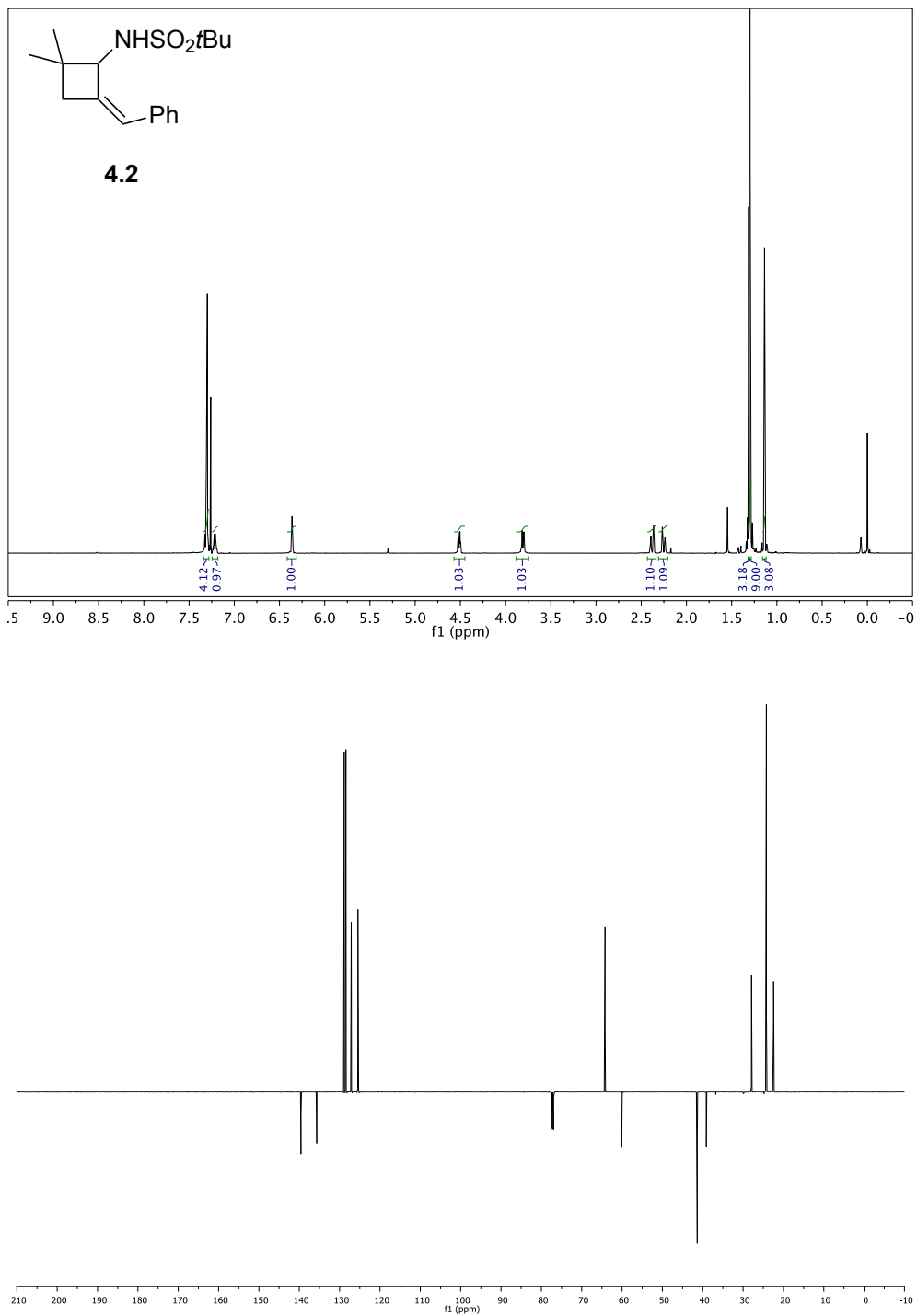
Peak #	RetTime [min]	Type	Width [min]	Area [mAU*s]	Height [mAU]	Area %
1	12.575	MM	0.6412	1.40125e4	364.20401	93.6899
2	14.188	MM	0.4403	943.74670	35.72705	6.3101

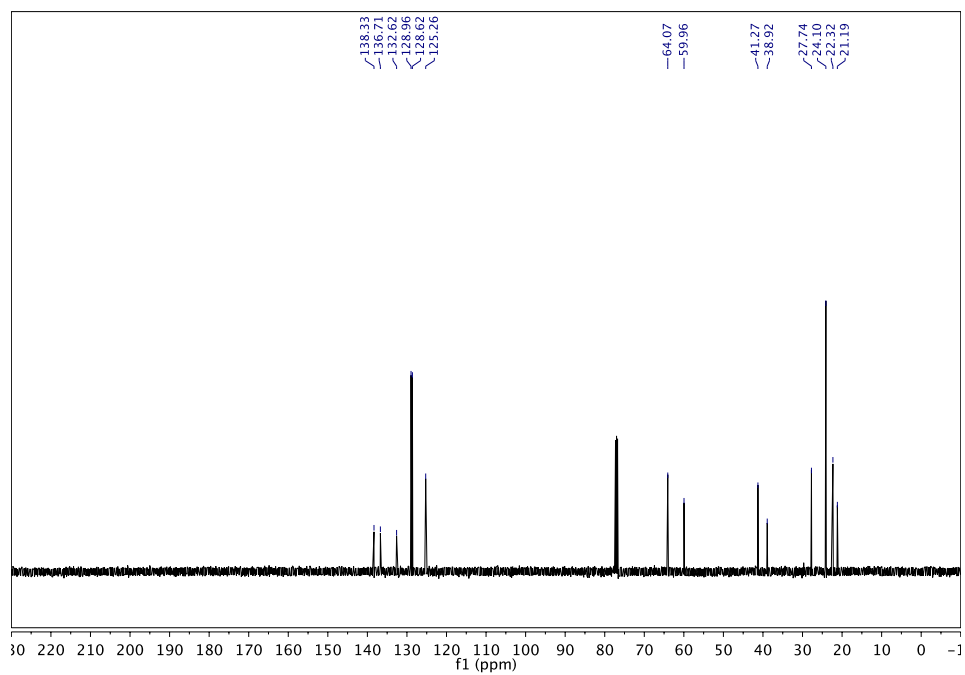
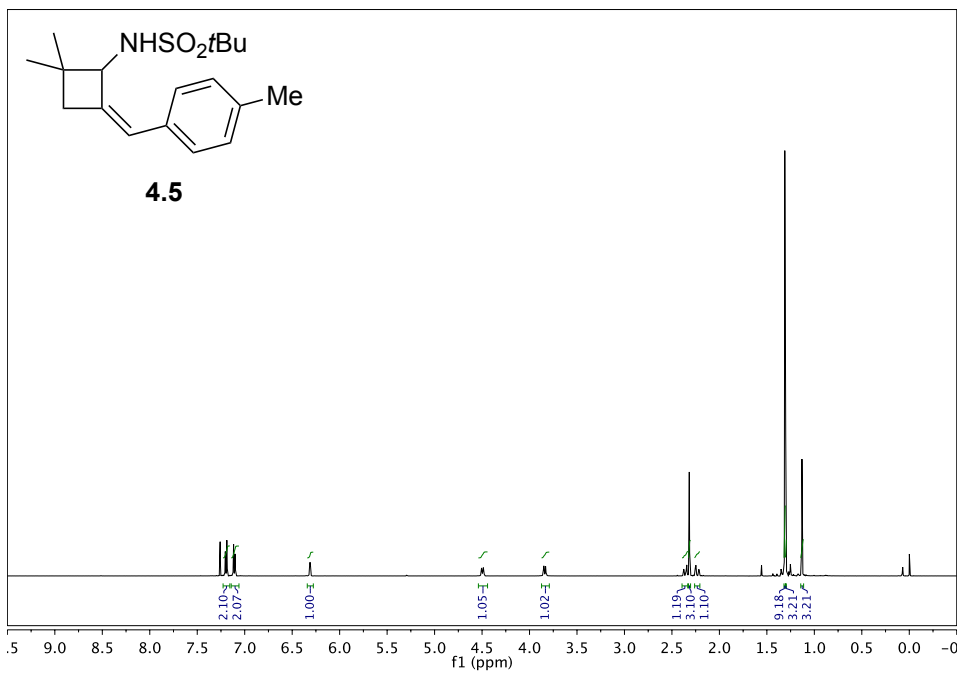
Totals : 1.49562e4 399.93106

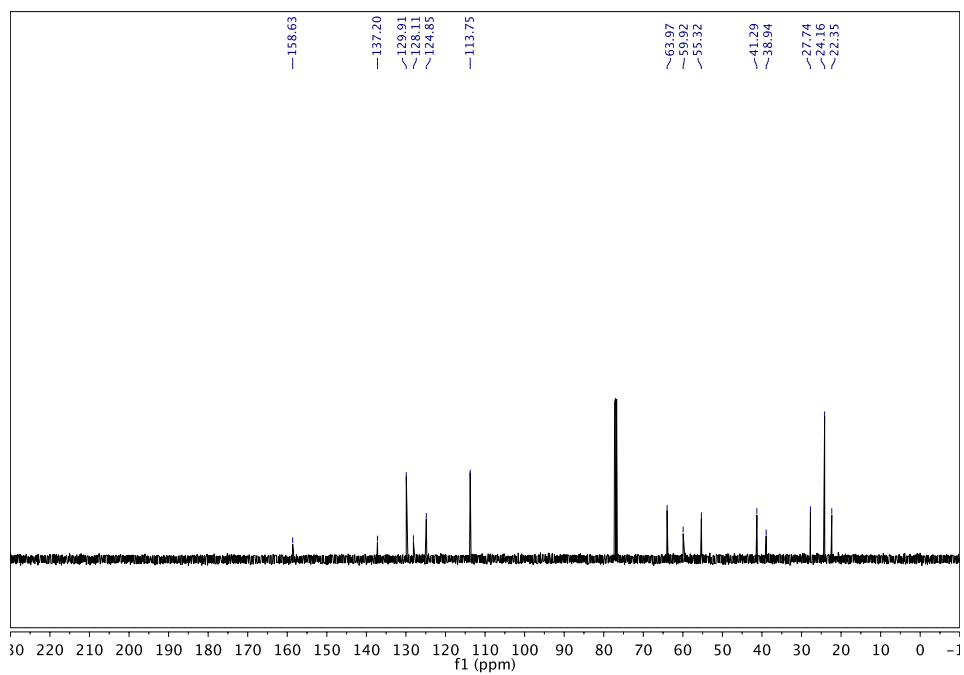
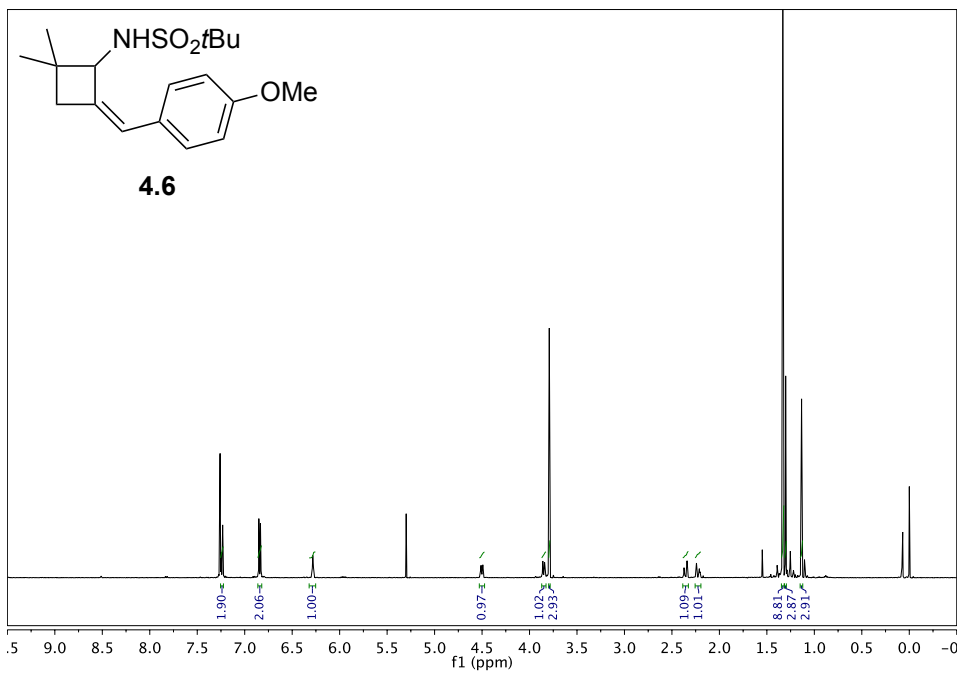
Chapter 4

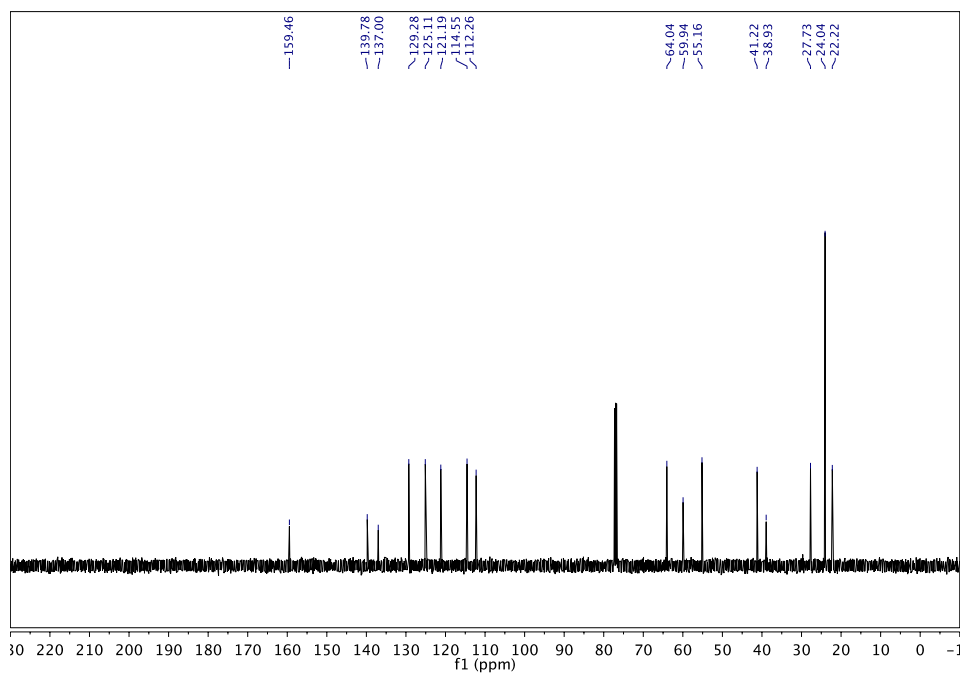
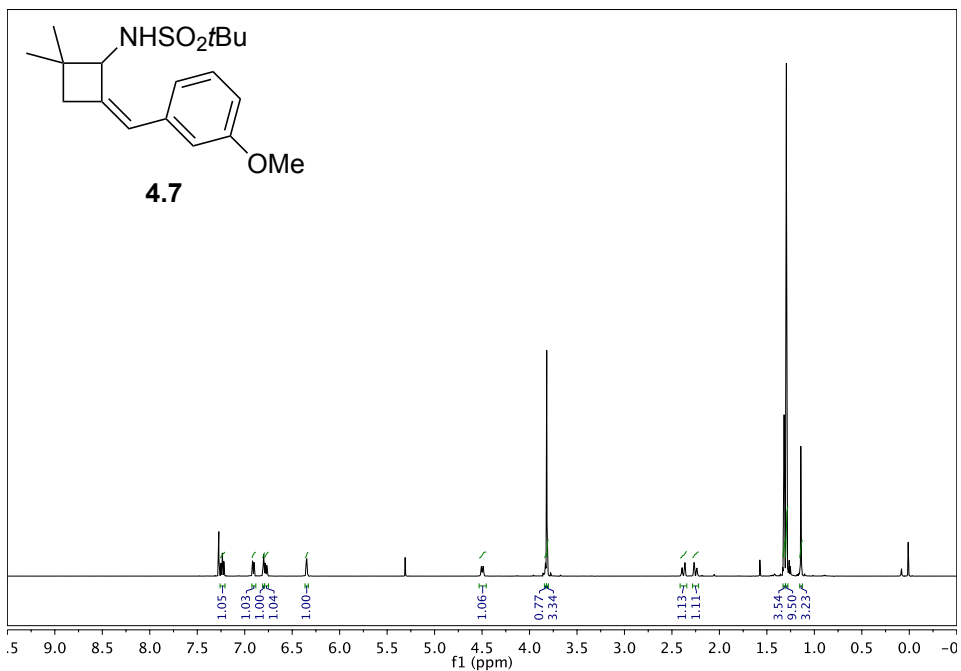
NMR spectra

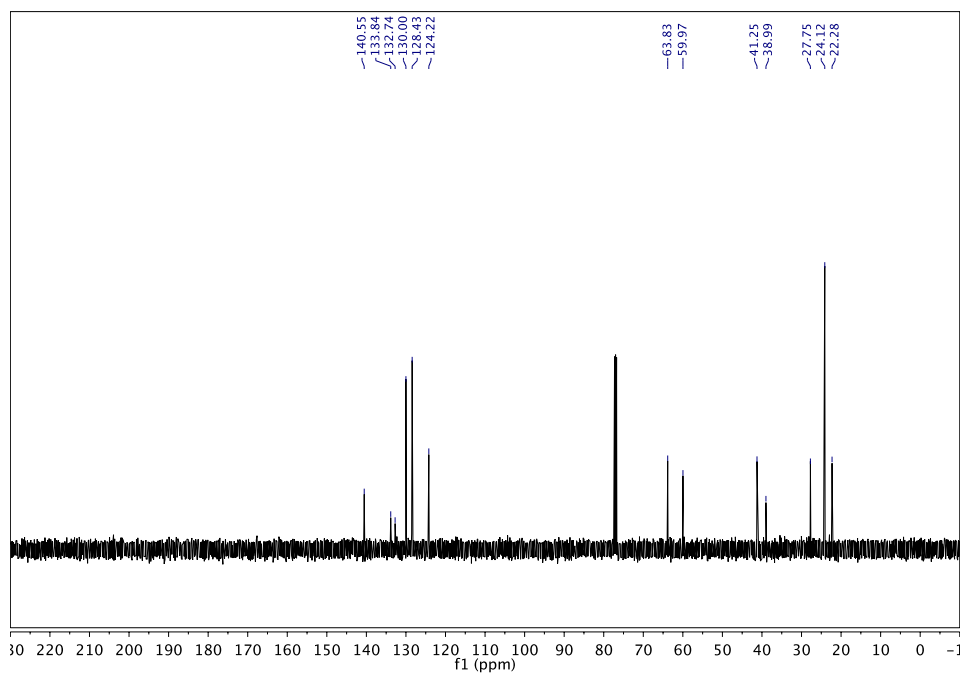
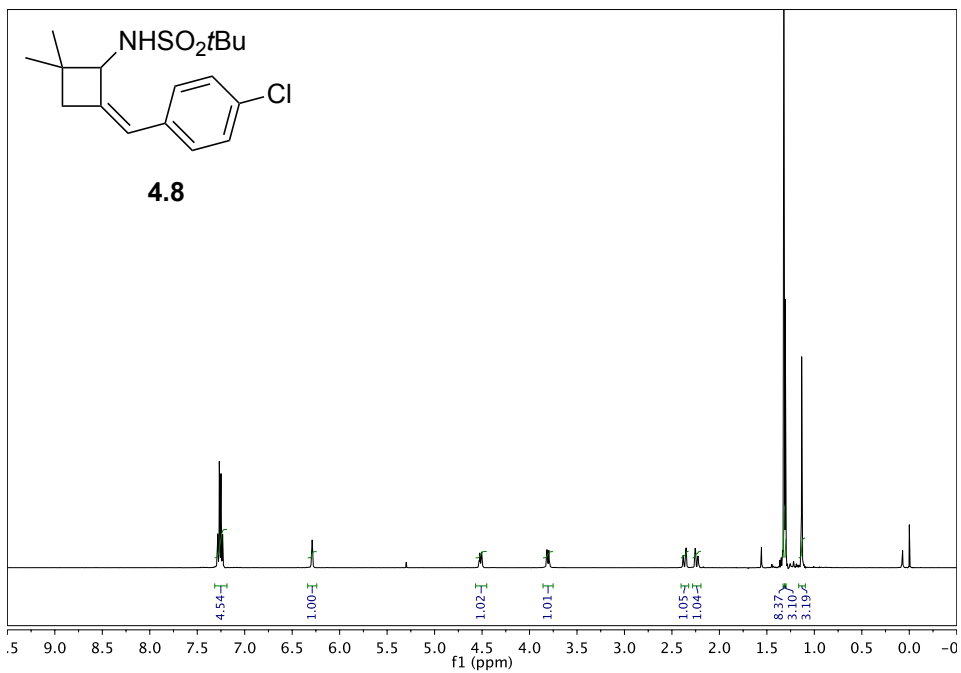


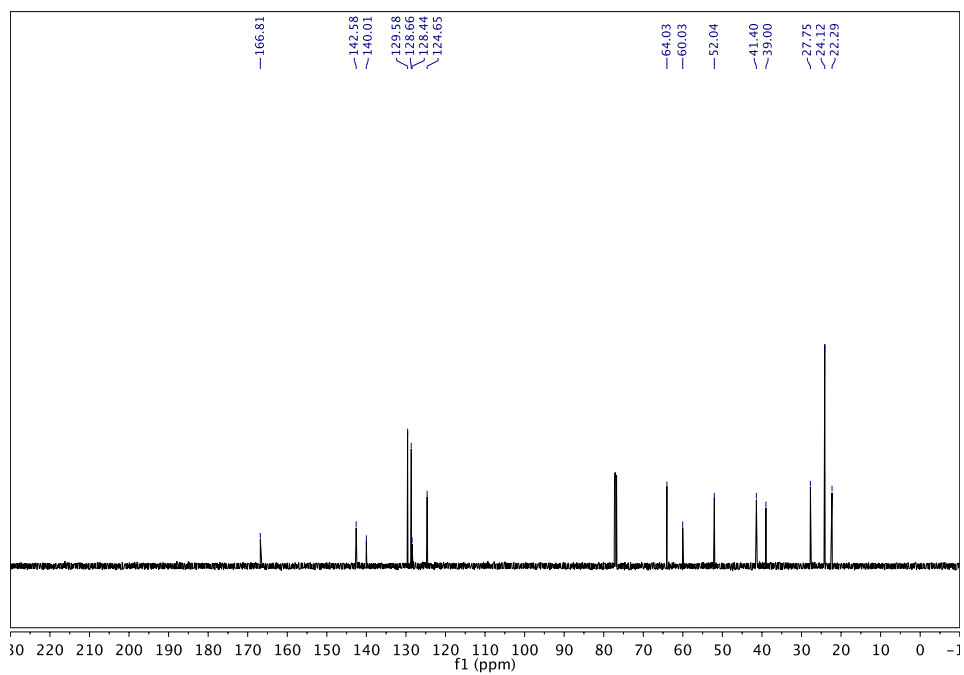
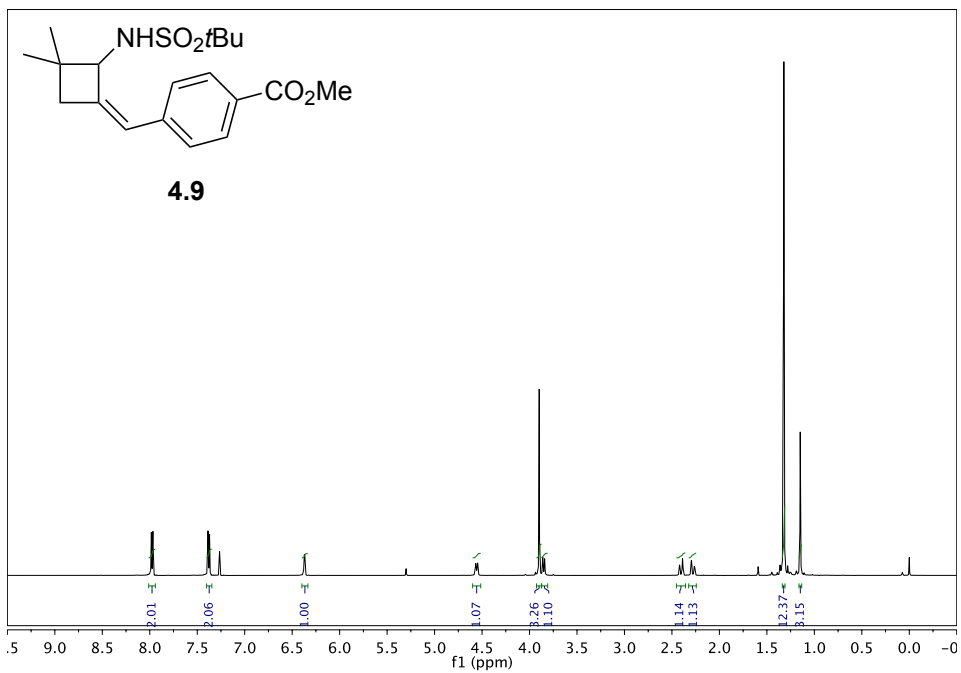


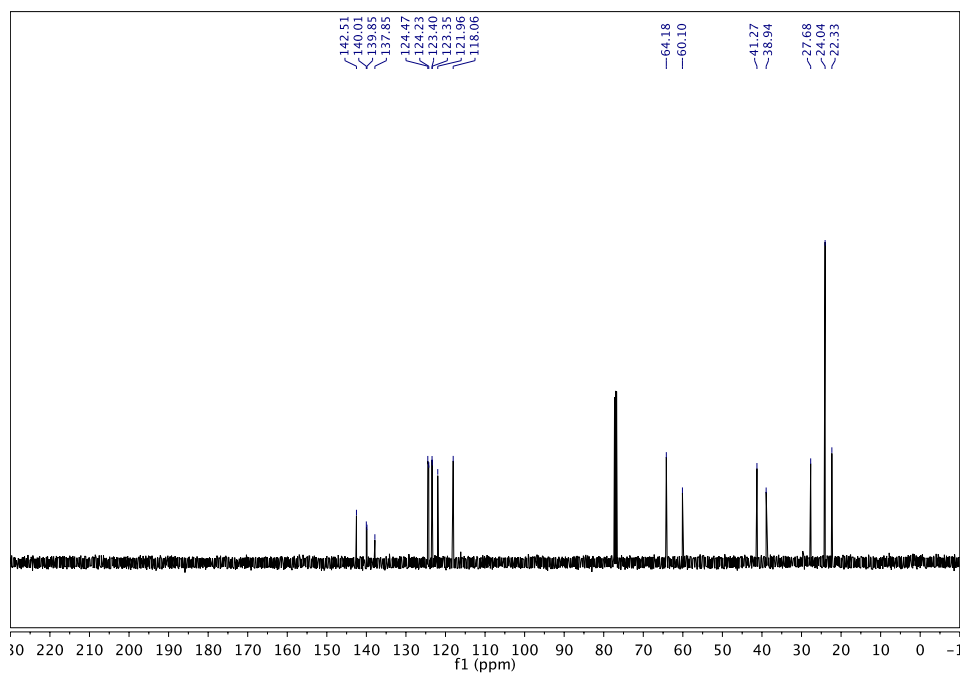
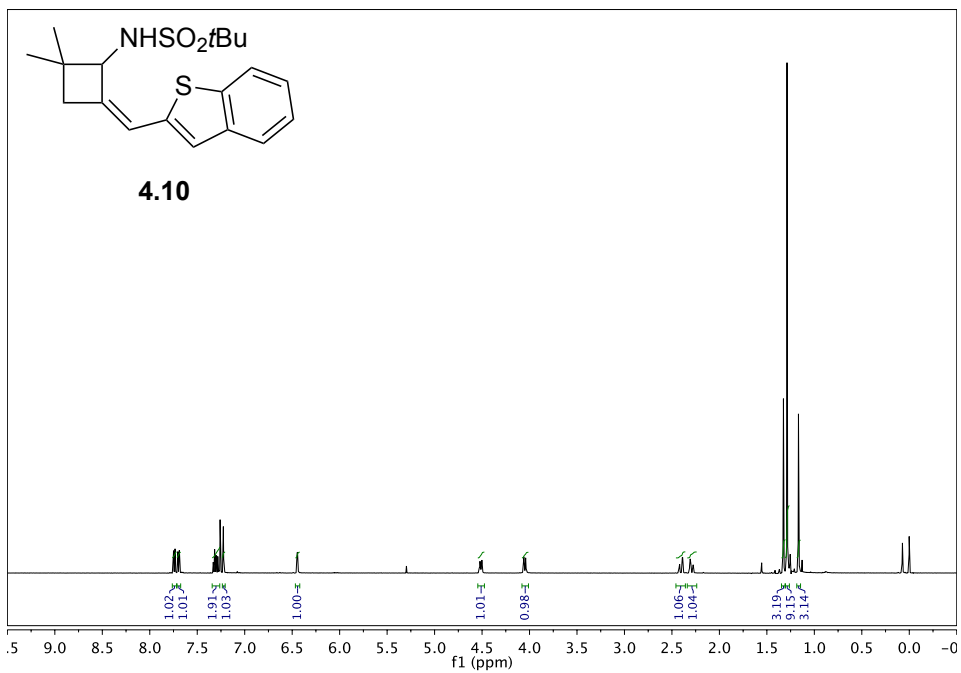


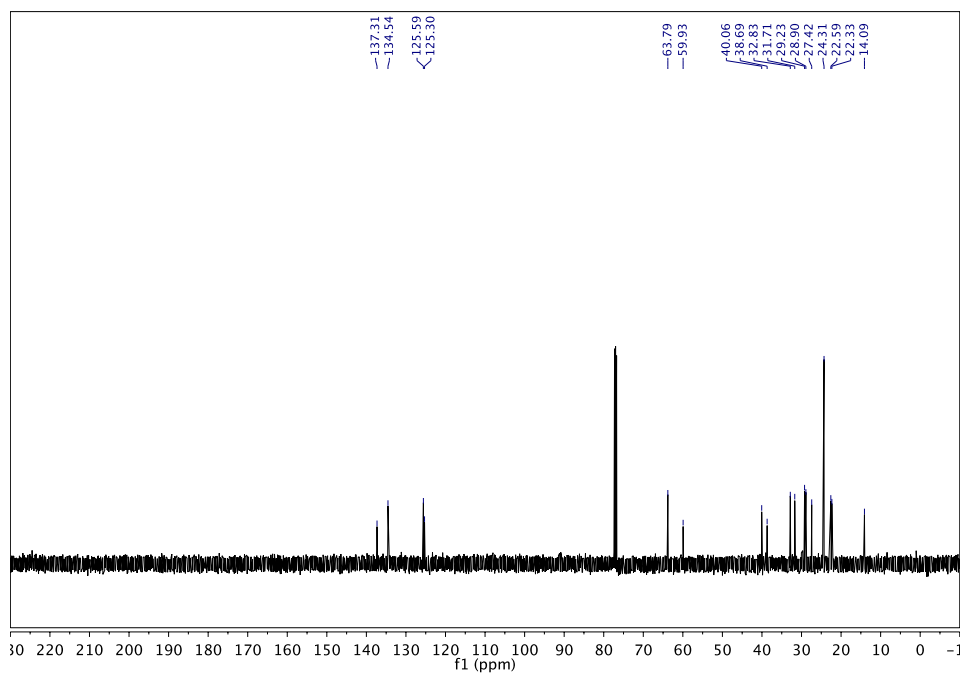
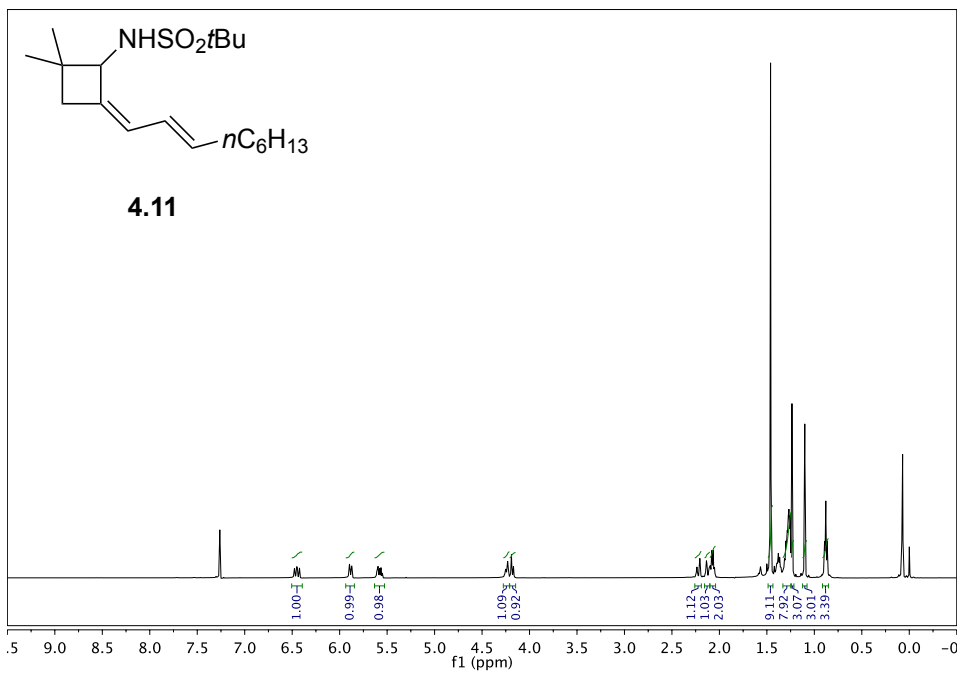


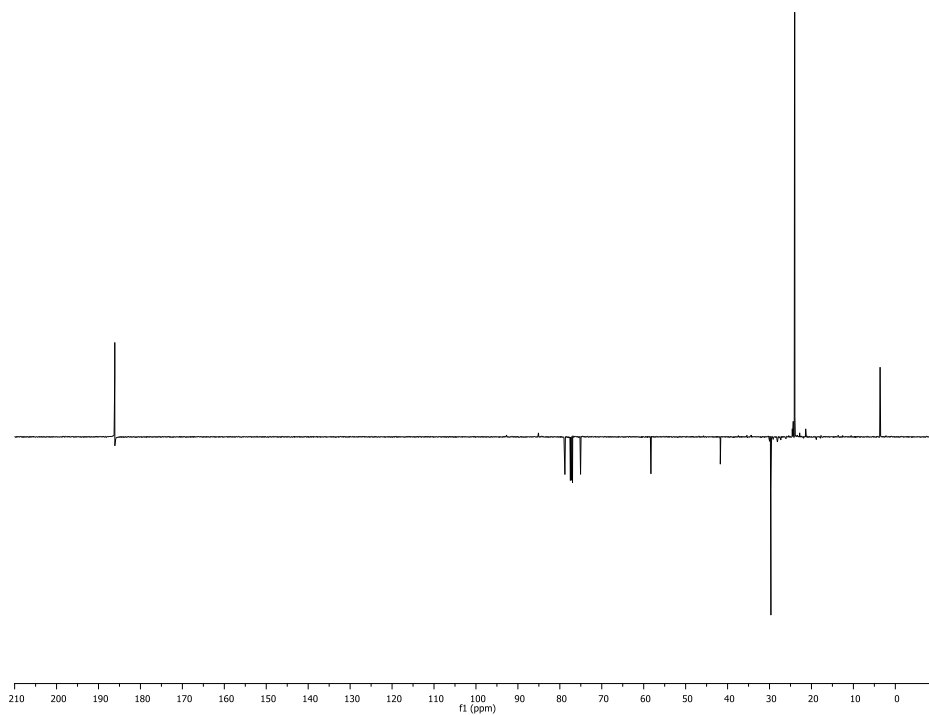
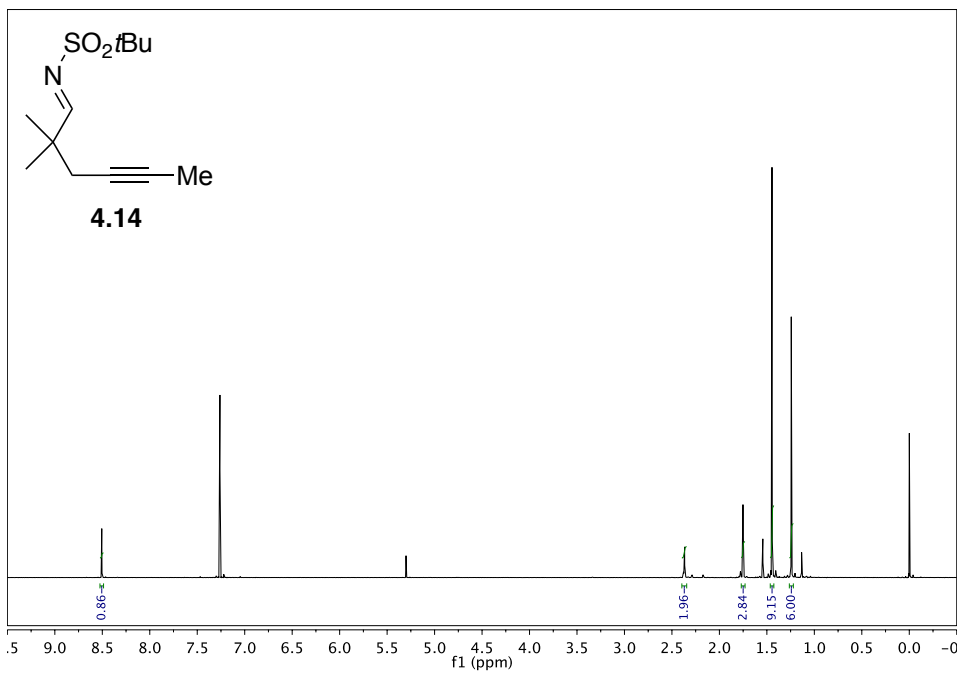


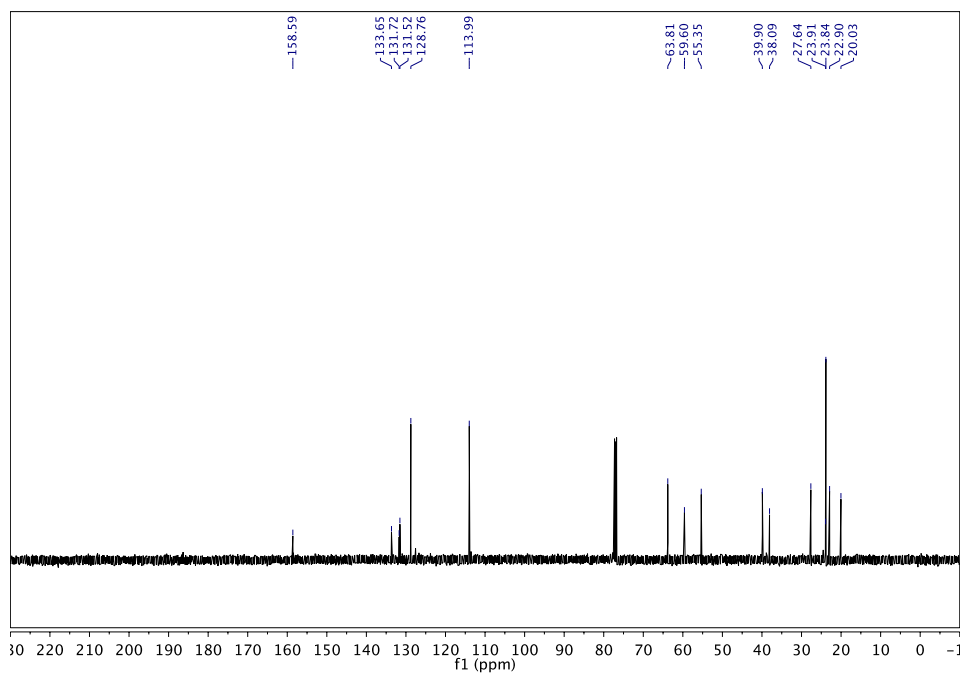
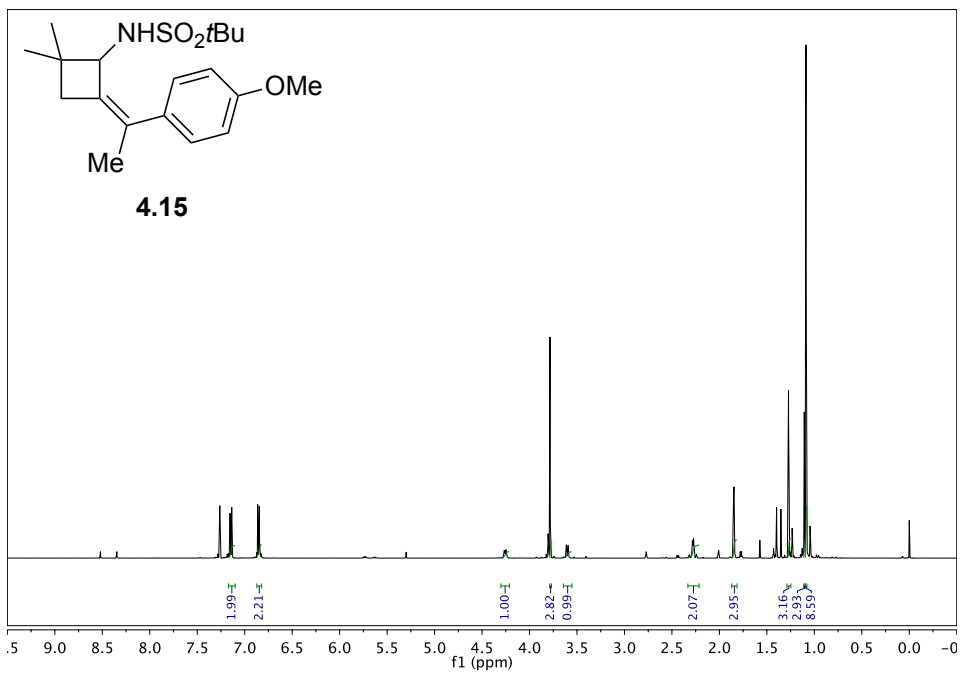


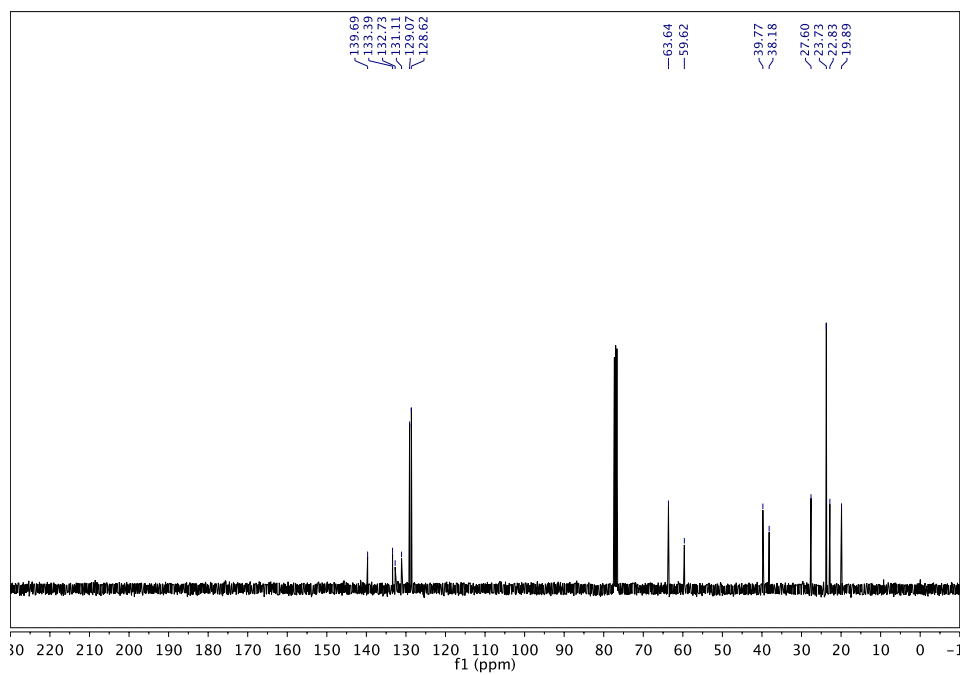
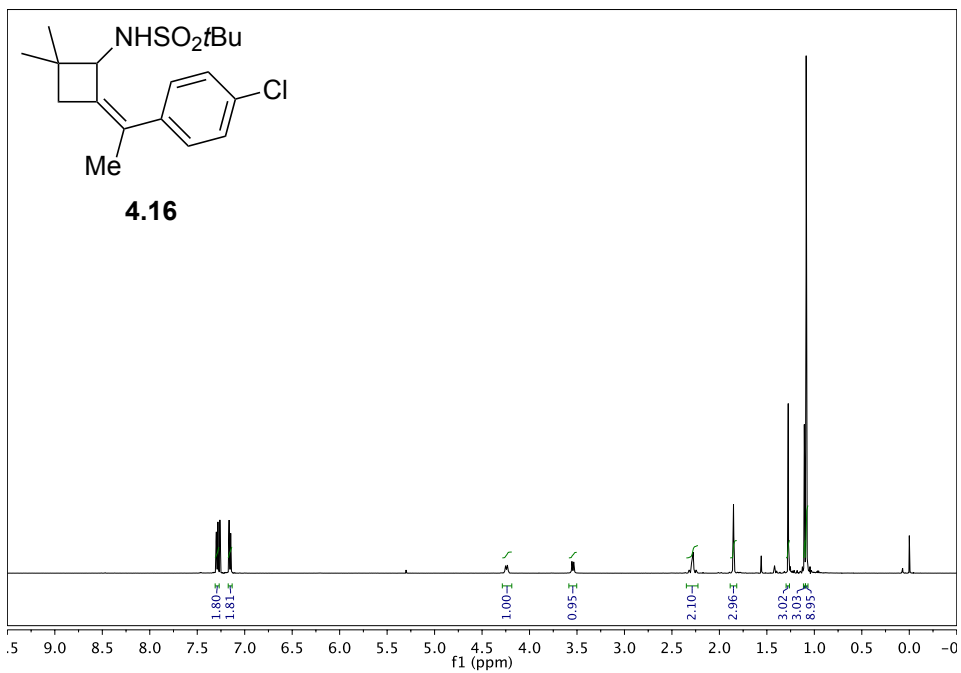












Chiral HPLC data

1. Analytical Method of 4.2

Column: Chiralpak IA

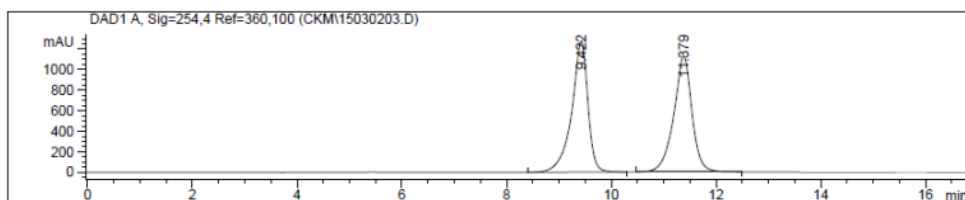
Eluent: Hexane/isopropyl alcohol = 99:1

Flow rate: 1.0 ml/min

Detection Wavelength: 254 nm

2. Chromatographic Traces

2-1. A racemic sample

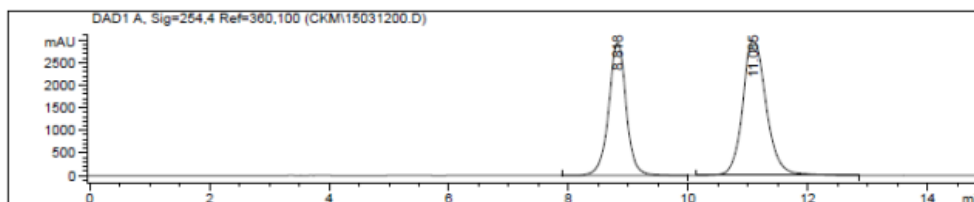


Signal 1: DAD1 A, Sig=254,4 Ref=360,100

Peak #	RetTime [min]	Type	Width [min]	Area [mAU*s]	Height [mAU]	Area %
1	9.422	BB	0.3126	2.73981e4	1275.48242	50.1063
2	11.379	BB	0.3539	2.72819e4	1129.06958	49.8937

Totals : 5.46800e4 2404.55200

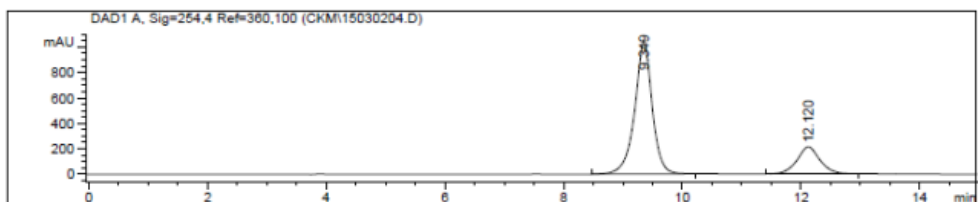
2-2. A chiral sample using 4.22 (16% ee)



Signal 1: DAD1 A, Sig=254,4 Ref=360,100

Peak #	RetTime [min]	Type	Width [min]	Area [mAU*s]	Height [mAU]	Area %
1	8.818	VB	0.3066	6.00103e4	2934.57300	42.2243
2	11.085	BB	0.4164	8.21124e4	2971.57202	57.7757
Totals :				1.42123e5	5906.14502	

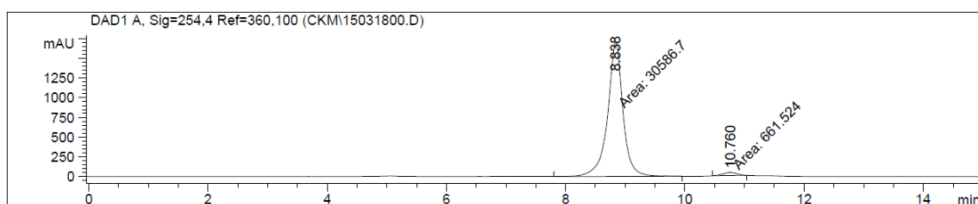
2-3. A chiral sample using 4.23 (58% ee)



Signal 1: DAD1 A, Sig=254,4 Ref=360,100

Peak #	RetTime [min]	Type	Width [min]	Area [mAU*s]	Height [mAU]	Area %
1	9.349	BB	0.2972	2.14737e4	1047.20630	78.9673
2	12.120	BB	0.3937	5719.45605	212.68799	21.0327
Totals :				2.71932e4	1259.89429	

2-4. A chiral sample using 4.24 (96% ee)

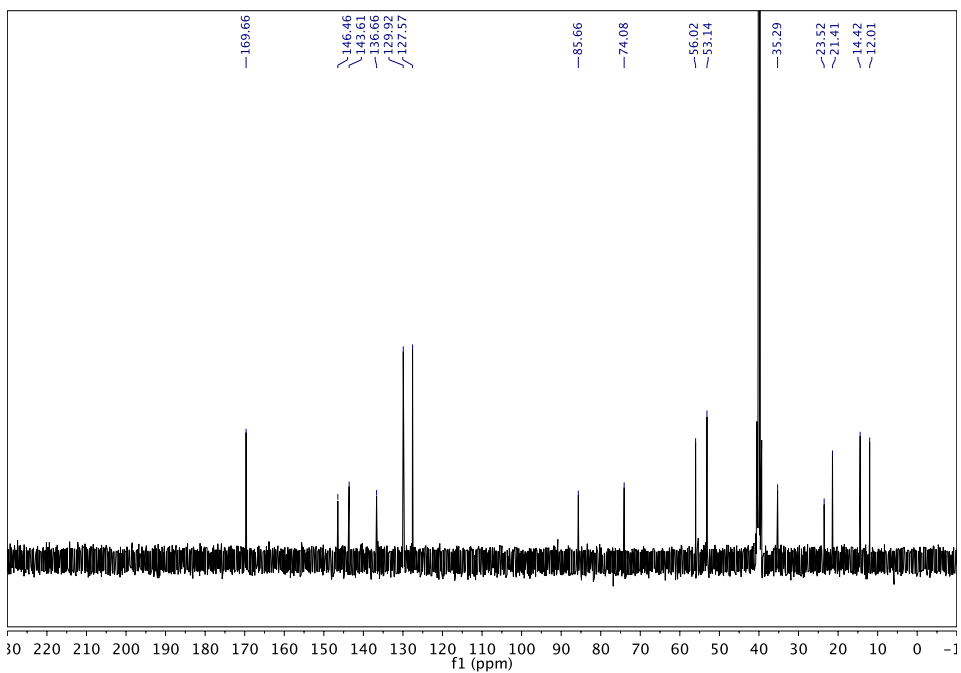
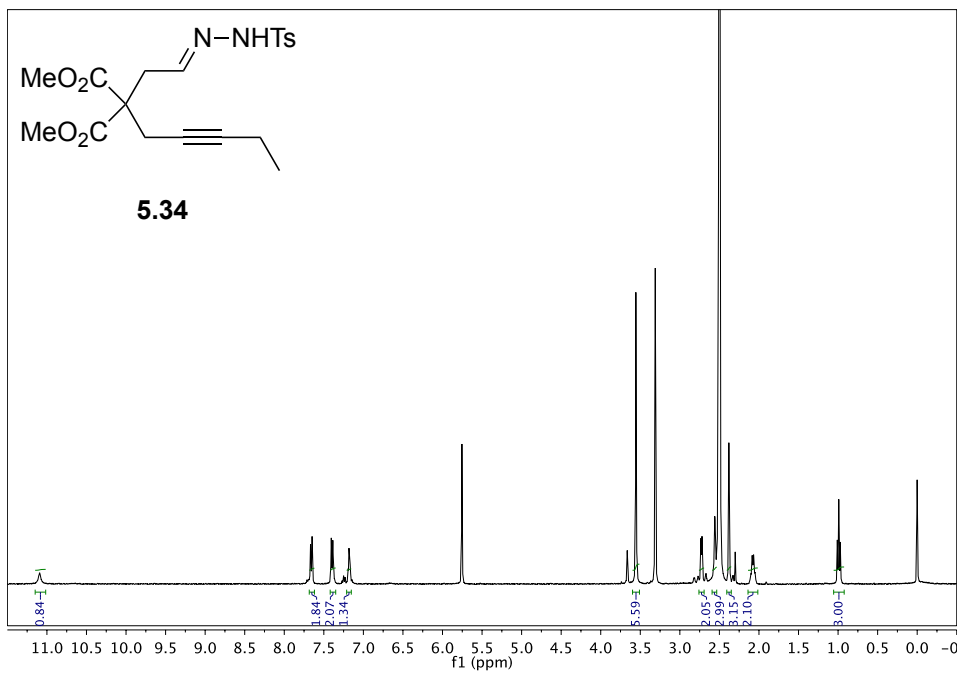


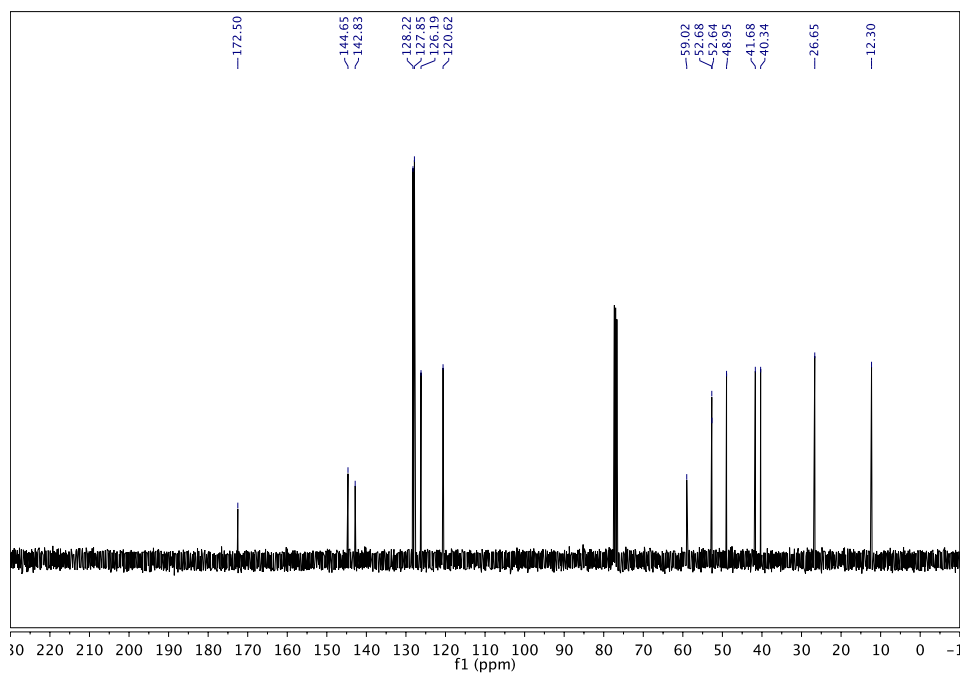
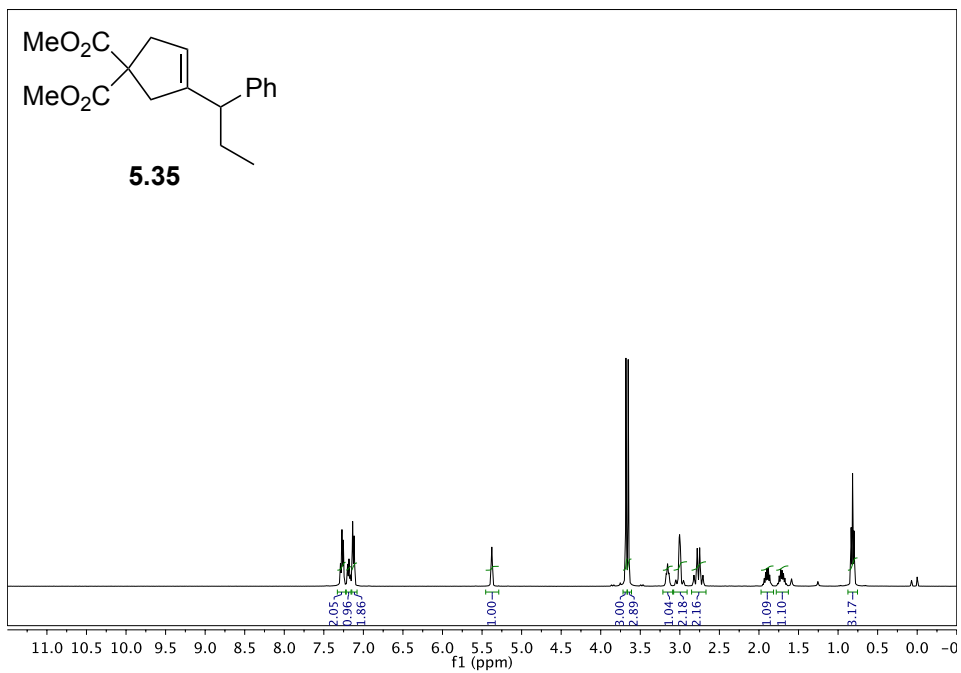
Signal 1: DAD1 A, Sig=254,4 Ref=360,100

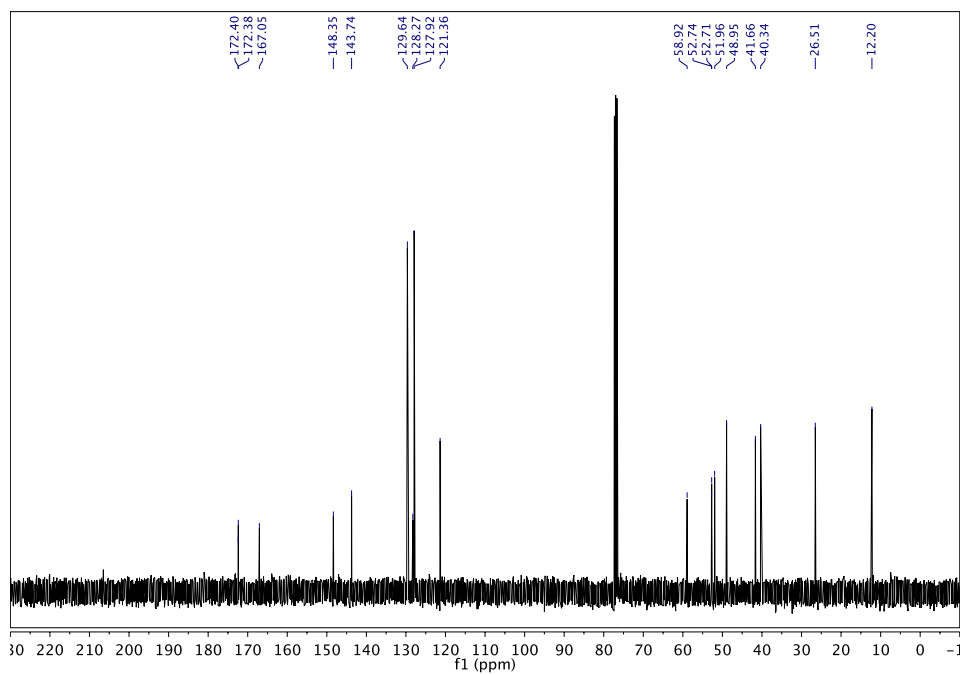
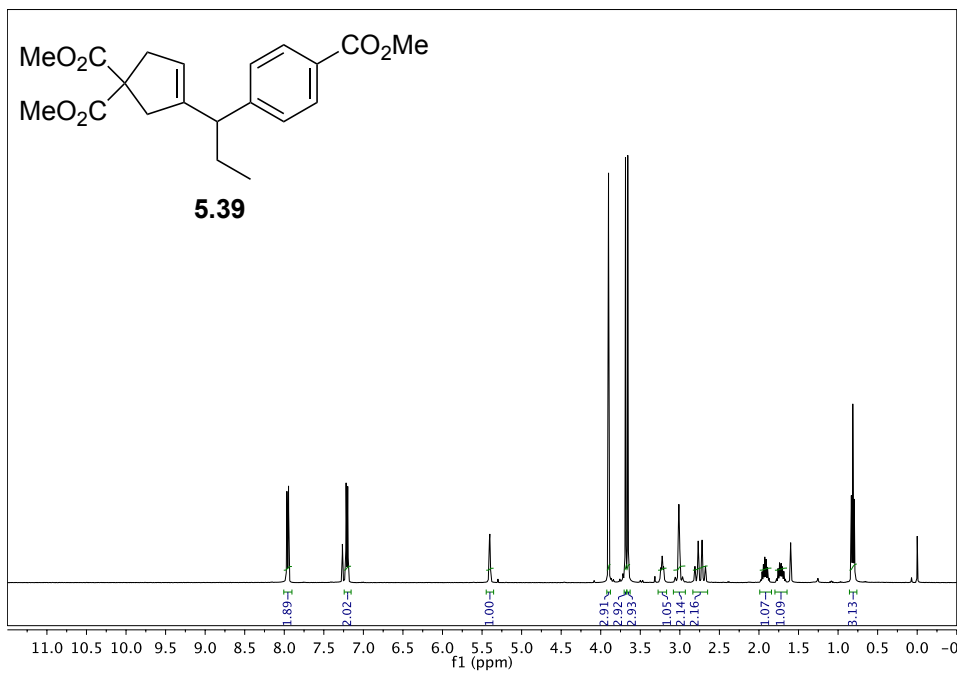
Peak #	RetTime [min]	Type	Width [min]	Area [mAU*s]	Height [mAU]	Area %
1	8.838	MM	0.3000	3.05867e4	1699.50024	97.8830
2	10.760	MM	0.2750	661.52374	40.09766	2.1170
Totals :				3.12483e4	1739.59790	

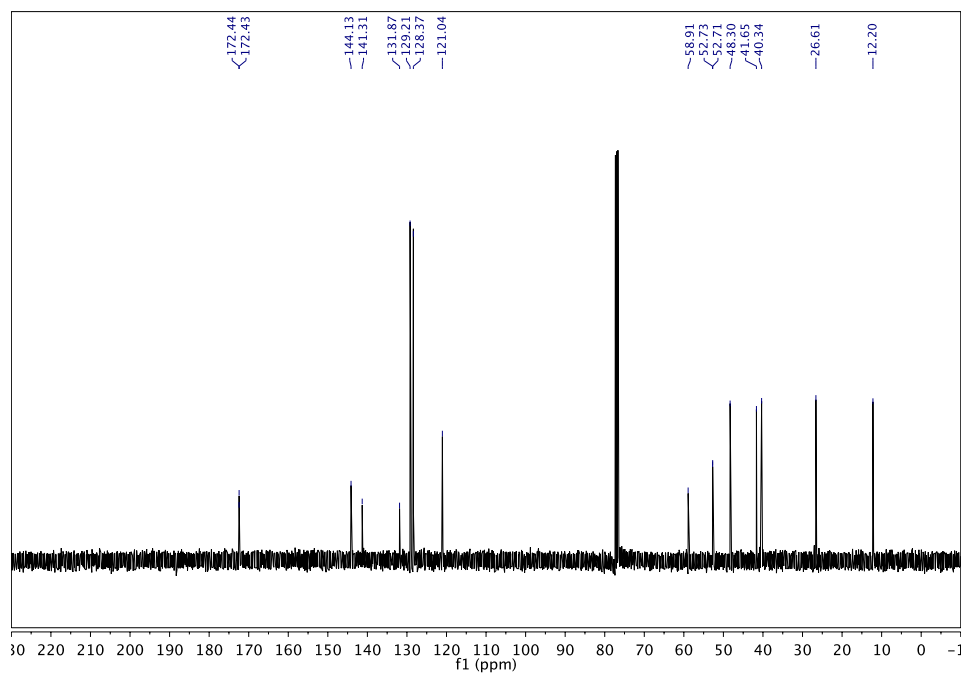
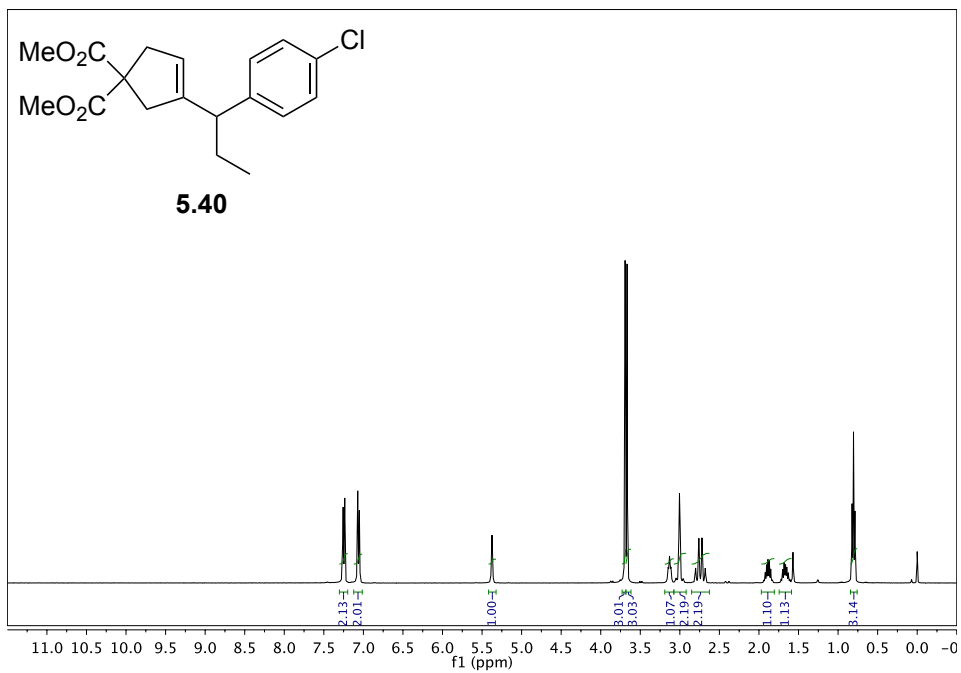
Chapter 5

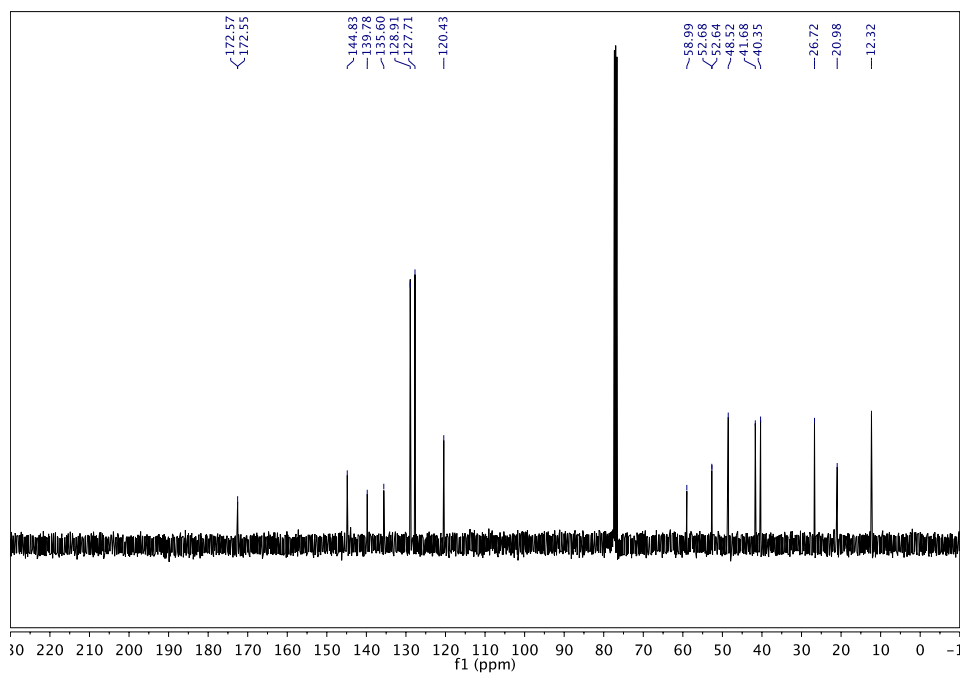
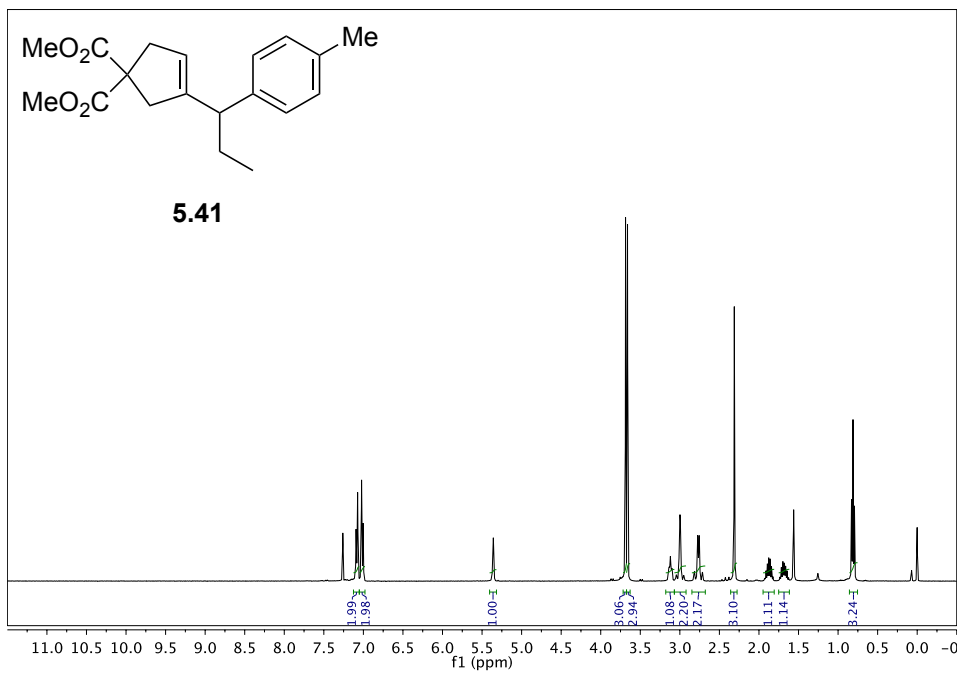
NMR Spectra

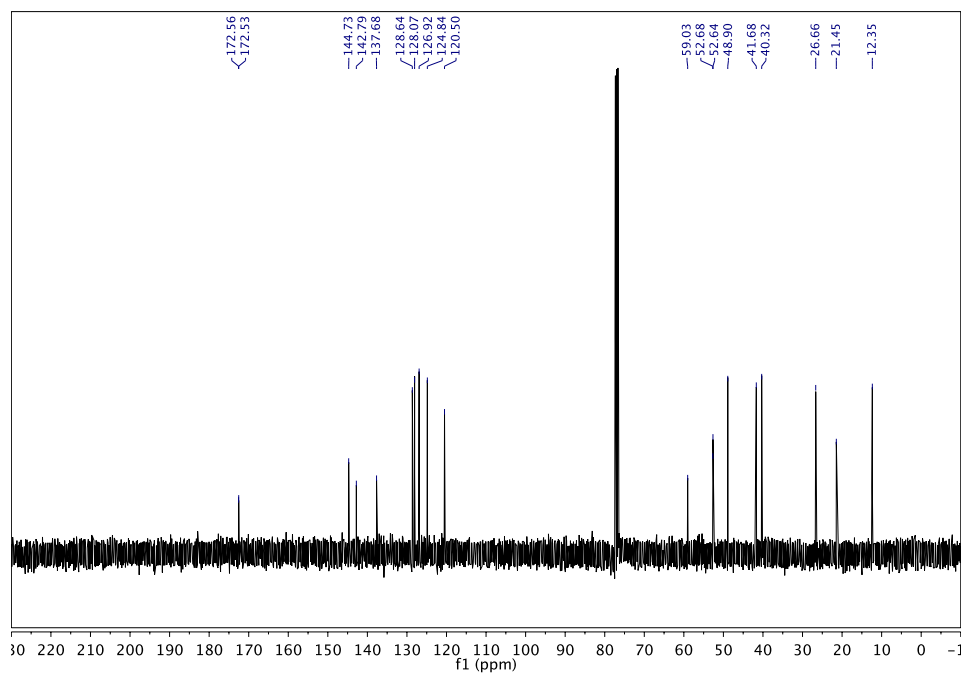
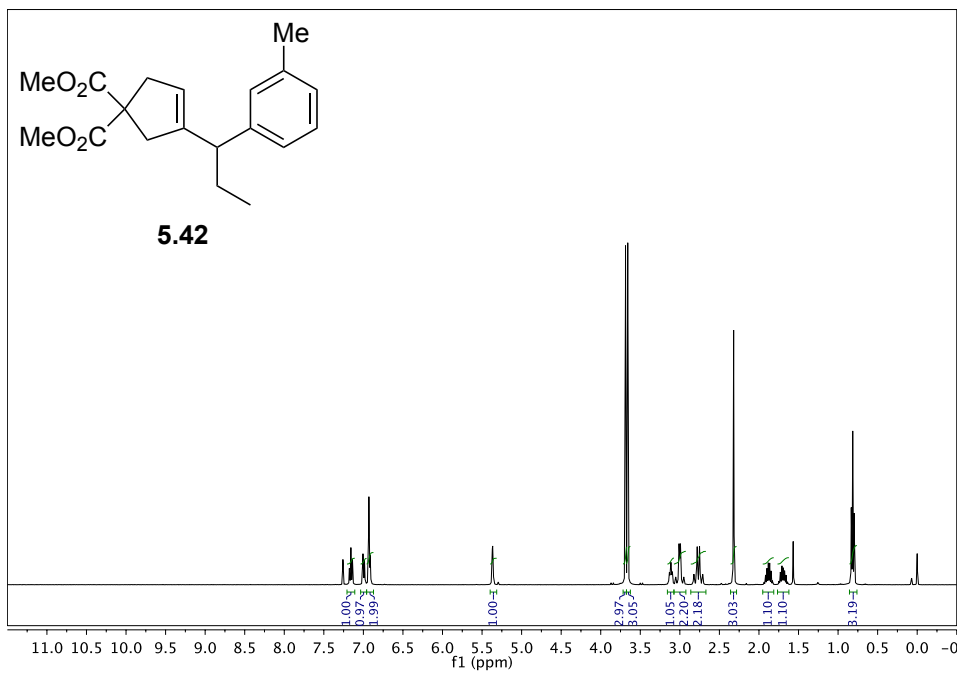


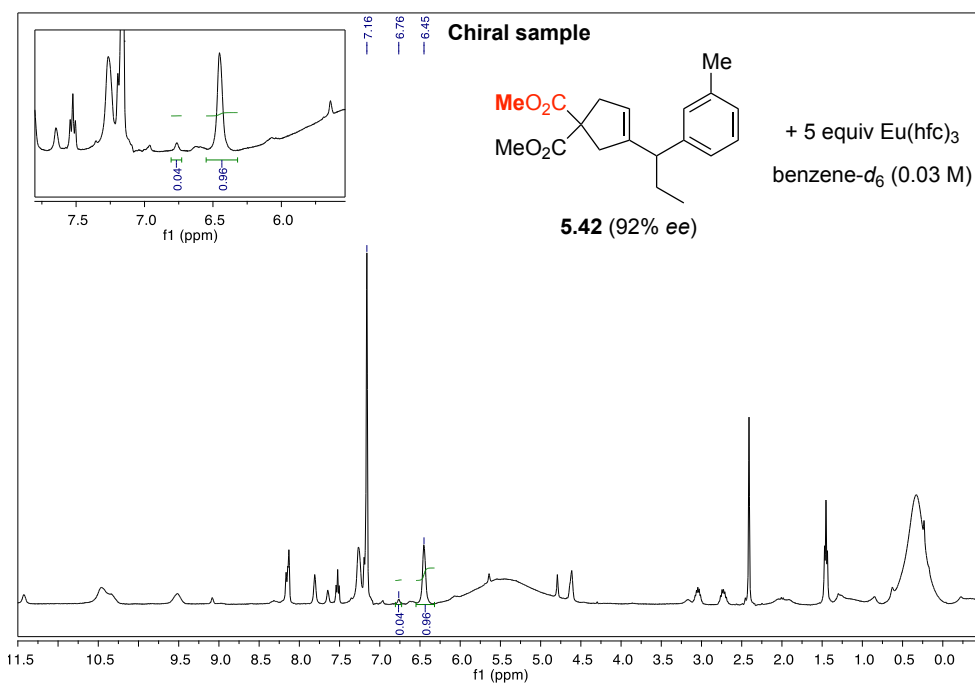
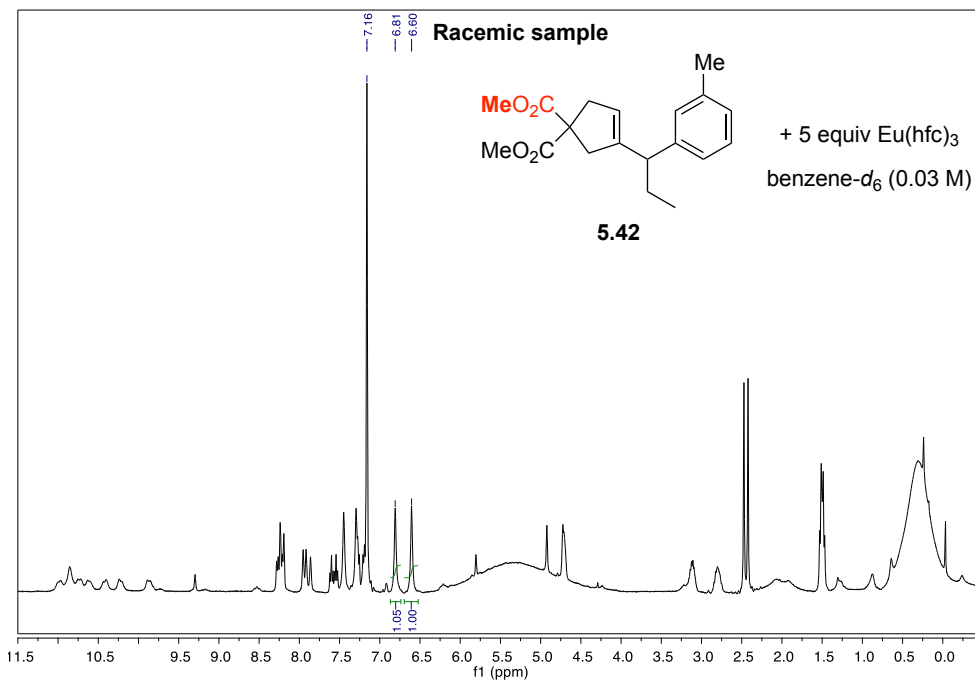


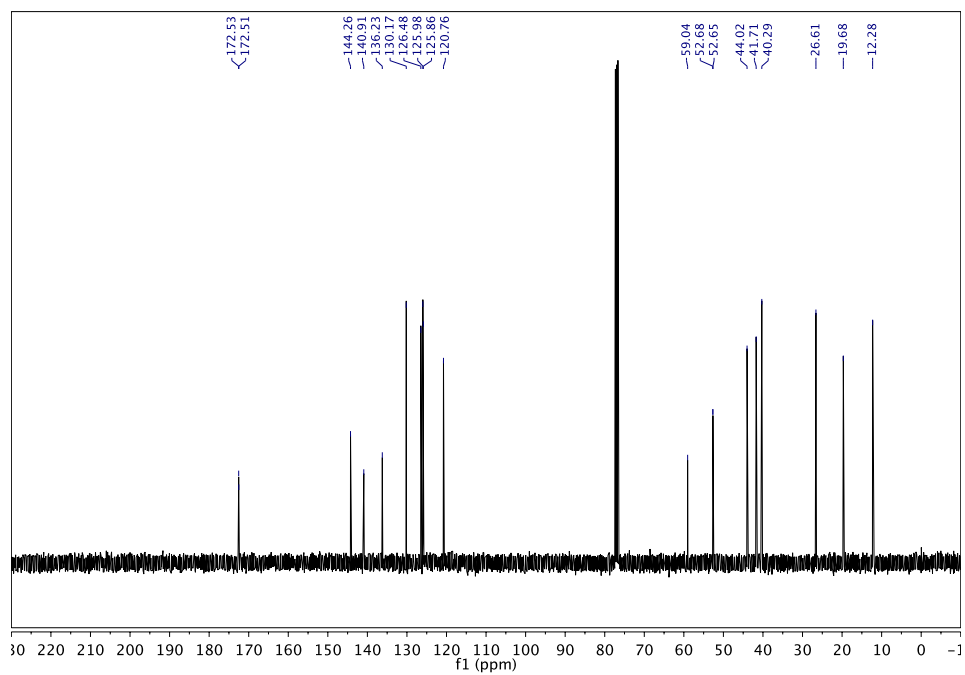
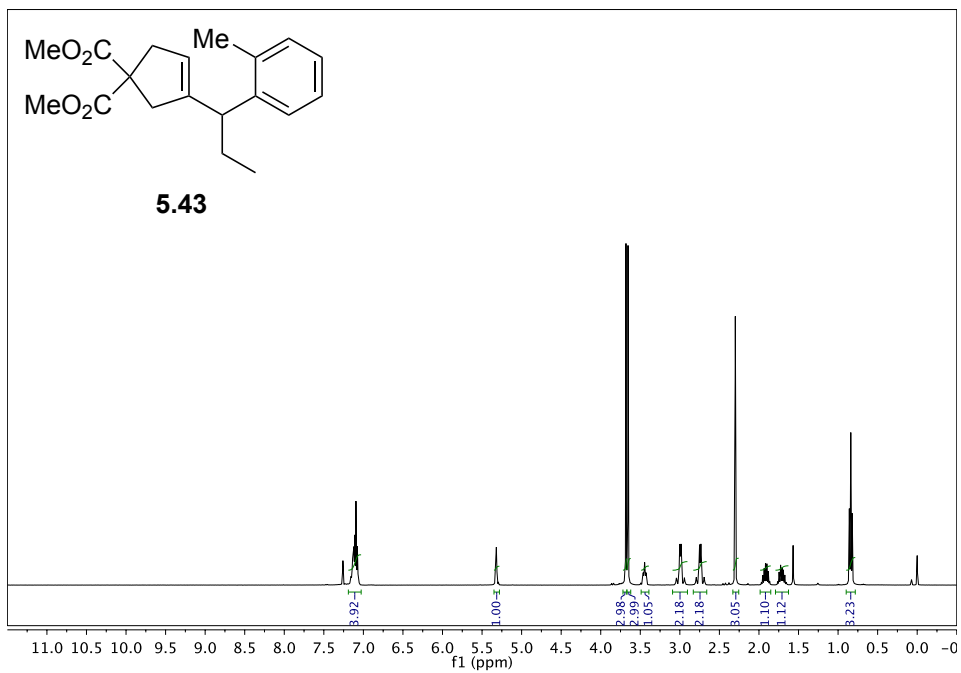


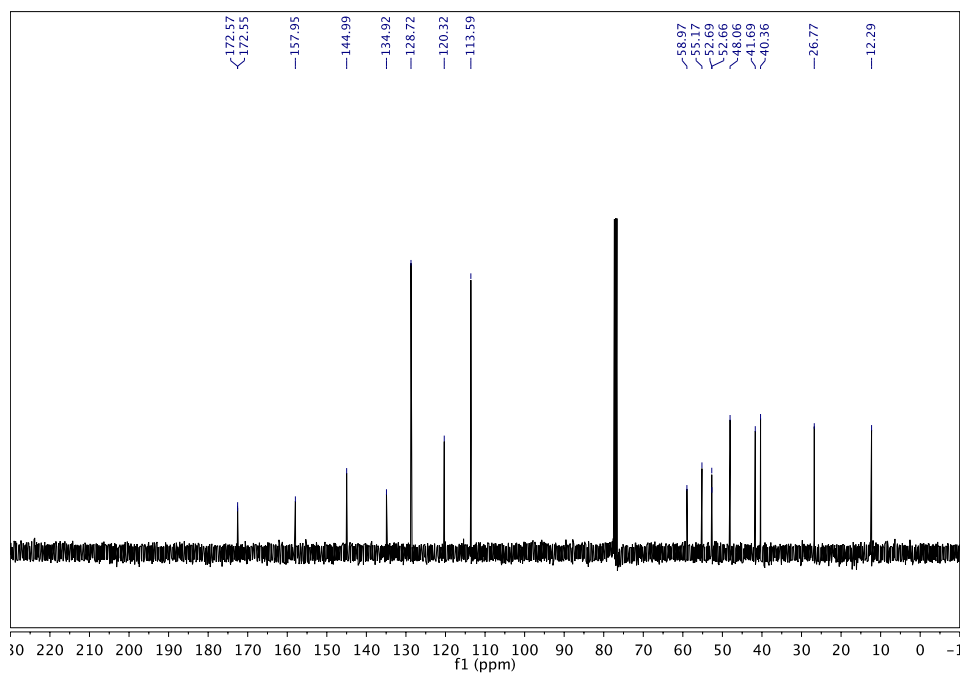
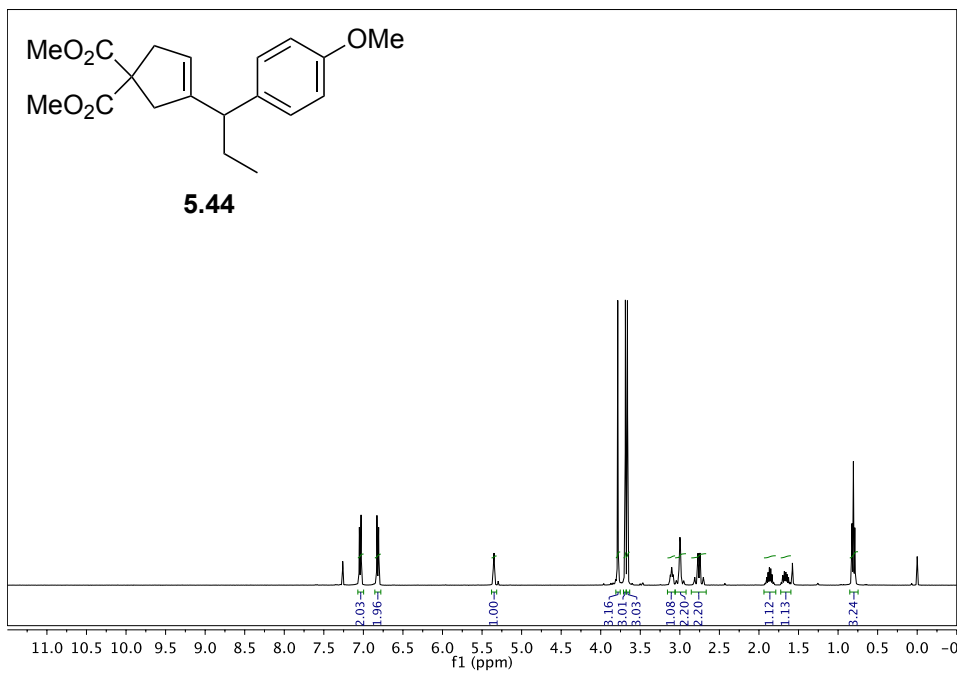


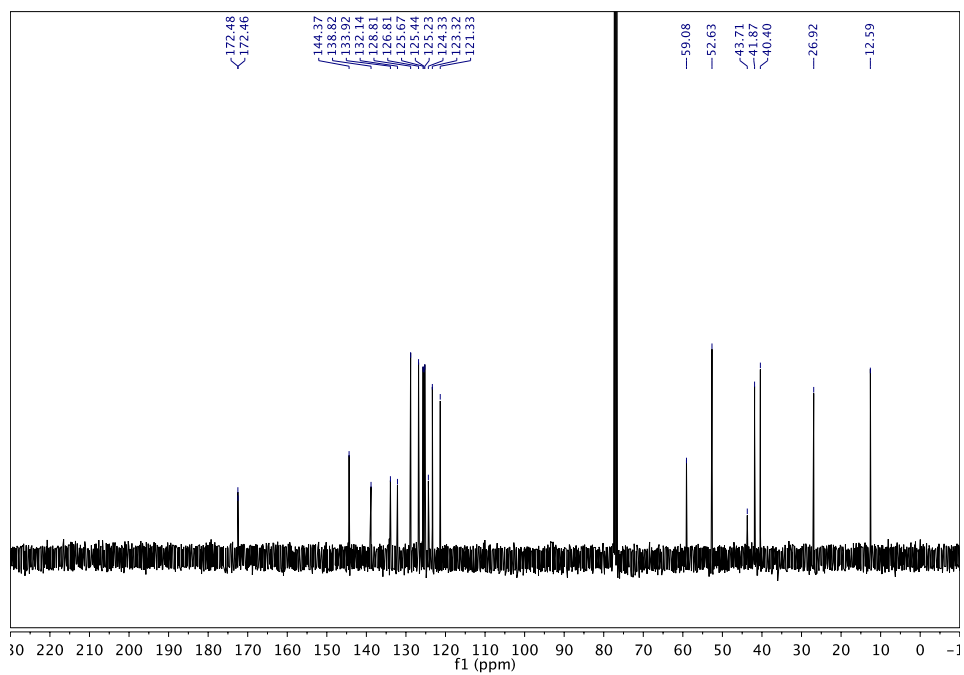
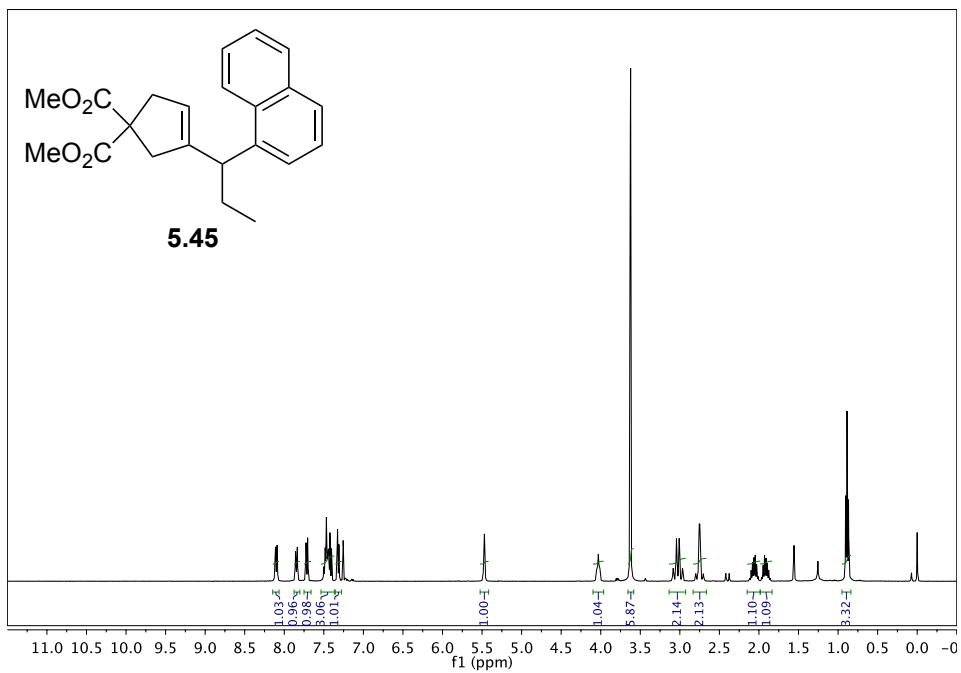


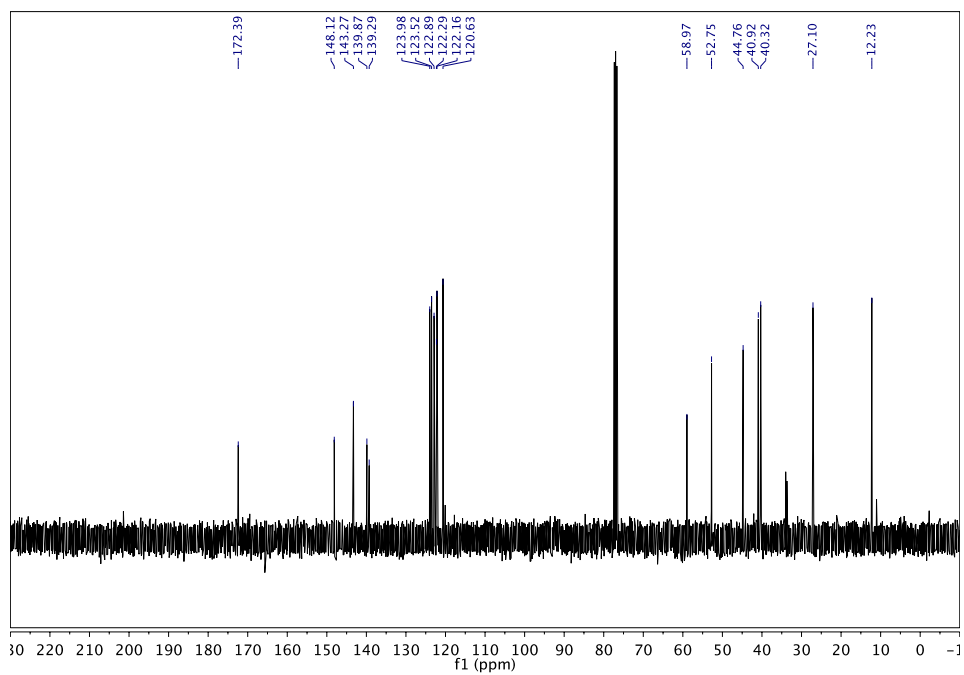
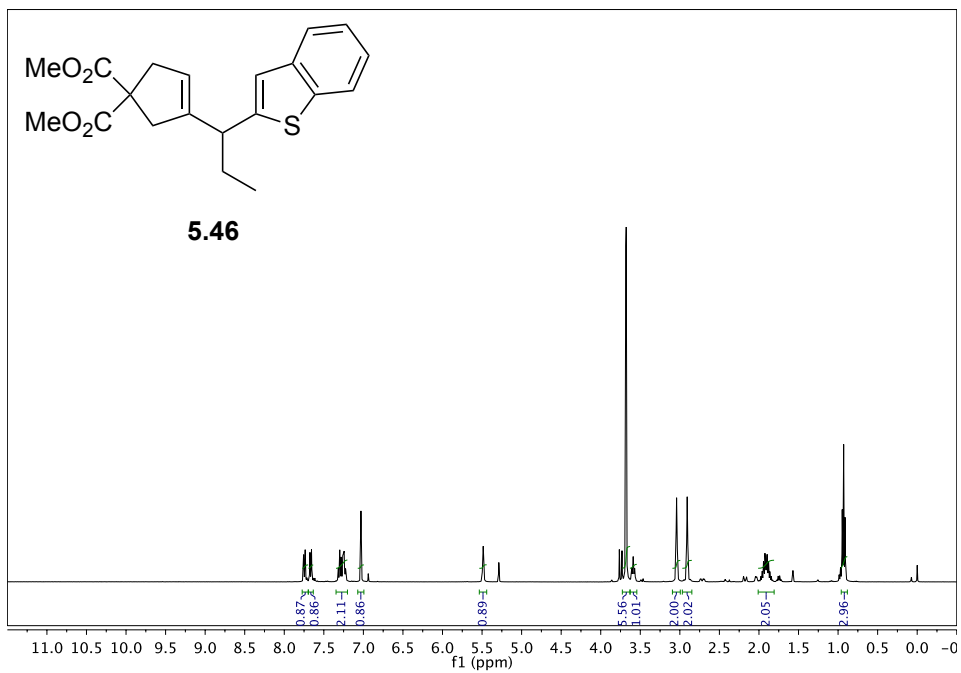


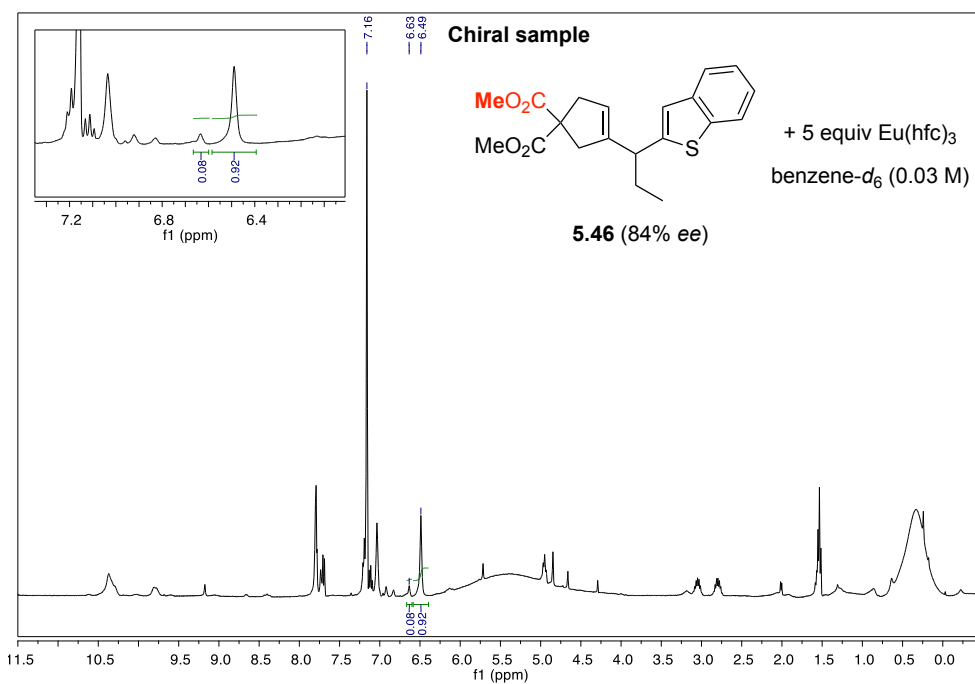
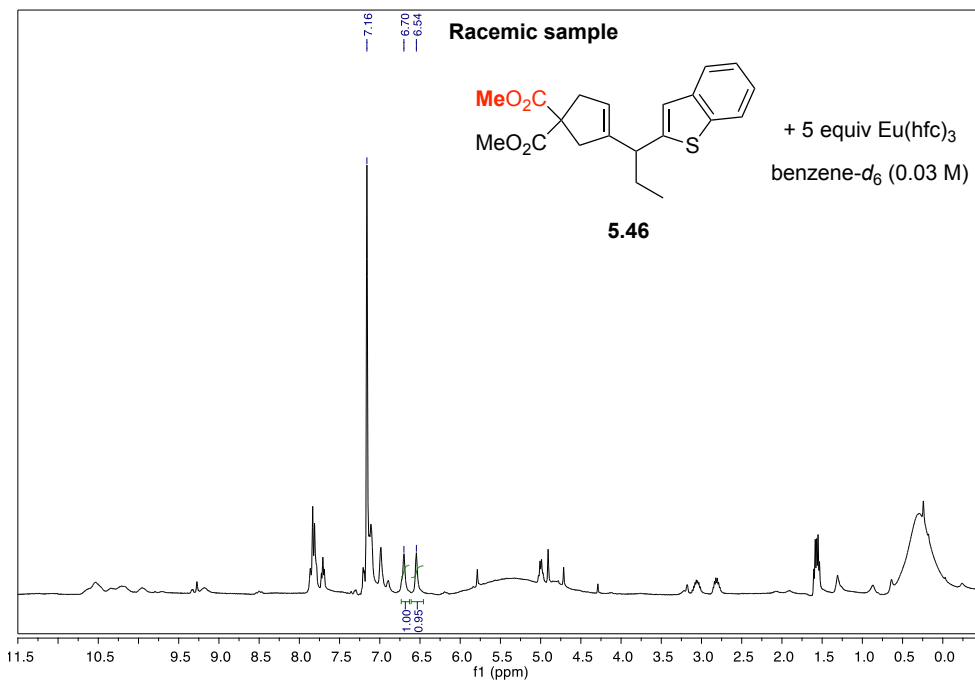


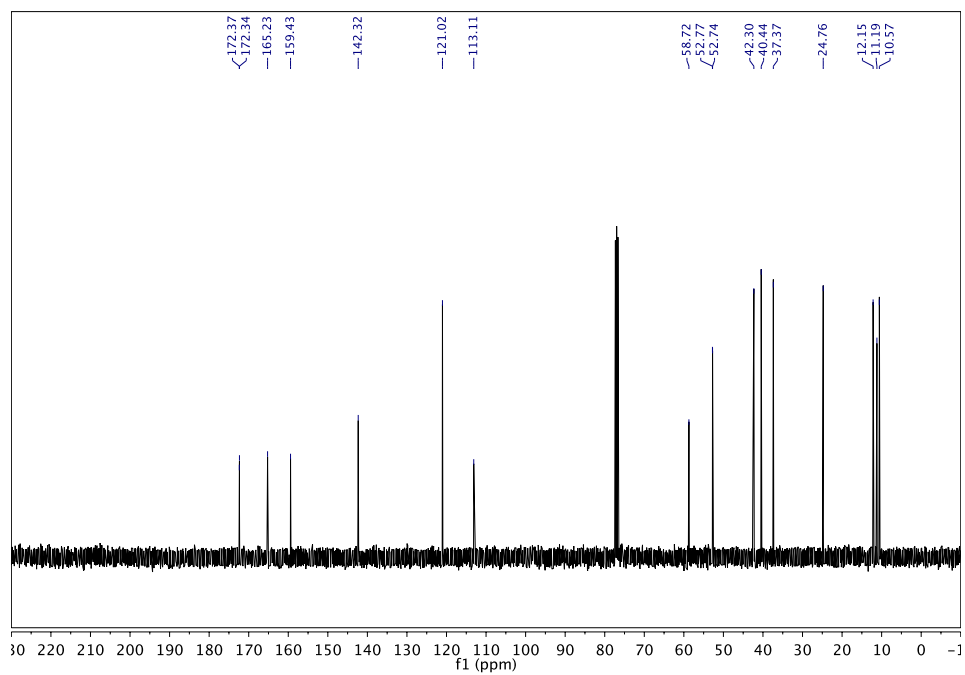
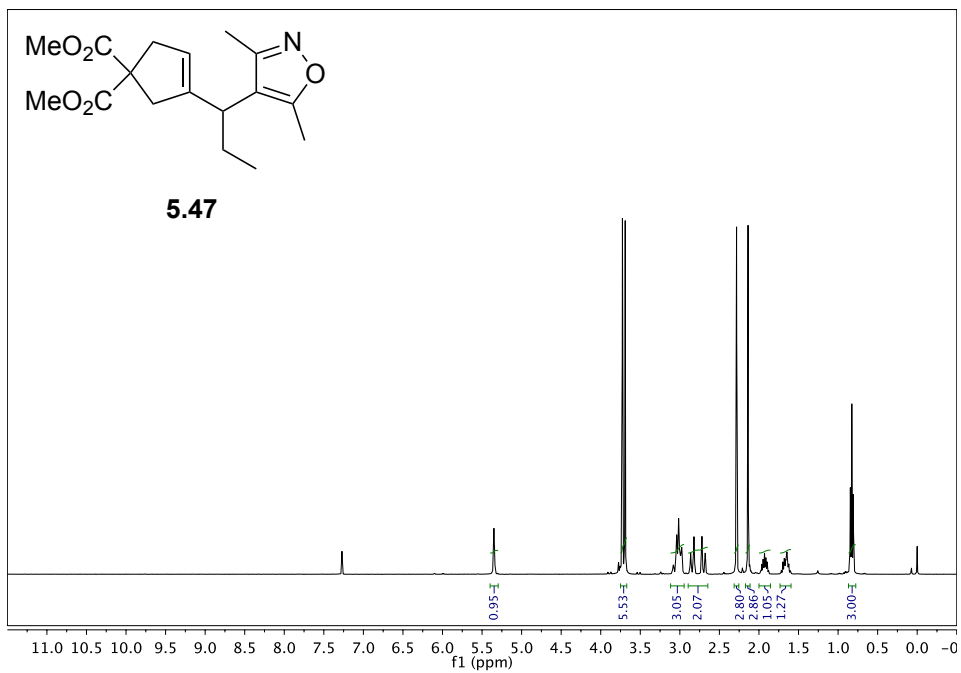


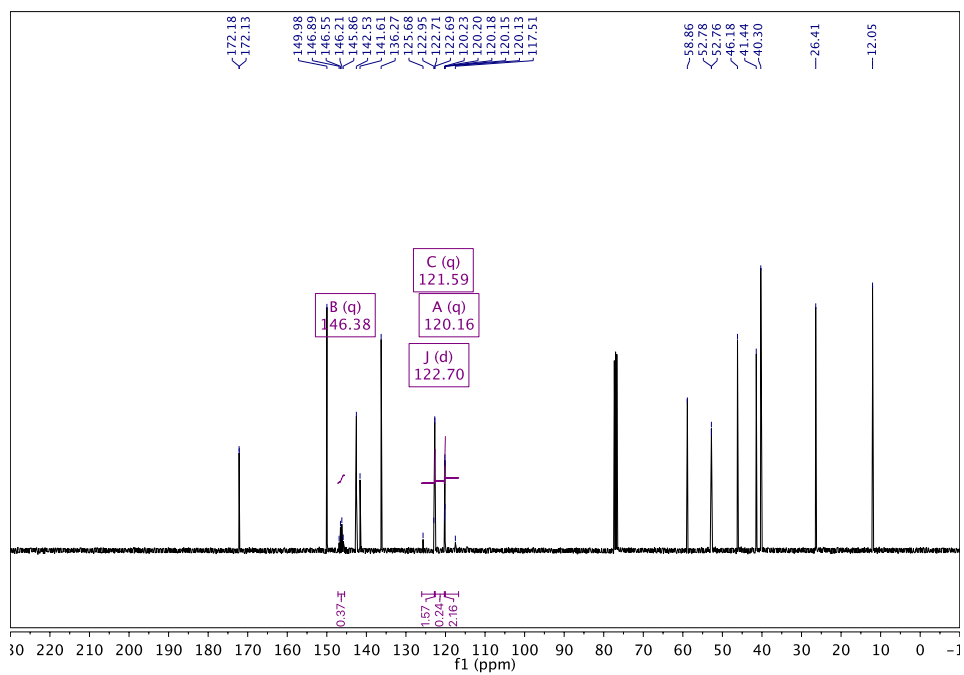
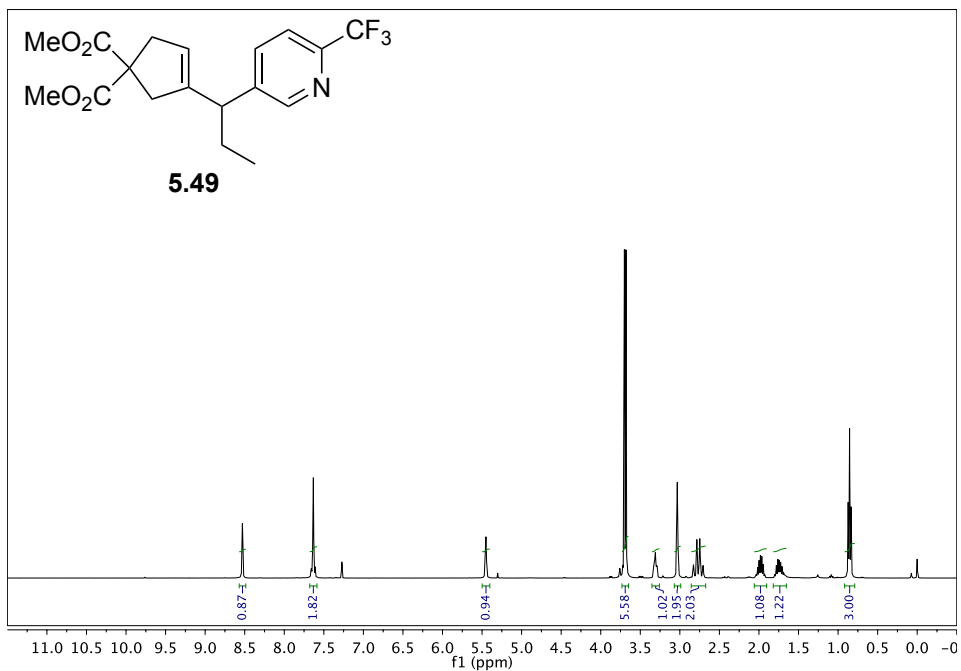


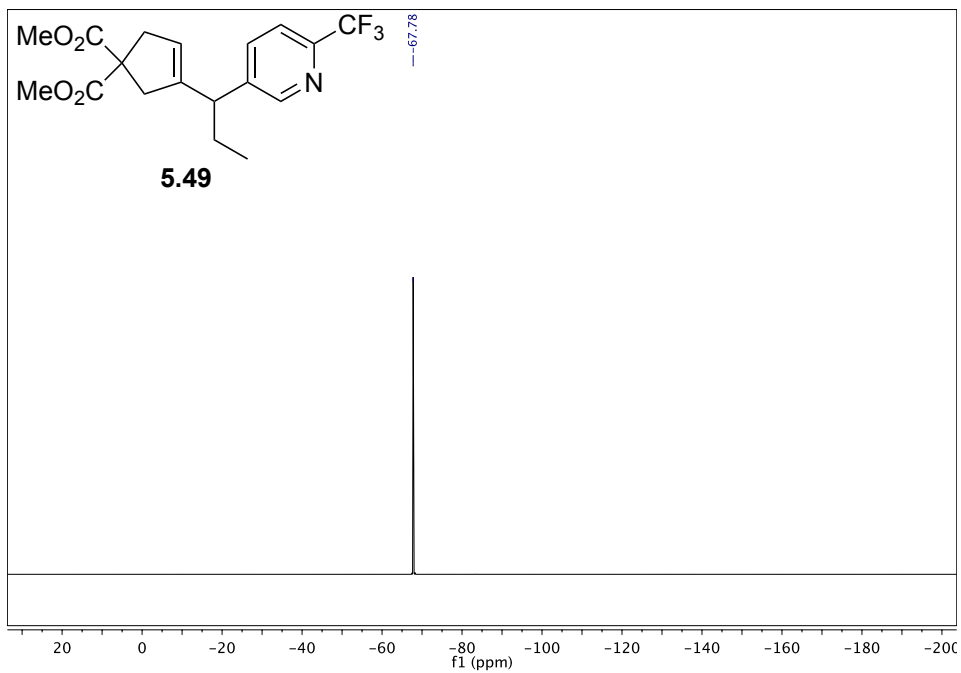


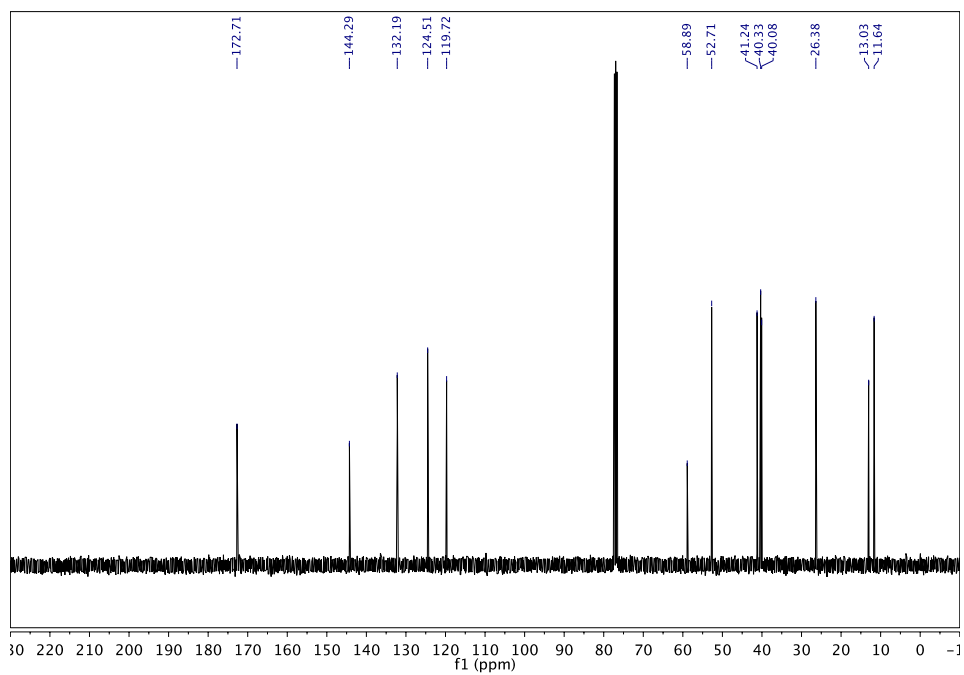
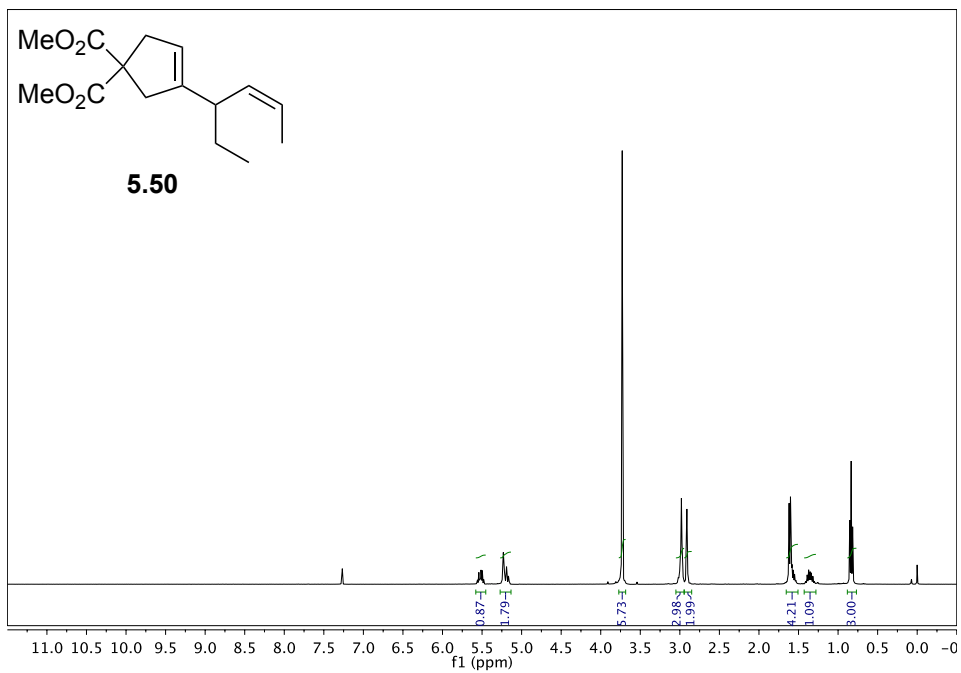


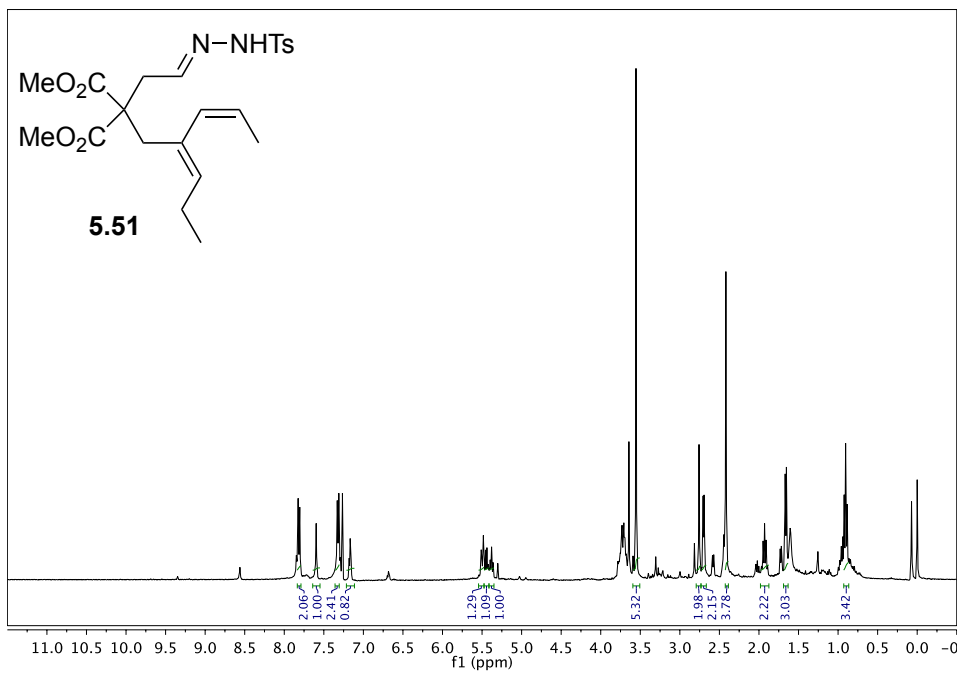


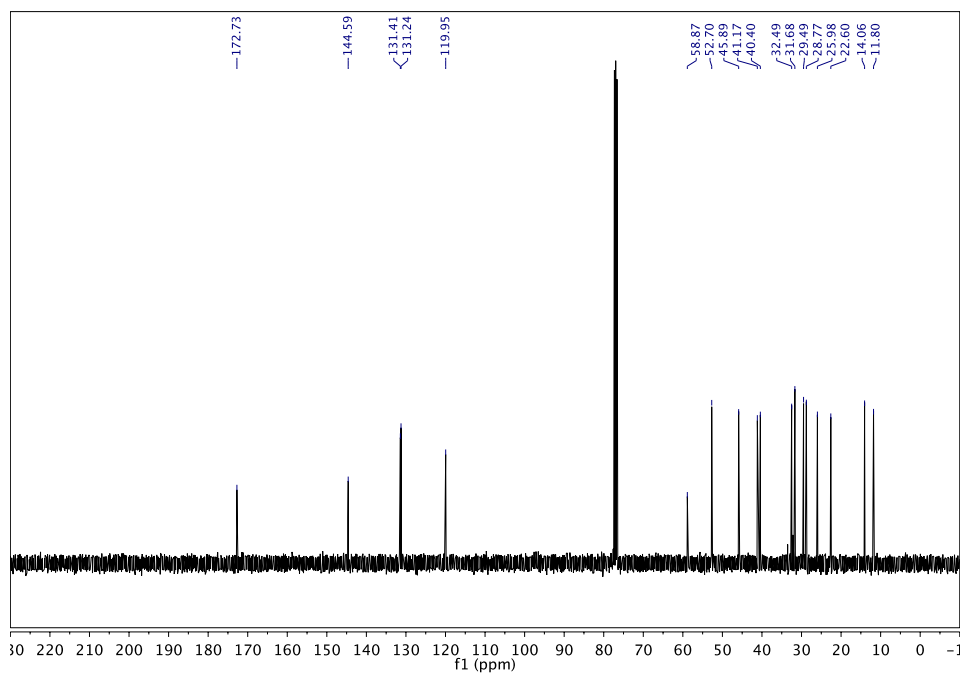
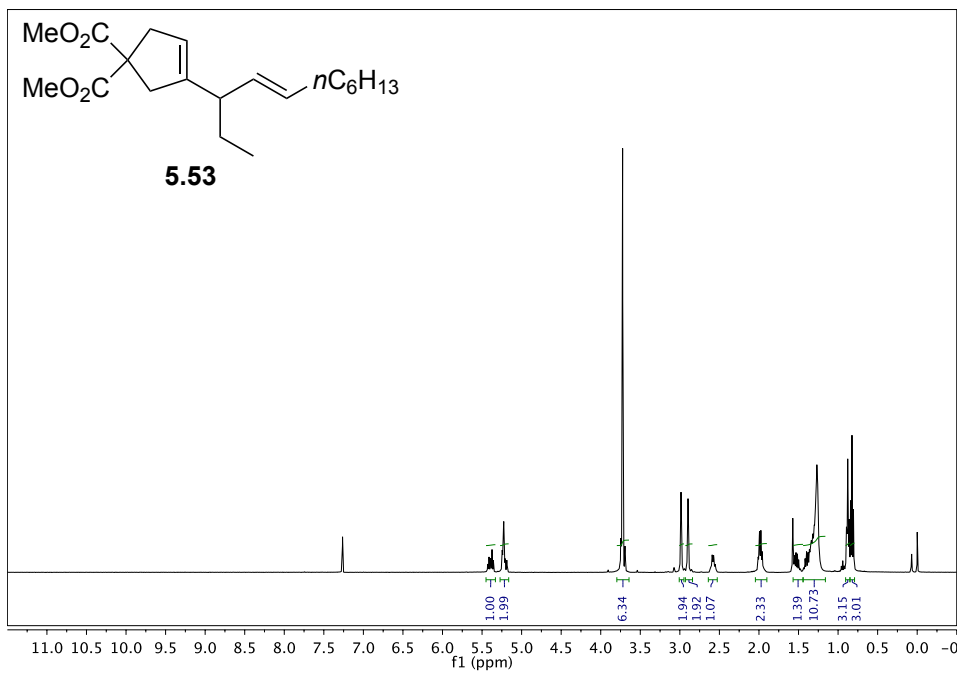


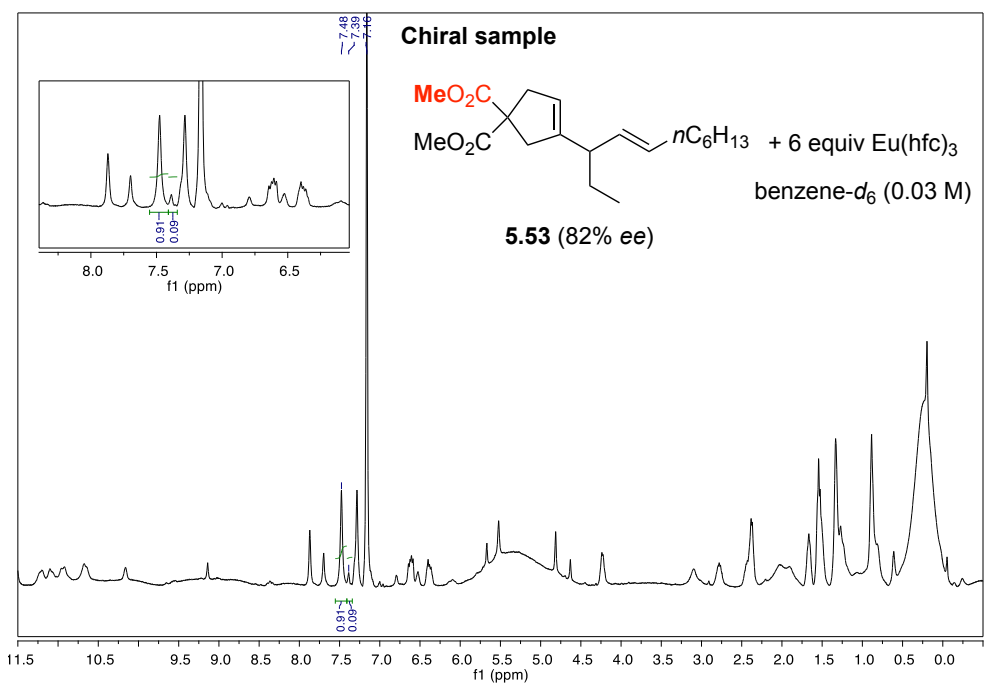
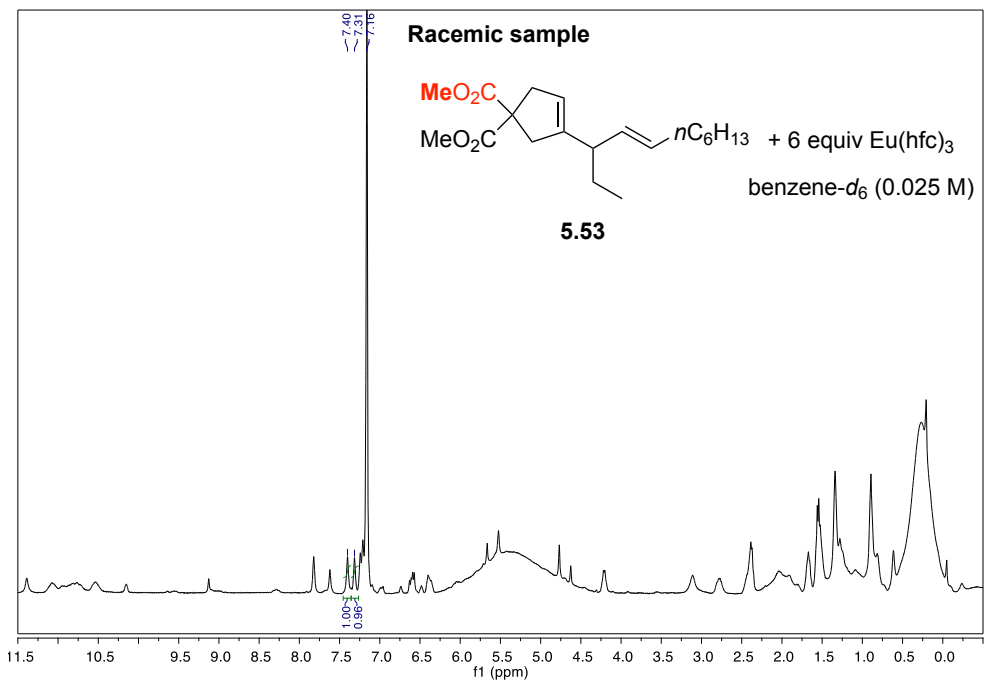


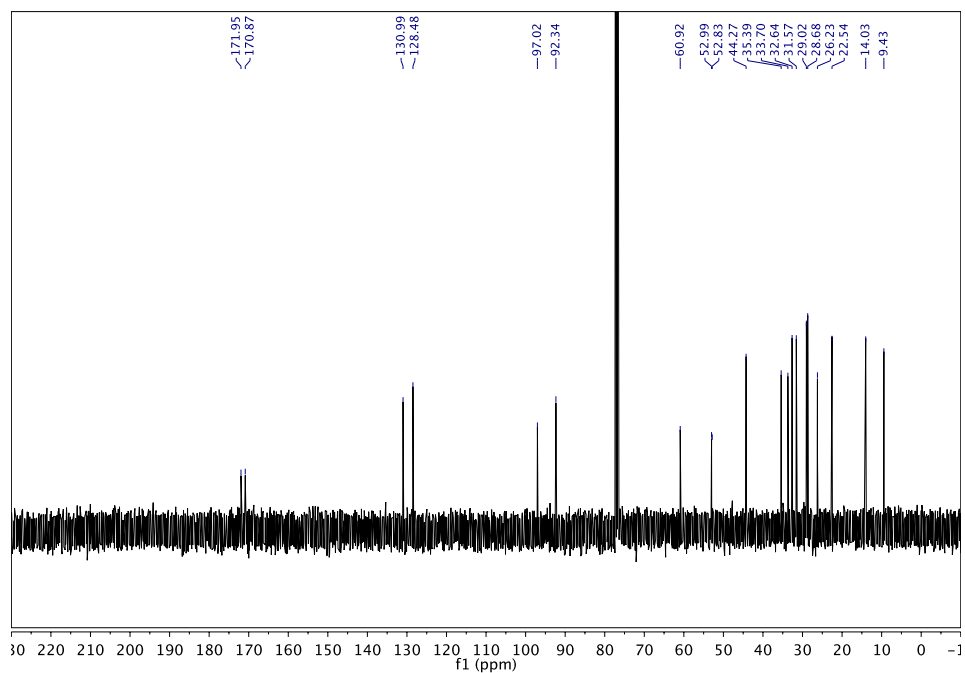
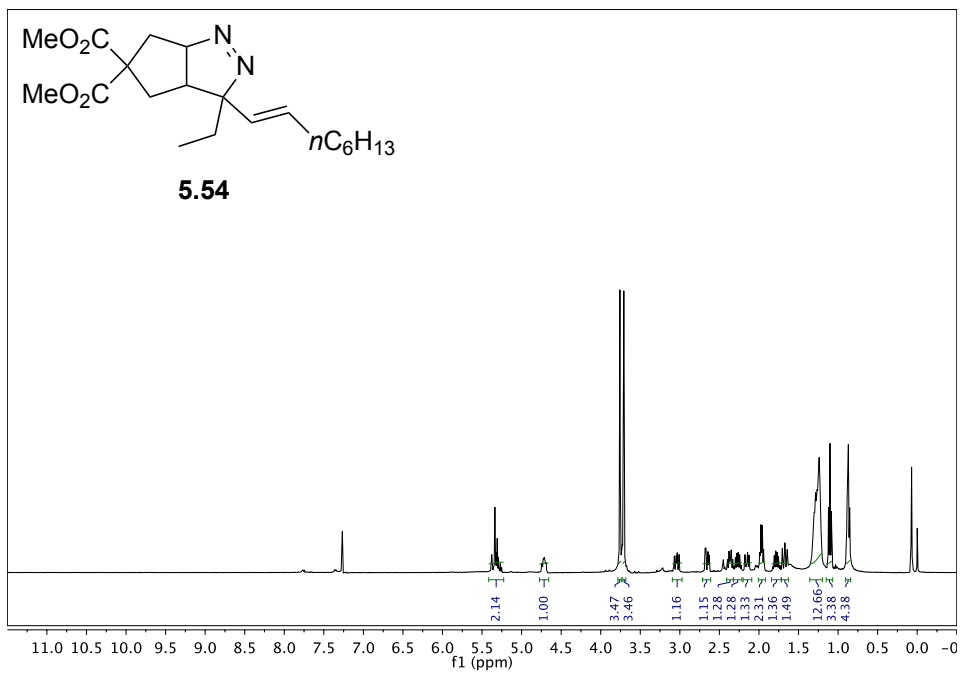


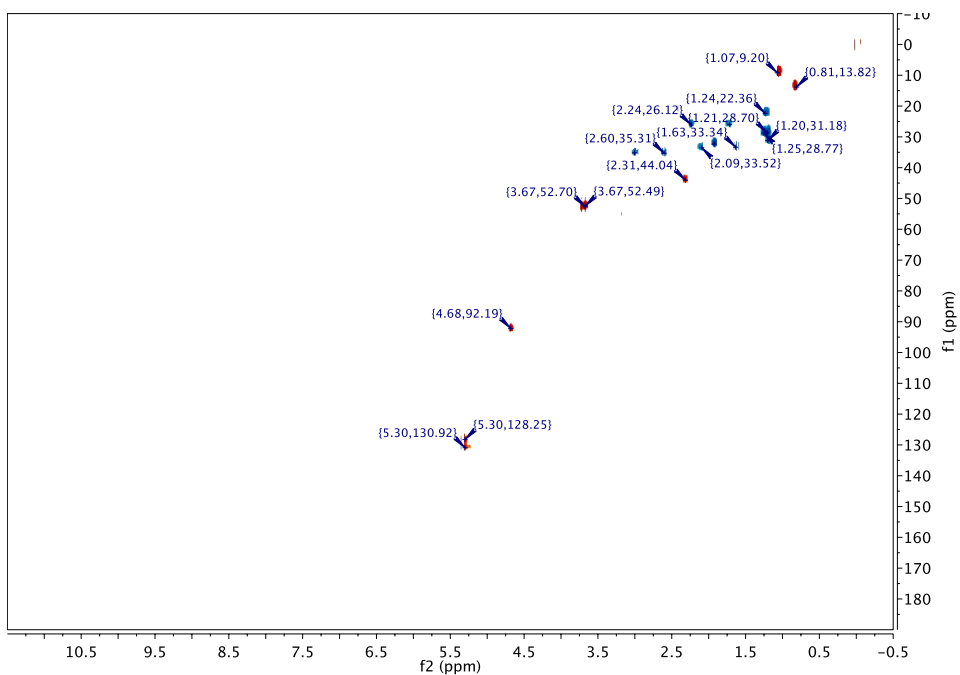
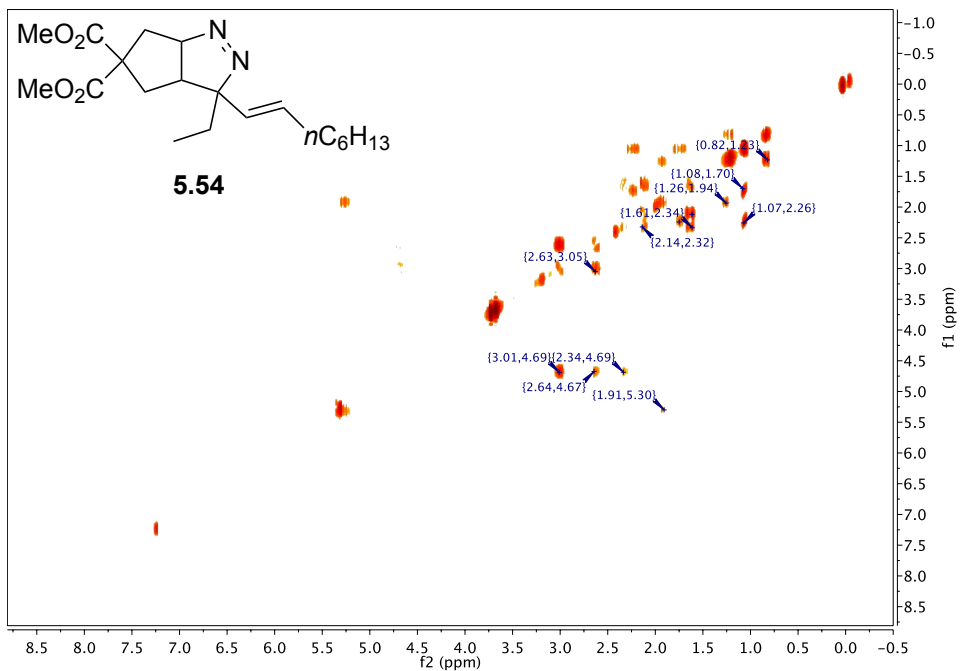


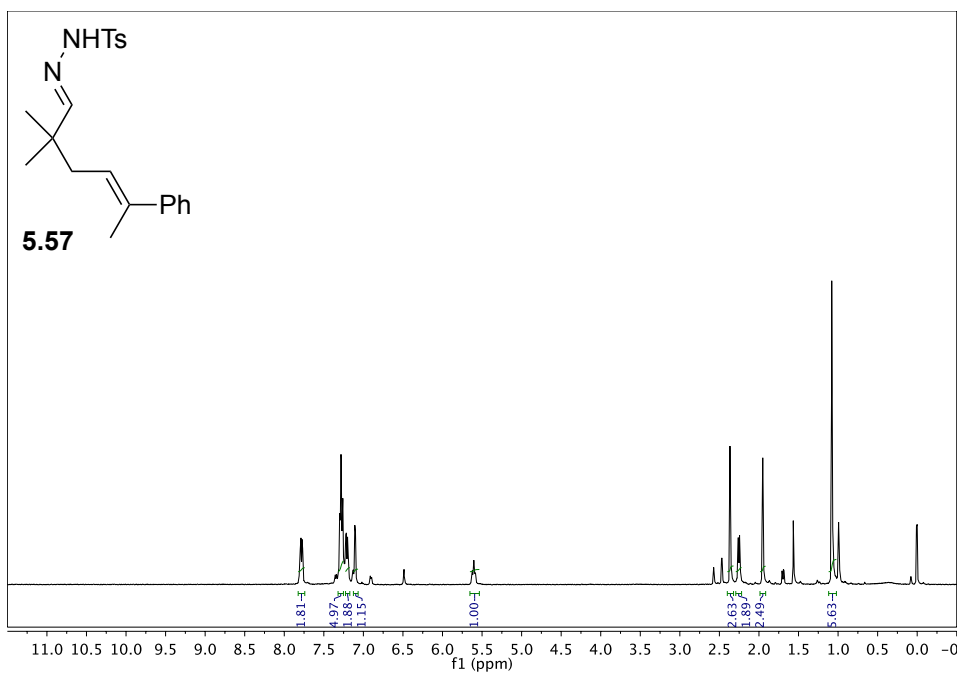
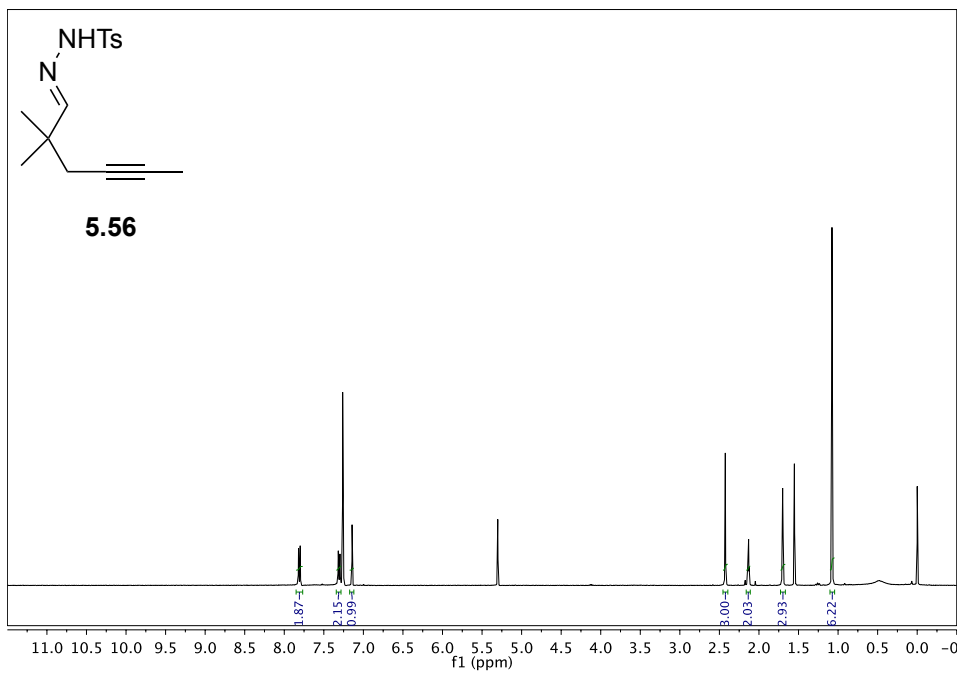


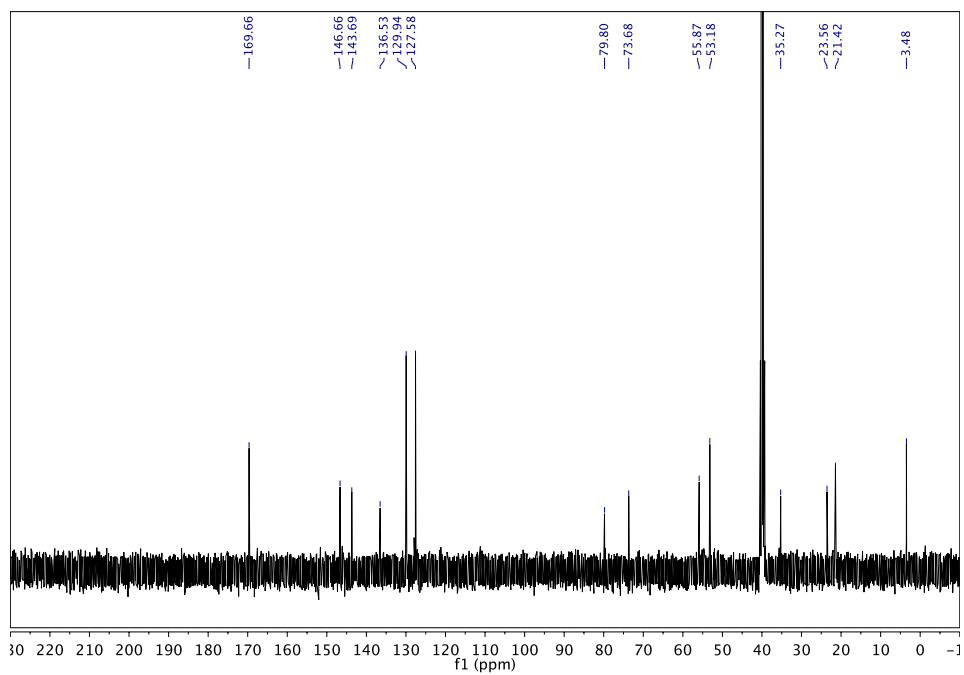
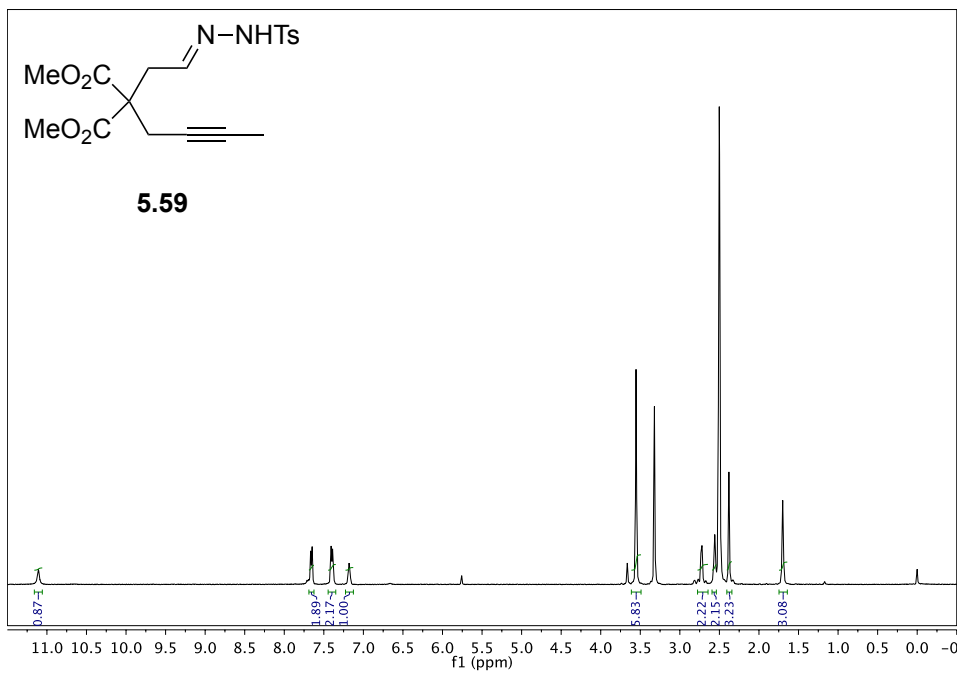


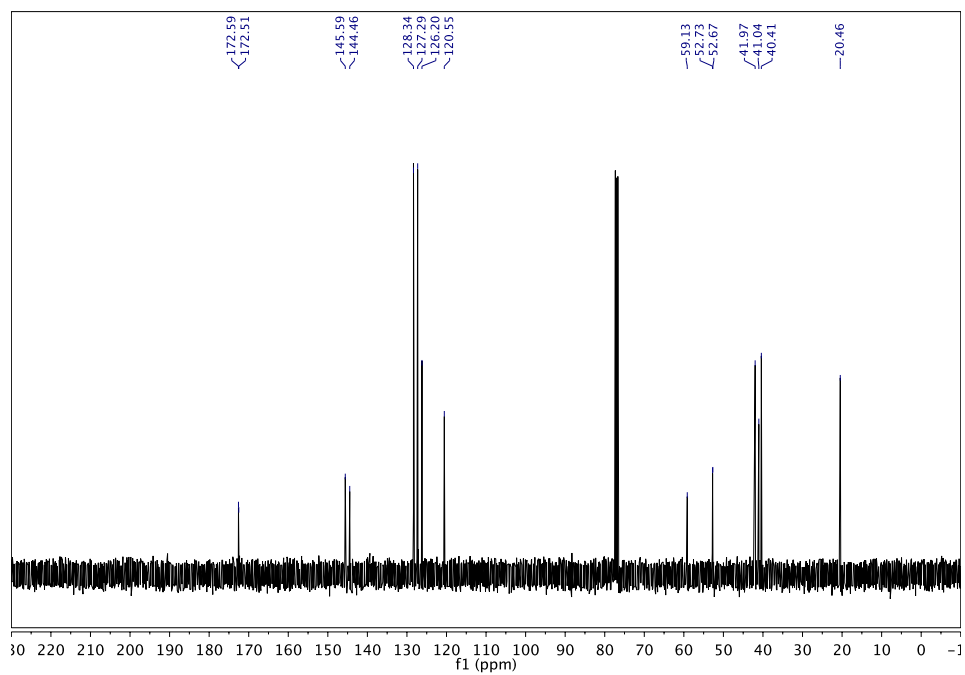
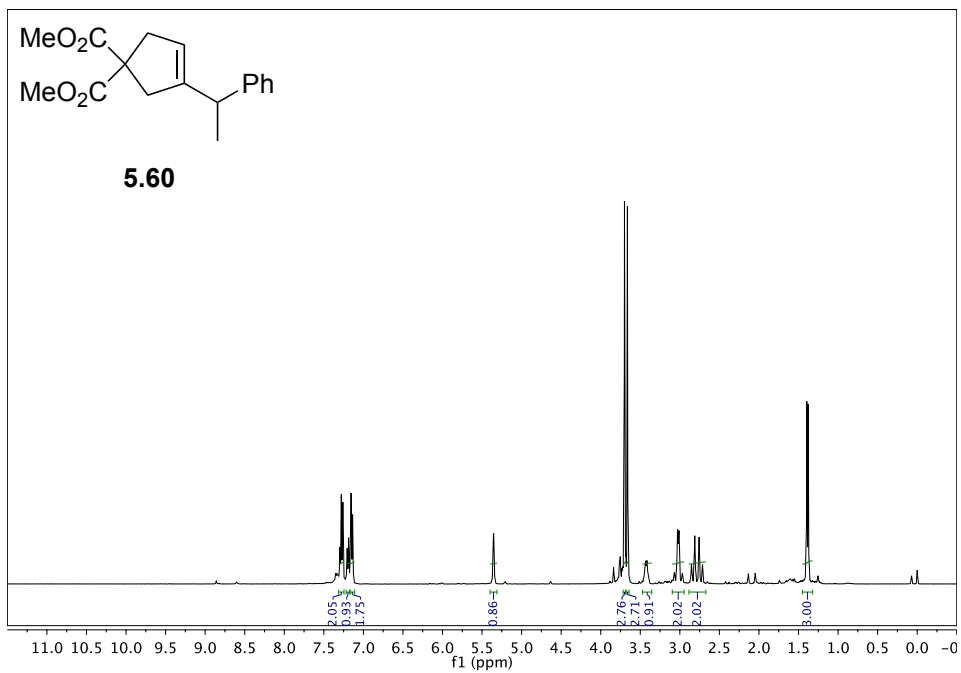


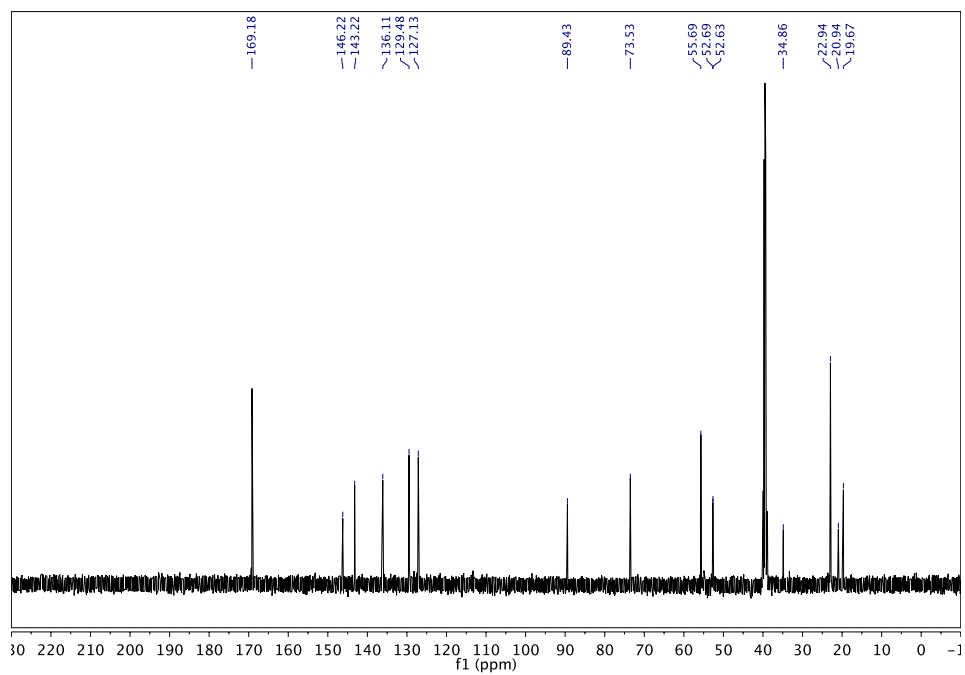
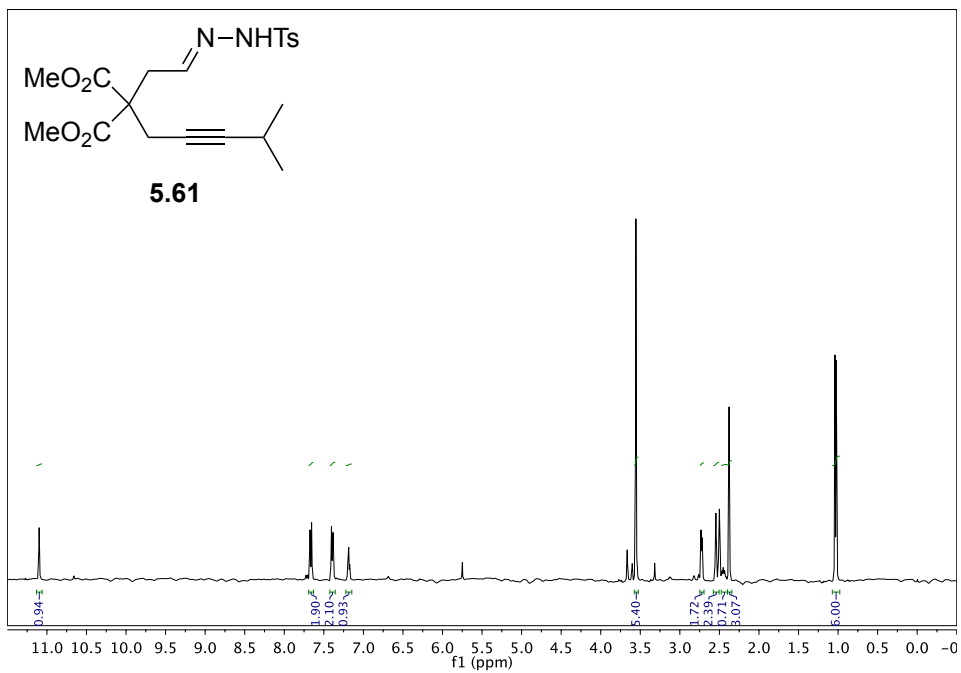


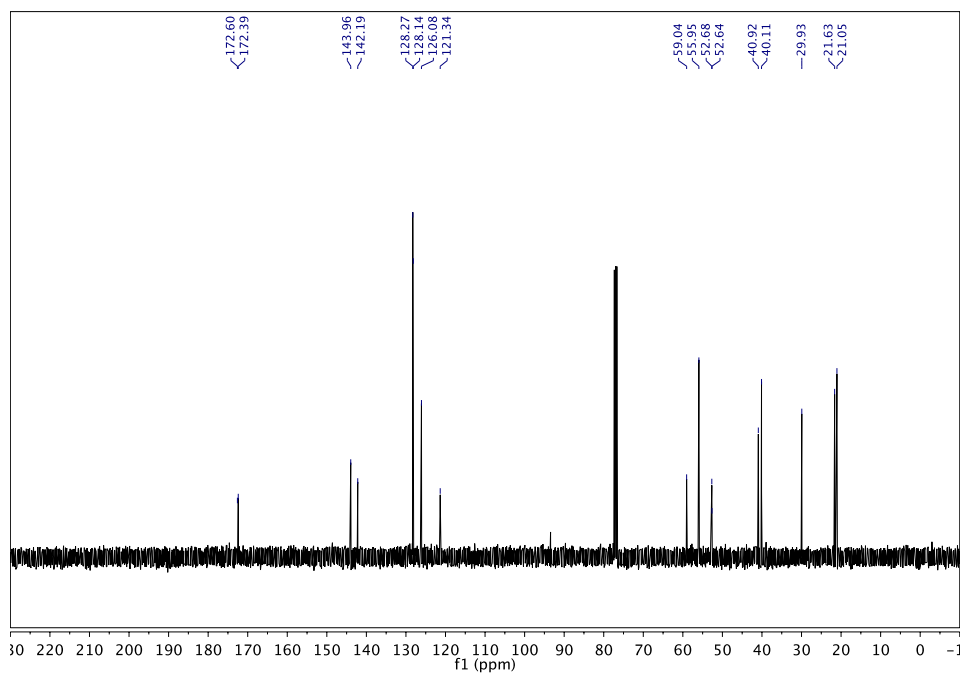
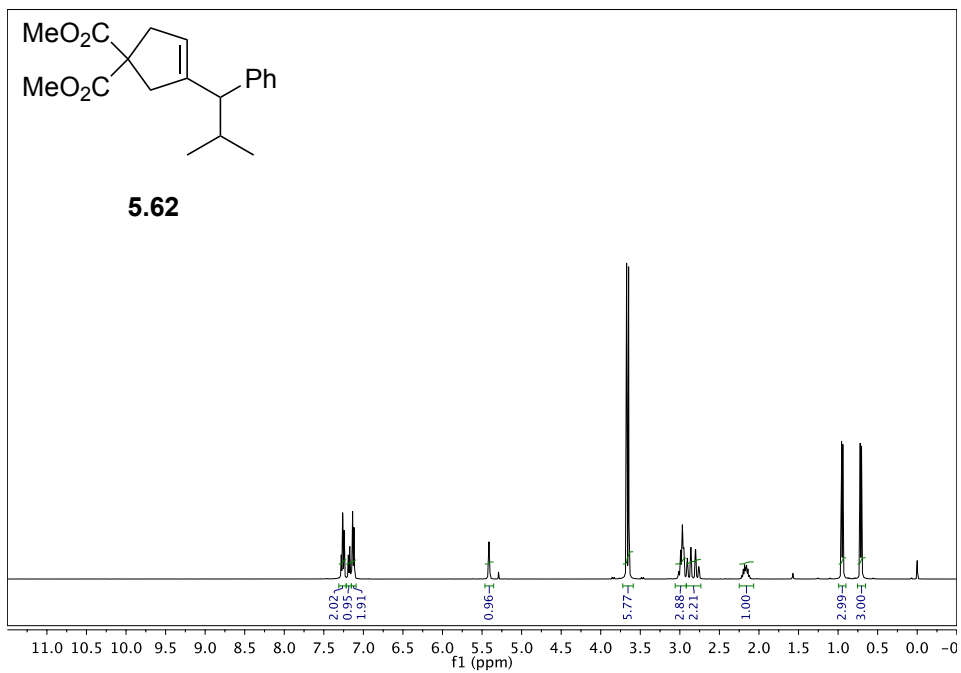


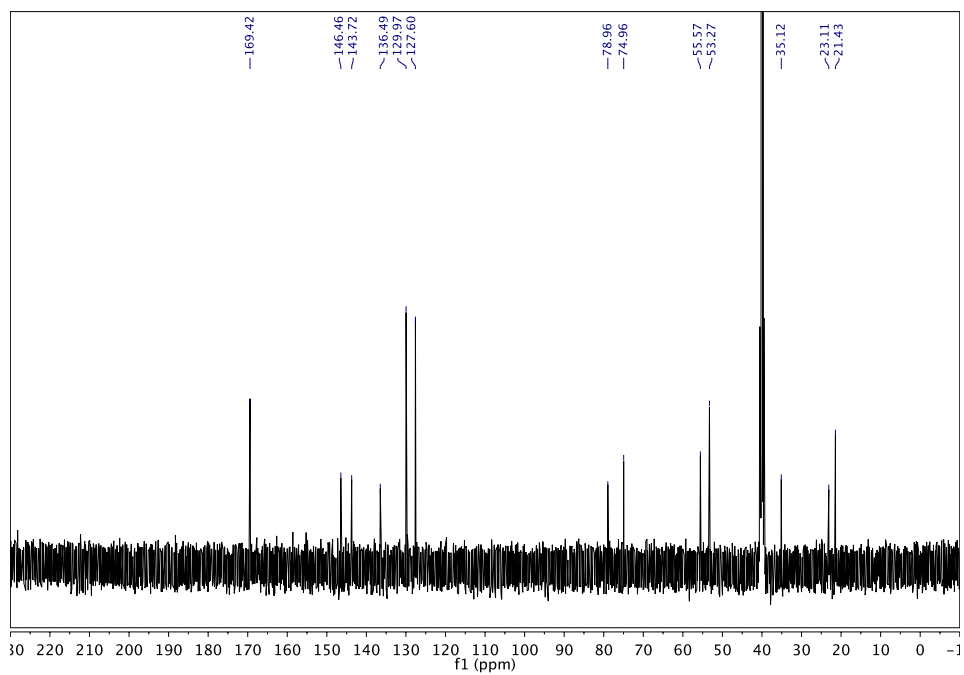
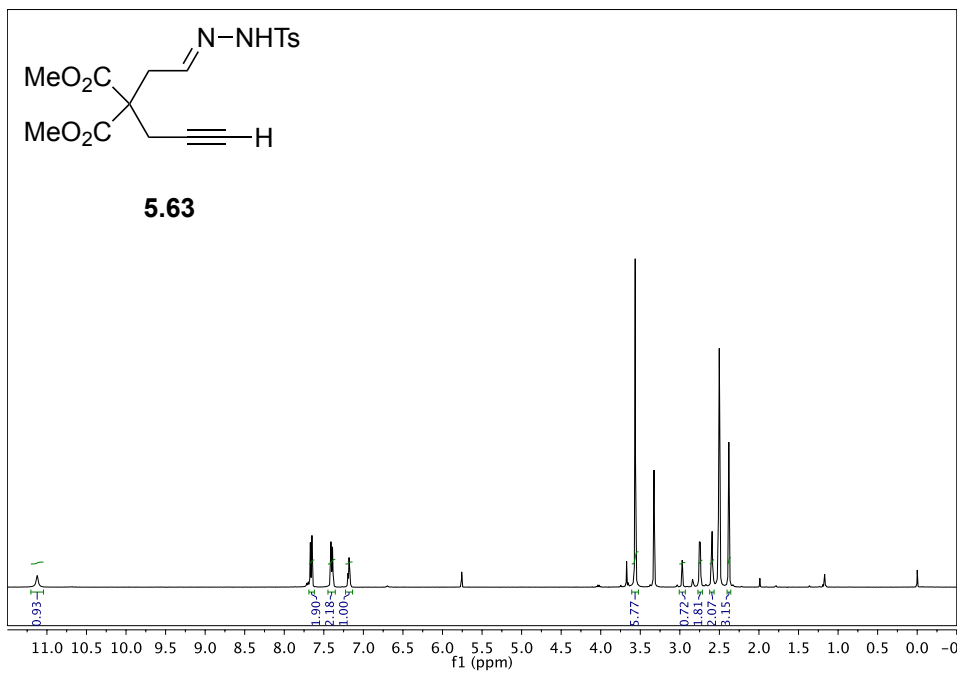


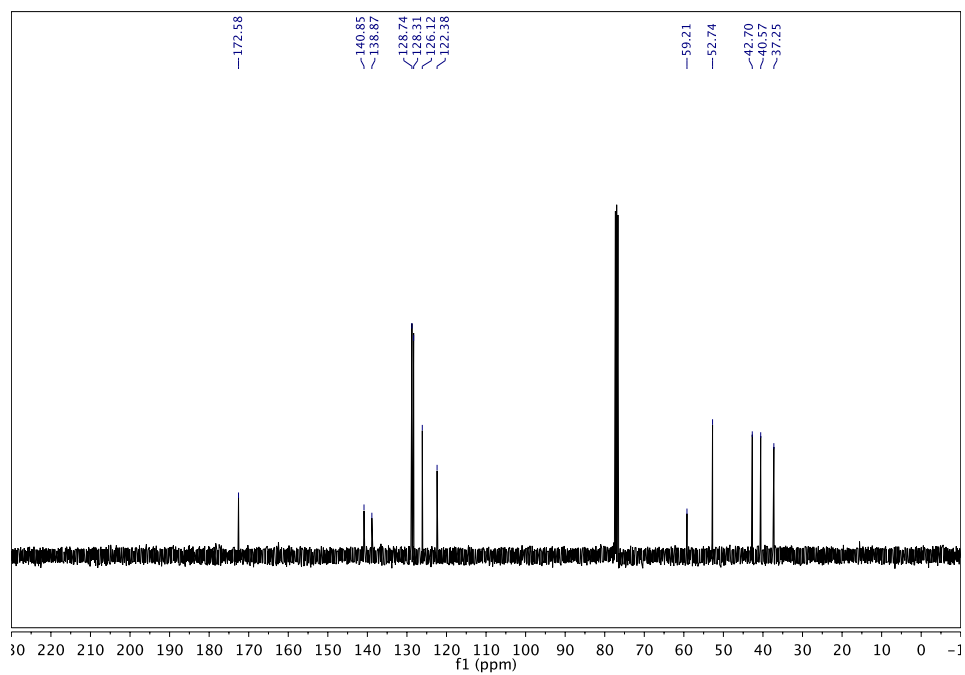
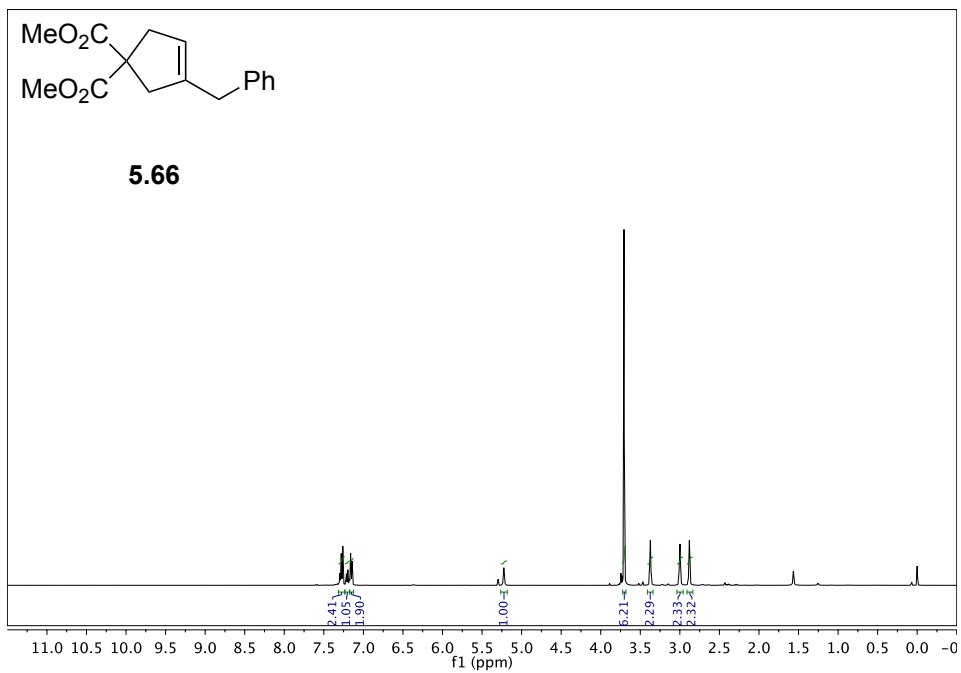


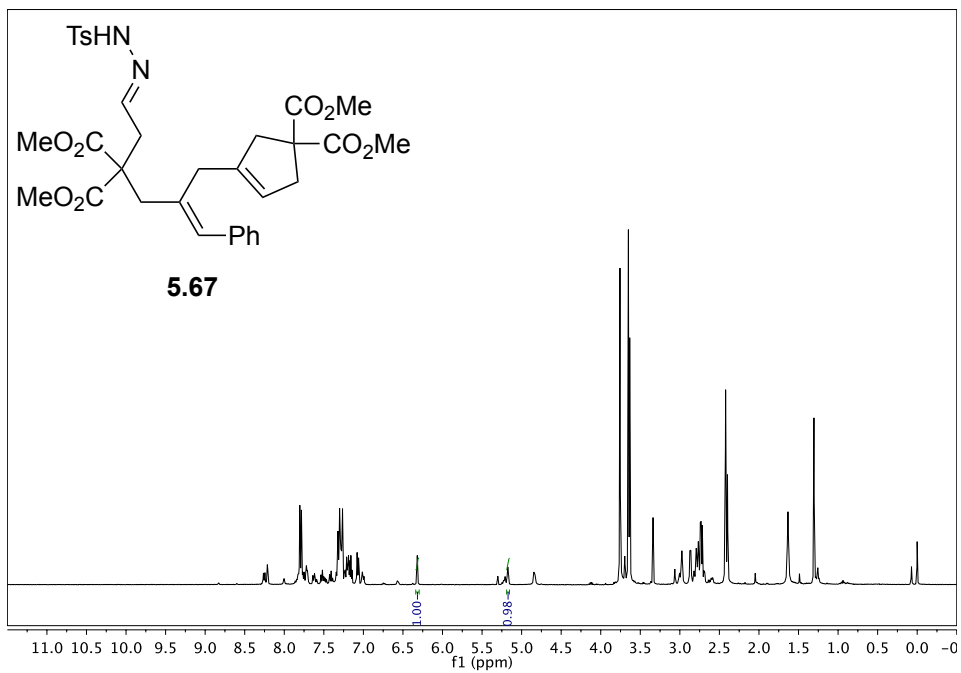


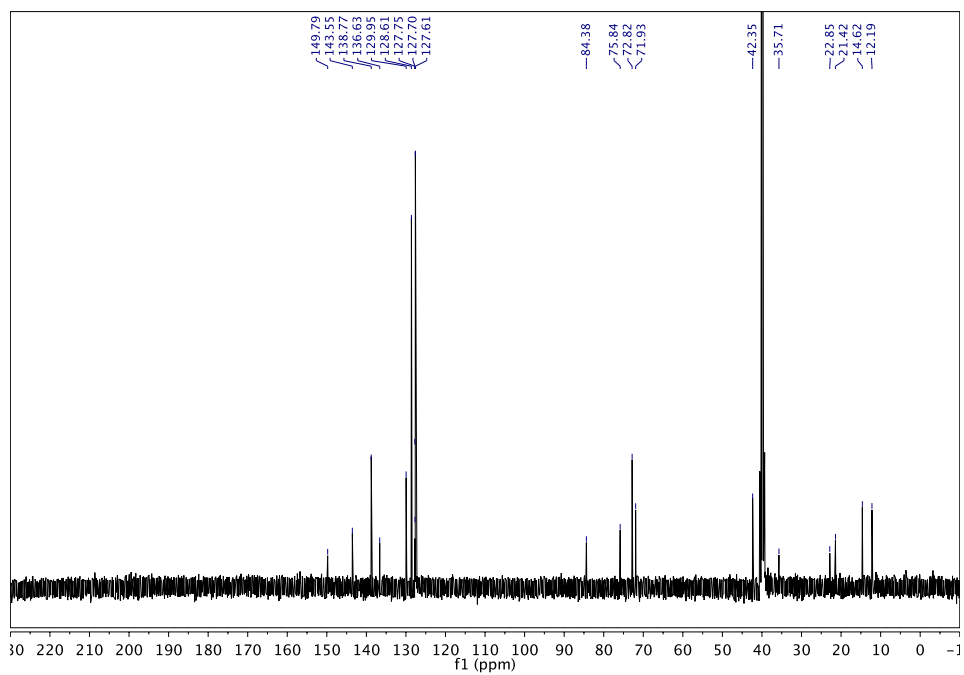
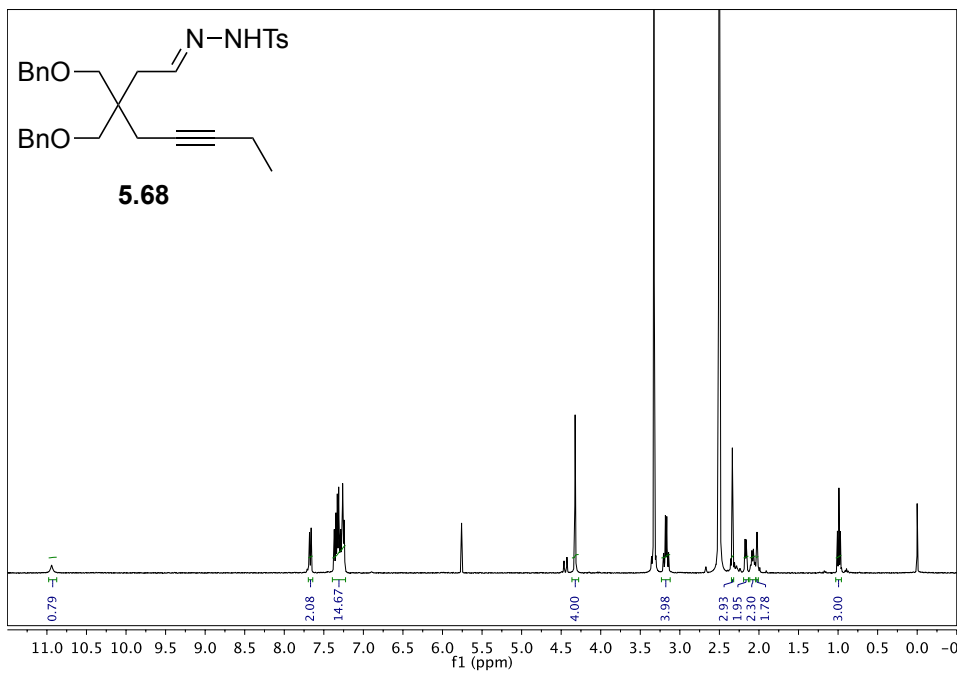


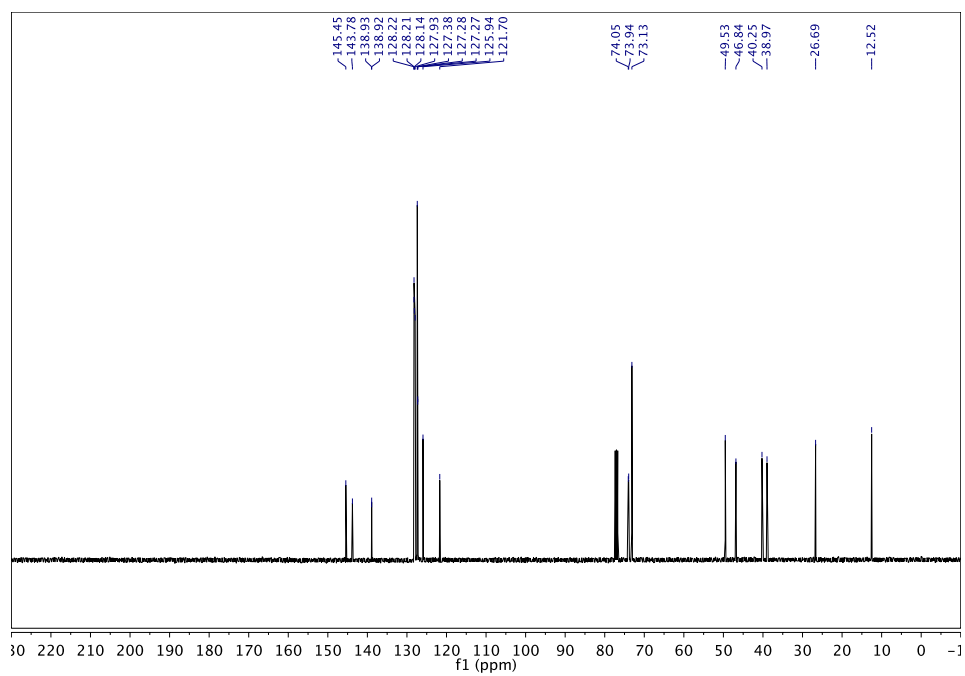
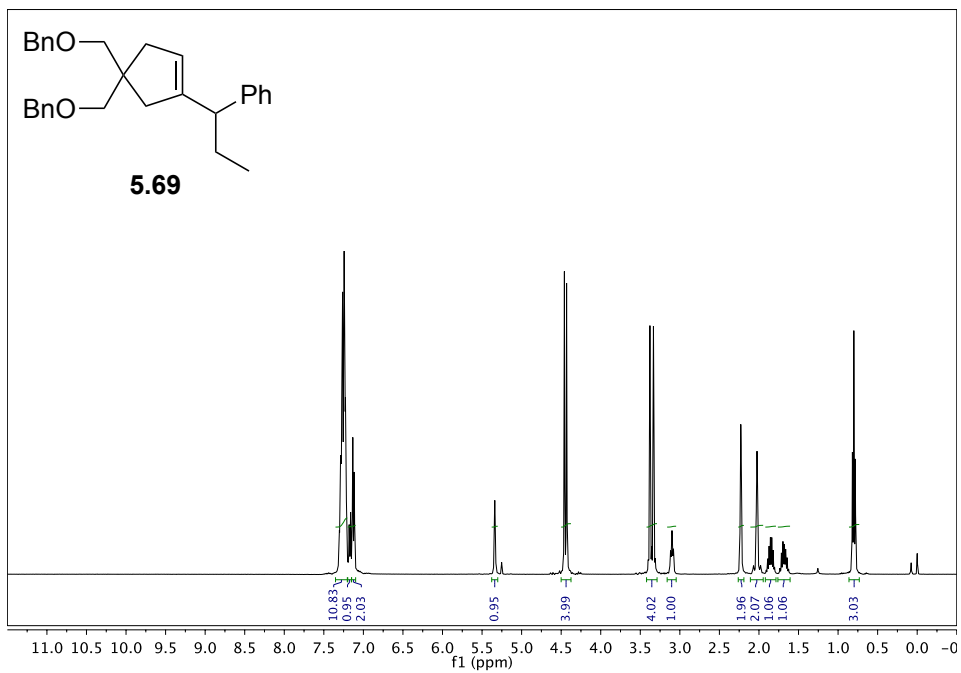


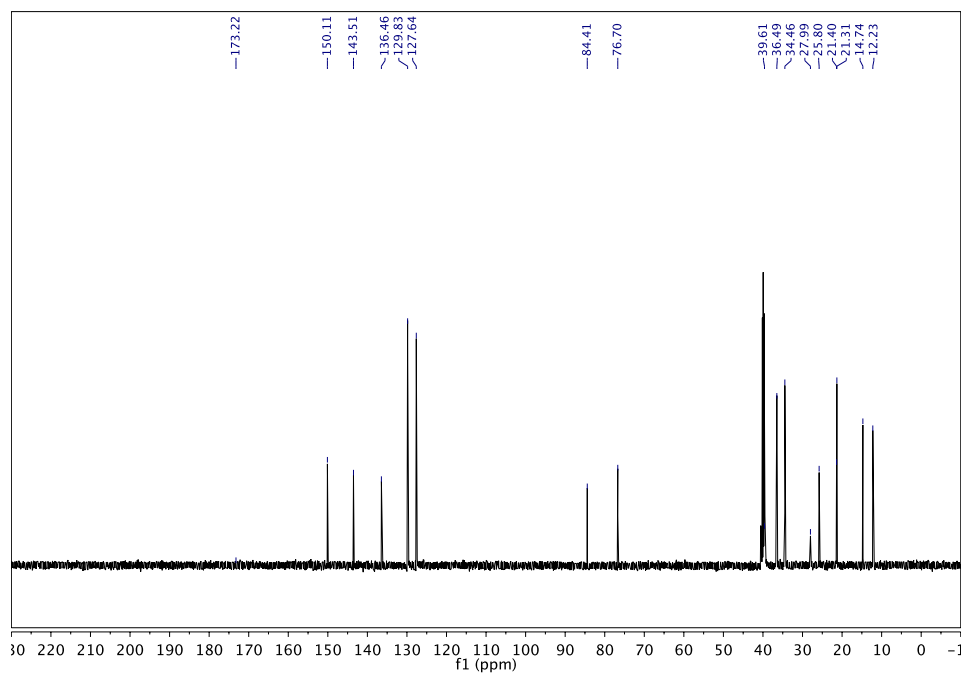
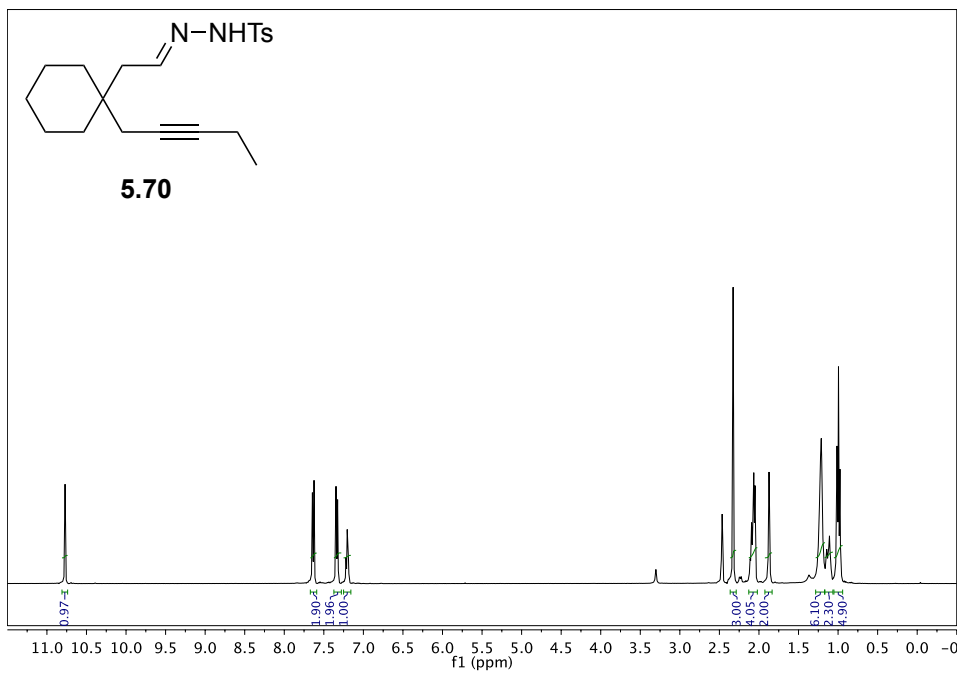


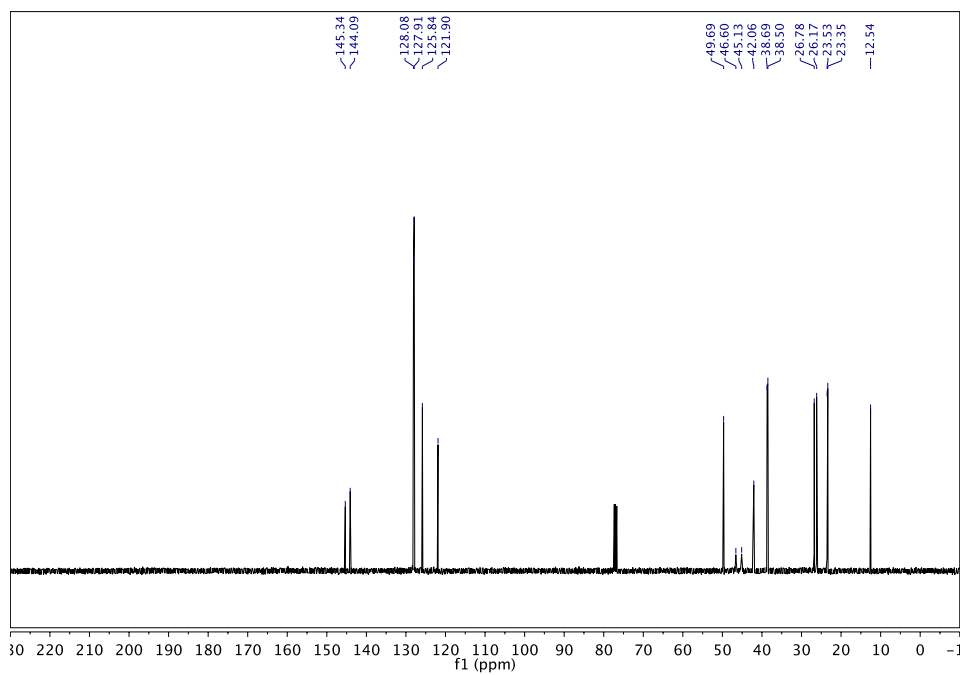
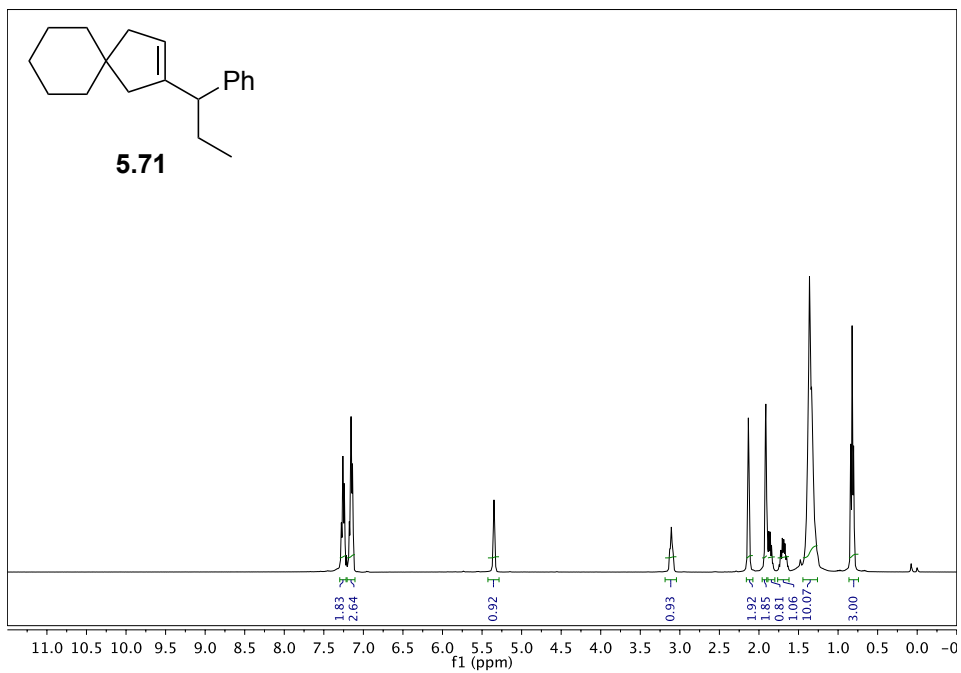


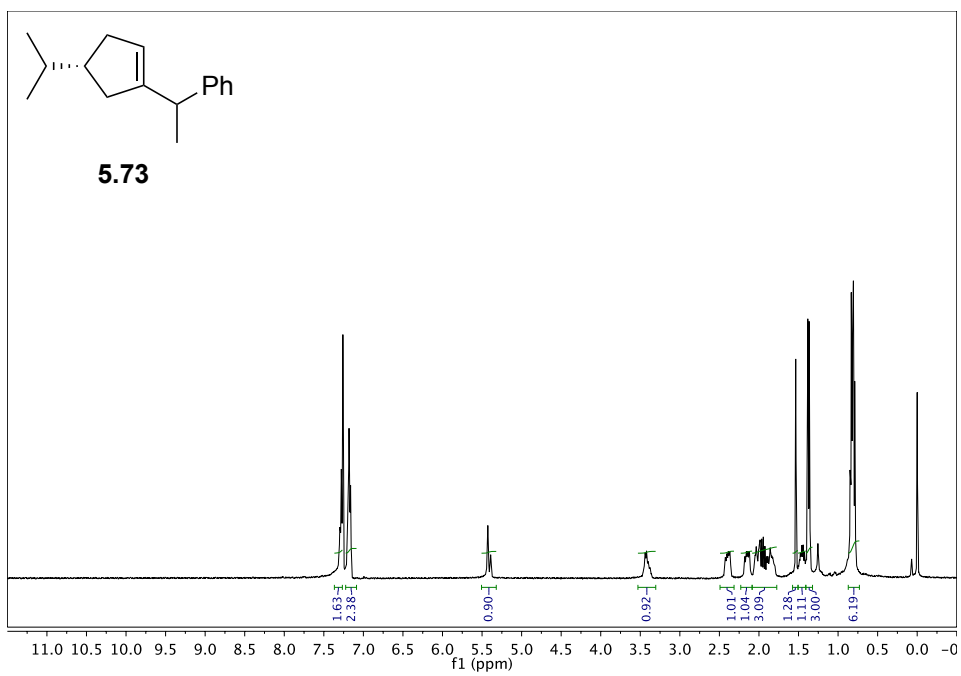
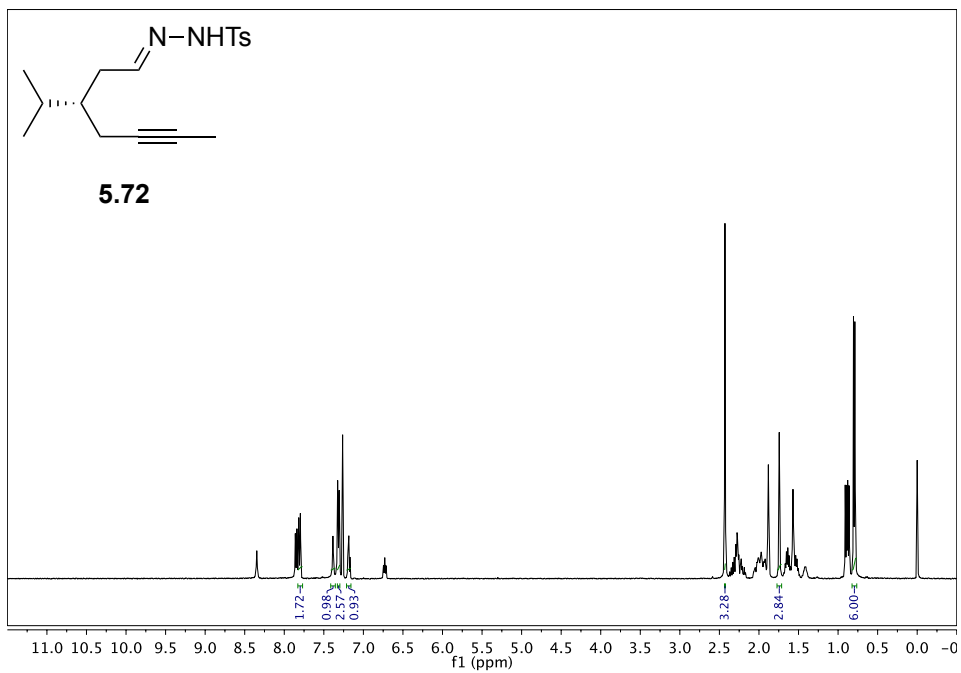


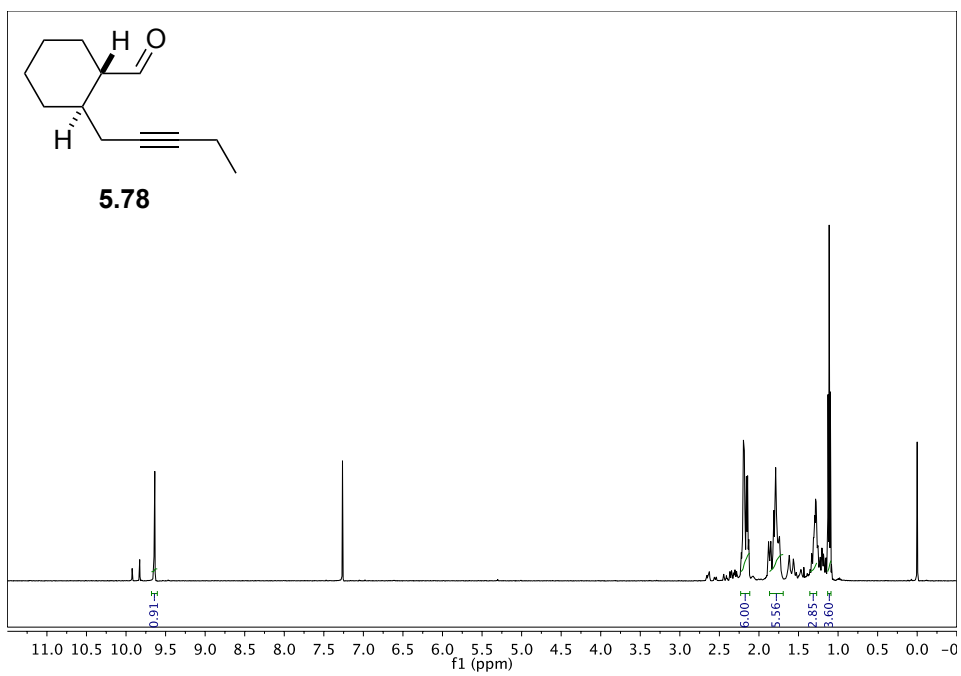
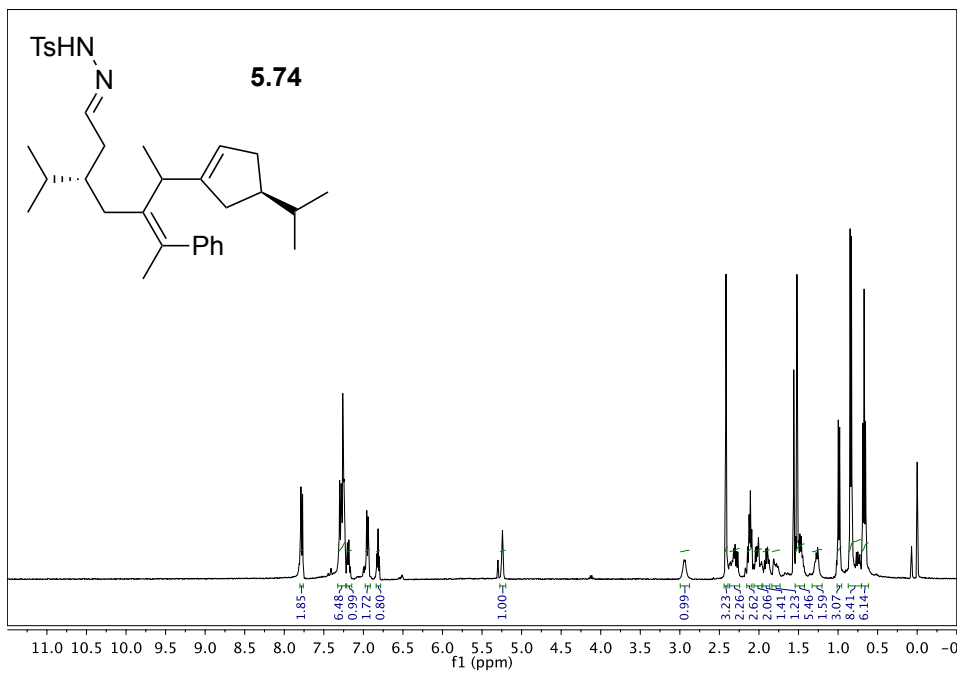


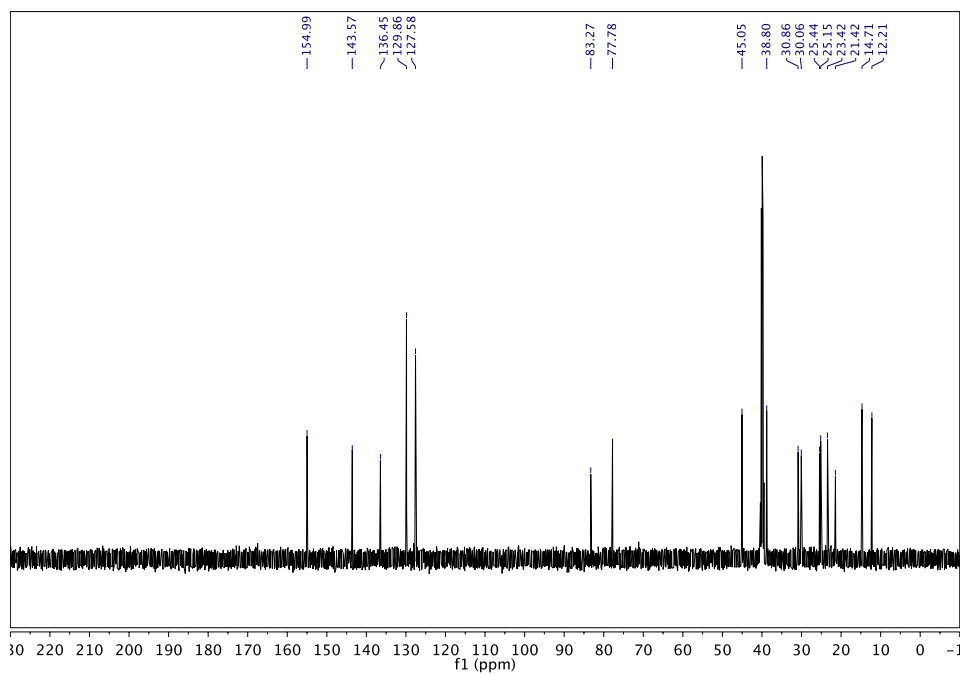
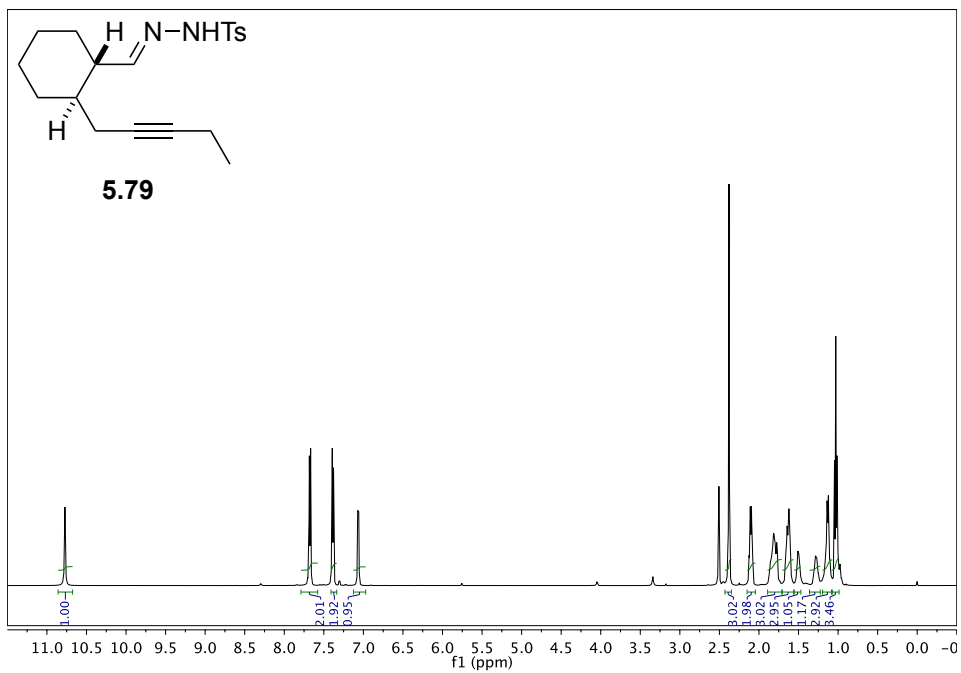


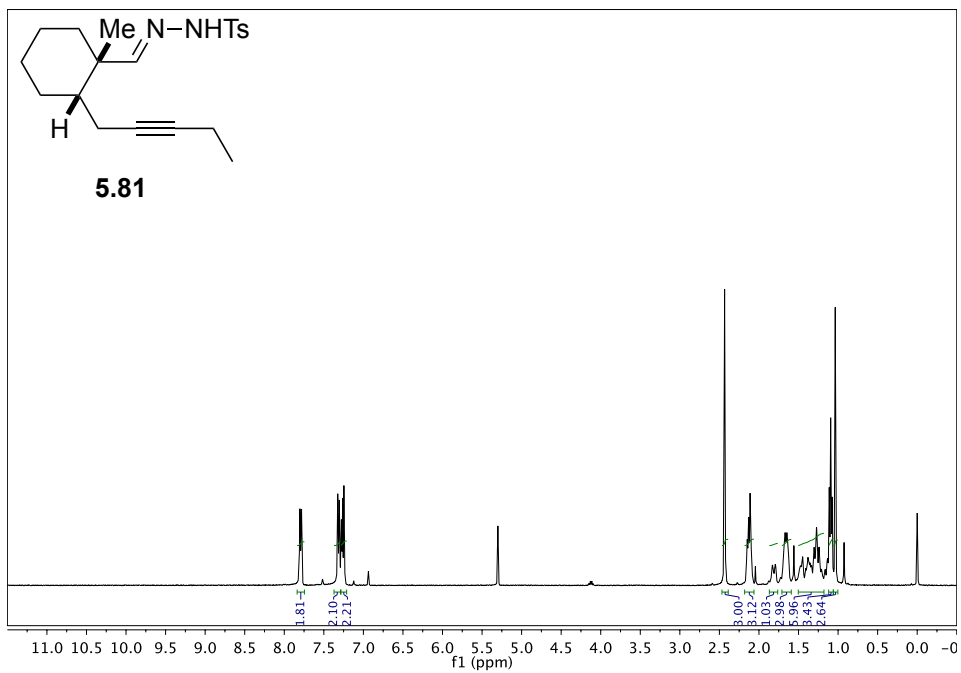


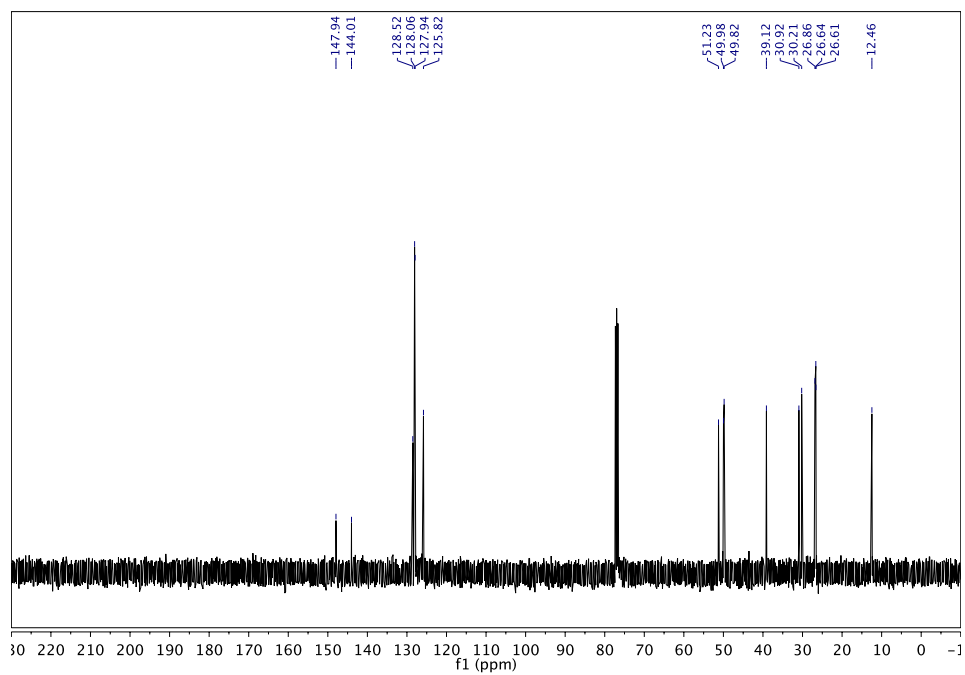
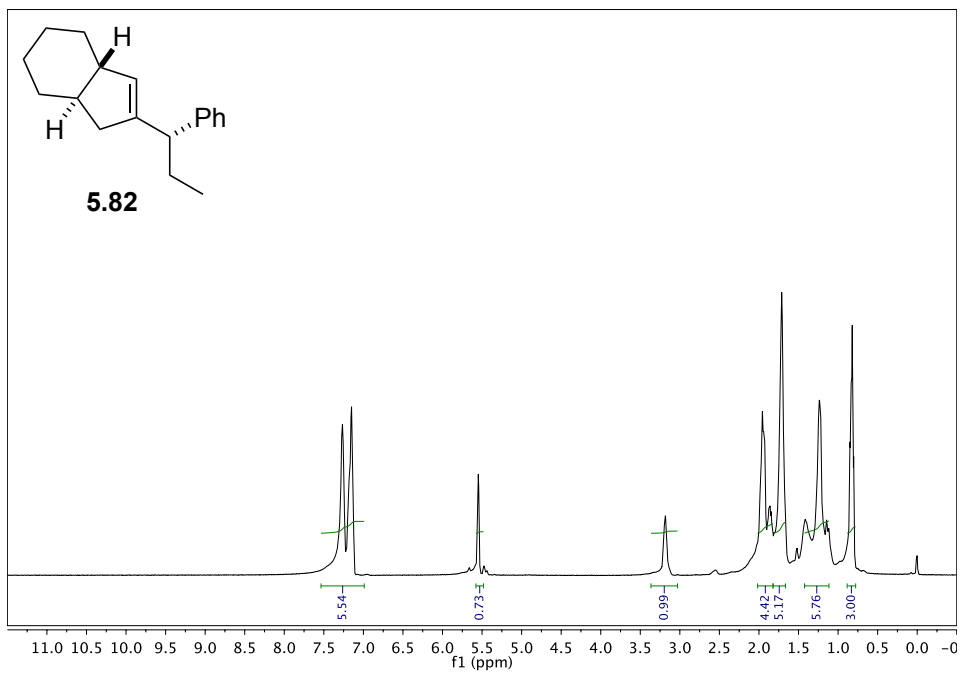


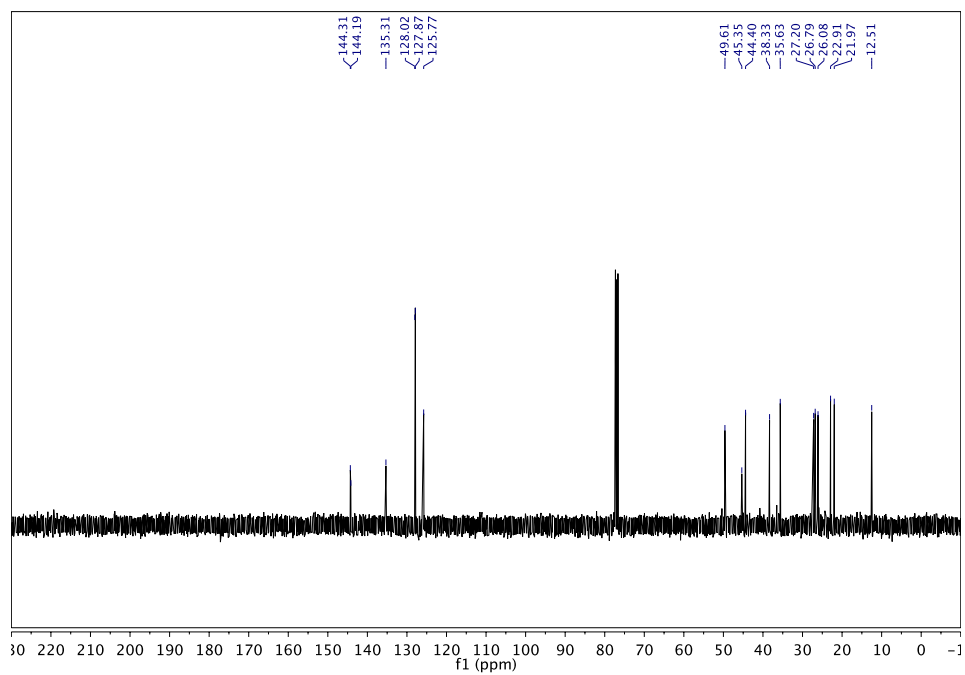
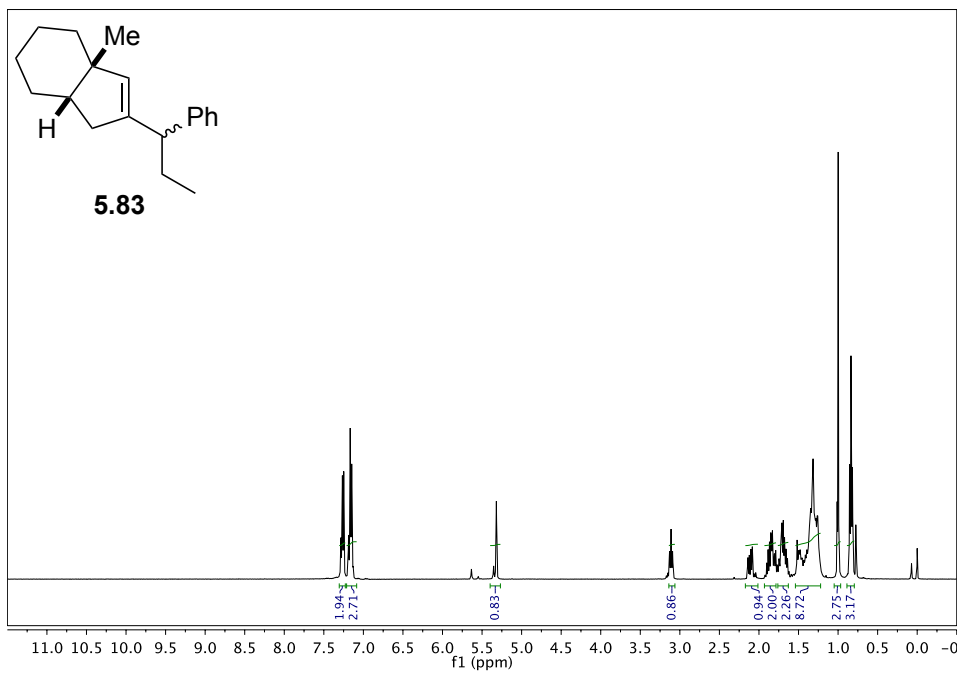


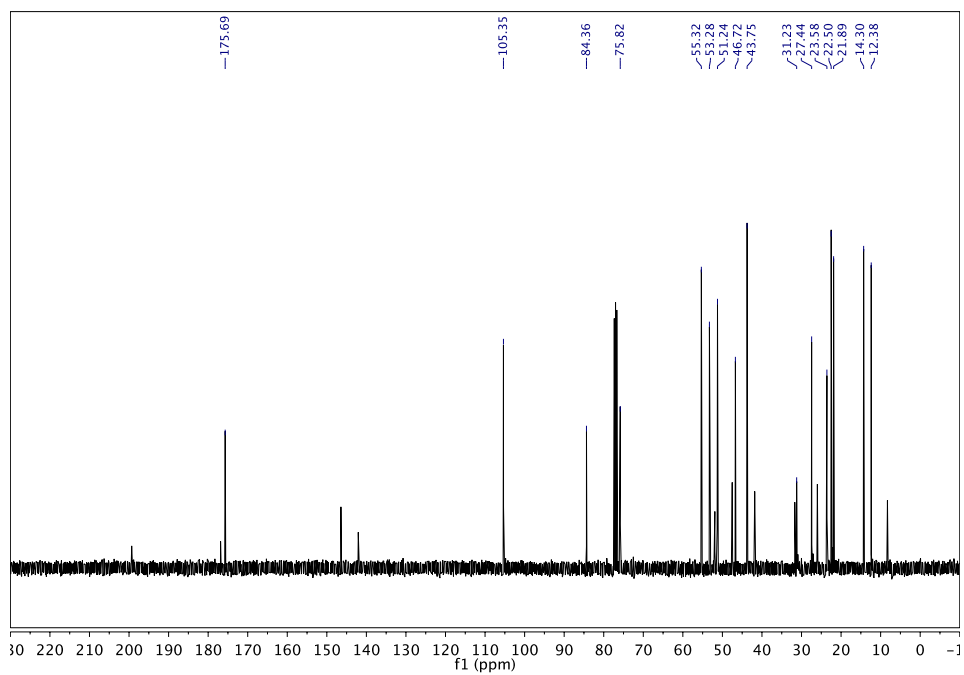
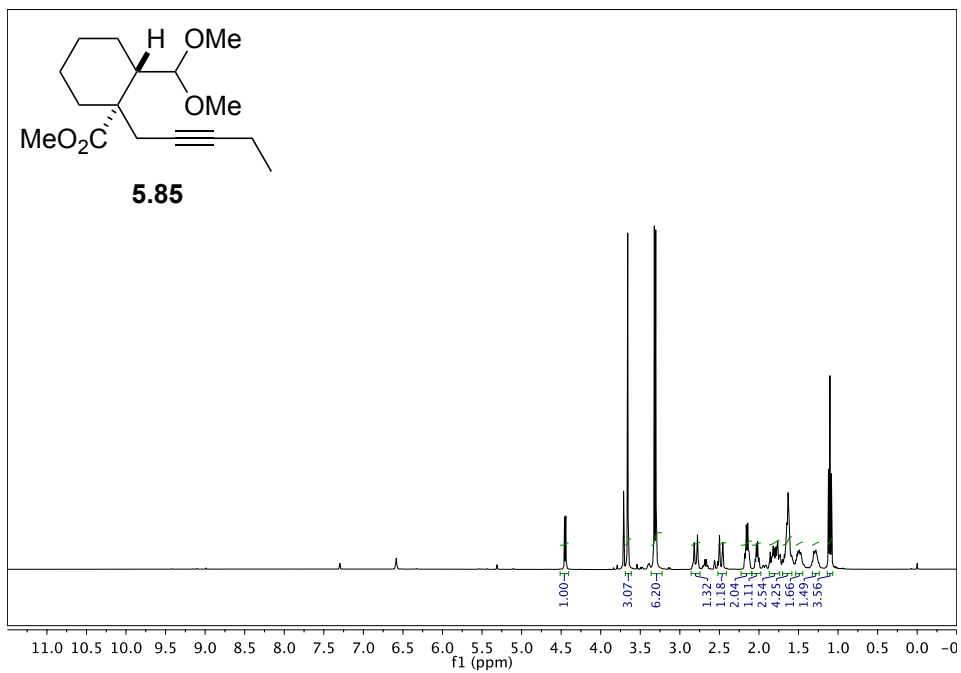


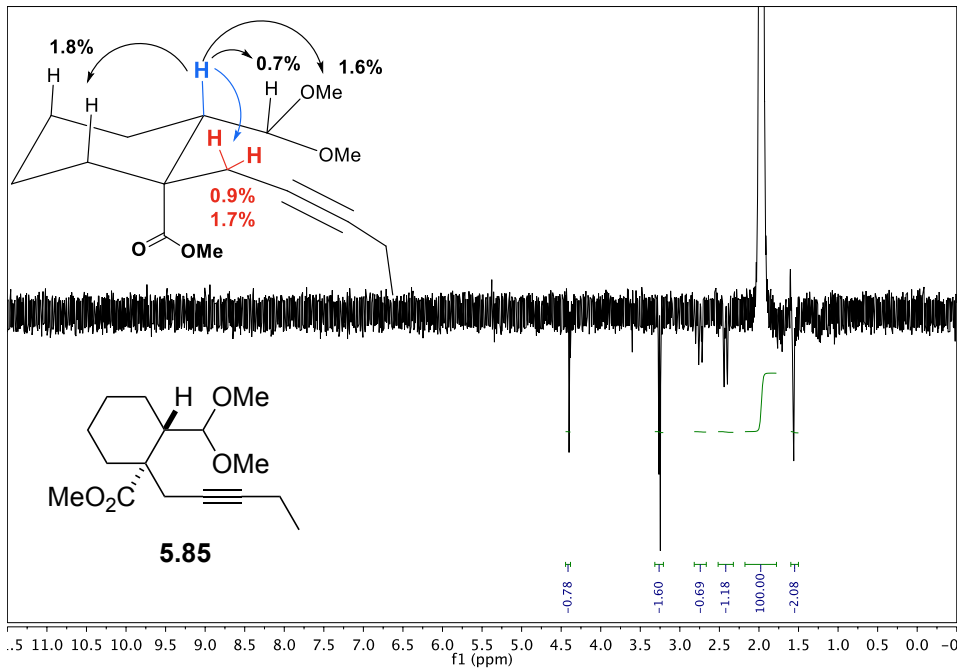


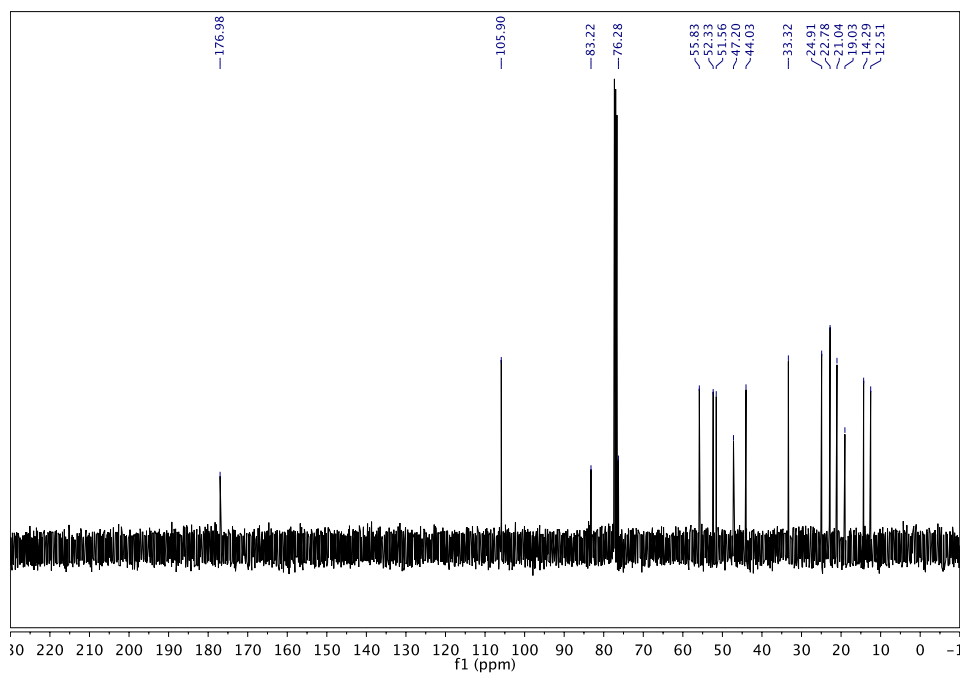
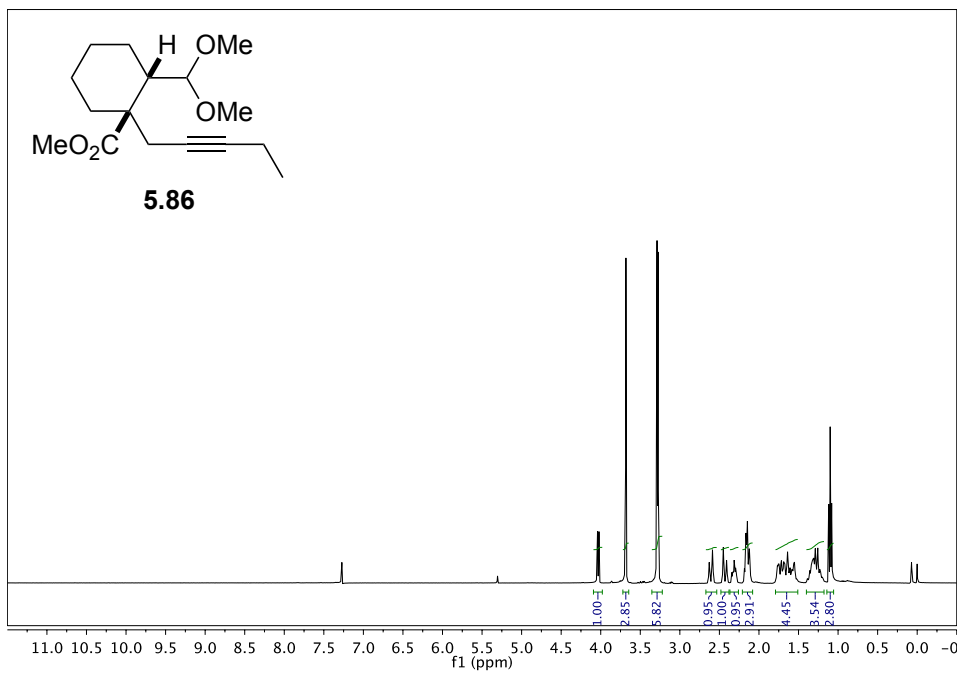


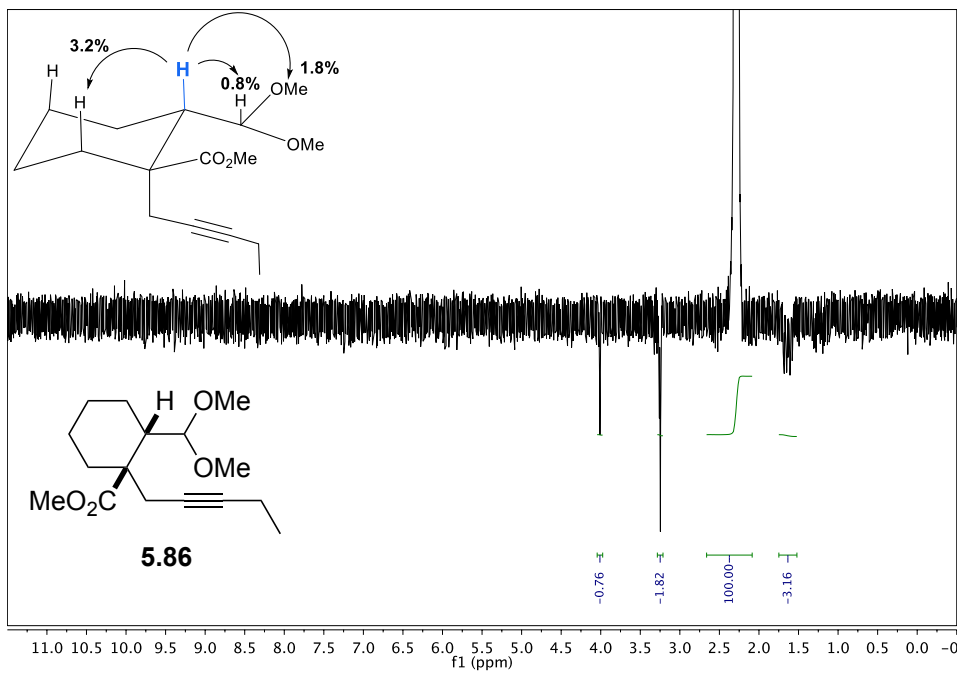


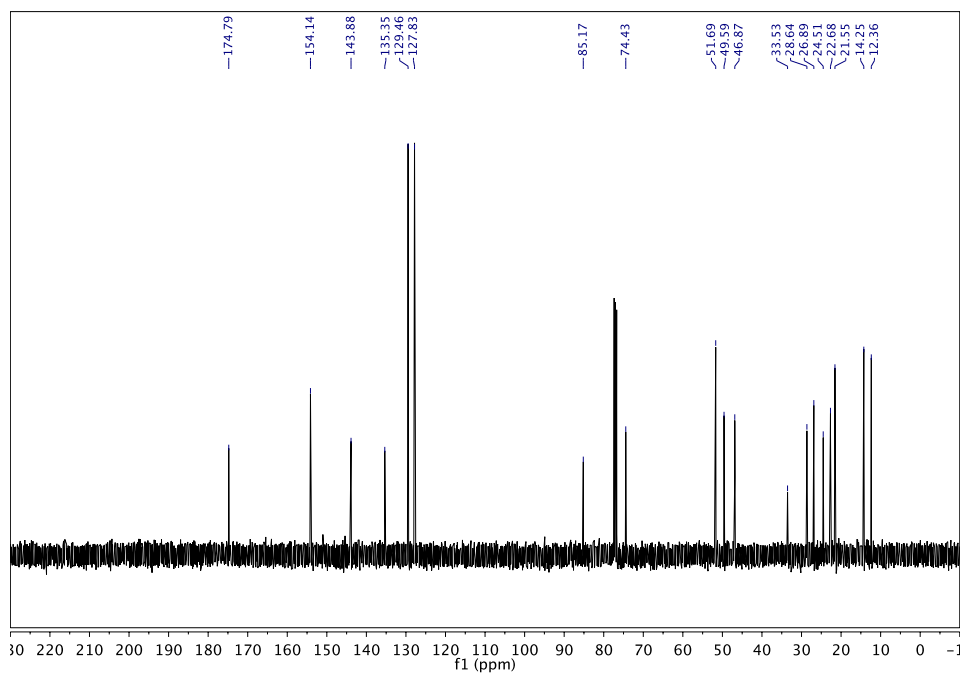
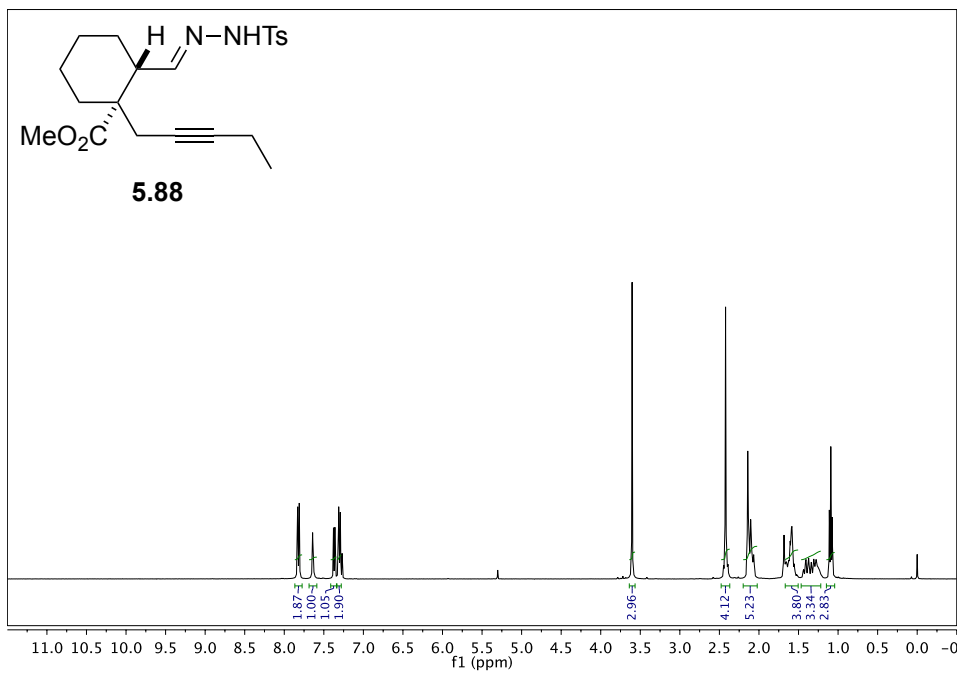


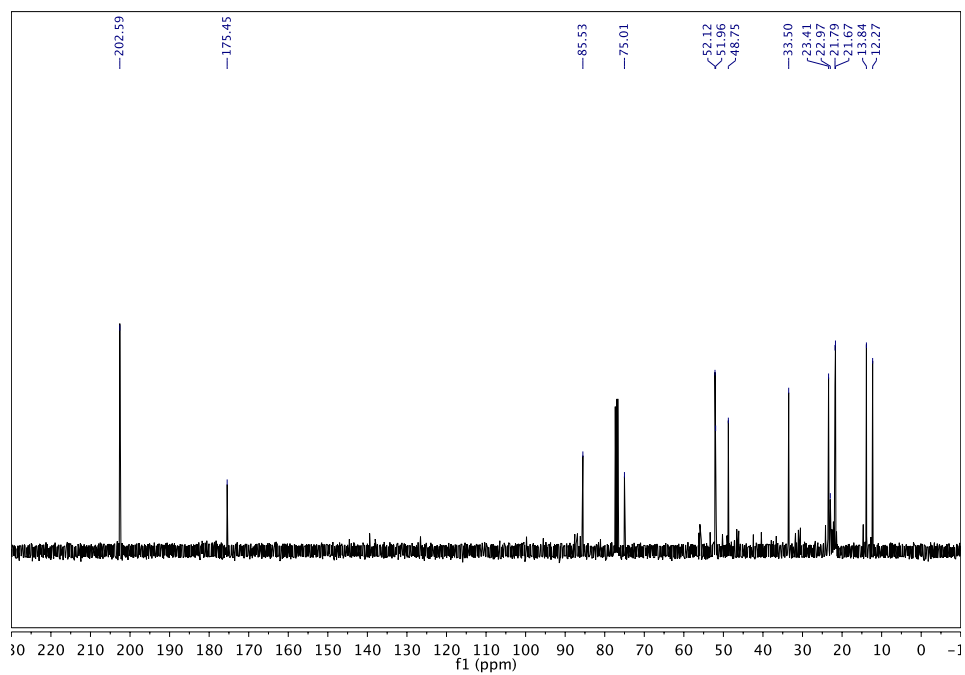
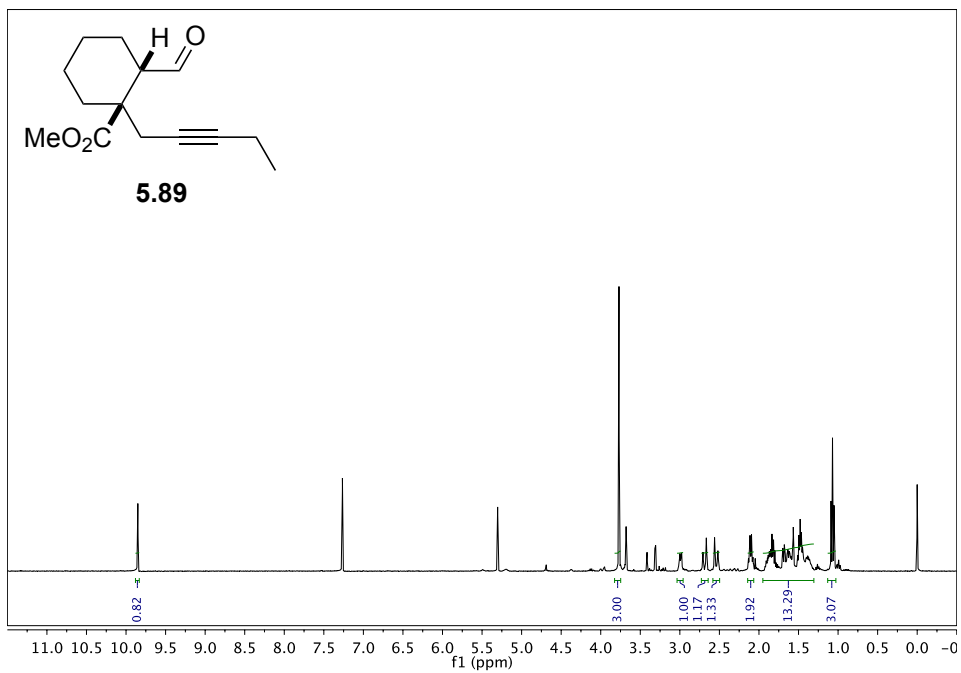


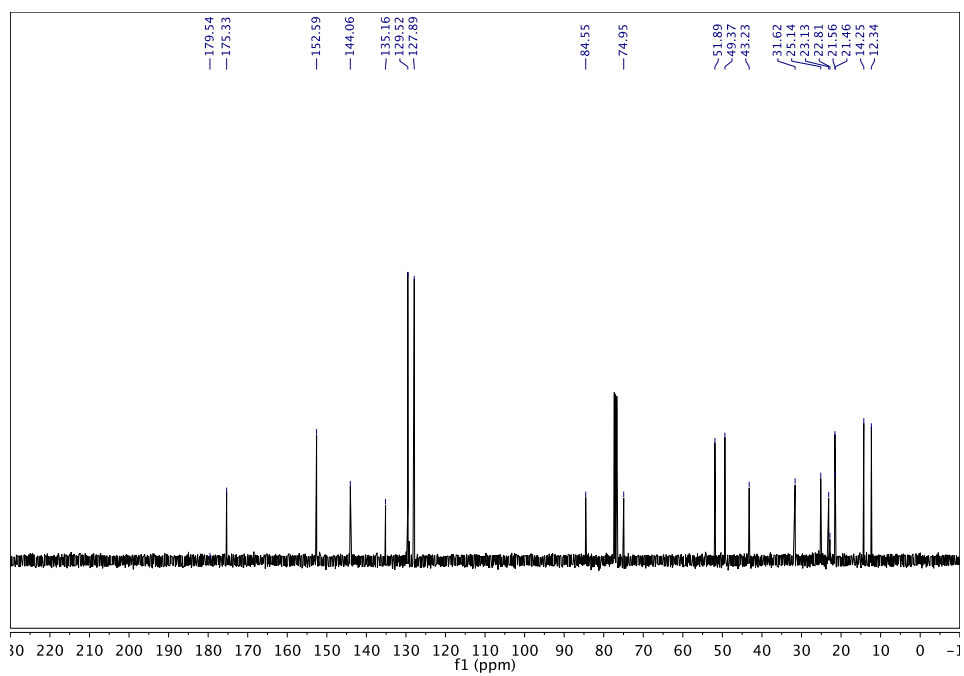
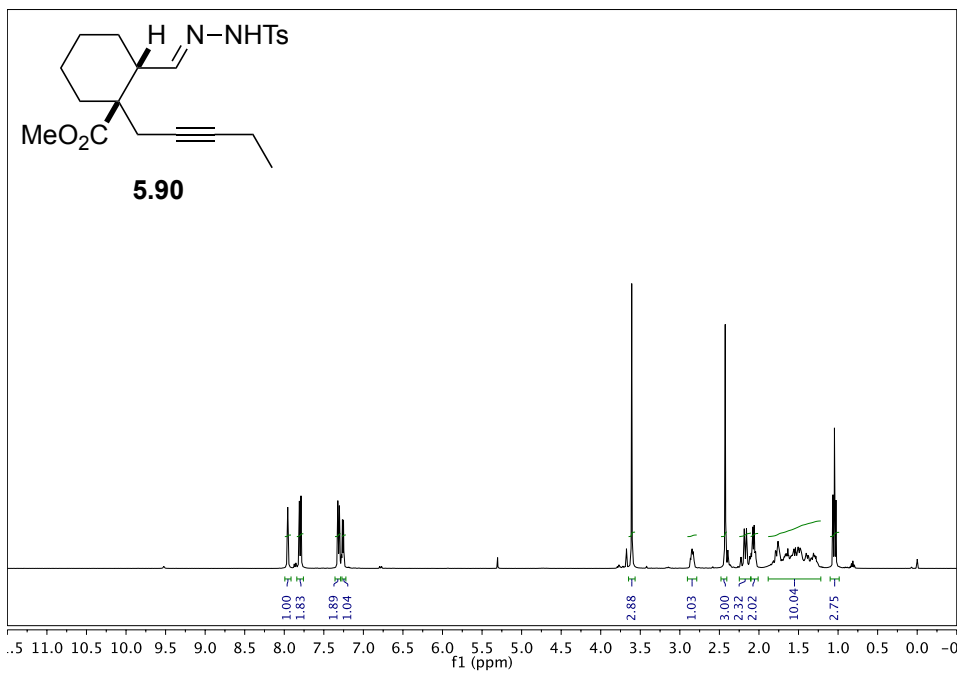


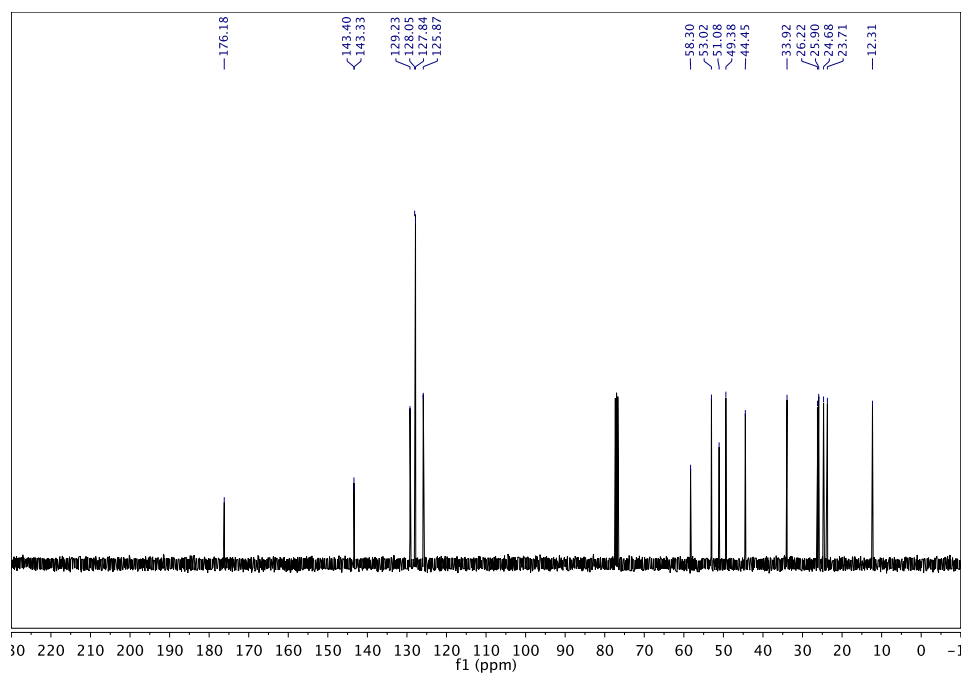
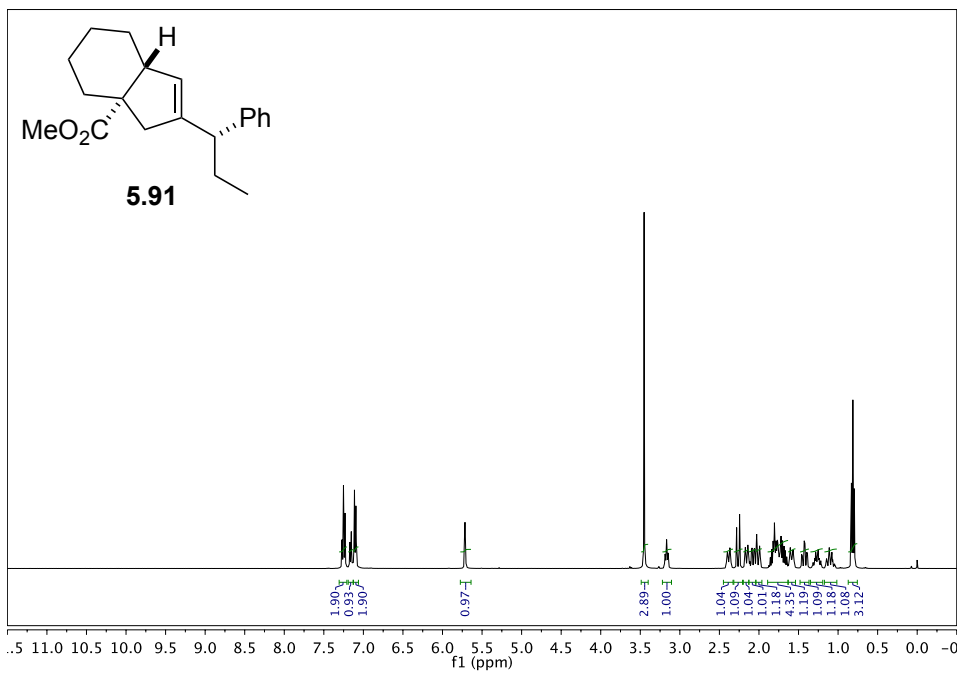


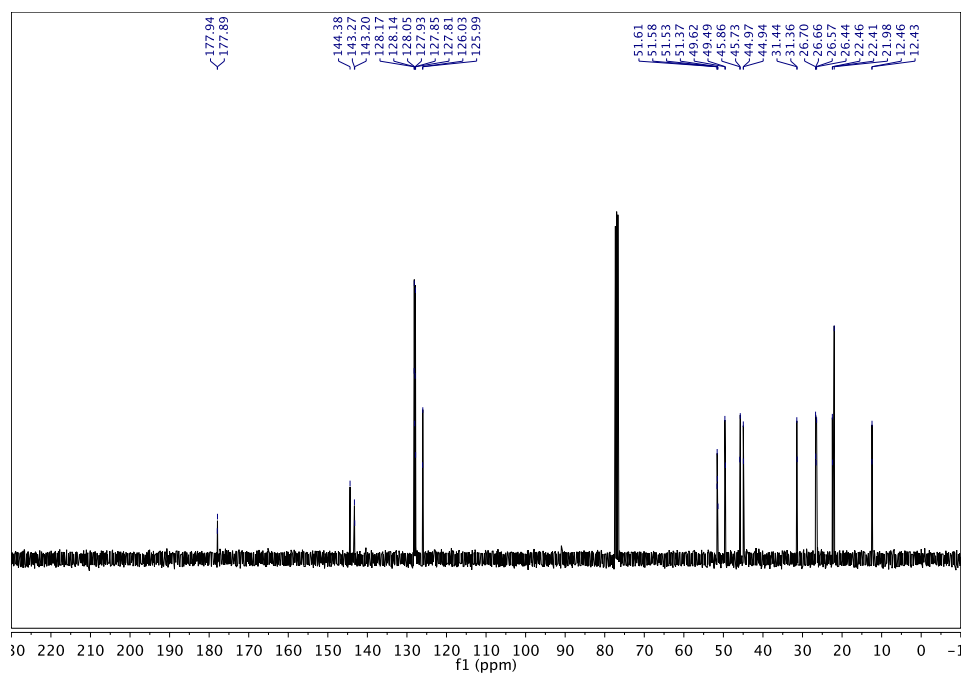
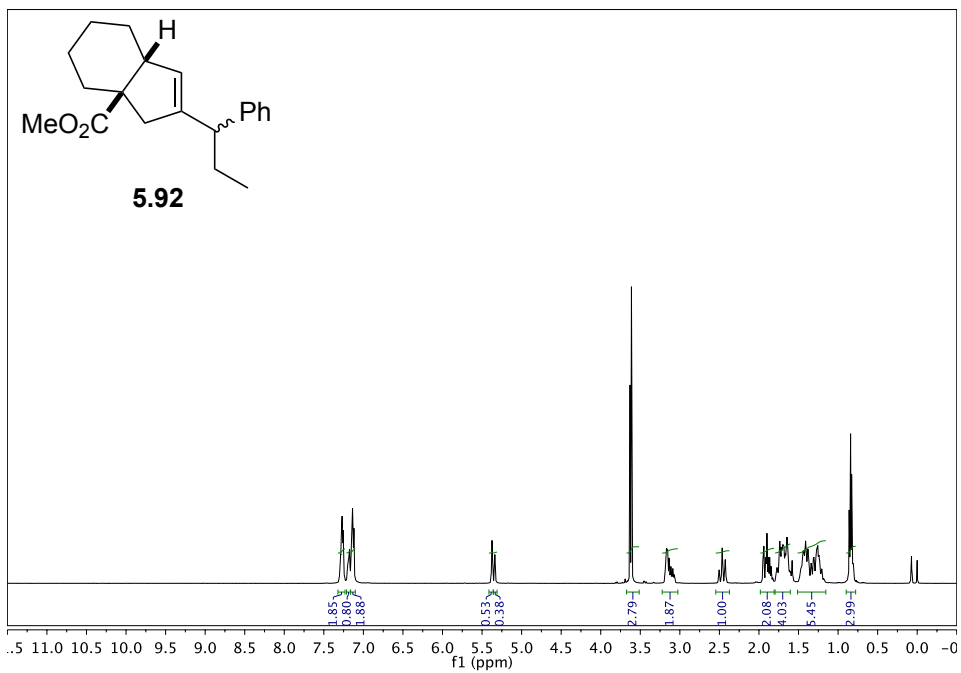


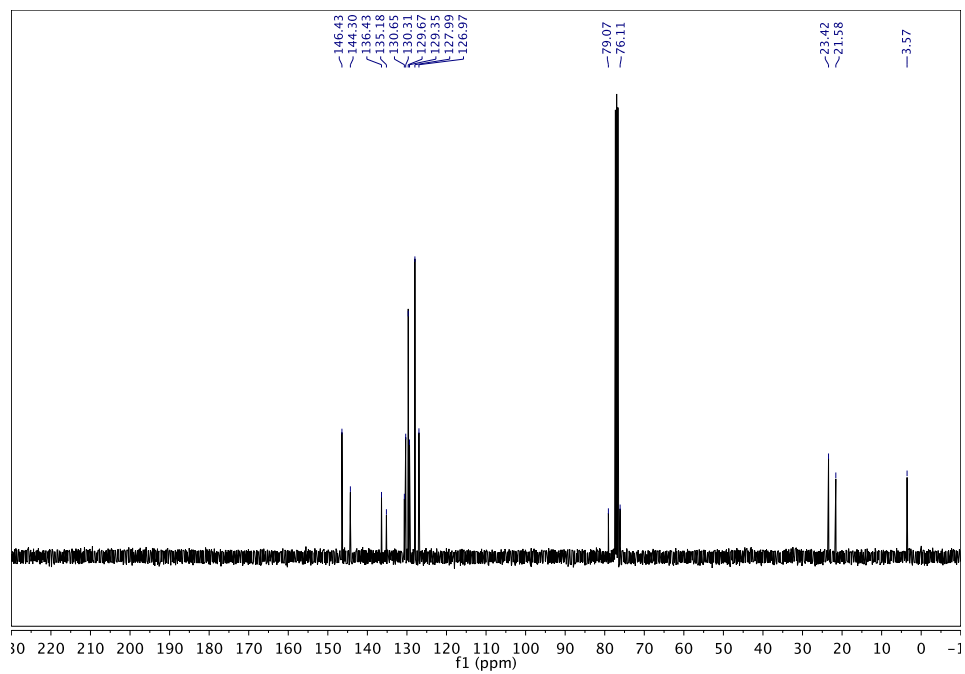
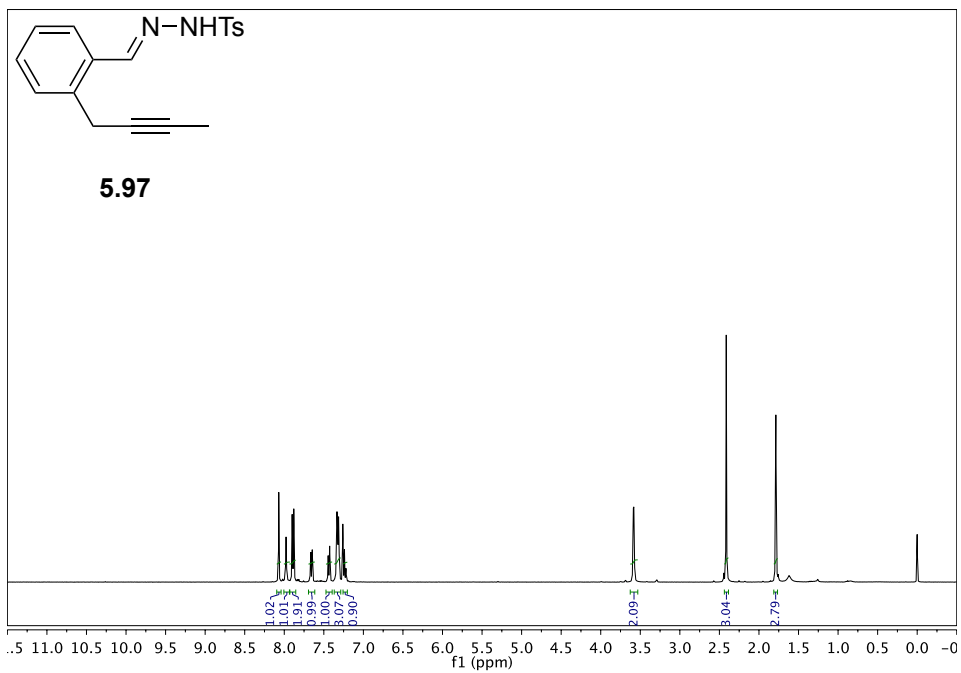


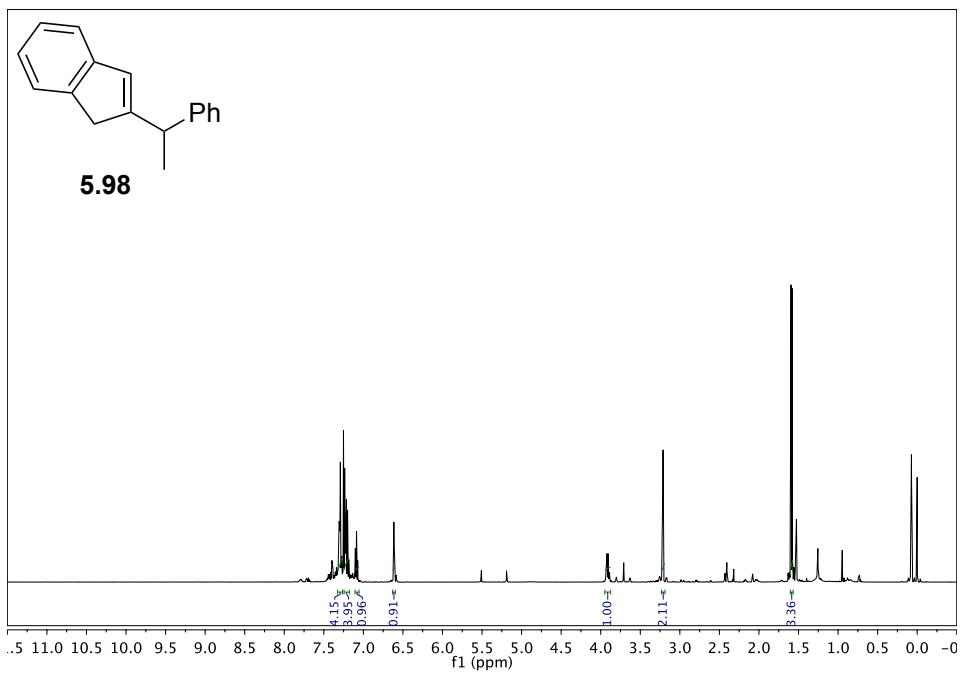


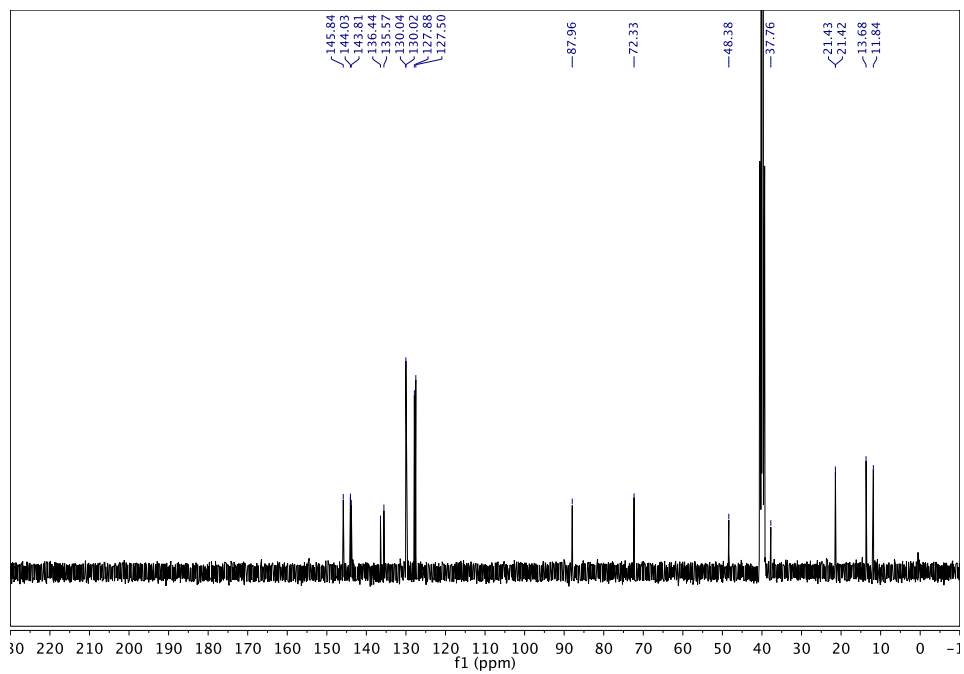
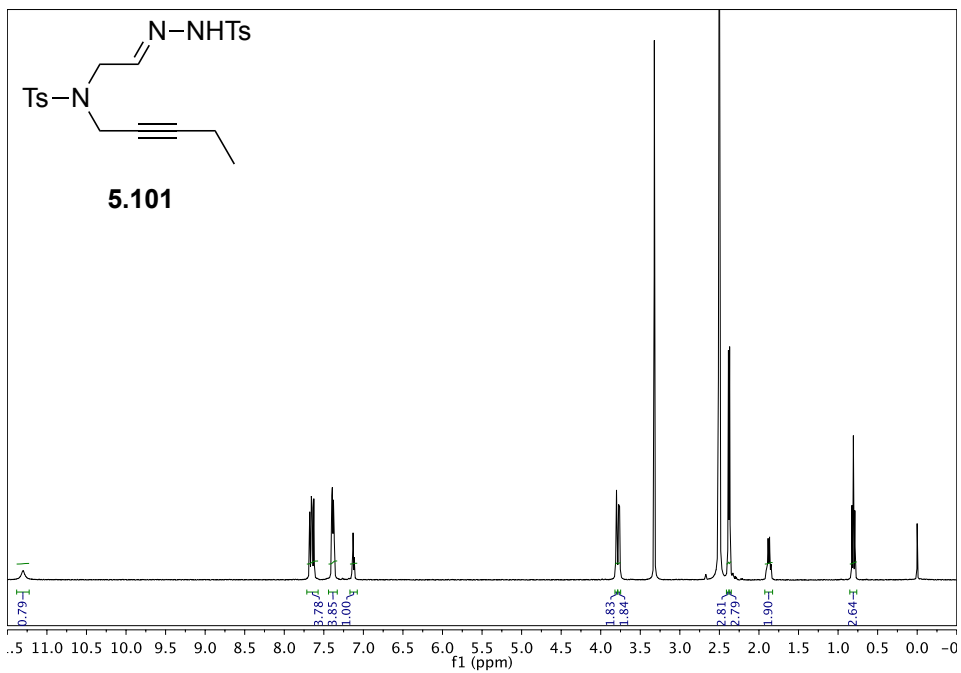


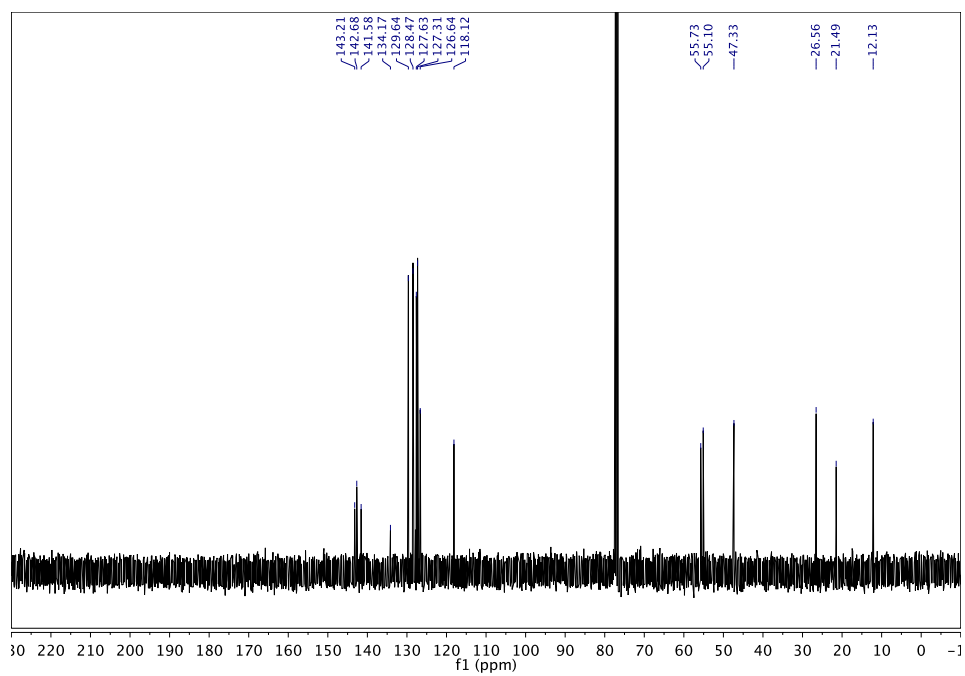
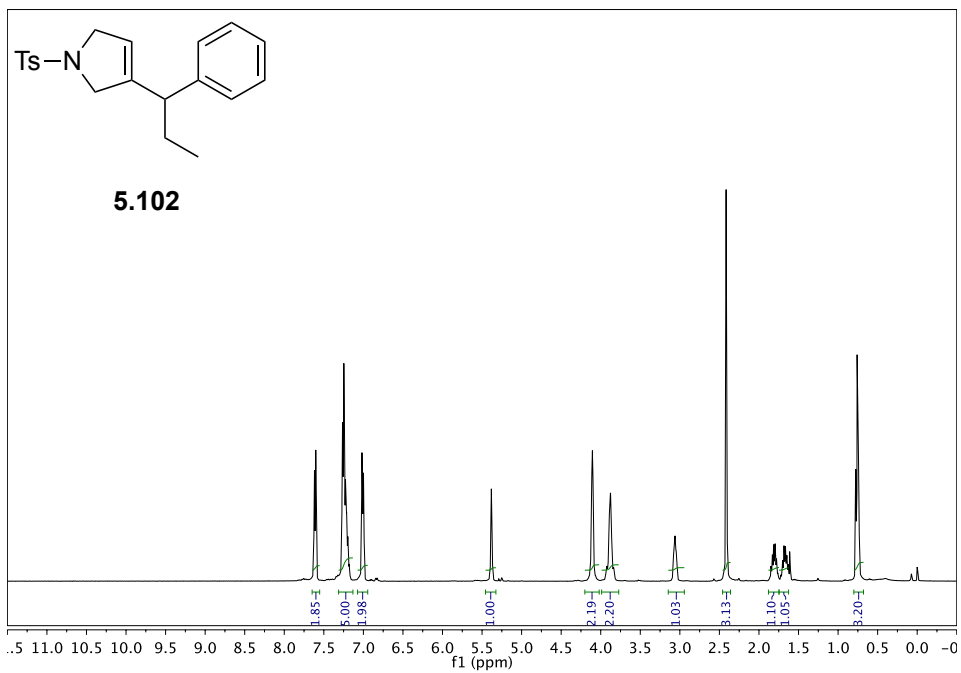


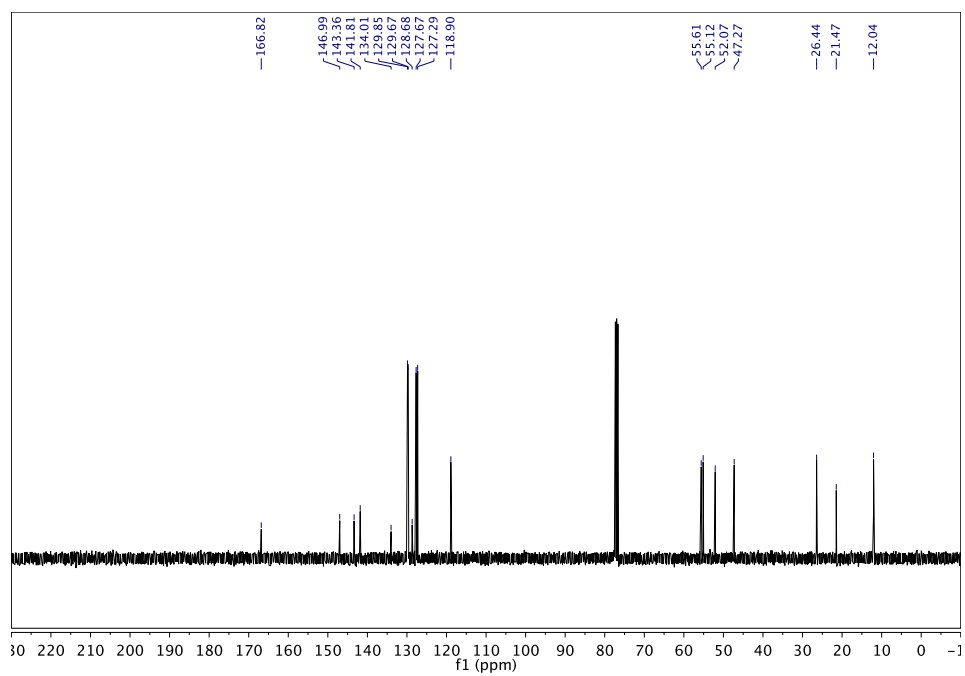
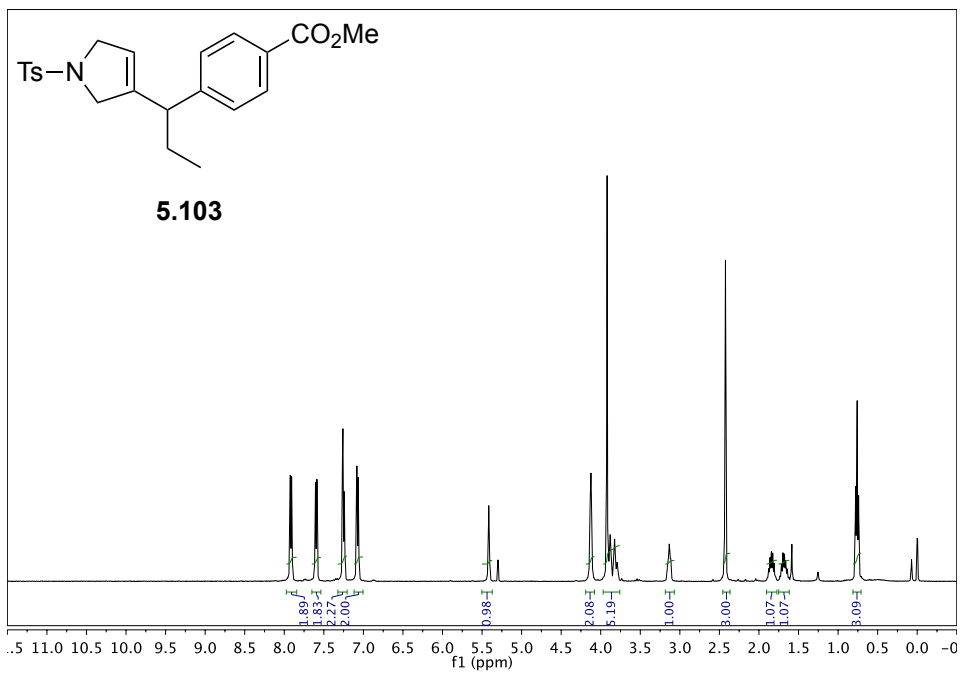


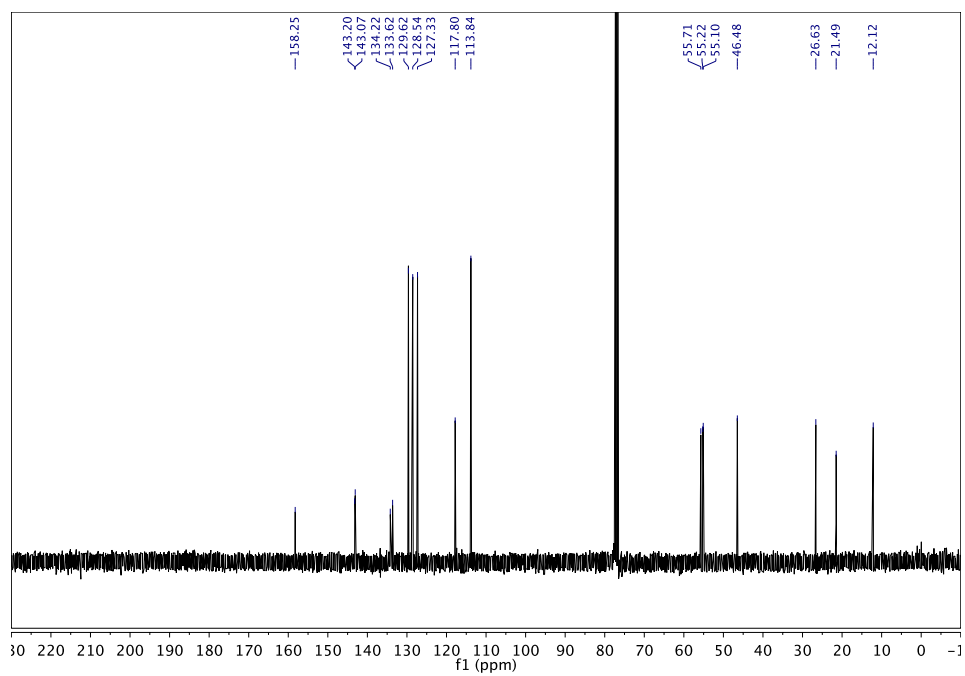
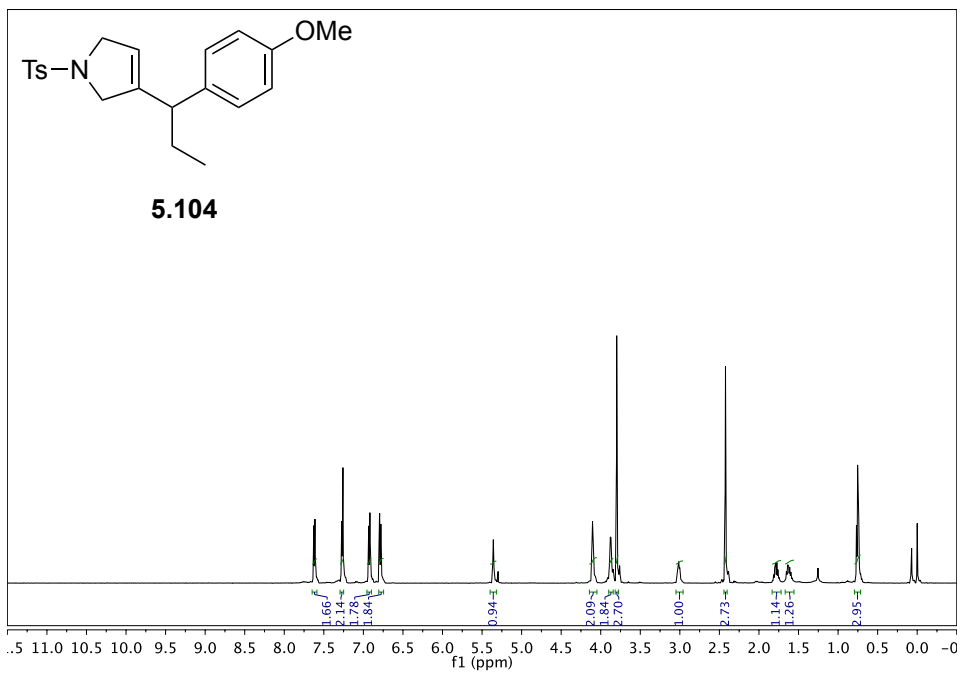


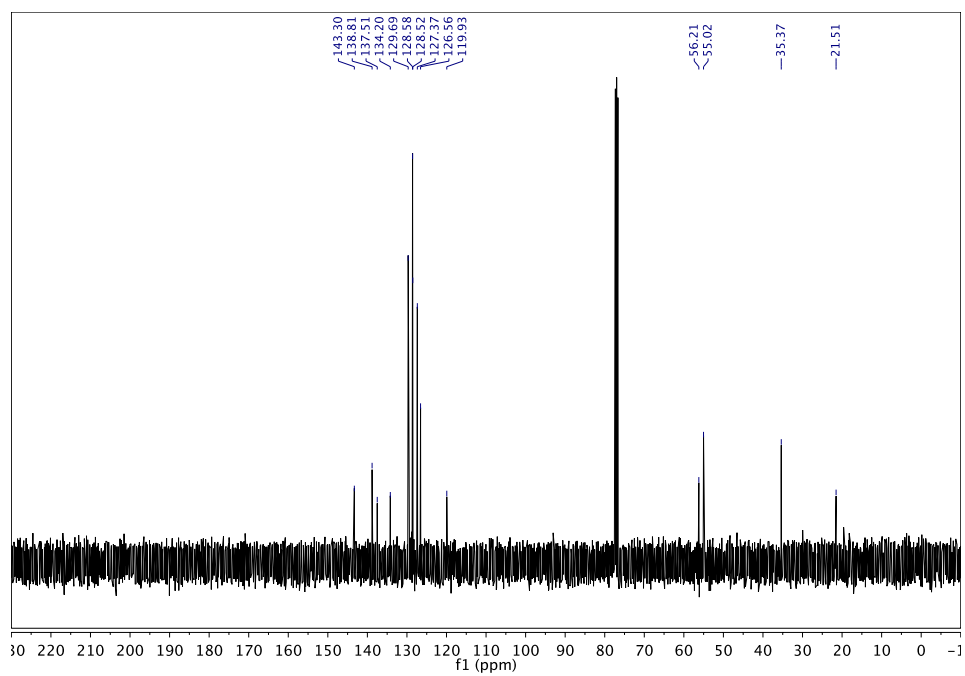
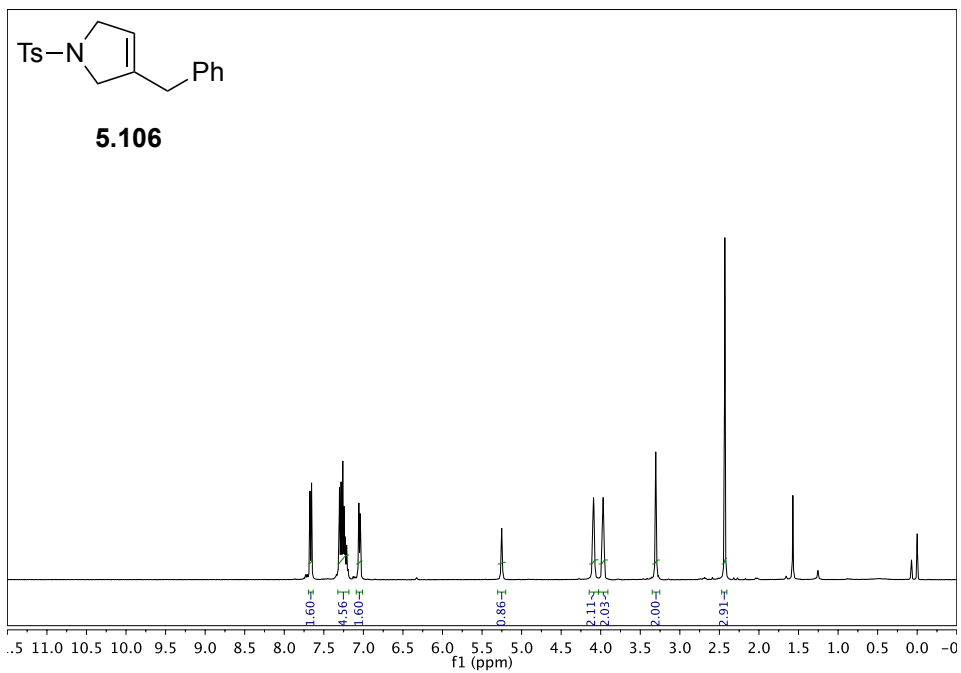


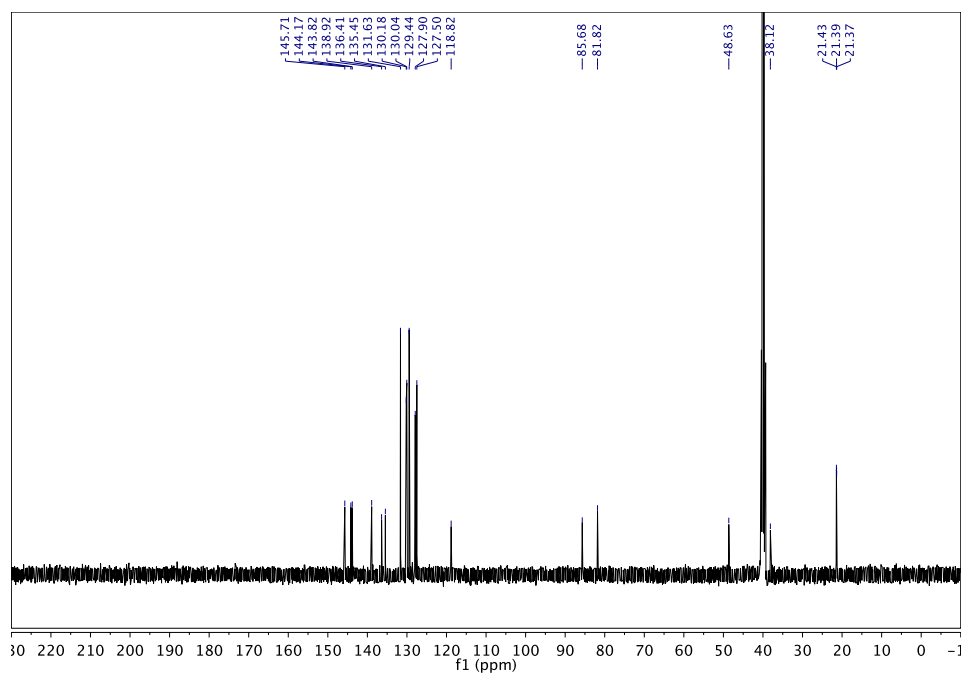
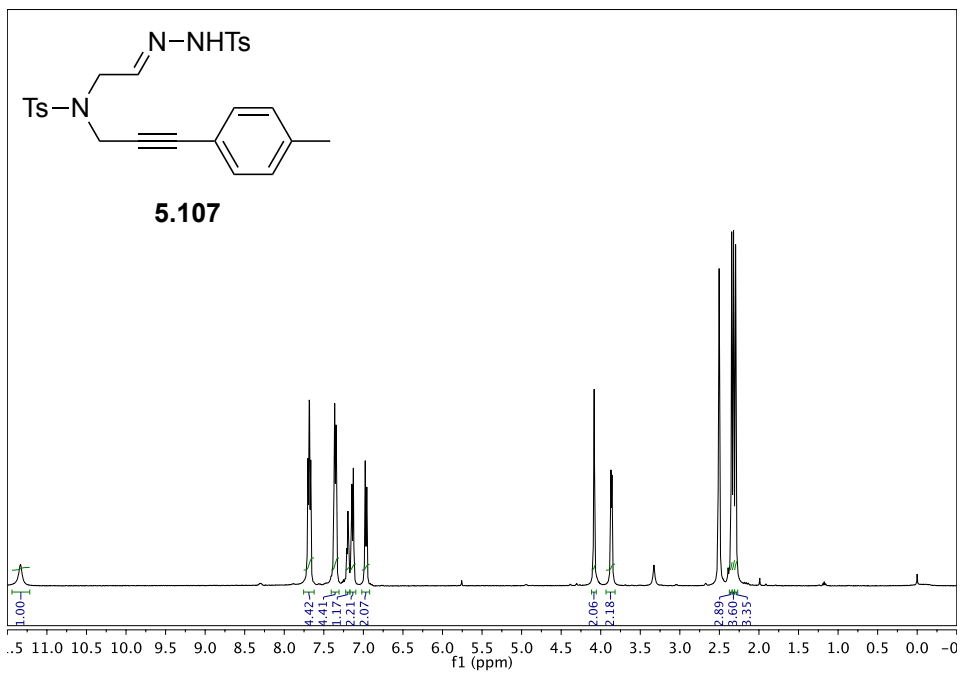


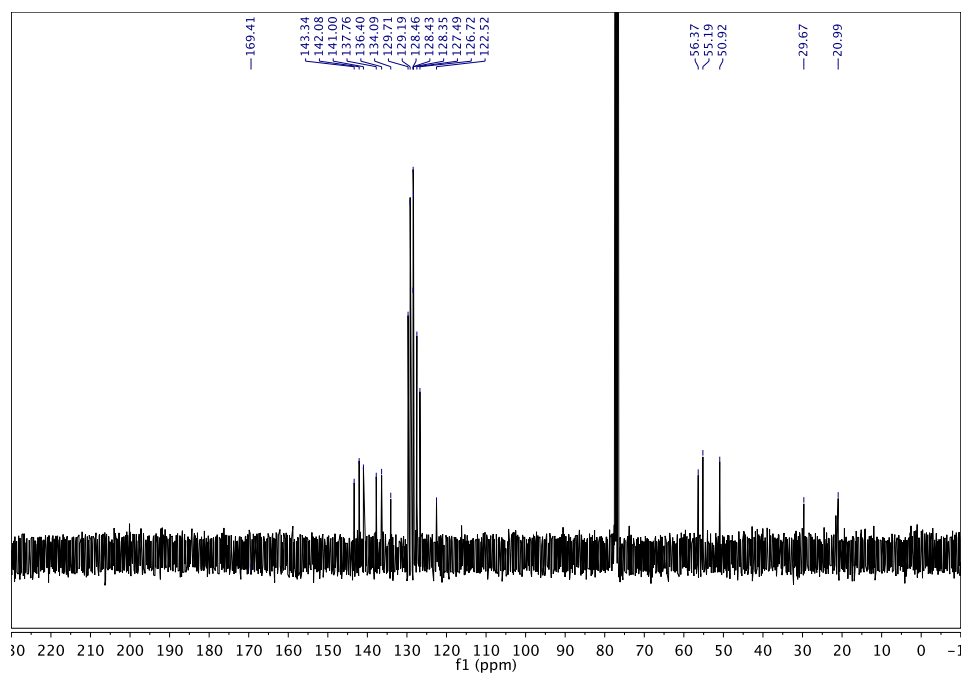
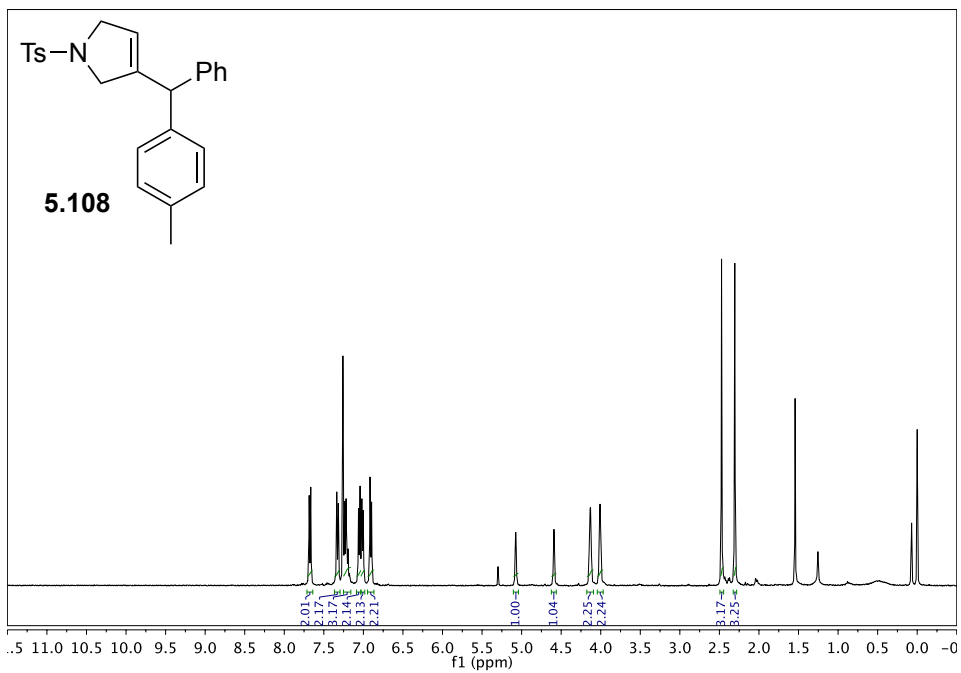


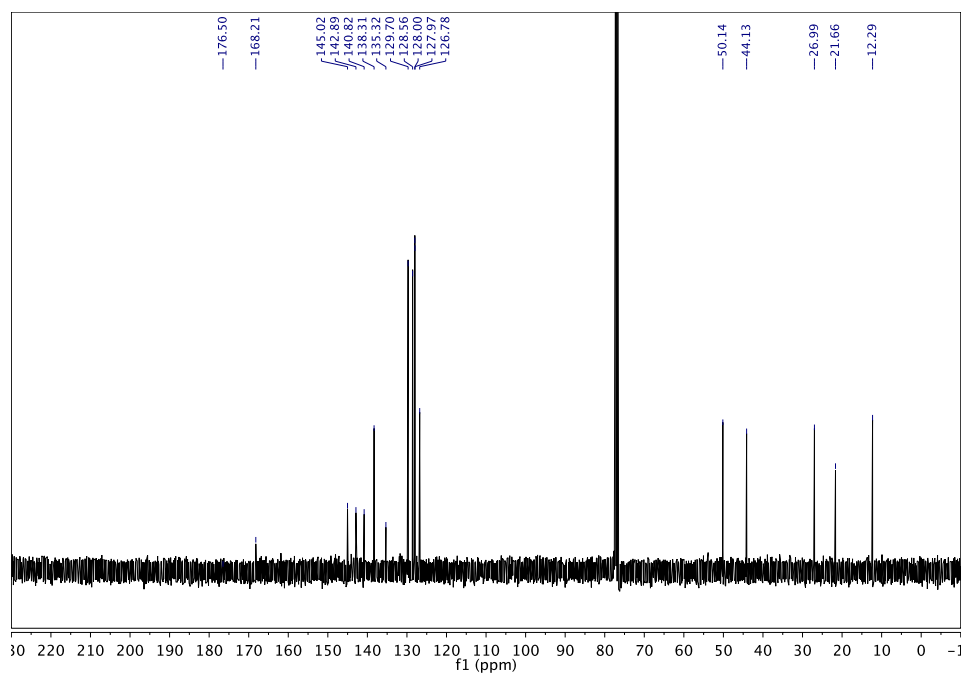
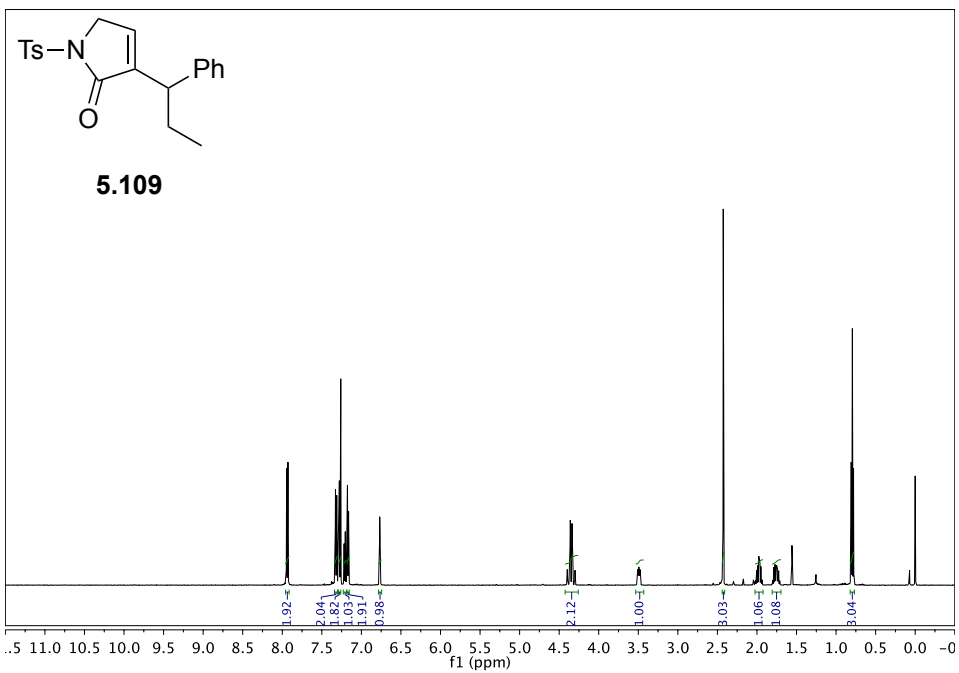


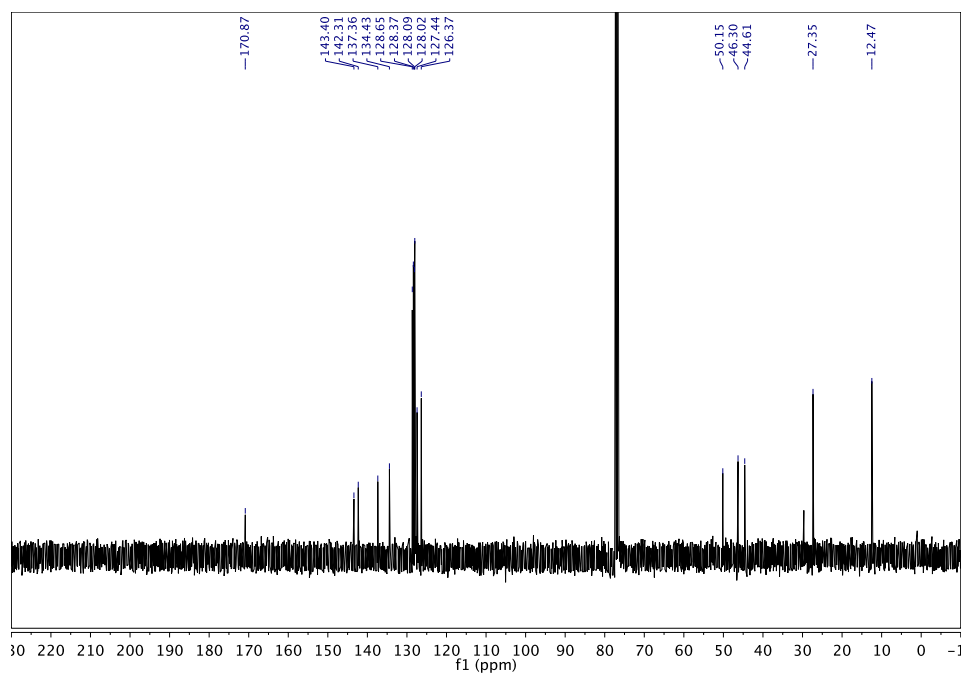
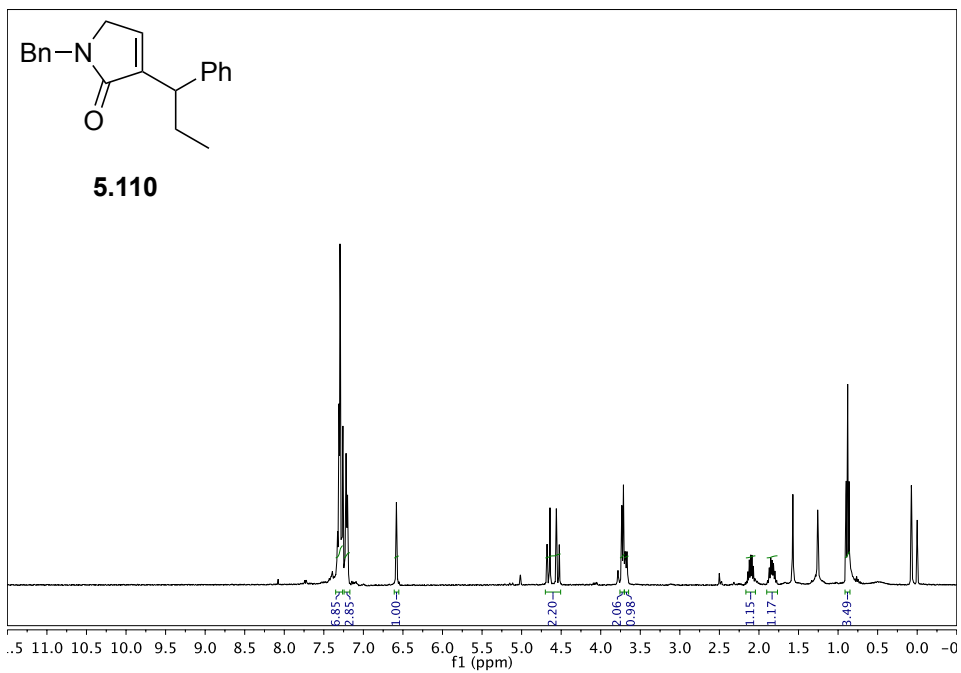


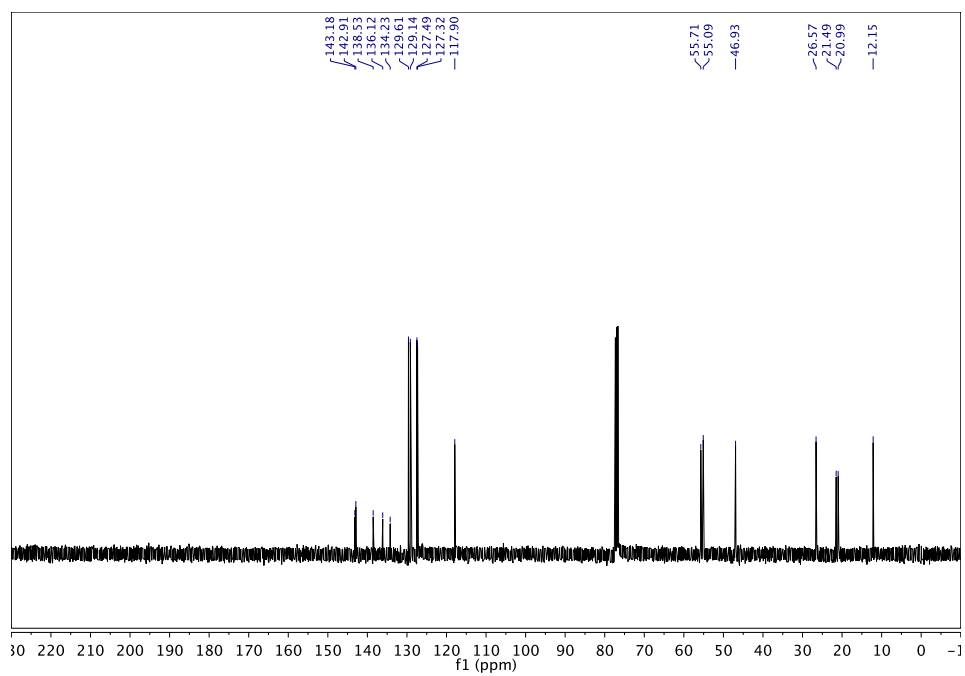
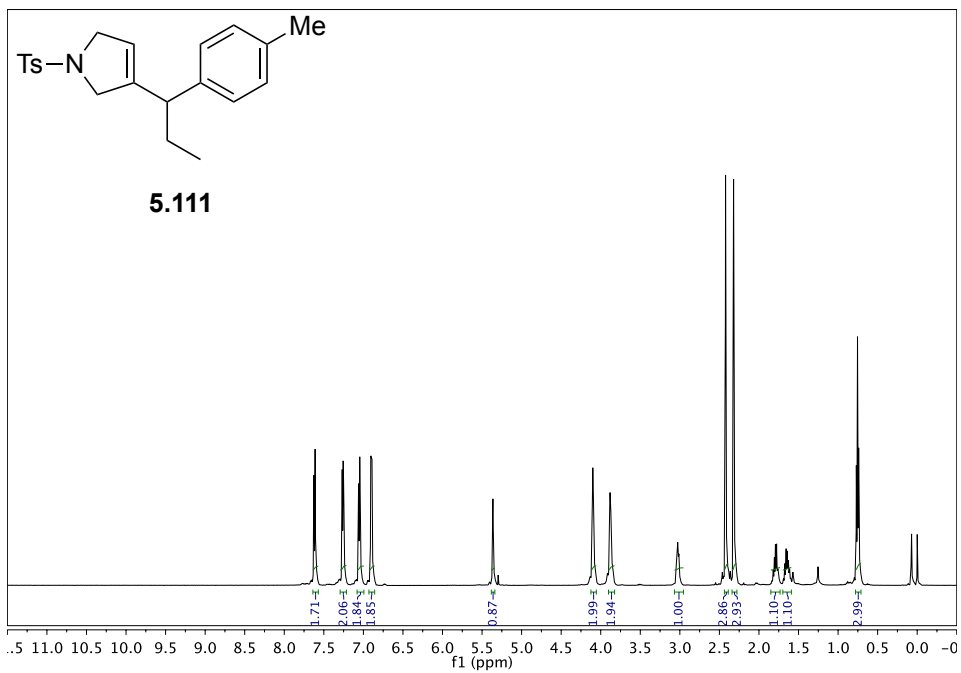


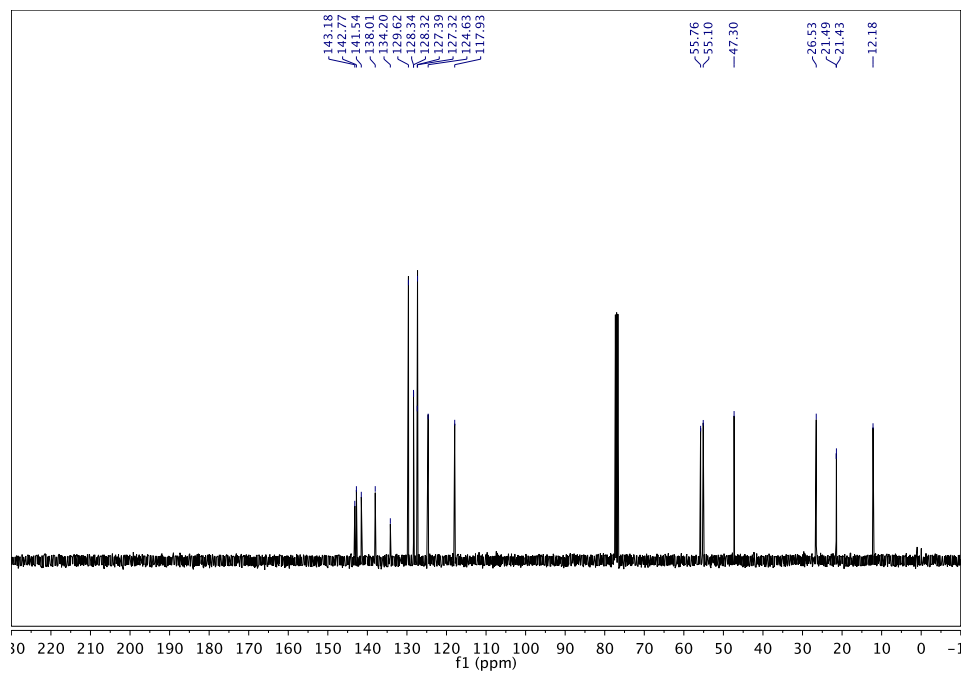
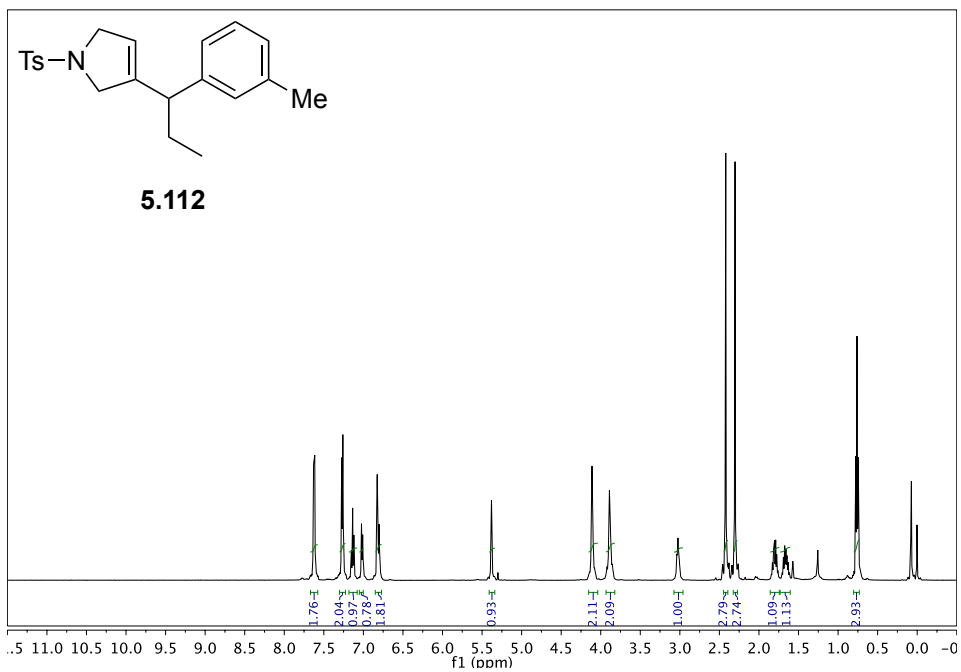


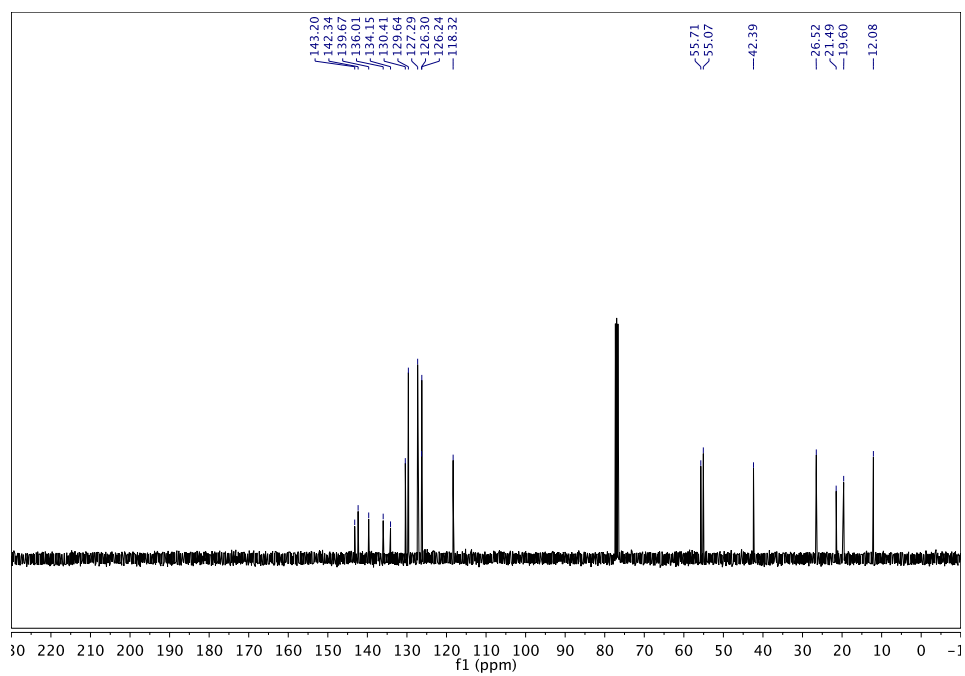
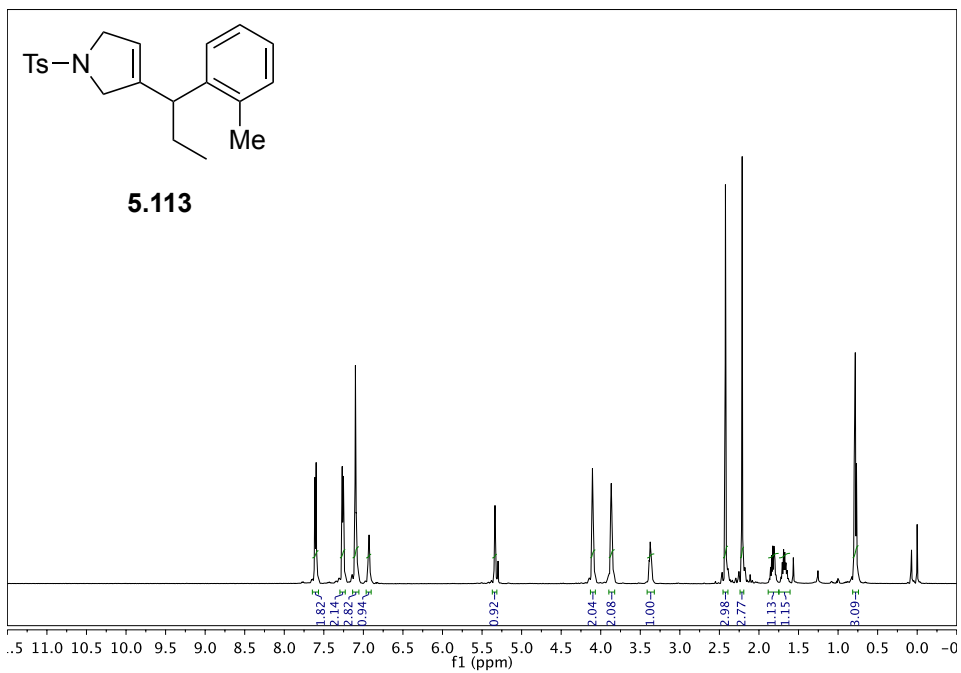


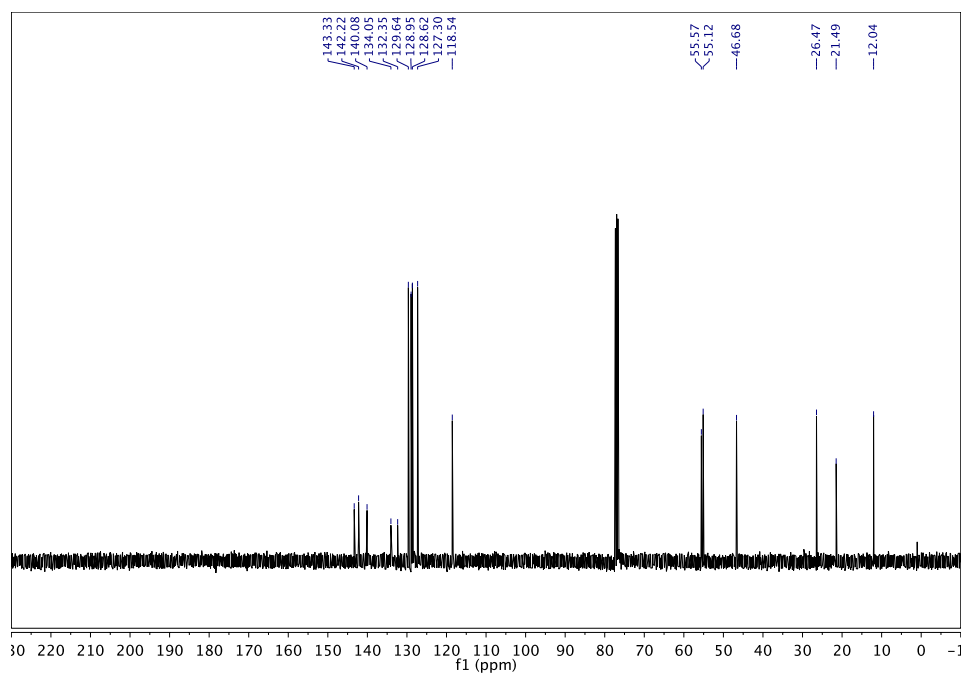
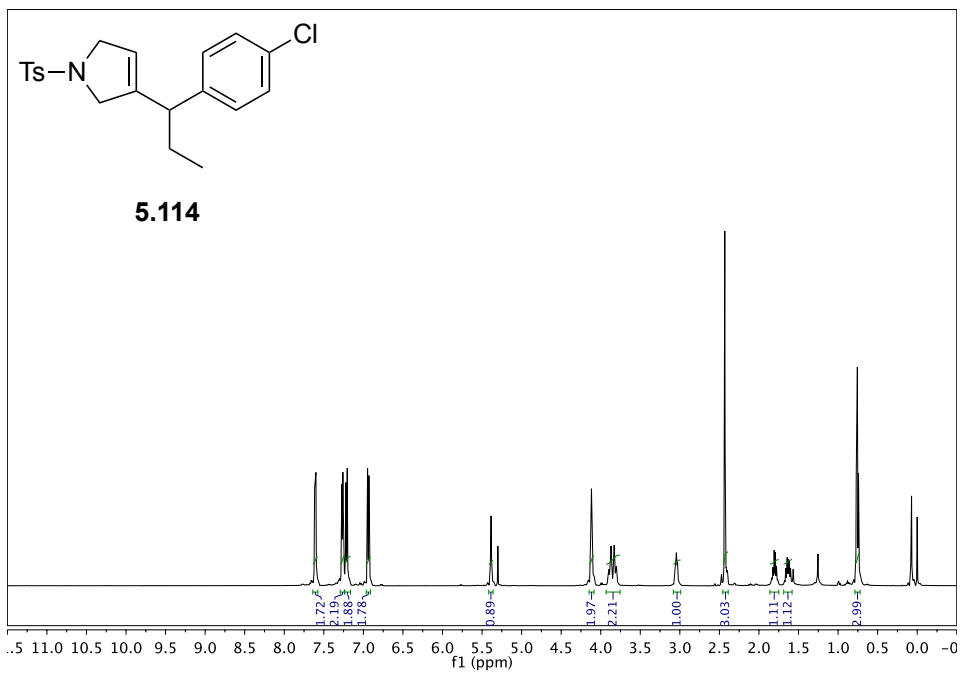


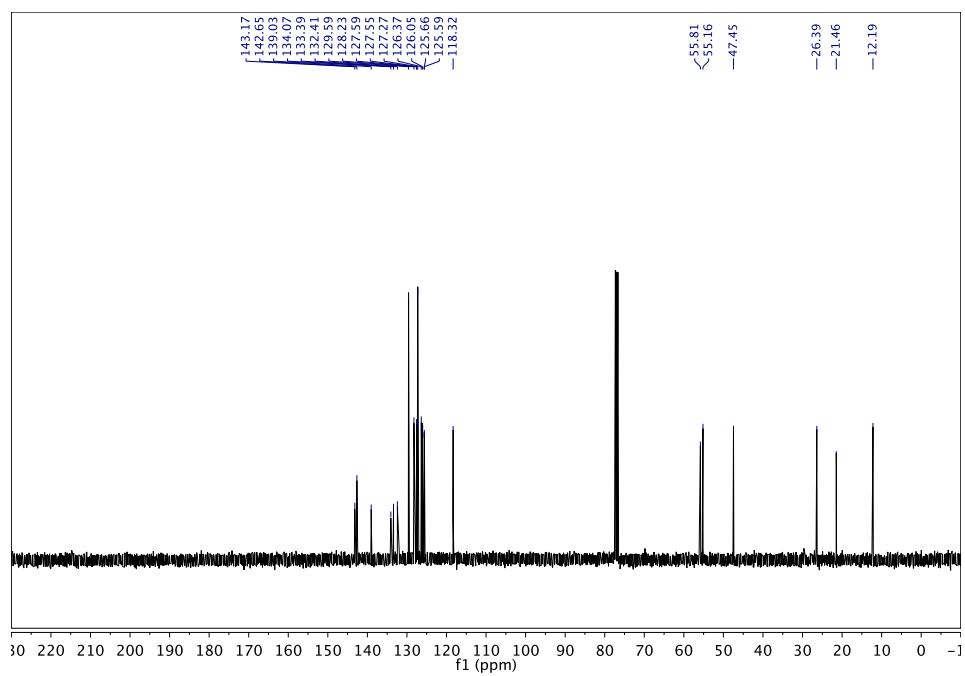
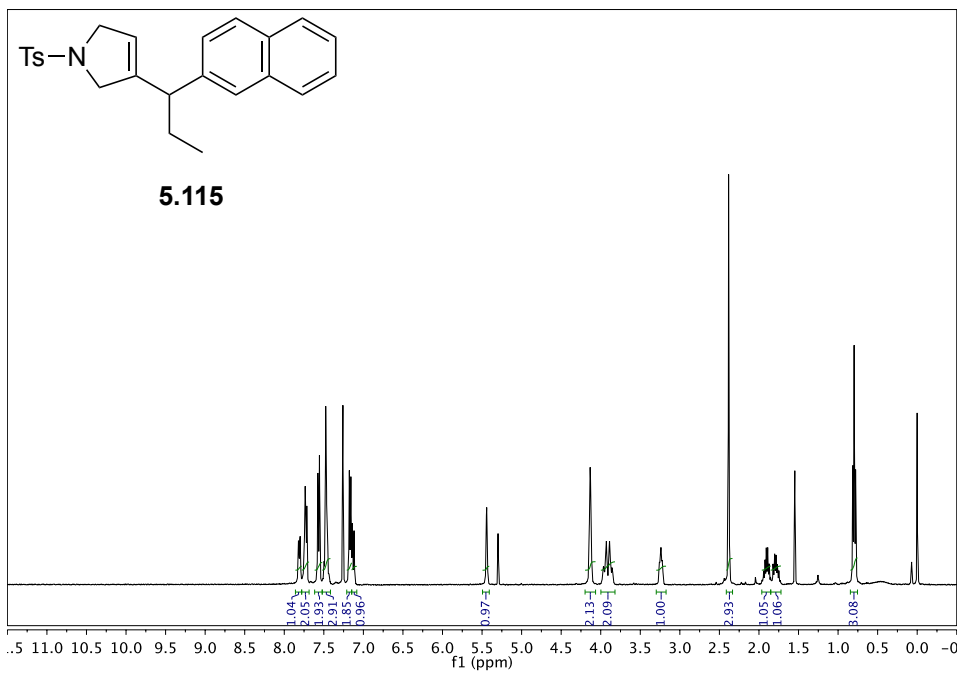


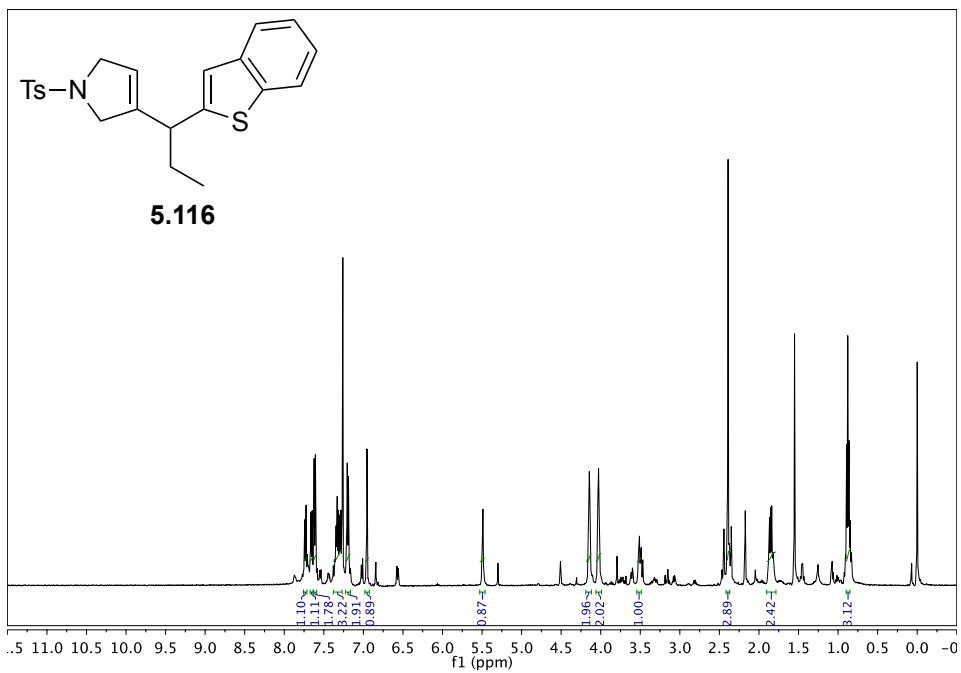


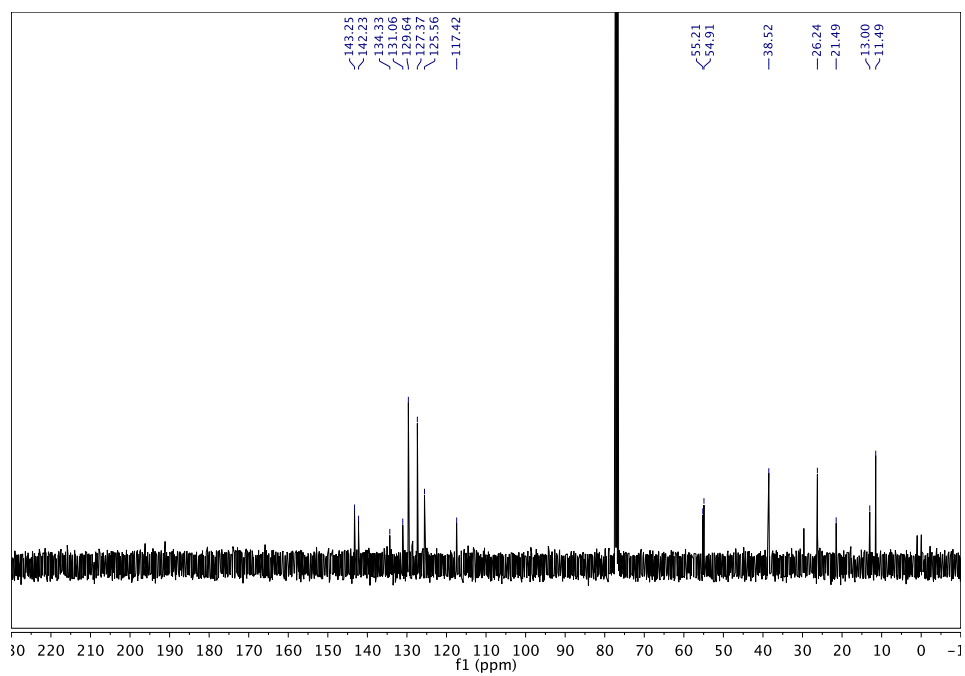
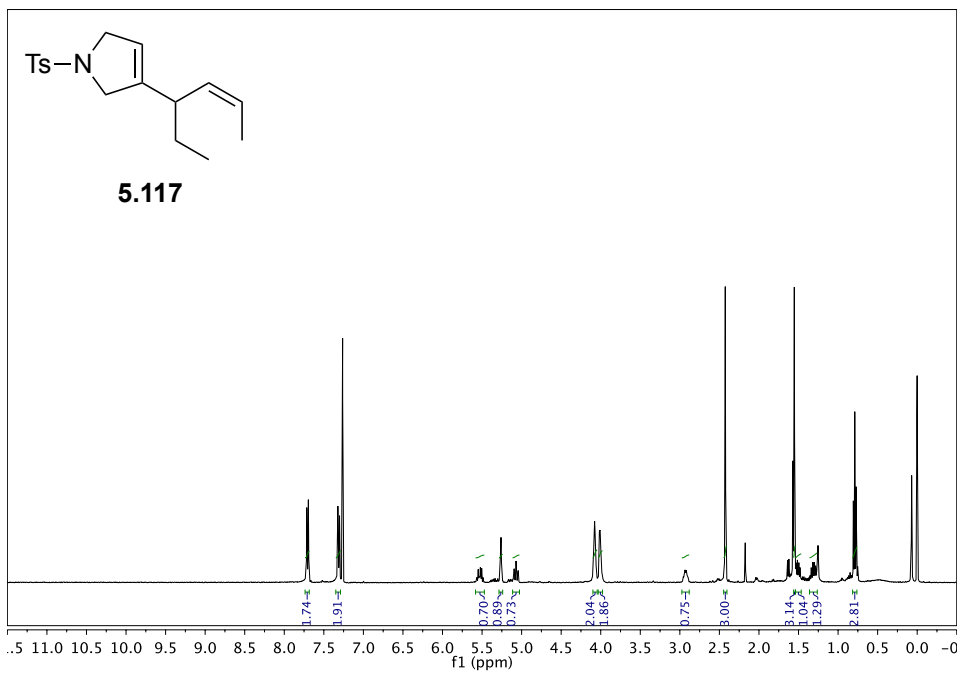


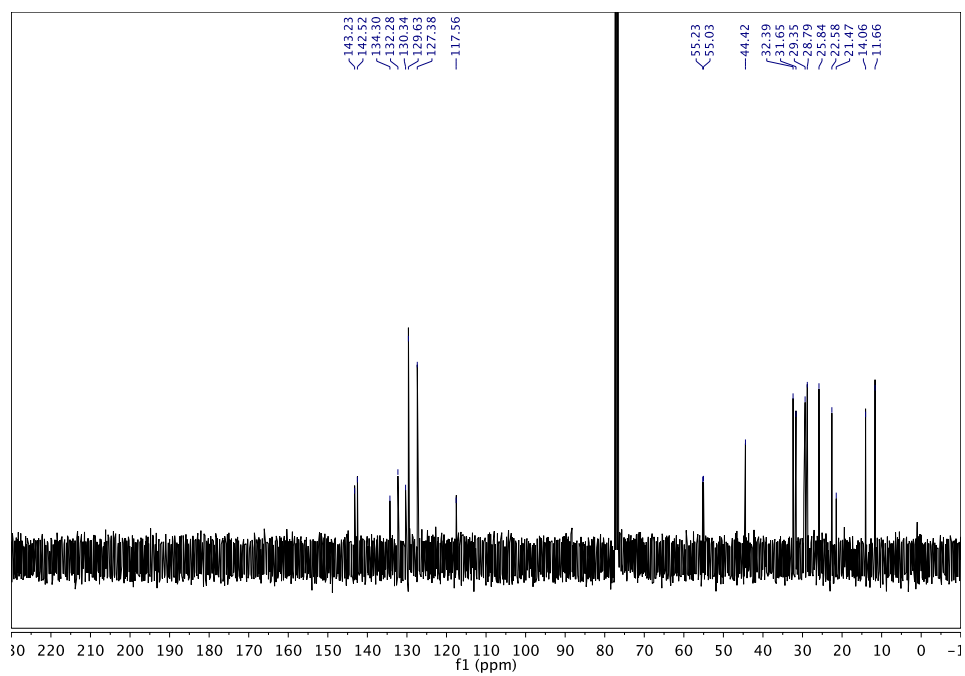
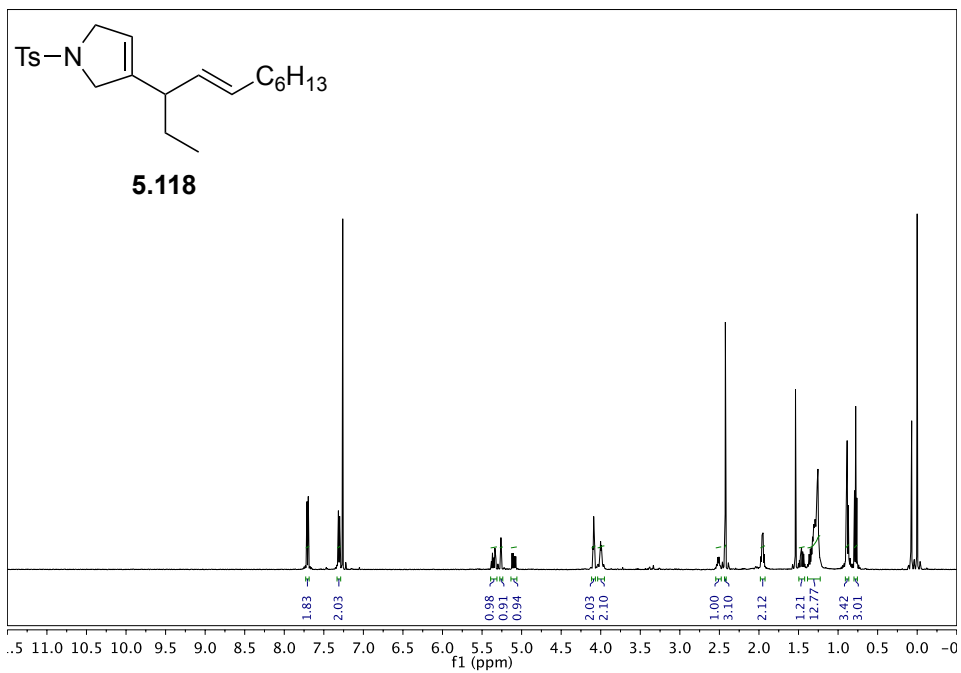


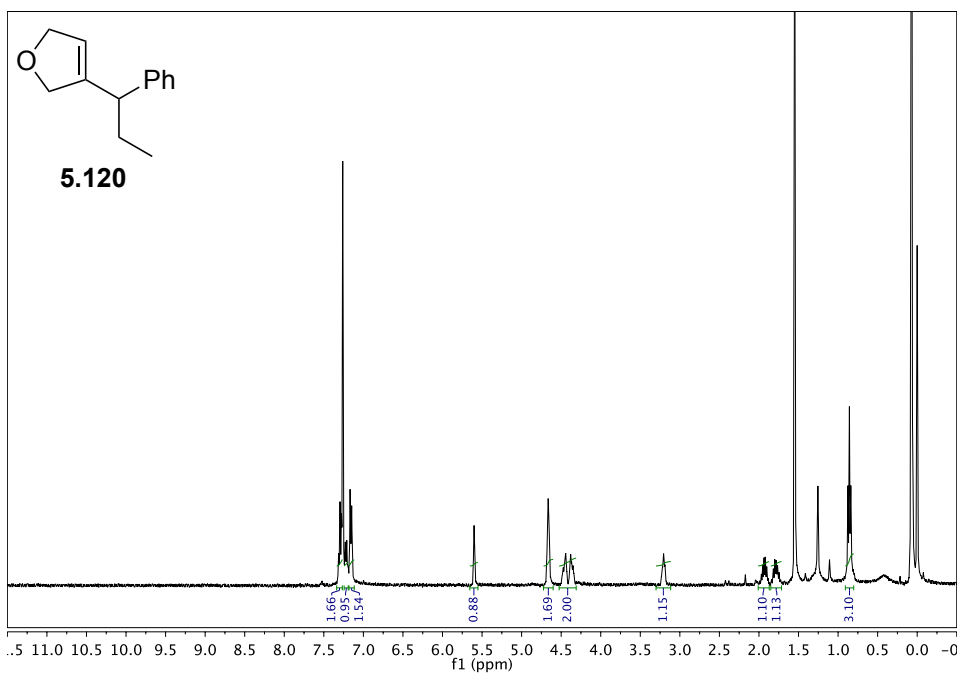
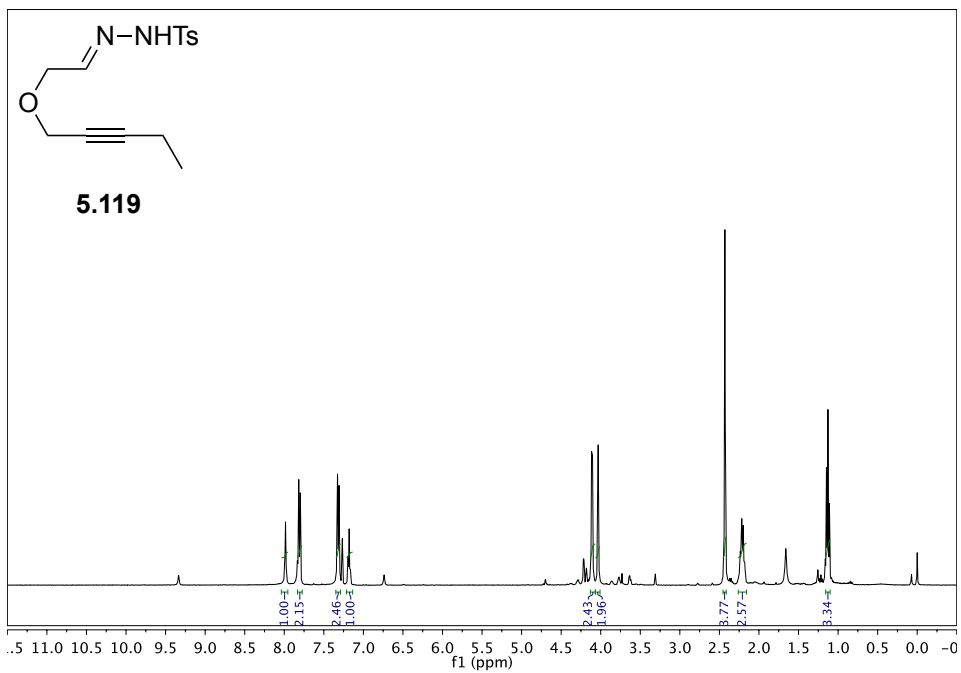


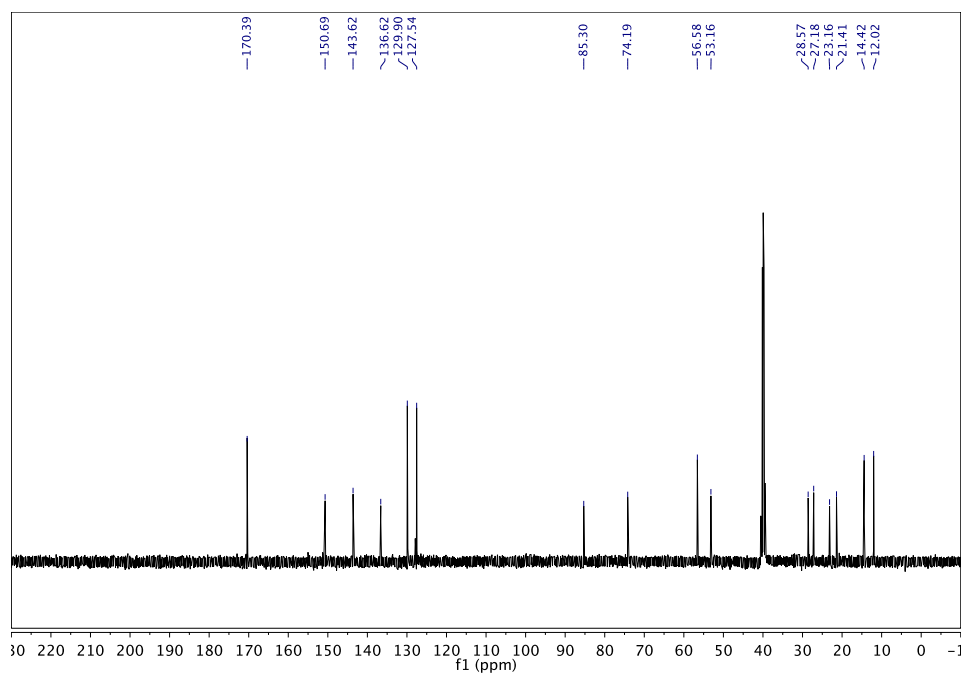
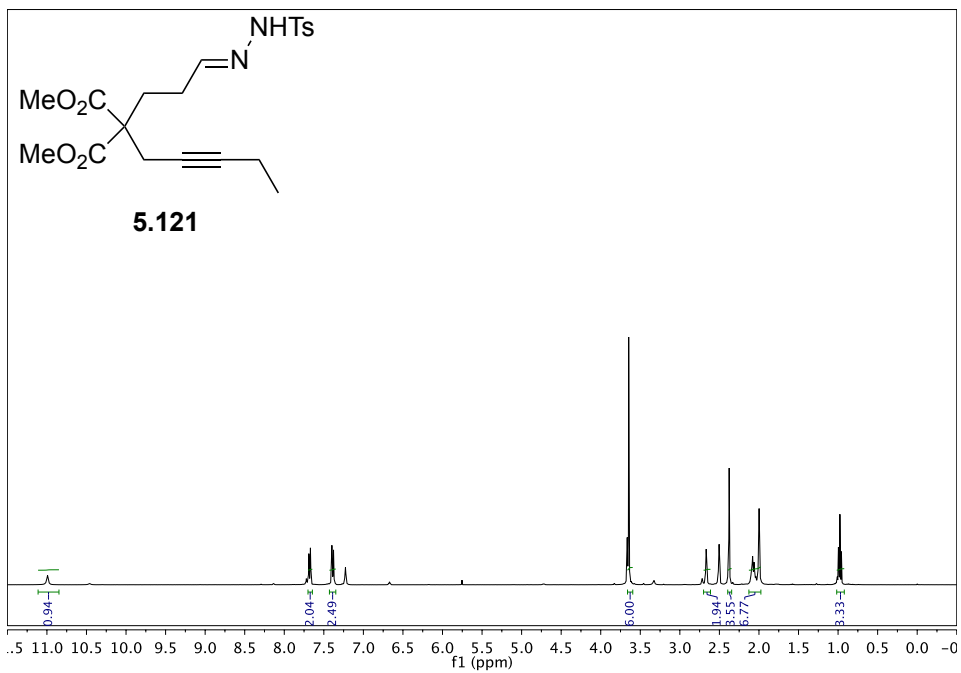


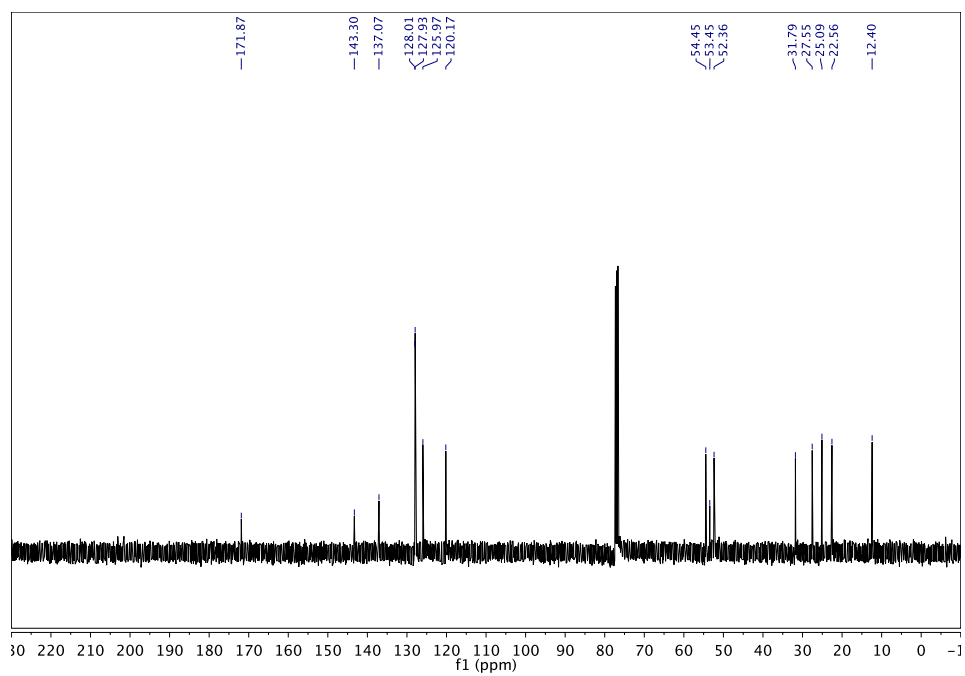
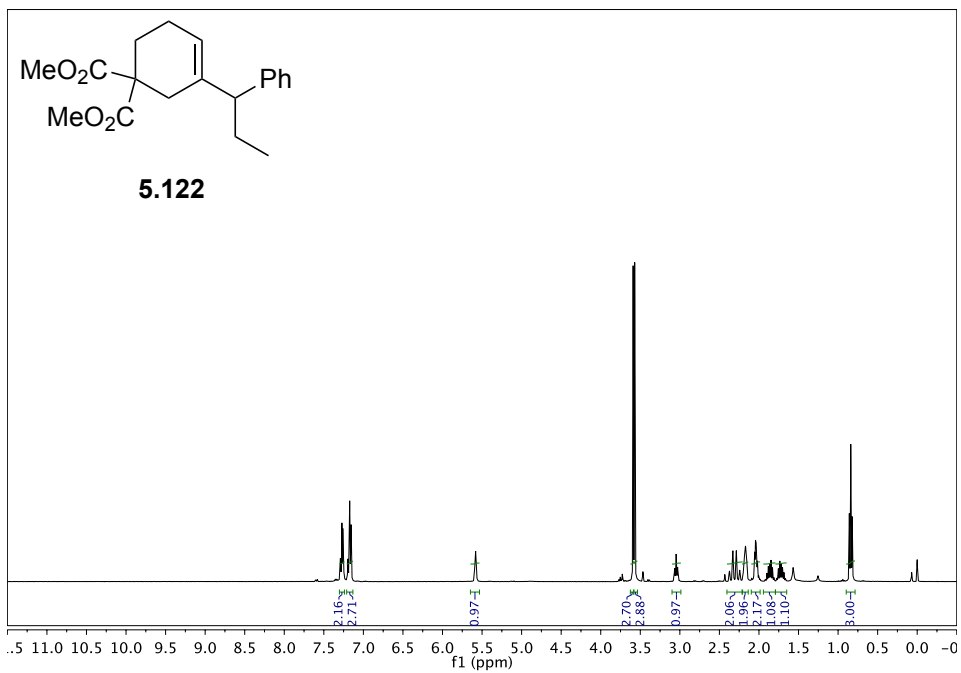


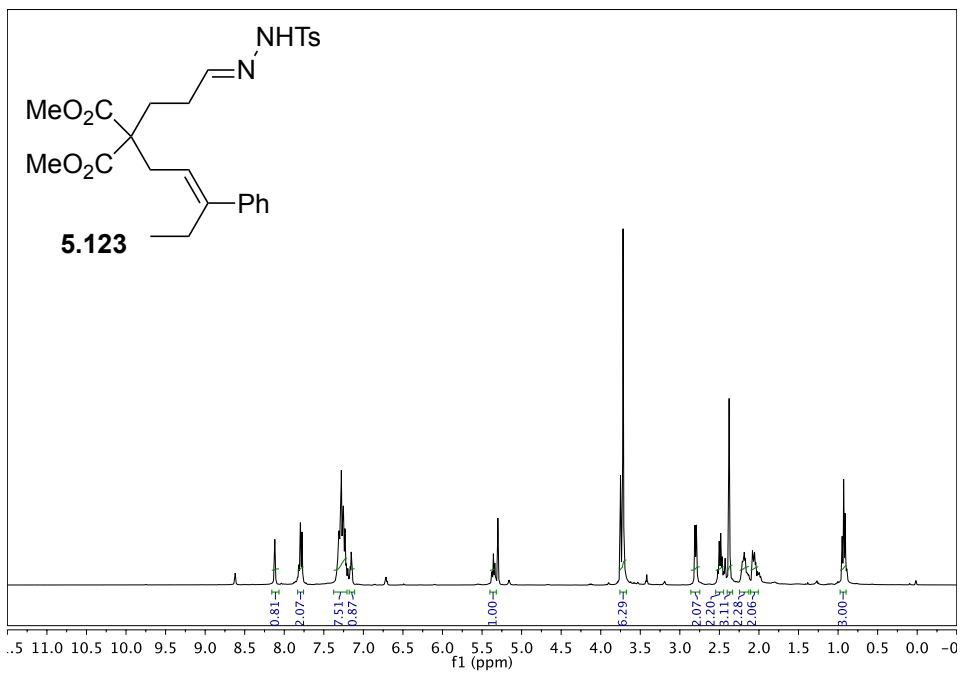


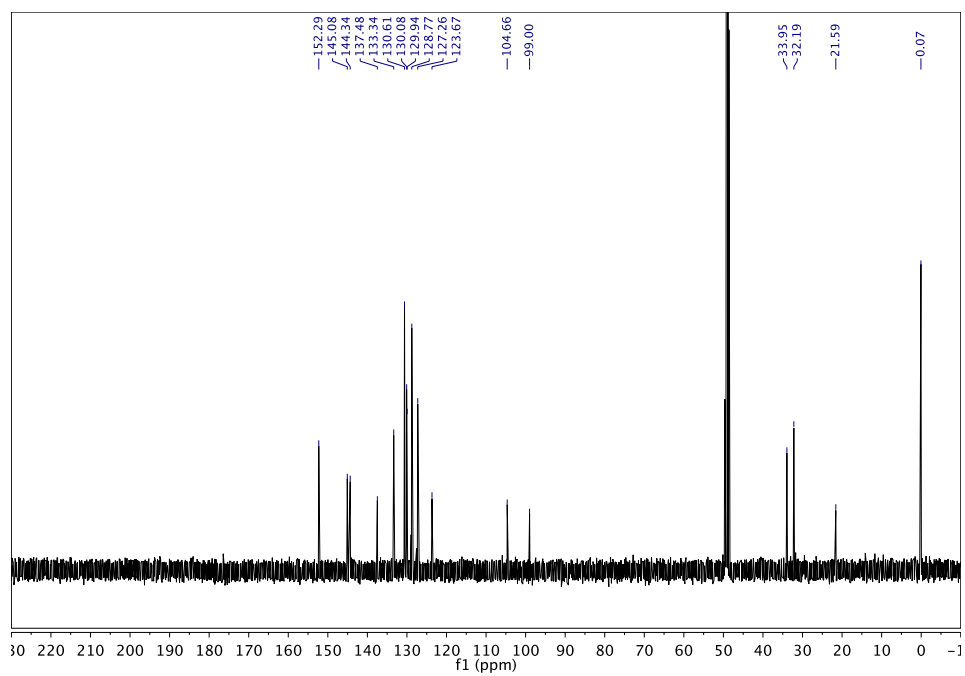
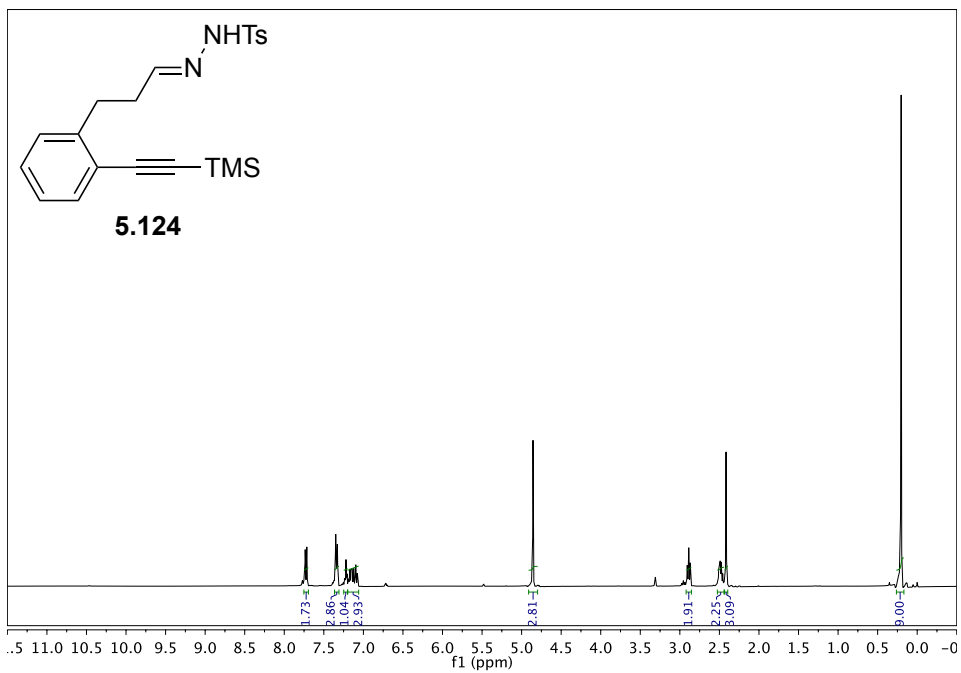


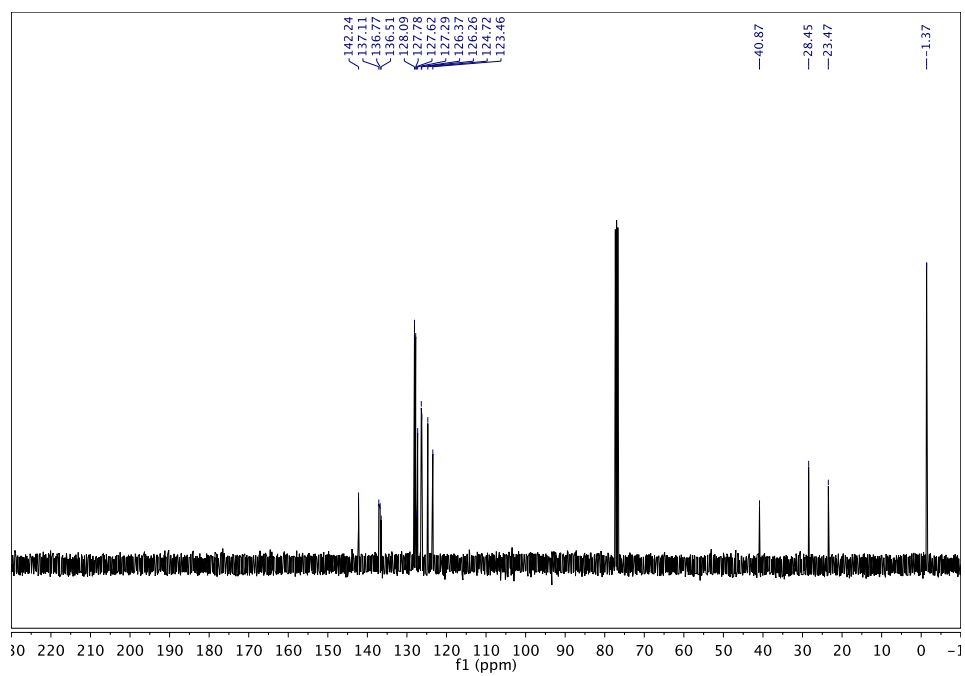
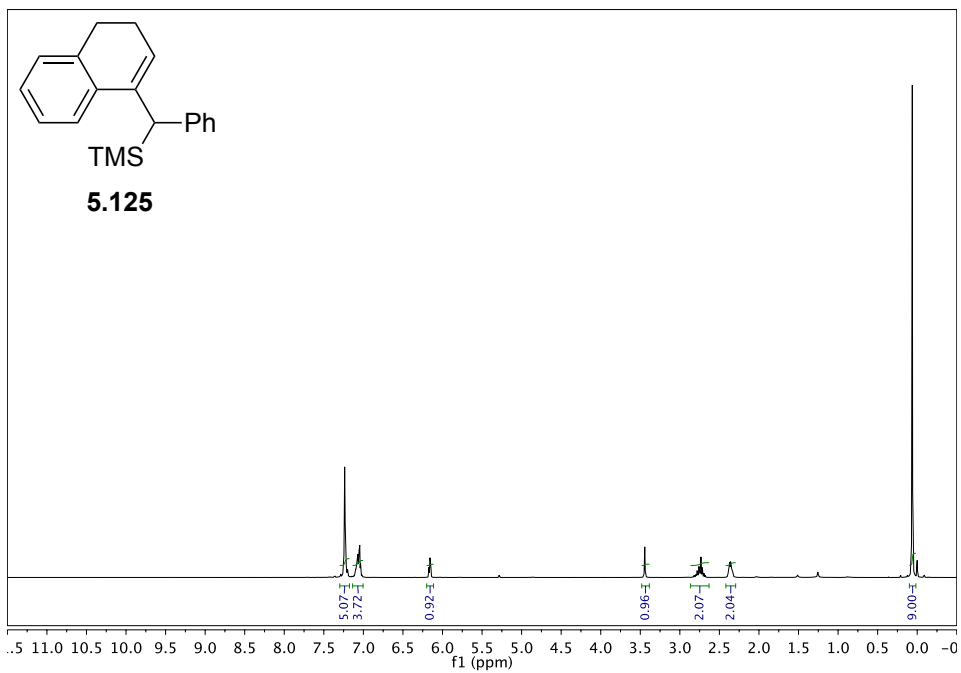


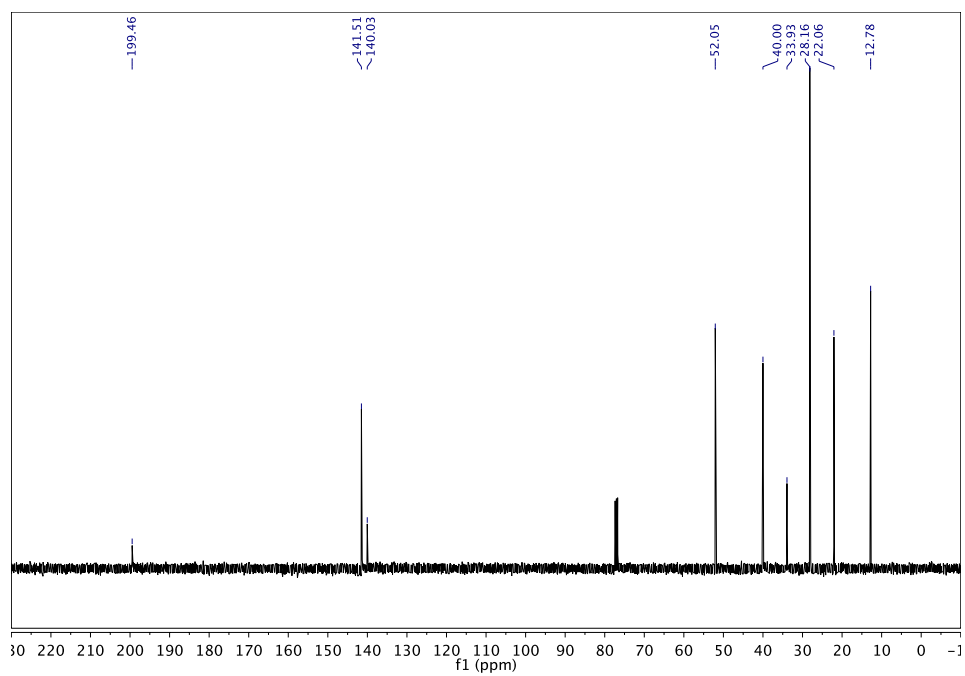
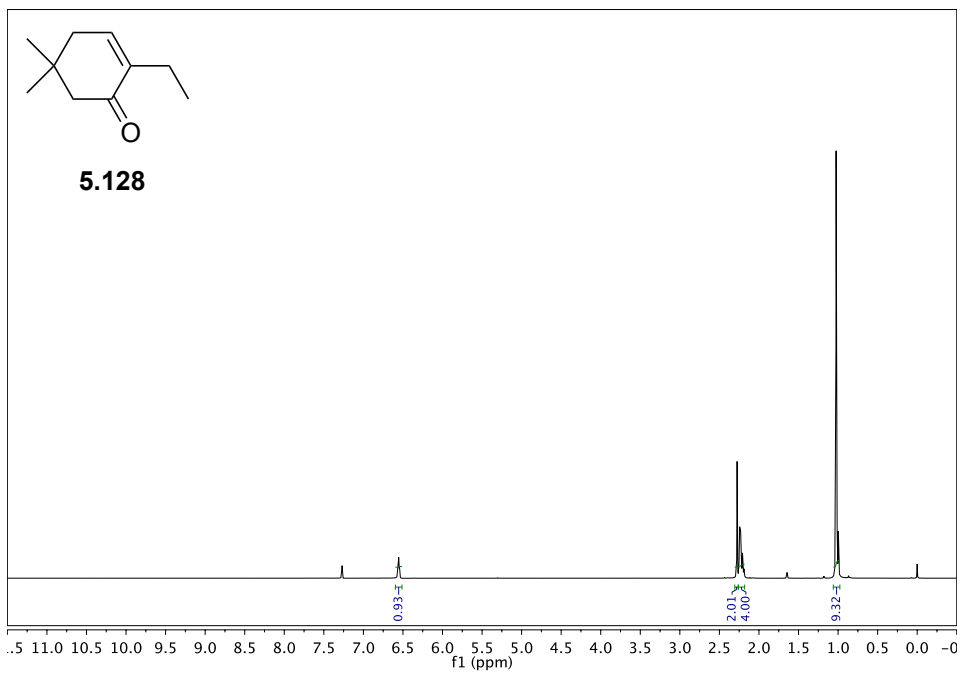


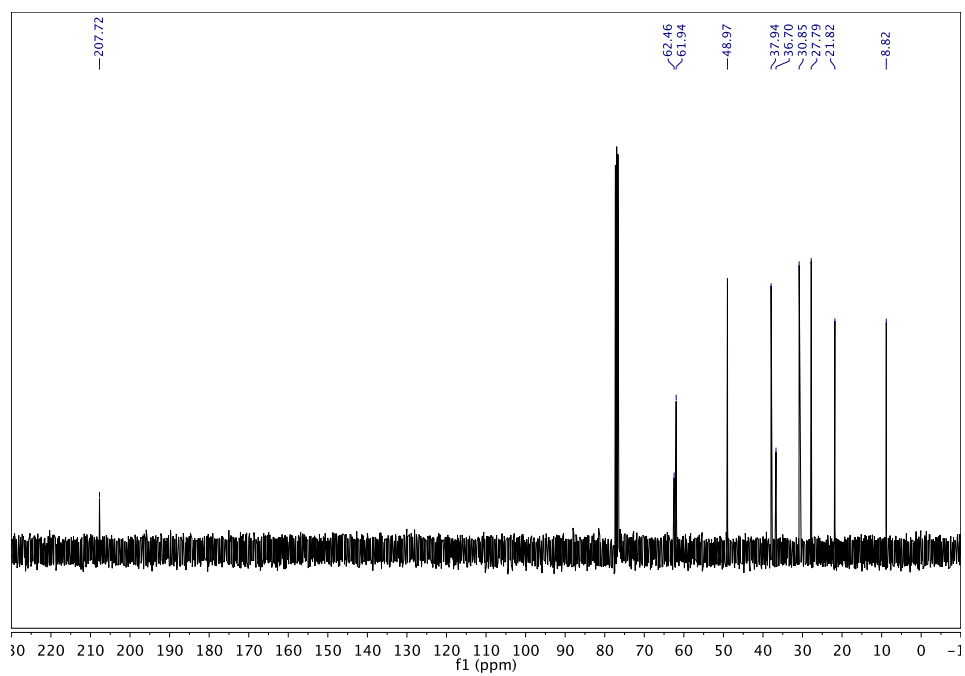
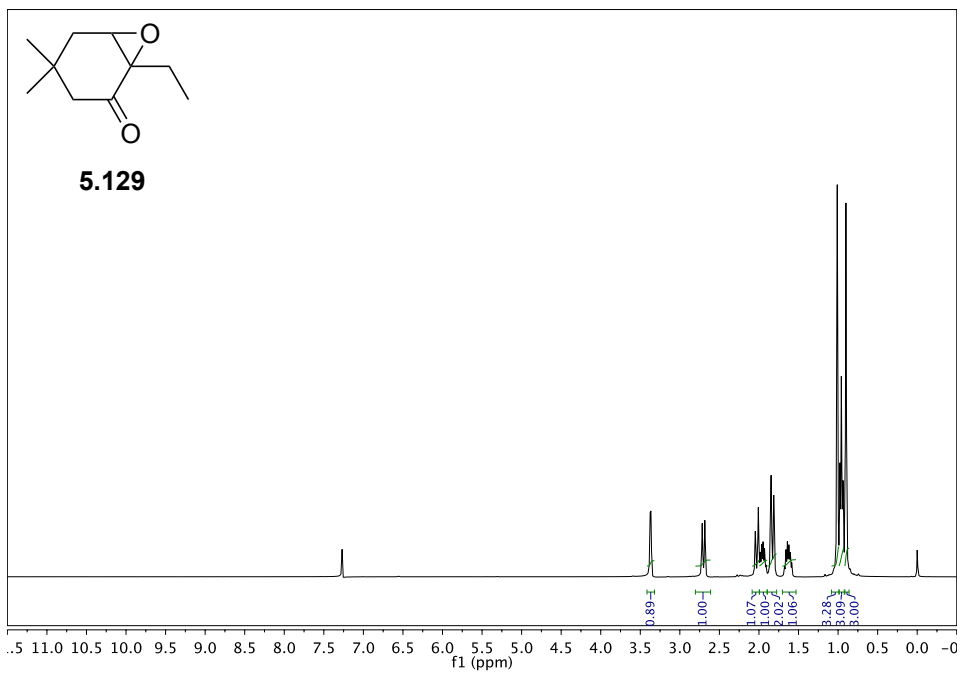


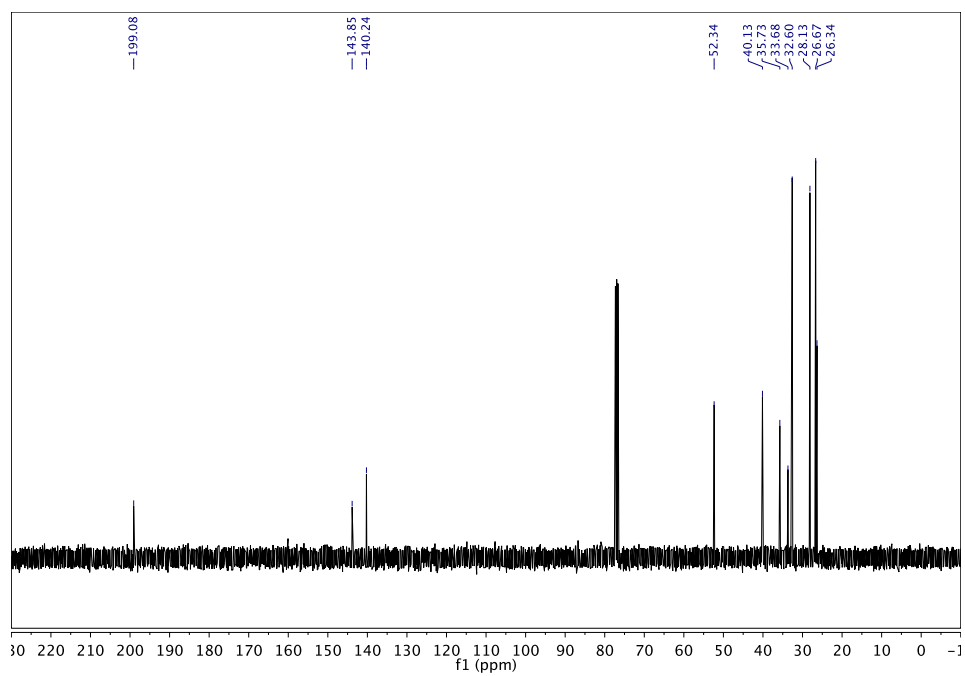
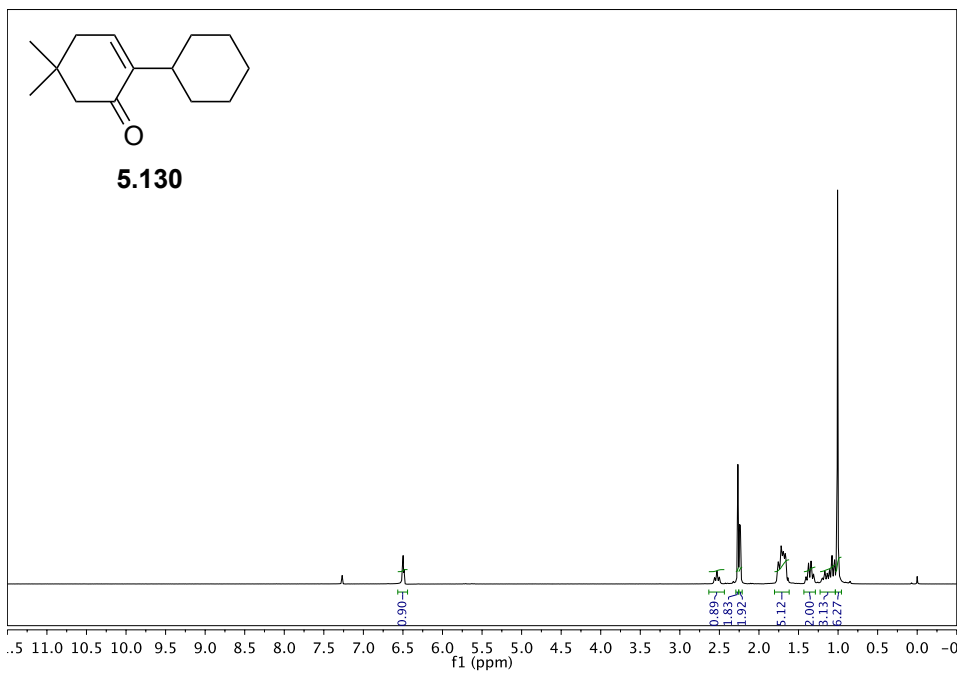


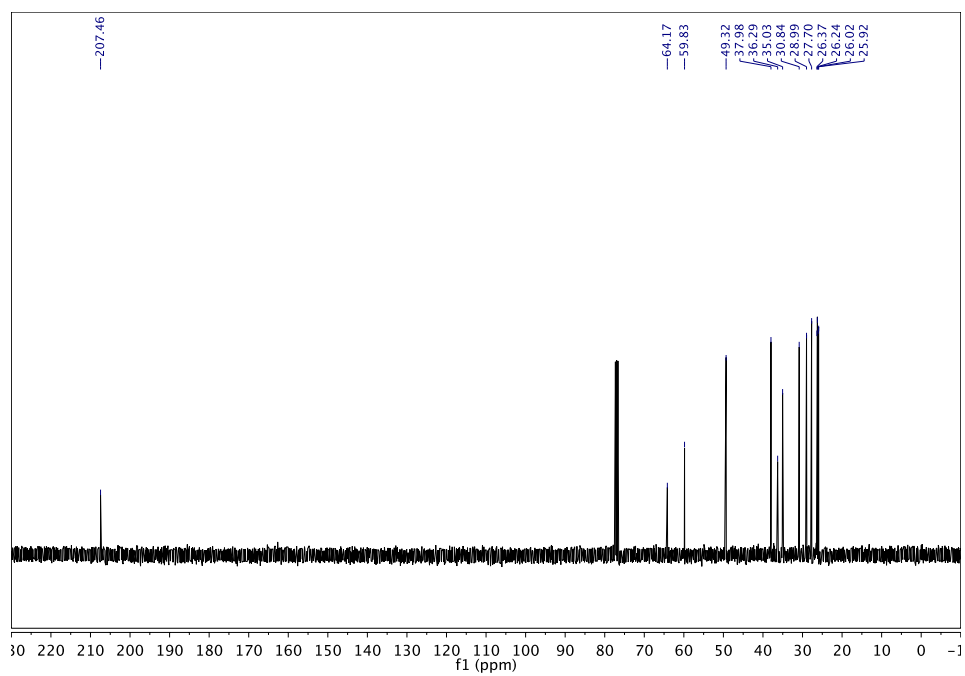
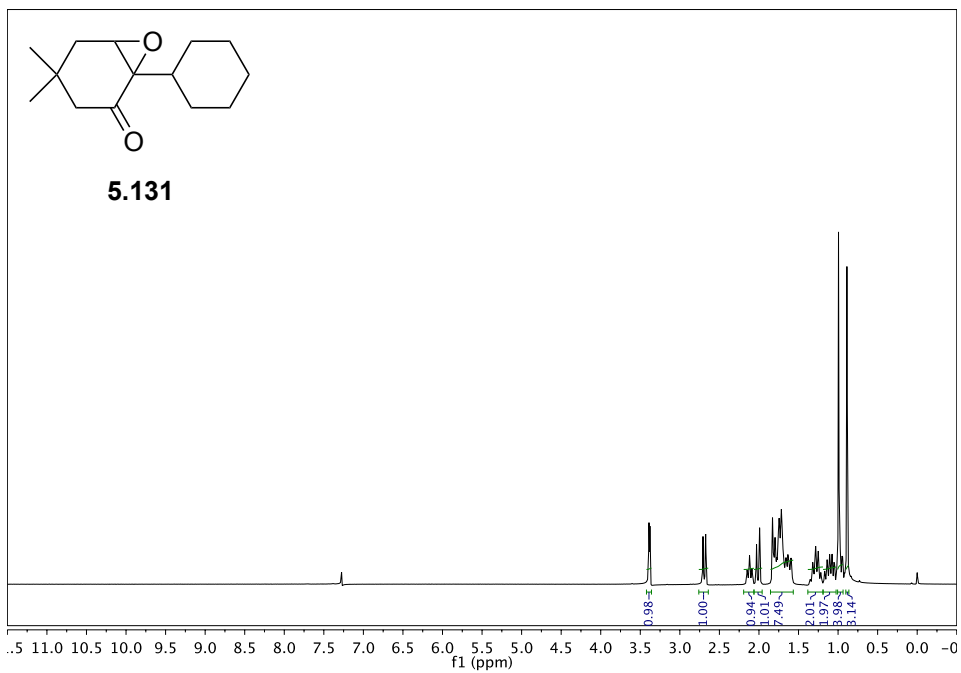


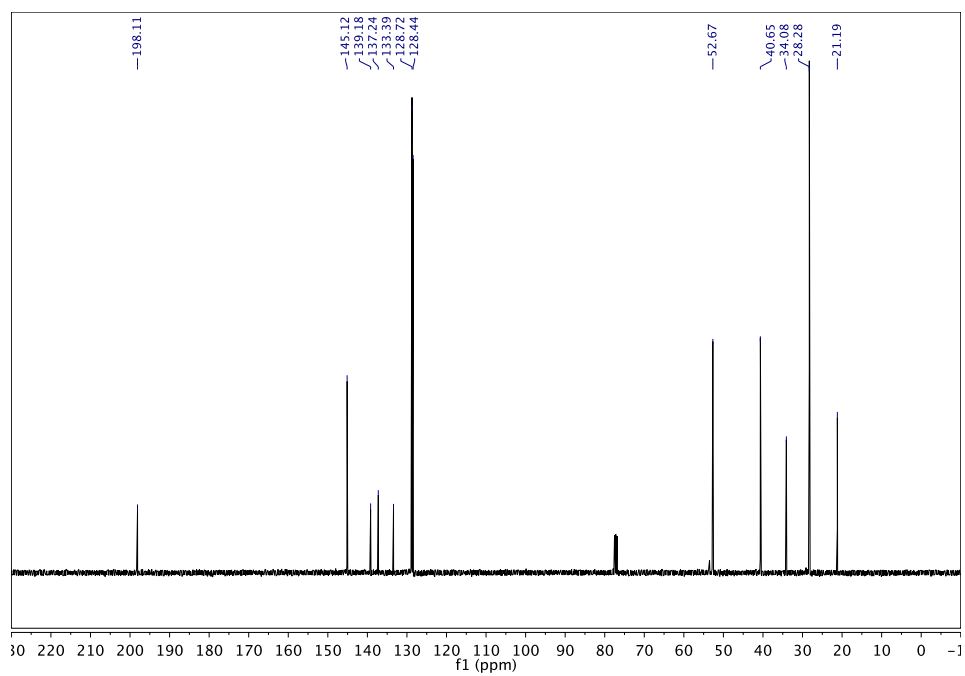
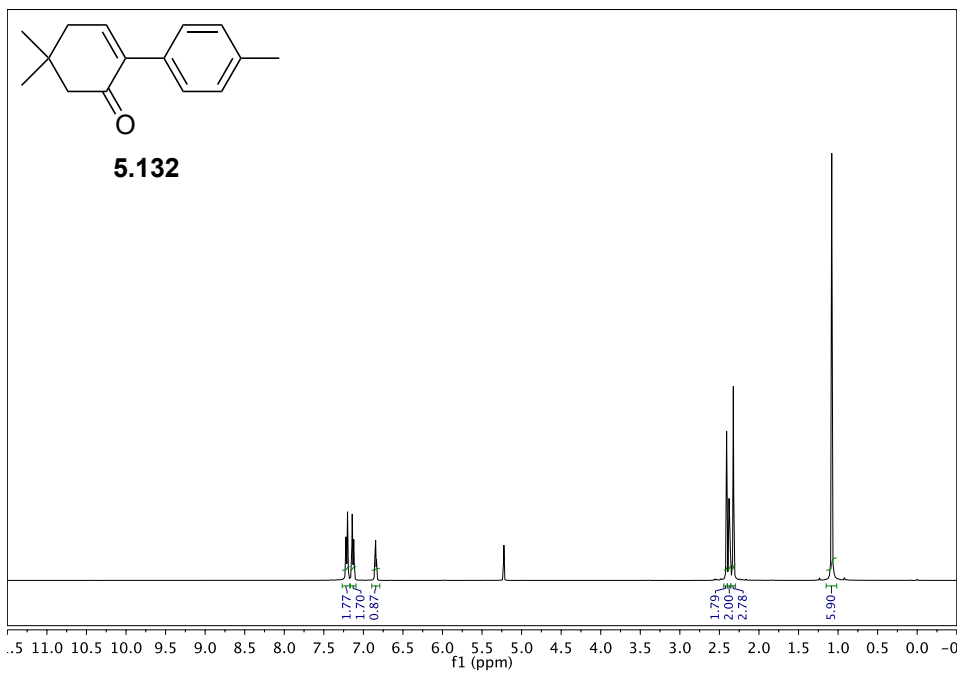


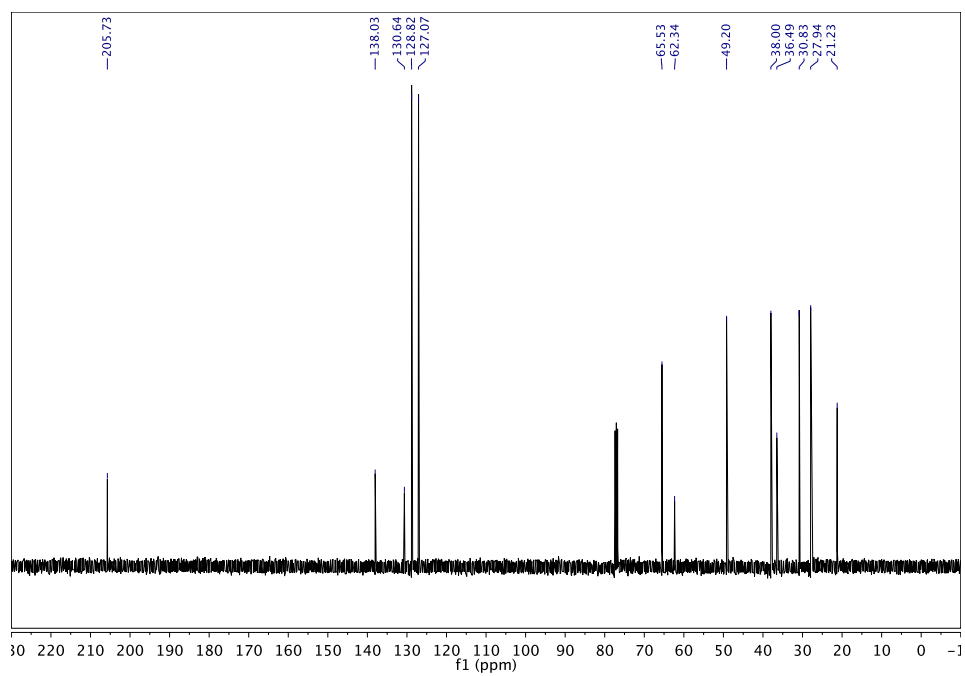
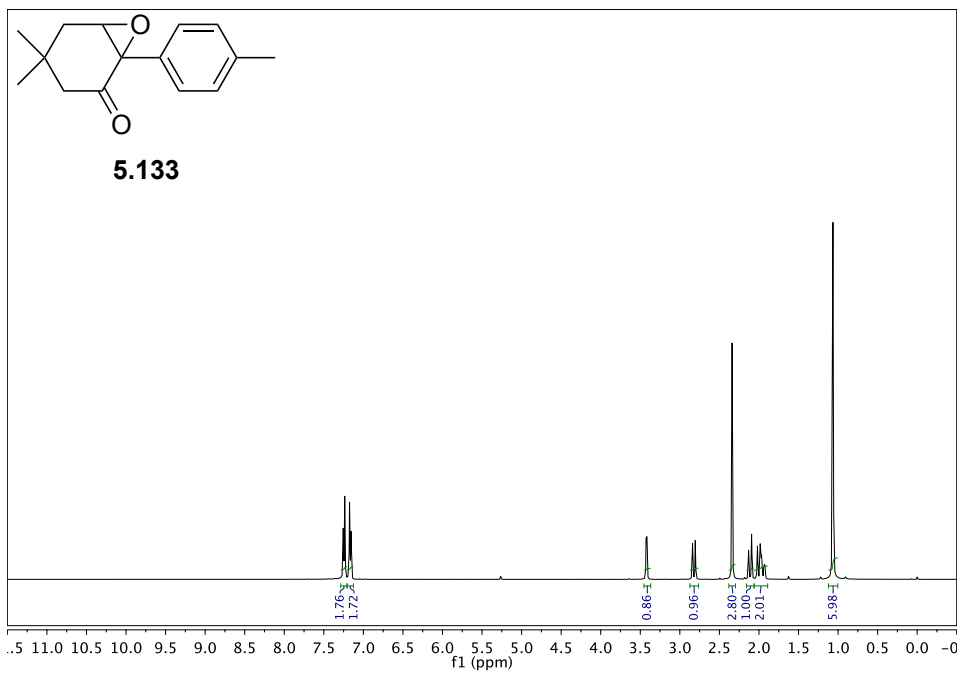


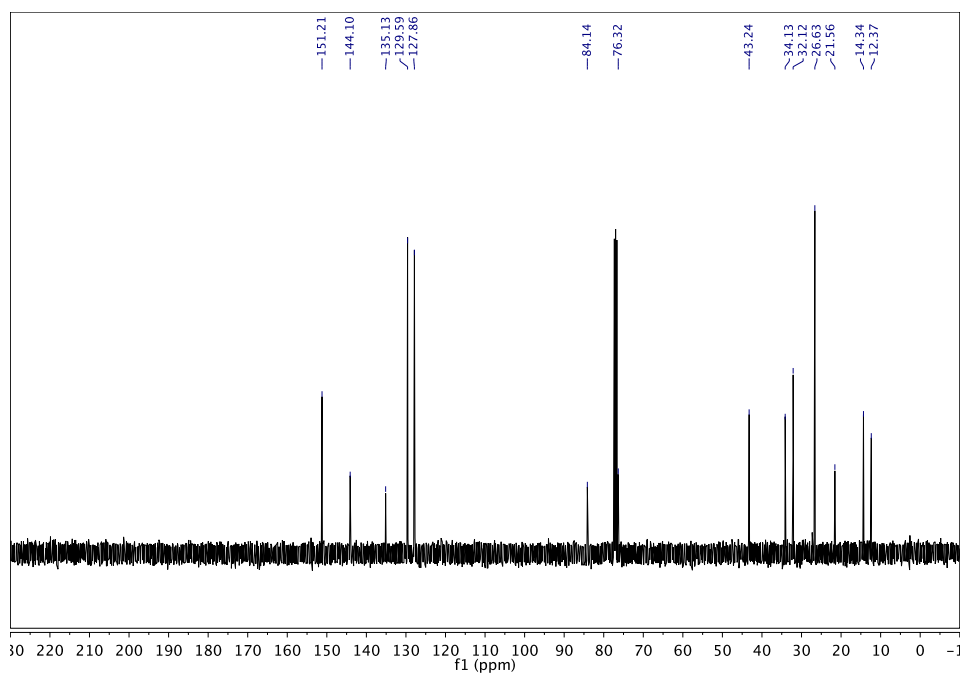
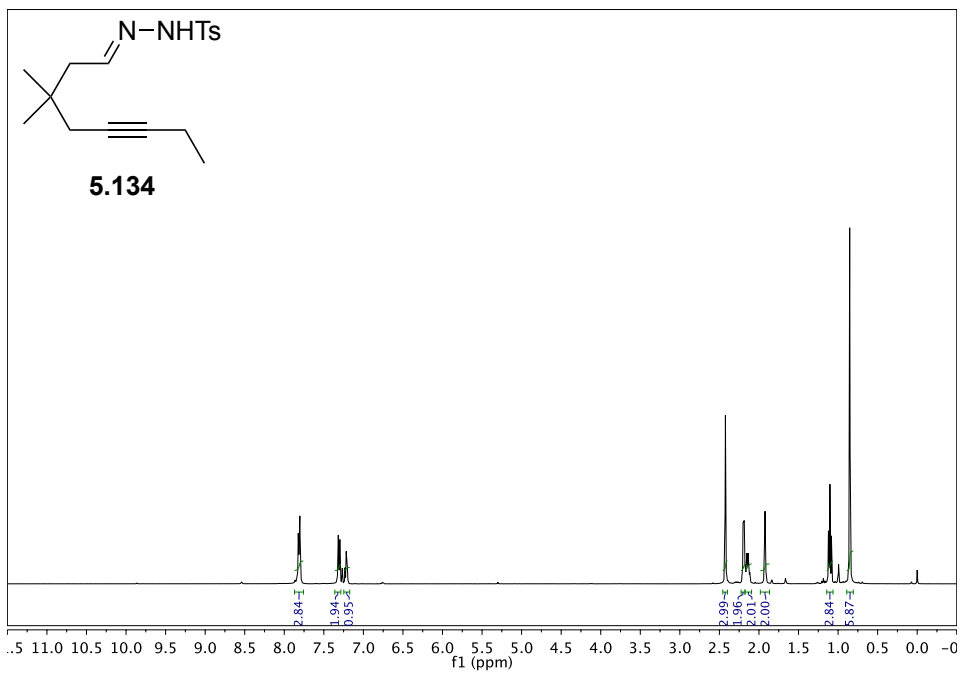


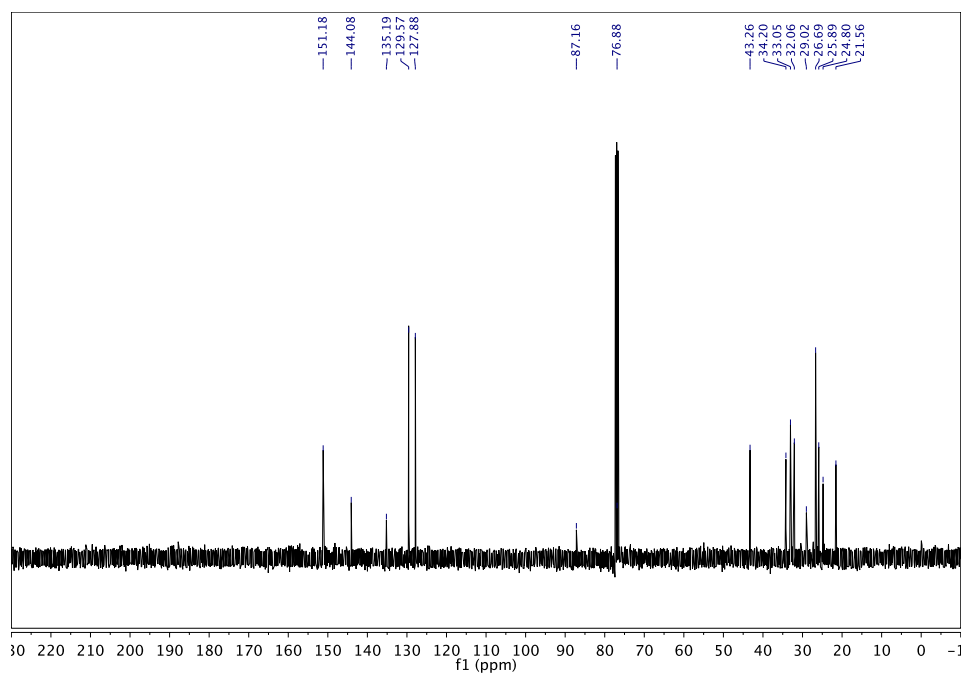
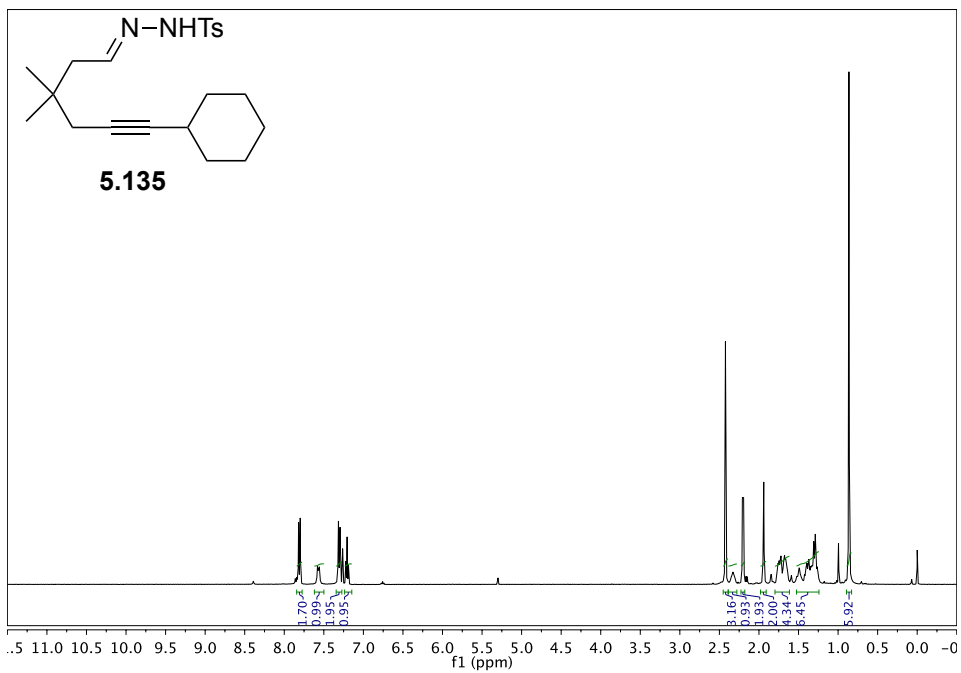


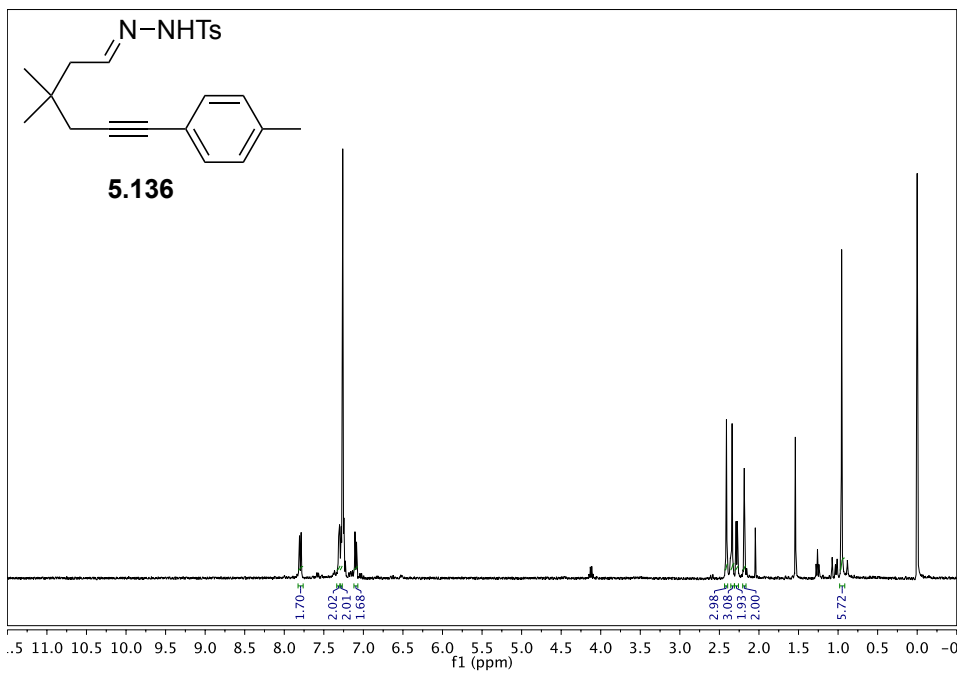


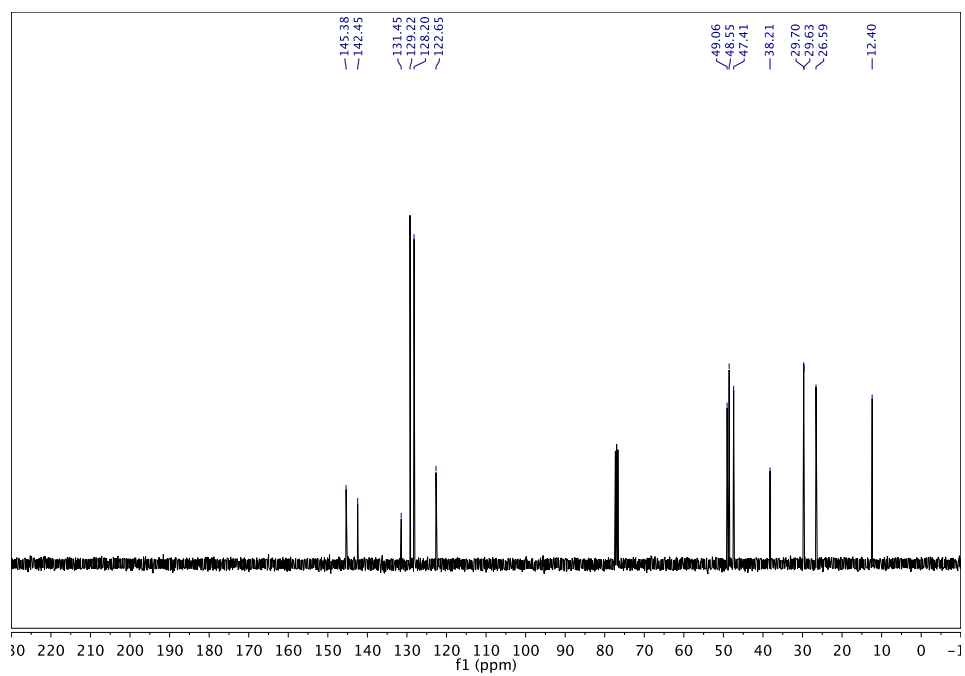
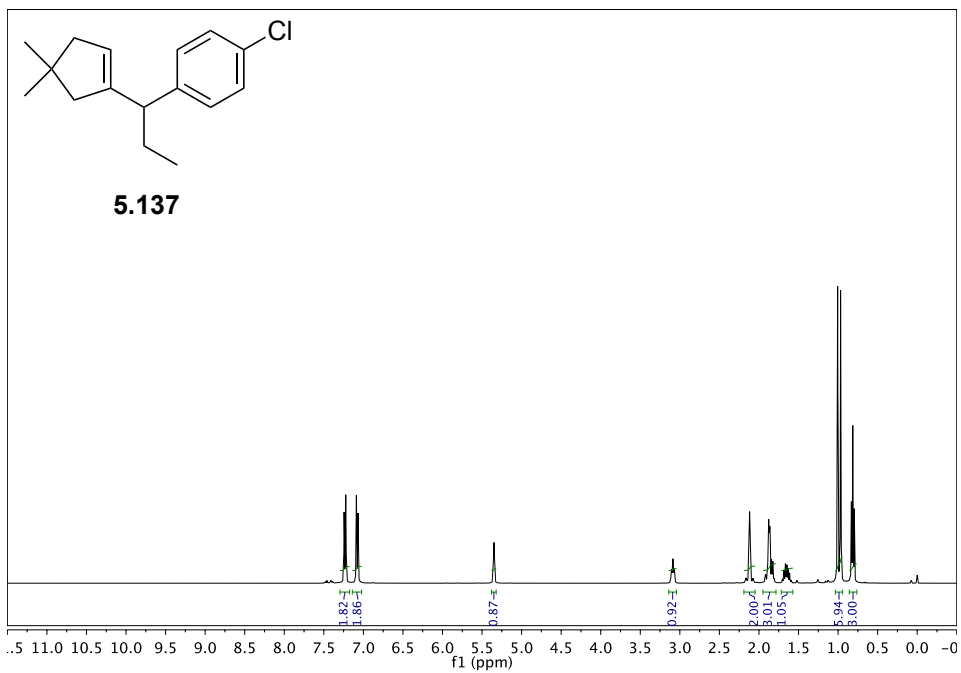


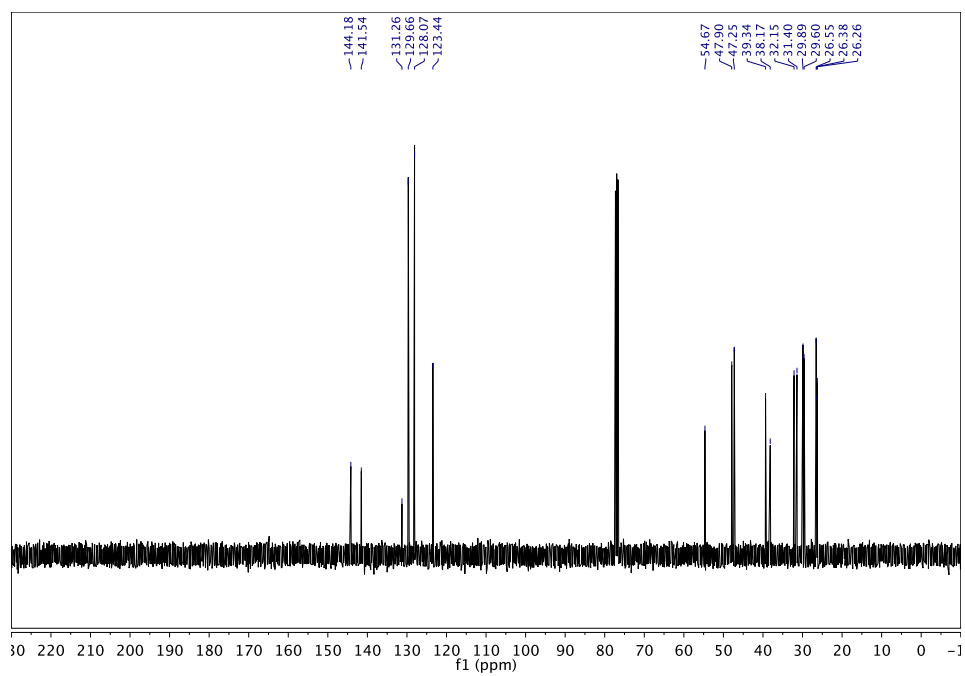
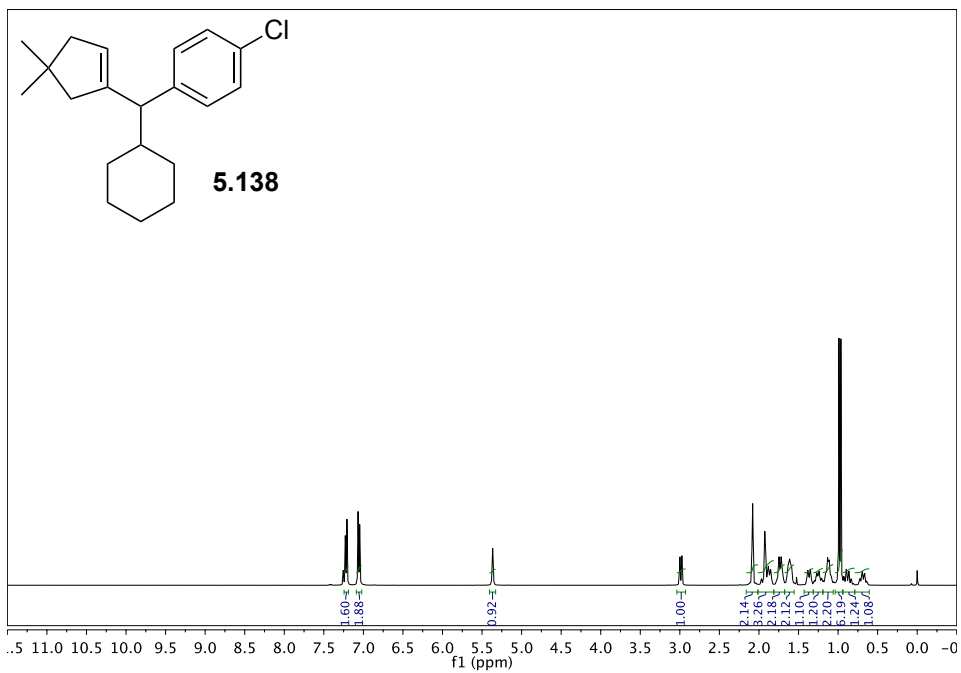


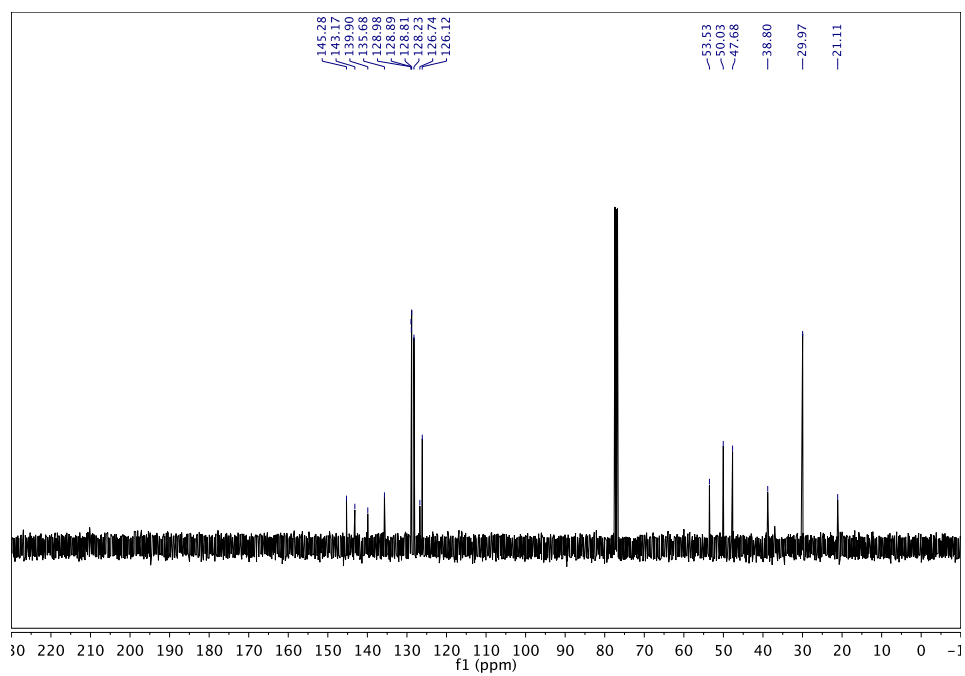
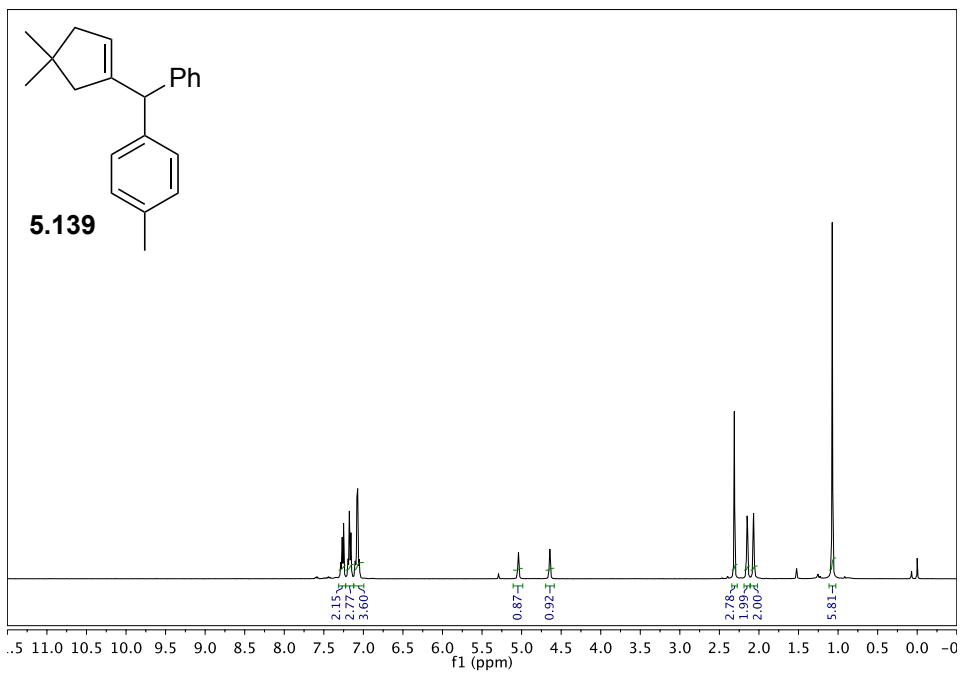


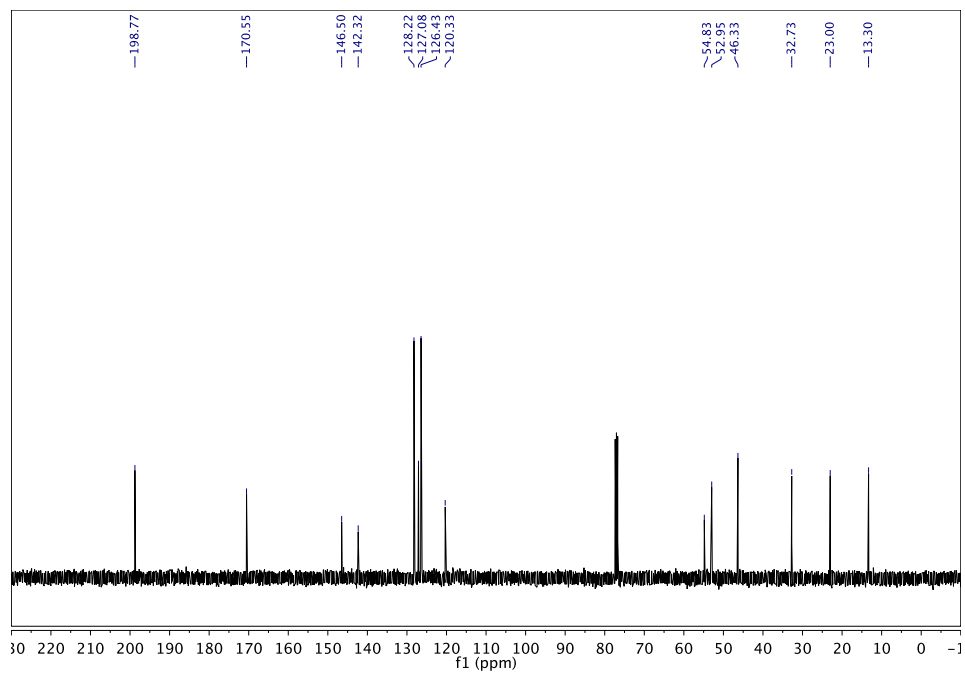
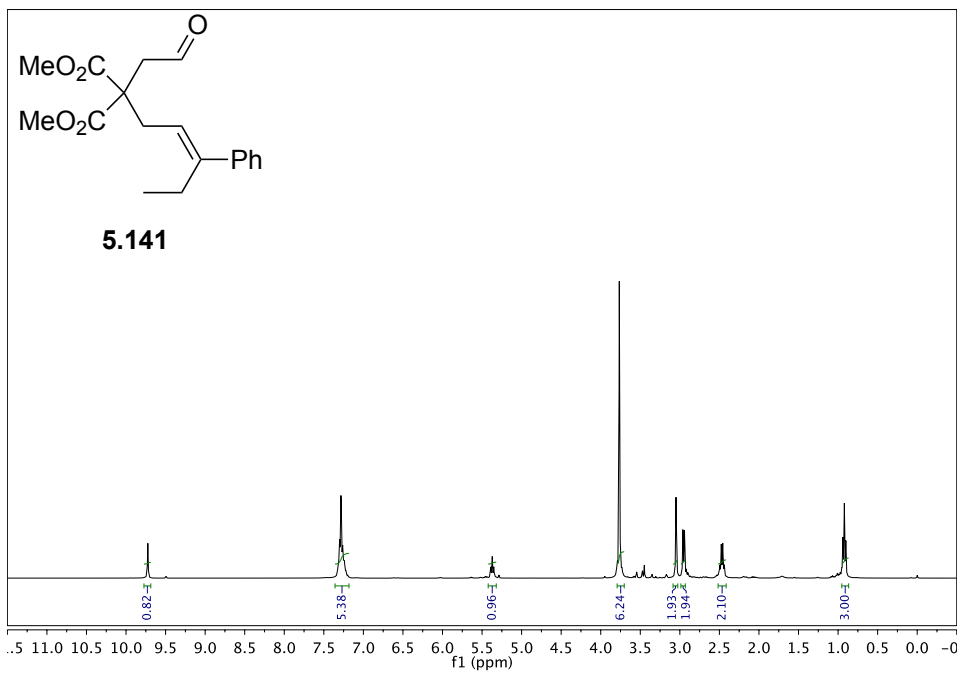


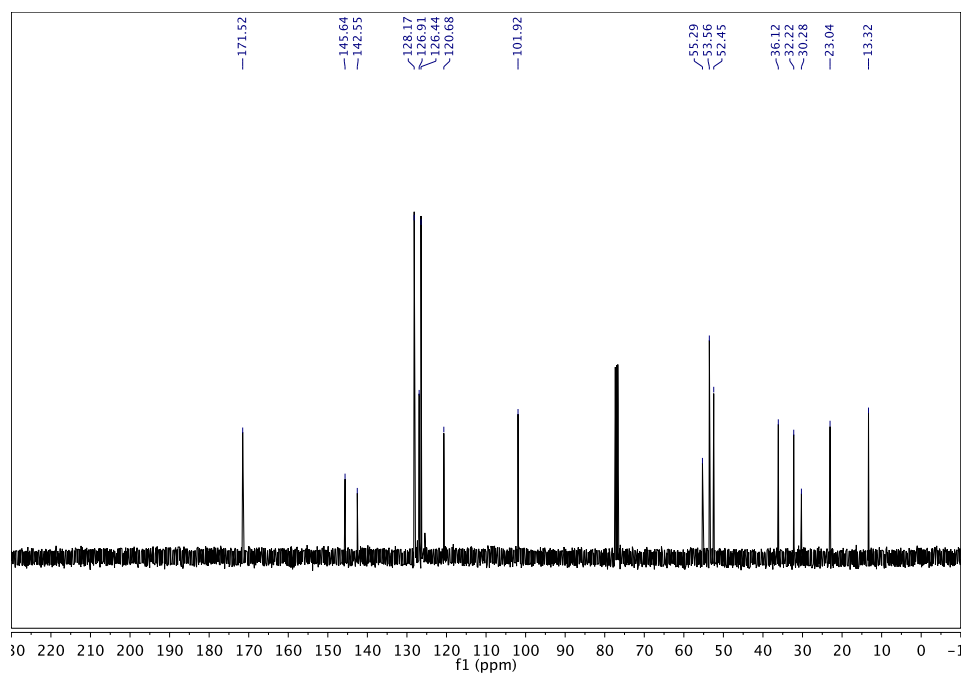
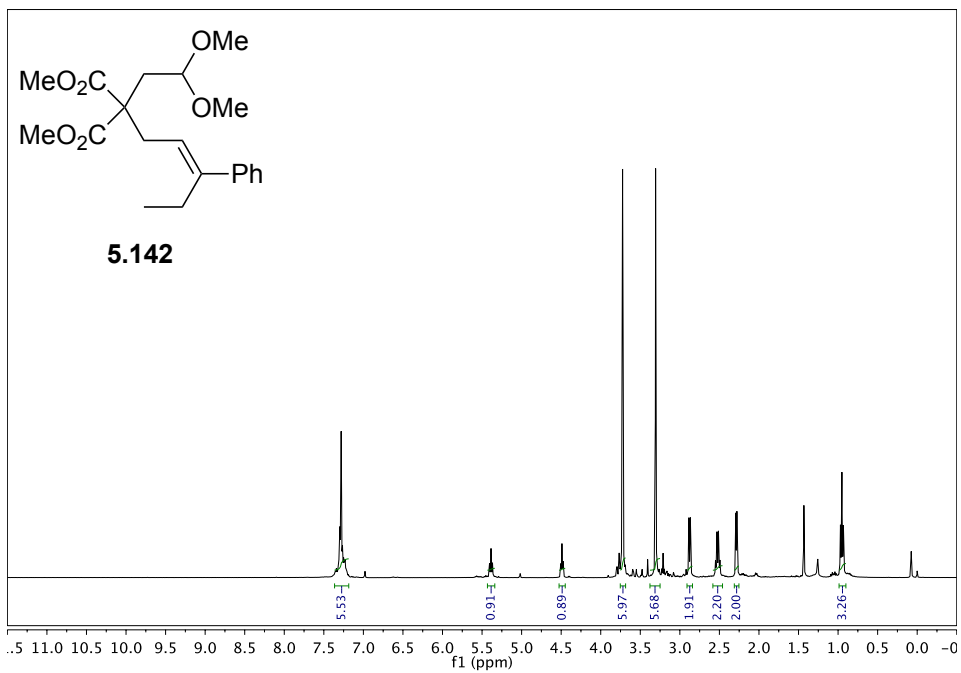


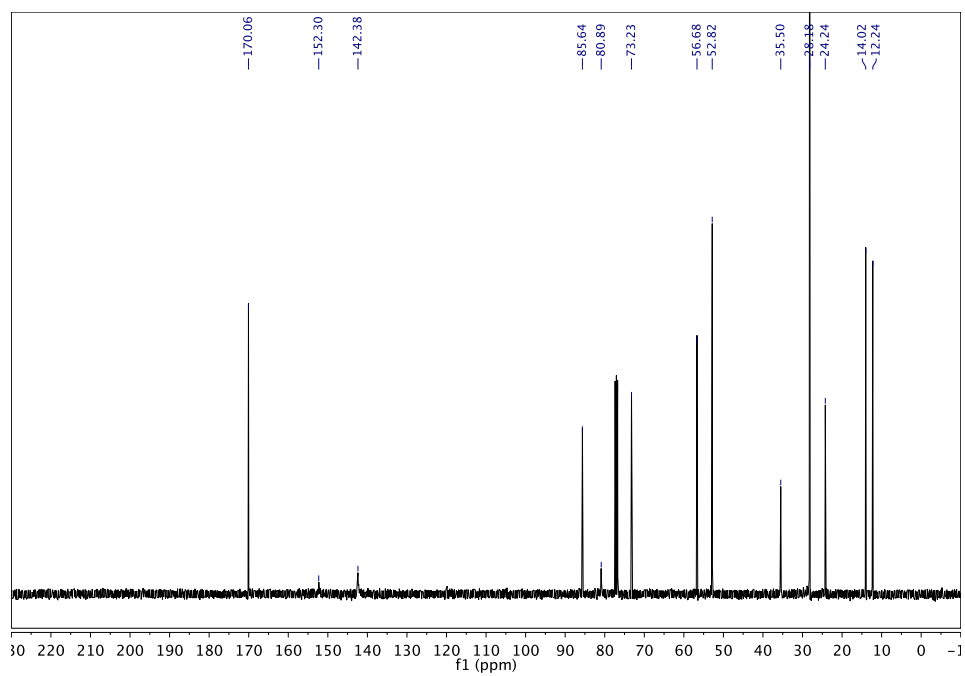
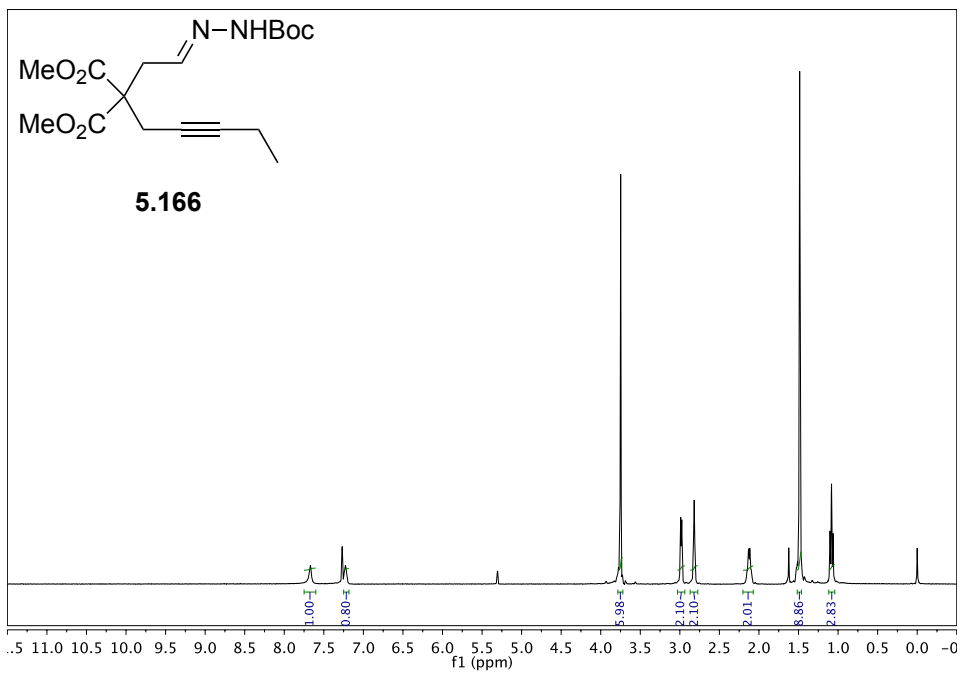


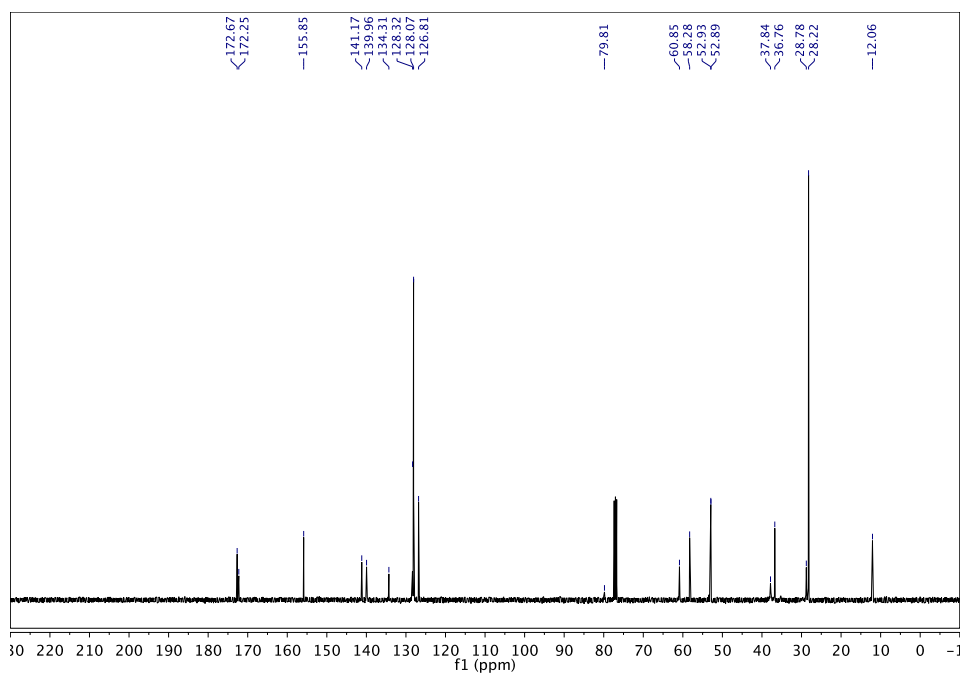
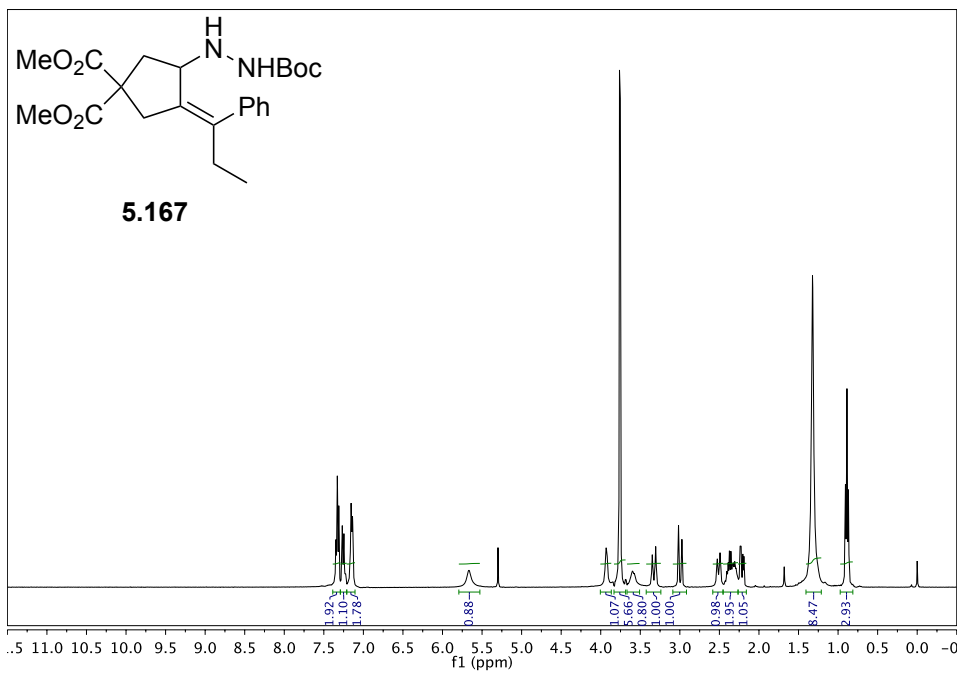


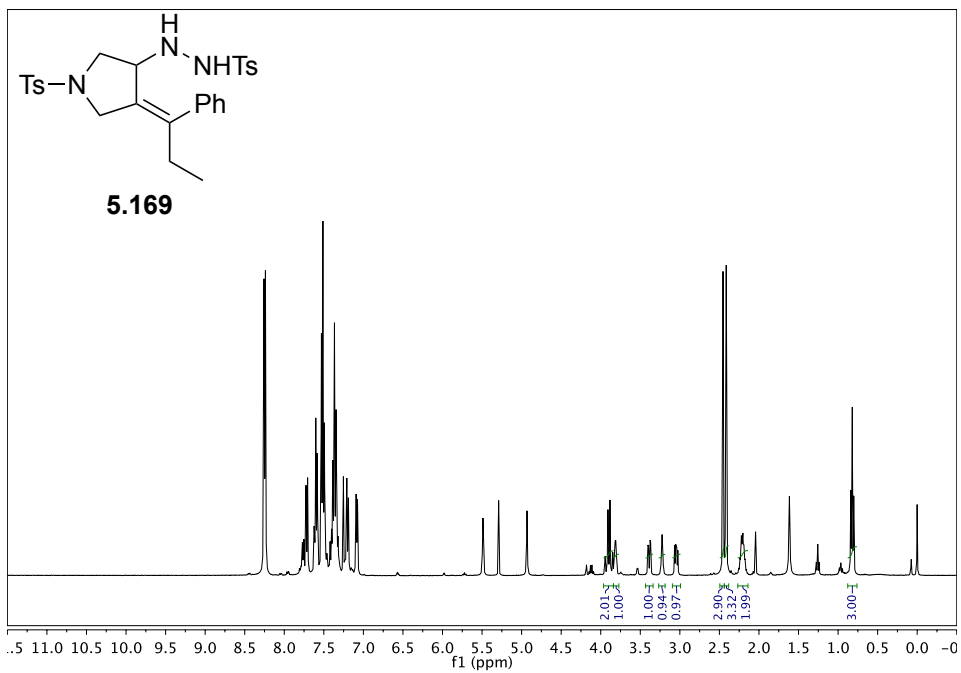


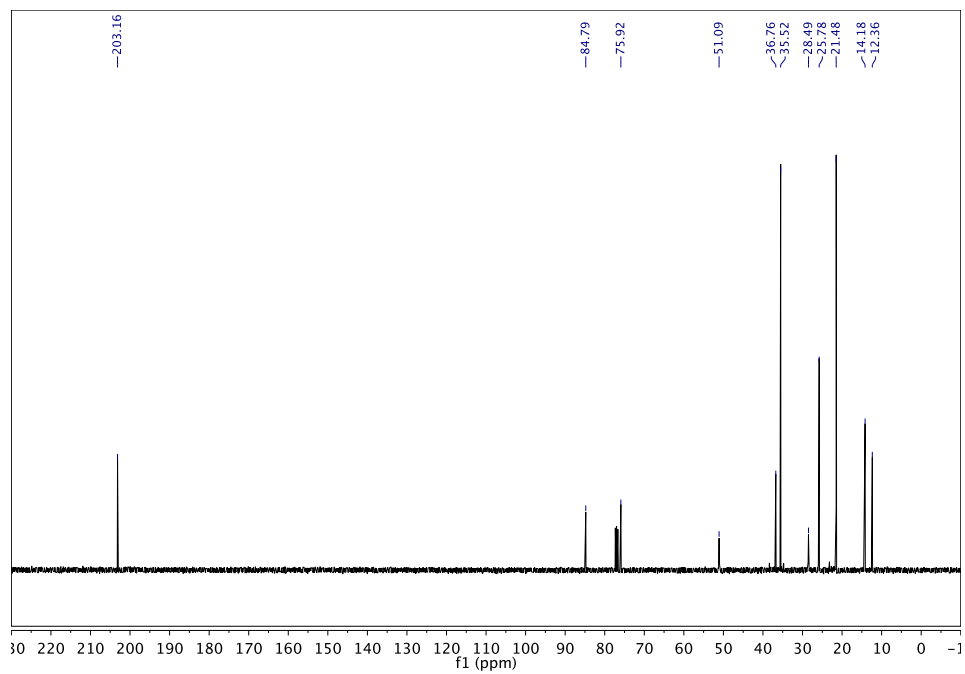
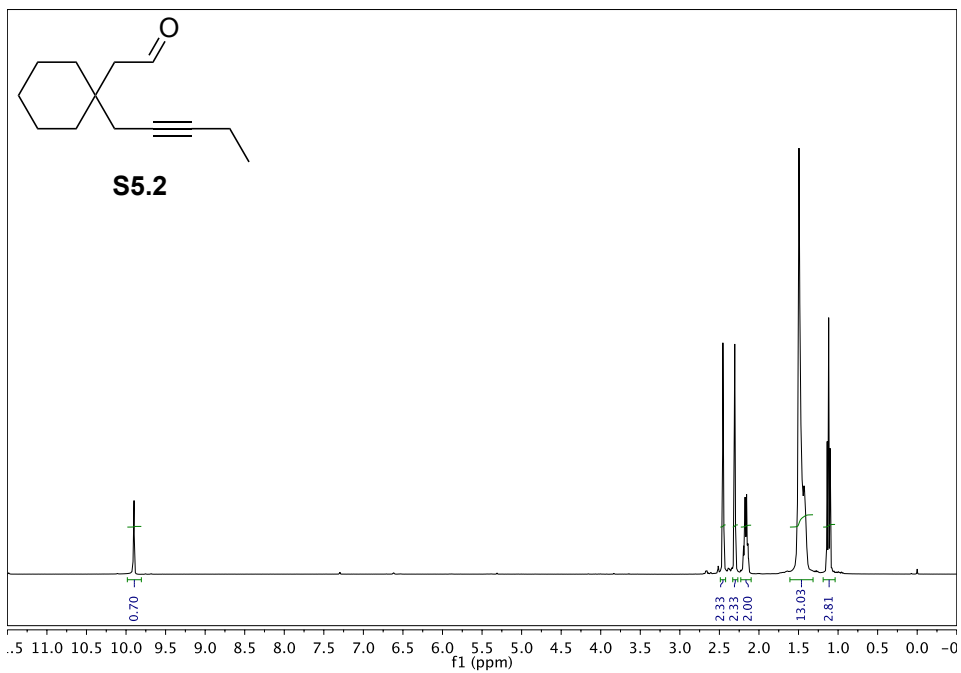


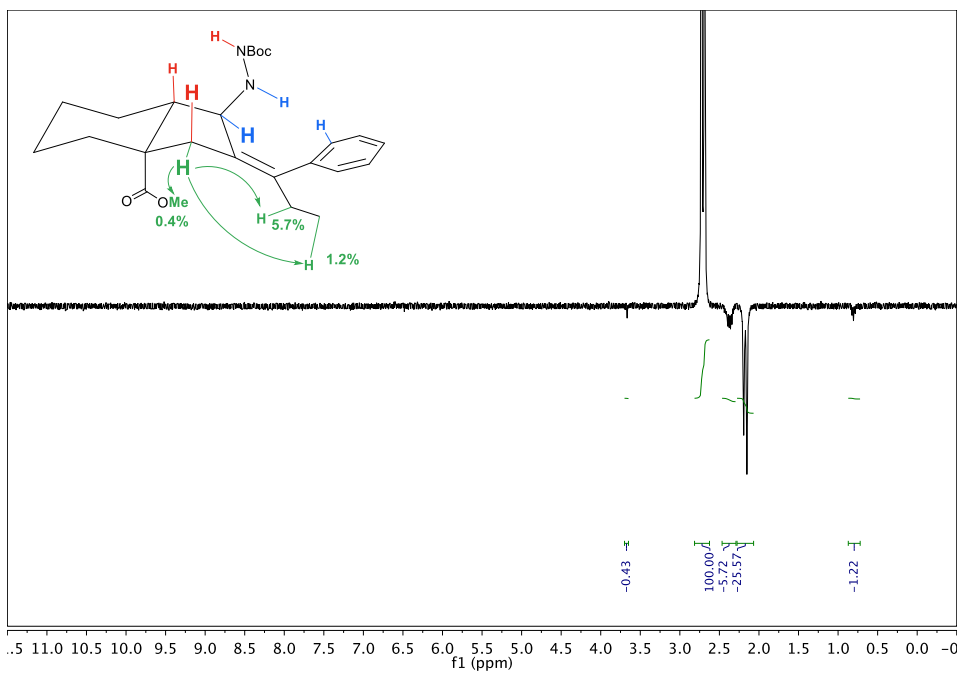
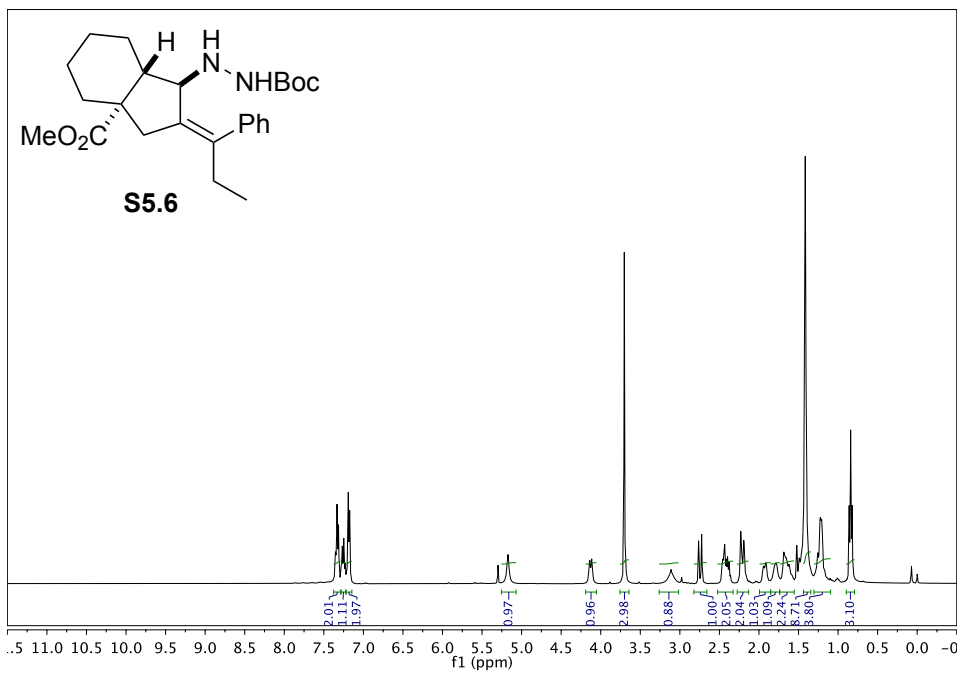


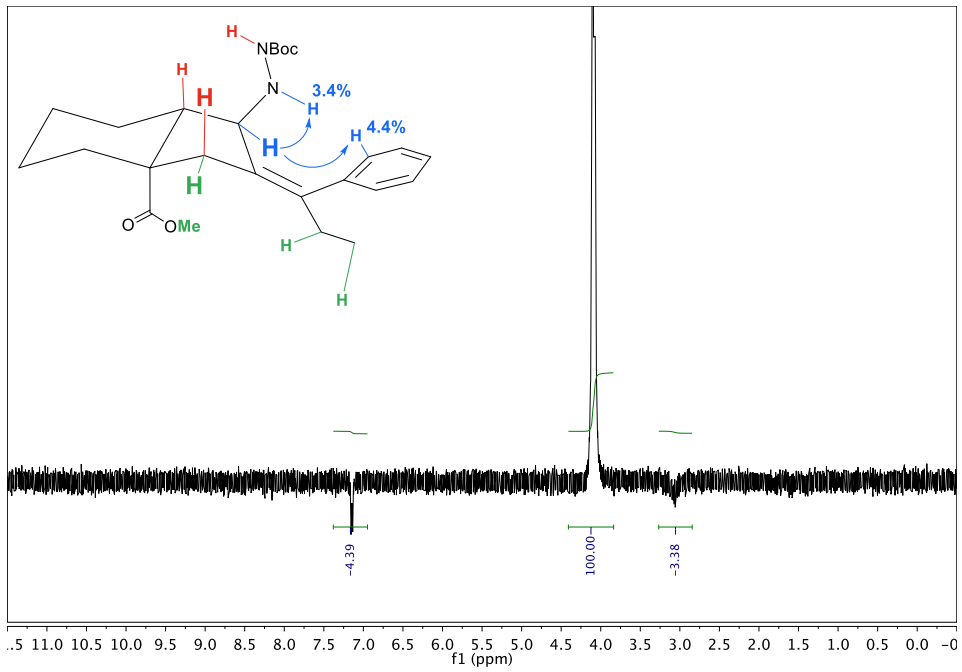
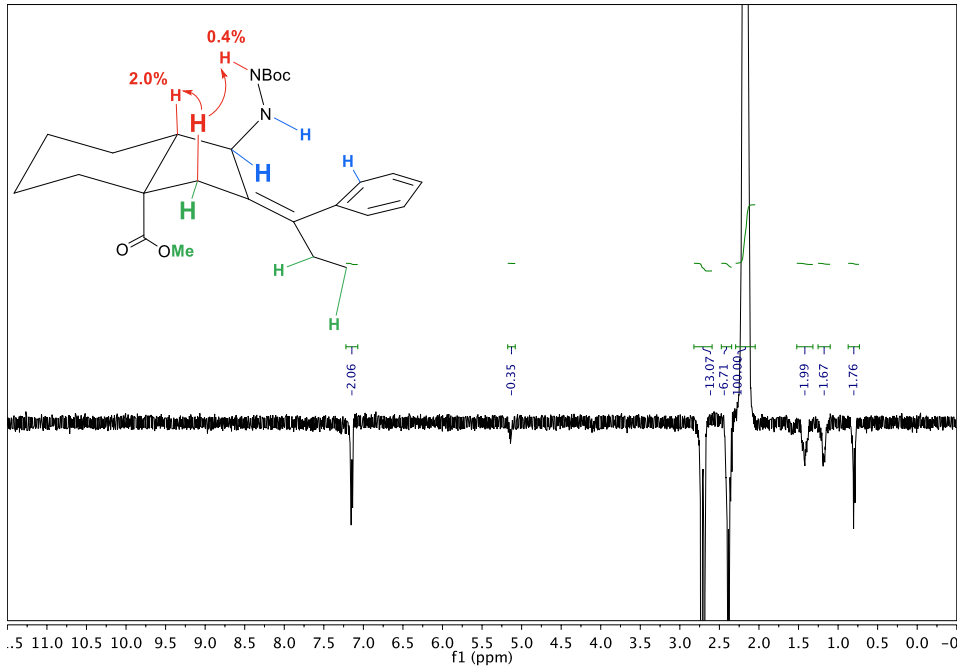


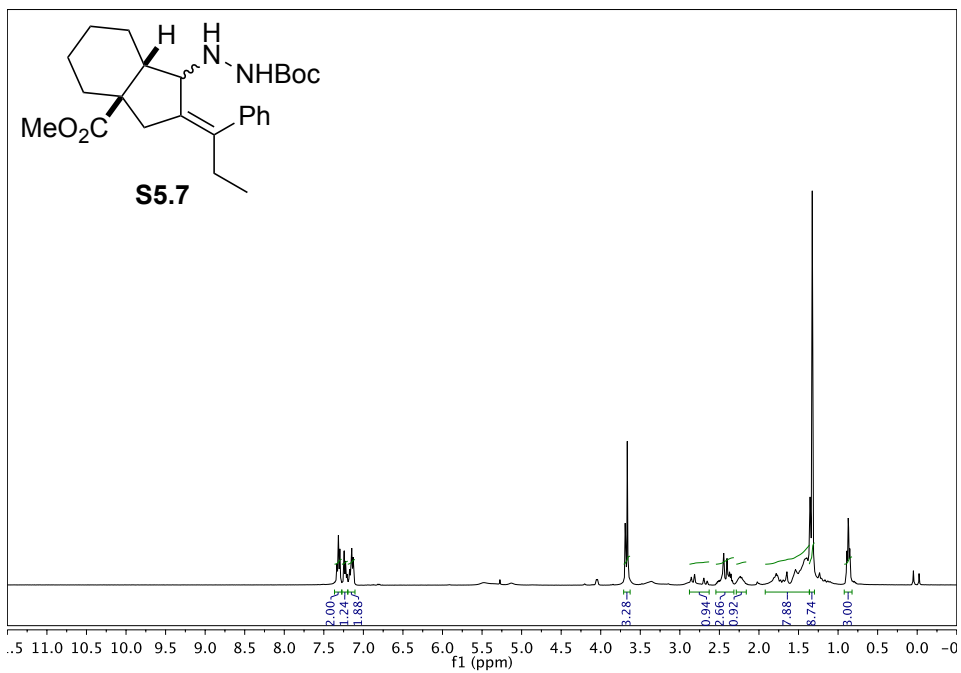


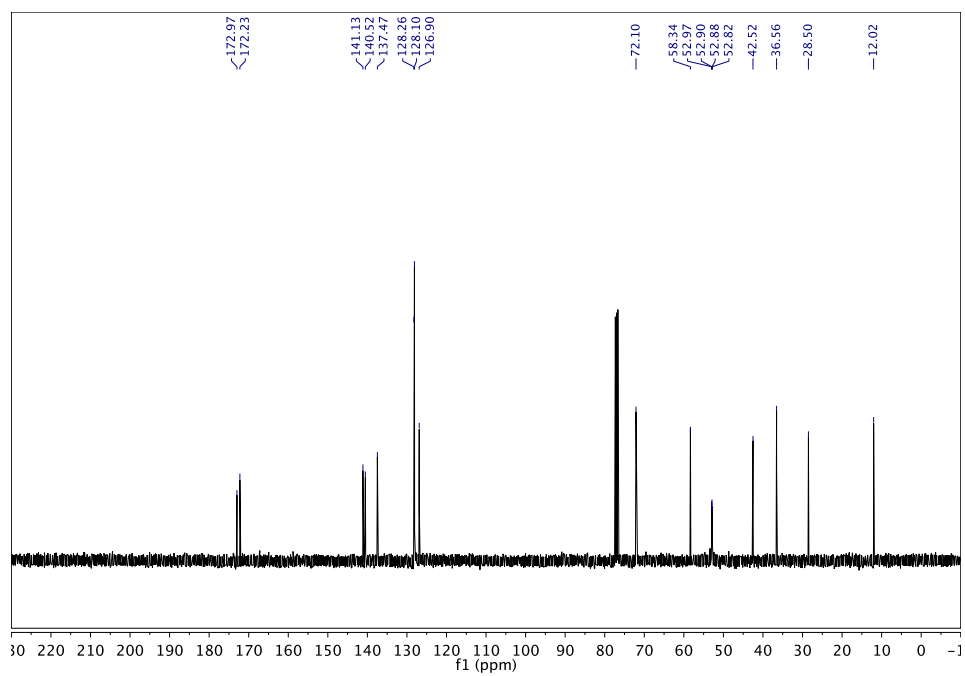
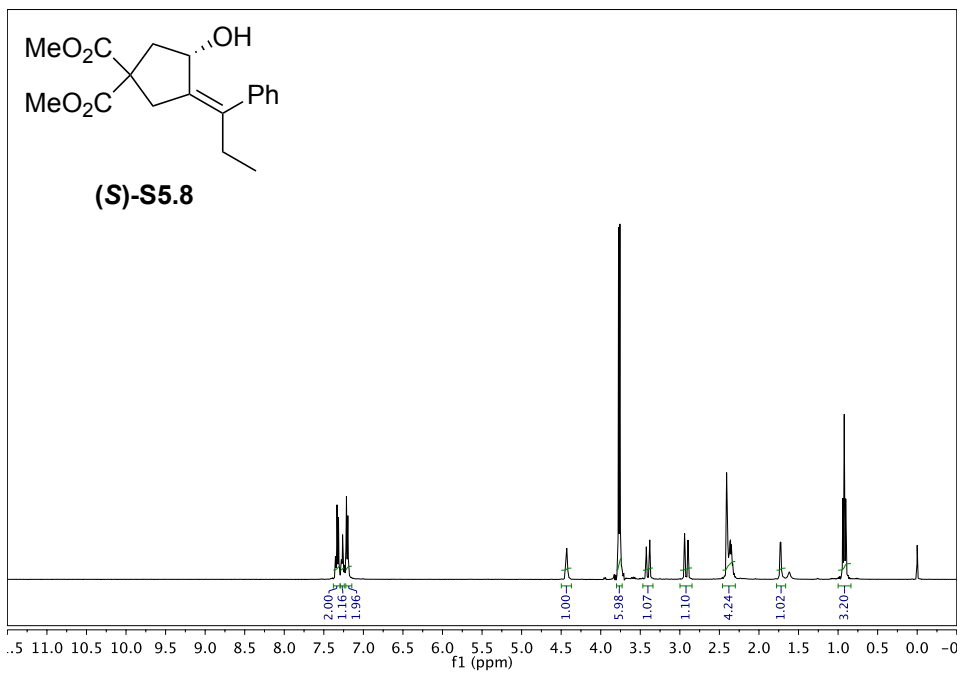




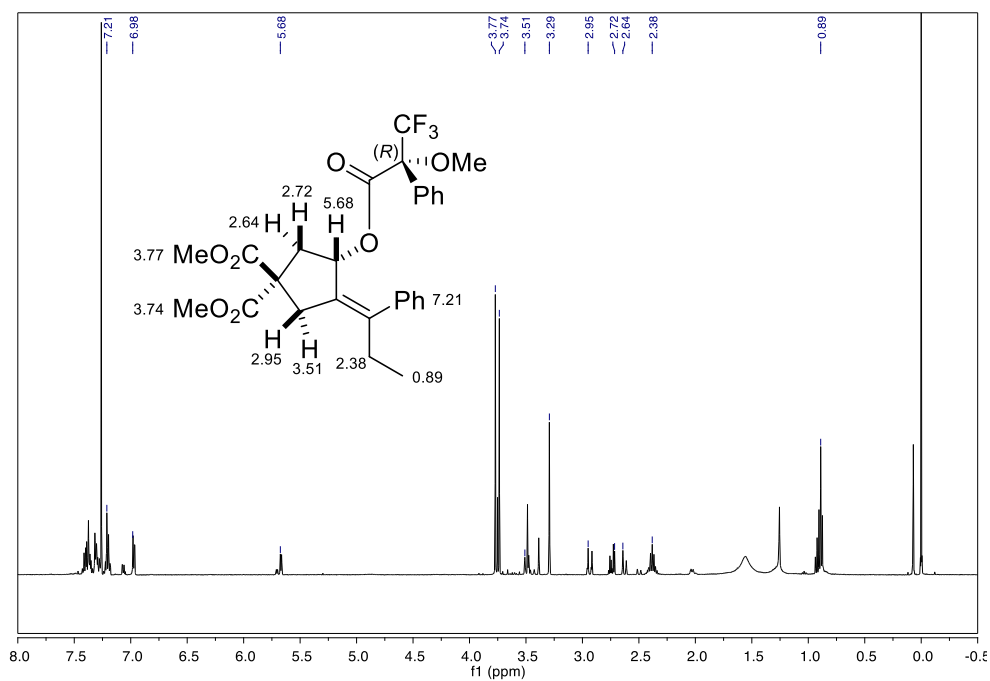
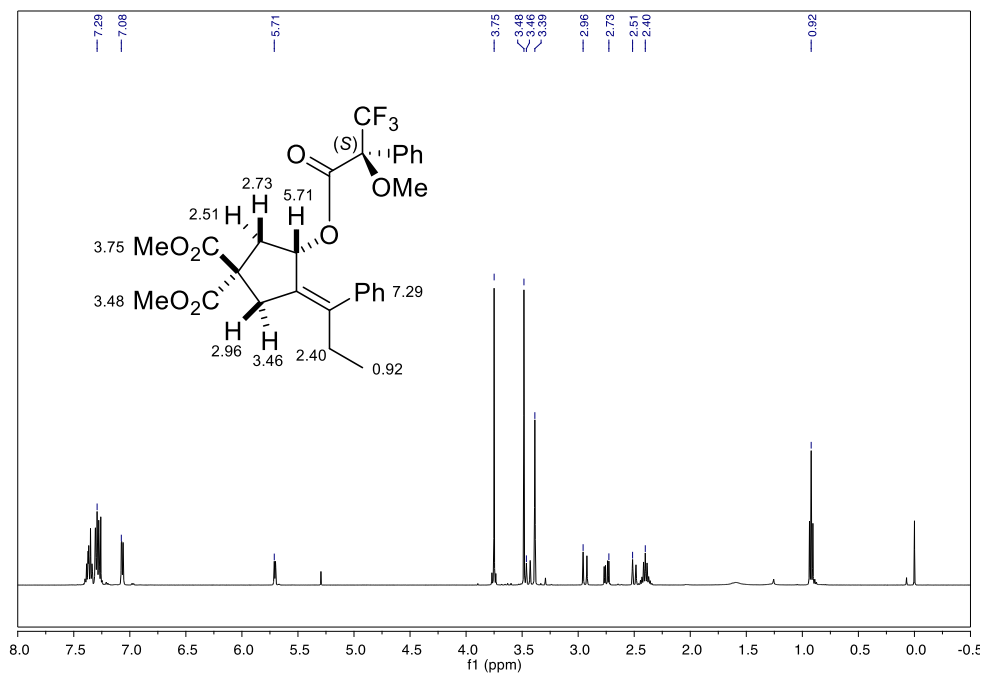


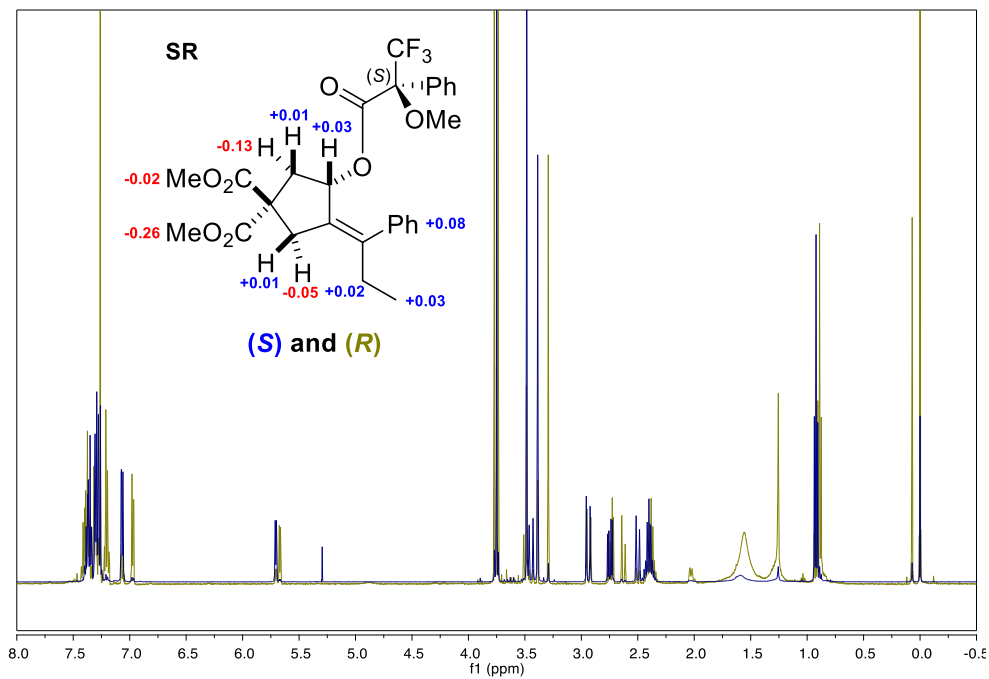






Copies of ^1H NMR spectra of MTPA esters of (*S*)-**S5.8**





Chiral HPLC data

1. Analytical Method

Column: Chiralpak IA

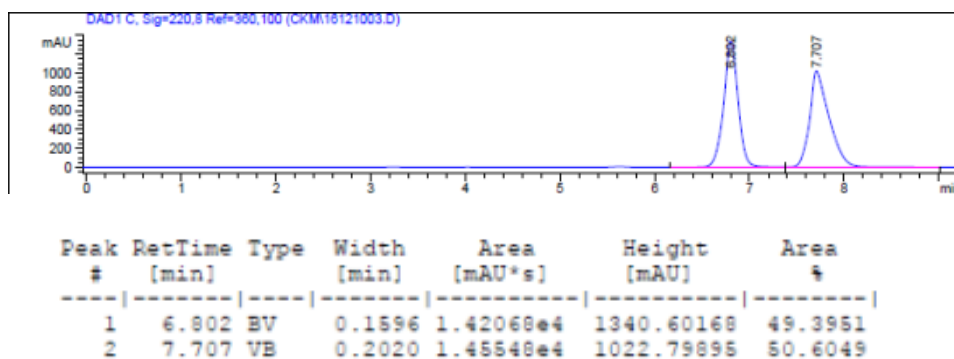
Eluent: Hexane/isopropyl alcohol

Flow rate: 1.0 ml/min or 0.5 ml/min

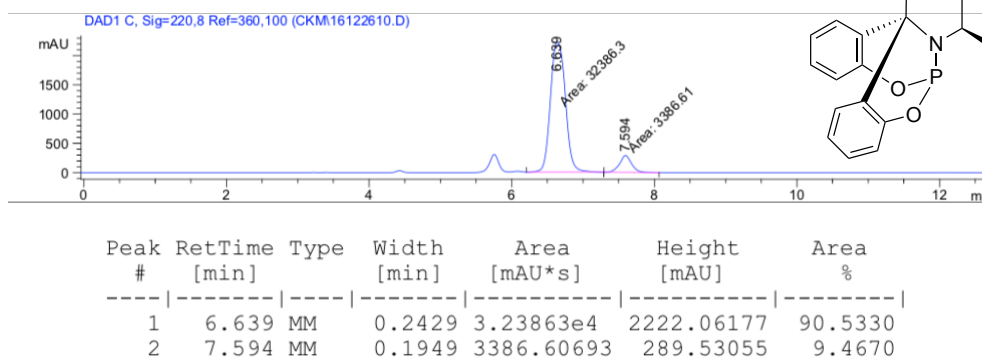
Detection Wavelength: 220 nm or 230 nm

2. Chromatographic Traces of **5.35** (methanol solvent)

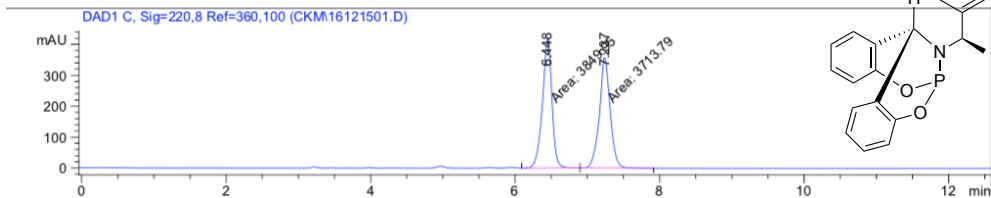
2-1. A racemic sample



2-2. A chiral sample **5.35** using **5.145** in MeOH (81% ee)

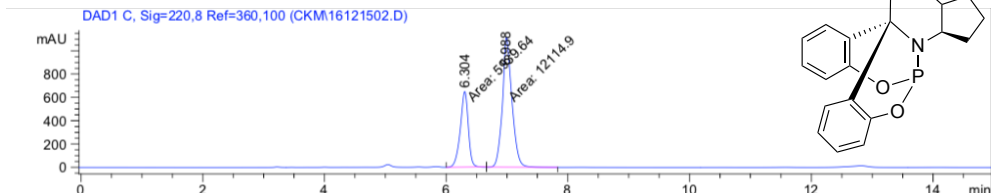


2-3. A chiral sample **5.35** using **5.146** in MeOH (2% ee)



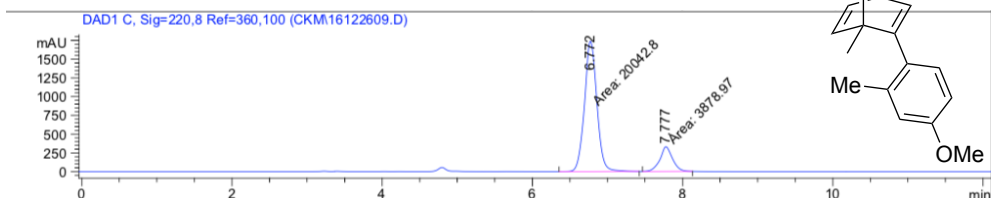
Peak #	RetTime [min]	Type	Width [min]	Area [mAU*s]	Height [mAU]	Area %
1	6.448	MM	0.1523	3849.95313	421.43491	50.9001
2	7.237	MM	0.1730	3713.78760	357.87796	49.0999

2-4. A chiral sample **5.35** using **5.147** in MeOH (-34% ee)



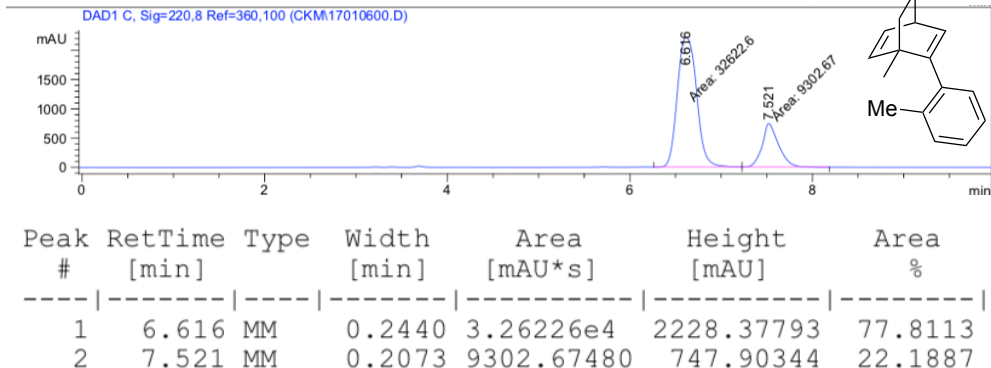
Peak #	RetTime [min]	Type	Width [min]	Area [mAU*s]	Height [mAU]	Area %
1	6.304	MM	0.1522	5939.63623	650.38916	32.8983
2	6.988	MM	0.1807	1.21149e4	1117.38843	67.1017

2-5. A chiral sample **5.35** using **5.148** in MeOH (68% ee)

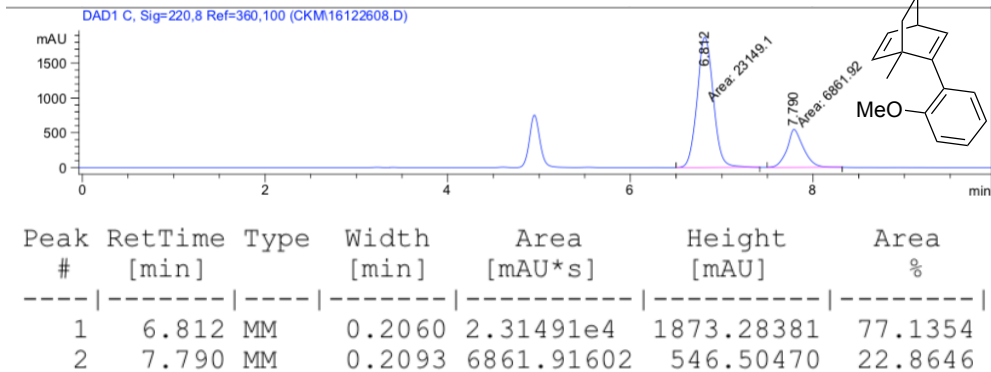


Peak #	RetTime [min]	Type	Width [min]	Area [mAU*s]	Height [mAU]	Area %
1	6.772	MM	0.1918	2.00428e4	1741.38721	83.7848
2	7.777	MM	0.1951	3878.96655	331.44174	16.2152

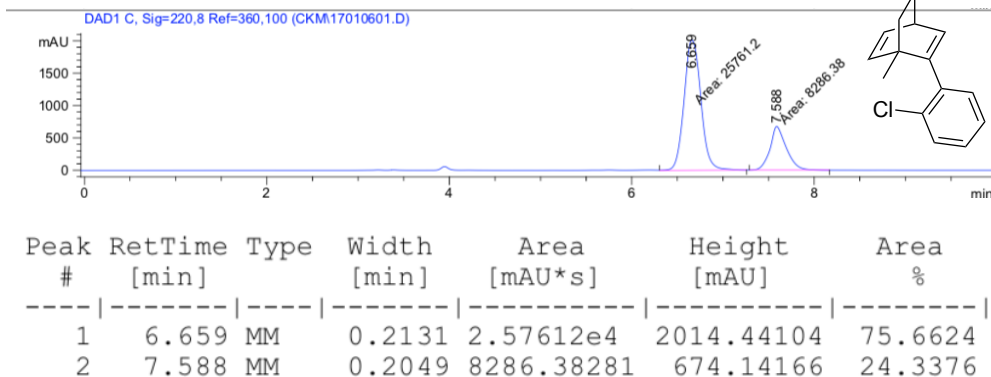
2-6. A chiral sample **5.35** using **5.149** in MeOH (56% *ee*)



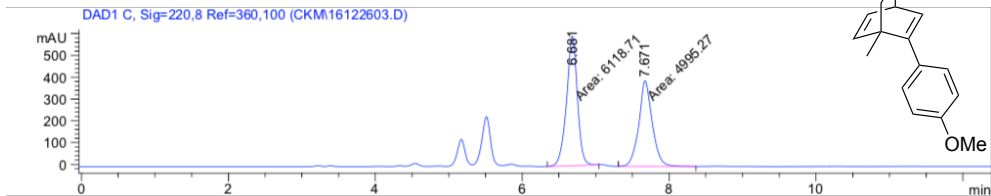
2-7. A chiral sample **5.35** using **5.150** in MeOH (54% *ee*)



2-8. A chiral sample **5.35** using **5.151** in MeOH (51% *ee*)

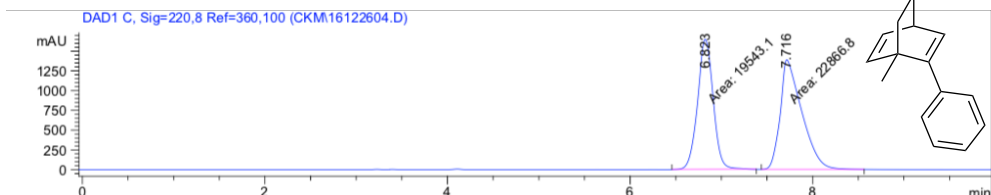


2-9. A chiral sample **5.35** using **5.152** in MeOH (10% ee)



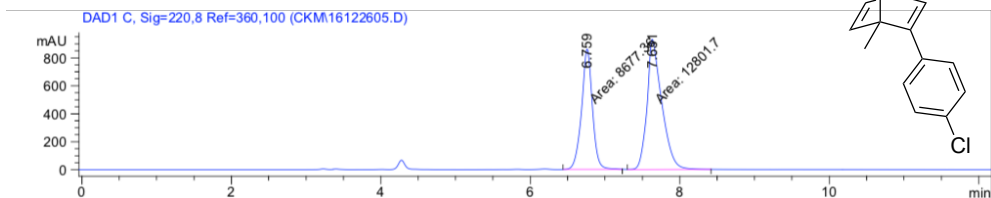
Peak #	RetTime [min]	Type	Width [min]	Area [mAU*s]	Height [mAU]	Area %
1	6.681	MM	0.1716	6118.71240	594.16510	55.0542
2	7.671	MM	0.2117	4995.27148	393.31033	44.9458

2-10. A chiral sample **5.35** using **5.153** in MeOH (-8% ee)



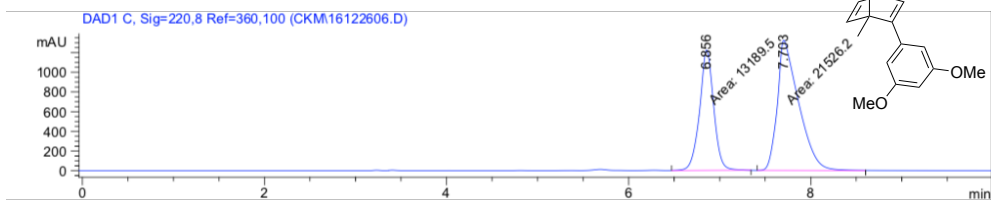
Peak #	RetTime [min]	Type	Width [min]	Area [mAU*s]	Height [mAU]	Area %
1	6.823	MM	0.1976	1.95431e4	1648.14087	46.0815
2	7.716	MM	0.2739	2.28668e4	1391.34985	53.9185

2-11. A chiral sample **5.35** using **5.154** in MeOH (-19% ee)



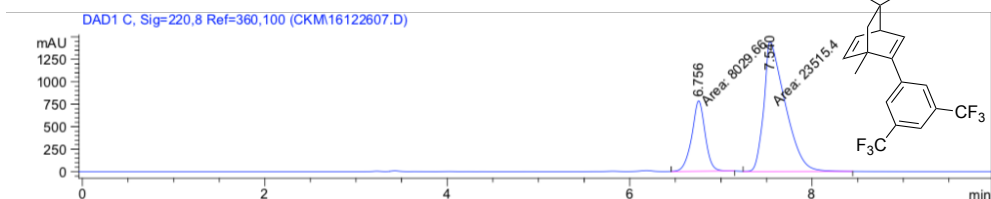
Peak #	RetTime [min]	Type	Width [min]	Area [mAU*s]	Height [mAU]	Area %
1	6.759	MM	0.1679	8677.36133	861.44305	40.3991
2	7.631	MM	0.2287	1.28017e4	932.84998	59.6009

2-12. A chiral sample **5.35** using **5.155** in MeOH (-24% ee)



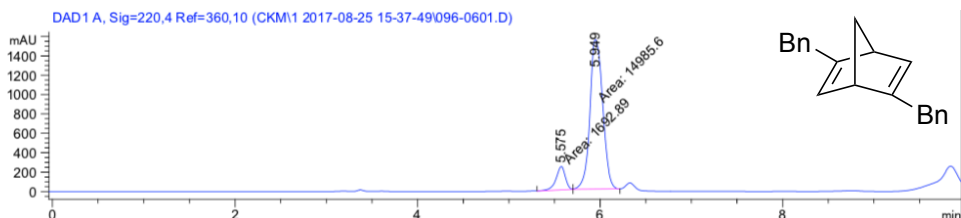
Peak #	RetTime [min]	Type	Width [min]	Area [mAU*s]	Height [mAU]	Area %
1	6.856	MM	0.1795	1.31895e4	1224.82166	37.9929
2	7.703	MM	0.2710	2.15262e4	1323.82764	62.0071

2-13. A chiral sample **5.35** using **5.156** in MeOH (-49% ee)



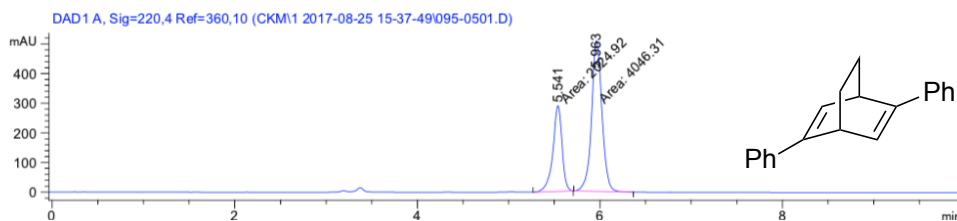
Peak #	RetTime [min]	Type	Width [min]	Area [mAU*s]	Height [mAU]	Area %
1	6.756	MM	0.1702	8029.66309	786.06592	25.4545
2	7.540	MM	0.2703	2.35154e4	1450.06165	74.5455

2-14. A chiral sample **5.35** using **5.158** in MeOH (-80% ee)



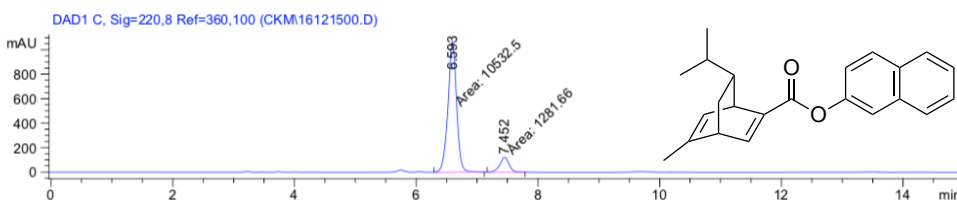
Peak #	RetTime [min]	Type	Width [min]	Area [mAU*s]	Height [mAU]	Area %
1	5.575	MM	0.1168	1692.88611	241.50577	10.1501
2	5.949	MM	0.1619	1.49856e4	1542.64355	89.8499

2-15. A chiral sample **5.35** using **5.159** in MeOH (-33% *ee*)



Peak #	RetTime [min]	Type	Width [min]	Area [mAU*s]	Height [mAU]	Area %
1	5.541	MM	0.1165	2024.92224	289.63043	33.3527
2	5.963	MM	0.1325	4046.30933	508.99167	66.6473

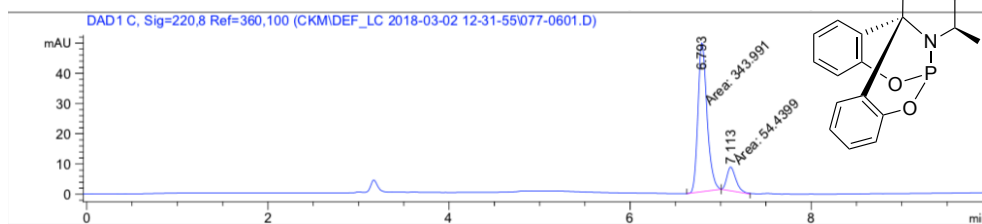
2-16. A chiral sample **5.35** using **5.160** in MeOH (78% *ee*)



Peak #	RetTime [min]	Type	Width [min]	Area [mAU*s]	Height [mAU]	Area %
1	6.593	MM	0.1637	1.05325e4	1072.29187	89.1515
2	7.452	MM	0.1748	1281.66028	122.17838	10.8485

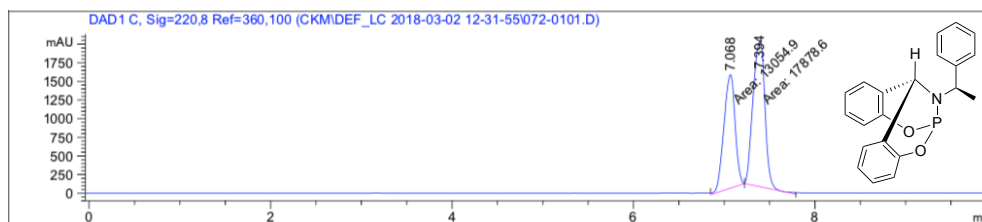
3. Chromatographic Traces of **5.35** (aqueous toluene solvent)

3-1. A chiral sample **5.35** using **5.145** in toluene/H₂O (73% *ee*)



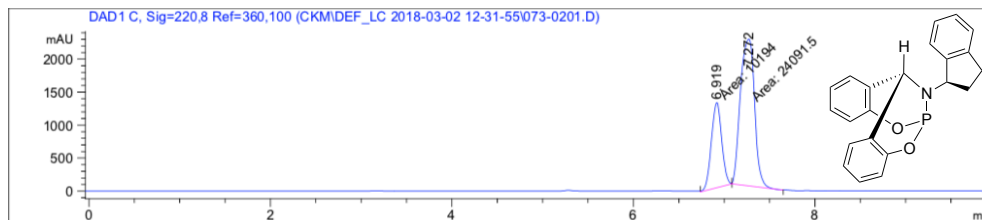
Peak #	RetTime [min]	Type	Width [min]	Area [mAU*s]	Height [mAU]	Area %
1	6.793	MM	0.1163	343.99088	49.27545	86.3364
2	7.113	MM	0.1150	54.43990	7.89144	13.6636

3-2. A chiral sample **5.35** using **5.146** in toluene/H₂O (-16% *ee*)



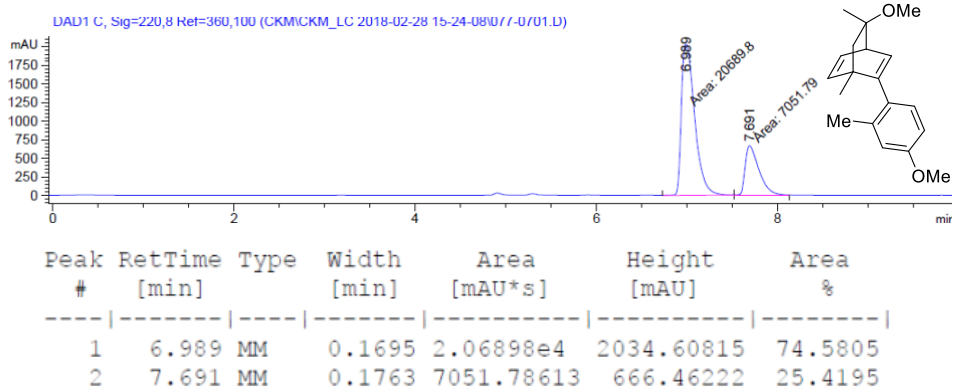
Peak #	RetTime [min]	Type	Width [min]	Area [mAU*s]	Height [mAU]	Area %
1	7.068	MM	0.1427	1.30549e4	1524.74780	42.2032
2	7.394	MM	0.1534	1.78786e4	1942.85889	57.7968

3-3. A chiral sample **5.35** using **5.147** in toluene/H₂O (-41% *ee*)

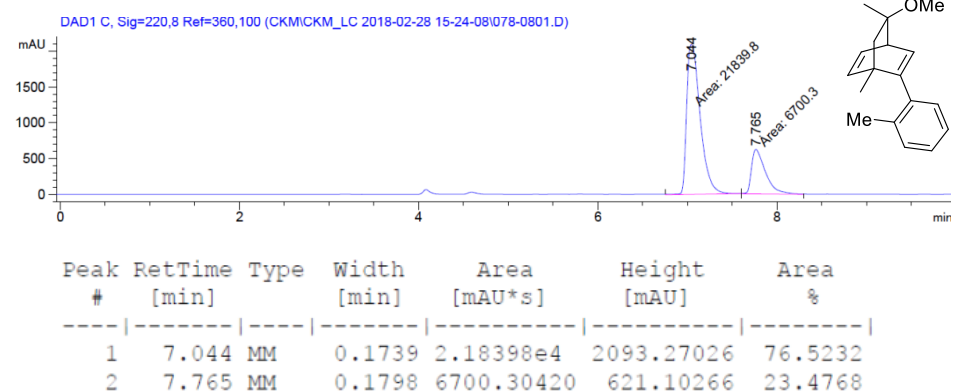


Peak #	RetTime [min]	Type	Width [min]	Area [mAU*s]	Height [mAU]	Area %
1	6.919	MM	0.1316	1.01940e4	1290.66931	29.7328
2	7.272	MM	0.1805	2.40915e4	2224.61694	70.2672

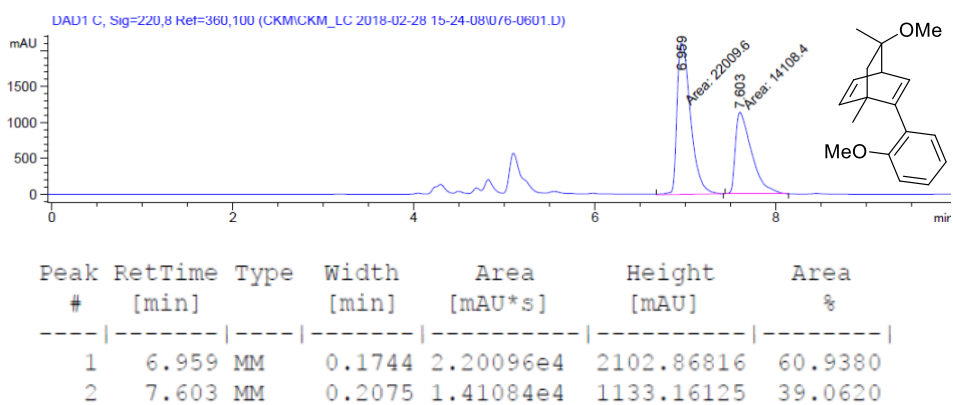
3-4. A chiral sample **5.35** using **5.148** in toluene/H₂O (49% *ee*)



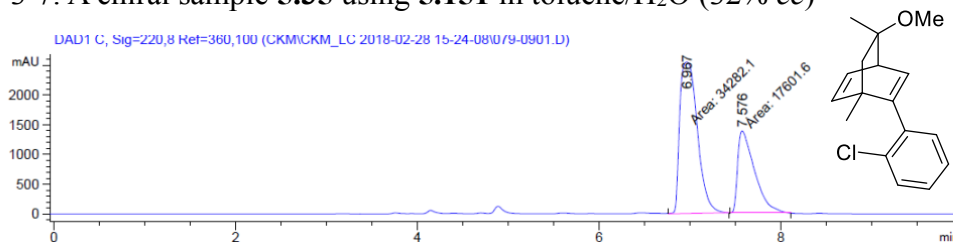
3-5. A chiral sample **5.35** using **5.149** in toluene/H₂O (53% *ee*)



3-6. A chiral sample **5.35** using **5.150** in toluene/H₂O (22% *ee*)

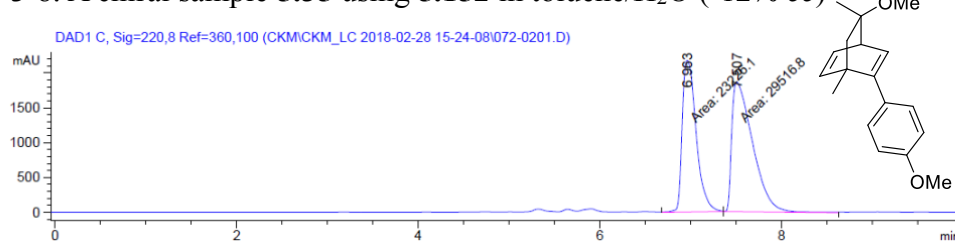


3-7. A chiral sample **5.35** using **5.151** in toluene/H₂O (32% *ee*)



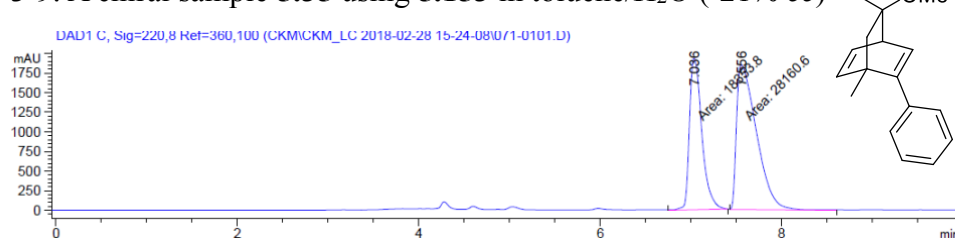
Peak #	RetTime [min]	Type	Width [min]	Area [mAU*s]	Height [mAU]	Area %
1	6.967	MM	0.2240	3.42821e4	2550.56299	66.0749
2	7.576	MM	0.2134	1.76016e4	1374.89014	33.9251

3-8. A chiral sample **5.35** using **5.152** in toluene/H₂O (-12% *ee*)



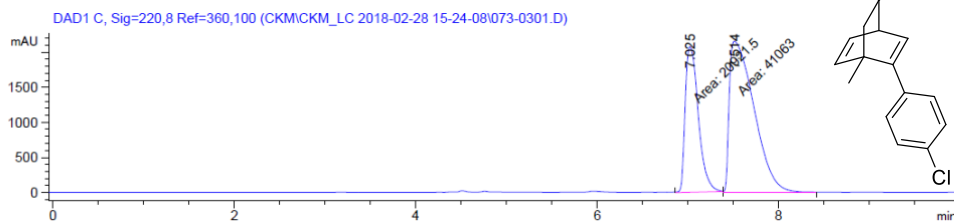
Peak #	RetTime [min]	Type	Width [min]	Area [mAU*s]	Height [mAU]	Area %
1	6.963	MM	0.1779	2.32261e4	2175.85840	44.0365
2	7.507	MM	0.2648	2.95168e4	1857.70129	55.9635

3-9. A chiral sample **5.35** using **5.153** in toluene/H₂O (-21% *ee*)



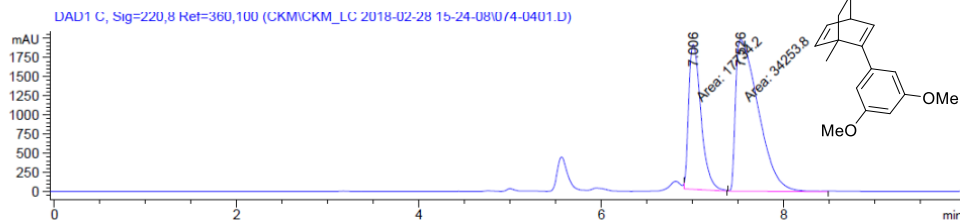
Peak #	RetTime [min]	Type	Width [min]	Area [mAU*s]	Height [mAU]	Area %
1	7.036	MM	0.1584	1.83538e4	1931.58826	39.4584
2	7.556	MM	0.2541	2.81606e4	1847.08655	60.5416

3-10. A chiral sample **5.35** using **5.154** in toluene/H₂O (-32% ee)



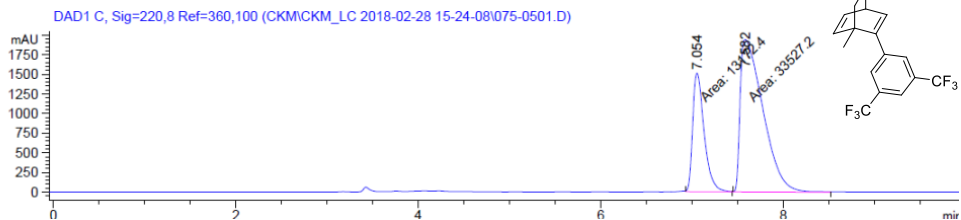
Peak #	RetTime [min]	Type	Width [min]	Area [mAU*s]	Height [mAU]	Area %
1	7.025	MM	0.1677	2.09215e4	2079.51563	33.7528
2	7.514	MM	0.3165	4.10630e4	2162.35327	66.2472

3-11. A chiral sample **5.35** using **5.155** in toluene/H₂O (-32% ee)



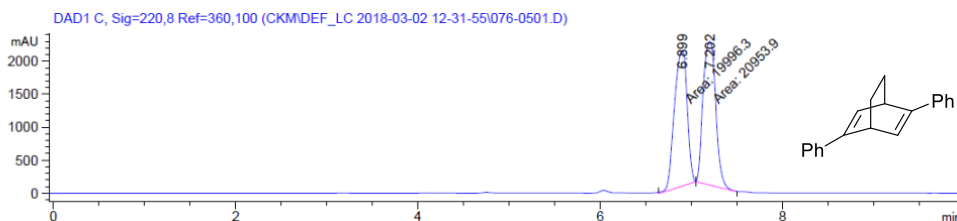
Peak #	RetTime [min]	Type	Width [min]	Area [mAU*s]	Height [mAU]	Area %
1	7.006	MM	0.1562	1.77342e4	1892.03809	34.1122
2	7.526	MM	0.2880	3.42538e4	1981.94885	65.8878

3-12. A chiral sample **5.35** using **5.156** in toluene/H₂O (-44% ee)



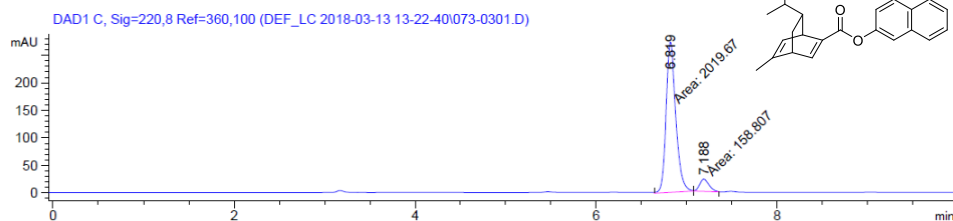
Peak #	RetTime [min]	Type	Width [min]	Area [mAU*s]	Height [mAU]	Area %
1	7.054	MM	0.1453	1.31724e4	1511.09302	28.2067
2	7.582	MM	0.2876	3.35272e4	1942.95154	71.7933

3-13. A chiral sample **5.35** using **5.159** in toluene/H₂O (-2% ee)



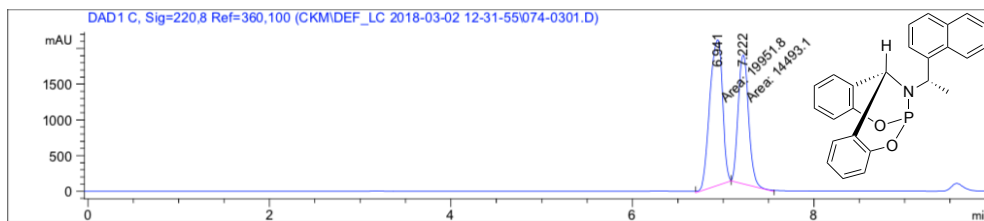
Peak #	RetTime [min]	Type	Width [min]	Area [mAU*s]	Height [mAU]	Area %
1	6.899	MM	0.1625	1.99963e4	2050.92529	48.8308
2	7.202	MM	0.1606	2.09539e4	2174.30176	51.1692

3-14. A chiral sample **5.35** using **5.160** in toluene/H₂O (85% ee)



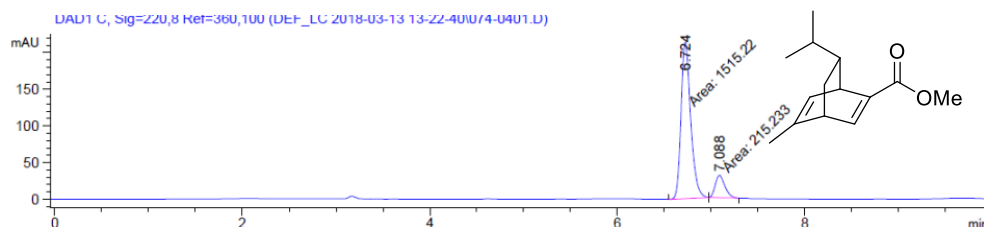
Peak #	RetTime [min]	Type	Width [min]	Area [mAU*s]	Height [mAU]	Area %
1	6.819	MM	0.1228	2019.67017	274.01099	92.7102
2	7.188	MM	0.1183	158.80652	22.38255	7.2898

3-15. A chiral sample **5.35** using **5.161** in toluene/H₂O (16% ee)



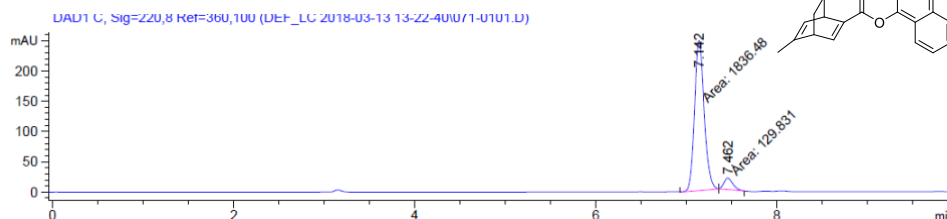
Peak #	RetTime [min]	Type	Width [min]	Area [mAU*s]	Height [mAU]	Area %
1	6.941	MM	0.1629	1.99518e4	2040.89270	57.9237
2	7.222	MM	0.1337	1.44931e4	1806.71802	42.0763

3-16. A chiral sample **5.35** using **5.162** in toluene/H₂O (75% *ee*)



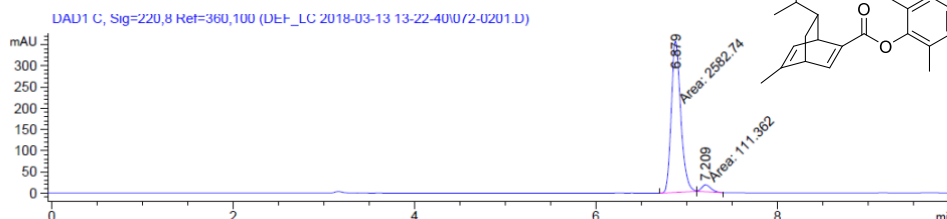
Peak #	RetTime [min]	Type	Width [min]	Area [mAU*s]	Height [mAU]	Area %
1	6.724	MM	0.1184	1515.22314	213.31847	87.5621
2	7.088	MM	0.1174	215.23308	30.54273	12.4379

3-17. A chiral sample **5.35** using **5.163** in toluene/H₂O (87% *ee*)



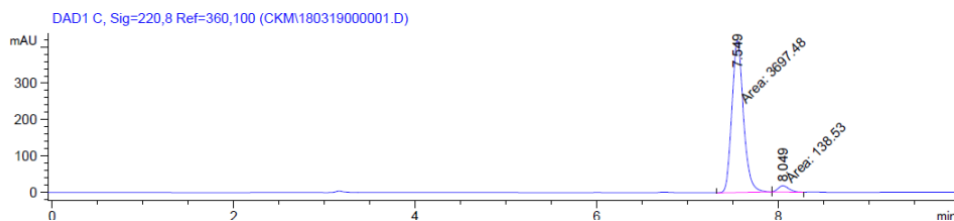
Peak #	RetTime [min]	Type	Width [min]	Area [mAU*s]	Height [mAU]	Area %
1	7.142	MM	0.1233	1836.48218	248.29167	93.3972
2	7.462	MM	0.1140	129.83121	18.98735	6.6028

3-18. A chiral sample **5.35** using **5.164** in toluene/H₂O (92% *ee*)



Peak #	RetTime [min]	Type	Width [min]	Area [mAU*s]	Height [mAU]	Area %
1	6.879	MM	0.1206	2582.74292	357.00864	95.8664
2	7.209	MM	0.1137	111.36246	16.32810	4.1336

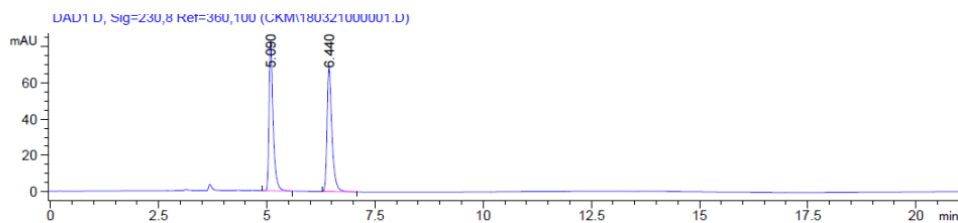
3-19. A chiral sample **5.35** using **5.165** in toluene/H₂O (93% *ee*)



Peak #	RetTime [min]	Type	Width [min]	Area [mAU*s]	Height [mAU]	Area %
1	7.549	MM	0.1475	3697.47681	417.89795	96.3887
2	8.049	MM	0.1346	138.52971	17.15647	3.6113

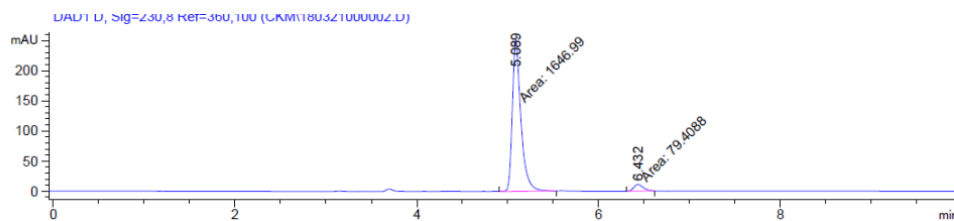
4. Chromatographic Traces of **5.39**

4-1. A racemic sample



Peak #	RetTime [min]	Type	Width [min]	Area [mAU*s]	Height [mAU]	Area %
1	5.090	BB	0.0977	538.11230	82.92719	50.0890
2	6.440	BB	0.1171	536.20099	68.63211	49.9110

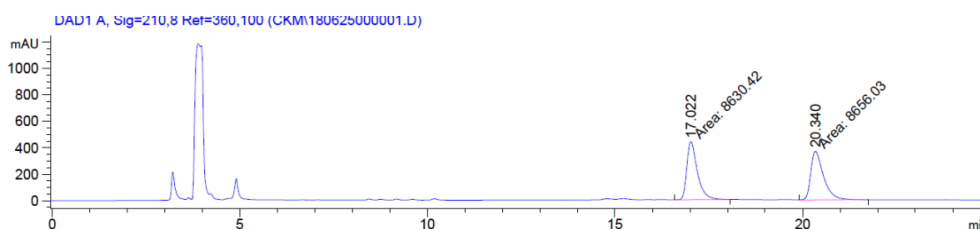
4-2. A chiral sample (91% *ee*)



Peak #	RetTime [min]	Type	Width [min]	Area [mAU*s]	Height [mAU]	Area %
1	5.089	MM	0.1090	1646.98633	251.84337	95.4003
2	6.432	MM	0.1186	79.40883	11.15847	4.5997

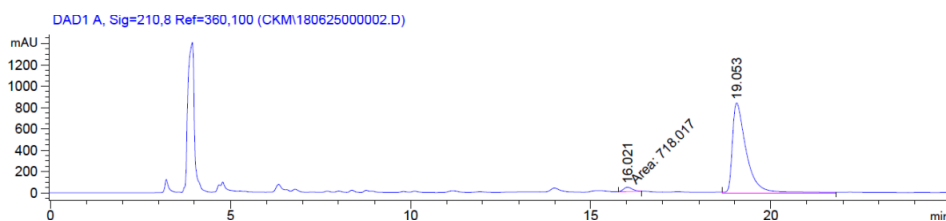
5. Chromatographic Traces of 5.40-diol

5-1. A racemic sample



Peak #	RetTime [min]	Type	Width [min]	Area [mAU*s]	Height [mAU]	Area %
1	17.022	MM	0.3277	8630.41797	438.91748	49.9259
2	20.340	MM	0.3931	8656.03223	366.96918	50.0741

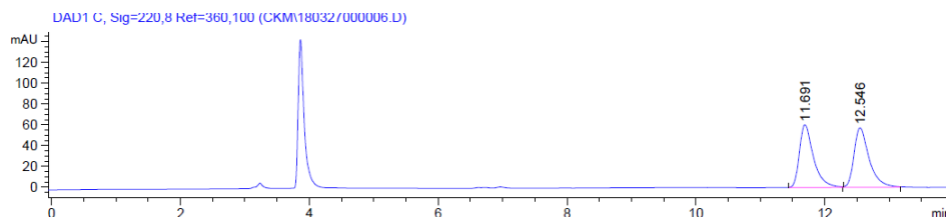
5-2. A chiral sample (94% ee)



Peak #	RetTime [min]	Type	Width [min]	Area [mAU*s]	Height [mAU]	Area %
1	16.021	MM	0.2883	718.01672	41.51555	3.0545
2	19.053	VV	0.3957	2.27890e4	842.18390	96.9455

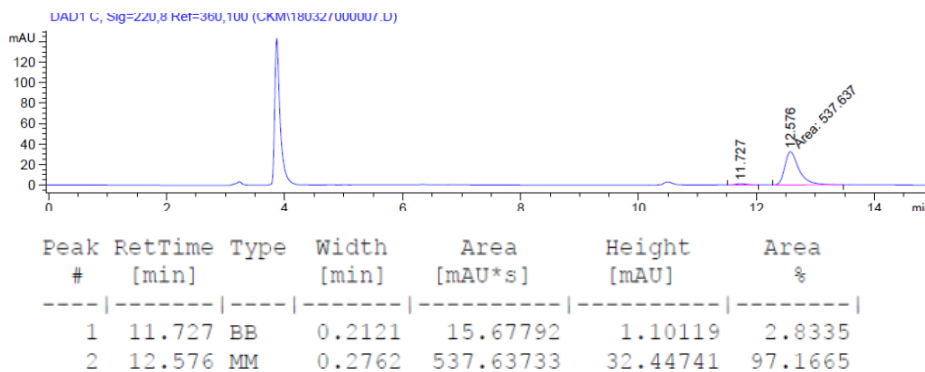
6. Chromatographic Traces of 5.41-diol

6-1. A racemic sample



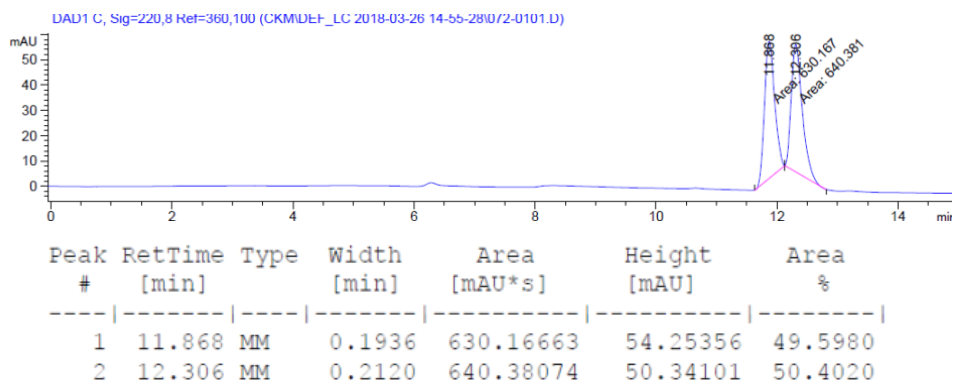
Peak #	RetTime [min]	Type	Width [min]	Area [mAU*s]	Height [mAU]	Area %
1	11.691	BB	0.2272	918.32672	60.45929	49.5331
2	12.546	BB	0.2445	935.63763	57.30799	50.4669

6-2. A chiral sample (93% ee)

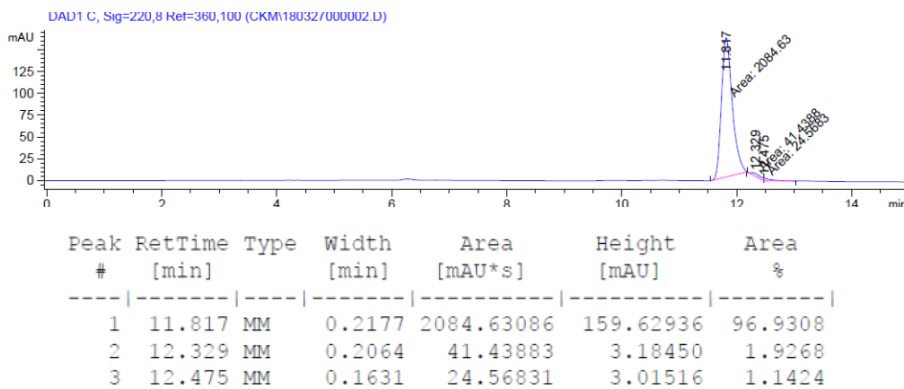


7. Chromatographic Traces of 5.42

7-1. A racemic sample

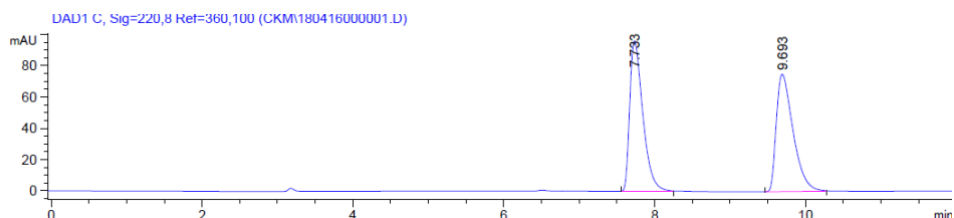


7-2. A chiral sample (94% ee)



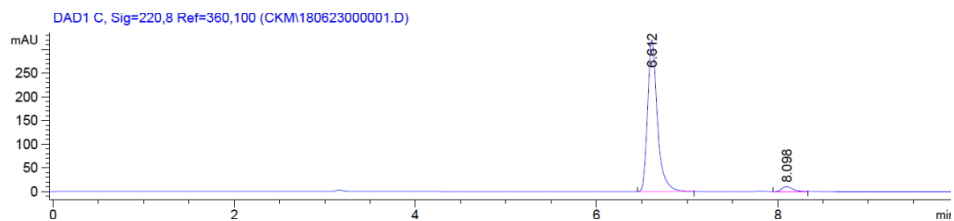
8. Chromatographic Traces of 5.43

8-1. A racemic sample



Peak #	RetTime [min]	Type	Width [min]	Area [mAU*s]	Height [mAU]	Area %
1	7.733	BB	0.1850	1162.98792	96.23158	50.1090
2	9.693	BB	0.2360	1157.92969	75.05307	49.8910

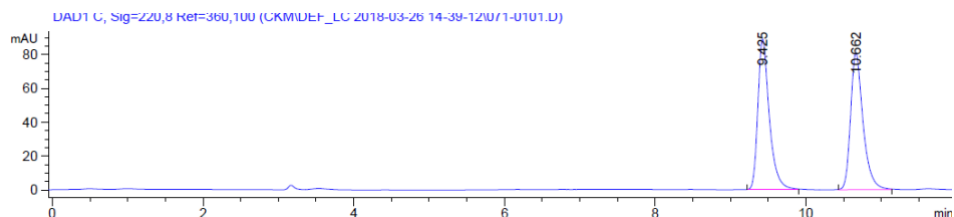
8-2. A chiral sample (93% ee)



Peak #	RetTime [min]	Type	Width [min]	Area [mAU*s]	Height [mAU]	Area %
1	6.612	BB S	0.1136	2401.12256	319.63507	96.5759
2	8.098	VB	0.1233	85.13108	10.42209	3.4241

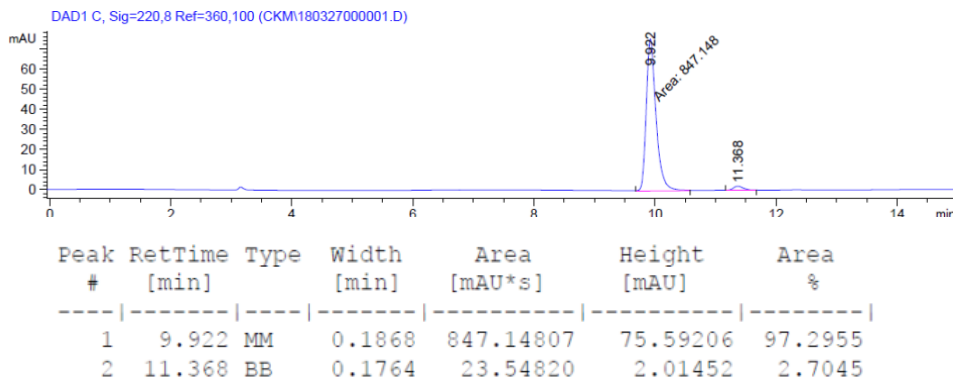
9. Chromatographic Traces of 5.44

9-1. A racemic sample



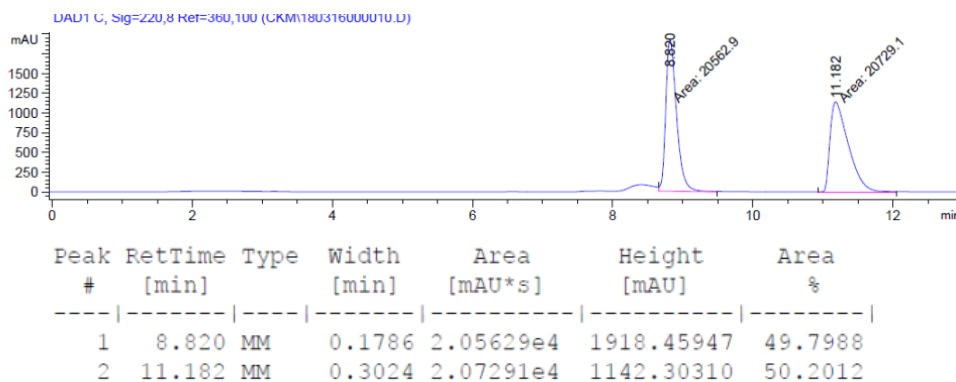
Peak #	RetTime [min]	Type	Width [min]	Area [mAU*s]	Height [mAU]	Area %
1	9.425	BB	0.1569	937.52679	89.00380	50.2105
2	10.662	BB	0.1740	929.66425	80.91231	49.7895

9-2. A chiral sample (95% *ee*)

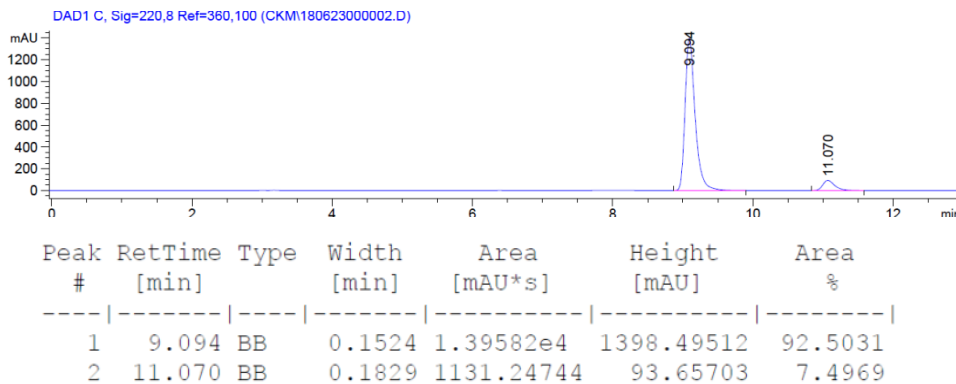


10. Chromatographic Traces of 5.45

10-1. A racemic sample

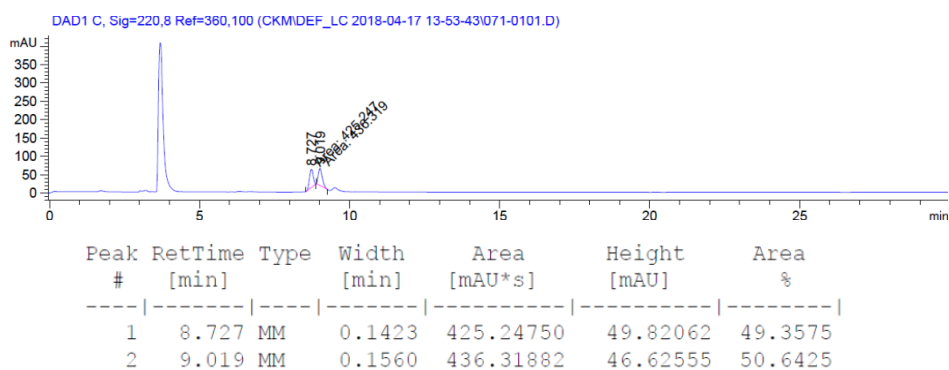


10-2. A chiral sample (85% *ee*)

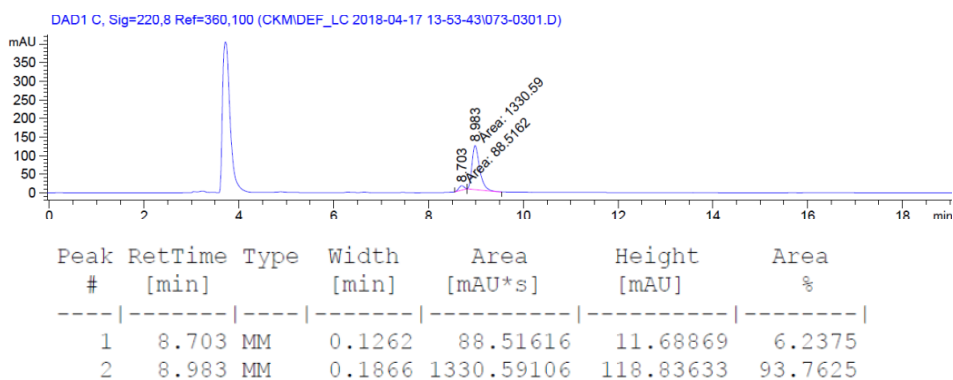


11. Chromatographic Traces of 5.46-diol

11-1. A racemic sample

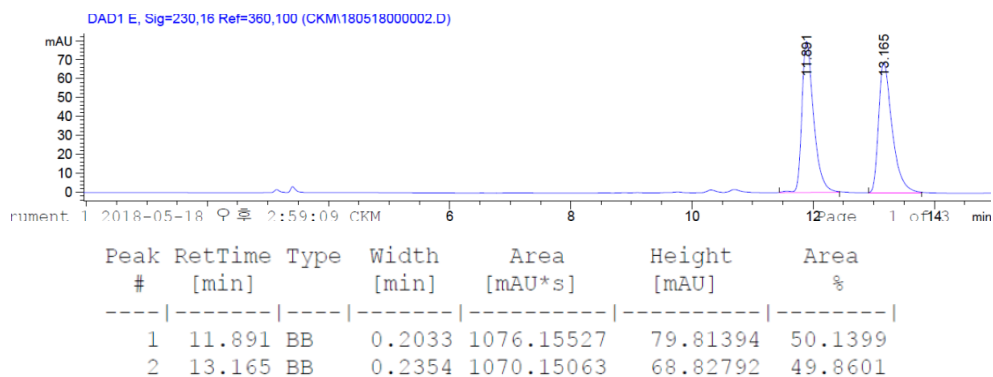


11-2. A chiral sample (88 % ee)

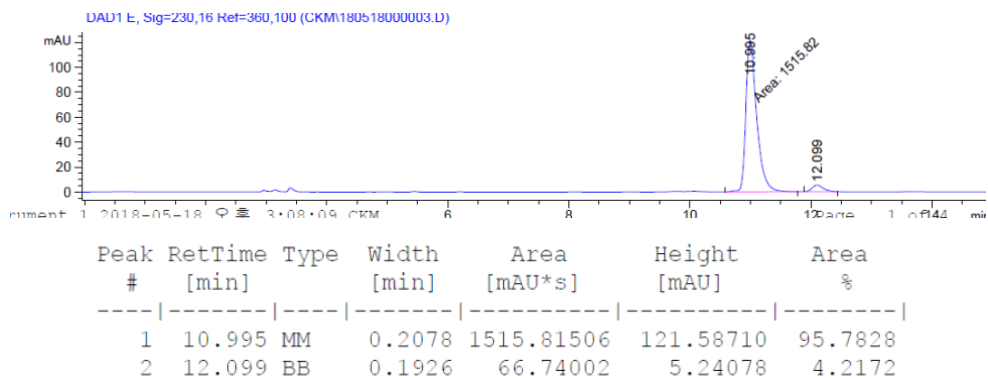


12. Chromatographic Traces of 5.49

12-1. A racemic sample

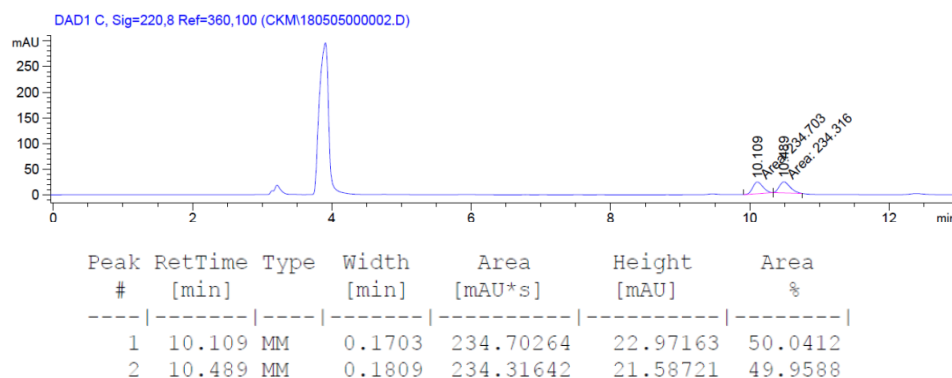


12-2. A chiral sample (92% ee)

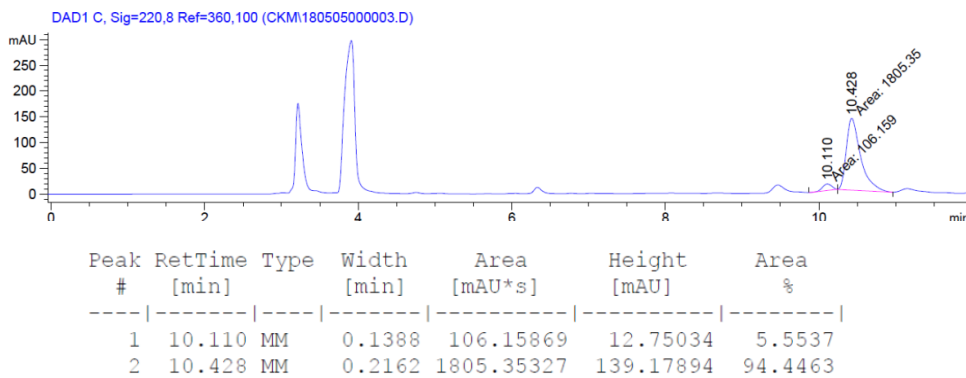


13. Chromatographic Traces of 5.50-diol

13-1. A racemic sample

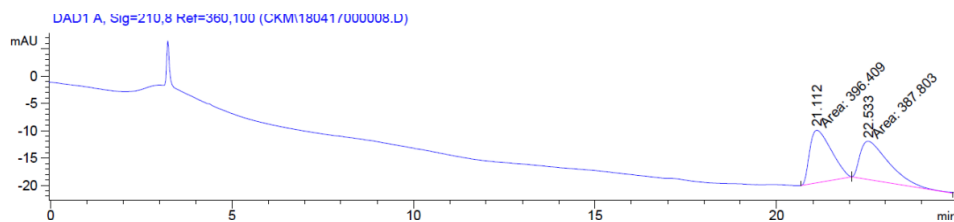


13-2. A chiral sample (89% ee)



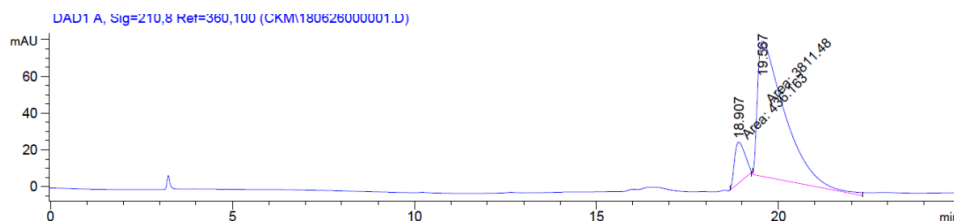
14. Chromatographic Traces of 5.53

14-1. A racemic sample



Peak #	RetTime [min]	Type	Width [min]	Area [mAU*s]	Height [mAU]	Area %
1	21.112	MM	0.6865	396.40930	9.62378	50.5487
2	22.533	MM	0.9226	387.80298	7.00554	49.4513

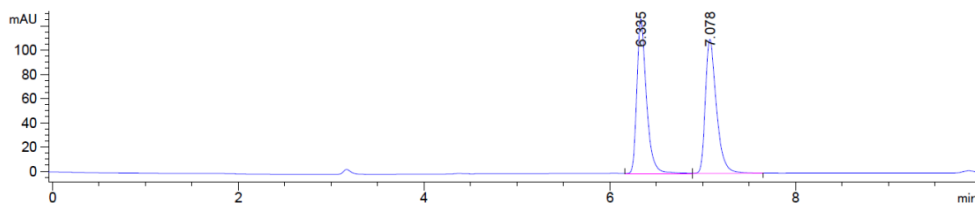
14-2. A chiral sample (80% ee)



Peak #	RetTime [min]	Type	Width [min]	Area [mAU*s]	Height [mAU]	Area %
1	18.907	MM	0.3269	436.16278	22.23916	10.2684
2	19.567	MM	0.8619	3811.47559	73.70274	89.7316

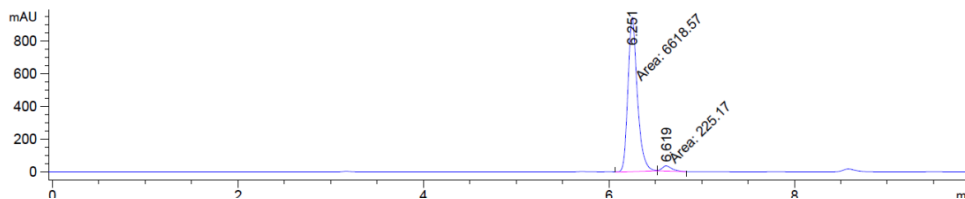
15. Chromatographic Traces of 5.62

15-1. A racemic sample



Peak #	RetTime [min]	Type	Width [min]	Area [mAU*s]	Height [mAU]	Area %
1	6.335	VV	0.1078	916.03076	127.47469	50.0593
2	7.078	VB	0.1263	913.86176	110.67357	49.9407

15-2. A chiral sample (93% ee)



Peak #	RetTime [min]	Type	Width [min]	Area [mAU*s]	Height [mAU]	Area %
1	6.251	MM	0.1169	6618.57373	943.32916	96.7098
2	6.619	MM	0.1204	225.16957	31.16169	3.2902

16. Chromatographic Traces of **5.167**

16-1. Analytical Method

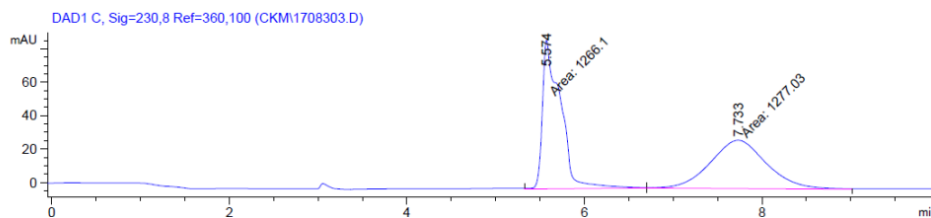
Column: Chiralcel OD-H

Eluent: Hexane/isopropyl alcohol = 95:5

Flow rate: 1.0 ml/min

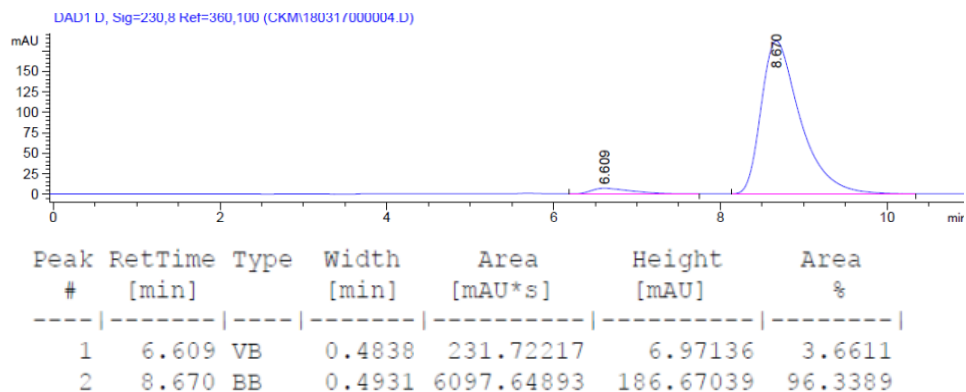
Detection Wavelength: 230 nm

16-2. A racemic sample

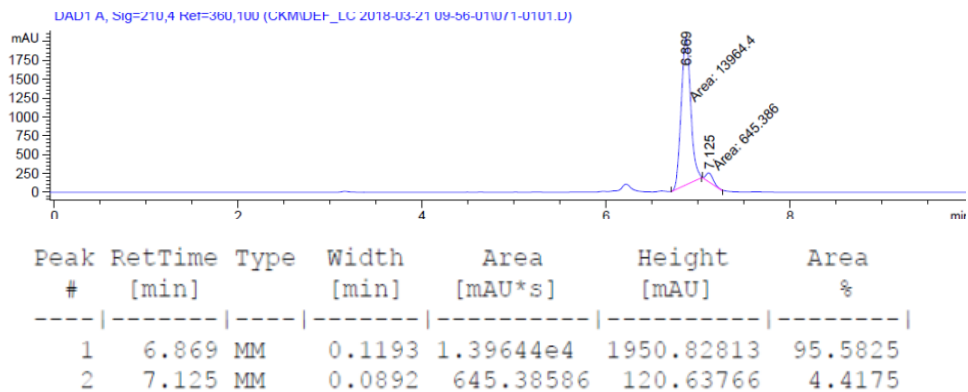


Peak #	RetTime [min]	Type	Width [min]	Area [mAU*s]	Height [mAU]	Area %
1	5.574	MM	0.2365	1266.09631	89.22665	49.7850
2	7.733	MM	0.7360	1277.03296	28.91824	50.2150

16-3. A chiral sample (93% *ee*)



16-4. A chiral sample **5.35** from a chiral sample **5.167** (91% *ee*)



17. Chromatographic Traces of S5.8

17-1. Analytical Method

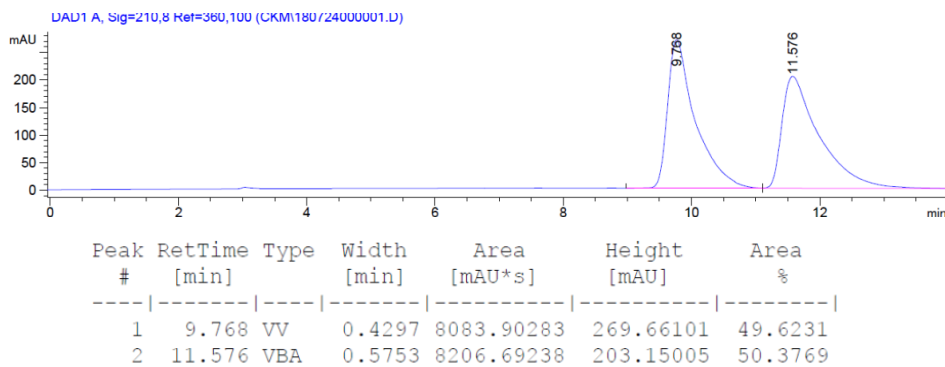
Column: Chiralcel OD-H

Eluent: Hexane/isopropyl alcohol = 95:5

Flow rate: 1.0 ml/min

Detection Wavelength: 210 nm

17-2. A racemic sample



17-3. A chiral sample (90% ee)

